frontiers | Research Topics

Insights in immunological tolerance and regulation 2022

Edited by
Lucienne Chatenoud, Stephen Robert Daley, Julia Y. Wang and Joanna Davies

Published in
Frontiers in Immunology

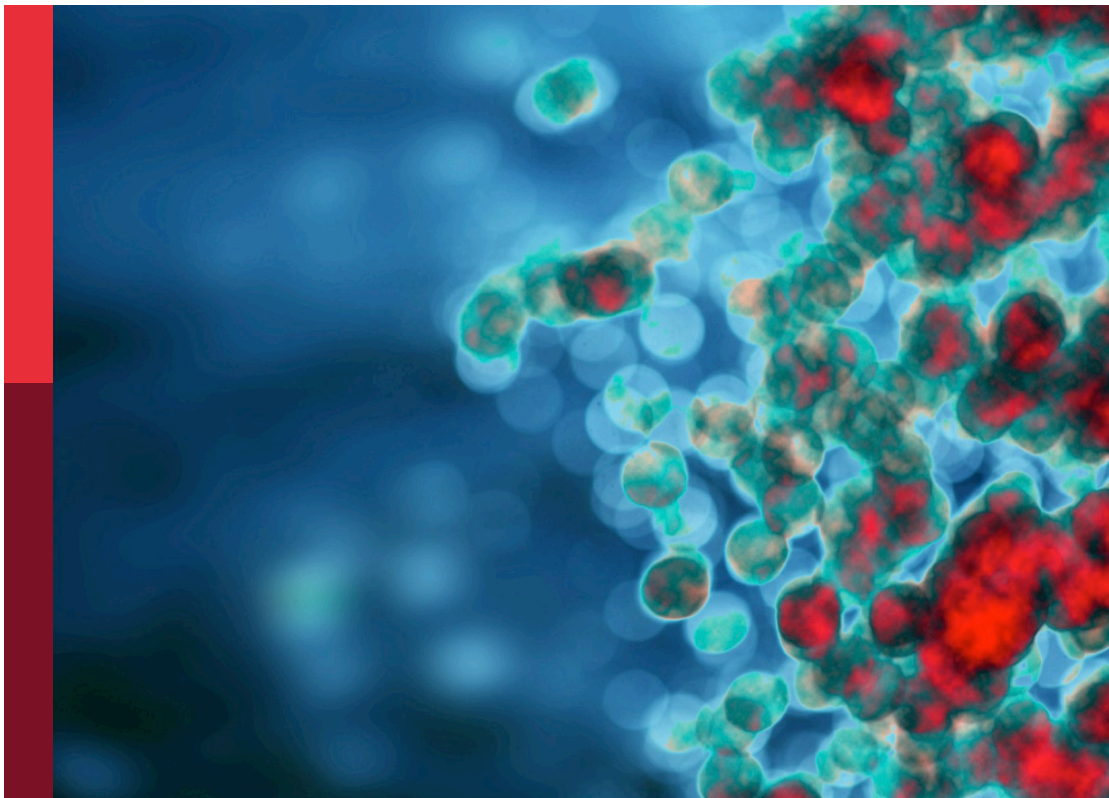

ISSN 1664-8714
ISBN 978-2-8325-3625-4
DOI 10.3389/978-2-8325-3625-4

About Frontiers

Frontiers is more than just an open access publisher of scholarly articles: it is a pioneering approach to the world of academia, radically improving the way scholarly research is managed. The grand vision of Frontiers is a world where all people have an equal opportunity to seek, share and generate knowledge. Frontiers provides immediate and permanent online open access to all its publications, but this alone is not enough to realize our grand goals.

Frontiers journal series

The Frontiers journal series is a multi-tier and interdisciplinary set of open-access, online journals, promising a paradigm shift from the current review, selection and dissemination processes in academic publishing. All Frontiers journals are driven by researchers for researchers; therefore, they constitute a service to the scholarly community. At the same time, the *Frontiers journal series* operates on a revolutionary invention, the tiered publishing system, initially addressing specific communities of scholars, and gradually climbing up to broader public understanding, thus serving the interests of the lay society, too.

Dedication to quality

Each Frontiers article is a landmark of the highest quality, thanks to genuinely collaborative interactions between authors and review editors, who include some of the world's best academicians. Research must be certified by peers before entering a stream of knowledge that may eventually reach the public - and shape society; therefore, Frontiers only applies the most rigorous and unbiased reviews. Frontiers revolutionizes research publishing by freely delivering the most outstanding research, evaluated with no bias from both the academic and social point of view. By applying the most advanced information technologies, Frontiers is catapulting scholarly publishing into a new generation.

What are Frontiers Research Topics?

Frontiers Research Topics are very popular trademarks of the *Frontiers journals series*: they are collections of at least ten articles, all centered on a particular subject. With their unique mix of varied contributions from Original Research to Review Articles, Frontiers Research Topics unify the most influential researchers, the latest key findings and historical advances in a hot research area.

Find out more on how to host your own Frontiers Research Topic or contribute to one as an author by contacting the Frontiers editorial office: frontiersin.org/about/contact

Insights in immunological tolerance and regulation: 2022

Topic editors

Lucienne Chatenoud — Université Paris Cité, France
Stephen Robert Daley — Queensland University of Technology, Australia
Julia Y. Wang — Curandis Inc, United States
Joanna Davies — San Diego Biomedical Research Institute, United States

Citation

Chatenoud, L., Daley, S. R., Wang, J. Y., Davies, J., eds. (2023). *Insights in immunological tolerance and regulation: 2022*. Lausanne: Frontiers Media SA. doi: 10.3389/978-2-8325-3625-4

Table of contents

frontiers | Frontiers in Immunology

TYPE Review
PUBLISHED 19 August 2022
DOI 10.3389/fimmu.2022.962552

OPEN ACCESS

EDITED BY
Joanna Davies,
San Diego Biomedical Research Institute, United States

REVIEWED BY
Bartosz Puła,
Institute of Hematology and Transfusiology (IHT), Poland
Stefania Gobessi,
Gadeta BV, Netherlands

*CORRESPONDENCE
Yongping Song
songyongping0001@126.com
Qingsong Yin
jnyinqingsong@163.com

SPECIALTY SECTION
This article was submitted to Immunological Tolerance and Regulation, a section of the journal Frontiers in Immunology

RECEIVED 06 June 2022
ACCEPTED 28 July 2022
PUBLISHED 19 August 2022

CITATION
Liu Y, Song Y and Yin Q (2022) Effects of ibrutinib on T-cell immunity in patients with chronic lymphocytic leukemia. *Front. Immunol.* 13:962552. doi: 10.3389/fimmu.2022.962552

Effects of ibrutinib on T-cell immunity in patients with chronic lymphocytic leukemia

Yanyan Liu, Yongping Song* and Qingsong Yin*

Department of Hematology, The Affiliated Cancer Hospital of Zhengzhou University and Henan Cancer Hospital, Zhengzhou, China

Chronic lymphocytic leukemia (CLL), a highly heterogeneous B-cell malignancy, is characterized by tumor microenvironment disorder and T-cell immune dysfunction, which play a major role in the proliferation and survival of CLL cells. Ibrutinib is the first irreversible inhibitor of Bruton's tyrosine kinase (BTK). In addition to targeting B-cell receptor (BCR) signaling to kill tumor cells, increasing evidence has suggested that ibrutinib regulates the tumor microenvironment and T-cell immunity in a direct and indirect manner. For example, ibrutinib not only reverses the tumor microenvironment by blocking cytokine networks and toll-like receptor signaling but also regulates T cells in number, subset distribution, T-cell receptor (TCR) repertoire and immune function by inhibiting interleukin-2 inducible T-cell kinase (ITK) and reducing the expression of inhibitory receptors, and so on. In this review, we summarize the current evidence for the effects of ibrutinib on the tumor microenvironment and cellular immunity of patients with CLL, particularly for the behavior and function of T cells, explore its potential mechanisms, and provide a basis for the clinical benefits of long-term ibrutinib treatment and combined therapy based on T-cell-based immunotherapies.

KEYWORDS

chronic lymphocytic leukemia, ibrutinib, T-cell immunity, tumor microenvironment, immune regulation

Introduction

Chronic lymphocytic leukemia (CLL) is a malignancy of small, mature B lymphocytes that clonally expand into secondary lymphoid organs, bone marrow, and peripheral blood, resulting in lymphadenopathy, splenomegaly, and hematopoietic failure (1, 2). Tumor microenvironment disorder and T-cell immune dysfunction are prominent characteristics of CLL that are clinically manifested as increased susceptibility to opportunistic infections such as viruses and fungi and an increased incidence of autoimmune diseases and secondary malignant tumors (2), which are also the main causes of failure of T-cell-based immunotherapies and drug resistance (3, 4). T cells in

CLL patients, as major supporting cells in the tumor microenvironment and particularly $CD4^+$ T cells, nourish CLL cells through complex cytokine networks or direct contact (5). Moreover, $CD8^+$ T cells demonstrate an "exhausted" phenotype with progressive loss of effector function and impaired memory T-cell potential (6, 7). Therefore, reversing microenvironment disorders and reconstituting T-cell immunity may be critical to improving the outcome of CLL patients (8, 9).

The B-cell receptor (BCR) signaling pathway in CLL cells is reportedly overactivated; thus, targeting the key kinases of the BCR pathway is a promising anti-leukemia therapy. BCR signaling is initiated through upstream kinases, including SYK, BTK, and PI3K, and these can be inhibited by corresponding small-molecule kinase inhibitors (10). First-generation BTK inhibitors (BTKis), such as ibrutinib, acalabrutinib, and zanubrutinib, are irreversible at the C418 site of BTK (11). Second-generation BTKis, such as fenibrutinib, vecabrutinib, and nembrolizumab, can reversibly inhibit BTK and to some extent overcome the drug resistance of first-generation BTKis (11). Ibrutinib, as the first BTKi, has profoundly altered the treatment paradigm of CLL patients, particularly relapsed/refractory CLL (R/R CLL) and high-risk patients with TP53 aberrations (12–14). Both acalabrutinib and zanubrutinib have demonstrated higher selectivity and fewer off-target effects than ibrutinib (11, 15, 16). Nevertheless, previous studies have shown that ibrutinib not only inhibits BCR and nuclear factor kappa B (NF-κB) signaling (17–19) but also plays multiple roles in regulating the tumor microenvironment and T-cell immunity in CLL patients (20–22). This activity has been confirmed by significant improvement in the efficacy of CAR-T cells and the bispecific antibody blinatumomab in the clinic (3, 23–25). However, to date, the effect of ibrutinib on the microenvironment and T-cell immunity of patients with CLL is not completely clear.

Therefore, this article reviews the effects of ibrutinib on the microenvironment and cellular immunity of patients with CLL, particularly on the behavior and function of T cells, and their potential mechanisms, to provide a basis for the clinical benefits of long-term ibrutinib treatment and the further design of combined therapy based on T-cell-based immunotherapies.

Overall regulation of ibrutinib on CLL microenvironment

Secondary lymphoid organs, which are also called proliferation centers, have a more complex microenvironment that is more conducive to CLL cell survival (18), and this is where the BCR signaling activity of CLL cells is upregulated, and the proliferative activity of CLL cells is also increased (18, 26). Stromal cells, nurse-like cells (NLCs), and T cells are three supporting cells in the CLL microenvironment (27) (Figure 1A) that mediate the activation, homing, proliferation, and survival of CLL cells *via* direct contact and the secretion of chemokine/cytokines and adhesion molecules as well as their ligand–receptor interactions (28–33). Together, these constitute complex cytokine networks (33, 34) that in turn recruit the migration of T cells (35), including Th2 cells and Tregs, and induce T–cell immune tolerance, T-cell anergy, and the immune escape of CLL cells (36, 37). Additionally, toll-like receptors (TLRs) interact with BTK, connecting the BCR signal with TLR signals and activating the NF-κB signaling pathway, eventually promoting the proliferation and survival of CLL cells (38, 39). Moreover, TLR signaling also increases the immune escape of CLL cells by inducing Treg expansion and producing immunosuppressive molecules (40).

Accumulating studies have demonstrated that ibrutinib regulates the disordered microenvironment in CLL patients (18, 34). Specifically, ibrutinib directly inhibits the activation and proliferation of CLL cells by blocking the BCR and the NF-κB signaling pathways (18, 19, 31). Moreover, ibrutinib blocks the close "crosstalk" between CLL cells and supporting cells in the microenvironment to prevent their protection of CLL cells by blocking complex cytokine networks and direct contact (27, 39). For instance, ibrutinib not only inhibits the secretion of cytokines, such as CCL3, CCL4, CXCL12, and CXCL13, from CLL cells and their supporting cells within the microenvironment, it also inhibits the TLR signaling pathway (38, 41), which prevents the homing and residence of CLL cells and dissociates these cells from the protective microenvironment (31, 41, 42).

The effects of ibrutinib on circulating T-cell counts

Increasing studies have shown that $CD4^+$ and $CD8^+$ T cells are enriched in the peripheral blood of CLL patients (43). Specifically, the absolute numbers of $CD3^+$, $CD4^+$, and $CD8^+$ T cells significantly increased in the peripheral blood of R/R and naïve CLL patients before ibrutinib treatment (22, 28, 34, 44, 45), particularly $CD8^+$ T cells (20, 44), which resulted in a decreased CD4:CD8 ratio (28, 45) (Figure 2A).

Burger and colleagues described for the first time that ibrutinib treatment induces lymphocyte redistribution using 2H-labeling experiments, which results in increased absolute lymphocyte counts in peripheral blood and significant shrinkage of lymph nodes (46). Subsequently, numerous studies have focused on the effects of ibrutinib on the number of T cells and distribution of T-cell subpopulations, but these results remain controversial. Parry et al. found that $CD3^+$ and $CD8^+$ T-cell counts significantly decreased in R/R and naïve CLL patients who were treated with ibrutinib for 6 months (47). Niemann et al. found that the proportion of $CD4^+$ and $CD8^+$ T cells decreased dramatically after 6 months (34). Yin et al. found that the increased $CD3^+$, $CD4^+$, and $CD8^+$ T cells were significantly decreased in R/R CLL patients after 3 months of

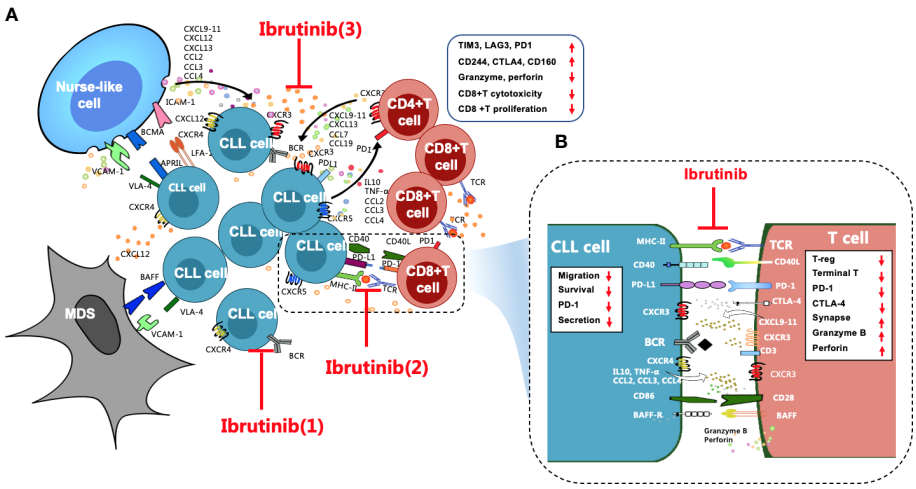

FIGURE 1
Overall regulation of ibrutinib on the CLL microenvironment, particularly T cell immunity, is important. **(A)** Stromal cells, NLCs, and T cells are the three key supporting cells in the CLL microenvironment. They crosstalk with CLL cells through direct contact and chemokines/cytokines and their ligand-receptor interactions, such as CXCR4/CXCL12, CXCR3/CXCL9,10,11, and CXCR5/CXCL13, to mediate the activation, homing, proliferation, and survival of CLL cells, which leads to T-cell immune dysfunction, particularly for $CD8^+$ T cells, which are excessively activated, expanded, and gradually pseudo-exhausted. Exhausted $CD8^+$ T cells highly express a variety of inhibitory receptors, such as PD1, CTLA4, CD244, TIM3, and LAG3. The cytotoxicity and proliferation activity of $CD8^+$ T cells decrease. Ibrutinib regulates the CLL microenvironment by (1) blocking BCR signaling, (2) preventing direct contact between CLL cells and T cells and repairing impaired immune synapses, and (3) inhibiting cytokine networks. **(B)** These effects contribute to improving the activity of effector T cells in CLL patients, such as increased granzyme B and perforin secretion, reduced inhibitory receptors, etc. In addition, ibrutinib inhibits the cytokine secretion, migration, proliferation, and survival of CLL cells.

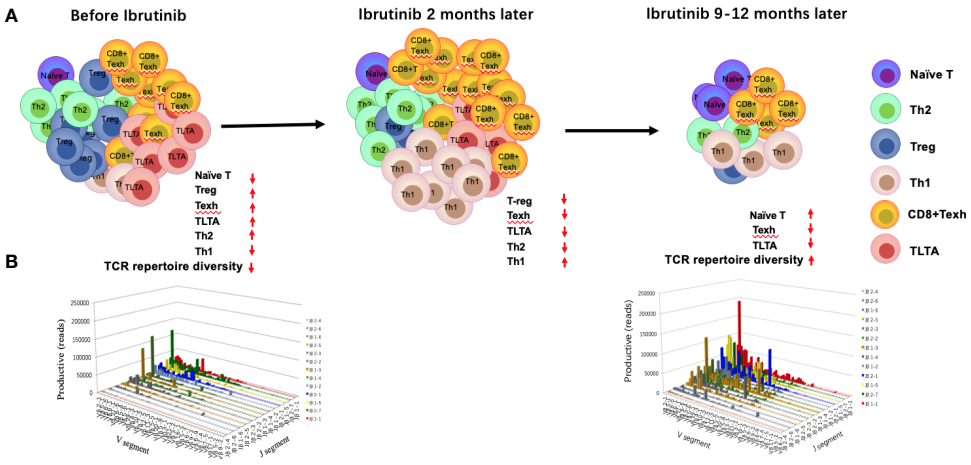

FIGURE 2
Changes in the T-cell compartment and T-cell repertoire before and during ibrutinib treatment. The absolute numbers and percentage of $CD4^+$ and $CD8^+$ T cells increase in the peripheral blood, particularly for $CD8^+$ T cells. However, the distribution of T-cell subgroups is abnormal, which leads to the imbalance of Th1/Th2, an increase in T-regs, long-term activated T cells (TLTAs), and terminally differentiated T cells such as effector memory T cells (T_{EM}) and exhausted T cells (Texh cells), and a decrease in naïve T cells (A, left penal). There is a severely skewed T-cell repertoire in patients with CLL **(B)**. After 1–2 months of ibrutinib treatment, the number of T cells demonstrates a transient increase and then decreases gradually after 6 months (**(A)** middle penal). The distribution of the T-cell subgroups is near to the normal level at 12 months, in parallel with partial reconstruction of the T-cell repertoire diversity [**(A)** right penal; **(B)**].

ibrutinib treatment and then dropped to the normal range after 12 months (22). However, Long et al. noted a progressive increase in T-cell counts until 6 months of ibrutinib treatment in R/R and primary CLL patients (21). Single-cell sequencing also showed that the percentage of T-cell subgroups changed after treatment with ibrutinib, particularly the percentage of $CD8^+$T cells, which increased gradually until 4 months, while $CD4^+$T cells decreased gradually, which coincided with the progressive reduction of CLL cells (20). Differences in the above results may be related to disease status, tumor burden, and time point after ibrutinib treatment. Recently, a study with more intensive detection time points demonstrated there was a transient increase in the T-cell number in CLL patients at about 2 months after ibrutinib treatment, followed by a decrease after 6–10 months that gradually returned to normal levels at 1 year (42).

The reason for the transient increase in T-cell counts after ibrutinib treatment is completely unclear. It may be related to the redistribution of T and CLL cells to the peripheral blood after ibrutinib treatment (48, 49), followed by a simultaneous decline in both T and CLL cells (22, 47–50). Additionally, ibrutinib can reduce activation-induced cell death (AICD) by inhibiting interleukin-2 inducible T cell kinase (ITK) activity, causing a short-term increase in circulating T-cell counts (21). Sun et al. also confirmed this finding in an ITK-deficient mouse model (51).

The regulation of ibrutinib on the differentiation of T-cell subpopulations

T cells are key adaptive immune effector cells that can be mainly classified into multi-functional helper T cells (Th cells), immunosuppressive Tregs, and cytotoxic T cells (CTLs). Acute antigen stimulation drives naïve T-cell differentiation and rapid expansion of effector T cells (Figure 3A). However, prolonged exposure to an antigen from chronic viral infections or cancer induces exhaustion in the responding $CD8^+$ effector T-cell populations (52). Moreover, the differentiation of T-cell subgroups is unbalanced in patients with CLL (Figures 3B, C).

Th1 and Th2 cells

In CLL patients, TCR signaling activation triggers a signaling cascade to activate ITK, promoting the differentiation of Th2 and Treg cells and inhibiting the differentiation of Th1 and cytotoxic $CD8^+$ T cells (53, 54). Additionally, a series of cytokines/chemokines, such as IL6, IL4, and IL10, which are produced by CLL and Th2 cells, can promote immune system skewing toward Th2 cells and inhibit Th1 differentiation (55)

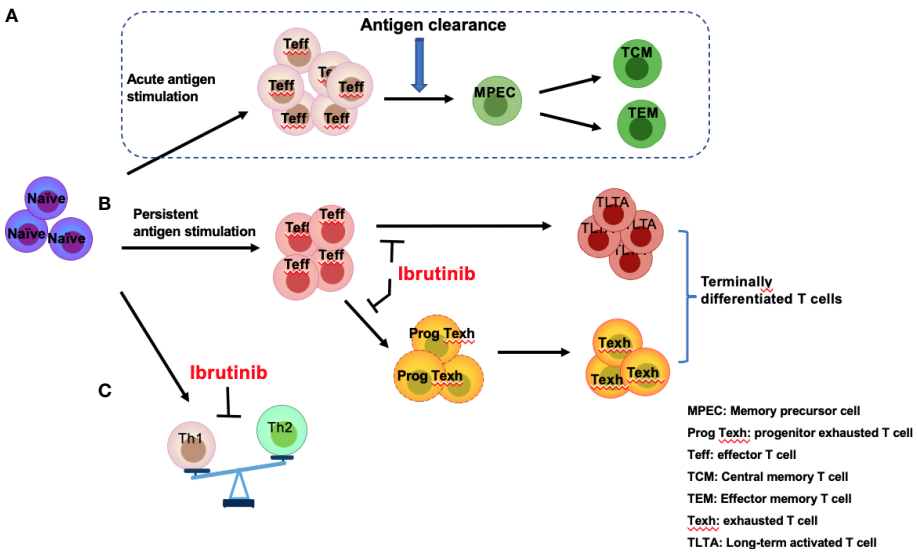

FIGURE 3
Effects of ibrutinib on effector T-cell subgroups. Antigen stimulation drives naïve T cells to differentiate into effector T cells (Teff) followed by rapid expansion of effector T cells, which eventually produce memory precursor cells (MPECs) after antigen clearance, further differentiating into central memory T cells (TCM) and effector memory T cells (TEM) **(A)**. However, persistent antigen stimulation from infections or CLL-related antigens induces over-activation of T cells and promotes progenitor exhausted T (Prog Texh) cells to differentiate into exhausted T (Texh) cells, which leads to the accumulation of terminally differentiated T cells, including TLTA and Texh cells **(B)**. In addition, Th1 and Th2 differentiation is unbalanced **(C)**. Ibrutinib reverses the pseudo-exhaustion of T cells and promotes the activity of effector T cells and the predominant differentiation of Th1 cells in CLL patients.

(Figure 3C). Therefore, compared with healthy subjects, the number of Th1 and Th2 cells in CLL patients increases (56), but the distribution is unbalanced, demonstrating the dominant differentiation of Th2 cells (53), which results in a tumor-promoting environment and a reduced role for Th1 in tumor monitoring (54, 57). Several studies have shown that ITK deficiency promotes T-bet expression and blocks ITK-dependent Th2 cell differentiation (53, 58, 59), while Th1 cell differentiation can be triggered by the substitution of another lymphocyte kinase (RLK) (59). Therefore, ibrutinib can irreversibly bind to ITK to suppress Th2 cell differentiation, restoring the balance between Th1 and Th2 (53).

Tregs and Th17 cells

Tregs and IL-17-producing $CD4^+$ (Th17) cells play an important role in immune tolerance and homeostasis (8, 60). In CLL, Tregs may facilitate a tumor-promoting microenvironment and tumor progression (61, 62). Nevertheless, Th17 cells in anti-tumor immunity are negatively correlated with Tregs and positively correlated with invariant natural killer T cells (NKTs) (63). Disease progression in CLL patients and in the Eμ-TCL1 CLL mouse model is usually accompanied by a reduction in Th17 cells and Treg expansion and its immunosuppressive effector function (64–66), which demonstrates the different roles of these T cell subsets in CLL proliferation and survival. It has been reported that the frequency and absolute number of Tregs are significantly higher in CLL patients, which is related to high tumor burden and advanced disease (66, 67), and an increase in Tregs also indicates shorter overall survival (OS) (66). In contrast, Tregs were more suppressive in CLL patients than in healthy individuals, and the decrease in Tregs contributed to effective anti-tumor effects in animal models (68, 69). Fortunately, the absolute count and percentage of Treg were significantly reduced in CLL patients as early as 30 days after ibrutinib treatment (70). Animal models also revealed the effects of ibrutinib on Treg differentiation (71).

Th17 cells are an important component in CLL anti-tumor immune monitoring (72). Most studies have reported that a high Th17 cell number is positively associated with OS and negatively related to disease progression (65, 73–76), suggesting that Th17 has anti-tumor effects in CLL. Jadidi-Niaragh and colleagues found that CLL patients, including progressive and indolent patients, had a significantly lower frequency of Th17 cells compared with healthy subjects (65), which was consistent with the finding from Yousefi et al. (61). However, other studies also found that the frequency and absolute count of Th17 cells increased in CLL patients (56, 73, 74), particularly at early disease stages (8, 63). A previous study has demonstrated that the Th17 cells increased in patients with ibrutinib treatment by decreasing the FAS-mediated AICD (21). Moreover, ibrutinib reduced the number of Tregs, which also contributed to the expansion of Th17 cells to maintain the balance between Th17 cells and Tregs (73). However, contradictory findings, with decreased frequency and absolute number of Th17 T cells in patients with CLL receiving ibrutinib, have been reported (34, 55), and the possible reason was that ibrutinib impaired Th17 differentiation (77). It is speculated that these contradictory findings may be associated with the difference in the timing of detection and previous treatment history (3).

Naïve T cells and terminally differentiated T cells

Patients with CLL experience abnormal T-cell differentiation due to persistent antigen stimulation from tumor antigens or infections, leading to over-activation of T cells with high expression of the activation markers CD38 and HLA-DR and the accumulation of long-term activated T cells (TLTAs) and terminally differentiated T cells (78, 79). There is also an increase in effector memory T cells (T_{EM}), CD45RA-positive memory effector T cells (T_{EMRA}), and exhausted T cells (Texh cells) (Figures 2A, 3C), particularly during disease progression (45). Additionally, a significant decrease in naïve T cells and central memory T cells (T_{CM}) (80), largely limits the immune function of T cells (45). Moreover, TLTAs reportedly maintain the ability to secrete cytokines and remain in a state of pseudo-exhaustion (50). These TLTAs and Texh cells are characterized by progressive loss in effector function, poor proliferative capacity (81) and upregulation of multiple inhibitory receptors, such as CD160, CD244, PD-1, TIM3, and cytotoxic T lymphocyte antigen 4 (CTLA-4) (44, 50, 81–83).

Accumulating data have demonstrated that ibrutinib can directly inhibit the expression of inhibitory receptors (21, 44, 50, 82, 84) and reduce the number of terminally differentiated T cells, such as TLTA, Texh, T_{EM}, and T_{EMRA} cells (79, 84) but remain naïve T cells (79). Niemann et al. found that PD-1 expression significantly decreased at 4 weeks after ibrutinib treatment in CLL patients (34). Similarly, Solman et al. found that increased TLTA and Texh cell pre-treatment gradually decreased in R/R and primary CLL patients; specifically, the number of TLTA cells was significantly reduced after 2 months of ibrutinib and near normal at 9 months, and Texh cells decreased to the normal range at 5 months after ibrutinib treatment (79). Furthermore, studies have found that naïve $CD4^+$ T cells increase in CLL patients with ibrutinib treatment (21, 79), and a large proportion of naïve T cells in CLL (greater than 10%) express T-BET or EOMES (21), indicating the differentiation is skewed to Th1 cells. Taken together, ibrutinib can inhibit the pseudo-exhaustion of T cells, thus reducing the

number of TLTA and Texh cells and reversing the unbalanced T cell subgroups.

Unconventional T cells

Unconventional T cells mainly include γδ T cells, NKT cells, and mucosal associated invariant T (MAIT) cells. γδ T cells account for about 10% of the T cells in peripheral blood, and 90% of γδ T cells carry the Vγ9Vδ2 TCR, which recognizes natural killer group 2D (NKG2D) and modulates γδ T-cell-driven immune responses (85). In CLL patients, both the absolute count and percentage of γδ T cells significantly increased (86), particularly the phenotype and function of Vγ9Vδ2-T cells changed. Specifically, compared with healthy individuals, CLL-derived Vγ9Vδ2 T cells were in a higher state of differentiation and had a lower ability to produce cytokines and degranulate, resulting in impaired granzyme-dependent cytotoxicity (87, 88). Ibrutinib treatment restored their function and cytotoxicity (88), which may be associated with the fact that ibrutinib promotes the phenotype of Vδ2Vγ9 T cells skewing toward Th1 cells in CLL patients by inhibiting ITK (87, 88).

In addition, NKT cells play a key role in regulating anti-tumor immunity (89). The frequency of NKT cells decreased with the development of CLL and could be a marker for immune monitoring and prognosis in CLL (90, 91). However, other studies found an increased absolute count of NKT cells in untreated CLL patients (42, 79), and a transient continuous increase at 3 months of ibrutinib treatment (79), and then the number of NKT cells displayed a gradual decrease and reached normal levels after 1 year (79).

MAIT cells exist in the liver and mucosal tissues, accounting for 1%–10% of peripheral blood T cells. MAIT cells are mainly involved in antibacterial immunity by producing a series of cytokines and lytic molecules, but little is known about their role in tumor immunity (92). Wallace et al. reported MAIT cell deficiency in CLL (93). However, so far, the regulatory effect of ibrutinib on MAIT cells remains unclear.

The effects of ibrutinib on T cell functions

Generally, T cells are the key effector cells in anti-leukemia immunity. Nevertheless, in CLL patients, $CD4^+$ T cells stimulate CLL cell survival and proliferation by secreting multiple chemokines/cytokines and through direct contact with the CD40 ligand (27, 36, 94), and $CD8^+$ T cells are persistently activated and expanded within the CLL microenvironment and gradually become pseudo-exhausted (5, 50, 52), finally resulting in T-cell immune tolerance and the loss of their anti-tumor activity (27), which has been reported to be causative of the poor response to CAR-T cell therapies for CLL patients (95–97). Additionally, due to the damaged structure of effector T cells and the poor antigen presentation function of CLL cells, the formation of immune synapses between T and CLL cells is impaired (84, 98).

Clinical studies have found that ibrutinib regulates T-cell immunity through various mechanisms (Figure 1B). For instance, ibrutinib promotes immune synapse formation between T and tumor cells and restores immune function by enhancing F-actin polarization and protein tyrosine phosphorylation (99, 100). Moreover, long-term ibrutinib therapy is likely to reverse the pseudo-exhaustion of T cells and promote the activity of effector T cells in CLL patients by inhibiting ITK activity and reducing the expression of inhibitory receptors (53, 83, 84). Additionally, ibrutinib directly and indirectly blocks the interaction between CLL and T cells by inhibiting cytokine networks and reducing tumor burden (34). Recently, single-cell analysis has shown that ibrutinib significantly increases the expression of cytotoxic genes in $CD8^+$ T cells and enhances the function of CTLs with ibrutinib treatment (44, 101).

However, a contradictory finding demonstrated that there was reduced granzyme and IFNγ in $CD8^+$ T cells from ibrutinib-treated mice, implying poor cytotoxicity (102). Most studies have shown that ibrutinib treatment promotes the recovery of T-cell cytotoxicity. However, the mechanism of ibrutinib regulating T-cell immunity is not fully clear.

The impacts of ibrutinib on TCR repertoire diversity

More than 90% of T cells are αβ T cells in the peripheral blood. T-cell receptor (TCR) repertoire diversity is mainly determined by the diversity of the hypervariable complementary determining region 3 (CDR3) of the TCRα and β chains, which specifically recognize antigens presented by major histocompatibility complex (MHC) molecules. A diverse TCR repertoire is used to resist the invasion of various pathogens. However, the TCR repertoire in CLL patients is seriously skewed and exhibits oligoclonal or monoclonal expansion (22, 103, 104) (Figure 2B), suggesting a tumor-related antigen-mediated selection (104–106), in parallel with severe impairment of T-cell immunity (105–107). In fact, the pro-tumor and anti-tumor effects of these oligoclonal or monoclonal T cells remain unknown (6, 22, 105). Prior studies have confirmed that there are specific T-cell clones in patients with CLL (6, 104), but they cannot effectively play an anti-tumor role due to their small number and severe immunosuppressive microenvironment (8). Additionally, the diversity of the TCR repertoire is progressively impaired with disease progression and multiple chemotherapy regimens (99, 105). Therefore, the

reconstruction of the TCR repertoire may be key to restoring T-cell immune function and further improving the response to antitumor immunotherapy (22, 108).

Yin and colleagues found that the diversity of the TCRβ repertoire could be partially reconstituted in R/R CLL patients after 12 months of ibrutinib treatment, which was closely related to good treatment response and decreased infection rates (22), suggesting that ibrutinib contributes to promoting the reconstruction of the TCR repertoire diversity (Figure 2B). However, another study revealed that the clonality of the TCR repertoire increased with ibrutinib treatment in newly diagnosed CLL patients; nevertheless, the clonality disappeared with disease progression (103). These clonally expanded T cells after ibrutinib treatment cannot be excluded as tumor-specific T cells due to the stimulation from CLL-related antigens, which is consistent with previous studies displaying the existence of anti-tumor T-cell clones in CLL patients, suggesting to some extent the recovery of T-cell immunity of patients with CLL (6, 22, 105). The differences in the results of the above two studies may be due to the immune function of the subjects. The former is R/R patients, and the latter is naive patients. Moreover, the difference may also be due to analysis from different standpoints. The former is from the whole TCR repertoire, and the latter is from T-cell immune response in the TCR repertoire.

Conclusion and future prospects

Tumor microenvironment disorder and T-cell immune dysfunction are the main characteristics of CLL patients (37, 109). Long-term ibrutinib treatment promotes the restoration of immunity, particularly T-cell immunity, consistent with improved clinical outcomes observed in CLL patients (3, 42). Although single-agent ibrutinib has long-term efficacy and tolerability in CLL patients according to an 8-year follow-up (14), combined therapies are still needed to overcome drug resistance, further improve the efficacy of ibrutinib and reduce side effects, such as ibrutinib combined with immunochemotherapy or BCL2 inhibitor venetoclax (110, 111). However, the biggest challenge in the future is to find strategic combinations to overcome T-cell dysfunction, reverse the immunosuppressive environment, and improve the efficacy of targeted immunotherapies in CLL (37, 97, 112). Theoretically, ibrutinib combined with anti-CD20 antibody rituximab (113) or immune checkpoint blockade (ICB) can improve the efficacy of ibrutinib and enhance the anti-tumor effect (103, 114); however, these effects have not been confirmed in the clinic (115–117). Obinutuzumab reportedly appears to have improved antibody-dependent cellular toxicity over rituximab (118).

Recently, increasing studies have demonstrated that ibrutinib has beneficial effects on T-cell-based immunotherapies (23). Both preclinical and clinical studies have confirmed that ibrutinib pretreatment combined with CAR-T cells can promote the implantation and amplification of CAR-T cells and enhance its anti-tumor activity in CLL patients (3, 25, 119), even if in patients with ibrutinib-resistance (3, 25), and decreased toxicity of CAR-T cells (25, 119). There are several possible mechanisms. For instance, long-term ibrutinib treatment regulates the disordered microenvironment (18, 34), decreases the expression of inhibitory molecules in CLL (21, 44, 82, 84), and reverses the limited expansion of T cells (120, 121), particularly naïve-like T cells and stem cell memory-like T cells (122), which play an important role in the expansion and long-term maintenance of CAR-T cells (123, 124). Moreover, ibrutinib can promote the migration of CAR-T cells to the tumor by enhancing CD62L expression (122, 125), which is conducive to the anti-tumor effect of CAR-T cells. Likewise, ibrutinib combined with the bispecific antibody blinatumomab can promote T-cell-mediated anti-tumor effects by inducing T-cell activation and proliferation, triggering cytokine secretion and granzyme release (24, 126, 127). Moreover, emerging targeted therapies, such as CD3/CD20 bispecific antibodies, may provide further combined options (128).

Collectively, based on the effects of ibrutinib on the microenvironment and T-cell immunity, in addition to the benefits of long-term treatment with ibrutinib alone, the combination of ibrutinib with T-cell-based immunotherapies could become a promising treatment with deeper remission and longer survival for CLL patients in the future.

Author contributions

YL reviewed the literature and wrote the manuscript. YS contributed to manuscript revision. QY designed the review and revised the manuscript. YS and QY equally contributed to this work. All authors contributed to the article and approved the submitted version.

Funding

This study was supported by the Foundation for Young Teachers' Basal Research of Zhengzhou University (jc202050015).

Conflict of interest

The authors declare that the research was conducted in the absence of any commercial or financial relationships that could be construed as a potential conflict of interest.

Publisher's note

All claims expressed in this article are solely those of the authors and do not necessarily represent those of their affiliated

organizations, or those of the publisher, the editors and the reviewers. Any product that may be evaluated in this article, or claim that may be made by its manufacturer, is not guaranteed or endorsed by the publisher.

References

1. Wierda WG, Byrd JC, Abramson JS, Bilgrami SF, Bociek G, Brander D, et al. Chronic lymphocytic leukemia/small lymphocytic lymphoma, version 4. 2020, NCCN clinical practice guidelines in oncology. *J Natl Compr Canc Netw* (2020) 18 (2):185–217. doi: 10.6004/jnccn.2020.0006

2. Crassini KR, Best OG, Mulligan SP. Immune failure, infection and survival in chronic lymphocytic leukemia. *Haematologica* (2018) 103(7):e329. doi: 10.3324/haematol.2018.196543

3. Turtle CJ, Hay KA, Hanafi LA, Li D, Cherian S, Chen X, et al. Durable molecular remissions in chronic lymphocytic leukemia treated with CD19-specific chimeric antigen receptor-modified T cells after failure of ibrutinib. *J Clin Oncol* (2017) 35(26):3010–20. doi: 10.1200/JCO.2017.72.8519

4. Shah B, Zhao X, Silva AS, Shain KH, Tao J. Resistance to ibrutinib in b cell malignancies: one size does not fit all. *Trends Cancer* (2018) 4(3):197–206. doi: 10.1016/j.trecan.2018.01.004

5. Bagnara D, Kaufman MS, Calissano C, Marsilio S, Patten PE, Simone R, et al. A novel adoptive transfer model of chronic lymphocytic leukemia suggests a key role for T lymphocytes in the disease. *Blood* (2011) 117(20):5463–72. doi: 10.1182/blood-2010-12-324210

6. Hanna BS, Roessner PM, Yazdanparast H, Colomer D, Campo E, Kugler S, et al. Control of chronic lymphocytic leukemia development by clonally-expanded CD8(+) T-cells that undergo functional exhaustion in secondary lymphoid tissues. *Leukemia* (2019) 33(3):625–37. doi: 10.1038/s41375-018-0250-6

7. Roessner PM, Seiffert M. T-Cells in chronic lymphocytic leukemia: Guardians or drivers of disease? *Leukemia* (2020) 34(8):2012–24. doi: 10.1038/s41375-020-0873-2

8. Vlachonikola E, Stamatopoulos K, Chatzidimitriou A. T Cells in chronic lymphocytic leukemia: a two-edged sword. *Front Immunol* (2020) 11:612244. doi: 10.3389/fimmu.2020.612244

9. Liu YY, Zhou XX, Wang X. Targeting the tumor microenvironment in b-cell lymphoma: challenges and opportunities. *J Hematol Oncol* (2021) 14:125. doi: 10.1186/s13045-021-01134-x

10. Zain R, Vihinen M. Structure-function relationships of covalent and non-covalent BTK inhibitors. *Front Immunol* (2021) 12:694853. doi: 10.3389/fimmu.2021.694853

11. Robak T, Witkowska M, Smolewski P. The role of bruton's kinase inhibitors in chronic lymphocytic leukemia: current status and future directions. *Cancers (Basel)* (2022) 14(3):771. doi: 10.3390/cancers14030771

12. Burger JA, Barr PM, Robak T, Owen C, Ghia P, Tedeschi A, et al. Long-term efficacy and safety of first-line ibrutinib treatment for patients with CLL/SLL: 5 years of follow-up from the phase 3 RESONATE-2 study. *Leukemia* (2020) 34 (3):787–98. doi: 10.1038/s41375-019-0602-x

13. Patel K, Pagel JM. Current and future treatment strategies in chronic lymphocytic leukemia. *J Hematol Oncol* (2021) 14(1):69. doi: 10.1186/s13045-021-01054-w

14. Byrd JC, Furman RR, Coutre SE, Flinn IW, Burger JA, Blum K, et al. Ibrutinib treatment for first-line and relapsed/refractory chronic lymphocytic leukemia: final analysis of the pivotal phase Ib/II PCYC-1102 study. *Clin Cancer Res* (2020) 26(15):3918–27. doi: 10.1158/1078-0432.CCR-19-2856

15. Awan FT, Schuh A, Brown JR, Furman RR, Pagel JM, Hillmen P, et al. Acalabrutinib monotherapy in patients with chronic lymphocytic leukemia who are intolerant to ibrutinib. *Blood Adv* (2019) 3(9):1553–62. doi: 10.1182/bloodadvances.2018030007

16. Byrd JC, Woyach JA, Furman RR, Martin P, O'Brien S, Brown JR, et al. Acalabrutinib in treatment- naïve chronic lymphocytic leukemia. *Blood* (2021) 137 (24):3327–38. doi: 10.1182/blood.2020009617

17. Gaiti F, Chaligne R, Gu H, Brand RM, Kothen-Hill S, Schulman RC, et al. Epigenetic evolution and lineage histories of chronic lymphocytic leukaemia. *Nature* (2019) 569(7757):576–80. doi: 10.1038/s41586-019-1198-z

18. Herman SE, Mustafa RZ, Gyamfi JA, Pittaluga S, Chang S, Chang B, et al. Ibrutinib inhibits BCR and NF-κB signaling and reduces tumor proliferation in tissue-resident cells of patients with CLL. *Blood* (2014) 123(21):3286–95. doi: 10.1182/blood-2014-02-548610

19. Burger JA, Li KW, Keating MJ, Sivina M, Amer AM, Garg N, et al. Leukemia cell proliferation and death in chronic lymphocytic leukemia patients on therapy with the BTK inhibitor ibrutinib. *JCI Insight* (2017) 2(2):e89904. doi: 10.1172/jci.insight.89904

20. Rendeiro AF, Krausgruber T, Fortelny N, Zhao F, Penz T, Farlik M, et al. Chromatin mapping and single-cell immune profiling define the temporal dynamics of ibrutinib response in CLL. *Nat Commun* (2020) 11(1):577. doi: 10.1038/s41467-019-14081-6

21. Long M, Beckwith K, Do P, Mundy BL, Gordon A, Lehman AM, et al. Ibrutinib treatment improves T cell number and function in CLL patients. *J Clin Invest* (2017) 127(8):3052–64. doi: 10.1172/jci89756

22. Yin Q, Sivina M, Robins H, Yusko E, Vignali M, O'Brien S, et al. Ibrutinib therapy increases T cell repertoire diversity in patients with chronic lymphocytic leukemia. *J Immunol* (2017) 198(4):1740–7. doi: 10.4049/jimmunol.1601190

23. Vlachonikola E, Stamatopoulos K, Chatzidimitriou A. T Cell defects and immunotherapy in chronic lymphocytic leukemia. *Cancers (Basel)* (2021) 13 (13):3255. doi: 10.3390/cancers13133255

24. Long M, Williams E, Berard C, Cheney C, Hu E, Bhat SA, et al. Ibrutinib treatment in CLL patients improves T cell function and blinatumomab redirected cytotoxicity. *Blood* (2019) 134(Supplement_1):1049. doi: 10.1182/blood-2019-125417

25. Gauthier J, Hirayama AV, Purushe J, Hay KA, Lymp J, Li DH, et al. Feasibility and efficacy of CD19-targeted CAR T cells with concurrent ibrutinib for CLL after ibrutinib failure. *Blood* (2020) 135(19):1650–60. doi: 10.1182/blood.2019002936

26. Herndon TM, Chen SS, Saba NS, Valdez J, Emson C, Gatmaitan M, et al. Direct *in vivo* evidence for increased proliferation of CLL cells in lymph nodes compared to bone marrow and peripheral blood. *Leukemia* (2017) 31(6):1340–7. doi: 10.1038/leu.2017.11

27. Burger JA, Ghia P, Rosenwald A, Caligaris-Cappio F. The microenvironment in mature b-cell malignancies: a target for new treatment strategies. *Blood* (2009) 114(16):3367–75. doi: 10.1182/blood-2009-06-225326

28. Burger JA, Gribben JG. The microenvironment in chronic lymphocytic leukemia (CLL) and other b cell malignancies: insight into disease biology and new targeted therapies. *Semin Cancer Biol* (2014) 24:71–81. doi: 10.1016/j.semcancer.2013.08.011

29. Bürkle A, Niedermeier M, Schmitt-Gräff A, Wierda WG, Keating MJ, Burger JA. Overexpression of the CXCR5 chemokine receptor, and its ligand, CXCL13 in b-cell chronic lymphocytic leukemia. *Blood* (2007) 110(9):3316–25. doi: 10.1182/blood-2007-05-089409

30. Dubois N, Crompot E, Meuleman N, Bron D, Lagneaux L, Stamatopoulos B. Importance of crosstalk between chronic lymphocytic leukemia cells and the stromal microenvironment: direct contact, soluble factors, and extracellular vesicles. *Front Oncol* (2020) 10:1422. doi: 10.3389/fonc.2020.01422

31. Niemann CU, Wiestner A. B-cell receptor signaling as a driver of lymphoma development and evolution. *Semin Cancer Biol* (2013) 23(6):410–21. doi: 10.1016/j.semcancer.2013.09.001

32. Nishio M, Endo T, Tsukada N, Ohata J, Kitada S, Reed JC, et al. Nurse like cells express BAFF and APRIL, which can promote survival of chronic lymphocytic leukemia cells *via* a paracrine pathway distinct from that of SDF-1alpha. *Blood* (2005) 106(3):1012–20. doi: 10.1182/blood-2004-03-0889

33. Ten Hacken E, Burger JA. Microenvironment interactions and b-cell receptor signaling in chronic lymphocytic leukemia: implications for disease pathogenesis and treatment. *Biochim Biophys Acta* (2016) 1863(3):401–13. doi: 10.1016/j.bbamcr.2015.07.009

34. Niemann CU, Herman SE, Maric I, Gomez-Rodriguez J, Biancotto A, Chang BY, et al. Disruption of *in vivo* chronic lymphocytic leukemia tumor-microenvironment interactions by ibrutinib–findings from an investigator-initiated phase II study. *Clin Cancer Res* (2016) 22(7):1572–82. doi: 10.1158/1078-0432.Ccr-15-1965

35. van Attekum MH, Eldering E, Kater AP. Chronic lymphocytic leukemia cells are active participants in microenvironmental cross-talk. *Haematologica* (2017) 102(9):1469–76. doi: 10.3324/haematol.2016.142679

36. Ghia P, Strola G, Granziero L, Geuna M, Guida G, Sallusto F, et al. Chronic lymphocytic leukemia b cells are endowed with the capacity to attract CD4+, CD40L+ T cells by producing CCL22. *Eur J Immunol* (2002) 32(5):1403–13. doi: 10.1002/1521-4141(200205)32:5<1403::Aid-immu1403>3.0.Co;2-y

37. Griggio V, Perutelli F, Salvetti C, Boccellato E, Boccadoro M, Vitale C, et al. Immune dysfunctions and immune-based therapeutic interventions in chronic lymphocytic leukemia. *Front Immunol* (2020) 11:594556. doi: 10.3389/fimmu.2020.594556

38. Delvecchio VS, Sana I, Mantione ME, Vilia MG, Ranghetti P, Rovida A, et al. Interleukin-1 receptor-associated kinase 4 inhibitor interrupts toll-like receptor signalling and sensitizes chronic lymphocytic leukaemia cells to apoptosis. *Br J Haematol* (2020) 189(3):475–88. doi: 10.1111/bjh.16386

39. Svanberg R, Janum S, Patten PEM, Ramsay AG, Niemann CU. Targeting the tumor microenvironment in chronic lymphocytic leukemia. *Haematologica* (2021) 106(9):2312–24. doi: 10.3324/haematol.2020.268037

40. Isaza-Correa JM, Liang Z, van den Berg A, Diepstra A, Visser L. Toll-like receptors in the pathogenesis of human b cell malignancies. *J Hematol Oncol* (2014) 7:57. doi: 10.1186/s13045-014-0057-5

41. Dadashian EL, McAuley EM, Liu D, Shaffer AL3rd, Young RM, Iyer JR, et al. TLR signaling is activated in lymph node-resident CLL cells and is only partially inhibited by ibrutinib. *Cancer Res* (2019) 79(2):360–71. doi: 10.1158/0008-5472.CAN-18-0781

42. Solman IG, Blum LK, Burger JA, Kipps TJ, Dean JP, James DF, et al. Impact of long-term ibrutinib treatment on circulating immune cells in previously untreated chronic lymphocytic leukemia. *Leuk Res* (2021) 102:106520. doi: 10.1016/j.leukres.2021.106520

43. Forconi F, Moss P. Perturbation of the normal immune system in patients with CLL. *Blood* (2015) 126(5):573–81. doi: 10.1182/blood-2015-03-567388

44. Purroy N, Tong YE, Lemvigh CK, Cieri N, Li SQ, Parry EM, et al. Single-cell analysis reveals immune dysfunction from the earliest stages of CLL that can be reversed by ibrutinib. *Blood* (2022) 139(14):2252–6. doi: 10.1182/blood.2021013926

45. Nunes C, Wong R, Mason M, Fegan C, Man S, Pepper C. Expansion of a CD8(+)PD-1(+) replicative senescence phenotype in early stage CLL patients is associated with inverted CD4:CD8 ratios and disease progression. *Clin Cancer Res* (2012) 18(3):678–87. doi: 10.1158/1078-0432.CCR-11-2630

46. Burger JA, Li K, Keating M, Sivina M, Ferrajoli A, Jalayer A, et al. Functional evidence from deuterated water labeling that the bruton tyrosine kinase inhibitor ibrutinib blocks leukemia cell proliferation and trafficking and promotes leukemia cell death in patients with chronic lymphocytic leukemia and small lymphocytic lymphoma. *Blood* (2014) 124(21):326. doi: 10.1182/blood.V124.21.326.326

47. Parry HM, Mirajkar N, Cutmore N, Zuo J, Long H, Kwok M, et al. Long-term ibrutinib therapy reverses CD8+ T cell exhaustion in b cell chronic lymphocytic leukaemia. *Front Immunol* (2019) 10:2832. doi: 10.3389/fimmu.2019.02832

48. Herman SE, Niemann CU, Farooqui M, Jones J, Mustafa RZ, Lipsky A, et al. Ibrutinib-induced lymphocytosis in patients with chronic lymphocytic leukemia: correlative analyses from a phase II study. *Leukemia* (2014) 28(11):2188–96. doi: 10.1038/leu.2014.122

49. Mulder TA, Peña-Pérez L, Berglöf A, Meinke S, Estupiñán HY, Heimersson K, et al. Ibrutinib has time-dependent on- and off-target effects on plasma biomarkers and immune cells in chronic lymphocytic leukemia. *Hemasphere* (2021) 5(5):e564. doi: 10.1097/hs9.0000000000000564

50. Riches JC, Davies JK, McClanahan F, Fatah R, Iqbal S, Agrawal S, et al. T Cells from CLL patients exhibit features of T-cell exhaustion but retain capacity for cytokine production. *Blood* (2013) 121(9):1612–21. doi: 10.1182/blood-2012-09-457531

51. Sun Y, Peng I, Webster JD, Suto E, Lesch J, Wu X, et al. Inhibition of the kinase ITK in a mouse model of asthma reduces cell death and fails to inhibit the inflammatory response. *Sci Signal* (2015) 8(405):ra122. doi: 10.1126/scisignal.aab0949

52. McLane LM, Abdel-Hakeem MS, Wherry EJ. CD8 T cell exhaustion during chronic viral infection and cancer. *Annu Rev Immunol* (2019) 37:457–95. doi: 10.1146/annurev-immunol-041015-055318

53. Dubovsky JA, Beckwith KA, Natarajan G, Woyach JA, Jaglowski S, Zhong Y, et al. Ibrutinib is an irreversible molecular inhibitor of ITK driving a Th1-selective pressure in T lymphocytes. *Blood* (2013) 122(15):2539–49. doi: 10.1182/blood-2013-06-507947

54. Moreno C, Muñoz C, Terol MJ, Hernández-Rivas JÁ, Villanueva M. Restoration of the immune function as a complementary strategy to treat chronic lymphocytic leukemia effectively. *J Exp Clin Cancer Res* (2021) 40 (1):321. doi: 10.1186/s13046-021-02115-1

55. Puzzolo MC, Del Giudice I, Peragine N, Mariglia P, De Propris MS, Cappelli LV, et al. Th2/Th1 shift under ibrutinib treatment in chronic lymphocytic leukemia. *Front Oncol* (2021) 11:637186. doi: 10.3389/fonc.2021.637186

56. Palma M, Gentilcore G, Heimersson K, Mozaffari F, Näsman-Glaser B, Young E, et al. T Cells in chronic lymphocytic leukemia display dysregulated expression of immune checkpoints and activation markers. *Haematologica* (2017) 102(3):562–72. doi: 10.3324/haematol.2016.151100

57. Podhorecka M, Dmoszynska A, Rolinski J, Wasik E. T Type 1/type 2 subsets balance in b-cell chronic lymphocytic leukemia–the three-color flow cytometry analysis. *Leuk Res* (2002) 26(7):657–60. doi: 10.1016/s0145-2126(01)00194-1

58. Miller AT, Wilcox HM, Lai Z, Berg LJ. Signaling through ITK promotes T helper 2 differentiation *via* negative regulation of T-bet. *Immunity* (2004) 21(1):67–80. doi: 10.1016/j.immuni.2004.06.009

59. Pleyer C, Wiestner A, Sun C. Immunological changes with kinase inhibitor therapy for chronic lymphocytic leukemia. *Leuk Lymphoma* (2018) 59(12):2792–800. doi: 10.1080/10428194.2018.1457147

60. Knochelmann HM, Dwyer CJ, Bailey SR, Amaya SM, Elston DM, Mazza-McCrann JM, et al. When worlds collide: Th17 and treg cells in cancer and autoimmunity. *Cell Mol Immunol* (2018) 15(5):458–69. doi: 10.1038/s41423-018-0004-4

61. Yousefi M, Movassaghpour AA, Shamsasenjan K, Ghalamfarsa G, Sadreddini S, Jadidi-Niaragh F, et al. The skewed balance between tregs and Th17 in chronic lymphocytic leukemia. *Future Oncol* (2015) 11(10):1567–82. doi: 10.2217/fon.14.298

62. Dees S, Ganesan R, Singh S, Grewal IS. Regulatory T cell targeting in cancer: emerging strategies in immunotherapy. *Eur J Immunol* (2021) 51(2):280–91. doi: 10.1002/eji.202048992

63. Hus I, Bojarska-Junak A, Chocholska S, Tomczak W, Woś J, Dmoszyńska A, et al. Th17/IL-17A might play a protective role in chronic lymphocytic leukemia immunity. *PLoS One* (2013) 8(11):e78091. doi: 10.1371/journal.pone.0078091

64. Goral A, Firczuk M, Fidyt K, Sledz M, Simoncello F, Siudakowska K, et al. A specific CD44lo CD25lo subpopulation of regulatory T cells inhibits anti-leukemic immune response and promotes the progression in a mouse model of chronic lymphocytic leukemia. *Front Immunol* (2022) 13:781364. doi: 10.3389/fimmu.2022.781364

65. Jadidi-Niaragh F, Ghalamfarsa G, Memarian A, Asgarian-Omran H, Razavi SM, Sarrafnejad A, et al. Downregulation of IL-17-producing T cells is associated with regulatory T cell expansion and disease progression in chronic lymphocytic leukemia. *Tumour Biol* (2013) 34(2):929–40. doi: 10.1007/s13277-012-0628-4

66. D'Arena G, Laurenti L, Minervini MM, Deaglio S, Bonello L, De Martino L, et al. Regulatory T-cell number is increased in chronic lymphocytic leukemia patients and correlates with progressive disease. *Leuk Res* (2011) 35(3):363–8. doi: 10.1016/j.leukres.2010.08.010

67. Mpakou VE, Ioannidou HD, Konsta E, Vikentiou M, Spathis A, Kontsioti F, et al. Quantitative and qualitative analysis of regulatory T cells in b cell chronic lymphocytic leukemia. *Leuk Res* (2017) 60:74–81. doi: 10.1016/j.leukres.2017.07.004

68. Lad D, Hoeppli R, Huang Q, Garcia R, Xu L, Toze C, et al. Regulatory T-cells drive immune dysfunction in CLL. *Leuk Lymphoma* (2018) 59(2):486–9. doi: 10.1080/10428194.2017.1330475

69. Rissiek A, Schulze C, Bacher U, Schieferdecker A, Thiele B, Jacholkowski A, et al. Multidimensional scaling analysis identifies pathological and prognostically relevant profiles of circulating T-cells in chronic lymphocytic leukemia. *Int J Cancer* (2014) 135(10):2370–9. doi: 10.1002/ijc.28884

70. Podhorecka M, Goracy A, Szymczyk A, Kowal M, Ibanez B, Jankowska-Lecka O, et al. Changes in T-cell subpopulations and cytokine network during early period of ibrutinib therapy in chronic lymphocytic leukemia patients: the significant decrease in T regulatory cells number. *Oncotarget* (2017) 8 (21):34661–9. doi: 10.18632/oncotarget.16148

71. Eken A, Cansever M, Somekh I, Mizoguchi Y, Zietara N, Okus FZ, et al. Genetic deficiency and biochemical inhibition of ITK affect human Th17, treg, and innate lymphoid cells. *J Clin Immunol* (2019) 39(4):391–400. doi: 10.1007/s10875-019-00632-5

72. Purroy N, Wu CJ. Coevolution of leukemia and host immune cells in chronic lymphocytic leukemia. *Cold Spring Harb Perspect Med* (2017) 7(4): a026740. doi: 10.1101/cshperspect.a026740

73. Jain P, Javdan M, Feger FK, Chiu PY, Sison C, Damle RN, et al. Th17 and non-Th17 interleukin-17-expressing cells in chronic lymphocytic leukemia: delineation, distribution, and clinical relevance. *Haematologica* (2012) 97(4):599–607. doi: 10.3324/haematol.2011.047316

74. Lad DP, Varma S, Varma N, Sachdeva MU, Bose P, Malhotra P. Regulatory T-cell and T-helper 17 balance in chronic lymphocytic leukemia progression and autoimmune cytopenias. *Leuk Lymphoma* (2015) 56(8):2424–8. doi: 10.3109/10428194.2014.986479

75. Chatterjee S, Daenthanasanmak A, Chakraborty P, Wyatt MW, Dhar P, Selvam SP, et al. CD38-NAD+ axis regulates immunotherapeutic anti-tumor T cell response. *Cell Metab* (2018) 27(1):85–100.e8. doi: 10.1016/j.cmet.2017.10.006

76. Jung B, Ferrer G, Chiu PY, Aslam R, Ng A, Palacios F, et al. Activated CLL cells regulate IL-17F-producing Th17 cells in miR155-dependent and outcome-specific manners. *JCI Insight* (2022) 7(12):e158243. doi: 10.1172/jci.insight.158243

77. Elmore JP, McGee MC, Nidetz NF, Anannya O, Huang W, August A. Tuning T helper cell differentiation by ITK. *Biochem Soc Trans* (2020) 48(1):179–85. doi: 10.1042/BST20190486

78. Mahnke YD, Brodie TM, Sallusto F, Roederer M, Lugli E. The who's who of T-cell differentiation: human memory T-cell subsets. *Eur J Immunol* (2013) 43 (11):2797–809. doi: 10.1002/eji.201343751

79. Solman IG, Blum LK, Hoh HY, Kipps TJ, Burger JA, Barrientos JC, et al. Ibrutinib restores immune cell numbers and function in first-line and relapsed/refractory chronic lymphocytic leukemia. *Leuk Res* (2020) 97:106432. doi: 10.1016/j.leukres.2020.106432

80. Brusa D, Serra S, Coscia M, Rossi D, D'Arena G, Laurenti L, et al. The PD-1/PD-L1 axis contributes to T-cell dysfunction in chronic lymphocytic leukemia. *Haematologica* (2013) 98(6):953–63. doi: 10.3324/haematol.2012.077537

81. Thommen DS, Schumacher TN. T Cell dysfunction in cancer. *Cancer Cell* (2018) 33(4):547–62. doi: 10.1016/j.ccell.2018.03.012

82. Arruga F, Gyau BB, Iannello A, Vitale N, Vaisitti T, Deaglio S. Immune response dysfunction in chronic lymphocytic leukemia: dissecting molecular mechanisms and microenvironmental conditions. *Int J Mol Sci* (2020) 21 (5):1825. doi: 10.3390/ijms21051825

83. Wherry EJ. T Cell exhaustion. *Nat Immunol* (2011) 12(6):492–9. doi: 10.1038/ni.2035

84. Davis JE, Sharpe C, Mason K, Tam CS, Koldej RM, Ritchie DS. Ibrutinib protects T cells in patients with CLL from proliferation-induced senescence. *J Transl Med* (2021) 19(1):473. doi: 10.1186/s12967-021-03136-2

85. Simoes AE, Di Lorenzo B, Silva-Santos B. Molecular determinants of target cell recognition by human gammadelta T cells. *Front Immunol* (2018) 9:929. doi: 10.3389/fimmu.2018.00929

86. Zarobkiewicz MK, Bojarska-Junak AA. The mysterious actor-gammadelta T lymphocytes in chronic lymphocytic leukaemia (CLL). *Cells* (2022) 11(4):661. doi: 10.3390/cells11040661

87. de Weerdt I, Hofland T, Lameris R, Endstra S, Jongejan A, Moerland PD, et al. Improving CLL Vgamma9Vdelta2-t-cell fitness for cellular therapy by *ex vivo* activation and ibrutinib. *Blood* (2018) 132(21):2260–72. doi: 10.1182/blood-2017-12-822569

88. Long M. Gammadelta T cells for immunotherapy. *Blood* (2018) 132 (21):2212–3. doi: 10.1182/blood-2018-10-876078

89. Nair S, Dhodapkar MV. Natural killer T cells in cancer immunotherapy. *Front Immunol* (2017) 8:1178. doi: 10.3389/fimmu.2017.01178

90. Bojarska-Junak A, Hus I, Sieklucka M, Wasik-Szczepanek E, Mazurkiewicz T, Polak P, et al. Natural killer-like T CD3+/CD16+CD56+ cells in chronic lymphocytic leukemia: intracellular cytokine expression and relationship with clinical outcome. *Oncol Rep* (2010) 24(3):803–10. doi: 10.3892/or_00000924

91. Gorini F, Azzimonti L, Delfanti G, Scarfo L, Scielzo C, Bertilaccio MT, et al. Invariant NKT cells contribute to chronic lymphocytic leukemia surveillance and prognosis. *Blood* (2017) 129(26):3440–51. doi: 10.1182/blood-2016-11-751065

92. O'Neill C, Cassidy FC, O'Shea D, Hogan AE. Mucosal associated invariant T cells in cancer-friend or foe? *Cancers (Basel)* (2021) 13(7):1582. doi: 10.3390/cancers13071582

93. Wallace ME, Alcantara MB, Minoda Y, Kannourakis G, Berzins SP. An emerging role for immune regulatory subsets in chronic lymphocytic leukaemia. *Int Immunopharmacol* (2015) 28(2):897–900. doi: 10.1016/j.intimp.2015.03.047

94. Elston L, Fegan C, Hills R, Hashimdeen SS, Walsby E, Henley P, et al. Increased frequency of CD4+ PD-1+ HLA-DR+ T cells is associated with disease progression in CLL. *Br J Haematol* (2020) 188(6):872–80. doi: 10.1111/bjh.16260

95. Lemal R, Tournilhac O. State-of-the-art for CAR T-cell therapy for chronic lymphocytic leukemia in 2019. *J Immunother Cancer* (2019) 7(1):202. doi: 10.1186/s40425-019-0686-x

96. Man S, Henley P. Chronic lymphocytic leukaemia: the role of T cells in a b cell disease. *Br J Haematol* (2019) 186(2):220–33. doi: 10.1111/bjh.15918

97. Mehta PH, Fiorenza S, Koldej RM, Jaworowski A, Ritchie DS, Quinn KM. T Cell fitness and autologous CAR T cell therapy in haematologic malignancy. *Front Immunol* (2021) 12:780442. doi: 10.3389/fimmu.2021.780442

98. Ramsay AG, Johnson AJ, Lee AM, Gorgün G, Le Dieu R, Blum W, et al. Chronic lymphocytic leukemia T cells show impaired immunological synapse formation that can be reversed with an immunomodulating drug. *J Clin Invest* (2008) 118(7):2427–37. doi: 10.1172/jci35017

99. Vardi A, Vlachonikola E, Papazoglou D, Psomopoulos F, Kotta K, Ioannou N, et al. T-Cell dynamics in chronic lymphocytic leukemia under different treatment modalities. *Clin Cancer Res* (2020) 26(18):4958–69. doi: 10.1158/1078-0432.Ccr-19-3827

100. Papazoglou D, Lesnick CE, Wang V, Kay NE, Shanafelt TD, Ramsay AG. Ibrutinib-based therapy improves anti-tumor T cell killing function allowing effective pairing with anti-PD-L1 immunotherapy compared to traditional FCR chemoimmunotherapy; implications for therapy and correlative immune functional data from the phase III E1912 trial. *Blood* (2018) 132(Supplement 1):236. doi: 10.1182/blood-2018-99-118333

101. Cadot S, Valle C, Tosolini M, Pont F, Largeaud L, Laurent C, et al. Longitudinal CITE-seq profiling of chronic lymphocytic leukemia during ibrutinib treatment: evolution of leukemic and immune cells at relapse. *biomark Res* (2020) 8 (1):72. doi: 10.1186/s40364-020-00253-w

102. Hanna BS, Yazdanparast H, Demerdash Y, Roessner PM, Schulz R, Lichter P, et al. Combining ibrutinib and checkpoint blockade improves CD8+ T-cell function and control of chronic lymphocytic leukemia in em-TCL1 mice. *Haematologica* (2021) 106(4):968–77. doi: 10.3324/haematol.2019.238154

103. Baptista MJ, Basumallik N, Herman SEM, Cook EM, Ahn IE, Wiestner A, et al. Ibrutinib increases the clonality of TCR repertoire in patients with chronic lymphocytic leukemia. *Blood* (2018) 132(Supplement 1):238. doi: 10.1182/blood-2018-99-109847

104. Rezvany MR, Jeddi-Tehrani M, Wigzell H, Osterborg A, Mellstedt H. Leukemia-associated monoclonal and oligoclonal TCR-BV use in patients with b-cell chronic lymphocytic leukemia. *Blood* (2003) 101:1063–70. doi: 10.1182/blood-2002-03-0746

105. Vardi A, Agathangelidis A, Stalika E, Karypidou M, Siorenta A, Anagnostopoulos A, et al. Antigen selection shapes the T-cell repertoire in chronic lymphocytic leukemia. *Clin Cancer Res* (2016) 22(1):167–74. doi: 10.1158/1078-0432.Ccr-14-3017

106. Vardi A, Vlachonikola E, Karypidou M, Stalika E, Bikos V, Gemenetzi K, et al. Restrictions in the T-cell repertoire of chronic lymphocytic leukemia: high-throughput immunoprofiling supports selection by shared antigenic elements. *Leukemia* (2017) 31(7):1555–61. doi: 10.1038/leu.2016.362

107. Blanco G, Vardi A, Puiggros A, Gómez-Llonín A, Muro M, Rodríguez-Rivera M, et al. Restricted T cell receptor repertoire in CLL-like monoclonal b cell lymphocytosis and early stage CLL. *Oncoimmunology* (2018) 7(6):e1432328. doi: 10.1080/2162402x.2018.1432328

108. Li Y, Xu L. Evaluation of TCR repertoire diversity in patients after hematopoietic stem cell transplantation. *Stem Cell Investig* (2015) 2:17. doi: 10.3978/j.issn.2306-9759.2015.09.01

109. Peters FS, Strefford JC, Eldering E, Kater AP. T-Cell dysfunction in chronic lymphocytic leukemia from an epigenetic perspective. *Haematologica* (2021) 106 (5):1234–43. doi: 10.3324/haematol.2020.267914

110. Jain N, Thompson P, Burger J, Ferrajoli A, Takahashi K, Estrov Z, et al. Ibrutinib, fludarabine, cyclophosphamide, and obinutuzumab (iFCG) regimen for chronic lymphocytic leukemia (CLL) with mutated IGHV and without TP53 aberrations. *Leukemia* (2021) 35(12):3421–9. doi: 10.1038/s41375-021-01280-8

111. Wierda WG, Allan JN, Siddiqi T, Kipps TJ, Opat S, Tedeschi A, et al. Ibrutinib plus venetoclax for first-line treatment of chronic lymphocytic leukemia: primary analysis results from the minimal residual disease cohort of the randomized phase II CAPTIVATE study. *J Clin Oncol* (2021) 39(34):3853–65. doi: 10.1200/jco.21.00807

112. Mhibik M, Wiestner A, Sun C. Harnessing the effects of BTKi on T cells for effective immunotherapy against CLL. *Int J Mol Sci* (2019) 21(1):68. doi: 10.3390/ijms21010068

113. Kuo H-P, Hsieh S, Whang J, Huang Y, Sirisawad M, Chang BY. Ibrutinib potentiated NK cell-mediated cytotoxicity in mouse models of b-cell lymphomas. *Blood* (2016) 128(22):4140. doi: 10.1182/blood.V128.22.4140.4140

114. McClanahan F, Hanna B, Miller S, Clear AJ, Lichter P, Gribben JG, et al. PD-L1 checkpoint blockade prevents immune dysfunction and leukemia development in a mouse model of chronic lymphocytic leukemia. *Blood* (2015) 126(2):203–11. doi: 10.1182/blood-2015-01-622936

115. Woyach JA, Ruppert AS, Heerema NA, Zhao W, Booth AM, Ding W, et al. Ibrutinib regimens versus chemoimmunotherapy in older patients with untreated CLL. *N Engl J Med* (2018) 379(26):2517–28. doi: 10.1056/NEJMoa1812836

116. Ding W, LaPlant BR, Call TG, Parikh SA, Leis JF, He R, et al. Pembrolizumab in patients with CLL and Richter transformation or with relapsed CLL. *Blood* (2017) 129(26):3419–27. doi: 10.1182/blood-2017-02-765685

117. Younes A, Brody J, Carpio C, Lopez-Guillermo A, Ben-Yehuda D, Ferhanoglu B, et al. Safety and activity of ibrutinib in combination with nivolumab in patients with relapsed non-Hodgkin lymphoma or chronic lymphocytic leukaemia: a phase 1/2a study. *Lancet Haematol* (2019) 6(2):e67–78. doi: 10.1016/s2352-3026(18)30217-5

118. Sharman JP, Egyed M, Jurczak W, Skarbnik A, Pagel JM, Flinn IW, et al. Acalabrutinib with or without obinutuzumab versus chlorambucil and obinutuzmab for treatment-naive chronic lymphocytic leukaemia (ELEVATE TN): a randomised, controlled, phase 3 trial. *Lancet* (2020) 395(10232):1278–91. doi: 10.1016/S0140-6736(20)30262-2

119. Siddiqi T, Soumerai JD, Dorritie KA, Stephens DM, Riedell PA, Arnason JE, et al. Updated follow-up of patients with relapsed/refractory chronic lymphocytic leukemia/small lymphocytic lymphoma treated with lisocabtagene maraleucel in the phase 1 monotherapy cohort of transcend CLL 004, including high-risk and ibrutinib-treated patients. *Blood* (2020) 136(Supplement 1):40–1. doi: 10.1182/blood-2020-140491

120. Fraietta JA, Beckwith KA, Patel PR, Ruella M, Zheng Z, Barrett DM, et al. Ibrutinib enhances chimeric antigen receptor T-cell engraftment and efficacy in leukemia. *Blood* (2016) 127(9):1117–27. doi: 10.1182/blood-2015-11-679134

121. Kater AP, Melenhorst JJ. CAR-T and ibrutinib vs CLL: sequential or simultaneous? *Blood* (2020) 135(19):1611–2. doi: 10.1182/blood.2020005362

122. Fan F, Yoo HJ, Stock S, Wang L, Liu Y, Schubert ML, et al. Ibrutinib for improved chimeric antigen receptor T-cell production for chronic lymphocytic leukemia patients. *Int J Cancer* (2021) 148(2):419–28. doi: 10.1002/ijc.33212

123. Porter DL, Hwang WT, Frey NV, Lacey SF, Shaw PA, Loren AW, et al. Chimeric antigen receptor T cells persist and induce sustained remissions in relapsed refractory chronic lymphocytic leukemia. *Sci Transl Med* (2015) 7 (303):303ra139. doi: 10.1126/scitranslmed.aac5415

124. Gill SI, Vides V, Frey NV, Hexner E, Metzger S, O'Brien M, et al. Anti-CD19 CAR T cells in combination with ibrutinib for the treatment of chronic lymphocytic leukemia. *Blood Adv* (2022). doi: 10.1182/bloodadvances.2022007317

125. Masopust D, Schenkel JM. The integration of T cell migration, differentiation and function. *Nat Rev Immunol* (2013) 13(5):309–20. doi: 10.1038/nri3442

126. Mhibik M, Gaglione EM, Eik D, Kendall EK, Blackburn A, Keyvanfar K, et al. BTK inhibitors, irrespective of ITK inhibition, increase efficacy of a CD19/CD3-bispecific antibody in CLL. *Blood* (2021) 138(19):1843–54. doi: 10.1182/blood.2020009686

127. Robinson HR, Qi J, Cook EM, Nichols C, Dadashian EL, Underbayev C, et al. A CD19/CD3 bispecific antibody for effective immunotherapy of chronic lymphocytic leukemia in the ibrutinib era. *Blood* (2018) 132(5):521–32. doi: 10.1182/blood-2018-02-830992

128. Lejeune M, Kose MC, Duray E, Einsele H, Beguin Y, Caers J. Bispecific, T-cell-recruiting antibodies in b-cell malignancies. *Front Immunol* (2020) 11:762. doi: 10.3389/fimmu.2020.00762

frontiers | Frontiers in Immunology

TYPE Review
PUBLISHED 13 September 2022
DOI 10.3389/fimmu.2022.970508

OPEN ACCESS

EDITED BY
Lucienne Chatenoud,
UniversitéParis Descartes,
France

REVIEWED BY
Aggelos Banos,
Biomedical Research Foundation of the Academy of Athens (BRFAA),
Greece
Björn E. Clausen,
Johannes Gutenberg-University Mainz,
Germany

*CORRESPONDENCE
Hongbo Liu
liuhongbo6279@126.com

SPECIALTY SECTION
This article was submitted to Immunological Tolerance and Regulation, a section of the journal Frontiers in Immunology

RECEIVED 16 June 2022
ACCEPTED 01 August 2022
PUBLISHED 13 September 2022

CITATION
Li R, Li H, Yang X, Hu H, Liu P and Liu H (2022) Crosstalk between dendritic cells and regulatory T cells: Protective effect and therapeutic potential in multiple sclerosis. *Front. Immunol.* 13:970508. doi: 10.3389/fimmu.2022.970508

Crosstalk between dendritic cells and regulatory T cells: Protective effect and therapeutic potential in multiple sclerosis

Ruoyu Li[1], Hui Li[1], Xiaoyan Yang[1], Huiru Hu[1], Peidong Liu[2,3] and Hongbo Liu[1,3]*

[1]Department of Neurology, The First Affiliated Hospital of Zhengzhou University, Zhengzhou, China, [2]Department of Neurosurgery, First Affiliated Hospital of Zhengzhou University, Zhengzhou, China, [3]Translational Medicine Center, First Affiliated Hospital of Zhengzhou University, Zhengzhou, China

Multiple sclerosis (MS) is a chronic inflammatory disease of the central nervous system related to autoimmunity and is characterized by demyelination, neuroinflammation, and neurodegeneration. Cell therapies mediated by dendritic cells (DCs) and regulatory T cells (Tregs) have gradually become accumulating focusing in MS, and the protective crosstalk mechanisms between DCs and Tregs provide the basis for the efficacy of treatment regimens. In MS and its animal model experimental autoimmune encephalomyelitis, DCs communicate with Tregs to form immune synapses and complete a variety of complex interactions to counteract the unbalanced immune tolerance. Through different co-stimulatory/inhibitory molecules, cytokines, and metabolic enzymes, DCs regulate the proliferation, differentiation and function of Tregs. On the other hand, Tregs inhibit the mature state and antigen presentation ability of DCs, ultimately improving immune tolerance. In this review, we summarized the pivotal immune targets in the interaction between DCs and Tregs, and elucidated the protective mechanisms of DC-Treg cell crosstalk in MS, finally interpreted the complex cell interplay in the manner of inhibitory feedback loops to explore novel therapeutic directions for MS.

KEYWORDS

dendritic cell, regulatory T cell (Treg), immune tolerance, multiple sclerosis, experimental autoimmune encephalomyelitis

Introduction

Multiple sclerosis (MS) is an immune-mediated disease characterized by inflammatory demyelinating lesions in the central nervous system (CNS), which causes the youngs non-traumatic disability. The course of MS is characterized by recurrence and remission and MS is thus divided into three main clinical types: relapsing-remitting MS (RRMS), primary progressive MS (PPMS), and secondary progressive MS (SPMS). Existing studies have shown that MS is mainly mediated by myelin-specific autoreactive $CD4^+$T cells, whereas dendritic cells (DCs), regulatory T cells (Tregs), and other immune cells play auxiliary roles. When the peripheral immune tolerance is disordered due to Treg cell defects and/or the resistance of effector cells to Tregs, autoreactive $CD4^+$ T cells in the lymph nodes are activated and become aggressive effector cells, followed by entering into the peripheral blood and trafficking to the brain. Besides, DCs, memory T cells, and other immune cells, also cross the blood-brain barrier into the CNS under the action of chemokines (1, 2). Subsequently, activated DCs reactivate autoreactive $CD4^+$ T cells and memory T cells, and prompt their polarization into Teffs, such as T helper (Th) type 1 and Th17 *via* the different cytokine environment, followed by causing an inflammatory cascade reaction (3, 4). In addition, the activated T cells mediate the activation of macrophages as well as microglia and assist B cells to produce antibodies. When patients with MS enter the chronic phase, immune cell infiltration appears in the CNS and activated DCs, macrophages, and microglia further damage the myelin sheaths, axons, and neurons, which leads to the progression of MS (3) (Figure 1). Therefore, in individuals with MS, it appears that immune dysregulation originates from DCs with the activation phenotype that initiates adaptive immune responses (3). In addition, Tregs, as immune supervisors, can inhibit the inflammatory immune response mediated by activated DCs, pathogenic B cells, and T cells (5). Besides, a small number of potential tolerogenic DCs play a limited protective role in MS, such as inducing Treg cell generation and effector T cell (Teff) anergy. Consequently, the occurrence of MS might be related to the limited DC ability to induce normal Tregs or the insufficient monitoring of activated DCs by Tregs.

DC-Treg cell crosstalk has also been shown to affect animal model of MS-experimental autoimmune encephalomyelitis (EAE). For example, the number of CNS-infiltrating Tregs

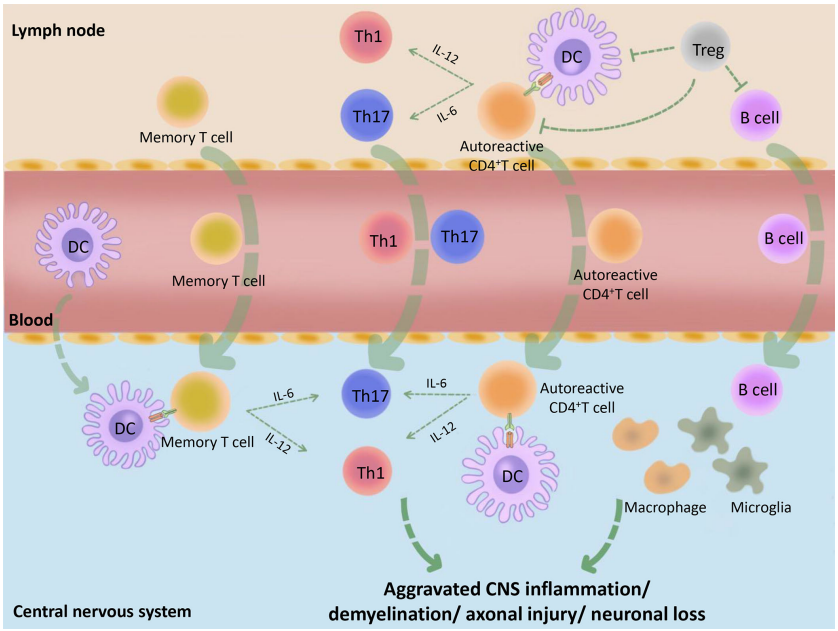

FIGURE 1
Basic immunopathological process of MS. Initially, the peripheral tolerance of MS patients is disordered (for example, the inhibitory function of Tregs is decreased or the Teffs are not sensitive to the inhibitory effect of Tregs) and the autoantigens, such as MBP, MOG and PLP, are incorrectly recognized as pathogens by DCs. These DCs combine with $CD4^+$ autoreactive T cells, which cause peripheral immune response. The activated immune cells make entering into the peripheral blood, then trafficking across the blood–CNS barrier. Subsequently, activated DCs in the CNS combine and reactivate with memory T cells or $CD4^+$ autoreactive T cells and promote their differentiation into Teffs, such as Th1 and Th17, followed by causing CNS inflammation. At the same time, B cells, macrophages, microglia and many other immune cells are also activated by the inflammatory context, followed by causing demyelination, axonal damage, and more serious CNS inflammation. MBP, myelin basic protein; PLP, proteolipid protein; MOG, myelin oligodendrocyte glycoprotein.

was decreased in DC deficient EAE mice (6). Similarly, during the initiation phase of activation in myelin-specific T cells, conditional ablation of $CD11c^+$ DCs selectively suspended the generation of induced Tregs (iTregs) and resulted in the aggravation of EAE (6, 7). In turn, Tregs also shaped the tolerance of plasmacytoid DCs (pDCs) in a steady state, which was conducive to maintaining the regulatory ability of Tregs during EAE (8). A basic study has shown that Tregs can reduce the stable contact between DCs and naive T cells and interfere with the initiation of $CD4^+$ T cells in the early immune response (9). Moreover, activated antigen-specific Tregs can also inhibit DC antigen presentation *via* the bystander effect (10). Detailed examinations of the crosstalk mechanisms of DC-Treg revealed that DCs influenced the proliferation, differentiation, and function of Tregs by reducing the expression of co-stimulatory molecules on the surface of the cell membrane, as well as by enhancing the expression of co-inhibitory molecules, metabolic enzymes, and the secretion of anti-inflammatory cytokines. Besides, Tregs can limit DC maturation and antigen presentation ability by secreting anti-inflammatory cytokines and boosting the formation of co-inhibitory signaling pathways. These processes can interfere with the metabolic pathways of DCs and even directly destroy DCs *via* cytolysis (11, 12). Various cell therapies for MS make full use of the DC-Treg cell crosstalk mechanism to achieve a therapeutic effect; these include tolerogenic dendritic cell (tolDC) therapy and regulatory T cell therapy (13). Tolerogenic dendritic cells mainly maintain highly specific immune tolerance by inducing the anergy and deletion of Teffs, and producing myelin-specific Tregs (13, 14). Similarly, Tregs can also establish antigen-specific immune tolerance by eliminating over-activated DCs and Teffs, and inducing the generation of tolDCs (10, 13). Although both cell therapies have broad application prospects in MS, there remain numerous barriers to the translation of knowledge into practical use. Thus, the protective DC-Treg cell crosstalk mechanism is crucial to inducing the immune tolerance in MS/EAE, and further in-depth studies will be instrumental to translate the protective mechanism into cell therapy.

By analyzing the co-stimulatory molecules, cytokines, and metabolic enzymes related to the DC-Treg cell interplay, this review comprehensively elucidates the protective effect of the DC-Treg cell crosstalk mechanism in MS/EAE and attempts to interpret the complex cell interaction *via* novel inhibitory feedback loops, with the further goal of exploring new research directions for protective autoimmune mechanisms and therapeutic schedules for MS.

Classification of DCs and Tregs

DCs are the most powerful antigen-presenting cells (APCs), which exist in almost all human peripheral tissues and link innate and adaptive immune responses. DCs can be divided into conventional DCs (cDCs), pDCs and monocyte-derived DCs (MoDCs) (15–18). And cDCs can be further divided into the type 1 (cDC1) and type 2 (cDC2) subsets (15, 16, 19–21) (Table 1). Based on the characteristics of cellular immune tolerance, DCs can also be divided into immunogenic DCs and tolDCs (22). At present, there is no specific surface markers for tolDCs, although it can be identified by several characteristics:1) low expression of co-stimulatory (CD83 and CD80/86) and major histocompatibility complex class II (MHC-II) molecules and pro-inflammatory cytokines (interleukin [IL]-6, IL-12); 2) high expression of co-inhibitory molecules (programmed cell death ligand 1 [PD-L1]), anti-inflammatory cytokines (IL-10, IL-35, and transforming growth factor [TGF]-β), and indoleamine 2,3-dioxygenase (IDO) (23). In the steady state, most DCs maintain in an immature condition, and the types of antigens (i.e., pathogen or self-antigen) encountered with DC (including immature DC and mature DC) usually determine whether it plays an immunogenic or tolerogenic role (20, 24). However, in MS, most DCs are regarded as immunogenicity because the immune system mistakenly recognizes the self-antigens (i.e., myelin basic protein [MBP], proteolipid protein [PLP] and myelin oligodendrocyte glycoprotein [MOG]) as pathogens. Intriguingly, in MS, several rare DC subsets expressing CD8, CD103, dendritic cell endocytic receptor (DEC205), B- and T-lymphocyte attenuator (BTLA) or secreting interleukin (IL)-10, IL-27, IL-35 might become the potential tolDC subsets that induce Tregs. Therefore, DCs have two main functions in MS: one is playing a role in antigen presentation, activating T cells, and initiating immune responses; the other is interacting with T cells, shaping the differentiation/development/function of T cells, and inducing immune tolerance (22). The antigen presentation ability of DCs, namely immunogenicity, can be compensated by macrophages and B cells; however, the tolerance function of DCs appears irreplaceable (6).

Tregs are a classical type of inhibitory T cell with an immune regulation function, which are primarily involved in the formation of immune tolerance. Tregs can be divided into two subsets: thymus derived Tregs (tTregs) and peripheral derived Tregs (pTregs). The main phenotype of tTregs is $CD4^+$ $CD25^+$ $CD127^-$ $Foxp3^+$ Tregs, while pTregs mainly include $CD4^+$ $CD25^+$ $Foxp3^-$ type 1 regulatory T cells (Tr1) that secrete a large amount of IL-10 and $CD4^+$ $CD25^{low}$ T helper type 3 cells (Th3), which produce significant amounts of TGF-β. In addition, there are many Treg subsets that have been named based on key surface molecules or transcription factors, such as $CD8^+$ Tregs and $FoxA1^+$ Tregs (25). The heterogeneity of Tregs makes their subsets complex, and we have summarized the main Treg cell subsets related to MS (25–32) (Table 2). Tregs not only interfere with the mature state and antigen presentation ability of DCs but also induce the generation of tolDCs. When DCs play an excessive role in antigen presentation, and attack both pathogenic cells and

TABLE 1 Human dendritic cell subsets related to multiple sclerosis.

	Function introduction		Marker	Ref.
cDC	cDCs initiate from the myeloid progenitors. In the process of cDC maturation, the ability to capture environmental- and cell-associated antigens, and initiate adaptive immune responses will be enhanced, while the ability of phagocytosis and elimination of pathogens will be relatively weakened. In the steady state (mouse), the marker combination, CD11c and MHCII, can distinguish migratory DCs ($CD11c^{int}MHCII^{hi}$) from lymph node resident DCs ($CD11c^{hi}MHCII^{int}$) phenotypically. During inflammation (mouse), CD8α on LN-resident cDC1s and CD103 on migratory cDC1s can be their own special mark, while such a marker does not exist in resident and migratory cDC2s.	cDC1	CD141(BDCA3), CLEC9A, XCR1, CD205(DEC-205) *	(15, 16, 19)
		cDC2	CD1c (BDCA1), CD301 (CLEC10A, MGL), CD172a (SIRPα), DCIR2*	(21)
pDC	pDCs, which are morphologically similar to plasma cells that produce antibodies, initiate from the lymphoid progenitors. pDCs demonstrate strong activation in response to viral and bacterial infections, secreting massive amounts of type I-IFN and acquiring the ability to present foreign antigens. pDCs express low levels of MHC-II, co-stimulatory molecules and the integrin CD11c in the steady state. When they are not stimulated, pDCs show a tolerogenic potential.		CD303 (BDCA2), CD123, CD304, CD45RA	(15, 16)
MoDC	Monocyte-derived DCs (MoDCs), which also named as "inflammatory DCs", arise from the myeloid progenitors, and play a complementary role to cDCs. Phenotypically, we can roughly distinguish cDCs and MoDCs with CD11b.		FCER1A, CD14, CD226, CD64, CD1a*, CD1b*, CD1c*	(17, 18)

BDCA3, blood DC antigen 3; CLEC9A, C-type lectin domain-containing 9A; XCR1, the chemokine XC receptor 1; MHC II, major histocompatibility complex class II; FCER1A, Fc epsilon receptor Ia. *: less important than the others.

normal cells, Tregs act as a negative regulator of these overactivated DCs and restrict the autoimmune response.

Defects in DCs and Tregs in MS

A recent study indicated that monocyte-to-DC differentiation was a process potentially influenced by MS risk single nucleotide polymorphisms (SNPs) (33). Moreover, previous studies showed that MS patients had DC defects. For example, the percentage of circulating myeloid DCs was decreased in patients with SPMS and PPMS, whereas a large number of DCs were found in the CNS lesion and cerebrospinal fluid (CSF) (34). The process of DC exiting the CNS to maintain immunological tolerance was perturbed in MS patients, which might contribute to the abnormal distribution of DCs in MS patients (2). In the CSF, pDCs percentage was higher in untreated-relapsing MS patients than those of patients in remission, whereas this result was not observed in the peripheral blood (35). In contrast, the expression of CD83, CD80, and CD86 on the surface of circulating DCs in patients with PPMS was downregulated, whereas the circulating cDCs of RRMS and SPMS patients showed an activated phenotype, suggesting an imbalance between tolerogenicity and

TABLE 2 Human regulatory T cell subsets related to multiple sclerosis.

Subset	Marker	Distribution	Characteristics	Ref.
Thymus-derived Treg cell (tTreg)	$CD4^+CD25^+Foxp3^+$	Thymus and peripheral tissues	They enter the Treg cell lineage as a consequence of intermediate or strong TCR signals during T cell maturation in the thymus.	(26)
Type 1 regulatory T cell (Tr1)	IL-10-producing $CD4^+$ $CD25^{-/low}$ $Foxp3^-$	Peripheral tissues	They secrete predominantly IL-10 and have a suppressor function independent from Foxp3. Memory Tr1 cells also regard LAG-3 and CD49b as biomarkers.	(27)
T helper type 3 cell (Th3)	TGF-β-producing $CD4^+CD25^{-/low}$	Peripheral tissues	They secrete predominantly TGF-β. The suppressive ability of Th3 and Tr1 cells is contact-independent and is based mainly on cytokines such as TGF-β and IL-10.	(28)
Th1-like, $Foxp3^+$ Treg cell	T helper type 1-like IFN-γ-secreting $Foxp3^+$	Peripheral blood	They show reduced suppressive activity. Moreover, Tregs associated with MS were excessively inclined to acquire Th1-Treg phenotype.	(29)
T follicular regulatory cell (Tfr)	$CXCR5^+$ $PD\text{-}1^+$ $BCL6^+$ $Foxp3^+$ $CD25^-$	Peripheral tissues	The traditional viewpoint is that Tfr cells are negative regulators of B cells and Tfh cells in germinal centers. However, the function of Tfr cells is multifaceted in fact, which may reflect the function of different subsets of Tfr cells.	(30, 31)
$CD8^+$ Treg cell	$Foxp3^+CD8^+$ $/CD8^+CD28^-$	Peripheral tissues and thymus	Presenting in the thymus, tonsils, and peripheral blood of human, $CD8^+$ Tregs can mitigate spontaneous germinal center reactions and various immune responses via suppressing Tfh cells and B cells.	(30, 32)
$FoxA1^+$ Treg cell	$CD4^+FoxA1^+CD47^+$ $CD69^+PD\text{-}L1^{hi}$ $FoxP3^-$	CNS and peripheral blood	$FoxA1^+$ Tregs develop primarily in the CNS and respond to autoimmune inflammation in a FoxA1- and PD-L1-dependent manner.	(25)

immunogenicity of DCs in MS patients (i.e., functional defects in DCs) (34, 36). In addition, the ability of pDCs to induce Tregs has been shown to be related to the occurrence of MS. Gene expression level of HSPA1A —which may influence the ability of pDCs to induce Tregs—was downregulated in MS patients and this probably resulted in alterations in the mature state and regulatory function of pDCs (37). Furthermore, the depletion of pDCs in healthy controls resulted in the reduction in $CD4^+$ $Foxp3^+$ Tregs, whereas the depletion of pDCs in MS patients did not influence the generation of Tregs (38). Taken together, these studies showed that DC deficiency was closely related to MS relapsing and remitting.

Treg cell defects also exist in MS patients. CD25, namely the IL-2 receptor α chain, is a pivotal surface marker of Tregs, and its SNPs are closely related to MS (39). Studies have demonstrated that Treg cell defects in MS patients were mainly reflected in cell quantity, subset changes, and dysfunction (40–43). For example, the percentage of Tregs in the peripheral blood of RRMS patients was significantly reduced and associated with the clinical severity of the disease (41). Moreover, a previous study has shown that the number of Tregs in the CSF, but not in the peripheral blood, was elevated in MS patients (42). In contrast, alterations in the proportion and dysfunction of Treg cell subsets were more marked in patients with MS (43). For example, the effector function of $CD4^+$ $CD25^{hi}$ Tregs in the peripheral blood was significantly downregulated in MS patients (44). Moreover, T helper type 1 (Th1)-like, interferon-γ (IFN-γ)-secreting $Foxp3^+$ T cells were elevated in RRMS patients, while their inhibitory function were weakened (29). A recent study showed that, compared with healthy donors, MS patients had lower resting $CD4^+$ $CD25^+$ $CD45RA^+$ $CCR7^+$ Tregs and more activated $CD4^+$ $CD25^{hi}$ $CD45RA^-$ $Foxp3^{hi}$ Tregs even before treatment (40). Therefore, Treg cell deficiency was one of the main causes of the autoimmune response in MS patients.

Bidirectional DC-Treg cell crosstalk in MS patients and EAE mice

Emerging myeloid cell research has been focused primarily on the regulatory effect of DCs on Tregs. However, the regulatory effect of Tregs on DCs is also worth investigating. We summarize three inhibitory feedback loops to explain the protective crosstalk mechanism between DCs and Tregs in the context of MS/EAE: the CD28/cytotoxic T lymphocyte antigen (CTLA)-4/B7 pathway, the PD-L1/PD-1 inhibitory feedback loop, and the lymphocyte activation gene 3 (LAG-3)/T cell receptor (TCR)/MHC-II inhibitory feedback loop (Figure 2). We also highlight three inhibitory feedback mechanisms related to DC-Treg cell crosstalk that may be involved in MS/EAE, including IL-10, IL-35, and TGF-β (Figure 3).

Surface molecules involved in DC-Treg cell crosstalk

Protean CD28/CTLA-4/B7pathway

CD28 and CTLA-4 (CD152) are members of the CD28 superfamily. They share common ligands, the B7 family molecule CD80/CD86 (B7-1/B7-2), on the surface of DCs. The CD28 molecules that are crucially expressed in most $CD4^+$ T cells (including Tregs) promote T cell activation, proliferation, and survival (45). Besides, the expression of CTLA-4 is pivotal in Tregs and is upregulated on the surface of activated T cells. CTLA-4 has considerably higher avidity for CD80/CD86 than CD28 and can reduce the expression of CD80/CD86 on the surface of DCs *via* trans-endocytosis. The co-expression of CD28 and CTLA-4 in Tregs, activated T cells, and their competitive combination with CD80/86 make the CD28/CTLA-4/B7 pathway play a more complex role in DC-Treg cell-mediated immune regulation (Figure 2).

The CD80/86-CD28 axis, the second signal-inducing Tregs produced by DCs, serves to lower the signaling threshold of the TCR, and induces the production of IL-2 that is essential for the development of $CD4^+$ $CD25^+$ Tregs. Besides, the CD80/86-CD28 axis also enables Treg cell homeostasis (7, 45, 46). Selectively targeting Tregs in normal Lewis rats with very low doses of the CD28 superagonist was shown to be sufficient to induce Treg cell proliferation *in vivo* and enable the effective treatment of EAE (47). Similarly, despite the normal number of $Foxp3^+$ cells in Treg cell-specific CD28 conditional knockout mice, CD28-deficient Tregs exhibited a pronounced proliferative/survival disadvantage. This result caused a severe autoimmunity and experimental allergic encephalomyelitis that is considered as animal models of MS (48). However, it has been reported that CD28 knockout mice were resistant to EAE induction because the CD28 signals of pathogenic T cells and Tregs were blocked simultaneously (49). Additionally, selective blocking of CD80/86-CD28 signal transduction in rhesus monkeys suppressed the activation of autoreactive T cells and B cells, thereby abrogating the induction of EAE (50). Therefore, despite the pivotal role that the CD80/86-CD28 axis plays in the development and proliferation of tTregs and pTregs, it is evident that, the activation of the CD28 signal is conducive to the pathogenesis of EAE/MS, based on the overall perspective of the $CD4^+$ T cell population. It's probably because the CD80/86-CD28 axis has a much greater effect on the activation of pathogenic T cells than on the induction of Tregs, and pathogenic T cells have obvious quantitative advantages.

The CTLA-4-CD80/86 axis is an important medium for the Treg cell inhibition effect, which indirectly influences the activation of Teffs by suppressing the antigen-presenting function of DCs (51). Furthermore, CTLA-4 is an immune checkpoint and therapeutic target in the development of MS (52). For germline knockout mice, the deletion of CTLA-4

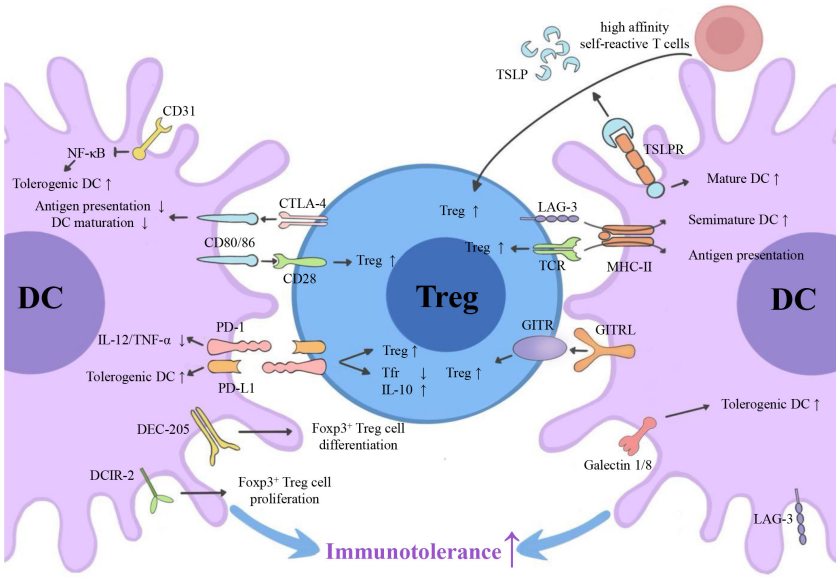

FIGURE 2
Surface molecules involved in DC-Treg cell crosstalk. *Via* the CD28/CTLA-4/B7 pathway, the PD-L1/PD-1 inhibitory feedback loop, and the potential LAG-3/TCR/MHC-II inhibitory feedback loop, DCs can affect the generation of Tregs, and Tregs can affect the tolerance of DCs. GITRL, TSLPR, DEC-205, DCIR-2, and CD31 are also key molecules for DC-dependent Treg cell generation. CTLA-4, cytotoxic T lymphocyte antigen 4; PD-L1, programmed cell death ligand 1; PD-1, programmed cell death receptor; LAG-3, lymphocyte activation gene 3; TCR, T cell receptor; MHC-II, major histocompatibility complex class II; GITR, glucocorticoid-induced tumor necrosis factor receptor; GITRL, glucocorticoid-induced tumor necrosis factor receptor ligand; TSLP, thymic stromal lymphopoietin; DCIR2, dendritic cell inhibitory receptor 2.

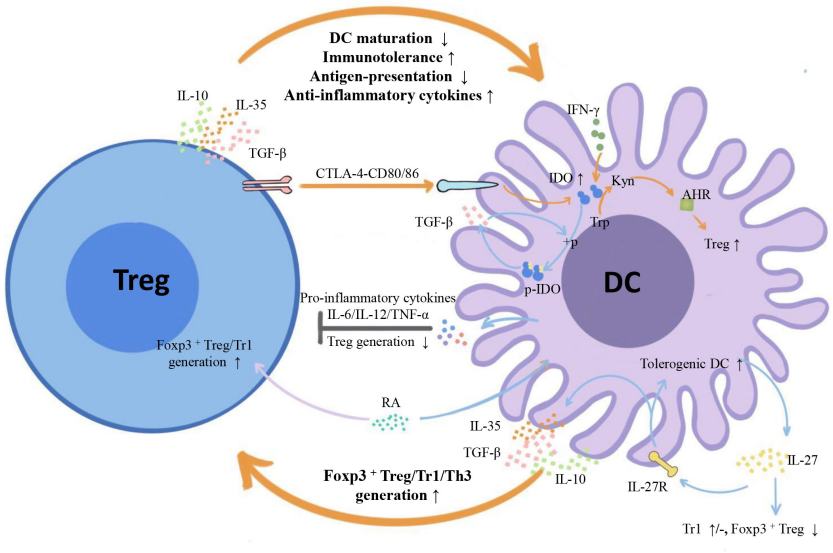

FIGURE 3
Inhibitory cytokines and metabolic enzymes involved in DC-Treg cell crosstalk. From the perspective of cytokines, both DCs and Tregs can secrete inhibitory cytokines IL-10/IL-35/TGF-β and form inhibitory feedback mechanisms: DCs promote the generation of different subtypes of Tregs, and Tregs inhibit the maturity and antigen presentation ability of DCs and improve their tolerance. From the perspective of metabolic enzymes, Tregs can induce IDO expression in DCs with the help of signals axes, such as CTLA-4-CD80/86, initiate the tryptophan metabolic pathway, trigger the generation of IDO-dependent Tregs, and form a negative feedback loop with IDO at the core. There is also unidirectional regulation of Tregs by DCs: DCs influence Treg generation by secreting IL-27, and IL-12/IL-6/TNF-α inhibits Treg cell proliferation. TGF-β, transforming growth factor-β; IFN- γ, Interferon- γ; IDO1, indoleamine 2,3-dioxygenase 1; + p, phosphorylation; P-IDO1, phosphorylated indoleamine 2,3-dioxygenase 1; Trp, tryptophan; Kyn, kynurenine; AHR, aromatic hydrocarbon receptor.

precipitates severe autoimmunity diseases (53). Real-time reverse transcription–PCR detection has shown that the expression of CTLA-4 in peripheral blood mononuclear cells (PBMCs) of MS patients was either decreased (54) or unchanged (55).These results, at least, could reflect the trend of CTLA-4 expression in Tregs of MS patients because CTLA-4 is mainly expressed by Tregs in PBMCs. In addition, a recent *in vitro* experiment demonstrated that when DCs were co-cultured with $CD4^+$ $CD25^-$ naive T cells and Tregs, Tregs always gathered around DCs, inhibited their activation, captured CD80/86 *via* trans-endocytosis of CTLA-4, and increased free PD-L1 expression on the surface of DCs (56, 57). This phenomenon influenced the antigen presentation ability of DCs, indirectly regulated the CD80/86-CD28 signaling pathway and inhibited the activation of T cells. Intriguingly, iTregs from CTLA-4-deficient mice failed to induce the downregulation of CD80/CD86, whereas DCs treated with iTregs from CTLA-4-deficient mice showed an impaired ability to activate naive T cells (57). Similarly, the CTLA-4-CD80/86 axis had the same effect on EAE mice, and the expression of CD80/86 and MHC-II on the surface of peripheral DCs was significantly elevated in Treg cell-specific CTLA-4-deficient mice (53). Thus, without the limiting effect of CTLA-4 on the Treg cell surface, the overall maturity and activation level of DC were enhanced. However, in the CNS of mouse, CTLA-4-deficient Tregs did not increase the expression of B7 on the surface of DCs (53). Moreover, in EAE/MS, Tregs can induce IDO expression in DCs *via* the CTLA-4-CD80/86 axis and improve their tolerance. Therefore, the CTLA-4-CD80/86 axis is of great significance in the DC-Treg cell crosstalk mechanism.

Although CTLA-4 is recognized as a co-inhibitory molecule, its effect on Tregs is highly complex. In general, it was thought that CTLA-4 promotes tTreg cell proliferation (51). For example, the lysine motif in the cytoplasmic domain of CTLA-4 was crucial for Foxp3 induction and EAE inhibition. Transporting the chimeric peptide containing the CTLA-4 cytoplasmic tail into T cells can induce Tregs *in vivo*, resulting in EAE remission (58). However, Paterson et al. (53) reported that CTLA-4 can limit the proliferation of Teffs and inhibit the expansion of pTregs, which is different from the role that CTLA-4 plays in the thymus. For example, a study showed that the deletion of CTLA-4 in adulthood promoted the activation and expansion of traditional $CD4^+$ $Foxp3^-$ T cell and regulatory $Foxp3^+$ T cell subsets that protect mice from EAE (53). Paradoxically, Wing et al. (51) have suggested that CTLA-4 is necessary for Tregs to exert an inhibitory effect, whereas Paterson et al. (53) have proposed the opposite: upregulating the expression of other inhibitory molecules (e.g., IL-10, LAG-3, and PD-1) compensated for the CTLA-4 deficiency. There are two possible explanations for these results: 1. CTLA-4 expression has different relative contributions to Tregs and Teffs; and 2. the intracellular and extracellular segments of CTLA-4 are responsible for different functions.

Interference of the CD28/CTLA-4/B7 pathway can concurrently influence two signaling pathways between DCs and Tregs; therefore, its function in EAE/MS might be complicated. Abatacept is a CTLA-4-immunoglobulin (Ig) fusion protein, which is composed of the extracellular region of CTLA-4 and the Fc portion of IgG. It can simultaneously bind to CD80/86 and block the CD28/CTLA-4/B7 pathway. Glatigny et al. (59) found that abatacept significantly reduces circulating Tregs, especially $CD45RO^+$ memory Tregs, in RRMS patients. Researchers suggested that the inhibition of CD28-mediated DC-Treg cell crosstalk was the primary mechanism underlying the reduction in human circulating Tregs following abatacept therapy (59). However, upon myelin reactive T cell activation, blocking B7 with CTLA-4-Ig can inhibit Tregs and aggravate EAE, resulting in more severe CNS inflammation and demyelination (60). It suggested that blocking the CD28/CTLA-4/B7 pathway primarily interferes with the CTLA-4-CD80/86 signal between DCs and Tregs, due to the reduced dependence of activated myelin-specific T cells on the CD28 signal. This interesting process caused Treg cell anergy and continuous activation of myelin-specific T cells, thus, promoting inflammation (60). In a phase II clinical trial called ACCLAIM (NCT01116427), abatacept provided no clinical benefit to patients with RRMS, which probably due to the mutual offset of the CD28 signal and the CTLA-4 downstream effect (61). Therefore, the final result of blocking the CD28/CTLA-4/B7 pathway in EAE/MS may depend on the relative strength of the CTLA-4 and CD28 signals as well as the blocking time point (61). However, no study to date has reported the effect of blocking the CD28/CTLA-4/B7 pathway in DCs in EAE/MS. Instead, studies in mouse models of rheumatoid arthritis have suggested that abatacept treatment induced a unique T cell phenotype to reduce DC antigen presentation (62).

In summary, in the context of MS/EAE, DCs rely on the CD80/CD86-CD28 axis to induce Treg cell generation, and Tregs rely on the CTLA-4-CD80/86 axis to inhibit DC immunogenicity, and induce the generation of tolDCs, thereby forming a protective signaling loop.

PD-L1/PD-1 inhibitory feedback loop

Similar to CTLA-4, the PD-L1/PD-1 axis also plays a pivotal role in inducing peripheral tolerance. However, the latter is distinct because it can be simultaneously expressed on the surface of DCs and Tregs (63, 64). Generally, cells with expression of PD-L1 play a regulatory role. $PD\text{-}L1^+$ DCs involve in regulating the differentiation and development of naive T cells. Besides, they preferentially induce the expression of Foxp3 and promote the differentiation of Tregs. $PD\text{-}L1^+$ DCs can also maintain Treg cell inhibitory function and promote the secretion of IL-10 by binding to PD-1 on the surface of Tregs (65). Simultaneously, PD-L1 can act inversely on DCs and inhibit DC maturation (6). In addition, PD-L1 constitutively

expressed by Tregs can mediate the inhibitory function of Tregs, improve the tolerogenicity of PD-1$^+$ DCs, and inhibit the secretion of proinflammatory cytokines, such as IL-6, IL-12 and tumor necrosis factor-alpha (TNF-α) (25, 66). Therefore, the PD-L1/PD-1 axis in DC-Treg cell crosstalk forms an inhibitory feedback loop and influences both cells simultaneously (Figure 2).

The PD-L1/PD-1 axis plays a similar protective role in MS. Numerous studies have reported the expression of PD-L1/PD-1 in MS patients or EAE mice from different perspectives, such as genes, peripheral blood, and brain tissue samples (66). Overall, the expression of PD-L1/PD-1 in healthy controls was highest, followed by MS patients or EAE mice in the remission stage, and finally those in the acute stage (66). However, exceptions also exist. For example, the expression level of PD-L1/PD-1 in MS plaques was higher than that in non-pathological human CNS tissue (67). Focusing on DCs/Tregs that are stimulated by MBPs, T cells expressing PD-1 and APC expressing PD-L1 in the peripheral blood of patients with acute MS were prominently increased compared with those of remitted patients with MS (68). A recent study also showed that the expression of PD-1 on the surface of CD4$^+$ and CD8$^+$ Tregs was reduced in patients with RRMS (69). Taken together, these studies suggested that the DC- or Treg cell-related PD-L1/PD-1 axis is involved in the occurrence and development of MS.

Tregs can improve DC tolerance *via* the PD-L1/PD-1 axis. As mentioned above, Tregs can release soluble PD-L1 on the surface of DCs when they endocytose CD80/86 in a CTLA-4-dependent manner, which boosts the tolerance of DCs (70). In addition, Liu et al. (25) found a new type of regulatory T cell subset: CD4$^+$ FoxA1$^+$ CD47$^+$ CD69$^+$ PD-L1^{hi} FoxP3$^-$ Tregs (FoxA1$^+$ Tregs). It was the main Treg cell subset that combats against EAE in the CNS and was induced by IFN-β. Transferring stable FoxA1$^+$ Tregs to mice suppressed EAE in a PD-L1-dependent manner, which was related to its reduction in pro-inflammatory cytokines (IL-12 and IL-17) secreted by DCs and its inhibition of PD-1$^+$ Teffs. Of note, FoxA1$^+$ Tregs are negative for expression of Foxp3, CTLA-4, TGF-β, IL-10, and IL-35, though FoxA1 is a key transcription factor for PD-L1 production. Hence, the main pathway in which Tregs regulate DCs changes alongside alterations in the cell subtype. However, whether other Treg cell subtypes induce tolDCs *via* PD-L1 remains to be verified experimentally.

The regulation of PD-L1$^+$ DCs on Treg proliferation, differentiation, and function in EAE/MS has attracted significant attention. A previous study in EAE has shown that steady-state DCs exhibited their suppressive capacity by promoting the development of Tregs, thereby improving CNS autoimmunity (6). Further research has demonstrated that the generation of DC-dependent Tregs was guided by the interaction between PD-L1 on DCs and PD-1 expressed by T Cells (6, 64). Paradoxically, one study showed that PD-L1 expressed on DCs was important for the inhibition of follicular regulatory T (Tfr) cell differentiation and maintenance (71). The study demonstrated that PD-L1 deficiency in DCs resulted in a higher percentage of Tfr cells in the draining lymph nodes and blood than in control mice. It can be preliminarily speculated that PD-L1$^+$ CD11c$^+$ DCs were responsible for inhibiting the development of CD4$^+$ICOS$^+$CXCR5$^+$CD19$^-$Foxp3$^+$Tfr cells, but the specific DC subset was still unclear (71). We hold that this contradiction might be due to the heterogeneity of DC and Treg cell subsets. Moreover, PD-L1$^+$ DCs have become a new therapeutic target for EAE/MS. Vitamin D3 (VitD3), IFN-β, hypomethylating agents, and other drugs can induce Tregs and alleviate EAE *via* PD-L1$^+$ DCs (72, 73). A recent study showed that the IFN-γ-JAK1-STAT1 signaling pathway was an inherent upstream pathway that enabled DCs to induce PD-L1, followed by causing a series of subsequent immune tolerance effects. Therefore, mice harboring a DC-specific JAK1 deletion exhibited decreased expression of PD-L1 in DCs, fewer Tregs, and a deterioration of EAE (74). These studies demonstrated that the PD-L1/PD-1 axis played a powerful immune tolerance role in the DC-Treg cell crosstalk in the context of EAE/MS.

Potential LAG-3/TCR/MHC-II inhibitory feedback loop

The LAG-3 (CD223) is an inhibitory immune receptor that is mainly expressed by Tregs, especially Tr1, and negatively regulates T cell activation. Both TCR and LAG-3 on the surface of Tregs can bind to MHC-II on the surface of DCs. TCR-MHC-II signal transduction in DC-Treg cell crosstalk is the first signal produced by DCs inducing Tregs, and LAG-3-MHC-II signal transduction is one of the important ways for Tregs to inhibit DC antigen presentation. These two signal axes interfere with each other and form an inhibitory feedback loop (Figure 2).

Generally speaking, the TCR-MHC-II axis, as the first signal of T cell activation, plays a pathogenic role in EAE. However, it also plays a protective role in DC-Treg cell crosstalk. For instance, upon EAE induction, pDCs were recruited to the lymph nodes and established MHC-II-dependent cross-linking with CD4$^+$ T cells to promote the selective amplification of myelin antigen-specific Tregs, thereby inhibiting the response of pathogenic T cells (75). DCs that express MHC-II at a low level facilitated a significant increase in the amount of nTregs and alleviated EAE (76). In turn, Tregs limited the antigen presentation ability of DCs by consuming the peptide-MHC class II complex on the surface of DCs. In addition, there was some evidence that LAG-3-MHC-II signal transduction in DC-Treg cell crosstalk had a protective effect in the context of autoimmunity disease. For example, basic studies and experiments on tumors had shown that LAG-3 competitively binded MHC-II with TCR, directly interfering with TCR signal transduction and blocking the DC-mediated immune response (77, 78). LAG-3 engagement with MHC-II inhibited DC activation and induced tolDC generation *via* the immunoreceptor tyrosine-based activation motif (ITAM)-

mediated inhibitory signaling pathway that involved FcγRγ and the ERK-mediated recruitment of SHP-1 (78).

In addition, the expression level of LAG-3 is closely related to the course of MS. It has been reported that SNPs of LAG-3 influenced MS susceptibility (79). The expression of LAG-3 messenger RNA (mRNA) in PBMCs at diagnosis in untreated MS patients was significantly lower than that in healthy controls. Another study has shown that the reduced expression of baseline LAG-3 in PBMCs predicted the MS course alongside paraclinical and clinical parameters and might also be an adverse prognostic factor for MS (55). In line with this finding, a recent study observed significant reduction in the expression of LAG-3 mRNA in major $CD4^+$ and $CD8^+$ T cell subsets in RRMS individuals (80). Due to the expression level of LAG-3 in MS patients and the pathological characteristics of immune diseases, it can be speculated that the LAG-3/MHC-II axis is involved in DC-Treg cell crosstalk in MS/EAE and that the LAG-3/TCR/MHC-II inhibitory feedback loop mediates DC-Treg cell interactions and plays a protective role in MS/EAE.

DC-Treg cell crosstalk-related inhibitory cytokines in MS/EAE

(Figure 3) Both DCs and Tregs can secrete IL-10/TGF-β/IL-35, and the secretion level is closely related to EAE/MS. It has been reported that the reduction in serum IL-10 level in patients with acute MS may be used as a marker of MS disease activity (81). As for cell subsets, the IL-10 secretion level of Tr1 is decreased in MS patients (82). In addition, increased TGF-β secretion in the peripheral blood of RRMS and SPMS patients has also been reported (83). Specifically, in MS patients, decreased gene expressions of key proteins in the TGF-β signal pathway of naive $CD4^+$ T cells, such as TGF-βRI, TGF-βRII, and drosophila mothers against decapentaplegic 4 (SMAD4), have been reported (84), and T cell lines in patients with stable MS produce more TGF-β than those in patients with active MS (85). A recent study has further shown that a variety of cell surface markers related to TGF-β signal transduction in the Tregs are differentially expressed in MS patients and healthy controls, and are closely related to disease severity (86). These results indicate that TGF-β and its downstream signal pathway play a momentous modulating role in MS. Regarding IL-35, a new member of the IL-12 family, two contradictory studies have reported that the serum IL-35 level of RRMS patients was either lower or higher than that of healthy controls (87, 88). The subjects of the first study included both RRMS patients and clinically isolated syndrome (CIS) patients who have not yet converted to MS, which might be responsible for the contradiction of IL-35 expression level in serum. In addition, another study demonstrated that MS patients treated with IFN-β or methylprednisolone had higher serum IL-35 levels, which suggested that the clinical therapeutic benefits of these drugs might be partly induced by the upregulation of IL-35 (89). Collectively, MS patients can active the protective compensatory mechanism by regulating the secretion of IL-35 after symptoms onset, which may be influenced by the Foxp3 gene polymorphism and the progression stage of MS.

The above studies indicate that IL-10/TGF-β/IL-35 is involved in the regulation of MS disease activity and demonstrate their regulatory role in DC-Treg cell crosstalk. In addition, once cytokines have been secreted into the internal environment, it is difficult to determine their source and aim. For example, DC- or Treg- derived IL-10/TGF-β/IL-35 can influence the generation of Tregs by paracrine, but it also influences its own mature state and antigen presentation ability by autocrine. However, in order to clearly ascertain their roles in DC-Treg cell crosstalk, we distinguished them to DCs- and Tregs-derived cytokines in the following paragraphs.

DC-derived IL-10/TGF-β/IL-35 can promote Treg generation

DC-derived IL-10 can promote Treg cell generation and play a neuroprotective role (Figure 3). A recent study demonstrated that the adoptive transfer of tolDCs with upregulated IL-10 expression to EAE mice reduced the percentage of Th1 and Th17 cells, promoted splenetic Treg cell generation, and restricted the development of EAE to some degree (90). Besides, curcumin can promote the generation of peripheral IL-10-producing tolDCs and Tregs, as well as alleviate EAE, whereas the neuroprotection was completely abrogated in IL-10 deficient mice (91). In MS patients, there is a signal pathway of IL-10-dependent Treg cell generation: IL-10 activates signal transducer and activator of transcription 3 (STAT3) and converts DCs into tolDCs; in the presence of IL-2, tolDCs further induce STAT5 phosphorylation in naive T cells and promote Treg cell generation (92). Therefore, there is an inhibitory feedback loop about IL-10 that participates in DC-Treg cell crosstalk in MS patients. In addition, IL-10 is a downstream molecule of IL-27, and both of them established intravenous tolerance in EAE mice (93–95). For example, intravenously (i.v.) injecting $MOG_{35–55}$ to wild-type (WT) mice infected with EAE can induce i.v. tolerance and reduce disease severity, whereas this administration was ineffective in IL-27 receptor (WSX-1) knockout mice. Moreover, research showed that distinct subsets of splenic DCs (i.e., $CD11b^+CD103^±$ and $CD11b^{hi}CD103^+$) contributed together to the induction of i.v. tolerance *via* promoting DC-drived IL-27, IL-10 and IFN-γ secretion, as well as suppressing IL-17 secretion (94).

DC-derived TGF-β promotes Treg cell generation *via* direct and indirect effects (Figure 3). It is well established that TGF-β is a popular inducer of Tregs *in vitro* that works independently of DC. In addition, several drugs alleviated EAE *via* the direct effect of TGF-β. For example, by targeting DCs to drive TGF-β1 upregulation, Tanshinone IIA(TSA) promoted the polarization of naïve $CD4^+$ T cells to Tregs and

significantly reduced the clinical severity of EAE (96). Apigenin shifted DC-modulated T cell responses from Th1 and Th17 types towards Treg cell-directed responses and curbed neuroinflammation in EAE by promoting the secretion of TGF-β and IL-10 (97). However, TGF-β can also promote the phosphorylation of IDO in DCs, a key enzyme in the tryptophan metabolic pathway, induce the DC tolerance phenotype, and indirectly facilitate Treg cell generation. For example, SMAD7 is an inhibitory SMAD protein that negatively regulates TGF-β signal pathway. Mice devoid of SMAD 7 in DCs were resistant to the induction of EAE. This result was predominantly caused by the high expression level of IDO and the elevated frequency of Tregs in secondary lymphoid organs and the CNS (98). Likewise, administration of the downstream tryptophan metabolite 3-hydroxyanthranillic acid enhanced the secretion of DC-derived TGF-β and the percentage of Tregs in IDO-deficient mice (99). Furthermore, the enhanced Treg cell response promoted the secretion of DC-derived TGF-β, formed an inhibitory feedback mechanism, and eventually reduced the clinical manifestations of EAE.

DC-derived IL-35 can promote Treg cell generation (Figure 3). IL-35-producing CD8α$^+$ DCs have limited antigen presentation capacity and high tolerance. Moreover, since antigen-pulsed IL-35$^+$ DCs possessed the ability to induce Tregs, their use can significantly reduce the severity of EAE, and Tregs induced by IL-35$^+$ DCs acquired a stronger inhibitory function than those induced by TGF-β/IL-2 (100). Furthermore, the α (IL-12p35) and β (Epstein-Barr Virus-Induced, EBI3) subunits of IL-35 can both alter Tregs. For example, IL-12p35 suppressed neuroinflammatory responses and ameliorated the pathology of EAE by boosting the expansion of IL-10-producing Tregs in the brain and spinal cord as well as by inhibiting the STAT1/STAT3 pathways, and pathogenic Th17 and Th1 cells (101). Conversely, EBI3-deficient mice immunized by the MOG peptide elicited stronger Th17/Th1 responses in the CNS with marginally enhanced EAE development (102). Strikingly, there was an increased number of CD4$^+$ Foxp3$^+$ Tregs in the peripheral lymphoid organs of EBI3-deficient mice, and the suppressive function of these Tregs was more potent than Tregs in WT mice. The authors explained that the EAE development was only modestly enhanced compared with WT mice in the presence of potent Th17 response, which may attribute to the enhanced Treg responses (102). It's indicated that the enhanced Treg responses was a comprehensive change of IL-35 and IL-27, because EBI3 is also the subunit of IL-27, which appears to have an inhibitory effect on Treg cell generation, as mentioned below. As a result, selectively knocking out IL-35-EBI3, while retaining IL-27-EBI3 may better reflect the effect of EBI3 subunit of IL-35 on Tregs.

Treg cell-derived IL-10/TGF-β/IL-35 can enhance the tolerance of DCs

Unfortunately, in the context of EAE/MS, there was little direct evidence for a distinct modulatory effect of Treg cell-derived IL-10/TGF-β/IL-35 on DC maturation and antigen presentation ability. Nevertheless, several basic experiments have shown that, in the context of immune tolerance, Treg cell-derived IL-10/TGF-β/IL-35 can acquire the capacity to inhibit DCs (Figure 3). For example, when Ag-specific iTregs were co-cultured with DCs in the absence of Teffs, iTreg cell-treated DCs had markedly impaired immunogenicity, which can be completely reversed by anti-IL-10 (57). Further research has shown that IL-10 can induce the degradation of CD86 and MHC-II on DCs and achieve the goal of suppressing the DC function by promoting the neutralization reaction between membrane associated ring-CH-type finger 1 (MARCH1, an E3 ubiquitin ligase) and CD83(a DC activation marker) (57). Another study reported that IL-10 can suppress immune responses by interfering with TLR- or IFNγ- mediated DC activation and directly inducing gene expression that inhibits APC function (103). Moreover, one study suggested that IL-10$^{-/-}$ iTregs lost their protective role in EAE, which may be due to the impaired mechanism of iTreg cell-derived IL-10 inhibiting the expression of co-stimulatory molecules in DCs (104). A recent study demonstrated that Treg-derived IL-10 in tumors was also required for imprinting the Treg cell-inducing capacity of tolDCs (105).

Strikingly, a very recent report indicated that CD4$^+$ Teff cell-derived IL-10 promoted CNS inflammation during the progression of EAE, *via* sustaining survival and proliferation of Th1 cells and, to a lesser degree, Th17 cells (106). However, IL-10 produced by Teffs did not exert its modulatory function by acting directly on APCs, and what affect such IL-10 may bear on the DCs remained open questions. Exploring the cellular source and targeted cell of cytokines seems to be important and meaningful. Besides, this study showed a hint: could Treg derived IL-10 also plays a pro-inflammatory role in a specific environment? This still needs further experiments and facts to prove. On the other hand, a study about gut inflammation also has reference value for MS because the microbiota-gut-brain axis is considered to participate in MS. For example, IL-10 signaling in CD11c$^+$ DCs can limit reactivation of local memory T cells thereby controlling gut immune homeostasis (107). As mentioned above, the reactivation of memory T cells migrating to CNS is a pivotal process causing MS (3). Therefore, we speculated that IL-10 signal between CNS-DCs and memory T cells might be of similar significance. In conclusion, these researches proved the importance of exploring the cellular source and aims of cytokines, because IL-10 from different cellular sources may have different effects and mechanisms of action.

Treg cell-derived TGF-β is also necessary for the induction of DC tolerogenic function. When human monocytes were cultured with normal $CD4^+Foxp3^+$ Tregs and Th cells, they polarized into tolDCs, with capable of generating induced Tregs from naïve T cells. In this process, Treg-derived TGF-β, IL-10 and CTLA-4 were all required for the phenotypic differentiation of tolDCs (105). Similarly, a classical basic study revealed that Tregs restricted the maturation and antigen-presenting capacity of DCs, which can be marginally reversed using anti-TGF-β antibodies to neutralize TGF-β (108). Besides, transforming growth factor receptor 1 (TGFβR1) had an indispensable role in the development of intestinal $CD103^+CD11b^+$ DCs, and influenced the amount of DC related $Foxp3^+$ Treg cells *in vitro* and *in vivo* (109). These phenomena confirmed that Treg cell-derived TGF-β affected DC tolerogenic phenotype. As for IL-35, IL-35-treated MoDCs are characterized by tolerance, with a strong inhibitory function on the proliferation of pathogenic T cells. The exogenous addition of IL-35 inhibited MoDC maturation and secretion of pro-inflammatory cytokines, and also partially inhibited the differentiation of MoDCs (110). It suggested that Treg cell-derived IL-35 may also have a similar inhibitory effect on DCs.

In autoimmune diseases, Tregs inhibit DC maturation and improve immune tolerance by secreting IL-10/TGF-β/IL-35; moreover, DC provides conditions for Treg cell generation *via* the production of IL-10/TGF-β/IL-35. As a result, these three inhibitory cytokines involved in DC-Treg cell crosstalk formed three negative feedback mechanisms to counteract the imbalance of immune tolerance. Considering the autoimmune mechanism and the expression of IL-10/TGF-β/IL-35 in EAE/MS, we speculated that Treg cell-derived IL-10/TGF-β/IL-35 have a similar inhibitory effect on DCs in EAE/MS. However, it requires further experimental verification to fill the knowledge gap regarding cytokines in DC-Treg cell crosstalk. In addition, most researches have focused on the compherehensive changes in cytokines, whereas little attention has been paid to cytokine production in specific cell subsets. Therefore, unequivocally detecting cytokines is a critical future direction in the study of the DC-Treg cell crosstalk mechanism.

Extracellular vesicles involved in DC-Treg cell crosstalk

Extracellular vesicles (EVs)—including exosomes that are wrapped with biological messengers, such as microRNAs and cytokines from DCs and Tregs—can complete cell interactions without direct contact (111, 112). Exosomes with membrane-associated TGF-β1 from gene-modified DCs can maintain the inhibitory function of Tregs, reduce the frequency of Th17 cells, and curb the progression of EAE (111, 112). Moreover, DC-derived exosomes can promote myelin regeneration (113). Conversely, with the help of EVs, Tregs can transport miRNA (especially mir-150-5p and mir-142-3p) into DCs to induce the tolerance phenotype (114). A previous study has shown that the inhibitory effect of Treg cell-derived exosomes in RRMS individuals was significantly weaker than that in healthy controls (115). Additionally, in a rat liver allograft model, exosomes from immature DCs were shown to retain numerous tolerogenic characteristics of immature DCs, and Tregs could be amplified in the presence of such exosomes to induce immune tolerance (116). Therefore, EVs are involved in DC-Treg cell crosstalk and are expected to become an emerging treatment strategy for MS.

IDO1-related negative feedback loop

IDO is the first rate-limiting catabolic enzyme in the degradation pathway of the essential amino acid tryptophan (23). IDO has two isozymes: IDO1 and IDO2. IDO1 converts L-tryptophan to kynurenine *via* the kynurenine pathway (KP), which plays a key role in MS, whereas IDO2 may not be related to MS (117). Expressed mainly in DCs (especially pDCs), IDO typically has low basal expression, and its upregulation primarily correlates with cytokines (IFN-γ, IFNα/β, and TGF-β) and co-stimulatory signals (CTLA-4 and glucocorticoid-induced tumor necrosis factor receptor [GITR]) (118), whereas IL-6 and IL-4 inhibit the expression of IDO in DCs (119, 120). IDO activation is considered an endogenous self-protection response that accompanies EAE/MS (120). For example, the expression of IDO1 in the PBMCs of patients with RRMS was higher during the recurrence period than in the remission period (121). During an EAE attack in mice, activating the Stimulator of IFN Genes (STING) signaling adaptor to stimulate IFN-I production induced IDO expression in DCs, effectively inhibited disease progression, and alleviated clinical symptoms (122). Similarly, the mild condition of MS patients during pregnancy was related to the promotion of IDO expression in DCs by estriol. However, this compensatory effect is limited, and the IDO expression level in DCs of pregnant MS patients may be still lower than that of healthy controls (123, 124).

IDO1 mediates DC-Treg cell crosstalk and plays a protective role *via* the related negative signal loop (Figure 3). When EAE/MS occurs, both the massive secretion of IFN-α/β, IFN- γ, and CTLA-4-CD80/86 between Tregs and DCs can be used as the upstream signal of IDO1 to enhance the expression of IDO1 in DCs, which initiates tryptophan catabolism. Since tryptophan is an essential amino acid for T cell activation and proliferation, IDO1-mediated tryptophan catabolism can lead to tryptophan starvation, inhibit specific immune responses, and promote T cell anergy (8, 125). The KP is the most important tryptophan metabolism pathway mediated by IDO1. A variety of IDO1 downstream products produced *via* the KP are positive regulators that induce Tregs, of which kynurenine is the most representative. A large amount of kynurenine is produced and

bound to AHR as a ligand, which promotes the generation of AHR-dependent Tregs (125). Moreover, such combination regulates the NF-kB pathway in DCs, further upregulates the gene expression level of IDO1, and improves the tolerance of DCs (119). In addition, long-term tryptophan catabolism is also conducive to promoting the differentiation of naive T cells into Tregs; and tolDCs can also enhance the inhibitory function of Tregs (119). Conversely, newly generated Tregs induce expression of IDO1 in DCs *via* CTLA-4, which further promotes the generation of tolDCs and forms the IDO1 related negative feedback loop. In addition, it has been demonstrated that in the steady state, Tregs induced the generation of IDO^+ tolDCs in advance, and tolDCs, in turn, promoted the inhibitory function and rapid proliferation of Tregs following inflammation (8). Treg cell- or DC-derived TGF-β in EAE also induced IDO phosphorylation, promoted the gene expression level of TGF-β in DCs, and induced Treg cell generation. In the allergic airway inflammation model, Tregs induced IDO *via* GITR-GITR ligand (GITRL) reverse signal transduction (118). Surprisingly, basic research has also shown that IDO^+ DCs can make IDO^- DCs tolerogenic *via* the bystander mechanism (126).

Compared with cDCs, pDCs have a stronger potential to induce Tregs in an IDO-dependent manner. However, the ability of pDCs to induce Tregs was significantly downregulated in MS patients, followed by destroying immune tolerance. Notably, IFN-β treatment can restore the Treg-inducing ability of pDCs (37). A newly developed DC-targeting IFN can specifically induce Tregs in an IDO-dependent manner to alleviate EAE (127). Its application eliminated the influence of IFN-β on other immune cells, which offered promise for providing an effective therapy. Furthermore, VitD3 and anti-malarial drug-primaquine, can also boost the expression level of IDO in $CD11c^+$ DCs and induce $Foxp3^+$ Tregs (128). The adoptive transfer of IDO^+ $CD11c^+$ DCs induced by VitD3 to EAE mice had the same therapeutic effect as oral or intraperitoneal injection of VitD3 (129). However, the role of IDO in EAE is variable. A recent study showed that the induction of EAE clinical signs was related to the activation of the neurotoxic metabolites of IDO and the KP, and the IDO inhibitor INCB024360 unexpectedly curbed the clinical symptoms and weight loss caused by EAE (120). The most likely explanation for this phenomenon is that IDO is a double-edged sword (130). In the early stage of inflammation, KP maintained immune tolerance by promoting the generation of $Foxp3^+$ Tregs and played a protective role in EAE. However, as the disease progresses, the infiltration of immune cells in the CNS intensified, and microglia produced neurotoxic metabolites of kynurenine, such as quinolinic acid (QUIN) and 3-hydroxykynurenine, downstream of IDO. These toxic substances accumulated in the prefrontal cortex, hippocampus, spinal cord, spleen, and lymph node of EAE mice, gradually offsetting the IDO-induced immune tolerance (120). Among these metabolites, QUIN connected neuroinflammation with neurodegeneration and guided EAE to develop in the direction of neurodegeneration-related chronic inflammation and neurotoxicity (120, 131). Therefore, IDO inhibitors are expected to become a new strategy for the treatment of advanced MS with neurodegenerative diseases; selecting the right time point to administer IDO inhibitors and treat autoimmune diseases will be a challenge in the future.

Unidirectional regulation of Tregs by DCs in MS/EAE

Various signal loops with surface molecules, cytokines, and metabolic enzymes as the core, as described above, explain the majority of the DC-Treg cell crosstalk mechanism; however, there are also other molecules, such as thymic stromal lymphopoietin (TSLP), GITRL, IL-27, and retinoic acid (RA), indirectly influence Tregs by inducing DC tolerogenicity. Unsatisfactorily, it has not been confirmed experimentally whether Tregs participate in the regulation of DC through these molecules.

Surface molecules involved in the DC regulation of Tregs

DCs can regulate Treg cell generation with the help of surface molecules (Figure 2). For example, TSLP-activated DCs can provide a strong survival signal for high-affinity autoreactive T cells and actively participate in their differentiation into Tregs (132). The expression level of the TSLP receptor (TSLPR) on the surface of myeloid DCs was decreased in peripheral blood of MS patients, and the function of DCs was altered, which resulted in abnormal Treg cell homeostasis and function. Upon immunomodulatory treatment with IFN-β and glatiramer acetate, TSLPRs on myeloid DCs were upregulated, and Treg cell homeostasis was restored (133). These studies demonstrated that TSLPRs were involved in the generation of DC-dependent Tregs.

The binding of GITRL on the DC surface and the corresponding receptor (i.e., GITR) on the Treg cell surface can improve the sensitivity of Treg precursor cells to IL-2 and provide co-stimulatory signals for Treg cell proliferation (134, 135). A recent study showed that the expression of GITRs on the surface of $CD4^+$ and $CD8^+$ Tregs was decreased in RRMS individuals (69). This might be one of the reasons that DC-Treg cell crosstalk is destroyed in MS patients, which limits the proliferation of DC-dependent Tregs. In addition, the GITR-GITRL axis was one of the mechanisms underlying the treatment effect of IFN-β on MS. It has been shown that in the presence of IL-2, IFN-β induced the expression of GITRL on DCs, enhanced the GITR-GITRL axis

signal transduction, promoted the proliferation of Tregs, and participated in the treatment of MS (136). The allergic airway inflammation model suggested that the reverse signal transduction of GITRL induced IDO expression in mouse pDCs (118). Thus, the GITR-GITRL axis might also play a bidirectional role in DC-Treg cell crosstalk in EAE/MS.

CD31 is a transhomophilic tyrosine-based inhibitory motif receptor expressed by DCs. Sustaining CD31/SHP-1 signaling during DC maturation resulted in reduced NF-κB nuclear translocation and enhanced tolerogenic functions of DCs that promoted the generation of antigen-specific Tregs (137). The adoptive transfer of CD31-conditioned MOG-loaded DCs can significantly increase the percentage of $CD4^+$ $CD25^+$ $Foxp3^+$ Tregs and offer immune tolerance against the subsequent development of MOG-induced EAE *in vivo* (137). Therefore, inducing Treg cell generation by regulating these DC surface molecules is a potentially promising treatment for MS.

Cytokines involved in the DC regulation of Tregs

DC-derived IL-27 induces Treg cell generation

IL-27 secreted by DCs has both anti-inflammatory and pro-inflammatory effects, and its production changes with the occurrence of MS/EAE (138). For example, plasma IL-27 secretion and IL-27 mRNA expression in PBMCs were significantly decreased in patients with progressive MS (139). The IL-27 subunit and its receptor were upregulated in the CNS inflammatory cells of EAE mice (140). These results suggested a clear correlation between IL-27 and EAE/MS.

Studies have shown that the IL-27 signaling pathway mediates protective DC-Treg cell crosstalk in EAE (141) (Figure 3). For example, IL-27 receptor knockout mice with EAE deteriorate significantly, accompanied by reductions in the frequency of $Foxp3^+$ and $IL\text{-}10^+$ $CD4^+$ T cells (141). Subsequent studies have shown that DC-derived IL-27 activated STAT1, STAT3, AHR, c-Maf, and other transcription factors, induced the production of IL-10, and, in turn, promoted the generation of Tr1 and Tregs (22, 93). Recent studies have revealed that the functioning way of IL-27 differed between the central and peripheral tolerance. Do et al. (142) used a Treg cell-specific IL-27 receptor knockout mouse model to illustrate that IL-27 signaling in $Foxp3^+$ Tregs was essential for Tregs to control autoimmune inflammation in the CNS. However, Thomé et al. (94) demonstrated that this classical IL-27 signaling mode in T cells was not necessary to induce peripheral tolerance in EAE mice. In contrast, the indirect way in which IL-27 promotes DC tolerance and induces Treg cell generation is more pivotal in peripheral tolerance. In addition to secreting IL-10, IL-27 plays an anti-inflammatory role in another two ways to induce tolDCs and prevent the development of CNS inflammation and EAE: 1) promote the expression of co-inhibitory molecules PD-L1 and CD39 on the surface of DCs (22, 141, 143, 144); 2) regulate the NF-κB signaling pathway in DCs to promote the expression of TGF-β1 and IDO (137).

IL-27 appears to have a dual effect on Treg cell generation in EAE mice (93, 145). For example, although the systemic delivery of IL-27 can effectively prevent the initiation of Th17 cells and the development of EAE, it enhanced the Th1 response, downregulated the frequency of $Foxp3^+$ Tregs in the spleen, and significantly inhibited Treg cell subsets of the CNS without influencing Tr1 cells (146). This phenomenon increased the risk of IL-27-based EAE treatment and suggested that IL-27 has an inhibitory effect on Treg cell generation. In addition, IL-27 in EAE also inhibits immune tolerance mediated by mature DCs and thus plays a pro-inflammatory role. In this process, mature DCs treated with IL-27 did not influence the expression of Treg cell-associated molecules on $CD4^+$ T cells *in vivo* or *in vitro* but induced the development of $CD4^+$ $CD127^+$ $3G11^+$ Tregs, which were considered an unprecedented pro-inflammatory Treg cell subset (138). Therefore, the mechanism of the pleiotropic molecule IL-27 in DC-Treg cell crosstalk has not been fully elucidated. At present, in the context of EAE/MS, most studies are devoted to the anti-inflammatory effect of IL-27 on the promotion of the generation of tolDCs and Tregs. However, the pro-inflammatory effect of IL-27 and its negative regulation of Treg cell generation also warrant further attention.

Other cytokines that induce Tregs in a DC-dependent manner

RA is produced by a variety of cells, including DCs and Tregs (Figure 3). Although numerous studies have shown that RA directly promotes Treg cell proliferation (147, 148), there is evidence that RA can also indirectly influence Tregs in a DC-dependent manner. For example, in an EAE model, all-trans-RA can impair the antigen-presenting ability of DCs, resulting in the reduction of pro-inflammatory Th1/Th17 cells and severity of EAE (149). Similarly, helminth-infected MS patients developed a relatively mild condition owing to the increased synthesis of RA in DCs, so that DCs were programmed to develop into tolDCs, which induce $Foxp3^+$ Tregs and inhibit the production of the suppressor of cytokine signaling 3-mediated pro-inflammatory cytokines (150). Furthermore, tolDCs induced by RA can induce the antigen-specific Treg cell response *in vitro*, and the liposomal co-delivery of antigen and RA might be a more targeted approach to induce antigen-specific tolerance in autoimmune and chronic inflammatory diseases (148). Thus, RA is of great significance for DC-dependent Treg cell generation.

Most galectins are critical mediators for the induction of peripheral tolerance, offering protective effects for MS patients and EAE mice. Galectin-1 is synthesized and secreted by Tregs, DCs, and other cells, which in turn boosts the generation of tolDCs. A previous study showed that galectin-1 induced

tolDCs, enhanced the development of Tr1 and Tregs, and participated in the induction of intravenous tolerance in MOG_{35-55} immunized EAE mice (151). In addition, EAE was exacerbated in Lgals8/Lac-Z knock-in mice lacking galectin-8 expression because of the increased immunogenicity of DCs and the disruption of the Treg cell-Th1/Th17 cell balance (152).

Possible pathways of tolDCs inducing Tregs

The contribution of the immunoglobulin-like transcript (ILT), CD83, and heme oxygenase 1 (HO-1) to DC-Treg cell crosstalk in MS/EAE has not been extensively reported. However, researches suggested that they indirectly participate in the DC-Treg cell interplay by inducing tolDCs.

The inhibitory receptors ILT3 and ILT4 are vital for inducing T cell tolerance, highly expressed in tolDCs, and independently prevent the activation of pathogenic T cells (14). The beneficial effect of IFN-β in MS patients was probably achieved partially by regulating the expression of ILT3 and ILT4 in DCs. VitD3 also increased the expression of ILT3 but not ILT4 (153). These studies suggested that a variety of drugs induce Tregs and treat MS by regulating the expression of ILTs on the surface of DCs. Besides, *via* secreting IFN-I, toll-like receptor 9-activated cDCs can regulate neutrophil and monocyte trafficking to the inflamed colon and restrain the inflammatory products of tissue macrophages, thereby inhibiting colonic inflammation independently of T cell (154). This reminds us that cDCs may further influence CNS inflammation in a similar way, with the help of gut-brain axis. In addition, CD83 is expressed in activated B cells, T cells, and especially Tregs, and its soluble form inhibits the maturation and function of DCs (155). CD83 transgenic mice recovered quickly from EAE with the enhanced activity of Tregs and the limited proliferation of pathogenic T cells (155). Therefore, CD83 probably induced Treg cell generation in a tolDC-dependent manner.

Surprisingly, numerous studies have shown that HO-1 has a protective effect on MS/EAE. HO-1 in EAE inhibited the expression of MHC-II in DCs and improved DC tolerogenecity (156–158). However, one study found that HO-1 did not regulate the number or function of infiltrated Tregs in the CNS; it showed that the protective effect of HO-1 on the CNS of EAE mice might not be related to DC-Treg cell crosstalk (159). Currently, it remains uncertain whether peripheral HO-1^+ DCs in EAE play a protective role *via* Tregs, because in the airway inflammation model, HO-1 expressed by DCs indeed promote the differentiation of Tregs (159).

Potential tolDC subsets can induce Tregs

There are a small number of dedicated so-called tolerogenic DC subsets, which are predestined to induce Tregs in a steady state (Table 3). Moreover, the generation of tolDC is closely related to the Wnt/beta-catenin pathway. A classical study in 2007 demonstrated that disruption of E-cadherin-mediated adhesion could induce peripheral T cell tolerance *in vivo* and protect against EAE (164). In this process, E-cadherin triggered Wnt/beta-catenin pathway, a classical pathway to induce DC tolerance and maturation, and these tolDCs further boosted IL-10-producing Treg cell generation and peripheral tolerance (164, 165). Of note, CD103 is a heterotypic ligand for E-cadherin, so some $CD103^+$DCs might be a potential tolDC subset. For example, Langerin$^+$CD103$^+$ migratory DCs had a superior ability to generate Tregs *in vivo*, which in turn drastically alleviated EAE (160). Besides, a recent study defined another tolDC subset: BTLA$^+$ DEC205$^+$ CD8$^+$ CD11c$^+$ DCs, which took advantage of the engagement of the herpesvirus entry mediator (HVEM), a receptor of BTLA, upregulated the expression of Foxp3 in a CD5-dependent manner, and promoted peripheral Treg cell transformation (161). This study suggested that the

TABLE 3 Potential tolDC subsets that can induce Treg cells.

TolDC phenotype	Key molecules	Relevant Treg cell phenotype	Distribution	Ref.
Langerin$^+$ CD103$^+$ migratory DC	Langerin and CD103	Foxp3$^+$Treg	Peripheral tissues	(160)
Interleukin-27-producing CD11b$^+$CD103$^{\pm}$/ CD11b^{hi}CD103$^+$DC	IL-27	Foxp3$^+$Treg and Tr1 cell	Spleen	(94)
BTLA$^+$DEC205$^+$CD8$^+$CD11c$^+$ DC	BTLA	CD4$^+$CD25$^+$Foxp3$^+$Treg	Lymph nodes and spleen	(161)
Interleukin-35-producing CD8α$^+$ DC	IL-35	IL-35$^+$ DC-regulated Tregs do not express Foxp3, but their suppressive capacity is more potent than TGF-β /IL-2-induced Tregs.	/	(100)
CD31$^+$ DC	CD31	CD4$^+$ CD25$^+$ Foxp3$^+$ Treg	Draining lymph nodes	(137)
DC-10: CD1a$^-$CD1c$^-$CD14$^+$ CD16$^+$ CD11c$^+$CD11b$^+$HLA-DR$^+$CD83$^+$ IL-10-producing DC (human) (include two subsets: CD83^{high} CCR7$^+$ DC and CD83^{low}CCR7$^-$ DC)	IL-10	IL-10-producing Tr1 cell	Peripheral blood and secondary lymphoid organs	(162, 163)

cross-linking of BTLA and HVEM was one of the key mechanisms for DC to induce peripheral Tregs in EAE. However, most $CD11c^+$ DCs are $BTLA^{neg}$ DCs and thus can't acquire tolerance even in a steady state. Moreover, IL-10-producing DC(DC-10) is also a classical tolDC subset, and most of the induced tolDCs in EAE/MS are recognized by the secretion of IL-10. Therefore, we deem that DC-10 is a potential tolDC subset, but its concept is not clearly proposed in EAE (162, 163). Moreover, it should be noted that tolDC subsets only exist in the steady state. Once inflammation occurs, tolDCs would play a pro-inflammatory role again and activate Teffs. At that time, induced-tolDC would be crucial in role of immune protection.

DC-Treg crosstalk mechanism can be applied to MS treatment

DC-Treg crosstalk is one of the pivotal mechanisms of drugs to alleviate MS, such as IFN-β, Vit D3, tanshinone IIA, primaquine and apigenin. Besides, as for DC-Treg crosstalk, the treatment of MS/EAE in the future can also be explored in the following aspects: 1) inhibitors, agonists, or specific antibodies of critical immune targets, e.g., DC-targeting CTLA-4-Ig and PD-L1/PD-1 agonists; 2) therapeutic interventions modulating IDO activity, e.g., IDO inducers/inhibitors and STING agonists. However, drug-based therapy mostly plays its role through non-specific immunity, which often leads to side effects such as decreased immunity and infection. Therefore, cellar-based therapy involving tolDCs and Tregs have become a new upsurge, such as peptide- and protein-based vaccines. It can reestablish antigen-specific immune tolerance towards CNS structures and control autoreactive T cells without inducing systemic immune suppression.

At present, peptide-based vaccines were advanced into human clinical trials. A phase I clinical trial (NCT02283671) starting at 2014, was for the first time to evaluate the tolerance and safety of tolDCs in treating patients with MS or neuromyelitis optica (NMO). The clinical use of tolDCs in a well-defined population of MS patients was evaluated in two subsequent phase I clinical trials (NCT02618902 and NCT02903537). These two clinical trials conducted dose-escalation studies and compared each other through intradermal and intranodal cell administration, followed by evaluating the safety and feasibility of tolDC administration, and exploring appropriate vaccine injection doses and DC delivery methods for the next phase II clinical trials (166). In addition, a phase II clinical trial (NCT04530318) about the treatment of MS with autologous peripheral blood differentiated tolDCs combined with immune regulation was started in 2020, which is expected to be completed in 2024. Surprisingly, the current experiment did not report any safety problems related to tolDC administration in MS patients (166).

Similarly, protein-based vaccines are also intriguing tolDC therapies that involve DC-specific antigen-targeting strategy. For instance, both DEC205 (CD205) and dendritic-cell inhibitory receptor-2 (DCIR2), are DC-specific endocytosis receptors, which can improve the antigen presentation efficiency of DCs (167, 168) (Figure 2). Delivering PLP to DCs using αDEC-205 fusion monoclonal antibodies or DCIR2 fusion monoclonal antibodies can induce Treg cell generation. Then these Tregs resulted in antigen-specific tolerance and amelioration of EAE (167, 169). Similarly, targeting migratory DCs with an anti-receptor-antigen fusing to MOG can provide the same result (160). Intriguingly, $\alpha DEC\text{-}205^+$ fusion antibodies cause extrathymic induction of a $Foxp3^+$ Treg cell phenotype in naïve $CD4^+$ $Foxp3^-$ T cells, whereas $DCIR2^+$ fusion antibodies result in the proliferative expansion of natural $Foxp3^+$ Tregs in EAE (167). Besides, many drugs are inducers of tolDCs, such as interferon, vitD3, statins, galectin-1, tofacitinib, etc (151, 170, 171). Combining these drugs with protein-based vaccines is also more conducive to the induction of tolDCs.

Conclusion

DC-Treg cell crosstalk involves a variety of surface molecules, cytokines, and metabolic enzymes *via* multiple inhibitory feedback loops and plays a key protective role in the silent progression of MS. Drugs influencing DC-Treg crosstalk and tolDC therapy are expected to emerge as promising treatment strategies for MS. However, selecting the appropriate time point and specifically targeting DCs/Tregs without affecting the immune state of other cells is worthy of future discussion, due to different onset times and the wide distribution/rich targets of these immune effector molecules. At present, the researches of functional molecules working comprehensively become more and more popular in the environment of CSF, PBMC or peripheral blood in MS patients. Although, these studies can well show the correlation between molecules and diseases, what unsatisfied was that they did not reflect the molecular changes in specific cell subtypes and we cannot distinguish the cellular source and targeted cells of functional molecules from those studies. Therefore, further research on the expression level of molecules based on cell subsets is conducive to a more comprehensive analysis and evaluation of molecular effects. In addition, the increased focusing on tolDC therapy has facilitated an upsurge in

research on DC-induced Tregs, whereas investigations on the effect of Tregs in DCs remain relatively scarce. There remain several knowledge gaps in the mechanism of DC-Treg cell crosstalk, and further research would be necessary to translate mechanisms into clinical therapy.

Author contributions

RL, PL, and HLiu conceived this review. RL performed specific database queries, generated the figures and tables, and wrote the manuscript. HLi, XY, HH, PL, and HLiu edited and revised the review. All authors contributed to the article and approved the submitted version.

Funding

This work was supported by Henan Provincial and Ministerial Co-construction Projects (No. SB201901018) and the National Natural Science Foundation of China (No. U2004128).

Acknowledgments

We thank the reviewers for their insightful and constructive comments on the manuscript. We are grateful to the translational medicine center of the First Affiliated Hospital of Zhengzhou University for support.

Conflict of interest

The authors declare that the research was conducted in the absence of any commercial or financial relationships that could be construed as a potential conflict of interest.

Publisher's note

References

1. Ruland C, Renken H, Kuzmanov I, Fattahi Mehr A, Schwarte K, Cerina M, et al. Chemokine CCL17 is expressed by dendritic cells in the CNS during experimental autoimmune encephalomyelitis and promotes pathogenesis of disease. *Brain Behav Immun* (2017) 66:382–93. doi: 10.1016/j.bbi.2017.06.010

2. De Laere M, Berneman ZN, Cools N. To the brain and back: Migratory paths of dendritic cells in multiple sclerosis. *J Neuropathol Exp Neurol* (2018) 77(3):178–92. doi: 10.1093/jnen/nlx114

3. Grigoriadis N, van Pesch V, Paradig MSG. A basic overview of multiple sclerosis immunopathology. *Eur J Neurol* (2015) 22 Suppl 2:3–13. doi: 10.1111/ene.12798

4. Yang X, Peng J, Huang X, Liu P, Li J, Pan J, et al. Association of circulating follicular helper T cells and serum CXCL13 with neuromyelitis optica spectrum disorders. *Front In Immunol* (2021) 12:677190. doi: 10.3389/fimmu.2021.677190

5. Dendrou CA, Fugger L, Friese MA. Immunopathology of multiple sclerosis. *Nat Rev Immunol* (2015) 15(9):545–58. doi: 10.1038/nri3871

6. Yogev N, Frommer F, Lukas D, Kautz-Neu K, Karram K, Ielo D, et al. Dendritic cells ameliorate autoimmunity in the CNS by controlling the homeostasis of PD-1 receptor(+) regulatory T cells. *Immunity* (2012) 37(2):264–75. doi: 10.1016/j.immuni.2012.05.025

7. Paterka M, Voss JO, Werr J, Reuter E, Franck S, Leuenberger T, et al. Dendritic cells tip the balance towards induction of regulatory T cells upon priming in experimental autoimmune encephalomyelitis. *J Autoimmun* (2017) 76:108–14. doi: 10.1016/j.jaut.2016.09.008

8. Lippens C, Duraes FV, Dubrot J, Brighouse D, Lacroix M, Irla M, et al. IDO-orchestrated crosstalk between pDCs and tregs inhibits autoimmunity. *J Autoimmun* (2016) 75:39–49. doi: 10.1016/j.jaut.2016.07.004

9. Tadokoro CE, Shakhar G, Shen S, Ding Y, Lino AC, Maraver A, et al. Regulatory T cells inhibit stable contacts between CD4+ T cells and dendritic cells in vivo. *J Exp Med* (2006) 203(3):505–11. doi: 10.1084/jem.20050783

10. Moorman CD, Sohn SJ, Phee H. Emerging therapeutics for immune tolerance: Tolerogenic vaccines, T cell therapy, and IL-2 therapy. *Front Immunol* (2021) 12:657768. doi: 10.3389/fimmu.2021.657768

11. Onishi Y, Fehervari Z, Yamaguchi T, Sakaguchi S. Foxp3+ natural regulatory T cells preferentially form aggregates on dendritic cells *in vitro* and actively inhibit their maturation. *Proc Natl Acad Sci USA* (2008) 105(29):10113–8. doi: 10.1073/pnas.0711106105

12. Grover P, Goel PN, Greene MI. Regulatory T cells: Regulation of identity and function. *Front Immunol* (2021) 12:750542. doi: 10.3389/fimmu.2021.750542

13. Perdigoto AL, Chatenoud L, Bluestone JA, Herold KC. Inducing and administering tregs to treat human disease. *Front In Immunol* (2015) 6:654. doi: 10.3389/fimmu

14. Maldonado RA, von Andrian UH. How tolerogenic dendritic cells induce regulatory T cells. *Adv Immunol* (2010) 108:111–65. doi: 10.1016/B978-0-12-380995-7.00004-5

15. Eisenbarth SC. Dendritic cell subsets in T cell programming: location dictates function. *Nat Rev Immunol* (2019) 19(2):89–103. doi: 10.1038/s41577-018-0088-1

16. Villar J, Segura E. Decoding the heterogeneity of human dendritic cell subsets. *Trends Immunol* (2020) 41(12):1062–71. doi: 10.1016/j.it.2020.10.002

17. Coillard A, Segura E. *In vivo* differentiation of human monocytes. *Front Immunol* (2019) 10:1907. doi: 10.3389/fimmu.2019.01907

18. Zanna MY, Yasmin AR, Omar AR, Arshad SS, Mariatulqabtiah AR, Nur-Fazila SH, et al. Review of dendritic cells, their role in clinical immunology, and distribution in various animal species. *Int J Mol Sci* (2021) 22(15):8044. doi: 10.3390/ijms22158044

19. Macri C, Pang ES, Patton T, O'Keeffe M. Dendritic cell subsets. *Semin Cell Dev Biol* (2018) 84:11–21. doi: 10.1016/j.semcdb.2017.12.009

20. Bourque J, Hawiger D. Variegated outcomes of T cell activation by dendritic cells in the steady state. *J Immunol* (2022) 208(3):539–47. doi: 10.4049/jimmunol.2100932

21. Heger L, Hofer TP, Bigley V, de Vries IJM, Dalod M, Dudziak D, et al. Subsets of CD1c(+) DCs: Dendritic cell versus monocyte lineage. *Front Immunol* (2020) 11:559166. doi: 10.3389/fimmu.2020.559166

22. Waisman A, Lukas D, Clausen BE, Yogev N. Dendritic cells as gatekeepers of tolerance. *Semin Immunopathol* (2017) 39(2):153–63. doi: 10.1007/s00281-016-0583-z

23. Mondanelli G, Albini E, Pallotta MT, Volpi C, Chatenoud L, Kuhn C, et al. The proteasome inhibitor bortezomib controls indoleamine 2,3-dioxygenase 1

breakdown and restores immune regulation in autoimmune diabetes. *Front In Immunol* (2017) 8:428. doi: 10.3389/fimmu.2017.00428

24. Lutz MB, Backer RA, Clausen BE. Revisiting current concepts on the tolerogenicity of steady-state dendritic cell subsets and their maturation stages. *J Immunol* (2021) 206(8):1681–9. doi: 10.4049/jimmunol.2001315

25. Liu Y, Carlsson R, Comabella M, Wang J, Kosicki M, Carrion B, et al. FoxA1 directs the lineage and immunosuppressive properties of a novel regulatory T cell population in EAE and MS. *Nat Med* (2014) 20(3):272–82. doi: 10.1038/nm.3485

26. Klein L, Robey EA, Hsieh C-S. Central CD4 T cell tolerance: deletion versus regulatory T cell differentiation. *Nat Rev Immunol* (2019) 19(1):7–18. doi: 10.1038/s41577-018-0083-6

27. Roncarolo MG, Gregori S, Bacchetta R, Battaglia M, Gagliani N. The biology of T regulatory type 1 cells and their therapeutic application in immune-mediated diseases. *Immunity* (2018) 49(6):1004–19. doi: 10.1016/j.immuni.2018.12.001

28. Jonuleit H, Schmitt E. The regulatory T cell family: distinct subsets and their interrelations. *J Immunol* (2003) 171(12):6323–7. doi: 10.4049/jimmunol.171.12.6323

29. Dominguez-Villar M, Baecher-Allan CM, Hafler DA. Identification of T helper type 1-like, Foxp3+ regulatory T cells in human autoimmune disease. *Nat Med* (2011) 17(6):673–5. doi: 10.1038/nm.2389

30. Gupta S, Demirdag Y, Gupta AA. Members of the regulatory lymphocyte club in common variable immunodeficiency. *Front Immunol* (2022) 13:864307. doi: 10.3389/fimmu.2022.864307

31. Fazilleau N, Aloulou M. Several follicular regulatory T cell subsets with distinct phenotype and function emerge during germinal center reactions. *Front Immunol* (2018) 9:1792. doi: 10.3389/fimmu.2018.01792

32. Mishra S, Srinivasan S, Ma C, Zhang N. CD8 regulatory T cell - a mystery to be revealed. *Front In Immunol* (2021) 12:708874. doi: 10.3389/fimmu.2021.708874

33. Mena J, Alloza I, Tulloch Navarro R, Aldekoa A, Díez García J, Villanueva Etxebarria A, et al. Genomic multiple sclerosis risk variants modulate the expression of the - gene region in immature dendritic cells. *Front In Immunol* (2021) 12:816930. doi: 10.3389/fimmu.2021.816930

34. Luessi F, Zipp F, Witsch E. Dendritic cells as therapeutic targets in neuroinflammation. *Cell Mol Life Sci* (2016) 73(13):2425–50. doi: 10.1007/s00018-016-2170-9

35. Longhini ALF, von Glehn F, Brandão CO, de Paula RFO, Pradella F, Moraes AS, et al. Plasmacytoid dendritic cells are increased in cerebrospinal fluid of untreated patients during multiple sclerosis relapse. *J Neuroinflammation* (2011) 8(1):2. doi: 10.1186/1742-2094-8-2

36. Lopez C, Comabella M, Al-zayat H, Tintore M, Montalban X. Altered maturation of circulating dendritic cells in primary progressive MS patients. *J Neuroimmunol* (2006) 175(1-2):183–91. doi: 10.1016/j.jneuroim.2006.03.010

37. Aung LL, Brooks A, Greenberg SA, Rosenberg ML, Dhib-Jalbut S, Balashov KE. Multiple sclerosis-linked and interferon-beta-regulated gene expression in plasmacytoid dendritic cells. *J Neuroimmunol* (2012) 250(1-2):99–105. doi: 10.1016/j.jneuroim.2012.05.013

38. Stasiolek M, Bayas A, Kruse N, Wieczarkowiecz A, Toyka KV, Gold R, et al. Impaired maturation and altered regulatory function of plasmacytoid dendritic cells in multiple sclerosis. *Brain* (2006) 129(Pt 5):1293–305. doi: 10.1093/brain/awl043

39. Hafler DA, Compston A, Sawcer S, Lander ES, Daly MJ, De Jager PL, et al. Risk alleles for multiple sclerosis identified by a genomewide study. *N Engl J Med* (2007) 357(9):851–62. doi: 10.1056/NEJMoa073493

40. Verma ND, Lam AD, Chiu C, Tran GT, Hall BM, Hodgkinson SJ. Multiple sclerosis patients have reduced resting and increased activated CD4(+)CD25(+)FOXP3(+)T regulatory cells. *Sci Rep* (2021) 11(1):10476. doi: 10.1038/s41598-021-88448-5

41. Bjerg L, Brosbol-Ravnborg A, Torring C, Dige A, Bundgaard B, Petersen T, et al. Altered frequency of T regulatory cells is associated with disability status in relapsing-remitting multiple sclerosis patients. *J Neuroimmunol* (2012) 249(1-2):76–82. doi: 10.1016/j.jneuroim.2012.04.012

42. Feger U, Luther C, Poeschel S, Melms A, Tolosa E, Wiendl H. Increased frequency of CD4+ CD25+ regulatory T cells in the cerebrospinal fluid but not in the blood of multiple sclerosis patients. *Clin Exp Immunol* (2007) 147(3):412–8. doi: 10.1111/j.1365-2249.2006.03271.x

43. Sambucci M, Gargano F, Guerrera G, Battistini L, Borsellino G. One, no one, and one hundred thousand: T regulatory cells' multiple identities in neuroimmunity. *Front Immunol* (2019) 10:2947. doi: 10.3389/fimmu.2019.02947

44. Viglietta V, Baecher-Allan C, Weiner HL, Hafler DA. Loss of functional suppression by CD4+CD25+ regulatory T cells in patients with multiple sclerosis. *J Exp Med* (2004) 199(7):971–9. doi: 10.1084/jem.20031579

45. Edner NM, Carlesso G, Rush JS, Walker LSK. Targeting co-stimulatory molecules in autoimmune disease. *Nat Rev Drug Discov* (2020) 19(12):860–83. doi: 10.1038/s41573-020-0081-9

46. Hsieh CS, Lee HM, Lio CW. Selection of regulatory T cells in the thymus. *Nat Rev Immunol* (2012) 12(3):157–67. doi: 10.1038/nri3155

47. Beyersdorf N, Gaupp S, Balbach K, Schmidt J, Toyka KV, Lin CH, et al. Selective targeting of regulatory T cells with CD28 superagonists allows effective therapy of experimental autoimmune encephalomyelitis. *J Exp Med* (2005) 202(3):445–55. doi: 10.1084/jem.20051060

48. Zhang R, Huynh A, Whitcher G, Chang J, Maltzman JS, Turka LA. An obligate cell-intrinsic function for CD28 in tregs. *J Clin Invest* (2013) 123(2):580–93. doi: 10.1172/JCI65013

49. Chang TT, Jabs C, Sobel RA, Kuchroo VK, Sharpe AH. Studies in B7-deficient mice reveal a critical role for B7 costimulation in both induction and effector phases of experimental autoimmune encephalomyelitis. *J Exp Med* (1999) 190(5):733–40. doi: 10.1084/jem.190.5.733

50. Haanstra KG, Dijkman K, Bashir N, Bauer J, Mary C, Poirier N, et al. Selective blockade of CD28-mediated T cell costimulation protects rhesus monkeys against acute fatal experimental autoimmune encephalomyelitis. *J Immunol* (2015) 194(4):1454–66. doi: 10.4049/jimmunol.1402563

51. Wing K, Onishi Y, Prieto-Martin P, Yamaguchi T, Miyara M, Fehervari Z, et al. CTLA-4 control over Foxp3+ regulatory T cell function. *Science* (2008) 322(5899):271–5. doi: 10.1126/science.1160062

52. Gerdes LA, Held K, Beltrán E, Berking C, Prinz JC, Junker A, et al. CTLA4 as immunological checkpoint in the development of multiple sclerosis. *Ann Neurol* (2016) 80(2):294–300. doi: 10.1002/ana.24715

53. Paterson AM, Lovitch SB, Sage PT, Juneja VR, Lee Y, Trombley JD, et al. Deletion of CTLA-4 on regulatory T cells during adulthood leads to resistance to autoimmunity. *J Exp Med* (2015) 212(10):1603–21. doi: 10.1084/jem.20141030

54. Mohammadzadeh A, Rad IA, Ahmadi-Salmasi B. CTLA-4, PD-1 and TIM-3 expression predominantly downregulated in MS patients. *J Neuroimmunol* (2018) 323:105–8. doi: 10.1016/j.jneuroim.2018.08.004

55. Lavon I, Heli C, Brill L, Charbit H, Vaknin-Dembinsky A. Blood levels of Co-inhibitory-Receptors: A biomarker of disease prognosis in multiple sclerosis. *Front Immunol* (2019) 10:835. doi: 10.3389/fimmu.2019.00835

56. Qureshi OS, Zheng Y, Nakamura K, Attridge K, Manzotti C, Schmidt EM, et al. Trans-endocytosis of CD80 and CD86: a molecular basis for the cell-extrinsic function of CTLA-4. *Science* (2011) 332(6029):600–3. doi: 10.1126/science.1202947

57. Chattopadhyay G, Shevach EM. Antigen-specific induced T regulatory cells impair dendritic cell function *via* an IL-10/MARCH1-dependent mechanism. *J Immunol* (2013) 191(12):5875–84. doi: 10.4049/jimmunol.1301693

58. Kim GR, Kim WJ, Lim S, Lee HG, Koo JH, Nam KH, et al. *In vivo* induction of regulatory T cells *Via* CTLA-4 signaling peptide to control autoimmune encephalomyelitis and prevent disease relapse. *Adv Sci (Weinh)* (2021) 8(14):2004973. doi: 10.1002/advs.202004973

59. Glatigny S, Hollbacher B, Motley SJ, Tan C, Hundhausen C, Buckner JH, et al. Abatacept targets T follicular helper and regulatory T cells, disrupting molecular pathways that regulate their proliferation and maintenance. *J Immunol* (2019) 202(5):1373–82. doi: 10.4049/jimmunol.1801425

60. Vogel I, Kasran A, Cremer J, Kim YJ, Boon L, Van Gool SW, et al. CD28/CTLA-4/B7 costimulatory pathway blockade affects regulatory T-cell function in autoimmunity. *Eur J Immunol* (2015) 45(6):1832–41. doi: 10.1002/eji.201445190

61. Khoury SJ, Rochon J, Ding L, Byron M, Ryker K, Tosta P, et al. ACCLAIM: A randomized trial of abatacept (CTLA4-ig) for relapsing-remitting multiple sclerosis. *Multiple scler* (2017) 23(5):686–95. doi: 10.1177/1352458516662727

62. Bonelli M, Scheinecker C. How does abatacept really work in rheumatoid arthritis? *Curr Opin Rheumatol* (2018) 30(3):295–300. doi: 10.1097/BOR.0000000000000491

63. Keir ME, Butte MJ, Freeman GJ, Sharpe AH. PD-1 and its ligands in tolerance and immunity. *Annu Rev Immunol* (2008) 26:677–704. doi: 10.1146/annurev.immunol.26.021607.090331

64. Ibañez-Vega J, Vilchez C, Jimenez K, Guevara C, Burgos PI, Naves R. Cellular and molecular regulation of the programmed death-1/programmed death ligand system and its role in multiple sclerosis and other autoimmune diseases. *J autoimmunity* (2021) 123:102702. doi: 10.1016/j.jaut.2021.102702

65. Francisco LM, Salinas VH, Brown KE, Vanguri VK, Freeman GJ, Kuchroo VK, et al. PD-L1 regulates the development, maintenance, and function of induced regulatory T cells. *J Exp Med* (2009) 206(13):3015–29. doi: 10.1084/jem.20090847

66. Mi Y, Han J, Zhu J, Jin T. Role of the PD-1/PD-L1 signaling in multiple sclerosis and experimental autoimmune encephalomyelitis: Recent insights and future directions. *Mol Neurobiol* (2021) 58(12):6249–71. doi: 10.1007/s12035-021-02495-7

67. Ortler S, Leder C, Mittelbronn M, Zozulya AL, Knolle PA, Chen L, et al. B7-H1 restricts neuroantigen-specific T cell responses and confines inflammatory CNS damage: implications for the lesion pathogenesis of multiple sclerosis. *Eur J Immunol* (2008) 38(6):1734–44. doi: 10.1002/eji.200738071

68. Trabattoni D, Saresella M, Pacei M, Marventano I, Mendozzi L, Rovaris M, et al. Costimulatory pathways in multiple sclerosis: distinctive expression of PD-1 and PD-L1 in patients with different patterns of disease. *J Immunol* (2009) 183 (8):4984–93. doi: 10.4049/jimmunol.0901038

69. Machcińska M, Kierasińska M, Michniowska M, Maruszewska-Cheruiyot M, Szewczak L, Rola R, et al. Reduced expression of PD-1 in circulating CD4+ and CD8+ tregs is an early feature of RRMS. *Int J Mol Sci* (2022) 23(6):3185. doi: 10.3390/ijms23063185

70. Tekguc M, Wing JB, Osaki M, Long J, Sakaguchi S. Treg-expressed CTLA-4 depletes CD80/CD86 by trogocytosis, releasing free PD-L1 on antigen-presenting cells. *Proc Natl Acad Sci USA* (2021) 118(30):e2023739118. doi: 10.1073/pnas.2023739118

71. Sage PT, Schildberg FA, Sobel RA, Kuchroo VK, Freeman GJ, Sharpe AH. Dendritic cell PD-L1 limits autoimmunity and follicular T cell differentiation and function. *J Immunol* (2018) 200(8):2592–602. doi: 10.4049/jimmunol.1701231

72. Cao Q, Zheng C, Xie Z, Liu L, Zhu J, Jin T. The change of PD1, PDL1 in experimental autoimmune encephalomyelitis treated by 1,25(OH)D. *J Neuroimmunol* (2020) 338:577079. doi: 10.1016/j.jneuroim.2019.577079

73. Schreiner B, Mitsdoerffer M, Kieseier BC, Chen L, Hartung HP, Weller M, et al. Interferon-beta enhances monocyte and dendritic cell expression of B7-H1 (PD-L1), a strong inhibitor of autologous T-cell activation: relevance for the immune modulatory effect in multiple sclerosis. *J Neuroimmunol* (2004) 155(1-2):172–82. doi: 10.1016/j.jneuroim.2004.06.013

74. Vogel A, Martin K, Soukup K, Halfmann A, Kerndl M, Brunner JS, et al. JAK1 signaling in dendritic cells promotes peripheral tolerance in autoimmunity through PD-L1-mediated regulatory T cell induction. *Cell Rep* (2022) 38 (8):110420. doi: 10.1016/j.celrep.2022.110420

75. Irla M, Kupfer N, Suter T, Lissilaa R, Benkhoucha M, Skupsky J, et al. MHC class II-restricted antigen presentation by plasmacytoid dendritic cells inhibits T cell-mediated autoimmunity. *J Exp Med* (2010) 207(9):1891–905. doi: 10.1084/jem.20092627

76. Ray A, Basu S, Miller NM, Chan AM, Dittel BN. An increase in tolerogenic dendritic cell and natural regulatory T cell numbers during experimental autoimmune encephalomyelitis in rras-/- mice results in attenuated disease. *J Immunol* (2014) 192(11):5109–17. doi: 10.4049/jimmunol.1302254

77. Kumar P, Bhattacharya P, Prabhakar BS. A comprehensive review on the role of co-signaling receptors and treg homeostasis in autoimmunity and tumor immunity. *J Autoimmun* (2018) 95:77–99. doi: 10.1016/j.jaut.2018.08.007

78. Liang B, Workman C, Lee J, Chew C, Dale BM, Colonna L, et al. Regulatory T cells inhibit dendritic cells by lymphocyte activation gene-3 engagement of MHC class II. *J Immunol* (2008) 180(9):5916–26. doi: 10.4049/jimmunol.180.9.5916

79. Zhang Z, Duvefelt K, Svensson F, Masterman T, Jonasdottir G, Salter H, et al. Two genes encoding immune-regulatory molecules (LAG3 and IL7R) confer susceptibility to multiple sclerosis. *Genes Immun* (2005) 6(2):145–52. doi: 10.1038/sj.gene.6364171

80. Jones BE, Maerz MD, Bahnson HT, Somasundaram A, McCarthy LH, Speake C, et al. Fewer LAG-3(+) T cells in relapsing-remitting multiple sclerosis and type 1 diabetes. *J Immunol* (2022) 208(3):594–602. doi: 10.4049/jimmunol.2100850

81. Sedeeq MS, El-Nahrery EMA, Shalaby N, Hussein M, Shehata H, El Aal RA, et al. Micro-RNA-96 and interleukin-10 are independent biomarkers for multiple sclerosis activity. *J Neurol Sci* (2019) 403:92–6. doi: 10.1016/j.jns.2019.06.022

82. Astier AL, Hafler DA. Abnormal Tr1 differentiation in multiple sclerosis. *J Neuroimmunol* (2007) 191(1-2):70–8. doi: 10.1016/j.jneuroim.2007.09.018

83. Pasquali L, Lucchesi C, Pecori C, Metelli MR, Pellegrini S, Iudice A, et al. A clinical and laboratory study evaluating the profile of cytokine levels in relapsing remitting and secondary progressive multiple sclerosis. *J Neuroimmunol* (2015) 278:53–9. doi: 10.1016/j.jneuroim.2014.12.005

84. Lee PW, Severin ME, Lovett-Racke AE. TGF-beta regulation of encephalitogenic and regulatory T cells in multiple sclerosis. *Eur J Immunol* (2017) 47(3):446–53. doi: 10.1002/eji.201646716

85. Sanjabi S, Oh SA, Li MO. Regulation of the immune response by TGF-beta: From conception to autoimmunity and infection. *Cold Spring Harb Perspect Biol* (2017) 9(6):a022236. doi: 10.1101/cshperspect.a022236

86. Tapia-Maltos MA, Trevino-Frenk I, Garcia-Gonzalez HB, Rosetti M, Barriga-Maldonado V, Morales-Ramirez F, et al. Identification of regulatory T cell molecules associated with severity of multiple sclerosis. *Mult Scler* (2021) 27 (11):1695–705. doi: 10.1177/1352458520977045

87. Badihian S, Shaygannejad V, Soleimani P, Mirmosayyeb O, Samee Z, Manouchehri N, et al. Decreased serum levels of interleukin-35 among multiple sclerosis patients may be related to disease progression. *J Biol Regul Homeost Agents* (2018) 32(5):1249–53.

88. Kamal A, Hosny M, Abd Elwahab A, Shawki Kamal Y, Shehata HS, Hassan A. FOXP3rs3761548 gene variant and interleukin-35 serum levels as biomarkers in patients with multiple sclerosis. *Rev Neurol (Paris)* (2021) 177(6):647–54. doi: 10.1016/j.neurol.2020.07.010

89. Jafarzadeh A, Jamali M, Mahdavi R, Ebrahimi HA, Hajghani H, Khosravimashizi A, et al. Circulating levels of interleukin-35 in patients with multiple sclerosis: evaluation of the influences of FOXP3 gene polymorphism and treatment program. *J Mol Neurosci MN* (2015) 55(4):891–7. doi: 10.1007/s12031-014-0443-z

90. Zhou Y, Leng X, Luo X, Mo C, Zou Q, Liu Y, et al. Regulatory dendritic cells induced by K313 display anti-inflammatory properties and ameliorate experimental autoimmune encephalitis in mice. *Front Pharmacol* (2019) 10:1579. doi: 10.3389/fphar.2019.01579

91. Tabares-Guevara JH, Jaramillo JC, Ospina-Quintero L, Piedrahíta-Ochoa CA, García-Valencia N, Bautista-Erazo DE, et al. IL-10-Dependent amelioration of chronic inflammatory disease by microdose subcutaneous delivery of a prototypic immunoregulatory small molecule. *Front In Immunol* (2021) 12:708955. doi: 10.3389/fimmu.2021.708955

92. Takeuchi H. Midkine and multiple sclerosis. *Br J Pharmacol* (2014) 171 (4):931–5. doi: 10.1111/bph.12499

93. Meka RR, Venkatesha SH, Dudics S, Acharya B, Moudgil KD. IL-27-induced modulation of autoimmunity and its therapeutic potential. *Autoimmun Rev* (2015) 14(12):1131–41. doi: 10.1016/j.autrev.2015.08.001

94. Thomé R, Moore JN, Mari ER, Rasouli J, Hwang D, Yoshimura S, et al. Induction of peripheral tolerance in ongoing autoimmune inflammation requires interleukin 27 signaling in dendritic cells. *Front In Immunol* (2017) 8:1392. doi: 10.3389/fimmu.2017.01392

95. Fitzgerald DC, Fonseca-Kelly Z, Cullimore ML, Safabakhsh P, Saris CJ, Zhang GX, et al. Independent and interdependent immunoregulatory effects of IL-27, IFN-beta, and IL-10 in the suppression of human Th17 cells and murine experimental autoimmune encephalomyelitis. *J Immunol* (2013) 190(7):3225–34. doi: 10.4049/jimmunol.1200141

96. Gong Y, Liu YC, Ding XL, Fu Y, Cui LJ, Yan YP. Tanshinone IIA ameliorates CNS autoimmunity by promoting the differentiation of regulatory T cells. *Neurotherapeutics* (2020) 17(2):690–703. doi: 10.1007/s13311-019-00789-2

97. Ginwala R, Bhavsar R, Moore P, Bernui M, Singh N, Bearoff F, et al. Apigenin modulates dendritic cell activities and curbs inflammation *Via* RelB inhibition in the context of neuroinflammatory diseases. *J Neuroimmun Pharmacol* (2021) 16(2):403–24. doi: 10.1007/s11481-020-09933-8

98. Lukas D, Yogev N, Kel JM, Regen T, Mufazalov IA, Tang Y, et al. TGF-β inhibitor Smad7 regulates dendritic cell-induced autoimmunity. *Proc Natl Acad Sci USA* (2017) 114(8):E1480–E9. doi: 10.1073/pnas.1615065114

99. Yan Y, Zhang GX, Gran B, Fallarino F, Yu S, Li H, et al. IDO upregulates regulatory T cells *via* tryptophan catabolite and suppresses encephalitogenic T cell responses in experimental autoimmune encephalomyelitis. *J Immunol* (2010) 185 (10):5953–61. doi: 10.4049/jimmunol.1001628

100. Haller S, Duval A, Migliorini R, Stevanin M, Mack V, Acha-Orbea H. Interleukin-35-Producing CD8alpha(+) dendritic cells acquire a tolerogenic state and regulate T cell function. *Front Immunol* (2017) 8:98. doi: 10.3389/fimmu.2017.00098

101. Choi JK, Dambuza IM, He C, Yu CR, Uche AN, Mattapallil MJ, et al. IL-12p35 inhibits neuroinflammation and ameliorates autoimmune encephalomyelitis. *Front Immunol* (2017) 8:1258. doi: 10.3389/fimmu.2017.01258

102. Liu JQ, Liu Z, Zhang X, Shi Y, Talebian F, Carl JWJr., et al. Increased Th17 and regulatory T cell responses in EBV-induced gene 3-deficient mice lead to marginally enhanced development of autoimmune encephalomyelitis. *J Immunol* (2012) 188(7):3099–106. doi: 10.4049/jimmunol.1100106

103. Mittal SK, Roche PA. Suppression of antigen presentation by IL-10. *Curr Opin Immunol* (2015) 34:22–7. doi: 10.1016/j.coi.2014.12.009

104. Verhagen J, Gabrysova L, Shepard ER, Wraith DC. Ctla-4 modulates the differentiation of inducible Foxp3+ treg cells but IL-10 mediates their function in experimental autoimmune encephalomyelitis. *PloS One* (2014) 9(9):e108023. doi: 10.1371/journal.pone.0108023

105. Zhang X, Zheng P, Prestwood TR, Zhang H, Carmi Y, Tolentino LL, et al. Human regulatory dendritic cells develop from monocytes in response to signals from regulatory and helper T cells. *Front In Immunol* (2020) 11:1982. doi: 10.3389/fimmu.2020.01982

106. Yogev N, Bedke T, Kobayashi Y, Brockmann L, Lukas D, Regen T, et al. CD4(+) T-cell-derived IL-10 promotes CNS inflammation in mice by sustaining effector T cell survival. *Cell Rep* (2022) 38(13):110565. doi: 10.1016/j.celrep.2022.110565

107. Girard-Madoux MJH, Ober-Blöbaum JL, Costes LMM, Kel JM, Lindenbergh-Kortleve DJ, Brouwers-Haspels I, et al. IL-10 control of CD11c+ myeloid cells is essential to maintain immune homeostasis in the small and large intestine. *Oncotarget* (2016) 7(22):32015–30. doi: 10.18632/oncotarget.8337

108. Misra N, Bayry J, Lacroix-Desmazes S, Kazatchkine MD, Kaveri SV. Cutting edge: human CD4+CD25+ T cells restrain the maturation and antigen-

presenting function of dendritic cells. *J Immunol* (2004) 172(8):4676–80. doi: 10.4049/jimmunol.172.8.4676

109. Bain CC, Montgomery J, Scott CL, Kel JM, Girard-Madoux MJH, Martens L, et al. TGFβR signalling controls CD103CD11b dendritic cell development in the intestine. *Nat Commun* (2017) 8(1):620.doi: 10.1038/s41467-017-00658-6

110. Chen X, Hao S, Zhao Z, Liu J, Shao Q, Wang F, et al. Interleukin 35: Inhibitory regulator in monocyte-derived dendritic cell maturation and activation. *Cytokine* (2018) 108:43–52. doi: 10.1016/j.cyto.2018.03.008

111. Yu L, Yang F, Jiang L, Chen Y, Wang K, Xu F, et al. Exosomes with membrane-associated TGF-beta1 from gene-modified dendritic cells inhibit murine EAE independently of MHC restriction. *Eur J Immunol* (2013) 43 (9):2461–72. doi: 10.1002/eji.201243295

112. Ji Q, Liu J, Dong Y, Wang L, Dong K, Setiz B, et al. Exosomes derived from thymic stromal lymphopoietin-treated dendritic cells regulate T helper 17/ regulatory T cell differentiation *via* miR-21/Smad7 axis. *Exp Cell Res* (2021) 398 (1):112393. doi: 10.1016/j.yexcr.2020.112393

113. Pusic AD, Pusic KM, Kraig RP. What are exosomes and how can they be used in multiple sclerosis therapy? *Expert Rev Neurother* (2014) 14(4):353–5. doi: 10.1586/14737175.2014.890893

114. Tung SL, Boardman DA, Sen M, Letizia M, Peng Q, Cianci N, et al. Regulatory T cell-derived extracellular vesicles modify dendritic cell function. *Sci Rep* (2018) 8(1):6065. doi: 10.1038/s41598-018-24531-8

115. Azimi M, Ghabaee M, Moghadasi AN, Noorbakhsh F, Izad M. Immunomodulatory function of treg-derived exosomes is impaired in patients with relapsing-remitting multiple sclerosis. *Immunol Res* (2018) 66(4):513–20. doi: 10.1007/s12026-018-9008-5

116. Ma B, Yang JY, Song WJ, Ding R, Zhang ZC, Ji HC, et al. Combining exosomes derived from immature DCs with donor antigen-specific treg cells induces tolerance in a rat liver allograft model. *Sci Rep* (2016) 6:32971. doi: 10.1038/srep32971

117. Correale J. Immunosuppressive amino-acid catabolizing enzymes in multiple sclerosis. *Front Immunol* (2020) 11:600428. doi: 10.3389/fimmu.2020.600428

118. Grohmann U, Volpi C, Fallarino F, Bozza S, Bianchi R, Vacca C, et al. Reverse signaling through GITR ligand enables dexamethasone to activate IDO in allergy. *Nat Med* (2007) 13(5):579–86. doi: 10.1038/nm1563

119. Proietti E, Rossini S, Grohmann U, Mondanelli G. Polyamines and kynurenines at the intersection of immune modulation. *Trends Immunol* (2020) 41(11):1037–50. doi: 10.1016/j.it.2020.09.007

120. Zarzecki MS, Cattelan Souza L, Giacomeli R, Silva MRP, Prigol M, Boeira SP, et al. Involvement of indoleamine-2,3-Dioxygenase and kynurenine pathway in experimental autoimmune encephalomyelitis in mice. *Neurochem Res* (2020) 45 (12):2959–77. doi: 10.1007/s11064-020-03144-6

121. Mancuso R, Hernis A, Agostini S, Rovaris M, Caputo D, Fuchs D, et al. Indoleamine 2,3 dioxygenase (IDO) expression and activity in relapsing-remitting multiple sclerosis. *PloS One* (2015) 10(6):e0130715. doi: 10.1371/journal.pone.0130715

122. Lemos H, Mohamed E, Ou R, McCardle C, Zheng X, McGuire K, et al. Co-Treatments to boost IDO activity and inhibit production of downstream catabolites induce durable suppression of experimental autoimmune encephalomyelitis. *Front Immunol* (2020) 11:1256. doi: 10.3389/fimmu.2020.01256

123. Nekrasova I, Shirshev S. Estriol in regulation of cell-mediated immune reactions in multiple sclerosis. *J Neuroimmunol* (2020) 349:577421. doi: 10.1016/j.jneuroim.2020.577421

124. Papenfuss TL, Powell ND, McClain MA, Bedarf A, Singh A, Gienapp IE, Shawler T, Whitacre CC. Estriol generates tolerogenic dendritic cells in vivo that protect against autoimmunity. *J Immunol* (2011) 186(6):3346–55. doi: 10.4049/jimmunol.1001322. Epub 2011 Feb 11.

125. Mezrich JD, Fechner JH, Zhang X, Johnson BP, Burlingham WJ, Bradfield CA. An interaction between kynurenine and the aryl hydrocarbon receptor can generate regulatory T cells. *J Immunol* (2010) 185(6):3190–8. doi: 10.4049/jimmunol.0903670

126. Belladonna ML, Grohmann U, Guidetti P, Volpi C, Bianchi R, Fioretti MC, et al. Kynurenine pathway enzymes in dendritic cells initiate tolerogenesis in the absence of functional IDO. *J Immunol* (2006) 177(1):130–7. doi: 10.4049/jimmunol.177.1.130

127. Cauwels A, Van Lint S, Catteeuw D, Pang S, Paul F, Rogge E, et al. Targeting interferon activity to dendritic cells enables *in vivo* tolerization and protection against EAE in mice. *J Autoimmun* (2019) 97:70–6. doi: 10.1016/j.jaut.2018.10.010

128. Thome R, Casella G, Lotfi N, Ishikawa LWL, Wang Q, Ciric B, et al. Primaquine elicits Foxp3(+) regulatory T cells with a superior ability to limit CNS autoimmune inflammation. *J Autoimmun* (2020) 114:102505. doi: 10.1016/j.jaut.2020.102505

129. Farias AS, Spagnol GS, Bordeaux-Rego P, Oliveira CO, Fontana AG, de Paula RF, et al. Vitamin D3 induces IDO+ tolerogenic DCs and enhances treg, reducing the severity of EAE. *CNS Neurosci Ther* (2013) 19(4):269–77. doi: 10.1111/cns.12071

130. Kwidzinski E, Bechmann I. IDO expression in the brain: a double-edged sword. *J Mol Med (Berl)* (2007) 85(12):1351–9. doi: 10.1007/s00109-007-0229-7

131. Sundaram G, Lim CK, Brew BJ, Guillemin GJ. Kynurenine pathway modulation reverses the experimental autoimmune encephalomyelitis mouse disease progression. *J Neuroinflammation* (2020) 17(1):176. doi: 10.1186/s12974-020-01844-y

132. Liu YJ, Soumelis V, Watanabe N, Ito T, Wang YH, Malefyt Rde W, et al. TSLP: an epithelial cell cytokine that regulates T cell differentiation by conditioning dendritic cell maturation. *Annu Rev Immunol* (2007) 25:193–219. doi: 10.1146/annurev.immunol.25.022106.141718

133. Haas J, Schwarz A, Korporal-Kuhnke M, Jarius S, Wildemann B. Myeloid dendritic cells exhibit defects in activation and function in patients with multiple sclerosis. *J Neuroimmunol* (2016) 301:53–60. doi: 10.1016/j.jneuroim.2016.10.007

134. Owen DL, Sjaastad LE, Farrar MA. Regulatory T cell development in the thymus. *J Immunol* (2019) 203(8):2031–41. doi: 10.4049/jimmunol.1900662

135. Mahmud SA, Manlove LS, Schmitz HM, Xing Y, Wang Y, Owen DL, et al. Costimulation *via* the tumor-necrosis factor receptor superfamily couples TCR signal strength to the thymic differentiation of regulatory T cells. *Nat Immunol* (2014) 15(5):473–81. doi: 10.1038/ni.2849

136. Chen M, Chen G, Deng S, Liu X, Hutton GJ, Hong J. IFN-beta induces the proliferation of CD4+CD25+Foxp3+ regulatory T cells through upregulation of GITRL on dendritic cells in the treatment of multiple sclerosis. *J Neuroimmunol* (2012) 242(1-2):39–46. doi: 10.1016/j.jneuroim.2011.10.014

137. Clement M, Fornasa G, Guedj K, Ben Mkaddem S, Gaston AT, Khallou-Laschet J, et al. CD31 is a key coinhibitory receptor in the development of immunogenic dendritic cells. *Proc Natl Acad Sci U S A* (2014) 111(12):E1101–10. doi: 10.1073/pnas.1314505111

138. Zhou F, Zhang GX, Rostami A. Distinct role of IL-27 in immature and LPS-induced mature dendritic cell-mediated development of CD4(+) CD127(+) 3G11(+) regulatory T cell subset. *Front Immunol* (2018) 9:2562. doi: 10.3389/fimmu.2018.02562

139. Tang SC, Fan XH, Pan QM, Sun QS, Liu Y. Decreased expression of IL-27 and its correlation with Th1 and Th17 cells in progressive multiple sclerosis. *J Neurol Sci* (2015) 348(1-2):174–80. doi: 10.1016/j.jns.2014.11.035

140. Li J, Gran B, Zhang GX, Rostami A, Kamoun M. IL-27 subunits and its receptor (WSX-1) mRNAs are markedly up-regulated in inflammatory cells in the CNS during experimental autoimmune encephalomyelitis. *J Neurol Sci* (2005) 232 (1-2):3–9. doi: 10.1016/j.jns.2004.12.013

141. Mascanfroni ID, Yeste A, Vieira SM, Burns EJ, Patel B, Sloma I, et al. IL-27 acts on DCs to suppress the T cell response and autoimmunity by inducing expression of the immunoregulatory molecule CD39. *Nat Immunol* (2013) 14 (10):1054–63. doi: 10.1038/ni.2695

142. Do J, Kim D, Kim S, Valentin-Torres A, Dvorina N, Jang E, et al. Treg-specific IL-27Ralpha deletion uncovers a key role for IL-27 in treg function to control autoimmunity. *Proc Natl Acad Sci U S A* (2017) 114(38):10190–5. doi: 10.1073/pnas.1703100114

143. Quintana FJ, Yeste A, Mascanfroni ID. Role and therapeutic value of dendritic cells in central nervous system autoimmunity. *Cell Death Differ* (2015) 22 (2):215–24. doi: 10.1038/cdd.2014.125

144. Casella G, Rasouli J, Thome R, Descamps HC, Vattikonda A, Ishikawa L, et al. Interferon-γ/Interleukin-27 axis induces programmed death ligand 1 expression in monocyte-derived dendritic cells and restores immune tolerance in central nervous system autoimmunity. *Front Immunol* (2020) 11:576752. doi: 10.3389/fimmu.2020.576752

145. Huber M, Steinwald V, Guralnik A, Brustle A, Kleemann P, Rosenplanter C, et al. IL-27 inhibits the development of regulatory T cells *via* STAT3. *Int Immunol* (2008) 20(2):223–34. doi: 10.1093/intimm/dxm139

146. Zhu J, Liu J-Q, Liu Z, Wu L, Shi M, Zhang J, et al. Interleukin-27 gene therapy prevents the development of autoimmune encephalomyelitis but fails to attenuate established inflammation due to the expansion of CD11bGr-1 myeloid cells. *Front Immunol* (2018) 9:873. doi: 10.3389/fimmu.2018.00873

147. Raverdeau M, Christofi M, Malara A, Wilk MM, Misiak A, Kuffova L, et al. Retinoic acid-induced autoantigen-specific type 1 regulatory T cells suppress autoimmunity. *EMBO Rep* (2019) 20(5):e47121. doi: 10.15252/embr.201847121

148. Ter Braake D, Benne N, Lau CYJ, Mastrobattista E, Broere F. Retinoic acid-containing liposomes for the induction of antigen-specific regulatory T cells as a treatment for autoimmune diseases. *Pharmaceutics* (2021) 13(11):1949. doi: 10.3390/pharmaceutics13111949

149. Zhan XX, Liu Y, Yang JF, Wang GY, Mu L, Zhang TS, et al. All-trans-retinoic acid ameliorates experimental allergic encephalomyelitis by affecting

dendritic cell and monocyte development. *Immunology* (2013) 138(4):333–45. doi: 10.1111/imm.12040

150. Correale J, Farez MF. Parasite infections in multiple sclerosis modulate immune responses through a retinoic acid-dependent pathway. *J Immunol* (2013) 191(7):3827–37. doi: 10.4049/jimmunol.1301110

151. Mari ER, Rasouli J, Ciric B, Moore JN, Conejo-Garcia JR, Rajasagi N, et al. Galectin-1 is essential for the induction of MOG35-55 -based intravenous tolerance in experimental autoimmune encephalomyelitis. *Eur J Immunol* (2016) 46 (7):1783–96. doi: 10.1002/eji.201546212

152. Pardo E, Carcamo C, Uribe-San Martin R, Ciampi E, Segovia-Miranda F, Curkovic-Pena C, et al. Galectin-8 as an immunosuppressor in experimental autoimmune encephalomyelitis and a target of human early prognostic antibodies in multiple sclerosis. *PloS One* (2017) 12(6):e0177472. doi: 10.1371/journal.pone.0177472

153. Waschbisch A, Sanderson N, Krumbholz M, Vlad G, Theil D, Schwab S, et al. Interferon beta and vitamin d synergize to induce immunoregulatory receptors on peripheral blood monocytes of multiple sclerosis patients. *PloS One* (2014) 9(12):e115488. doi: 10.1371/journal.pone.0115488

154. Abe K, Nguyen KP, Fine SD, Mo J-H, Shen C, Shenouda S, et al. Conventional dendritic cells regulate the outcome of colonic inflammation independently of T cells. *Proc Natl Acad Sci USA* (2007) 104(43):17022–7. doi: 10.1073/pnas.0708469104

155. Zinser E, Naumann R, Wild AB, Michalski J, Deinzer A, Stich L, et al. Endogenous expression of the human CD83 attenuates EAE symptoms in humanized transgenic mice and increases the activity of regulatory T cells. *Front Immunol* (2019) 10:1442. doi: 10.3389/fimmu.2019.01442

156. Agundez JA, Garcia-Martin E, Martinez C, Benito-Leon J, Millan-Pascual J, Diaz-Sanchez M, et al. Heme oxygenase-1 and 2 common genetic variants and risk for multiple sclerosis. *Sci Rep* (2016) 6:20830. doi: 10.1038/srep20830

157. Fagone P, Patti F, Mangano K, Mammana S, Coco M, Touil-Boukoffa C, et al. Heme oxygenase-1 expression in peripheral blood mononuclear cells correlates with disease activity in multiple sclerosis. *J Neuroimmunol* (2013) 261 (1-2):82–6. doi: 10.1016/j.jneuroim.2013.04.013

158. Chora AA, Fontoura P, Cunha A, Pais TF, Cardoso S, Ho PP, et al. Heme oxygenase-1 and carbon monoxide suppress autoimmune neuroinflammation. *J Clin Invest* (2007) 117(2):438–47. doi: 10.1172/JCI28844

159. Wong TH, Chen HA, Gau RJ, Yen JH, Suen JL. Heme oxygenase-1-Expressing dendritic cells promote Foxp3+ regulatory T cell differentiation and induce less severe airway inflammation in murine models. *PloS One* (2016) 11(12): e0168919. doi: 10.1371/journal.pone.0168919

160. Idoyaga J, Fiorese C, Zbytnuik L, Lubkin A, Miller J, Malissen B, et al. Specialized role of migratory dendritic cells in peripheral tolerance induction. *J Clin Invest* (2013) 123(2):844–54. doi: 10.1172/JCI65260

161. Jones A, Bourque J, Kuehm L, Opejin A, Teague RM, Gross C, et al. Immunomodulatory functions of BTLA and HVEM govern induction of extrathymic regulatory T cells and tolerance by dendritic cells. *Immunity* (2016) 45(5):1066–77. doi: 10.1016/j.immuni.2016.10.008

162. Gregori S, Tomasoni D, Pacciani V, Scirpoli M, Battaglia M, Magnani CF, et al. Differentiation of type 1 T regulatory cells (Tr1) by tolerogenic DC-10 requires the IL-10-dependent ILT4/HLA-G pathway. *Blood* (2010) 116(6):935–44. doi: 10.1182/blood-2009-07-234872

163. Comi M, Amodio G, Gregori S. Interleukin-10-Producing DC-10 is a unique tool to promote tolerance antigen-specific T regulatory type 1 cells. *Front In Immunol* (2018) 9:682. doi: 10.3389/fimmu.2018.00682

164. Jiang A, Bloom O, Ono S, Cui W, Unternaehrer J, Jiang S, et al. Disruption of e-Cadherin-Mediated adhesion induces a functionally distinct pathway of dendritic cell maturation. *Immunity* (2007) 27(4):610–24. doi: 10.1016/j.immuni.2007.08.015

165. Mellman I, Clausen BE. Immunology. beta-catenin balances immunity. *Science* (2010) 329(5993):767–9. doi: 10.1126/science.1194185

166. Willekens B, Presas-Rodríguez S, Mansilla MJ, Derdelinckx J, Lee W-P, Nijs G, et al. Tolerogenic dendritic cell-based treatment for multiple sclerosis (MS): a harmonised study protocol for two phase I clinical trials comparing intradermal and intranodal cell administration. *BMJ Open* (2019) 9(9):e030309. doi: 10.1136/bmjopen-2019-030309

167. Tabansky I, Keskin DB, Watts D, Petzold C, Funaro M, Sands W, et al. Targeting DEC-205(-)DCIR2(+) dendritic cells promotes immunological tolerance in proteolipid protein-induced experimental autoimmune encephalomyelitis. *Mol Med* (2018) 24(1):17. doi: 10.1186/s10020-018-0017-6

168. Dudziak D, Kamphorst AO, Heidkamp GF, Buchholz VR, Trumpfheller C, Yamazaki S, et al. Differential antigen processing by dendritic cell subsets in vivo. *Science* (2007) 315(5808):107–11. doi: 10.1126/science.1136080

169. Stern JNH, Keskin DB, Kato Z, Waldner H, Schallenberg S, Anderson A, et al. Promoting tolerance to proteolipid protein-induced experimental autoimmune encephalomyelitis through targeting dendritic cells. *Proc Natl Acad Sci USA* (2010) 107(40):17280–5. doi: 10.1073/pnas.1010263107

170. Zhou Y, Leng X, Luo S, Su Z, Luo X, Guo H, et al. Tolerogenic dendritic cells generated with tofacitinib ameliorate experimental autoimmune encephalomyelitis through modulation of Th17/Treg balance. *J Immunol Res* (2016) 2016:5021537. doi: 10.1155/2016/5021537

171. Chen Z, Yang D, Peng X, Lin J, Su Z, Li J, et al. Beneficial effect of atorvastatin-modified dendritic cells pulsed with myelin oligodendrocyte glycoprotein autoantigen on experimental autoimmune encephalomyelitis. *Neuroreport* (2018) 29(4):317–27. doi: 10.1097/WNR.0000000000000962

frontiers | Frontiers in Immunology

TYPE Review
PUBLISHED 26 September 2022
DOI 10.3389/fimmu.2022.988130

OPEN ACCESS

EDITED BY
Julia Y. Wang,
Curandis Inc, United States

REVIEWED BY
Ming-Qing Li,
Fudan University, China
Surendra Sharma,
Women & Infants Hospital of Rhode Island,
United States

*CORRESPONDENCE
Jie Zheng
471406854@qq.com
Aihua Liao
aihua_liao@sina.com

SPECIALTY SECTION
This article was submitted to Immunological Tolerance and Regulation, a section of the journal Frontiers in Immunology

RECEIVED 06 July 2022
ACCEPTED 09 September 2022
PUBLISHED 26 September 2022

CITATION
Liu H, Zheng J and Liao A (2022) The regulation and potential roles of m6A modifications in early embryonic development and immune tolerance at the maternal-fetal interface. *Front. Immunol.* 13:988130. doi: 10.3389/fimmu.2022.988130

The regulation and potential roles of m6A modifications in early embryonic development and immune tolerance at the maternal-fetal interface

Hong Liu[1], Jie Zheng[1]* and Aihua Liao[2]*

[1]Department of Reproduction, Maternal and Child Health Hospital of Hubei Province, Affiliated in Tongji Medical College, Huazhong University of Science and Technology, Wuhan, China, [2]Institute of Reproductive Health, Center for Reproductive Medicine, Tongji Medical College, Huazhong University of Science and Technology, Wuhan, China

The immune microenvironment at the maternal-fetal interface was determined by the crosstalk between the trophoblast and maternal-derived cells, which dynamically changed during the whole gestation. Trophoblasts act as innate immune cells and dialogue with maternal-derived cells to ensure early embryonic development, depending on the local immune microenvironment. Therefore, dysfunctions in trophoblasts and maternal decidual cells contribute to pregnancy complications, especially recurrent pregnancy loss in early pregnancy. Since many unknown regulatory factors still affect the complex immune status, exploring new potential aspects that could influence early pregnancy is essential. RNA methylation plays an important role in contributing to the transcriptional regulation of various cells. Sufficient studies have shown the crucial roles of N6-methyladenosine (m6A)- and m6A-associated-regulators in embryogenesis during implantation. They are also essential in regulating innate and adaptive immune cells and the immune response and shaping the local and systemic immune microenvironment. However, the function of m6A modifications at the maternal-fetal interface still lacks wide research. This review highlights the critical functions of m6A in early embryonic development, summarizes the reported research on m6A in regulating immune cells and tumor immune microenvironment, and identifies the potential value of m6A modifications in shaping trophoblasts, decidual immune cells, and the microenvironment at the maternal-fetal interface. The m6A modifications are more likely to contribute to embryogenesis, placentation and shape the immune microenvironment at the maternal-fetal interface. Uncovering these crucial regulatory mechanisms could provide novel therapeutic targets for RNA methylation in early pregnancy.

KEYWORDS

m6A methylation, embryo development, immune tolerance, maternal-fetal interface, early pregnancy

Introduction

Most mammalian genomes undergo RNA transcription, and many RNA transcripts can never be translated into proteins (1), which may lead to functional defects. RNA is not only an essential intermediate in the flux from DNA to proteins but also a regulatory molecule for fundamental cellular processes, the dysfunction of which contributes to important pathological processes (2). The coding and noncoding transcriptomes are widely and dynamically regulated by chemical modification, which adds new modifications of complexity and functionality to the emerging roles of RNAs in physiological and pathological conditions (3). Covalent modifications sense the changing environment directly and rapidly without changing the DNA and RNA sequences (4). In contrast to the epigenetic modifications on DNA and histones that work at the transcriptional level, RNA methylation has a notable effect on gene regulation at the posttranscriptional level (5). RNA modifications affect transcripts by altering the charge, base-pair potential, secondary structure and RNA–protein interactions, which, in turn, regulates gene expression *via* RNA processing, localization, translation and degradation (3). N6-methyladenosine (m6A) is the most abundant internal mRNA modification. Identifying of the proteins that mediate m6A modifications has elucidated the roles of mRNA modifications in nearly every aspect of the mRNA life cycle, as well as various cellular, developmental, and disease processes (3). In mammals, approximately 0.1%- 0.6% of adenines undergo m6A modification, with an average of 3-5 methylated sites in each mRNA. Remarkably, m6A modifications can be deposited onto transcripts in tissue- and cell-type-specific- manners (6). The m6A modifications commonly occur in yeast, plants, flies, bacteria, humans and other mammals, which implicates its multiple functions in RNA, including precursor mRNA (pre-mRNA) splicing, mRNA translation, stability, structure, export and decay, implying an association with several cellular processes, such as cell differentiation and reprogramming, further contributing to various human diseases (reviewed in (7)). For m6A detection, methods, including analytical chemistry, high-throughput sequencing, m6A-CLIP and miCLIP, have emerged to determine the specific methylation sites and the modification fractions at these sites to promote biological studies of RNA modifications (3, 8–11), which provided the available ways to study the roles of m6A modification proteins in physical and pathological processes.

Similar to DNA methylation, the deposition and removal of mRNA methylation also depend on a multiunit methyltransferase complex that was initially documented in 1994 (7). mRNA methylation is governed by three types of proteins, namely, methyltransferases as "writers", demethylases as "erasers", and specific m6A-binding proteins (YTHDF1-3) as "readers" (12). The deposition of m6A methylation is catalyzed by multicomponent methyltransferases, mainly methyltransferase-like 3 (METTL3), METTL14, Wilms' tumor 1-associated protein (WTAP), RNA-binding motif proteins 15 (RBM15s), virlike m6A methyltransferase associated (VIRMA/KIAA1429), zinc finger CCCH-Type containing 13 (ZC3H13) and METTL16 (13–19). METTL3 is the most important component of the m6A methyltransferase complex (MTC) and highly conserved in eukaryotes from yeast to humans (20); METTL3 forms a stable heterodimer core complex regulated by WTAP and catalyzes the transfer of meth1 groups (13, 21). Similar to WTAP, RBM15s have no catalytic function but bind to METTL3 and WTAP to guide these two proteins to specific RNA sites for m6A modification. KIAA1429-mediated m6A methylation of mRNAs takes place near the 3'-UTR and the stop codon (22). m6A modification occurs when METTL3 and METTL14 are recruited into the nucleus (14). Only METTL3 has methyltransferase activity in the MTC. METTL16 encodes S-adenosylmethionine (SAM) synthase and is expressed in most cells. However, METTL16-mediated m6A sites were located in introns or intron–exon boundaries, which is different from the common m6A sites in UTRs (19). The m6A demethylases as "erasers" make the m6A methylation dynamic and reversible, which could be passively removed from the transcriptome *via* degradation of the modified RNA or active demethylation by the m6A demethylases fat mass and obesity-associated (FTO) or a-ketoglutarate-dependent dioxygenase alkB homolog 5 (ALKBH5), both belonging to the AlkB family of dioxygenases known to demethylate N-methylated nucleic acids (23, 24). FTO was the first demethylase discovered in 2011 (23). The ALKBH5 catalytic domain can demethylate m6A-containing single-stranded RNA (ssRNA) and single-stranded DNA (ssDNA) (25).

The discovery of reader proteins has made great progress in elucidating the impact of m6A methylation in mammalian cells. Different 'readers' with different cellular localizations influence almost all aspects of RNA metabolism, such as YT521-B homology domain family proteins (YTHDFs), insulin-like growth factor 2 mRNA-binding proteins (IGF2BPs), eukaryotic translation initiation factor 3 (EIF3) and heterogeneous nuclear ribonucleoproteins (HNRNPs) (26–29). Proteins with YTH domains located in the cytoplasm (YTHDF1, YTHDF2 and YTHDF3) and nuclei (YTHDC1 and YTHDC2) directly recognize m6A marks (27, 30), which promote the degradation and translation of m6A-modified RNA. In contrast to YTHDFs, IGF2BPs promote the stability and storage of their target mRNAs in a m6A-dependent manner under normal stress conditions and therefore affect gene expression output (28). EIF3 directly binds a single 5' UTR m6A and recruits the 43S complex to initiate translation in a cap-dependent manner (26). Numerous studies have shown that m6A modifications play essential roles in multiple biological

and pathological processes: hematopoietic development, central nervous and system development, the adaptive and innate immune system, carcinogenesis and the tumor microenvironment, as well as gametogenesis and early embryo development, the dysfunction of which generally results in various diseases by abnormal m6A modifications of the target genes (31) (Figure 1). Currently, with the development of assisted reproductive technology (ART), which helps to exclude abnormalities in the embryo, there remains the occurrence of recurrent pregnancy loss (RPL) in child-bearing women (32). Embryo implantation into the endometrium successfully relies on strict and coordinated regulation of trophoblasts derived from the fetus and decidual stromal cells and immune cells derived from the maternal sides (33). Crosstalk could be regulated by molecules associated with implantation, including hormones, signaling molecules, transcription factors and cytokines (34). However, the occurrence of RPL remains high, and more efforts should be made to discover the mystery of embryo implantation. Emerging studies emphasize the essential roles of m6A modifications in embryo implantation, while their roles in trophoblasts and immune tolerance at the maternal-fetal interface are worthy of further investigation.

Successful blastocyst implantation was first established by normal embryo development after fertilization. Its further development relies on the dynamically coordinated balance between the fetal-derived invading trophoblasts and the receptive maternal decidua (35). Once implantation is initiated, the trophoblasts, originating from the outer layer of the blastocyst, will differentiate into invasive extravillous trophoblasts (EVTs) to attach and invade the maternal decidua and therefore promote placentation (36), making the first contact with the maternal immune system. The placenta not only mediates the hormonal, nutritional and oxygen support to the fetus but also plays an essential immunoregulatory role at the maternal-fetal interface (37). Blastocysts that take paternal antigens as semiallogeneic to the maternal side can be recognized and accepted by the immunosuppressive maternal immune system (38). After normal implantation, the implantation sites are infiltrated with diverse immune cells, which are mainly characterized by an anti-inflammatory Th2-type immune microenvironment (39). Previously, embryo quality was shown to contribute to adverse pregnancy complications. ART tools make the selection of high-quality embryos available; however, implantation rates and successful pregnancy with ART are still relatively low. This indicated that uterine receptivity might also play a crucial role in the establishment of normal pregnancy (40). Diverse mechanisms, including cytokine/chemokine and hormonal signaling as well as DNA modifications, contribute to the pathology of pregnancy complications (40), which is attributed to the abnormal gene expression of cytokines/chemokines and abnormal signaling in a specific time and space during placentation and further fetal development.

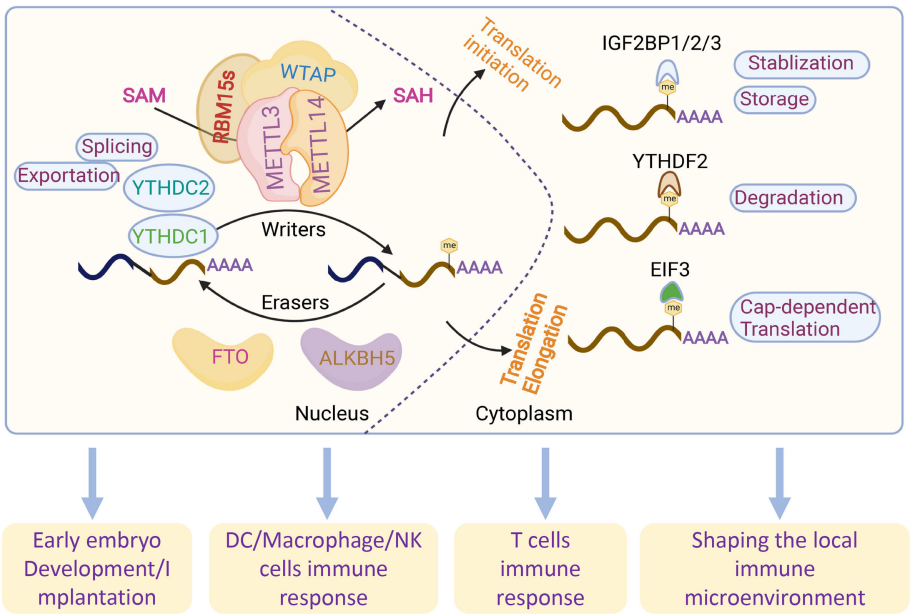

FIGURE 1
Overview of the reversible m6A RNA modifications and related functions. m6A modifications are regulated by m6A writers (METTL3, METTL14, RBM15s and WATP) and readers (FTO and ALKBH5). m6A methylation is recognized by different readers (YTHDC1-2, YTHDF1-3 and EIF3) by regulating RNA splicing, exportation, translation, degradation, stabilization and storage.

Early mammalian embryos are capable of strong pluripotent stemness, which could be reprogrammed by epigenetic modifications. m6A modification is highly conserved from yeast to mammals and can regulate gene expression output, determine stem cell fate and cell differentiation, and further shape the local microenvironment. Recent studies have shown that m6A modifications are associated with animal reproductive processes, including gametogenesis, maternal-zygote transition (MZT) and early embryonic development (41–45). In addition, m6A modifications also play an essential roles in fine-tuning the immune response, including innate and adaptive immune responses and immune system development (8). Here, we reviewed the potential roles and novel insights of m6A methylation in embryo development and immune tolerance during early pregnancy during maternal-fetal tolerance.

m6A functions in preimplantation embryogenesis

After fertilization, the newly generated zygote sustains a transcriptionally quiescent state and initiates early maternally programmed embryogenesis, following zygote genome activation (ZGA) with a clearance of maternal stores (RNA and DNA), which is termed the maternal-to-zygote transition (MZT) (46). The most important biological process, early embryonic development, is generally determined by a programmed transition into a totipotent and pluripotent embryonic state, followed by cell fate decisions and lineage-specific differentiation (47). Early embryogenesis relies on maternally inherited mRNA. Recently, emerging studies have reported that the epitranscriptomic mark m6A and its cofactors play critical roles in ensuring gene expression in an appropriate time and space in both preimplantation and postimplantation embryonic development (46, 47). In the murine preimplantation embryo, germinal vesicle (GV) oocyte-specific knockdown (KD) of *Mettl3* inhibited oocyte maturation and the MZT by disrupting maternal mRNA degradation (41). Additionally, *Mettl3* is mainly located in the intracisternal A particle (IAP)-type family of endogenous retroviruses. *Mettl3* knockout (KO) in mice blocked the integrity of multiple heterochromatin marks on METTL3-targeted IAPs. Mechanistically, the RNA transcripts in METTL3-bound IAPs are related to m6A-methylated chromatin, which is regulated by the m6A reader YTHDC1. This interaction, in turn, promotes the association of METTL3 with chromatin. Furthermore, METTL3 also interacts with the H3K9me3 methyltransferase SETDB1 and its cofactor TRIM28 (48). These results suggest an important role of METTL3-targeted IAP integrity in mouse embryonic stem cells. Downregulation of the m6A reader *HnRNPA2/B1*, which is regulated by *Mettl3*, blocked mouse embryonic development from the 4-cell stage by altering global gene expression involving the transcription, translation, cell cycle, embryonic stem cell differentiation, and RNA methylation pathways in *HnRNPA2/B1* KD blastocysts. Similar results were found in *Mettl3* KD blastocysts, which also showed that HnRNPA2/B1 is regulated in a Mettl3-dependent manner (49). In Mettl14 arginine 255 (R255me) mutant mice, embryonic stem cells (mESCs) led to decreased global mRNA m6A levels and preferentially affected endoderm differentiation in mESCs. Mettl14 R255me markedly enhances the interaction of Mettl3/Mettl14 with WTAP and binds to the substrate RNA. Moreover, protein arginine N-methyltransferase 1 (PRMT1) regulates Mettl14 at R255, which highlights the communication between protein and RNA methylation in regulating gene expression (50). Knockdown of Mettl3 and Mettl14 in mESCs led to similar phenotypes, with a lack of m6A RNA methylation and loss of self-renewal capability (27). WTAP, as part of the MTC, is essential for the blastocyst rate and global m6A levels of porcine early embryonic development, indicating the indispensable role of WTAP in porcine embryo development (51). An mRNA interactome capture study in zebrafish embryos identified the dramatic translocation of Hnrnpa1 accompanied by the movement from cytoplasmic to nuclear RNA targets and other pre-mRNA splicing factors to the nucleus in a transcription-dependent manner, indicating that Hnrnpa1 RNA-binding activities regulated RNA metabolism during early embryo development in a spatial and temporal manner (52). Accurately, one-third of zebrafish maternal mRNA is m6A modified, and m6A-binding protein promotes the clearance of maternal mRNAs, the removal of which slows down the decay of m6A-modified maternal mRNA and impairs ZGA, therefore blocking the initiation of the timely MZT and cell cycle and contributing to the overall delay of larval life (43). Additionally, the m6A reader protein YTHDF1-3, as a maternal mRNA-binding partner, was highly expressed in the zebrafish MZT process (3), suggesting that YTHDF protein-mediated m6A modification may regulate the MZT process. m6A-methylated maternal mRNA degradation impedes YTHDF2-deficient zebrafish embryos and therefore delays the timely MZT and leads to developmental interruption during the larval period (43). In addition, it was also reported that the m6A reader YTHDF2 is essential for oocyte maturation and embryo development (43, 53). The oocyte-specific deletion of YTHDF2 in mice also impeded the degradation of maternal mRNAs, thereby delaying the ZGA process. These results suggest that YTHDF2 plays important roles in the transcriptome transition by mediating m6A-dependent mRNA degradation. Similar to YTHDF2, the oocyte-specific deletion of VIRMA contributes to female-specific infertility in mice, which inhibits oocyte maturation by regulating pre-mRNA alternative splicing (54). In human ESCs, the ALKBH5 catalytic domain is fused to targeted RNA m6A erasure (TRME) and therefore

demethylates the target m6A sites and increases mRNA stability with limited off-target effects (55). However, the role of VIRMA in early embryonic development remains unknown and requires further investigation.

In contrast to YTHDF2 that promotes mRNA decay, IGF2BPs could work as a new class of cytoplasmic m6A readers that regulate the stability and storage of mRNAs (28). Downregulation of *Igf2bp1* in zebrafish parthenogenetic activation (PA) embryos decreased the cleavage and blastula rates, which induced cell apoptosis and could be rescued by augmenting the miR-670 inhibitor (56). Maternal deletion of *Igf2bp2* (also called *IMP2*) results in murine early embryo development arrest at the 2-cell stage *in vitro* by decreasing the expression of *Ccar1* and *Rps14*, both of which are essential for early embryonic developmental competence (57). However, the role of IGF2BP2 in regulating mRNA stability and degradation in ZGA as a m6A reader still needs to be clarified. Deletion of maternal *Igf2bp3* degraded maternal mRNAs prior to MZT and resulted in severe developmental defects of abnormal cytoskeleton organization and cell division and destabilized the Igf2bp3-bound mRNAs. Interestingly, *Igf2bp3* overexpression in wild-type embryos also causes a developmental delay. These results indicate the important functions of Igf2bp3 in regulating early zebrafish embryogenesis by binding and stabilizing maternal mRNAs (58). The above findings suggested that the function of IGF2BP3 is different from that of YTHDF2, but both are indispensable for early embryogenesis in various species (Figure 2).

m6A functions in postimplantation embryogenesis

After implantation, the blastocyst attaches to the uterus and initiates differentiation and development. The ectoderm of the blastocyst is the trophoblast stem cells, which differentiate into multiple trophoblast subsets and therefore promote placentation. The inner cell mass transitions from naïve state pluripotency to primed state pluripotency and is required for organogenesis and individual formation (47). A number of studies have reported that m6A determines the fate of embryonic stem cells (ESCs), losing m6A modifications causes pluripotent stem cells to display a state of hyperpluripotency and cannot differentiate into lineages, thus contributing to embryonic lethality (55, 59). Mechanistically, METTL3$^{-/-}$ ESCs exhibited poor differentiation potential that prevented KO teratomas from forming the three germ layers. The abnormal expression of NANOG from E5.5 to E7.5 in epiblasts led to embryonic lethality. *Mettl3* and *Mettl14* KO mice both exhibited embryonic lethality at E6.5 (59, 60). These findings indicate the important role of MELLT3/METTL14 in early embryogenesis. Another m6A writer, METTL16, regulates human MAT2A, and increasing METTL16 binding to the methionine

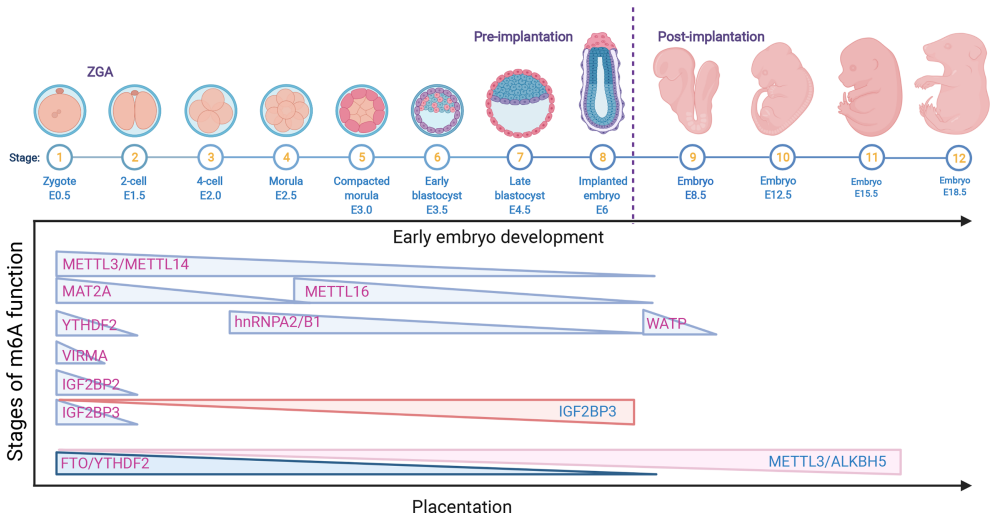

FIGURE 2
The role of m6A RNA modifications in early embryo development and placentation. The downregulation of the m6A RNA modifications METTL3, METTL14, METTL16, MAT2A, VIRMA, WATP, YTHDF2, hnRNPA2/B1 and IGF2BP2/3 is related to early embryo development; however, the upregulation of IGF2BP3 also causes a delay in late development. In addition, the decrease in FTO and YTHDF2 is associated with early placental dysfunction, while the overexpression of METTL3/ALKBH5 is related to late abnormal placentation.

adenosyltransferase 2A (MAT2A) 3'UTR could promote efficient splicing in a hairpin (hp1) m6A-dependent manner (19). However, the m6A modifications on MAT2A were recognized by YTHDC1 for mRNA degradation (61). Although normal morphology and genotyping ratios were observed in E2.5 and E3.5 blastocysts from WT and *Mettl16* KO mice, only 1.9% *Mettl16* KO embryos at E6.5 could be found in the *Mettl16*$^{-/-}$ mouse model, indicating that METTL16 deletion led to embryo lethality around implantation (42). Interestingly, the most decreased gene in E2.5 KO embryos was *Mat2a*, suggesting that *Mettl16* and *Mat2a* are essential for early embryonic development. Apart from METTLs, another m6A writer, WATP-deficient ESCs, failed to differentiate into endoderm and mesoderm. In addition, deficiency of WATP in embryos results in abnormal egg cylinders at the gastrulation stage and causes embryonic lethality at E10.5 in mice (62). However, the relevant mechanisms need further exploration. YTHDC1, as the only nuclear reader, regulates the alternative polyadenylation (APA), AS and nuclear export of m6A-modified mRNAs in mouse oocytes. In addition, YTHDC1 is essential for early embryonic development (63). These results indicated that YTHDC1 is not only critical for gametogenesis but also important for the viability of early embryo development. Interestingly, no colonies were found in hnRNPA2/B1 mouse KO blastocysts. Nonetheless, knockdown of hnRNPA2/B1 impeded embryonic development after the 4-cell stage and blocked further development, and a similar phenotype was observed in Mettl3 KD embryos. Furthermore, Mettl3 KD blastocysts showed enhanced mislocalization of hnRNPA2/B1 and reduced m6A methylation, which suggested that hnRNPA2/B1 is important for early embryogenesis by Mettl3-dependent m6A RNA methylation (49). Deficiency of m6A methylation writers, easers and readers generally leads to embryo lethality postimplantation. However, these mutants focus on the embryo itself and not the placenta. The results of deciphering the developmental disorders programmed for placental phenotypes in embryonic lethal and subviable mouse knockout lines showed that 68% of KO lines mainly exhibited placental dysmorphologies (64). Early embryo lethality is closely associated with placental malformation, which strongly correlates with abnormal brain, heart and vascular development (64). The critical role of the placenta in pregnancy was determined by the trophoblast lineage. In preeclampsia (PE), METTL3 and m6A methylation were upregulated in the placental trophoblast (65). The maturation of miR-497/195-5P mediated by METTL3 impeded trophoblast migration and invasion by targeting WWP1 in PE patients (66). In addition, the RNA demethylase FTO and HLA-G were significantly decreased in the trophoblasts of spontaneous abortion (SA) patients, and the mRNA expression of *VEGFA, VEGFR* and *MMP2* bound to YTHDF2 also decreased in SA patients, which indicated that FTO in the chorionic villi promotes immune tolerance and angiogenesis at the maternal-fetal interface due to aberrant methylation and oxidative stress and therefore leads to the occurrence of SA (67). Downregulation of ALKBH5 demethylase KDM3B mediated activated leukocyte cell adhesion molecule (ALCAM) by increasing PPARG mRNA m6A modification and activating the Wnt/β-catenin pathway, in turn relieving PE progression (68). In addition, Xiaocui Li et al. reported that global mRNA m6A methylation was significantly decreased in villi from RPL patients without affecting ALKBH5 expression. Besides, ALKBH5 KD in villous explants enhanced trophoblast invasion by upregulating the half-life of cysteine-rich angiogenic inducer 61 (CYR61) mRNA (69) (Figure 2). Although some m6A modifications are reported to be associated with the differentiation and function of trophoblasts, more explorations are needed to elucidate the other m6A enzymes in the biological and immunoregulatory functions of trophoblasts and provide broad RNA epigenetic regulatory patterns in physical and pathological pregnancies.

m6A functions in the innate immune response

Innate immunity provides the first line of defense against infections in a nonspecific manner. The innate immune cells at the maternal-fetal interface consist of macrophages (MΦs), natural killer (NK) cells and dendritic cells (DCs), which can sense invading pathogens and exogenous RNAs rapidly and thus respond in a timely manner to foreign pathogens (70). Innate immune cells comprise large populations of immune cells at the maternal-fetal interface (35). DC cells are the main antigen presentation cells (APCs) that can activate T cells and are equipped with the capacity to effectively take up, process and present antigens on the cell surface (71). Emerging studies have shown that m6A modification and m6A-associated proteins mediate innate immunity by regulating the recognition and responses to foreign pathogens, unmodified tRNAs, exogenous RNAs and aberrant endogenous RNAs. The recognition of foreign pathogens depends on several pattern-recognition receptors, such as plasma membrane receptors (Toll-like receptors, TLRs) and cytosolic sensors (RIG-I-like receptors, RIG-I and NLR proteins) (72). Kariko K et al. in 2005 reported that m6A modification decreased TLR3, TLR7, or TLR8 activation in monocyte-derived DCs (MDDCs), which was the first time that the regulatory effect on the process of RNA recognition was presented (73). Once RNA recognition occurs, the innate immune response immediately initiates and releases multiple cytokines, such as type I interferons (IFNs) and interferon-stimulated genes (ISGs) (74, 75). METTL14 depletion inhibited viral reproduction and promoted dsDNA- or HCMV-induced IFNB1 mRNA accumulation, while

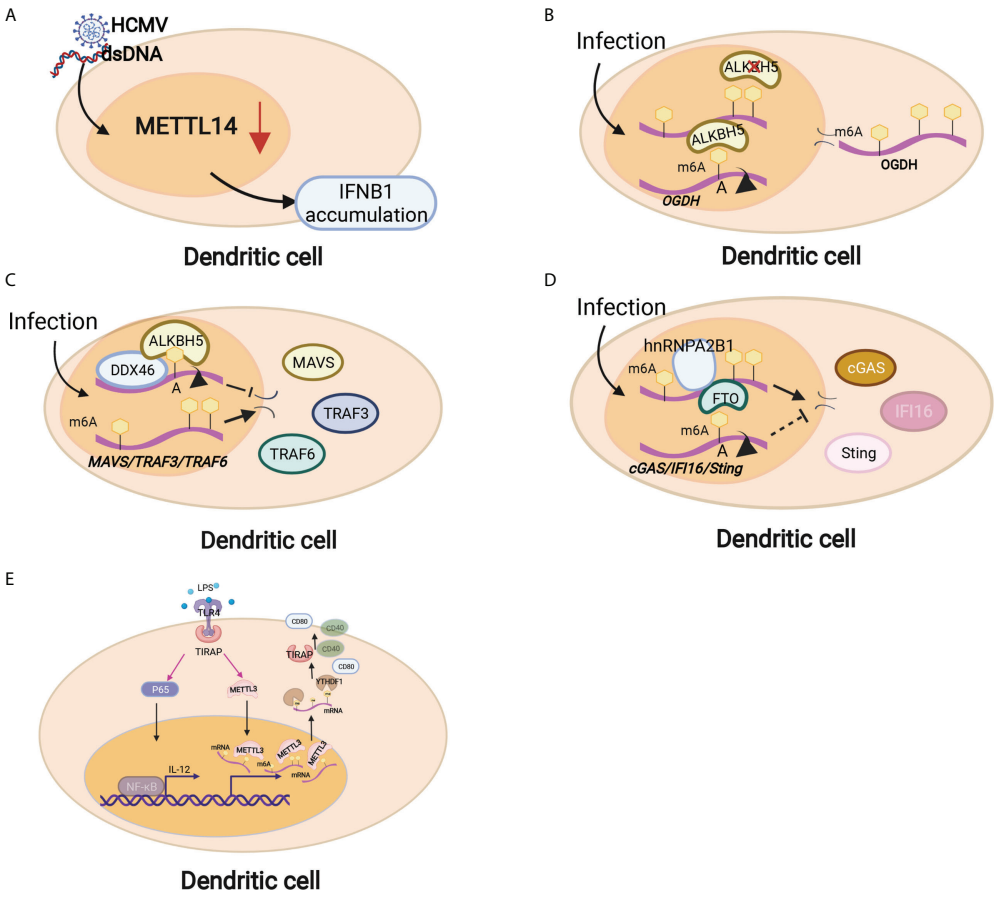

FIGURE 3
Dendritic cells are regulated by m6A modifications through different mechanisms. **(A)** METTL14 depletion inhibited viral reproduction and promoted dsDNA- or HCMV-induced IFNB1 mRNA accumulation. **(B)** Downregulation of ALBKH5 in DCs increased m6A modifications on OGDH mRNA and reduced its mRNA stability and protein expression, thereby inhibiting viral replication. **(C)** The RNA helicase DDX46 demethylates the antiviral proteins MAVS, TRAF3 and TRAF6 by recruiting ALBKH5. **(D)** hnRNPA2B1 recognizes viral DNA and facilitates m6A modification nucleocytoplasmic trafficking of CGAS, IFI16, and STING mRNAs by preventing FTO-mediated demethylation. **(E)** Mettl3-specific depletion in DCs results in delayed maturation in response to lipopolysaccharide (LPS) and impaired phenotypic and functional maturation of DCs. Mechanistically, the expression of the costimulatory molecules CD40 and CD80, the TLR4 signaling adaptor Tirap and the cytokine IL-12 decreased with a low capacity to stimulate T-cell responses.

ALKBH5 depletion exhibited the opposite effect (75)(Figure 3A). The RNA helicase DDX46 demethylates the antiviral proteins MAVS, TRAF3 and TRAF6 by recruiting ALBKH5 (76) (Figure 3C). hnRNPA2B1 recognizes viral DNA and facilitates the m6A modification nucleocytoplasmic trafficking of CGAS, IFI16, and STING mRNAs by preventing FTO-mediated demethylation, thereby amplifying IFN production and enhancing the antiviral effect on HSV-1 infection (77) (Figure 3D). In addition, m6A modification also mediates the metabolic program to promote host immunity against viral infection. Downregulation of ALBKH5 increases the m6A modifications on the mRNA of a-ketoglutarate dehydrogenase (OGDH) and reduces its mRNA stability and protein expression, which inhibits viral replication (Figure 3B). These studies suggest that m6A modifications exert a contributory effect on antiviral responses by targeting antiviral-specific genes and proteins and reprogramming the metabolic state of the host. In addition, mounting evidence has shown that m6A methylation plays a critical role in DC activation and function. Mettl3-specific depletion in DCs results in delayed maturation in response to lipopolysaccharide (LPS) and impaired phenotypic and functional maturation of DCs. Mechanistically, the expression of the costimulatory molecules CD40 and CD80, the TLR4 signaling adaptor Tirap and the cytokine IL-12 decreased with a low capacity to stimulate T-cell responses (78) (Figure 3E). Loss of classical DCs enhanced the cross-presentation of tumor antigen and cross-priming of CD8+ T cells *in vivo*. Binding of YTHDF1 to transcripts of lysosomal proteases increases the translation of lysosomal cathepsins in DCs. Moreover, blockade of the PD-L1 checkpoint is enhanced

in Ythdf1$^{-/-}$ mice, implicating YTHDF1 as a therapeutic target in cancer immunotherapy (79). These findings indicate that m6A methylation and its related proteins play major roles in the maturation and activation of DCs and promote the initiation of the adaptive immune response through antigen cross-presentation.

Macrophages serve as another main component of innate immune cells. RNA binding protein-focused CRISPR screening results showed that m6A writers were the top candidate genes in regulating LPS-activated macrophages. Mettl3 ablation macrophages produced little TNF-α with LPS stimulation (80) (Figure 4A). However, Mettl3 downregulation in macrophages significantly increased the proinflammatory cytokines TNF-α, IL-6 and NO. Mechanically, Mettl3 KO in macrophages promoted the expression and stability of NOD1 and RIPK2, which were mediated by YTHDF1 and YTHDF2, respectively (81) (Figure 4A). Additionally, Mettl3 and YTHDF2 cooperatively regulate PGC-1α mRNA degradation in oxidized low-density lipoprotein (ox-LDL)-induced monocytes (82) (Figure 4A). Mettl3 promotes the ox-LDL-induced inflammatory response in macrophages by modifying STAT1 mRNA, thereby polarizing macrophages to the M1 phenotype (83). The deletion of Mettl3 in myeloid cells promotes tumor growth and metastasis *in vivo*. Mechanistically, Mettl3-deficient mice showed increased M1/M2-like tumor-associated macrophage and regulatory T (Treg) cell infiltration in the local tumor microenvironment due to the impairment of YTHDF1-mediated SPRED2, which enhances the activation of nuclear factor κB (NF-κB) and STAT3 *via* the ERK pathway and consequently leads to tumor growth and metastasis. Furthermore, PD-1 checkpoint blockade was partially decreased in Mettl3-deficient mice, indicating the important role of Mettl3 in tumor immunotherapy (84). Additionally, myeloid lineage-restricted deletion of Mettl3 protects mice from age-related and diet-induced development of innate immunity-driven nonalcoholic fatty liver disease (NAFLD)

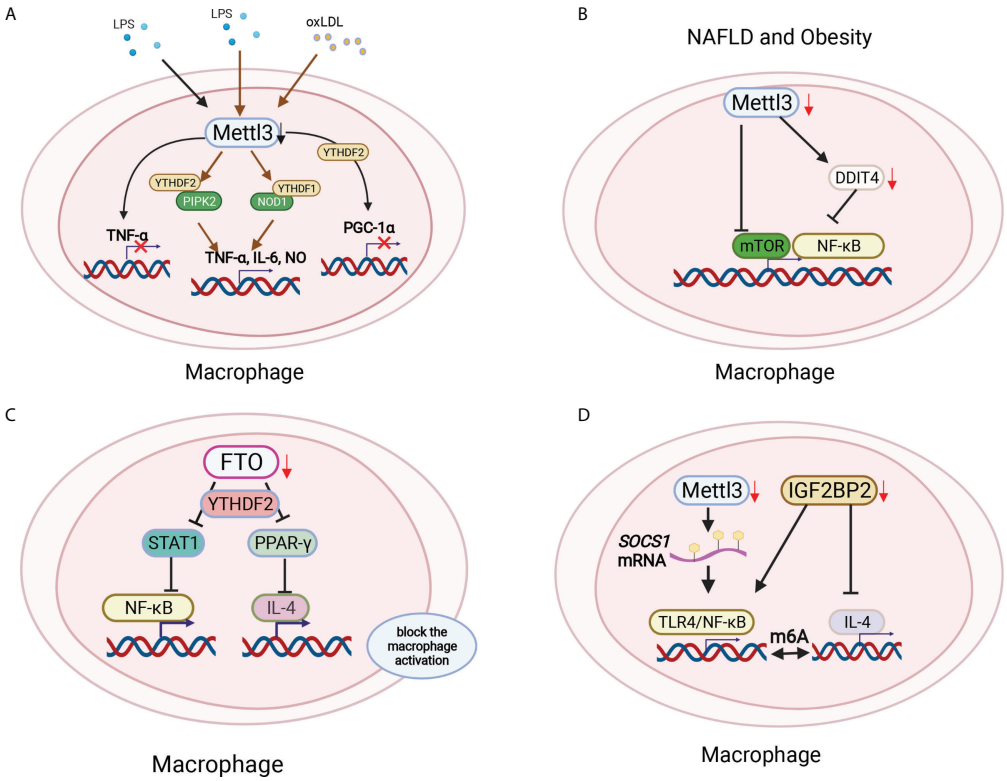

FIGURE 4
Macrophage polarization was modified by m6A methylation in different environments. **(A)** Mettl3 ablation macrophages produced little TNF-α with LPS stimulation. Mettl3 downregulation in macrophages significantly increased the proinflammatory cytokines TNF-α, IL-6 and NO by increasing NOD1 and RIPK2 *via* YTHDF1 and YTHDF2, respectively. Mettl3 and YTHDF2 cooperatively degraded PGC-1α mRNA in oxLDL-treated monocytes. **(B)** Myeloid lineage-restricted Mettl3 deletion protected mice from age-related and diet-induced development of innate immunity-driven nonalcoholic fatty liver disease (NAFLD) and obesity by decreasing mTOR expression and the NF-κB pathway by targeting DDIT4. **(C)** FTO deficiency inhibited both M1 and M2 polarization by suppressing the NF-κB signaling pathway and decreasing the stability of STAT and PPAR-γ *via* YTHDF2 involvement, therefore blocking macrophage activation. **(D)** The loss of Mettl14 decreased the demethylase Socs1 mRNA to activate TLR4/NF-κB signaling. In addition, IGF2BP2$^{-/-}$ macrophages were refractory to IL-4-induced activation to regulate the switch of M1 to M2 subtypes in a m6A-dependent manner.

and obesity. Mettl3 deficiency results in a notable increase in DNA damage inducible transcript 4 (DDIT4) mRNA. The decrease in mammalian target of rapamycin (mTOR) and NF-κB pathway activity in Mettl3-deficient macrophages could be restored by DDIT4 KD (85) (Figure 4B). These findings demonstrate the contribution of Mettl3-mediated m6A modification of DDIT4 to macrophage metabolic reprogramming in NAFLD and obesity. Lihui Dong et al. reported that macrophage-specific knockout of the m6A methyltransferase Mettl14 drives CD8+ T-cell differentiation with a dysfunctional trajectory, impairing CD8+ T cells to eliminate tumors (86). Silencing of the m6A eraser FTO markedly inhibited both M1 and M2 polarization by suppressing the NF-κB signaling pathway and decreasing the stability of STAT and PPAR-γ *via* YTHDF2 involvement, therefore blocking macrophage activation (87, 88) (Figure 4C). Mettl14 ablation in myeloid cells contributes to acute bacterial infection in mice by the continuous production of proinflammatory cytokines, which can be rescued by forced expression of Socs 1 in macrophages depleted of Mettl14 or YTHDF1. Loss of Mettl14 decreases demethylase expression, and Socs1 mRNA overactivates TLR4/NF-κB signaling. These findings highlight that m6A methylation-mediated SOCS1 expression is essential for the negative feedback control of macrophages on bacterial infection (89). YTHDF1 KD macrophages in rats improved the secretion of anti-inflammatory cytokines, highlighting the protective role of YTHDF1 KD macrophages in severe sepsis rats with ECMO (90). YTHDF2 KD in the mouse macrophage cell line Raw264.7 enhanced osteoclast formation and bone resorption (91). The m6A reader IGF2BP2-abated macrophages showed enhanced M1 polarization and promoted dextran sulfate sodium-induced colitis development. IGF2BP2$^{-/-}$ macrophages are refractory to IL-4-induced activation by targeting tuberous sclerosis 1 to regulate the switch of M1 to M2 subtypes in a m6A-dependent manner, which indicates the key role of IGF2BP2 in the regulation of macrophages (92) (Figure 4D). These results indicated that the differentiation and function of macrophages could be regulated by m6A methylation.

NK cells are a large population of innate lymphocytes involved in antitumour and antiviral immunity. The m6A reader YTHDF2 is markedly increased in NK cells when activated by cytokines, tumors and virus infection, which mediates NK-cell antitumour and terminal maturation related to modulating NK-cell trafficking and regulating Eomes, respectively, losing which affects the antitumour and antiviral function of NK cells *in vivo*. Mechanistically, YTHDF2 promotes the effector function of NK cells and is essential for IL-15-mediated NK-cell survival and proliferation by the STAT5-YTHDF2 positive feedback loop, highlighting the novel biological role of YTHDF2 in NK cells in antitumour immunity (93) (Figure 5A). In addition, inactivation of Mettle3 in NK cells changed the hemostasis, infiltration and function of NK cells in the tumor microenvironment, leading to accelerated tumor growth and short lifespan in mice by modifying SHP-2 mRNA, which rendered NK cells hyporesponsive to IL-15 (94) (Figure 5B). However, the role of m6A modifications in the development and function of macrophages and NK cells remains limited and is worthy of more focus and investigation.

m6A functions in the adaptive immune response

Adaptive immunity could be special in the clearance of specific pathogens, which are mainly mediated by the activation of antigen-specific T/B lymphocytes, and finally

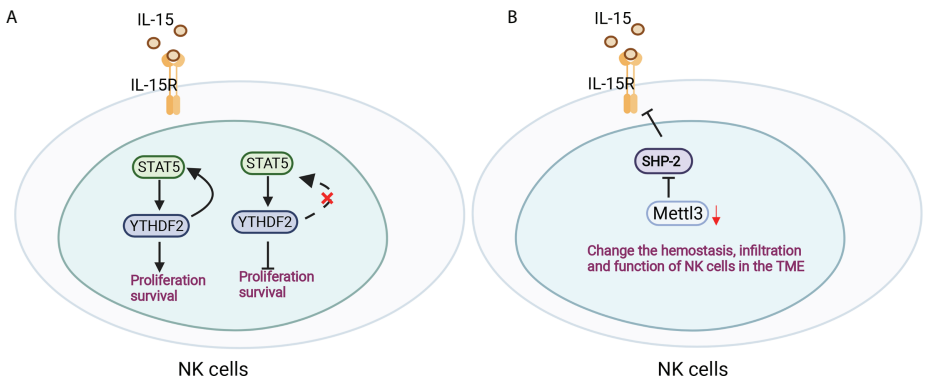

FIGURE 5
Antitumour immunity of NK cells was regulated by m6A modification. **(A)** YTHDF2 is essential for IL-15-mediated NK-cell survival and proliferation by the STAT5-YTHDF2 positive feedback loop. **(B)** Mettle3 ablation in NK cells changed the hemostasis, infiltration and function of NK cells by modifying SHP-2 mRNA in the tumor microenvironment.

establish long-term immunological memory against the given antigen. Recently, an increasing number of studies have shown that m6A exerts an important effect on adaptive immunity and modulates the differentiation and function of different subsets of T cells (70). Val1, expressed in all immune cells, is used as Cre recombinase with the Val1 promoter in studying the immune response. However, METTL3 deficiency in Val1-Cre mice led to nonviable progeny, indicating the critical role of METTL3 in immune cells. While CD4, CD11C and Foxp3 were used to construct cell-specific transgenic mice (95), a large amount of m6A was still detectable (78, 96), which reflected incomplete METTL3 deletion.

The generation and maturation of CD4+ T cells in the thymus highly depend on the T-cell receptor (TCR) and multiple costimulatory signals. Initially, deficiency of METTL3 in CD4+ T cells did not affect the generation, maturation or capacity to respond to TCR stimulation *in vitro*, which indicated that the basic TCR signals and downstream signal transduction did not depend on m6A methylation *in vitro* (96). In CD4+ T-cell-specific *Mettl3* KO mice, the proportion of naïve cells was higher, while the proportion of activating CD4+ T cells was lower than that in WT mice, and *Mettl3* KO mice developed spontaneous colitis, indicating that m6A helped to keep naïve cells quiescent. A similar phenotype was observed in *Mettl14* KO mice (96).

IL-7 is essential for homeostatic proliferation and long-term survival of naïve T cells (97). Likewise, the naïve T cells in *Mettl3* KO mice show a striking similarity to CD4+ T cells transferred to IL-7-deficient mice (98). The IL-7 receptor suppresses cytokine signaling of SOCS1 targets (98). Members of the SOCS family, including Socs1, Socs3 and Cish, bind the cytokine receptor and prevent STAT5 activation and downstream signaling (99) (Figure 6A). The SOCS genes were marked by m6A and showed slower mRNA degradation and higher protein expression in *Mettl3*-deficient T helper cells, which possibly impeded signal transduction through IL-7R (96). However, the role of m6A methylation in the response to cognate antigen recognition *in vitro* and pathogens *in vivo* cannot be excluded (8). T follicular helper (T_{fh}) cells are specialized effector CD4+ T cells required for humoral immunity. The conditional deletion of METTL3 in CD4+ T cells inhibits TFH cell differentiation and the germinal center response in a cell-intrinsic manner. TFH signature genes, including Tcf7, Bcl6, Icos and Cxcr5, and these effects rely on intact methyltransferase activity. Loss of METTL3 results in accelerated decay of Tcf7 transcripts, emphasizing the role of Mettl3 in stabilizing Tcf7 transcription *via* m6A modification and T_{fh} cell differentiation (100) (Figure 6B). Whether CD8+ T cells and TCR signaling *in vivo* are regulated by m6A requires further investigation.

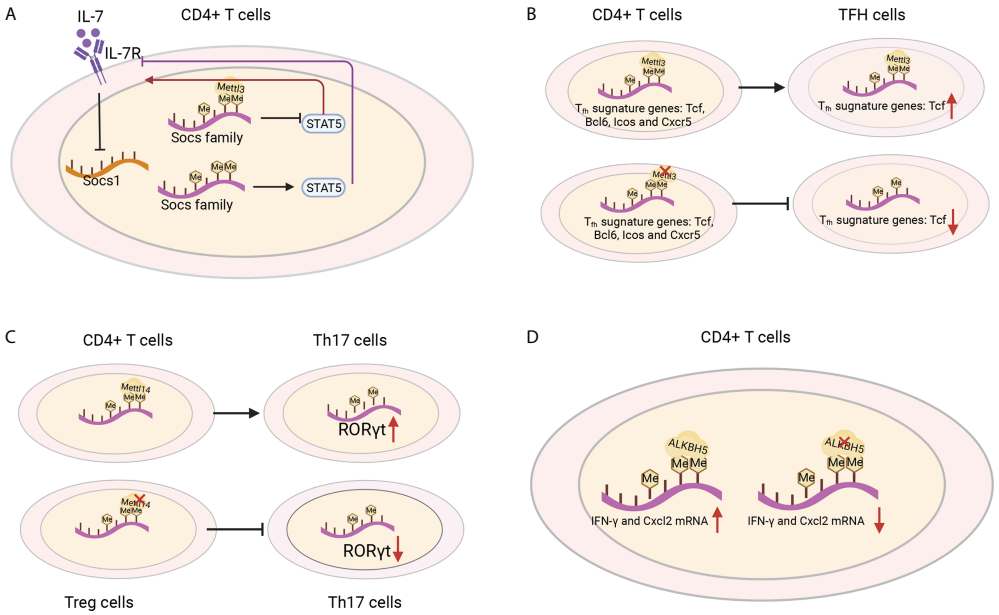

FIGURE 6
T-cell functions were shaped by m6A regulators. **(A)** IL-1R is a suppressor of SOCS1 targets. The Socs family prevents STAT5 activation and downstream signaling, which are marked by m6A and show slower mRNA degradation and higher protein expression in *Mettl3*-deficient T helper cells and blocked signal transduction through IL-7R. **(B)** Loss of METTL3 in CD4+ T cells leads to the degradation of the T_{fh} signature gene Tcf7 and inhibits T_{fh} cell differentiation. **(C)** Mettl14 ablation in Treg cells decreases RORγt expression and blocks the differentiation of naïve T cells into Th17 cells. **(D)** ALKBH5 deficiency in CD4+ T cells increases the m6A modification of IFN-γ and CXCL2 mRNA, thus decreasing their mRNA stability and protein expression in CD4+ T cells.

CD4+ regulatory T (Treg) cells represent differentiated CD4+ T cells that are transcribed by Foxp3, mediate immunosuppressive function and prevent the emergence of deleterious autoimmune diseases. Treg cells express high levels of IL-2R, which activates STAT5 and is essential for their immunosuppressive function (101–103). Although in Treg-specific *Mettl3* KO mice, the frequency of Treg cells was normal, both female and male mice developed severe autoimmune diseases and were infertile. Moreover, the mice died from 8-9 weeks and increased the mRNA levels of *SOCS* genes. These results suggest the important role of METTL3 in the immunosuppressive function of Treg cells (104). T-cell-specific Mettl14 deficiency induced spontaneous colitis in mice by increasing inflammatory cell infiltration, Th1/Th17 cytokines and the colonic weight-to-length ratio, which could be rescued by adoptive transfer of WT Treg cells. Mettl14-deficient Treg cells showed downregulated RORγt expression and blocked the differentiation of naïve T cells into Th17 cells (105)(Figure 6C). ALKBH5, not FTO, promotes naïve CD4+ T cells to induce adoptive transfer colitis. Additionally, T-cell-specific knockout ALKBH5 protects mice against EAE due to the increased m6A modification of interferon-γ and C-X-C motif chemokine ligand 2 (CXCL2) mRNA, thus decreasing their mRNA stability and protein expression in CD4+ T cells (Figure 6D). These changes resulted in an attenuated CD4+ T-cell response and diminished recruitment of neutrophils into the central nervous system, revealing the unexpected specific role of ALKBH5 in regulating the pathogenicity of CD4+ T cells in autoimmune disease (106). These studies highlighted some of the m6A modifiers in their therapeutic potential in antitumour and autoimmunity, and it would be interesting to decipher the regulatory networks in T cells and the functions of other RNA methylations in controlling T-cell differentiation, clonal expansion and their subsequent effector functions (107).

m6A functions in shaping the local immune microenvironment

Emerging studies have shown that the local tumor microenvironment (TME) required for tumor growth and survival plays important roles in tumor development and progression. TME is complex and contains not only cancer cells and stromal cells but also macrophages and distant recruited cells, such as infiltrating immune cells, characterized by hypoxia, immune escape, metabolic dysregulation and chronic inflammation (108, 109). m6A has been widely investigated in regulating oncogenes or tumor suppressor genes in various cancers. Accumulating studies have recently reported a new role of m6A in the antitumour immune response. In addition to affecting classical immunotherapy, m6A also affects tumor-associated immune cell activation and infiltration and cytokine secretion in the tumor microenvironment, which play important roles in tumor initiation, progression, metastasis, and treatment response (110, 111). The tumor immune microenvironment (TIME) generally consists of the infiltration of multiple immunosuppressive cells, especially MDSCs and Treg cells, and is often absent of antitumour immune cells (111, 112).

In recent years, emerging studies have deciphered the vital role of m6A modifications in the regulation of the local and systemic TIME, which mediate tumor progression and response to immunotherapy (113). The analysis of the m6A-related signatures from The Cancer Genome Atlas (TCGA), Genotype-Tissue Expression (GTEx) and the Gene Expression Omnibus (GEO) database revealed a significant relationship between the diverse m6A clusters and the TIME (114, 115). In glioma, m6A signatures were associated with classification, including prognosis, grade, isocitrate dehydrogenase (IDH) status and 1p19q status. Patients in the high-risk group showed enhanced stroma and immune scores and a higher abundance of immune infiltration (116–119). Silencing ALKBH5 in glioblastoma multiforme (GBM) notably suppresses hypoxia-induced tumor-associated macrophage (TAM) recruitment and immunosuppression in allograft tumors by regulating CXCL8/IL-8 secretion (120). Reduced METTL3 in hepatocellular carcinoma (HCC) results in increased infiltration of DCs in the TIME, which leads to the overall upregulation of major histocompatibility complex (MHC) molecules, costimulatory molecules, and adhesion molecules and is closely related to the prognoses of HCC (121). In addition, overexpressed YTHDF1 in HCC was associated with low CD3+ and CD8+ T-cell infiltration (122). ALKBH5 regulated PD-L1 mRNA in a YTHDF2-dependent manner on monocytes/macrophages and infiltration of myeloid-derived suppressor-like cells in the TIME of intrahepatic cholangiocarcinoma (ICC) (123). Alkbh5 in melanoma and colorectal cancers (CRC) regulates the metabolism/cytokines and infiltration of immunosuppressive Treg cells and MDSCs, therefore enhancing PD-1 immunotherapy and GVAX vaccination therapy (124, 125). In addition, Alkbh5 was related to the infiltration of monocytes in periodontitis, of which regulated m6A mediated the immune reaction of TNF-family-member receptors and cytokines, indicating the crucial roles of m6A in the diversity and complexity of the immune microenvironment of periodontitis (126). Additionally, Mettl3- or Mettl14-deficient tumors upregulated cytotoxic tumor-infiltrating CD8+ T cells and increased the production of IFN-γ, Cxcl9 and Cxcl10 in the TIME of CRC *in vivo*, thereby enhancing the response to anti-PD-1 treatment (127). METTL3, WTAP, IGF2BP3, YTHDF1, HNRNPA2B1 and HNRNPC were markedly increased in esophageal squamous cell carcinoma (ESCC) and positively related to the expression of PD-1, whose copy number dynamically affects the enrichment of tumor-infiltrating immune cells (128). Consensus clustering for 15 m6A regulators identified two molecular subtypes (clusters 1/2) in

head and neck squamous cell carcinoma (HNSCC). Cluster 1 was enriched with G2 M checkpoint, mTORC1 signaling, and PI3K/AKT/mTOR signaling, while cluster 2 was associated with favorable prognosis, increased PD-L1, higher immune score and distinct immune cell infiltration (129). High-risk pancreatic adenocarcinoma (PAAD) contributed to the enhanced infiltration of M0 and M2 macrophages and decreased B cells, naïve T cells, CD8+ T cells and Treg cells (130–133). IGF2BPs, as functional downstream modulators of circNDUFB2, regulate the secretion of CXCL10, CXCL11, CCL5, and IFNβ in non-small cell lung cancer (NSCLC) (134, 135). In addition, m6A-related genes in peripheral blood leukocytes are noninvasive biomarkers for NCCLC patients (136). Nucleophosmin 1 (NPM1) is a chameleon protein that shuttles between the nucleus and cytoplasm. NPM1 is overexpressed in lung adenocarcinoma (LUAD) and effectively distinguishes LUAD from normal samples. The expression level of NPM1 in LUAD is markedly related to tumor stage and prognosis. Multiple database analysis showed that NPM1 is negatively related to B cells and NK cells. Moreover, NPM1 expression was significantly correlated with one m6A modifier-related gene YTHDF2 and five glycolysis-related genes (ENO1, HK2, LDHA, LDHB and SLC2A1) (137, 138). Four immune-related genes (IRGs), including CD274, CD8A, GZMA and PRF1, were screened and were consistent with the enrichment of CD8+ T cells and activated memory CD4+ T cells in the TIME of multiple cancers (132). In breast cancer, the three m6A clusters (writers, erasers and readers) are correlated with subsets of the infiltrating immune landscape, including activated CD8+ T cells, NK cells, activated DCs, macrophages and Treg cells. The low m6Ascore contributes to the increased mutation burden, immune activation and survival rates and is associated with an enhanced response to anti-PD-1/PD-L1 immunotherapy (139–141). In bladder cancer, 9 m6A-related lncRNAs were dramatically associated with overall survival outcomes of bladder cancer. The risk score of bladder cancer was correlated with the infiltration levels of multiple immune cells, including B cells, plasma cells, Tfh cells, Treg cells, resting NK cells, neutrophils, and M0, M1 and M2 macrophages, which indicated the important role of m6A-related lncRNAs in prognosis and shaping the tumor immune microenvironment (142, 143), which was also found in papillary thyroid carcinoma (PTC) (114) and HCC (144). The above studies indicated that m6A methylation and m6A-related modifications play essential roles in the differentiation and function of immune cells and secretion of cytokines, therefore shaping the TIME and further regulating the response to immunotherapy (Figure 7).

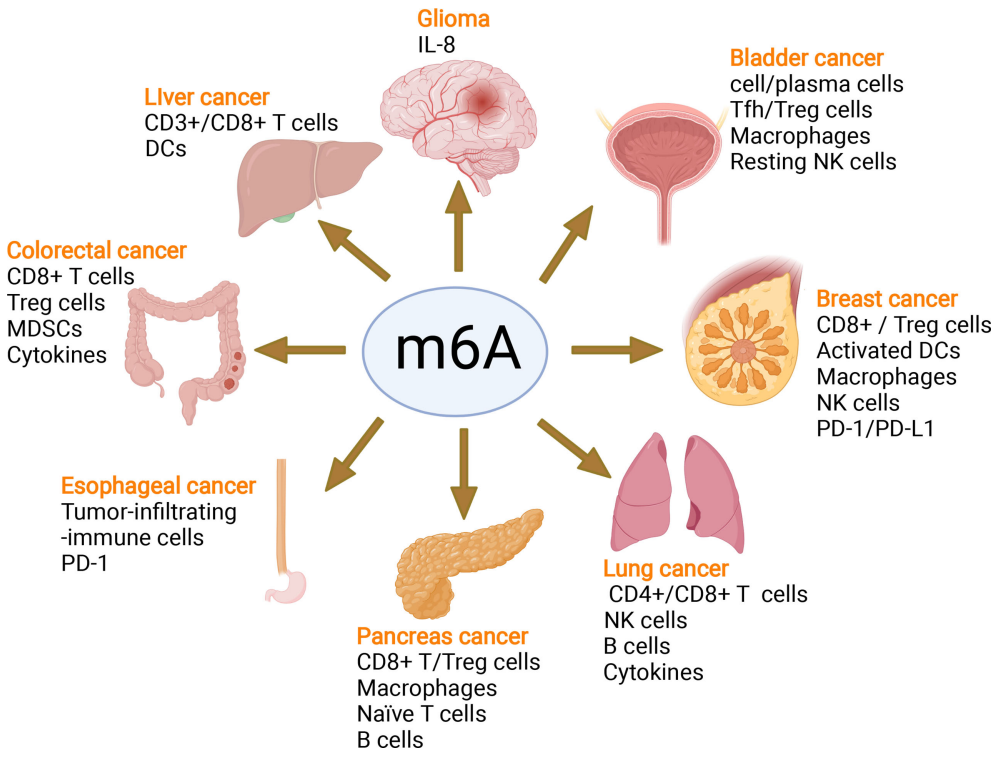

FIGURE 7
m6A modifies the tumor immune microenvironment and regulates tumor progression. m6A writers, erasers and readers regulate the tumor immune microenvironment in glioma, liver cancer, colorectal cancer, esophageal cancer, pancreatic cancer, lung cancer, breast cancer, and bladder cancer by controlling different immune cells and the PD-1/PD-L1 immune checkpoint mediating the efficacy of immune therapy.

The m6A modifications in the tumor immune microenvironment have been extensively studied (Figure 8). In addition, emerging studies have reported that m6A modifications can regulate the functions of multiple immune cells and cytokine secretion and shape the TIME, thus participating in the progression of cancer. Currently, RNA modification has become a new direction for studying embryo development and maternal-fetal immune tolerance. m6A modifications in the endometrium and ovary have been reported to be related to multiple gynecological diseases, including gynecological cancers, adenomyosis, endometriosis, polycystic ovary syndrome and premature ovarian failure, which generally contribute to RPL (145, 146). Researchers have proposed that receptivity at the maternal-fetal interface is more reminiscent of cancer immunology (35, 147). Trophoblasts and tumor cells share many similarities, including invasion, angiogenesis, and immunosuppressive environments, both of which are supported by an abetting microenvironment. However, the immunosuppressive environment in tumors severely influences antitumour therapy, which is different from the decidual immune environment (147). Emerging studies of m6A in tumors have shown potential value and strengthened the functions of m6A in the decidual local immune microenvironment. The crosstalk between trophoblasts and decidual immune cells, including decidual NK cells, macrophages and T cells, determines the local immune microenvironment at the maternal-fetal interface, the imbalance of which may lead to adverse pregnancy outcomes, such as RPL/RIF and preeclampsia (148). Although little is known about m6A methylation in trophoblast and decidual immune cells, knowledge of m6A modifications in shaping multiple immune cells and the TIME would inspire us to explore the potential roles of m6A functions in maternal-fetal immune tolerance by targeting trophoblasts and decidual NK cells, T cells and macrophages as well as cytokine secretion to shape the local immune microenvironment, thus affecting placentation and immune tolerance at the maternal-fetal interface, the imbalance of which may affect placentation and disrupt the receptive microenvironment and further lead to adverse pregnancy, including RPL and RIF. However, trophoblast cells are more precisely regulated than tumor cells, and the regulatory mechanisms of m6A in trophoblast and decidual immune cells remains unknown and requires further investigation (Figure 8).

Conclusions and future perspectives

Numerous studies have elucidated the crucial roles of m6A- and m6A-associated regulators in embryogenesis during

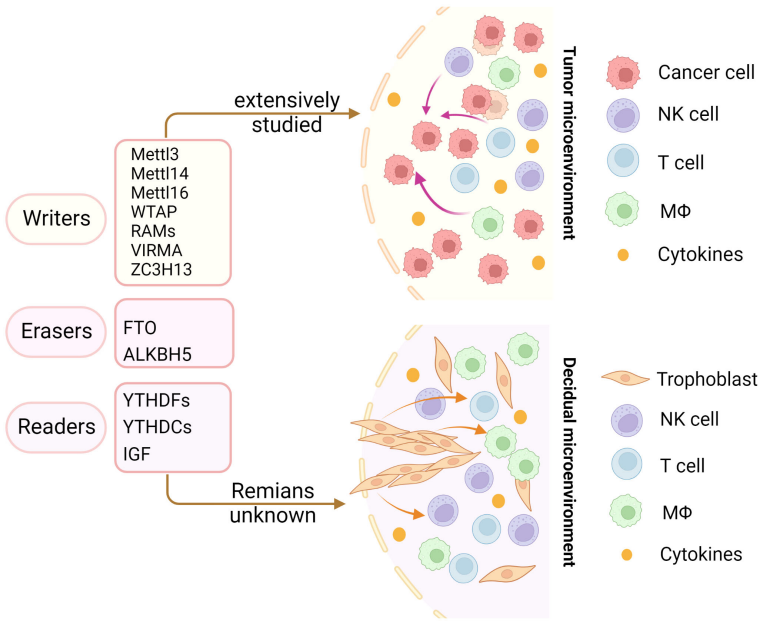

FIGURE 8
Insights into m6A modification in the tumor and decidual microenvironment. The m6A modifications in the tumor immune microenvironment have been extensively studied. However, the role of m6A modifications in decidual immune cells remains largely unknown. The same immune trajectory of decidual and tumor immune microenvironments encouraged us to study the mechanisms of m6A in decidual immune cells.

implantation. Additionally, other authors uncovered their essential roles in the differentiation and function of innate and adaptive immune cells as well as in shaping the local and systemic immune microenvironment. Indeed, m6A- and m6A-associated- regulators target cytokine secretion and multiple immune cells in the development and metastasis of various cancers by mediating the response to immunotherapy. Interestingly, the process of blastocyst implantation was similar to the metastasis of tumors; currently, the occurrence of RIF and RPL still disturbs child-bearing age women with unknown pathologies (35, 149). It is essential to determine the potential unknown factors causing RPL and RIF to provide clear targets for reproductive physicians. Although it is relatively straightforward to diagnose RPL, the progress of predicting and preventing RPL has been hampered by a lack of a standardized definition, uncertainties around the pathogenesis and highly variable clinical presentation. Moreover, the effectiveness of many medical interventions is controversial due to the available treatments targeting the putative risk factors for RPL (150). Therefore, it is urgent to explore the underlying pathologies that lead to RPL. Dysfunction of trophoblasts, stromal cells and decidual immune cells contributes to RPL and RIF. The m6A- and m6A-related-regulators participate in embryogenesis and shape the local microenvironment, which draws inspiration from studies in tumors and provides novel insight for investigating the potential pathologies causing RPL and RIF. Although some studies have reported the role of m6A- and m6A-related-regulators in the function of trophoblasts and are therefore correlated with pathological pregnancies, the relationship between m6A-and m6A-related- regulators and maternal decidual cells and the local immune microenvironment at the maternal-fetal interface is still unknown and needs further exploration, which would fill the gap in m6A in the shaping microenvironment at the maternal-fetal interface.

Author contributions

HL: conceptualization, investigation, data curation, writing – original draft, visualization, funding acquisition. JZ: data curation, writing – review & editing. AL: conceptualization, writing – review & editing. All authors have read and approved the final manuscript.

Funding

This work is supported by the Women and Children's Hospital of Hubei Province (2021SFYY002).

Acknowledgments

We thank Kahinho P Muyayalo and Zhibing Zhang for the language editing. The figures in this paper were created with BioRender.com.

Conflict of interest

The authors declare that the research was conducted in the absence of any commercial or financial relationships that could be construed as a potential conflict of interest.

Publisher's note

References

1. Consortium EP An integrated encyclopedia of DNA elements in the human genome. *Nature* (2012) 489:57–74. doi: 10.1038/nature11247

2. Li S, Mason CE. The pivotal regulatory landscape of RNA modifications. *Annu Rev Genomics Hum Genet* (2014) 15:127–50. doi: 10.1146/annurev-genom-090413-025405

3. Roundtree IA, Evans ME, Pan T, He C. Dynamic RNA modifications in gene expression regulation. *Cell* (2017) 169:1187–200. doi: 10.1016/j.cell.2017.05.045

4. Aguilo F, Walsh MJ. The N(6)-methyladenosine RNA modification in pluripotency and reprogramming. *Curr Opin Genet Dev* (2017) 46:77–82. doi: 10.1016/j.gde.2017.06.006

5. Yu F, Wei J, Cui X, Yu C, Ni W, Bungert J, et al. Post-translational modification of RNA m6A demethylase ALKBH5 regulates ROS-induced DNA damage response. *Nucleic Acids Res* (2021) 49:5779–97. doi: 10.1093/nar/gkab415

6. An S, Huang W, Huang X, Cun Y, Cheng W, Sun X, et al. Integrative network analysis identifies cell-specific trans regulators of m6A. *Nucleic Acids Res* (2020) 48:1715–29. doi: 10.1093/nar/gkz1206

7. Zhao BS, Roundtree IA, He C. Post-transcriptional gene regulation by mRNA modifications. *Nat Rev Mol Cell Biol* (2017) 18:31–42. doi: 10.1038/nrm.2016.132

8. Shulman Z, Stern-Ginossar N. The RNA modification N(6)-methyladenosine as a novel regulator of the immune system. *Nat Immunol* (2020) 21:501–12. doi: 10.1038/s41590-020-0650-4

9. Grozhik AV, Linder B, Olarerin-George AO, Jaffrey SR. Mapping m(6)A at individual-nucleotide resolution using crosslinking and immunoprecipitation (miCLIP). *Methods Mol Biol* (2017) 1562:55–78. doi: 10.1007/978-1-4939-6807-7_5

10. Linder B, Grozhik AV, Olarerin-George AO, Meydan C, Mason CE, Jaffrey SR. Single-nucleotide-resolution mapping of m6A and m6Am throughout the transcriptome. *Nat Methods* (2015) 12:767–72. doi: 10.1038/nmeth.3453

11. Ke S, Alemu EA, Mertens C, Gantman EC, Fak JJ, Mele A, et al. A majority of m6A residues are in the last exons, allowing the potential for 3' UTR regulation. *Genes Dev* (2015) 29:2037–53. doi: 10.1101/gad.269415.115

12. Zaccara S, Ries RJ, Jaffrey SR. Reading, writing and erasing mRNA methylation. *Nat Rev Mol Cell Biol* (2019) 20:608–24. doi: 10.1038/s41580-019-0168-5

13. Liu J, Yue Y, Han D, Wang X, Fu Y, Zhang L, et al. A METTL3-METTL14 complex mediates mammalian nuclear RNA N6-adenosine methylation. *Nat Chem Biol* (2014) 10:93–5. doi: 10.1038/nchembio.1432

14. Ping XL, Sun BF, Wang L, Xiao W, Yang X, Wang WJ, et al. Mammalian WTAP is a regulatory subunit of the RNA N6-methyladenosine methyltransferase. *Cell Res* (2014) 24:177–89. doi: 10.1038/cr.2014.3

15. Schumann U, Shafik A, Preiss T. METTL3 gains R/W access to the epitranscriptome. *Mol Cell* (2016) 62:323–4. doi: 10.1016/j.molcel.2016.04.024

16. Patil DP, Chen CK, Pickering BF, Chow A, Jackson C, Guttman M, et al. m(6)A RNA methylation promotes XIST-mediated transcriptional repression. *Nature* (2016) 537:369–73. doi: 10.1038/nature19342

17. Schwartz S, Mumbach MR, Jovanovic M, Wang T, Maciag K, Bushkin GG, et al. Perturbation of m6A writers reveals two distinct classes of mRNA methylation at internal and 5' sites. *Cell Rep* (2014) 8:284–96. doi: 10.1016/j.celrep.2014.05.048

18. Wen J, Lv R, Ma H, Shen H, He C, Wang J, et al. Zc3h13 regulates nuclear RNA m(6)A methylation and mouse embryonic stem cell self-renewal. *Mol Cell* (2018) 69:1028–1038.e6. doi: 10.1016/j.molcel.2018.02.015

19. Pendleton KE, Chen B, Liu K, Hunter OV, Xie Y, Tu BP, et al. The U6 snRNA m(6)A methyltransferase METTL16 regulates SAM synthetase intron retention. *Cell* (2017) 169:824–835.e14. doi: 10.1016/j.cell.2017.05.003

20. Bokar JA, Shambaugh ME, Polayes D, Matera AG, Rottman FM. Purification and cDNA cloning of the AdoMet-binding subunit of the human mRNA (N6-adenosine)-methyltransferase. *RNA* (1997) 3:1233–47.

21. Wang P, Doxtader KA, Nam Y. Structural basis for cooperative function of Mettl3 and Mettl14 methyltransferases. *Mol Cell* (2016) 63:306–17. doi: 10.1016/j.molcel.2016.05.041

22. Knuckles P, Lence T, Haussmann IU, Jacob D, Kreim N, Carl SH, et al. Zc3h13/Flacc is required for adenosine methylation by bridging the mRNA-binding factor Rbm15/Spenito to the m(6)A machinery component Wtap/Fl(2)d. *Genes Dev* (2018) 32:415–29. doi: 10.1101/gad.309146.117

23. Jia G, Fu Y, Zhao X, Dai Q, Zheng G, Yang Y, et al. N6-methyladenosine in nuclear RNA is a major substrate of the obesity-associated FTO. *Nat Chem Biol* (2011) 7:885–7. doi: 10.1038/nchembio.687

24. Zheng G, Dahl JA, Niu Y, Fedorcsak P, Huang CM, Li CJ, et al. ALKBH5 is a mammalian RNA demethylase that impacts RNA metabolism and mouse fertility. *Mol Cell* (2013) 49:18–29. doi: 10.1016/j.molcel.2012.10.015

25. Xu C, Liu K, Tempel W, Demetriades M, Aik W, Schofield CJ, et al. Structures of human ALKBH5 demethylase reveal a unique binding mode for specific single-stranded N6-methyladenosine RNA demethylation. *J Biol Chem* (2014) 289:17299–311. doi: 10.1074/jbc.M114.550350

26. Meyer KD, Patil DP, Zhou J, Zinoviev A, Skabkin MA, Elemento O, et al. 5' UTR m(6)A promotes cap-independent translation. *Cell* (2015) 163:999–1010. doi: 10.1016/j.cell.2015.10.012

27. Wang X, Lu Z, Gomez A, Hon GC, Yue Y, Han D, et al. N6-methyladenosine-dependent regulation of messenger RNA stability. *Nature* (2014) 505:117–20. doi: 10.1038/nature12730

28. Huang H, Weng H, Sun W, Qin X, Shi H, Wu H, et al. Recognition of RNA N(6)-methyladenosine by IGF2BP proteins enhances mRNA stability and translation. *Nat Cell Biol* (2018) 20:285–95. doi: 10.1038/s41556-018-0045-z

29. Liu N, Dai Q, Zheng G, He C, Parisien M, Pan T. N(6)-methyladenosine-dependent RNA structural switches regulate RNA-protein interactions. *Nature* (2015) 518:560–4. doi: 10.1038/nature14234

30. Dominissini D, Moshitch-Moshkovitz S, Schwartz S, Salmon-Divon M, Ungar L, Osenberg S, et al. Topology of the human and mouse m6A RNA methylomes revealed by m6A-seq. *Nature* (2012) 485:201–6. doi: 10.1038/nature11112

31. Jiang X, Liu B, Nie Z, Duan L, Xiong Q, Jin Z, et al. The role of m6A modification in the biological functions and diseases. *Signal Transduct Target Ther* (2021) 6:74. doi: 10.1038/s41392-020-00450-x

32. Vomstein K, Feil K, Strobel L, Aulitzky A, Hofer-Tollinger S, Kuon RJ, et al. Immunological risk factors in recurrent pregnancy loss: Guidelines versus current state of the art. *J Clin Med* (2021) 10:869–89. doi: 10.3390/jcm10040869

33. Fukui Y, Hirota Y, Matsuo M, Gebril M, Akaeda S, Hiraoka T, et al. Uterine receptivity, embryo attachment, and embryo invasion: Multistep processes in embryo implantation. *Reprod Med Biol* (2019) 18:234–40. doi: 10.1002/rmb2.12280

34. Ojosnegros S, Seriola A, Godeau AL, Veiga A. Embryo implantation in the laboratory: an update on current techniques. *Hum Reprod Update* (2021) 27:501–30. doi: 10.1093/humupd/dmaa054

35. Mor G, Aldo P, Alvero AB. The unique immunological and microbial aspects of pregnancy. *Nat Rev Immunol* (2017) 17:469–82. doi: 10.1038/nri.2017.64

36. West RC, Ming H, Logsdon DM, Sun J, Rajput SK, Kile RA, et al. Dynamics of trophoblast differentiation in peri-implantation-stage human embryos. *Proc Natl Acad Sci U.S.A.* (2019) 116:22635–44. doi: 10.1073/pnas.1911362116

37. PrabhuDas M, Bonney E, Caron K, Dey S, Erlebacher A, Fazleabas A, et al. Immune mechanisms at the maternal-fetal interface: perspectives and challenges. *Nat Immunol* (2015) 16:328–34. doi: 10.1038/ni.3131

38. Yang F, Zheng Q, Jin L. Dynamic function and composition changes of immune cells during normal and pathological pregnancy at the maternal-fetal interface. *Front Immunol* (2019) 10:2317. doi: 10.3389/fimmu.2019.02317

39. Abelius MS, Janefjord C, Ernerudh J, Berg G, Matthiesen L, Duchen K, et al. The placental immune milieu is characterized by a Th2- and anti-inflammatory transcription profile, regardless of maternal allergy, and associates with neonatal immunity. *Am J Reprod Immunol* (2015) 73:445–59. doi: 10.1111/aji.12350

40. Cakmak H, Taylor HS. Implantation failure: molecular mechanisms and clinical treatment. *Hum Reprod Update* (2011) 17:242–53. doi: 10.1093/humupd/dmq037

41. Sui X, Hu Y, Ren C, Cao Q, Zhou S, Cao Y, et al. METTL3-mediated m(6)A is required for murine oocyte maturation and maternal-to-zygotic transition. *Cell Cycle* (2020) 19:391–404. doi: 10.1080/15384101.2019.1711324

42. Mendel M, Chen KM, Homolka D, Gos P, Pandey RR, McCarthy AA, et al. Methylation of structured RNA by the m(6)A writer METTL16 is essential for mouse embryonic development. *Mol Cell* (2018) 71:986–1000.e11. doi: 10.1016/j.molcel.2018.08.004

43. Zhao BS, Wang X, Beadell AV, Lu Z, Shi H, Kuuspalu A, et al. m(6)A-dependent maternal mRNA clearance facilitates zebrafish maternal-to-zygotic transition. *Nature* (2017) 542:475–8. doi: 10.1038/nature21355

44. Du H, Zhao Y, He J, Zhang Y, Xi H, Liu M, et al. YTHDF2 destabilizes m(6)A-containing RNA through direct recruitment of the CCR4-NOT deadenylase complex. *Nat Commun* (2016) 7:12626. doi: 10.1038/ncomms12626

45. Fang F, Wang X, Li Z, Ni K, Xiong C. Epigenetic regulation of mRNA N6-methyladenosine modifications in mammalian gametogenesis. *Mol Hum Reprod* (2021) 27:gaab0025–36. doi: 10.1093/molehr/gaab025

46. Song P, Tayier S, Cai Z, Jia G. RNA Methylation in mammalian development and cancer. *Cell Biol Toxicol* (2021) 37:811–31. doi: 10.1007/s10565-021-09627-8

47. Zhang M, Zhai Y, Zhang S, Dai X, Li Z. Roles of N6-methyladenosine (m(6)A) in stem cell fate decisions and early embryonic development in mammals. *Front Cell Dev Biol* (2020) 8:782. doi: 10.3389/fcell.2020.00782

48. Xu W, Li J, He C, Wen J, Ma H, Rong B, et al. METTL3 regulates heterochromatin in mouse embryonic stem cells. *Nature* (2021) 591:317–21. doi: 10.1038/s41586-021-03210-1

49. Kwon J, Jo YJ, Namgoong S, Kim NH. Functional roles of hnRNPA2/B1 regulated by METTL3 in mammalian embryonic development. *Sci Rep* (2019) 9:8640. doi: 10.1038/s41598-019-44714-1

50. Liu X, Wang H, Zhao X, Luo Q, Wang Q, Tan K, et al. Arginine methylation of METTL14 promotes RNA N(6)-methyladenosine modification and endoderm differentiation of mouse embryonic stem cells. *Nat Commun* (2021) 12:3780. doi: 10.1038/s41467-021-24035-6

51. Hao J, Huang S, Wang D, Jin Y, Zhang M, Zhang J, et al. Loss of WTAP impairs early parthenogenetic embryo development. *Anim (Basel)* (2021) 11:1675–84. doi: 10.3390/ani11061675

52. Despic V, Dejung M, Gu M, Krishnan J, Zhang J, Herzel L, et al. Dynamic RNA-protein interactions underlie the zebrafish maternal-to-zygotic transition. *Genome Res* (2017) 27:1184–94. doi: 10.1101/gr.215954.116

53. Ivanova I, Much C, Di Giacomo M, Azzi C, Morgan M, Moreira PN, et al. The RNA m(6)A reader YTHDF2 is essential for the post-transcriptional regulation of the maternal transcriptome and oocyte competence. *Mol Cell* (2017) 67:1059–1067.e4. doi: 10.1016/j.molcel.2017.08.003

54. Yue Y, Liu J, Cui X, Cao J, Luo G, Zhang Z, et al. VIRMA mediates preferential m(6)A mRNA methylation in 3'UTR and near stop codon and associates with alternative polyadenylation. *Cell Discovery* (2018) 4:10. doi: 10.1038/s41421-018-0019-0

55. Chen X, Zhao Q, Zhao YL, Chai GS, Cheng W, Zhao Z, et al. Targeted RNA N(6) -methyladenosine demethylation controls cell fate transition in human pluripotent stem cells. *Adv Sci (Weinh)* (2021) 8:e2003902. doi: 10.1002/advs.202003902

56. Hao J, Hu H, Jiang Z, Yu X, Li C, Chen L, et al. microRNA-670 modulates Igf2bp1 expression to regulate RNA methylation in parthenogenetic mouse embryonic development. *Sci Rep* (2020) 10:4782. doi: 10.1038/s41598-020-61816-3

57. Liu HB, Muhammad T, Guo Y, Li MJ, Sha QQ, Zhang CX, et al. RNA-Binding protein IGF2BP2/IMP2 is a critical maternal activator in early zygotic genome activation. *Adv Sci (Weinh)* (2019) 6:1900295. doi: 10.1002/advs.201900295

58. Ren F, Lin Q, Gong G, Du X, Dan H, Qin W, et al. Igf2bp3 maintains maternal RNA stability and ensures early embryo development in zebrafish. *Commun Biol* (2020) 3:94. doi: 10.1038/s42003-020-0827-2

59. Geula S, Moshitch-Moshkovitz S, Dominissini D, Mansour AA, Kol N, Salmon-Divon M, et al. Stem cells. m6A mRNA methylation facilitates resolution of naive pluripotency toward differentiation. *Science* (2015) 347:1002–6. doi: 10.1126/science.1261417

60. Meng TG, Lu X, Guo L, Hou GM, Ma XS, Li QN, et al. Mettl14 is required for mouse postimplantation development by facilitating epiblast maturation. *FASEB J* (2019) 33:1179–87. doi: 10.1096/fj.201800719R

61. Shima H, Matsumoto M, Ishigami Y, Ebina M, Muto A, Sato Y, et al. S-adenosylmethionine synthesis is regulated by selective N(6)-adenosine methylation and mRNA degradation involving METTL16 and YTHDC1. *Cell Rep* (2017) 21:3354–63. doi: 10.1016/j.celrep.2017.11.092

62. Fukusumi Y, Naruse C, Asano M. Wtap is required for differentiation of endoderm and mesoderm in the mouse embryo. *Dev Dyn* (2008) 237:618–29. doi: 10.1002/dvdy.21444

63. Kasowitz SD, Ma J, Anderson SJ, Leu NA, Xu Y, Gregory BD, et al. Nuclear m6A reader YTHDC1 regulates alternative polyadenylation and splicing during mouse oocyte development. *PloS Genet* (2018) 14:e1007412. doi: 10.1371/journal.pgen.1007412

64. Perez-Garcia V, Fineberg E, Wilson R, Murray A, Mazzeo CI, Tudor C, et al. Placentation defects are highly prevalent in embryonic lethal mouse mutants. *Nature* (2018) 555:463–8. doi: 10.1038/nature26002

65. Gu Y, Chu X, Morgan JA, Lewis DF, Wang Y. Upregulation of METTL3 expression and m6A RNA methylation in placental trophoblasts in preeclampsia. *Placenta* (2021) 103:43–9. doi: 10.1016/j.placenta.2020.10.016

66. Li R, Qiu X, He M, Qiao J, He J, Zhong M. METTL3-mediated mature miR-497-5p/195-5p inhibits trophoblast migration and invasion by targeting WWP1 in preeclampsia. *Cell Cycle* (2021) 21:1–16. doi: 10.1080/15384101.2021.1982527

67. Qiu W, Zhou Y, Wu H, Lv X, Yang L, Ren Z, et al. RNA Demethylase FTO mediated RNA m(6)A modification is involved in maintaining maternal-fetal interface in spontaneous abortion. *Front Cell Dev Biol* (2021) 9:617172. doi: 10.3389/fcell.2021.617172

68. Guo Y, Song W, Yang Y. Inhibition of ALKBH5-mediated m(6) a modification of PPARG mRNA alleviates H/R-induced oxidative stress and apoptosis in placenta trophoblast. *Environ Toxicol* (2022) 37:910–24. doi: 10.1002/tox.23454

69. Li XC, Jin F, Wang BY, Yin XJ, Hong W, Tian FJ. The m6A demethylase ALKBH5 controls trophoblast invasion at the maternal-fetal interface by regulating the stability of CYR61 mRNA. *Theranostics* (2019) 9:3853–65. doi: 10.7150/thno.31868

70. Tang L, Wei X, Li T, Chen Y, Dai Z, Lu C, et al. Emerging perspectives of RNA n (6)-methyladenosine (m(6)A) modification on immunity and autoimmune diseases. *Front Immunol* (2021) 12:630358. doi: 10.3389/fimmu.2021.630358

71. Qi H, Kastenmuller W, Germain RN. Spatiotemporal basis of innate and adaptive immunity in secondary lymphoid tissue. *Annu Rev Cell Dev Biol* (2014) 30:141–67. doi: 10.1146/annurev-cellbio-100913-013254

72. Wu J, Chen ZJ. Innate immune sensing and signaling of cytosolic nucleic acids. *Annu Rev Immunol* (2014) 32:461–88. doi: 10.1146/annurev-immunol-032713-120156

73. Kariko K, Buckstein M, Ni H, Weissman D. Suppression of RNA recognition by toll-like receptors: the impact of nucleoside modification and the evolutionary origin of RNA. *Immunity* (2005) 23:165–75. doi: 10.1016/j.immuni.2005.06.008

74. Winkler R, Gillis E, Lasman L, Safra M, Geula S, Soyris C, et al. m(6)A modification controls the innate immune response to infection by targeting type I interferons. *Nat Immunol* (2019) 20:173–82. doi: 10.1038/s41590-018-0275-z

75. Rubio RM, Depledge DP, Bianco C, Thompson L, Mohr I. RNA m(6) a modification enzymes shape innate responses to DNA by regulating interferon beta. *Genes Dev* (2018) 32:1472–84. doi: 10.1101/gad.319475.118

76. Zheng Q, Hou J, Zhou Y, Li Z, Cao X. The RNA helicase DDX46 inhibits innate immunity by entrapping m(6)A-demethylated antiviral transcripts in the nucleus. *Nat Immunol* (2017) 18:1094–103. doi: 10.1038/ni.3830

77. Wang L, Wen M, Cao X. Nuclear hnRNPA2B1 initiates and amplifies the innate immune response to DNA viruses. *Science* (2019) 365:eaav0758. doi: 10.1126/science.aav0758

78. Wang H, Hu X, Huang M, Liu J, Gu Y, Ma L, et al. Mettl3-mediated mRNA m(6)A methylation promotes dendritic cell activation. *Nat Commun* (2019) 10:1898. doi: 10.1038/s41467-019-09903-6

79. Han D, Liu J, Chen C, Dong L, Liu Y, Chang R, et al. Anti-tumour immunity controlled through mRNA m(6)A methylation and YTHDF1 in dendritic cells. *Nature* (2019) 566:270–4. doi: 10.1038/s41586-019-0916-x

80. Tong J, Wang X, Liu Y, Ren X, Wang A, Chen Z, et al. Pooled CRISPR screening identifies m(6)A as a positive regulator of macrophage activation. *Sci Adv* (2021) 7:eabd4742–eabd4753. doi: 10.1126/sciadv.abd4742

81. Cai Y, Yu R, Kong Y, Feng Z, Xu Q. METTL3 regulates LPS-induced inflammatory response *via* the NOD1 signaling pathway. *Cell Signal* (2022) 93:110283. doi: 10.1016/j.cellsig.2022.110283

82. Zhang X, Li X, Jia H, An G, Ni J. The m(6)A methyltransferase METTL3 modifies PGC-1alpha mRNA promoting mitochondrial dysfunction and oxLDL-induced inflammation in monocytes. *J Biol Chem* (2021) 297:101058. doi: 10.1016/j.jbc.2021.101058

83. Li Z, Xu Q, Huangfu N, Chen X, Zhu J. Mettl3 promotes oxLDL-mediated inflammation through activating STAT1 signaling. *J Clin Lab Anal* (2022) 36:e24019. doi: 10.1002/jcla.24019

84. Yin H, Zhang X, Yang P, Zhang X, Peng Y, Li D, et al. RNA m6A methylation orchestrates cancer growth and metastasis *via* macrophage reprogramming. *Nat Commun* (2021) 12:1394. doi: 10.1038/s41467-021-21514-8

85. Qin Y, Li B, Arumugam S, Lu Q, Mankash SM, Li J, et al. m(6)A mRNA methylation-directed myeloid cell activation controls progression of NAFLD and obesity. *Cell Rep* (2021) 37:109968. doi: 10.1016/j.celrep.2021.109968

86. Dong L, Chen C, Zhang Y, Guo P, Wang Z, Li J, et al. The loss of RNA N(6)-adenosine methyltransferase Mettl14 in tumor-associated macrophages promotes CD8(+) T cell dysfunction and tumor growth. *Cancer Cell* (2021) 39:945–957.e10. doi: 10.1016/j.ccell.2021.04.016

87. Gu X, Zhang Y, Li D, Cai H, Cai L, Xu Q. N6-methyladenosine demethylase FTO promotes M1 and M2 macrophage activation. *Cell Signal* (2020) 69:109553. doi: 10.1016/j.cellsig.2020.109553

88. Liu Y, Liu Z, Tang H, Shen Y, Gong Z, Xie N, et al. The N(6)-methyladenosine (m(6)A)-forming enzyme METTL3 facilitates M1 macrophage polarization through the methylation of STAT1 mRNA. *Am J Physiol Cell Physiol* (2019) 317:C762–75. doi: 10.1152/ajpcell.00212.2019

89. Du J, Liao W, Liu W, Deb DK, He L, Hsu PJ, et al. N(6)-adenosine methylation of Socs1 mRNA is required to sustain the negative feedback control of macrophage activation. *Dev Cell* (2020) 55:737–753.e7. doi: 10.1016/j.devcel.2020.10.023

90. Xing Y, Cheng D, Shi C, Shen Z. The protective role of YTHDF1-knock down macrophages on the immune paralysis of severe sepsis rats with ECMO. *Microvasc Res* (2021) 137:104178. doi: 10.1016/j.mvr.2021.104178

91. Fang C, He M, Li D, Xu Q. YTHDF2 mediates LPS-induced osteoclastogenesis and inflammatory response *via* the NF-kappaB and MAPK signaling pathways. *Cell Signal* (2021) 85:110060. doi: 10.1016/j.cellsig.2021.110060

92. Wang X, Ji Y, Feng P, Liu R, Li G, Zheng J, et al. The m6A reader IGF2BP2 regulates macrophage phenotypic activation and inflammatory diseases by stabilizing TSC1 and PPARgamma. *Adv Sci (Weinh)* (2021) 8:2100209. doi: 10.1002/advs.202100209

93. Ma S, Yan J, Barr T, Zhang J, Chen Z, Wang LS, et al. The RNA m6A reader YTHDF2 controls NK cell antitumor and antiviral immunity. *J Exp Med* (2021) 218:e20210279. doi: 10.1084/jem.20210279

94. Song H, Song J, Cheng M, Zheng M, Wang T, Tian S, et al. METTL3-mediated m(6)A RNA methylation promotes the anti-tumour immunity of natural killer cells. *Nat Commun* (2021) 12:5522. doi: 10.1038/s41467-021-25803-0

95. Silva SL, Albuquerque AS, Matoso P, Charmeteau-de-Muylder B, Cheynier R, Ligeiro D, et al. IL-7-Induced proliferation of human naive CD4 T-cells relies on continued thymic activity. *Front Immunol* (2017) 8:20. doi: 10.3389/fimmu.2017.00020

96. Li HB, Tong J, Zhu S, Batista PJ, Duffy EE, Zhao J, et al. m(6)A mRNA methylation controls T cell homeostasis by targeting the IL-7/STAT5/SOCS pathways. *Nature* (2017) 548:338–42. doi: 10.1038/nature23450

97. Tan JT, Dudl E, LeRoy E, Murray R, Sprent J, Weinberg KI, et al. IL-7 is critical for homeostatic proliferation and survival of naive T cells. *Proc Natl Acad Sci U.S.A.* (2001) 98:8732–7. doi: 10.1073/pnas.161126098

98. Seki Y, Yang J, Okamoto M, Tanaka S, Goitsuka R, Farrar MA, et al. IL-7/STAT5 cytokine signaling pathway is essential but insufficient for maintenance of naive CD4 T cell survival in peripheral lymphoid organs. *J Immunol* (2007) 178:262–70. doi: 10.4049/jimmunol.178.1.262

99. Palmer DC, Restifo NP. Suppressors of cytokine signaling (SOCS) in T cell differentiation, maturation, and function. *Trends Immunol* (2009) 30:592–602. doi: 10.1016/j.it.2009.09.009

100. Yao Y, Yang Y, Guo W, Xu L, You M, Zhang YC, et al. METTL3-dependent m(6)A modification programs T follicular helper cell differentiation. *Nat Commun* (2021) 12:1333. doi: 10.1038/s41467-021-21594-6

101. Sakaguchi S, Sakaguchi N, Asano M, Itoh M, Toda M. Immunologic self-tolerance maintained by activated T cells expressing IL-2 receptor alpha-chains (CD25). breakdown of a single mechanism of self-tolerance causes various autoimmune diseases. *J Immunol* (1995) 155:1151–64 doi: 10.1038/s41591-018-0014-x.

102. Lio CW, Hsieh CS. A two-step process for thymic regulatory T cell development. *Immunity* (2008) 28:100–11. doi: 10.1016/j.immuni.2007.11.021

103. Chinen T, Kannan AK, Levine AG, Fan X, Klein U, Zheng Y, et al. An essential role for the IL-2 receptor in treg cell function. *Nat Immunol* (2016) 17:1322–33. doi: 10.1038/ni.3540

104. Tong J, Cao G, Zhang T, Sefik E, Amezcua Vesely MC, Broughton JP, et al. m(6)A mRNA methylation sustains treg suppressive functions. *Cell Res* (2018) 28:253–6. doi: 10.1038/cr.2018.7

105. Lu TX, Zheng Z, Zhang L, Sun HL, Bissonnette M, Huang H, et al. A new model of spontaneous colitis in mice induced by deletion of an RNA m(6)A methyltransferase component METTL14 in T cells. *Cell Mol Gastroenterol Hepatol* (2020) 10:747–61. doi: 10.1016/j.jcmgh.2020.07.001

106. Zhou J, Zhang X, Hu J, Qu R, Yu Z, Xu H, et al. m(6)A demethylase ALKBH5 controls CD4(+) T cell pathogenicity and promotes autoimmunity. *Sci Adv* (2021) 7:eabg0470. doi: 10.1126/sciadv.abg0470

107. Chao Y, Li HB, Zhou J. Multiple functions of RNA methylation in T cells: A review. *Front Immunol* (2021) 12:627455. doi: 10.3389/fimmu.2021.627455

108. Zhang B, Wu Q, Li B, Wang D, Wang L, Zhou YL. m(6)A regulator-mediated methylation modification patterns and tumor microenvironment infiltration characterization in gastric cancer. *Mol Cancer* (2020) 19:53. doi: 10.1186/s12943-020-01170-0

109. Gu Y, Wu X, Zhang J, Fang Y, Pan Y, Shu Y, et al. The evolving landscape of N(6)-methyladenosine modification in the tumor microenvironment. *Mol Ther* (2021) 29:1703–15. doi: 10.1016/j.ymthe.2021.04.009

110. Surendran V, Rutledge D, Colmon R, Chandrasekaran A. A novel tumor-immune microenvironment (TIME)-on-Chip mimics three dimensional neutrophil-tumor dynamics and neutrophil extracellular traps (NETs)-mediated collective tumor invasion. *Biofabrication* (2021) 13:10.1088. doi: 10.1088/1758-5090/abe1cf

111. Binnewies M, Roberts EW, Kersten K, Chan V, Fearon DF, Merad M, et al. Understanding the tumor immune microenvironment (TIME) for effective therapy. *Nat Med* (2018) 24:541–50. doi: 10.1038/s41591-018-0014-x

112. Berger Y, Giurcanu M, Vining CC, Schuitevoerder D, Posner MC, Roggin KK, et al. Cytoreductive surgery for selected patients whose metastatic gastric cancer was treated with systemic chemotherapy. *Ann Surg Oncol* (2021) 28:4433–43. doi: 10.1245/s10434-020-09475-6

113. Guo L, Yang H, Zhou C, Shi Y, Huang L, Zhang J. N6-methyladenosine RNA modification in the tumor immune microenvironment: Novel implications for immunotherapy. *Front Immunol* (2021) 12:773570. doi: 10.3389/fimmu.2021.773570

114. Tang R, Zhang Y, Liang C, Xu J, Meng Q, Hua J, et al. The role of m6A-related genes in the prognosis and immune microenvironment of pancreatic adenocarcinoma. *PeerJ* (2020) 8:e9602. doi: 10.7717/peerj.9602

115. Jin Y, Wang Z, He D, Zhu Y, Hu X, Gong L, et al. Analysis of m6A-related signatures in the tumor immune microenvironment and identification of clinical prognostic regulators in adrenocortical carcinoma. *Front Immunol* (2021) 12:637933. doi: 10.3389/fimmu.2021.637933

116. Xu S, Tang L, Dai G, Luo C, Liu Z. Expression of m6A regulators correlated with immune microenvironment predicts therapeutic efficacy and prognosis in gliomas. *Front Cell Dev Biol* (2020) 8:594112. doi: 10.3389/fcell.2020.594112

117. Lin S, Xu H, Zhang A, Ni Y, Xu Y, Meng T, et al. Prognosis analysis and validation of m(6)A signature and tumor immune microenvironment in glioma. *Front Oncol* (2020) 10:541401. doi: 10.3389/fonc.2020.541401

118. Du J, Ji H, Ma S, Jin J, Mi S, Hou K, et al. m6A regulator-mediated methylation modification patterns and characteristics of immunity and stemness in low-grade glioma. *Brief Bioinform* (2021) 22:bbab013. doi: 10.1093/bib/bbab013

119. Liu W, Li C, Wu Y, Xu W, Chen S, Zhang H, et al. Integrating m6A regulators-mediated methylation modification models and tumor immune microenvironment characterization in Caucasian and Chinese low-grade gliomas. *Front Cell Dev Biol* (2021) 9:725764. doi: 10.3389/fcell.2021.725764

120. Dong F, Qin X, Wang B, Li Q, Hu J, Cheng X, et al. ALKBH5 facilitates hypoxia-induced paraspeckle assembly and IL8 secretion to generate an immunosuppressive tumor microenvironment. *Cancer Res* (2021) 81:5876–88. doi: 10.1158/0008-5472.CAN-21-1456

121. Shen S, Yan J, Zhang Y, Dong Z, Xing J, He Y. N6-methyladenosine (m6A)-mediated messenger RNA signatures and the tumor immune microenvironment can predict the prognosis of hepatocellular carcinoma. *Ann Transl Med* (2021) 9:59. doi: 10.21037/atm-20-7396

122. Li J, Wang W, Zhou Y, Liu L, Zhang G, Guan K, et al. m6A regulator-associated modification patterns and immune infiltration of the tumor microenvironment in hepatocarcinoma. *Front Cell Dev Biol* (2021) 9:687756. doi: 10.3389/fcell.2021.687756

123. Qiu X, Yang S, Wang S, Wu J, Zheng B, Wang K, et al. M(6)A demethylase ALKBH5 regulates PD-L1 expression and tumor immunoenvironment in intrahepatic cholangiocarcinoma. *Cancer Res* (2021) 81:4778–93. doi: 10.1158/0008-5472.CAN-21-0468

124. Li N, Kang Y, Wang L, Huff S, Tang R, Hui H, et al. ALKBH5 regulates anti-PD-1 therapy response by modulating lactate and suppressive immune cell accumulation in tumor microenvironment. *Proc Natl Acad Sci U.S.A.* (2020) 117:20159–70. doi: 10.1073/pnas.1918986117

125. Chen H, Yao J, Bao R, Dong Y, Zhang T, Du Y, et al. Cross-talk of four types of RNA modification writers defines tumor microenvironment and pharmacogenomic landscape in colorectal cancer. *Mol Cancer* (2021) 20:29. doi: 10.1186/s12943-021-01322-w

126. Zhang X, Zhang S, Yan X, Shan Y, Liu L, Zhou J, et al. m6A regulator-mediated RNA methylation modification patterns are involved in immune microenvironment regulation of periodontitis. *J Cell Mol Med* (2021) 25:3634–45. doi: 10.1111/jcmm.16469

127. Wang L, Hui H, Agrawal K, Kang Y, Li N, Tang R, et al. m(6) a RNA methyltransferases METTL3/14 regulate immune responses to anti-PD-1 therapy. *EMBO J* (2020) 39:e104514. doi: 10.15252/embj.2020104514

128. Guo W, Tan F, Huai Q, Wang Z, Shao F, Zhang G, et al. Comprehensive analysis of PD-L1 expression, immune infiltrates, and m6A RNA methylation regulators in esophageal squamous cell carcinoma. *Front Immunol* (2021) 12:669750. doi: 10.3389/fimmu.2021.669750

129. Yi L, Wu G, Guo L, Zou X, Huang P. Comprehensive analysis of the PD-L1 and immune infiltrates of m(6)A RNA methylation regulators in head and neck squamous cell carcinoma. *Mol Ther Nucleic Acids* (2020) 21:299–314. doi: 10.1016/j.omtn.2020.06.001

130. Xu F, Zhang Z, Yuan M, Zhao Y, Zhou Y, Pei H, et al. M6A regulatory genes play an important role in the prognosis, progression and immune microenvironment of pancreatic adenocarcinoma. *Cancer Invest* (2021) 39:39–54. doi: 10.1080/07357907.2020.1834576

131. Wang L, Zhang S, Li H, Xu Y, Wu Q, Shen J, et al. Quantification of m6A RNA methylation modulators pattern was a potential biomarker for prognosis and associated with tumor immune microenvironment of pancreatic adenocarcinoma. *BMC Cancer* (2021) 21:876. doi: 10.1186/s12885-021-08550-9

132. Guo Y, Wang R, Li J, Song Y, Min J, Zhao T, et al. Comprehensive analysis of m6A RNA methylation regulators and the immune microenvironment to aid immunotherapy in pancreatic cancer. *Front Immunol* (2021) 12:769425. doi: 10.3389/fimmu.2021.769425

133. Liu Y, Li G, Yang Y, Lu Z, Wang T, Wang X, et al. Analysis of N6-methyladenosine modification patterns and tumor immune microenvironment in pancreatic adenocarcinoma. *Front Genet* (2021) 12:752025. doi: 10.3389/fgene.2021.752025

134. Li B, Zhu L, Lu C, Wang C, Wang H, Jin H, et al. circNDUFB2 inhibits non-small cell lung cancer progression *via* destabilizing IGF2BPs and activating anti-tumor immunity. *Nat Commun* (2021) 12:295. doi: 10.1038/s41467-020-20527-z

135. Zhu J, Jiang Y, Wang T, Wu A, Zhou T, Zhang A, et al. Integrative analysis of m6A RNA methylation regulators and the tumor immune microenvironment in non-Small-Cell lung cancer. *Dis Markers* (2022) 2022:2989200. doi: 10.1155/2022/2989200

136. Pei Y, Lou X, Li K, Xu X, Guo Y, Xu D, et al. Peripheral blood leukocyte N6-methyladenosine is a noninvasive biomarker for non-small-cell lung carcinoma. *Onco Targets Ther* (2020) 13:11913–21. doi: 10.2147/OTT.S267344

137. Liu XS, Zhou LM, Yuan LL, Gao Y, Kui XY, Liu XY, et al. NPM1 is a prognostic biomarker involved in immune infiltration of lung adenocarcinoma and associated with m6A modification and glycolysis. *Front Immunol* (2021) 12:724741. doi: 10.3389/fimmu.2021.724741

138. Zhou H, Zheng M, Shi M, Wang J, Huang Z, Zhang H, et al. Characteristic of molecular subtypes in lung adenocarcinoma based on m6A RNA methylation modification and immune microenvironment. *BMC Cancer* (2021) 21:938. doi: 10.1186/s12885-021-08655-1

139. Dong M, Shen W, Yang G, Yang Z, Li X. Analysis of m6A methylation modification patterns and tumor immune microenvironment in breast cancer. *Front Cell Dev Biol* (2022) 10:785058. doi: 10.3389/fcell.2022.785058

140. Liu F, Yu X, He G. m6A-mediated tumor invasion and methylation modification in breast cancer microenvironment. *J Oncol* (2021) 2021:9987376. doi: 10.1155/2021/9987376

141. Du A, Wu X, Gao Y, Jiang B, Wang J, Zhang P, et al. m6A regulator-mediated methylation modification patterns and tumor microenvironment infiltration characterization in acute myeloid leukemia. *Front Immunol* (2021) 12:789914. doi: 10.3389/fimmu.2021.789914

142. Li Z, Li Y, Zhong W, Huang P. m6A-related lncRNA to develop prognostic signature and predict the immune landscape in bladder cancer. *J Oncol* (2021) 2021:7488188. doi: 10.1155/2021/7488188

143. Zhu H, Jia X, Wang Y, Song Z, Wang N, Yang Y, et al. M6A classification combined with tumor microenvironment immune characteristics analysis of bladder cancer. *Front Oncol* (2021) 11:714267. doi: 10.3389/fonc.2021.714267

144. Li L, Xie R, Lu G. Identification of m6A methyltransferase-related lncRNA signature for predicting immunotherapy and prognosis in patients with hepatocellular carcinoma. *Biosci Rep* (2021) 41:BSR20210760. doi: 10.1042/BSR20210760

145. Zhai J, Li S, Sen S, Opoku-Anane J, Du Y, Chen ZJ, et al. m(6)A RNA methylation regulators contribute to eutopic endometrium and myometrium dysfunction in adenomyosis. *Front Genet* (2020) 11:716. doi: 10.3389/fgene.2020.00716

146. Chen J, Fang Y, Xu Y, Sun H. Role of m6A modification in female infertility and reproductive system diseases. *Int J Biol Sci* (2022) 18:3592–604. doi: 10.7150/ijbs.69771

147. Krstic J, Deutsch A, Fuchs J, Gauster M, Gorsek Sparovec T, Hiden U, et al. (Dis)similarities between the decidual and tumor microenvironment. *Biomedicines* (2022) 10:1065. doi: 10.3390/biomedicines10051065

148. Wang XQ, Li DJ. The mechanisms by which trophoblast-derived molecules induce maternal-fetal immune tolerance. *Cell Mol Immunol* (2020) 17:1204–7. doi: 10.1038/s41423-020-0460-5

149. Franasiak JM, Alecsandru D, Forman EJ, Gemmell LC, Goldberg JM, Llarena N, et al. A review of the pathophysiology of recurrent implantation failure. *Fertil Steril* (2021) 116:1436–48. doi: 10.1016/j.fertnstert.2021.09.014

150. Dimitriadis E, Menkhorst E, Saito S, Kutteh WH, Brosens JJ. Recurrent pregnancy loss. *Nat Rev Dis Primers* (2020) 6:98. doi: 10.1038/s41572-020-00228-z

frontiers | Frontiers in Immunology

TYPE Original Research
PUBLISHED 21 October 2022
DOI 10.3389/fimmu.2022.1030976

OPEN ACCESS

EDITED BY
Stephen Robert Daley,
Queensland University of Technology,
Australia

REVIEWED BY
Carlos Ernesto Fernández-García,
Princess University Hospital, Spain
Matthew Dale Woolard,
Louisiana State University,
United States

*CORRESPONDENCE
Li Liu
liuli011258@sina.com
Xingshou Pan
pan8602@sina.com

†These authors have contributed equally to this work

SPECIALTY SECTION
This article was submitted to Immunological Tolerance and Regulation, a section of the journal Frontiers in Immunology

RECEIVED 29 August 2022
ACCEPTED 10 October 2022
PUBLISHED 21 October 2022

CITATION
He B, Zhan Y, Cai C, Yu D, Wei Q, Quan L, Huang D, Liu Y, Li Z, Liu L and Pan X (2022) Common molecular mechanism and immune infiltration patterns of thoracic and abdominal aortic aneurysms.
Front. Immunol. 13:1030976.
doi: 10.3389/fimmu.2022.1030976

Common molecular mechanism and immune infiltration patterns of thoracic and abdominal aortic aneurysms

Bin He[1†], Ya Zhan[2†], Chunyu Cai[1†], Dianyou Yu[1], Qinjiang Wei[3], Liping Quan[1], Da Huang[3], Yan Liu[3], Zhile Li[3], Li Liu[3,4*] and Xingshou Pan[3*]

[1]Graduate School of Youjiang Medical University for Nationalities, Baise, China, [2]The Third Hospital of MianYang, Sichuan Mental Health Center, MianYang, China, [3]Department of Cardiology, Affiliated Hospital of Youjiang Medical University for Nationalities, Baise, China, [4]College of Clinical Medicine, Youjiang Medical University for Nationalities, Baise, China

Background: Aortic disease (aortic aneurysm (AA), dissection (AD)) is a serious threat to patient lives. Little is currently known about the molecular mechanisms and immune infiltration patterns underlying the development and progression of thoracic and abdominal aortic aneurysms (TAA and AAA), warranting further research.

Methods: We downloaded AA (includes TAA and AAA) datasets from the GEO database. The potential biomarkers in TAA and AAA were identified using differential expression analysis and two machine-learning algorithms. The discrimination power of the potential biomarkers and their diagnostic accuracy was assessed in validation datasets using ROC curve analysis. Then, GSEA, KEGG, GO and DO analyses were conducted. Furthermore, two immuno-infiltration analysis algorithms were utilized to analyze the common immune infiltration patterns in TAA and AAA. Finally, a retrospective clinical study was performed on 78 patients with AD, and the serum from 6 patients was used for whole exome sequencing (WES).

Results: The intersection of TAA and AAA datasets yielded 82 differentially expressed genes (DEGs). Subsequently, the biomarkers (*CX3CR1* and *HBB*) were acquired by screening using two machine-learning algorithms and ROC curve analysis. The functional analysis of DEGs showed significant enrichment in inflammation and regulation of angiogenic pathways. Immune cell infiltration analysis revealed that adaptive and innate immune responses were closely linked to AA progression. However, neither *CX3CR1* nor *HBB* was associated with B cell-mediated humoral immunity. *CX3CR1* expression was correlated with macrophages and *HBB* with eosinophils. Finally, our retrospective clinical study revealed a hyperinflammatory environment in aortic disease. The WES study identified disease biomarkers and gene variants, some of which may be druggable.

10.3389/fimmu.2022.1030976

Conclusion: The genes *CX3CR1* and *HBB* can be used as common biomarkers in TAA and AAA. Large numbers of innate and adaptive immune cells are infiltrated in AA and are closely linked to the development and progression of AA. Moreover, *CX3CR1* and *HBB* are highly correlated with the infiltration of immune cells and may be potential targets of immunotherapeutic drugs. Gene mutation research is a promising direction for the treatment of aortic disease.

KEYWORDS

aortic aneurysms, machine-learning, biomarkers, immune cell infiltration, whole exome sequencing

Introduction

Aortic aneurysms (AA) are the second most common aortic disease after atherosclerosis and can involve almost any part of the aorta. Older age, smoking, male gender and genetic susceptibility are strongly associated with the progression of AA. As the world's population ages, the incidence of AA is increasing dramatically. Once an aortic aneurysm ruptures, it can be rapidly life-threatening, but patients are usually asymptomatic until the rupture event occurs (1, 2). Therefore, early diagnosis of AA and prevention of AA rupture are particularly important. The current treatment for AA includes both non-surgical and surgical treatment. Non-surgical treatment focuses on smoking cessation and blood pressure control. It has been established that the diameter, growth rate and symptoms of AA are important aspects in considering whether to operate. Surgical treatments include an open (AA resection and artificial vessel grafting) and an endovascular (endovascular abdominal aortic repair (EVAR) and less invasive endovascular stenting) approach (3). Over the years, these modalities have effectively reduced and prevented AA dilatation and rupture, which has saved the lives of many patients with AA. However, dilemmas are faced clinically, such as the lack of specific drugs targeting the pathogenesis of AA and the serious complications associated with surgical treatment (4). Thus, understanding the molecular mechanisms and immune pathways of AA can contribute to the development of drug targets and drug therapy for this deadly disease.

AA mainly includes two types in the thoracic or abdominal sections [thoracic and abdominal aortic aneurysms (TAA and AAA)]. The formation of AA is a complex and chronic process that results from the interplay of inherited and environmental factors. TAA and AAA are significantly different in terms of risk factors and pathophysiology. In this respect, current evidence suggests that the vascular smooth muscle cells (VSMCs) in the ascending aorta originate from the neural crest, whereas the abdominal aorta VSMCs originate from the endothelium and mesoderm (5, 6). Generally, TAA has a more solid genetic background than AAA since TAA can occur with Marfan and Loeys-Dietz syndrome due to autosomal gene mutation, while AAA is more associated with atherosclerosis (7). Despite these significant differences, they share many common features, such as a pathologically dilated aortic phenotype, loss of smooth muscle cells, inflammatory response, and altered extracellular matrix (8). However, whether TAA and AAA involve common molecular mechanisms such as immune infiltration during pathogenesis remains unclear. Indeed, understanding these mechanisms is critical for managing and treating AA. In this study, we innovatively combined TAA and AAA to explore potential key biomarkers or immune infiltration cells of AA progression compared to non-AA individuals by machine-learning and immuno-infiltration analysis algorithms.

In recent years, high-throughput sequencing and machine-learning algorithms have been widely applied in scientific research to identify novel genes associated with a variety of diseases, such as COVID19 (9), heart attack (10), atrial fibrillation (11) and cancer (12). These genes may serve as drug targets, disease diagnostic and prognostic biomarkers (13). In our study, we integrated two machine-learning algorithms (least absolute shrinkage and selection operator (LASSO) and support vector machine-recursive feature elimination (SVM-RFE)) to increase the accuracy of the signature genes for screening and further validated the diagnostic value of the identified biomarkers using receiver-operating characteristic (ROC) curve analysis. Moreover, we utilized two cutting-edge immune infiltration analysis algorithms, "CIBERSORT" and "ssGSEA" to deepen our understanding of the level of immune infiltration in TAA and AAA. In addition, the correlation between biomarkers and infiltrating immune cells was assessed using spearman's rank correlation test. Overall, we identified biomarkers associated with the pathogenesis of immune infiltration in AA and provided the foothold for further research on drugs targeting characteristic molecules and immune cells.

Finally, we retrospectively assessed serum inflammation biomarkers and lipid levels in patients with AD, which revealed activation of the inflammatory milieu in aortic disease. The WES study provided further insight into gene mutations and whether biomarkers are abnormally mutated in aortic disease (14). Importantly, the sequencing analysis allowed the prediction of druggable variants of genes, which may lead to breakthroughs in treating aortic diseases.

Materials and methods

Data download and introduction

The microarray expression datasets (GSE47472, GSE57691 and GSE26155) related to AAA and TAA were downloaded from the Gene Expression Omnibus (GEO) database (http://www.ncbi.nlm.nih.gov/geo/) (15). The GSE57691 (16) and GSE26155 (17) datasets of AAA and TAA were used for the training group, and dataset GSE47472 (18) of AAA was used for the validation group. The training dataset of GSE57691 contained 49 cases of AAA, and 10 cases of controls, based on the GPL10058 platform. In addition, dataset GSE26155, based on the GPL5175 platform, contained 43 cases of TAA and 13 cases of controls. The validation dataset of GSE47472 contained 14 cases of AAA, and 8 cases of controls. The 92 AA (Treat, including 43 TAA and 49 AAA) samples belonging to the training group and the 14 AAA samples belonging to the validation group were derived from aortic wall tissue biopsy specimens, while the 23 controls (Con, including 13 TAA and 10 AAA) belonging to the training group and the 8 controls belonging to the validation group were derived from normal aortic tissue of organ donors. In the training dataset, samples that did not meet the diagnostic criteria for AAA and TAA were removed (3). Specifically, we removed the sample of 9 patients with aortic occlusive disease from the GSE57691 dataset and 30 patients with non-dilated aorta diameter (<40 mm) and 10 patients with aortic dilatation at borderline from the GSE26155 dataset. The mean maximum aorta diameter of AA and characteristics of the three datasets are presented in Table 1.

Data merging, preprocessing, and screening of DEGs

The "sva" and "limma" R software packages (version 4.2.0) were used to merge, probe-annotate, normalize and batch-correct the data from GSE57691 and GSE26155 datasets (19, 20). Platform annotation files were utilized to convert probes in each dataset into gene symbols. The "combat" function of the "SVA" package was utilized to eliminate batch effects between the two datasets (21). Probes with the same gene symbol were averaged to define the gene expression for a given sample. Subsequently, the DEGs were identified based on the merged and preprocessed data files. The "pheatmap" package and "ggplot2" package were deployed to create DEGs heatmaps and volcano plots, respectively (22). The thresholds for DEGs included a log2 fold change (FC) > 1 and adjusted P-value < 0.05.

Functional enrichment analysis

Gene Ontology (GO), Kyoto Encyclopedia of Genes and Genomes (KEGG) and Disease Ontology (DO) enrichment analyses were conducted on DEGs using the "clusterProfiler", "enrichplot" and "DOSE" packages of the R software (23). "c2.cp.kegg.v7.4.symbols.gmt" and "c5.go.v7.4.symbols.gmt" obtained from the Molecular Signature Database (GSEA | MSigDB (gsea-msigdb.org)) were used for Gene Set Enrichment (GSEA) (24). The top five significantly enriched pathways gene sets were displayed. Adjusted P-values < 0.05 were statistically significant.

Identification and verification of potential biomarkers in AAA and TAA

To identify potential biomarkers for AAA and TAA, the two machine-learning algorithms ("LASSO" and "SVM-RFE") were applied to the DEGs of the training group. The "LASSO" algorithm was performed based on the R package "glmnet" and could identify genes significantly associated with AA and

TABLE 1 Characteristics of the three AA datasets.

Datasets	Disease Type/groups	Contains	mean maximum aorta diameter, mm
GSE47472	AAA/validation	14 AAA 8 controls	62.6 ± 18.0 mm
GSE57691	AAA/training	49 AAA (29 large, 20 small) 10 controls	68.4 ± 14.3 (large)mm 54.3 ± 2.3 (small) mm
GSE26155	TAA/training	43 TAA 13 controls	53.6 ± 7.5mm

non-AA using ten-fold cross-validation (25). The "SVM-RFE" algorithm was performed based on the R package "e1071" to identify genes with a significantly strong distinguishing power (26). The genes obtained by these machine-learning methods were intersected. Subsequently, in the validation dataset of AAA, the expression levels of the overlapping genes were compared between the AA and control groups using a boxplot. The accuracy of the intersected genes as potential biomarkers for AA and control groups was assessed using ROC curve analysis.

Immune infiltration analysis and potential biomarkers correlation with infiltrating immune cells

The R software's "CIBERSORT" package was used to assess the level of immune cell infiltration based on 22 immune cell types of the "LM22" document (https://cibersort.stanford.edu/index.php) (27), The results were filtered using the screening criteria: P value< 0.05. The "ssGSEA" algorithm was used to assess the correlation of all gene expression profiles with the 28 immune cell types of "immune.gmt" based on R software's "GSVA" packages (28). Depending on the results obtained by these two immuno-infiltration assays, the differential expression levels of 22 and 28 immune infiltrating cell types in the AA and non-AA were visualized using heatmaps and violin plots. The correlation analysis of 22 infiltrating immune cell types was visualized by the R software's "corrplot" package. The degree of association between the 22 immune cell types and potential biomarkers was evaluated by "Spearman" correlation and visualized using R software's "ggplot2" package.

A retrospective clinical study of AD patients

Blood samples were collected from 78 patients with aortic dissection (AD) who were hospitalized at the Affiliated Hospital of Youjiang Medical University for Nationalities from 2007-2019. We retrospectively studied patient clinical information and serum inflammation markers and lipid levels. Serum inflammatory markers and lipid levels are tested using the Sysmex XN-1000^{TM} Hematology Analyzer and Roche Cobas C702 fully automated biochemistry analyzer. The aortic computed tomography angiography (CTA) results of all included cases met the diagnostic criteria for AD (29). All patients provided written informed consent. The baseline characteristics of the patients and information after grouping according to Stanford classification were presented in Table 2. The Stanford classification divides dissections by the most proximal involvement into types A and B. The DeBakey classification divides AD into types I, II, and III based on the location of the primary rupture and the extent of entrapment. Our study was approved by the Ethics Committee of Affiliated Hospital of Youjiang Medical University for Nationalities (YYFY-LL-2016-06) and was in accordance with the principles of the Declaration of Helsinki.

Whole Exome Sequencing

The peripheral blood samples of six patients with AD at the Affiliated Hospital of Youjiang Medical University for Nationalities were collected and underwent WES sequencing

TABLE 2 Baseline characteristics table of AD based on the Stanford classification.

Features/ Groups	Participants (%) N=78	Stanford A (%) N=30	Stanford B (%) N=48	p-value
Gender:				0.499
Female	14 (17.9%)	7 (23.3%)	7 (14.6%)	
Male	64 (82.1%)	23 (76.7%)	41 (85.4%)	
Age(years)	54.5 ± 14.8	55.7 ± 17.0	53.7 ± 13.4	0.578
Ethnicity:				0.350
Buyei	4 (5.13%)	3 (10.0%)	1 (2.08%)	
Han	18 (23.1%)	8 (26.7%)	10 (20.8%)	
Yao	1 (1.28%)	0 (0.00%)	1 (2.08%)	
Zhuang	55 (70.5%)	19 (63.3%)	36 (75.0%)	
Smoking	34 (43.6%)	13 (43.3%)	21 (43.8%)	1.000
Hypertension	66 (84.6%)	20 (66.7%)	46 (95.8%)	0.001
Debakey:				<0.001
I	26 (33.3%)	26 (86.7%)	0 (0.00%)	
II	4 (5.13%)	4 (13.3%)	0 (0.00%)	
III	48 (61.5%)	0 (0.00%)	48 (100%)	

The Stanford A involves any part of the aorta proximal to the origin of the left subclavian artery (A affects ascending aorta). The Stanford B arises distal to the left subclavian artery origin.

by Wuhan Huada Medical Laboratory Co. The six AD patients included five male patients and one female patient, two of whom (one male and one female) had lesions involving the thorax and abdomen, while the other four patients had lesions involving the thorax only. Subsequently, the Genome Reference Consortium Human Build 37 (GRCh37/hg19) was used to annotate the WES sequencing data. The mutation annotation results were further filtered using the following filters: ExAC_ALL, ESP6500, 1000G_EAS mutation frequency < 0.01 and VAF threshold > 0.05. The filtered mutation data were converted to the Mutation Annotation Format (maf) and further visualized using the "maftools" package in R (30). Finally, the Drug Gene Interaction Database (DGIdb) was applied to make predictions of potentially druggable genes based on the "drugInteractions" function of "maftools".

Results

Data curation and DEGs screening in AAA and TAA

Based on the research design, we downloaded and organized the list of gene symbols matrix information of training (GSE57691 and GSE26155) and validation (GSE47472) datasets (Supplementary File 1). Then, the training data from GSE57691 and GSE26155 datasets were merged, intersected, normalized and batch-corrected (Supplementary File 2). Based on the filtering criteria (log2 fold change (FC) > 1 and adjusted P-value < 0.05) for significant DEGs, a total of 82 DEGs were obtained. DEGs expression in the samples was visualized in a heatmap and volcano plot (Figures 1A, B). Collated results for all genes and DEGs are provided in Supplementary File 3.

Functional correlation analysis

GO, KEGG and DO enrichment analyses were conducted on DEGs to understand biological functions, signaling pathways, and disease mechanisms in AAA and TAA. Based on the screening criterion of adjusted P-value < 0.05, we obtained 606, 42 and 214 terms for the GO, KEGG and DO enrichment analyses, respectively (Supplementary Files 4–6). The top ten GO terms associated with biological process (BP), cellular components (CC) and molecular function (MF)) are shown in Figures 2A, B. The KEGG and DO analyses of the top 30 terms are displayed in Figures 2C–F. Significantly enriched BP terms included leukocyte cell-cell adhesion, leukocyte migration, regulation of angiogenesis, regulation of vasculature development and regulation of immune effector process. Significantly enriched CC and MF GO terms included external side of the plasma membrane, tertiary granule, vacuolar lumen, immune receptor activity and integrin binding. KEGG analysis showed significant enrichment in Leishmaniasis, Tuberculosis, Th17 cell differentiation, Leukocyte transendothelial migration and cell adhesion molecules. DO analysis showed that lung disease, coronary artery disease, myeloma and bone marrow cancer were highly associated with the DEGs.

GSEA analysis

We further performed GSEA enrichment analysis on all DEGs to better understand their potential functions and signaling pathways in AA (Treat) and non-AA (Con) cases (Supplementary File 7). Huntington's disease and oxidative phosphorylation were significantly enriched in the Con group (Figure 3A). In contrast, the complement and coagulation

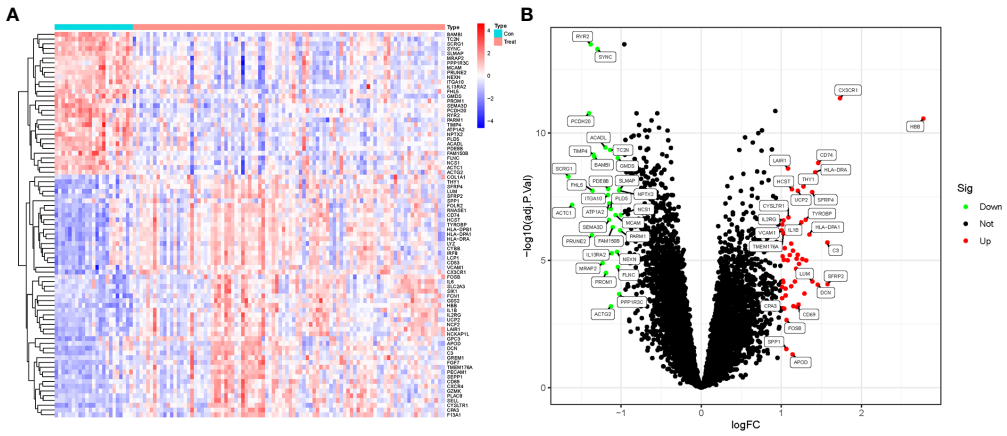

FIGURE 1
DEGs screening in AAA and TAA. **(A)** Heatmap of DEGs expression in aortic aneurysm (Treat) and non-aortic aneurysm (Con) groups. **(B)** Volcano plots of DEGs expression in Treat and Con groups.

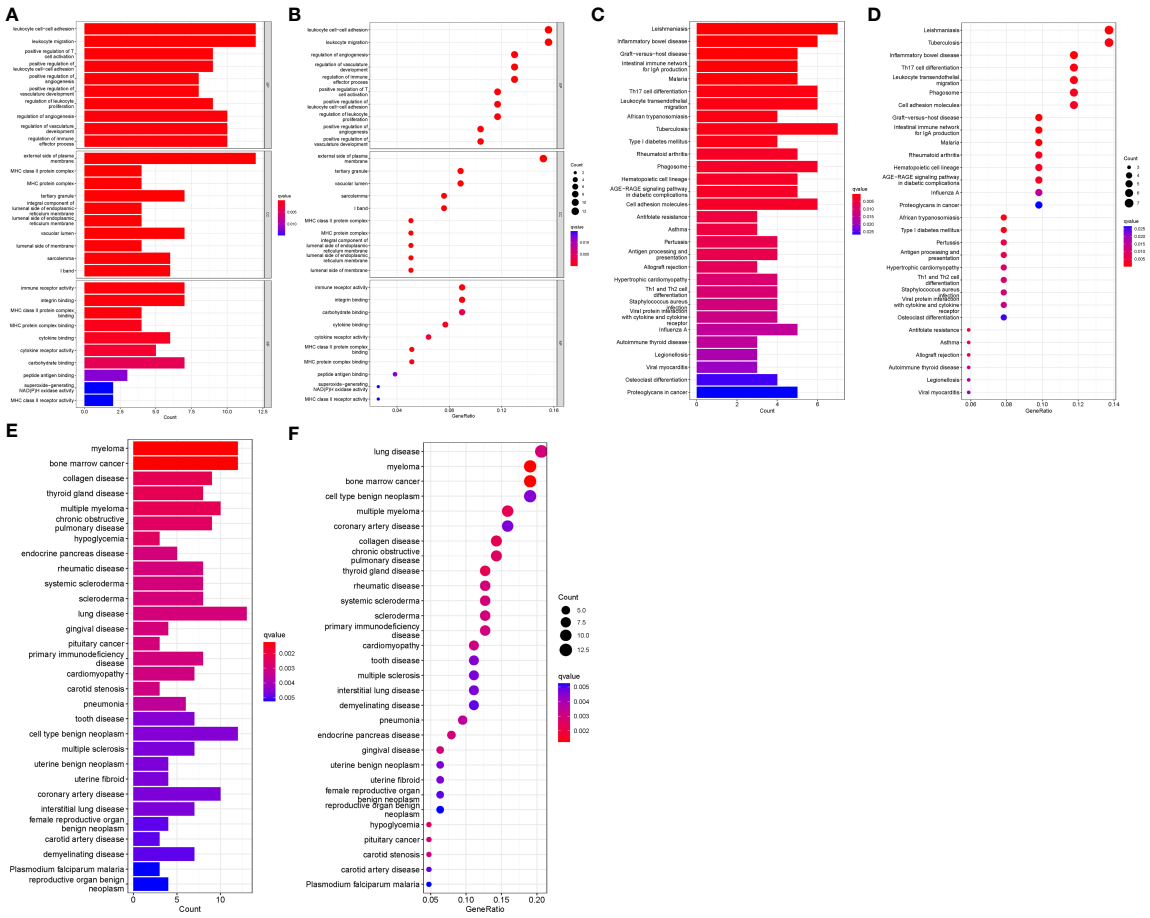

FIGURE 2
GO, KEGG and DO enrichment analyses. **(A)** Histogram of GO analysis. Enrichment significance increases with red color intensity. **(B)** Bubble plot representing GO analysis. Bubble size is proportional to the number of enriched genes. Red bubble color intensity increases with enrichment significance. **(C)** Histogram of KEGG analysis. **(D)** Bubble diagram representing KEGG analysis. **(E)** Histogram of DO analysis. **(F)** Bubble plot representing DO analysis.

cascades, cytokine-cytokine receptor interaction, hematopoietic cell lineage, Leishmania infections, and systemic lupus erythematosus were significantly enriched in the Treat group (Figure 3B).

Identification of potential biomarkers in AAA and TAA by two machine-learning algorithms

To identify common potential biomarkers in AAA and TAA, the DEGs obtained above were further screened using two machine-learning ("LASSO" and "SVM-RFE") algorithms. 12 genes were screened by "LASSO" and 6 genes were screened by "SVM-RFE" algorithms (Figures 4A, B). The intersection of the results of the two algorithms yielded three genes (*SYNC*, *CX3CR1* and *HBB*) (Figure 4C).

Verification of the discrimination power of the potential biomarkers and their diagnostic accuracy

The expression levels of the three potential biomarkers between AA (Treat) and non-AA (Con) in the validation dataset GSE47472 were visualized in boxplots (Figure 4D). The expression levels of *CX3CR1* and *HBB* were significantly higher in the Treat group than in the Con group ($P < 0.001$). In contrast, *SYNC* did not differ between the two groups with a P value of 0.27. The diagnostic accuracy of the three potential biomarkers between the Treat and Con groups was assessed by ROC curve analysis in the training and validation datasets. In the training datasets, the AUC values of *CX3CR1*, *HBB*, and *SYNC* genes were 0.938, 0.917 and 0.943, respectively (Figure 5A). In the validation datasets, the AUC values of *CX3CR1*, *HBB* and *SYNC* were 0.920, 0.938, and 0.652, respectively (Figure 5B).

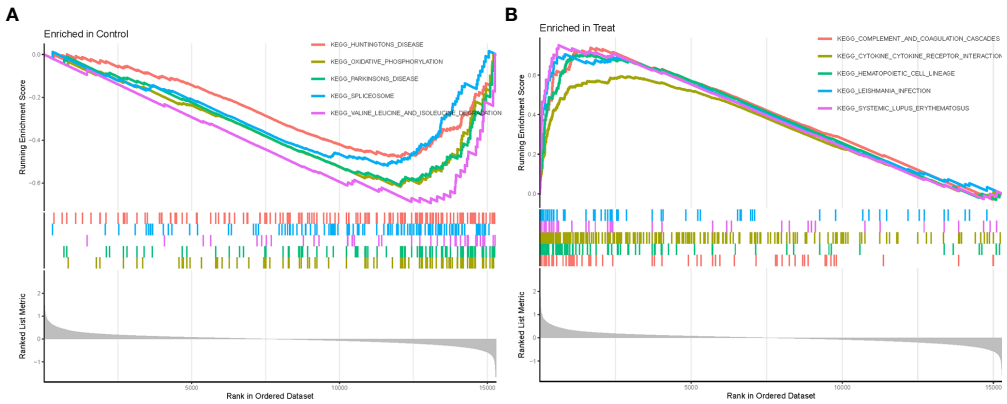

FIGURE 3
GSEA enrichment analysis. **(A)** KEGG pathway set scores enriched in the control group. **(B)** KEGG pathway set scores enriched in the Treat group.

These results suggest that *CX3CR1* and *HBB* have higher discrimination power and diagnostic accuracy and can be used as common biomarkers for AAA and TAA.

Immune infiltration analysis and the correlation between infiltrating immune cell types

Based on the normalized and merged gene expression data (Supplementary File 2), we compared Treat and Con groups by imputing the composition of immune cell populations using two algorithms, "CIBERSORT" and "ssGSEA" (Figures 6A, B; Supplementary Files 8, 9). The correlations between the infiltrating immune cell types of "CIBERSORT" are shown in Figure 6C. Finally, a violin plot was generated to visualize the differences in immune infiltrating cell types of "ssGSEA" between the Treat and Con groups (Figure 6D, Supplementary File 10). The results showed a positive correlation between resting mast cells and resting memory CD4 T cells (r=0.50), while a negative correlation was found between regulatory T cells (Tregs) and resting memory CD4 T cells and resting mast cells (r=-0.59 and -0.53). In addition, both adaptive (activated CD4+ T cells, CD8+ T cells, activated B cell, effector memory CD4 + T cells and so on) and innate immune cells (activated dendritic cell, MDSC, natural killer cell and so on) were significantly higher in the Treat group than in the Con group. In contrast, infiltrations of neutrophils, effector memory CD8+ T cells and immature dendritic cells did not differ between the two groups.

Correlation analysis between biomarkers (*CX3CR1* and *HBB*) and infiltrating immune cell types

The correlations between the biomarkers *CX3CR1* and *HBB* and infiltrating immune cell types were assessed based on the results of "ssGSEA" (Figure 7A) and "CIBERSORT" analysis (Figures 7B–L). The correlation results of ssGSEA showed that macrophage ($p<0.001$), mast cell ($p<0.05$), MDSC ($p<0.01$), dendritic cell ($p<0.01$), monocytes ($p<0.05$), Tregs ($p<0.001$), CD56bright natural killer cell ($p<0.001$), central memory CD4 T cell ($p<0.001$), activated CD8 T cell ($p<0.05$), gamma delta T cell ($p<0.001$), T follicular helper cells ($p<0.001$), and type 1 T helper cell ($p<0.01$) were highly correlated with *CX3CR1*. In contrast, eosinophil ($p<0.001$), mast cell ($p<0.001$), neutrophil ($p<0.001$), dendritic cell ($p<0.01$), monocyte ($p<0.001$), Treg ($p<0.01$), natural killer cell ($p<0.001$), MDSC ($p<0.001$), activated CD4 T cell ($p<0.01$), activated CD8 T cell ($p<0.01$), effector memory CD4 T cell ($p<0.01$) and T helper cell ($p<0.001$) were highly correlated with *HBB*. "CIBERSORT" analysis showed that *CX3CR1* was positively correlated with resting mast cells ($p<0.001$), resting memory CD4 T cells ($p<0.006$), monocytes ($p<0.008$), M2 macrophages ($p<0.043$) and gamma delta T cells ($p<0.047$), and negatively correlated with CD8T cells ($p<0.002$) and Tregs ($p<0.003$) (Supplementary File 11). *HBB* was positively correlated with activated dendritic cells ($p<0.001$) and eosinophils ($p<0.044$) and negatively with M1 macrophages ($p<0.005$) (Supplementary File 12).

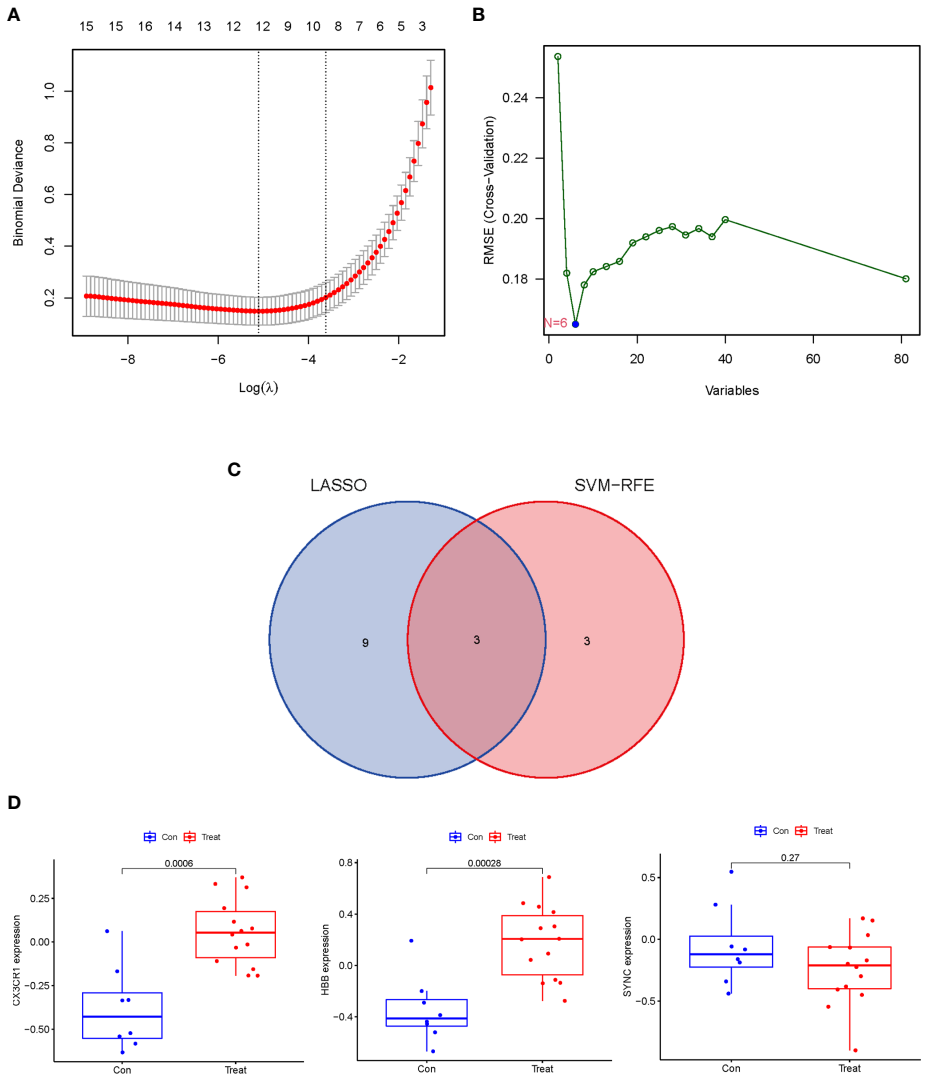

FIGURE 4
Identification and Verification of the discriminating power of potential biomarkers in AA. **(A)** Tuning feature selection in the "LASSO" model. The DEGs evaluated by 10-fold cross-validation in the "LASSO" regression model yielded 12 potential biomarkers. **(B)** The biomarkers screened by the SVM-RFE algorithm yielded 6 potential biomarkers. **(C)** Venn plot of potential biomarkers identified by "LASSO" and "SVM-RFE" algorithms. **(D)** The discrimination power of 3 potential biomarkers was verified in the validation dataset (GSE47472).

Baseline characteristics and serum markers analysis in patients with AD

Analysis of the baseline patient characteristics (Table 2) showed that the prevalence was 82.1% and 17.9% in males and females, respectively, and the age of onset was 54.5 ± 14.8 years. 43.6% (n=34) of patients had a previous smoking history. 66.49% (n=66) of patients had a previous history of hypertension, of whom 95.8% (n=46) were Stanford type B patients ($P < 0.001$). Subsequently, we analyzed the statistics of serum inflammation and lipid levels in 78 patients with AD in Table 3 and visualized them by box plots (Figures 8A–F). The median of white blood cell count (WBC) and neutrophil ratio (NEUT%) values in patients with AD were 11.0×10^9/L and 78.1%, respectively. 63% (n=49) and 79% (n=62) of cases had WBC and NEUT% values greater than the upper limit of normal. The median of the four lipid indicators LDL-C, HDL-C, TC and TG, were 2.13 mmol/L, 1.32 mmol/L, 4.47 mmol/L, and 1.00 mmol/L, with 6% (n=5), 9% (n=7), 6% (n=5) and 18% (n=14) of cases with values above the upper limit of normal, respectively.

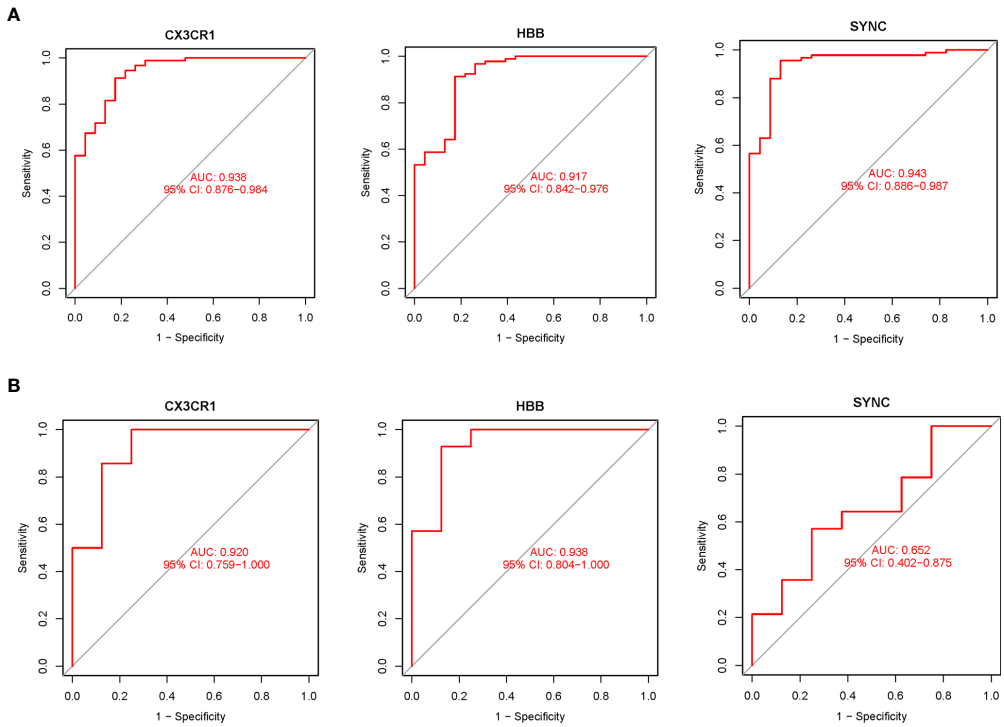

FIGURE 5
The diagnostic accuracy of the 3 potential biomarkers was assessed using ROC curve analysis. **(A)** Diagnostic ability of potential biomarkers in the training datasets. The AUC represents the diagnostic ability in Treat and Con groups. **(B)** Diagnostic accuracy of potential biomarkers in the validation datasets. The AUC represents the diagnostic accuracy in Treat and Con groups.

Whole exome sequencinganalysis

As a preliminary investigation of genetic variation in aortic disease, peripheral blood samples from 6 AD patients were subjected to whole exome sequencing. The distribution density of unfiltered single-nucleotide variant (SNV) and INDEL in chromosomes following WES analysis is shown in Figure 9A. The overall characteristics of the filtered mutation data are shown in Figure 9B. The top 100 high-frequency mutation genes are shown in Figure 9C. The top 30 high-frequency mutation genes and their corresponding mutation types are shown in Figure 9D. Transitions (Ti), Transversions (Tv) and the overall distribution of the six different Ti/Tv are shown in Figure 9E. The mutations in biomarkers (*CX3CR1* and *HBB*) in the 6 samples are shown in Figure 9F. Correlation analysis of the top 13 mutated genes is shown in Figure 9G. Potentially druggable genes are shown in Figure 9H. It could be found that missense mutations accounted for the major part; the frequency of SNP was higher than that of insertions or deletions; C>T was the most common mutation in SNV, with a mutation frequency of about 40%, followed by T>C, with a mutation frequency of about 25%. The ratio of Ti to Tv in the six sequenced samples was approximately 2:1, and the median variance per sample was 495.5. Among the top mutated genes, 100% mutation frequency was observed for *ATN1*, *HRCT1*, *KRT4*, *LNP1*, *MUC4*, *RP1L1* and *TRBV7-6* and 83% for *TTN* and *KDM6B*. Insertion frameshift mutation, nonsense mutation and missense mutation were the main types of forward mutations. In contrast, the biomarkers *CX3CR1* and *HBB* were not found to have abnormal mutations in the six sequenced samples. In addition, the correlation analysis of 13 mutated genes in six samples showed no significant correlation. Finally, the potentially druggable genes in the Drug-Gene Interaction Database (DGIdb) included *ARSD, ASPN, MUC16, MUC4, and TTN*.

Discussion

The development of high-throughput sequencing technology has brought medical research into the era of big data, while bioinformatics and artificial intelligence in medicine has enabled researchers to better analyze large amounts of sequencing data (31, 32). The combination of advanced machine-learning algorithms and medical research has led to tremendous advances in the pathogenesis, diagnosis, prognosis

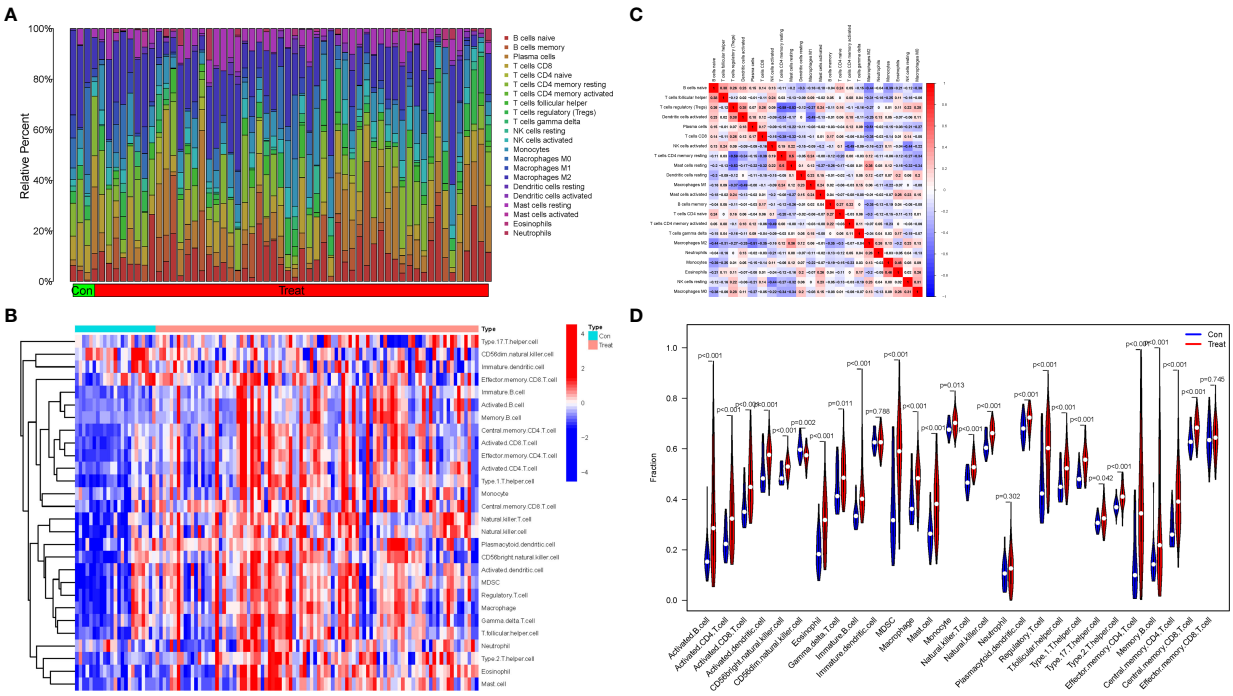

FIGURE 6
Immune infiltration analysis and the correlations between the infiltrating immune cell types. **(A)** The proportion of 22 infiltrating immune cell types in Treat and Con groups. **(B)** The distribution of the 28 infiltrating immune cell types in Treat and Con groups. **(C)** The correlations heatmap between the infiltrating immune cell types. **(D)** Violin plot demonstrating the differences between the 28 immune cell types in the Treat and Con groups.

and treatment of various diseases (33). In this study, we innovatively merged TAA and AAA data and identified three potential biomarkers by two machine-learning algorithms ("LASSO" and "SVM-RFE"). Subsequently, we validated the discrimination power and diagnostic accuracy of the potential biomarkers in a validation dataset using ROC curve analysis. *CX3CR1* and *HBB* were finally identified as accurate and reliable biomarkers of AA. These biomarkers provide novel insights into the molecular mechanisms underlying the development and progression of TAA and AAA. However, in this study we only compared biomarkers in the AA and non-AA groups. In the future, more researchers and scientists may be able to compare different sexes, different sizes of mean maximum aorta diameter and different age groupings, and thus the results obtained will further deepen the understanding of the disease at different levels.

The pathology of AA is thought to involve localized chronic inflammatory response with persistent angiogenesis and imbalance in extracellular matrix protein hydrolysis, leading to progressive weakening and dilatation of the aortic wall (34, 35). During chronic vascular inflammation, chemokines play a crucial role by mediating the activation of inflammatory and immune cells and their aggregation to the vessel wall (36, 37). Current evidence suggests that *CX3CL1* (also known as fractalkine), a specific member of the chemokine family, can act as an adhesion molecule through a membrane-bound form and as a chemoattractant in vascular inflammatory processes through a soluble form (38, 39). Interestingly, it has been shown that *CX3CR1* is a receptor for *CX3CL1* and is expressed on the surface of a variety of innate and adaptive immune cells, such as T lymphocytes, monocytes, natural killer cells, mast cells, platelets, and vascular smooth muscle cells (40–43). Moreover, *CX3CL1* on cell surfaces can play an important role in inflammatory vascular diseases by promoting migration, adhesion and proliferation of these immune cells expressing *CX3CR1* receptors (44, 45). For example, *CX3CR1*-expressing NK cells and cytotoxic T lymphocyte cells contain perforin and granzyme B, and *CX3CL1*-expressing vascular endothelial cells can effectively activate these immune cells, leading to the release of perforin and granzyme B and ultimately inducing vascular injury (46, 47). In addition, both *CX3CL1* and its receptor *CX3CR1* are expressed in vascular smooth muscle cells and can further attract macrophages to aggregate blood vessels, thereby inducing matrix metalloproteinase (MMP)-mediated extracellular matrix protein hydrolysis as well as promoting smooth muscle cell migration to endothelial cells, ultimately mediating vascular injury (48–50). Notably, the involvement of macrophages, smooth muscle cells, and MMP in the

10.3389/fimmu.2022.1030976

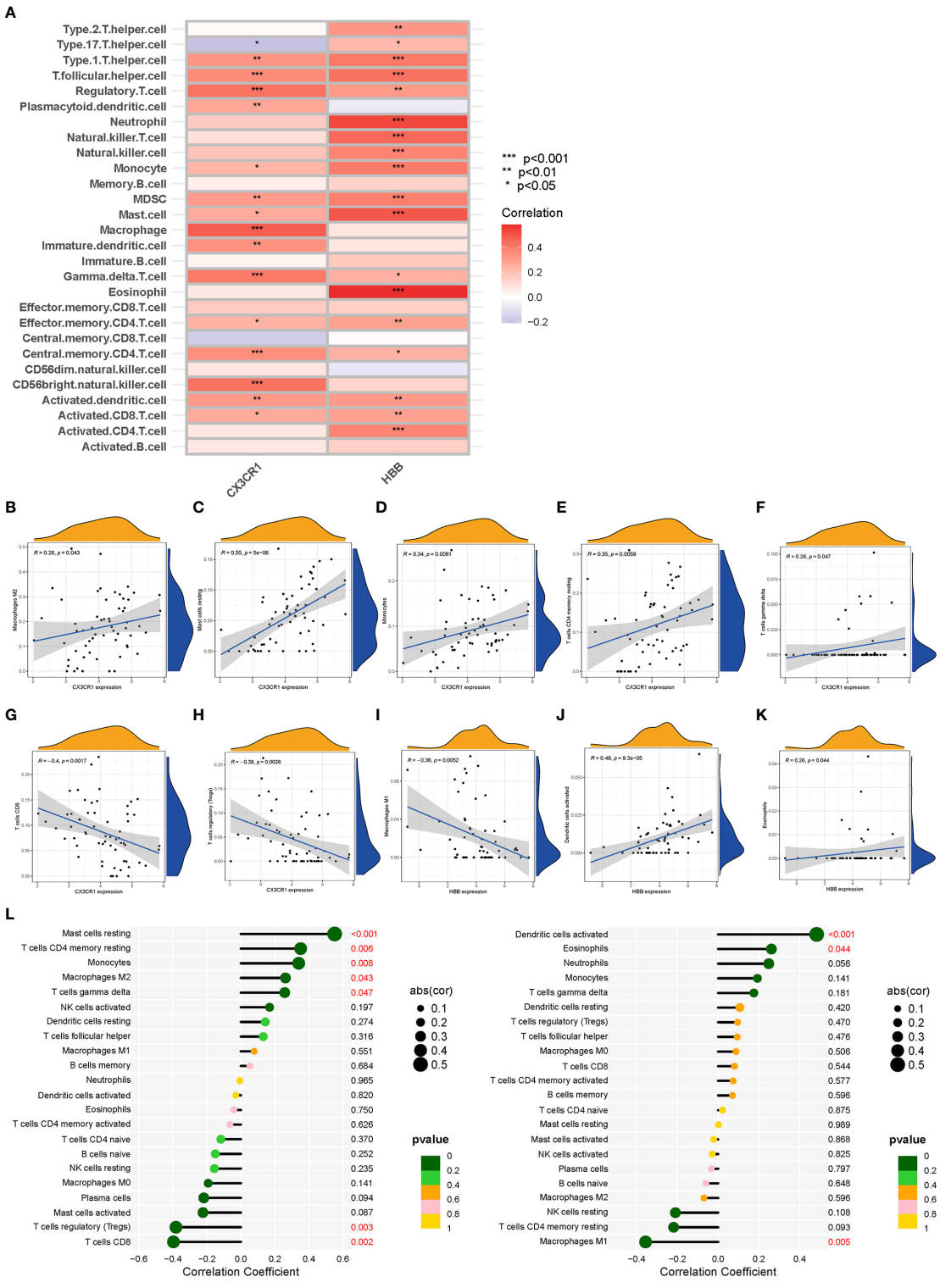

FIGURE 7
Correlation analysis between biomarkers (*CX3CR1* and *HBB*) and infiltrating immune cell types. **(A)** The relationship between 28 infiltrating immune cell types and two biomarkers; the redder the color, the more significant the difference. "***", "**", "*" represent P< (0.001, 0.01, 0.05). **(B–H)** Correlation between *CX3CR1* expression and infiltrating immune cell types. **(I–K)** Correlation between *HBB* expression and infiltrating immune cell types. **(L)** Correlation between *CX3CR1* and *HBB* and infiltrating immune cell types. The larger the dot, the stronger the correlation (cor). Numbers with P-value < 0.05 are marked red.

10.3389/fimmu.2022.1030976

TABLE 3 The serum inflammatory and lipid levels in patients with AD.

Serum markers	Participants n=78M[IQR]	Conditions	Number n=78 (%)
WBC (10^9/L)	11.0 [9.10;13.4]	>=10.0 *10^9/L	49 (63%)
		<10.0 *10^9/L	29 (37%)
NEUT (%)	78.1 [71.8;84.0]	>=70%	62 (79%)
		<70%	16 (21%)
LDL-C (mmol/L)	2.13 [1.54;2.69]	>=3.36mmol/L	5 (6%)
		<3.36 mmol/L	73 (94%)
HDL-C (mmol/L)	1.32 [1.10;1.55]	>=2.19 mmol/L	7 (9%)
		<2.19 mmol/L	71 (91%)
TC (mmol/L)	4.47 [3.96;5.06]	>=6.2 mmol/L	5 (6%)
		<6.2 mmol/L	73 (94%)
TG (mmol/L)	1.005 [0.78;1.54]	>=1.81 mmol/L	14 (18%)
		<1.81 mmol/L	64 (82%)

The serum inflammatory indicators include: white blood cell count (WBC) and neutrophil ratio (NEUT%); the reference values are: WBC (4.0~10) *10^9/L and NEUT% (50%~70%), respectively. The lipid panel includes: Low-density lipoprotein cholesterol (LDL-C), High-density lipoprotein cholesterol (HDL-C), Total cholesterol (TC), and Triglycerides (TG); the reference values are: LDL -C (0~3.36mmol/L), HDL-C (0.9~2.19 mmol/L), TC (3.1~6.2 mmol/L), and TG (0.30~1.81 mmol/L).M(Median), IQR (InterQuartile Range).

pathological alteration of AA and AA progression has been extensively studied (51–53). It was shown that by inhibiting *CX3CR1*-mediated signaling in smooth muscle cells, the formation of the neointima after arterial injury could be effectively reduced (54). Therefore, *CX3CL1* and its receptor *CX3CR1* cells are present in AA disease, and their interaction contributes to the recruitment and activation of multiple immune inflammatory cells in AA tissue, ultimately promoting AA progression (55). In our study, *CX3CR1* expression was significantly higher in AA tissues than in non-AA tissues, suggesting it could be used as a biomarker for AA. Based on a review of the literature and our previous studies, we have every reason to believe that *CX3CL1* and its receptor *CX3CR1* are potential pharmacological targets for AA treatment.

The *HBB* gene encodes a protein called beta-globin, a subunit of hemoglobin located within red blood cells.

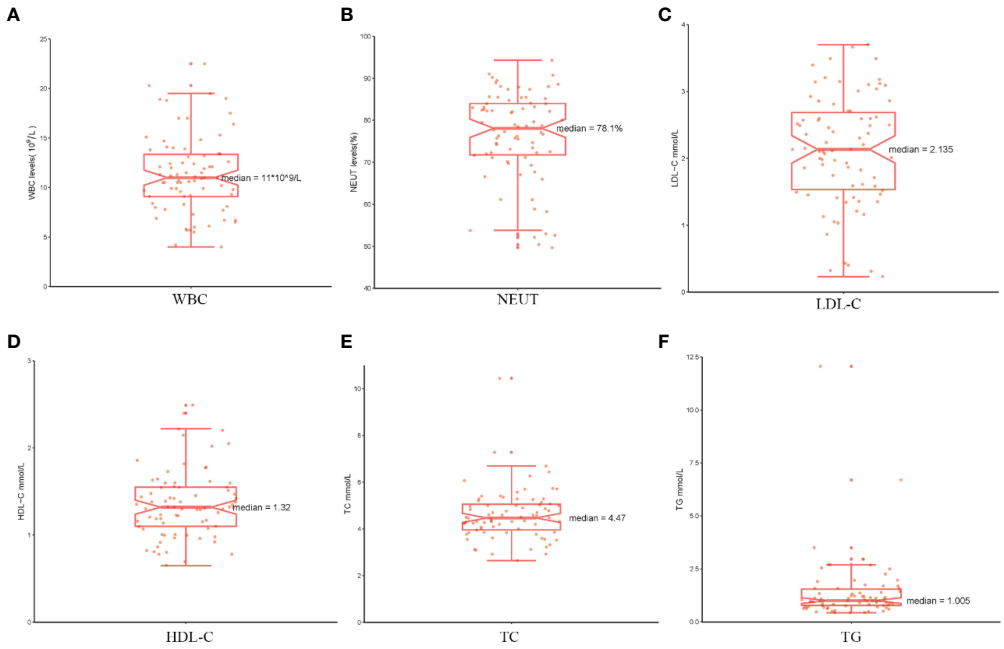

FIGURE 8
The serum markers analysis in patients with AD. **(A–F)** The serum levels of WBC, NEUT%, LDL-C, HDL-C, TC and TG are shown separately using box plots.

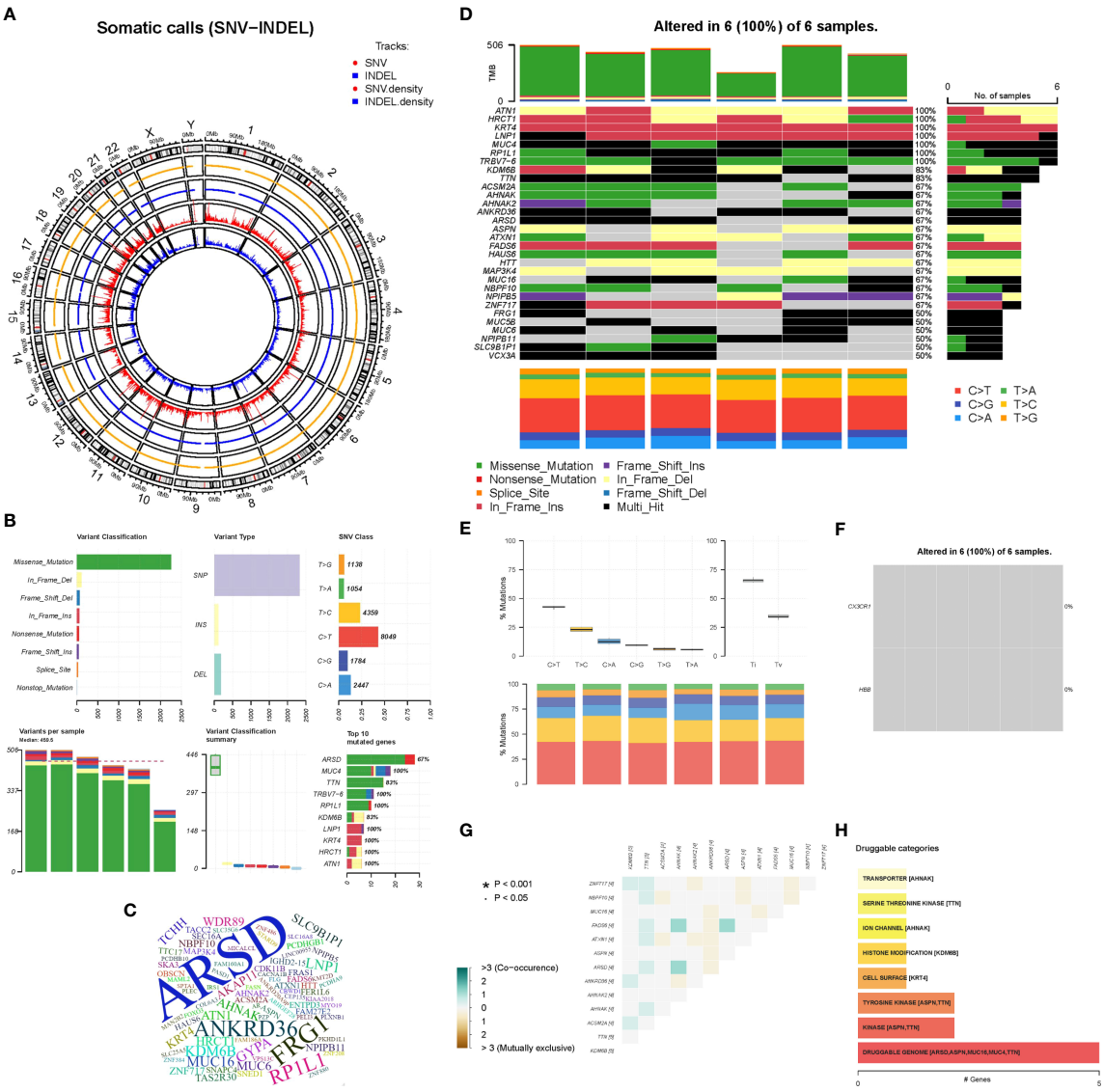

FIGURE 9
Whole Exome Sequencing analysis. **(A)** The circos plot of SNV-INDEL, the two outer tracks show the position of SNV and INDEL on the chromosome, and the two inner tracks show the distribution density. **(B)** The overall characteristics of the filtered mutation data. **(C)** The word cloud of the top 100 genes, the larger the font, the higher the variation frequency. **(D)** The oncoplot belongs to the top mutated 30 genes in each sample, different colors represent different variant classifications. **(E)** The overall distribution of the six different Ti/Tv in six samples. **(F)** The mutations of biomarkers (*CX3CR1* and *HBB*) in six samples. **(G)** Relevance Heatmap of the top 13 mutated genes. **(H)** The bar chart of potentially druggable variants genes.

Hemoglobin can usually move through the bloodstream and carries oxygen to tissues throughout the body. It has been shown that hypoxic environments may promote hemoglobin-oxygen binding and angiogenesis in Tibetan pigs through transcriptional upregulation of *HBB* expression to adapt to the plateau environment (56). In AAA, *HBB* is considered a potential biomarker in plasma samples from AAA patients (57). Our study substantiated that *HBB* gene expression is higher in AA than in non-AA tissues and may serve as a biomarker for AA. However, it is worth noting that detailed and in-depth studies of the *HBB* gene in AA tissues are still lacking, and it is well-established that *HBB* gene mutations are associated with several severe hemoglobinopathies, such as sickle cell anemia and β-thalassemia (58). We believe that the role of the *HBB* gene in AA warrants further attention, which may facilitate understanding of the molecular mechanisms underlying AA progression and the development of potential drug targets.

In the present study, the microarray expression data of TAA and AAA were merged to obtain common DEGs. We further performed GO, KEGG, DO and GSEA analyses to understand the common biological functions, signaling pathways and disease mechanisms involved in AAA and TAA. GO analysis exhibited significant enrichment in BP, including leukocyte cell-cell adhesion, leukocyte migration, regulation of angiogenesis, regulation of vasculature development and regulation of immune effector process, which is consistent with findings of previous study that chronic inflammation and regulation of angiogenesis play a crucial role in the pathology of AA (34, 35). KEGG analysis showed significant enrichment in Leishmaniasis, Tuberculosis, Th17 cell differentiation, Leukocyte transendothelial migration and cell adhesion molecules. We further performed GSEA analysis to identify the signaling pathways involved in AA and non-AA and found that complement and coagulation cascades, cytokine-cytokine receptor interaction, hematopoietic cell lineage, Leishmania infection, and systemic lupus erythematosus were significantly enriched in AA. The above analyses suggested that inflammatory factor chemotaxis, complement and coagulation cascades, and cell adhesion were commonly involved signaling pathways in AA. An increasing body of evidence suggests that AA is a chronic inflammatory disease involving extensive inflammatory cell infiltration into the arterial wall from the luminal lining to the periaortic epithelium (59, 60), and infiltration of inflammatory factors is closely associated with cytokine chemotaxis and cell adhesion (61, 62). In addition, in our study, complement and coagulation cascades were significantly enriched in AA. The complement system is widely acknowledged to be part of innate immunity. In AA, activation of the innate immune response by auto or foreign antigens further activates the complement system and induces a series of inflammatory cascades in the body, thus promoting disease progression in AA (63, 64). For instance, serum C5a complement levels were significantly elevated in AA patients and correlated with AA diameter (65). In addition, the complement system can be involved in AAA progression by participating in vascular remodeling (66). In the coagulation cascade, fibrinogen and platelet activation play an essential role in the formation of AA (67–69). Anticoagulants, such as low molecular heparin and rivaroxaban, have also been shown to inhibit the progression of AA (70). In summary, these results provide a deeper understanding of the mechanisms of AA progression and provide a basis and direction for further studies in the future.

The broad activation of the immune system in AA has been demonstrated (71, 72), but the mechanisms of co-immune infiltration in TAA and AAA remain largely unclear. Previous researchers have used algorithms such as “CIBERSORT” or “ssGSEA” when assessing the level of immune cell types infiltration in tissues. Such results may not be comprehensive and insightful. However, in our study, these two algorithms, “CIBERSORT” and “ssGSEA” were applied to assess the level of immune infiltration in AA compared to non-AA and biomarkers associated with immune infiltrating cell types. Our results suggest that the innate and adaptive immune systems are heavily activated in AA compared to non-AA, consistent with the literature (73). However, no significant difference in neutrophils, effector memory CD8+ T cells and immature dendritic cells were found between the two groups. Furthermore, resting mast cells positively correlated with resting memory CD4 T cells, while regulatory T cells negatively correlated with resting memory CD4 T cells and resting mast cells. Regulatory T cells (Tregs) are a specific T cell subtype, CD4+Foxp3+, that play an important role in regulating inflammatory responses and maintaining immune homeostasis. Studies have shown that Tregs are involved in protecting against AA through multiple mechanisms (74, 75). Mast cells are another inflammatory cell type found in aortic lesions. The mast cell protease, active chymase, is involved in the activation of MMP, which has been detected in patients positive for this enzyme in AA (76). Besides, mast cells can release pro-inflammatory chemokines involved in the progression of AA (77). Finally, we assessed the correlations between the biomarkers *CX3CR1* and *HBB* and infiltrating immune cells. Indeed, a deeper understanding of this correlation is essential to break the vicious cycle caused by immune-inflammatory activation in AA and identify new therapeutic targets. In our study, *CX3CR1* was highly correlated with macrophage, mast cell, MDSC, dendritic cell, monocytes, Tregs, CD56 bright natural killer cell, central memory CD4 T cell, activated CD8 T cell, gamma delta T cell, T follicular helper cells, and type 1 T helper cell. Moreover, it has a positive correlation with resting mast cells, resting memory CD4 T cells, monocytes, M2 macrophages and gamma delta T cells and a negative correlation with CD8 T cells and Tregs. Besides, *HBB* was highly correlated with eosinophils, mast cells, neutrophils, dendritic cells, monocytes, Tregs, natural killer cells, MDSC, activated CD4 T cells, activated CD8 T cells, effector memory CD4 T cells and T helper cells. It has a positive correlation with activated dendritic cells and eosinophils and a negative correlation with M1 macrophages. Combining the results of both immune infiltration analyses, we found that neither *CX3CR1* nor *HBB* was involved in B cell-induced humoral immunity. Furthermore, a higher correlation was found between *CX3CR1* and macrophages and HBB and eosinophils. In summary, we used two immune infiltration analysis algorithms to adequately assess the level of immune cell types infiltration in AA and to determine the relationship between infiltrating immune cell types and biomarkers. This study provides novel insights into immune mechanisms and designing new immunotherapeutic targets.

Aortic dissection (AD) is usually caused by diseases that can lead to medial degeneration and increased stress on the aortic wall, such as AA and hypertension. AD is also a serious complication of AA. In this process, chronic inflammation,

immune activation and stable degradation of extracellular matrix proteins are the key pathological changes that lead to dramatic changes in the aortic wall structure and ultimately to aneurysm formation and AD (1). Therefore, 78 patients with AD were selected for further evaluation of their clinical characteristics, serum inflammation and lipid levels. According to our results, the incidence was higher in men than in women, with a concentration of age of onset in the 50-60 years. Those with a previous history of hypertension had a high incidence and were more likely to be Stanford type B patients with AD. These findings are consistent with the epidemiological studies of aortic disease guidelines and suggest that hypertension is an important causative factor in AD (29, 78). Furthermore, in our study, serum levels of the four lipids were more often in the normal range in patients with AD, indicating that although statins are beneficial for other cardiovascular diseases, they may be less beneficial for patients with AD, especially since the 2018 AAA guidelines clearly stated that they do not reduce the risk of AAA diameter growth (3). In addition, we further assessed the level of inflammation in AA progression to AD at the clinical serum level compared to the previous analysis of immune infiltration at the AA tissue level. We found significantly elevated inflammatory markers (WBC and NEUT%) in patients with AD, which is consistent with previous studies indicating the critical involvement of inflammation in the progression of AD (1). In summary, inflammation and immunity play an important role in aortic disease and are key in studying drugs for treating aortic disease. However, some limitations of this retrospective study should be considered, for instance, the sample size, emphasizing the need for validation in prospective and larger sample studies. In addition, only the inflammatory markers and lipid levels at the time of hospitalization were counted in this study.

It has been established that genetic variants predispose individuals to these thoracic and abdominal aortic diseases: aortic aneurysms (AAA and TAA), aortic dissections (AD), and aortic ruptures (7, 79). Whole-exome sequencing was used to characterize gene mutations in aortic disease and assess whether the screened biomarkers (*CX3CR1* and *HBB)* were mutated. The sequencing of 6 patients with AD showed that the Ti/Tv ratio was close to 2, indicating no large bias in the variant calling process. In addition, the mutated genes screened by the mutation frequency database ESP6500, ExAC and 1000 Genomes were meaningful and valuable. Among the top mutated genes, *ARSD* exhibited the highest number of mutations. Moreover, 100% mutation frequency of *ATN1*, *HRCT1*, *KRT4*, *LNP1*, *MUC4*, *RP1L1* and *TRBV7-6* was observed in 6 samples and 83% for *TTN* and *KDM6B*, while the biomarkers *CX3CR1* and *HBB* were not mutated in the six sequenced samples. Although we identified highly mutated genes in the six samples, few studies have reported mutations in these genes in aortic disease. Moreover, the correlation analysis of 13 mutated genes in 6 samples showed no correlation. Finally, we used DGIdb to make predictions of potentially druggable genes (80), and the results showed that the top 5 genes (*ARSD, ASPN, MUC16, MUC4, TTN)* were highly associated with druggable properties. The development of drugs for aortic diseases from a genetic variant perspective is very promising and may lead to breakthroughs in treating aortic diseases. However, this limitation is similar to our retrospective clinical study in which the sample size of this sequencing was too small, and a prospective study with a larger sample is required to validate our conclusions. In addition, the characteristics of the population, environmental factors and differences in genetic susceptibility may impact the conclusions.

Conclusion

Overall, we innovatively merged the TAA and AAA data sets to identify two biomarkers (*CX3CR1* and *HBB*) based on two machine-learning algorithms and ROC curves. Furthermore, we conducted different bioinformatics analyses, including GO, KEGG, DO, GSEA and two immuno-infiltration analysis algorithms ("CIBERSORT" and "ssGSEA"). This study demonstrated the common molecular mechanisms and immune infiltration patterns associated with TAA and AAA, the correlations between the biomarkers and infiltrating immune cells, and provided insights into the underlying development of potential immunotherapeutic drugs. Finally, a retrospective clinical study revealed the presence of a hyper-inflammatory environment in aortic disease. The WES study identified mutated genes, biomarkers, and druggable variants genes. Due to the study limitations, further validation in prospective and larger sample studies is warranted for a deeper understanding of the pathological process, immune infiltration mechanisms, targeted drug development and variant genes in aortic disease.

Data availability statement

The WES data presented in the study are deposited in the NCBI SRA repository (https://www.ncbi.nlm.nih.gov/sra/), accession numbers SRR21846217, SRR21846218, SRR21846219, SRR21846220, SRR21846221 and SRR21846222.

Ethics statement

The studies involving human participants were reviewed and approved by the Ethics Committee of Affiliated Hospital of Youjiang Medical University for Nationalities (YYFY-LL-2016-06). The patients/participants provided their written informed consent to participate in this study.

Author contributions

BH was engaged to write and conceptualize the original draft. BH and YZ were responsible for methodology. CC, DY, QW, LQ, DH, YL, and ZL were responsible for software. LL and XP were responsible for reviewing and editing. All authors contributed to the article and approved the submitted version.

Funding

This study was sponsored by funds from the Chinese National Natural Science Foundation of China (81560076), Guangxi Natural Science Foundation Youth Program(2018JJB140358), Middle-Aged and Young Teachers in Colleges and Universities in Guangxi Basic Ability Promotion Project (2021KY0534), the First Batch of High-level Talent Scientific Research Projects of the Affiliated Hospital of Youjiang Medical University for Nationalities in 2019(R20196316).

Acknowledgments

It was the GEO network and the Affiliated Hospital of Youjiang Medical University for Nationalities that helped make this study possible. We are very grateful to the patients hospitalized at the Affiliated Hospital of Youjiang Medical University for Nationalities for agreeing to our study. We are also very grateful to the GEO database for providing free data. In additional, we have asked the researcher's house for help with the language. Thanks to FreeScience (https://www.home-for-researchers.com) for helping with the English language.

Conflict of interest

The authors declare that the research was conducted in the absence of any commercial or financial relationships that could be construed as a potential conflict of interest.

Publisher's note

Supplementary material

The Supplementary Material for this article can be found online at: https://www.frontiersin.org/articles/10.3389/fimmu.2022.1030976/full#supplementary-material

References

1. Goldfinger JZ, Halperin JL, Marin ML, Stewart AS, Eagle KA, Fuster V. Thoracic aortic aneurysm and dissection. *J Am Coll Cardiol* (2014) 64:1725–39. doi: 10.1016/j.jacc.2014.08.025

2. Guo DC, Papke CL, He R, Milewicz DM. Pathogenesis of thoracic and abdominal aortic aneurysms. *Ann N Y Acad Sci* (2006) 1085:339–52. doi: 10.1196/annals.1383.013

3. Wanhainen A, Verzini F, Van Herzeele I, Allaire E, Bown M, Cohnert T, et al. Editor's choice - European society for vascular surgery (ESVS) 2019 clinical practice guidelines on the management of abdominal aorto-iliac artery aneurysms. *Eur J Vasc Endovasc Surg* (2019) 57:8–93. doi: 10.1016/j.ejvs.2018.09.020

4. Liu B, Granville DJ, Golledge J, Kassiri Z. Pathogenic mechanisms and the potential of drug therapies for aortic aneurysm. *Am J Physiol Heart Circ Physiol* (2020) 318:H652–h670. doi: 10.1152/ajpheart.00621.2019

5. Gittenberger-de Groot AC, DeRuiter MC, Bergwerff M, Poelmann RE. Smooth muscle cell origin and its relation to heterogeneity in development and disease. *Arterioscler Thromb Vasc Biol* (1999) 19:1589–94. doi: 10.1161/01.atv.19.7.1589

6. Bergwerff M, Verberne ME, DeRuiter MC, Poelmann RE, Gittenberger-de Groot AC. Neural crest cell contribution to the developing circulatory system: Implications for vascular morphology? *Circ Res* (1998) 82:221–31. doi: 10.1161/01.res.82.2.221

7. Pinard A, Jones GT, Milewicz DM. Genetics of thoracic and abdominal aortic diseases. *Circ Res* (2019) 124:588–606. doi: 10.1161/CIRCRESAHA.118.312436

8. Quintana RA, Taylor WR. Cellular mechanisms of aortic aneurysm formation. *Circ Res* (2019) 124:607–18. doi: 10.1161/CIRCRESAHA.118.313187

9. Snider JM, You JK, Wang X, Snider AJ, Hallmark B, Zec MM, et al. Group IIA secreted phospholipase A2 is associated with the pathobiology leading to COVID-19 mortality. *J Clin Invest* (2021) 131:e149236. doi: 10.1172/JCI149236

10. Rajkomar A, Dean J, Kohane I. Machine learning in medicine. *N Engl J Med* (2019) 380:1347–58. doi: 10.1056/NEJMc1906060

11. Han L, Askari M, Altman RB, Schmitt SK, Fan J, Bentley JP, et al. Atrial fibrillation burden signature and near-term prediction of stroke: A machine learning analysis. *Circ Cardiovasc Qual Outcomes* (2019) 12:e005595. doi: 10.1161/CIRCOUTCOMES.118.005595

12. Barnes BM, Nelson L, Tighe A, Burghel GJ, Lin IH, Desai S, et al. Distinct transcriptional programs stratify ovarian cancer cell lines into the five major histological subtypes. *Genome Med* (2021) 13:140. doi: 10.1186/s13073-021-00952-5

13. Qi H, Wang F, Tao SC. Proteome microarray technology and application: Higher, wider, and deeper. *Expert Rev Proteomics* (2019) 16:815–27. doi: 10.1080/14789450.2019.1662303

14. Doreille A, Raymond L, Mesnard L. Exome sequencing as part of a multidisciplinary approach to diagnosis. *JAMA* (2020) 324:2445. doi: 10.1001/jama.2020.21506

15. Barrett T, Wilhite SE, Ledoux P, Evangelista C, Kim IF, Tomashevsky M, et al. NCBI GEO: Archive for functional genomics data sets–update. *Nucleic Acids Res* (2013) 41:D991–5. doi: 10.1093/nar/gks1193

16. Biros E, Gäbel G, Moran CS, Schreurs C, Lindeman JH, Walker PJ, et al. Differential gene expression in human abdominal aortic aneurysm and aortic occlusive disease. *Oncotarget* (2015) 6:12984–96. doi: 10.18632/oncotarget.3848

17. Folkersen L, Wågsäter D, Paloschi V, Jackson V, Petrini J, Kurtovic S, et al. Unraveling divergent gene expression profiles in bicuspid and tricuspid aortic valve patients with thoracic aortic dilatation: the ASAP study. *Mol Med* (2011) 17:1365–73. doi: 10.2119/molmed.2011.00286

18. Biros E, Moran CS, Rush CM, Gäbel G, Schreurs C, Lindeman JH, et al. Differential gene expression in the proximal neck of human abdominal aortic aneurysm. *Atherosclerosis* (2014) 233:211–8. doi: 10.1016/j.atherosclerosis.2013.12.017

19. Ritchie ME, Phipson B, Wu D, Hu Y, Law CW, Shi W, et al. Limma powers differential expression analyses for RNA-sequencing and microarray studies. *Nucleic Acids Res* (2015) 43:e47. doi: 10.1093/nar/gkv007

20. Davis S, Meltzer PS. GEOquery: a bridge between the gene expression omnibus (GEO) and BioConductor. *Bioinformatics* (2007) 23:1846–7. doi: 10.1093/bioinformatics/btm254

21. Chen C, Grennan K, Badner J, Zhang D, Gershon E, Jin L, et al. Removing batch effects in analysis of expression microarray data: an evaluation of six batch adjustment methods. *PloS One* (2011) 6:e17238. doi: 10.1371/journal.pone.0017238

22. Ito K, Murphy D. Application of ggplot2 to pharmacometric graphics. *CPT Pharmacometrics Syst Pharmacol* (2013) 2:e79. doi: 10.1038/psp.2013.56

23. Wu T, Hu E, Xu S, Chen M, Guo P, Dai Z, et al. clusterProfiler 4.0: A universal enrichment tool for interpreting omics data. *Innovation (Camb)* (2021) 2:100141. doi: 10.1016/j.xinn.2021.100141

24. Liberzon A, Subramanian A, Pinchback R, Thorvaldsdóttir H, Tamayo P, Mesirov JP. Molecular signatures database (MSigDB) 3.0. *Bioinformatics* (2011) 27:1739–40. doi: 10.1093/bioinformatics/btr260

25. Cai W, van der Laan M. Nonparametric bootstrap inference for the targeted highly adaptive least absolute shrinkage and selection operator (LASSO) estimator. *Int J Biostat* (2020) 16(2):20170070. doi: 10.1515/ijb-2017-0070

26. Nedaie A, Najafi AA. Support vector machine with dirichlet feature mapping. *Neural Netw* (2018) 98:87–101. doi: 10.1016/j.neunet.2017.11.006

27. Newman AM, Liu CL, Green MR, Gentles AJ, Feng W, Xu Y, et al. Robust enumeration of cell subsets from tissue expression profiles. *Nat Methods* (2015) 12:453–7. doi: 10.1038/nmeth.3337

28. Bindea G, Mlecnik B, Tosolini M, Kirilovsky A, Waldner M, Obenauf AC, et al. Spatiotemporal dynamics of intratumoral immune cells reveal the immune landscape in human cancer. *Immunity* (2013) 39:782–95. doi: 10.1016/j.immuni.2013.10.003

29. Bossone E, LaBounty T M, Eagle KA. Acute aortic syndromes: diagnosis and management, an update. *Eur Heart J* (2018) 39:739–749d. doi: 10.1093/eurheartj/ehx319

30. Mayakonda A, Lin DC, Assenov Y, Plass C, Koeffler HP. Maftools: efficient and comprehensive analysis of somatic variants in cancer. *Genome Res* (2018) 28:1747–56. doi: 10.1101/gr.239244.118

31. Reuter JA, Spacek DV, Snyder MP. High-throughput sequencing technologies. *Mol Cell* (2015) 58:586–97. doi: 10.1016/j.molcel.2015.05.004

32. Bülow RD, Dimitrov D, Boor P, Saez-Rodriguez J. How will artificial intelligence and bioinformatics change our understanding of IgA nephropathy in the next decade? *Semin Immunopathol* (2021) 43:739–52. doi: 10.1007/s00281-021-00847-y

33. Deo RC. Machine learning in medicine. *Circulation* (2015) 132:1920–30. doi: 10.1161/CIRCULATIONAHA.115.001593

34. Shen YH, LeMaire SA, Webb NR, Cassis LA, Daugherty A, Lu HS. Aortic aneurysms and dissections series. *Arterioscler Thromb Vasc Biol* (2020) 40:e37–46. doi: 10.1161/ATVBAHA.120.313991

35. Dale MA, Ruhlman MK, Baxter BT. Inflammatory cell phenotypes in AAAs: their role and potential as targets for therapy. *Arterioscler Thromb Vasc Biol* (2015) 35:1746–55. doi: 10.1161/ATVBAHA.115.305269

36. Rizas KD, Ippagunta N, Tilson MD. Immune cells and molecular mediators in the pathogenesis of the abdominal aortic aneurysm. *Cardiol Rev* (2009) 17:201–10. doi: 10.1097/CRD.0b013e3181b04698

37. Pisano C, Balistreri CR, Ricasoli A, Ruvolo G. Cardiovascular disease in ageing: An overview on thoracic aortic aneurysm as an emerging inflammatory disease. *Mediators Inflammation* (2017) 2017:1274034. doi: 10.1155/2017/1274034

38. Bazan JF, Bacon KB, Hardiman G, Wang W, Soo K, Rossi D, et al. A new class of membrane-bound chemokine with a CX3C motif. *Nature* (1997) 385:640–4. doi: 10.1038/385640a0

39. Umehara H, Imai T. Role of fractalkine in leukocyte adhesion and migration and in vascular injury. *Drug News Perspect* (2001) 14:460–4. doi: 10.1358/dnp.2001.14.8.858415

40. Imai T, Hieshima K, Haskell C, Baba M, Nagira M, Nishimura M, et al. Identification and molecular characterization of fractalkine receptor CX3CR1, which mediates both leukocyte migration and adhesion. *Cell* (1997) 91:521–30. doi: 10.1016/s0092-8674(00)80438-9

41. Landsman L, Bar-On L, Zernecke A, Kim KW, Krauthgamer R, Shagdarsuren E, et al. CX3CR1 is required for monocyte homeostasis and atherogenesis by promoting cell survival. *Blood* (2009) 113:963–72. doi: 10.1182/blood-2008-07-170787

42. Schulz C, Schäfer A, Stolla M, Kerstan S, Lorenz M, von Brühl ML, et al. Chemokine fractalkine mediates leukocyte recruitment to inflammatory endothelial cells in flowing whole blood: a critical role for p-selectin expressed on activated platelets. *Circulation* (2007) 116:764–73. doi: 10.1161/CIRCULATIONAHA.107.695189

43. Lucas AD, Bursill C, Guzik TJ, Sadowski J, Channon KM, Greaves DR. Smooth muscle cells in human atherosclerotic plaques express the fractalkine receptor CX3CR1 and undergo chemotaxis to the CX3C chemokine fractalkine (CX3CL1). *Circulation* (2003) 108:2498–504. doi: 10.1161/01.CIR.0000097119.57756.EF

44. Umehara H, Bloom E, Okazaki T, Domae N, Imai T. Fractalkine and vascular injury. *Trends Immunol* (2001) 22:602–7. doi: 10.1016/s1471-4906(01)02051-8

45. Damås JK, Boullier A, Waehre T, Smith C, Sandberg WJ, Green S, et al. Expression of fractalkine (CX3CL1) and its receptor, CX3CR1, is elevated in coronary artery disease and is reduced during statin therapy. *Arterioscler Thromb Vasc Biol* (2005) 25:2567–72. doi: 10.1161/01.ATV.0000190672.36490.7b

46. Nishimura M, Umehara H, Nakayama T, Yoneda O, Hieshima K, Kakizaki M, et al. Dual functions of fractalkine/CX3C ligand 1 in trafficking of perforin +/granzyme b+ cytotoxic effector lymphocytes that are defined by CX3CR1 expression. *J Immunol* (2002) 168:6173–80. doi: 10.4049/jimmunol.168.12.6173

47. Umehara H, Bloom ET, Okazaki T, Nagano Y, Yoshie O, Imai T. Fractalkine in vascular biology: from basic research to clinical disease. *Arterioscler Thromb Vasc Biol* (2004) 24:34–40. doi: 10.1161/01.ATV.0000095360.62479.1F

48. Ludwig A, Berkhout T, Moores K, Groot P, Chapman G. Fractalkine is expressed by smooth muscle cells in response to IFN-gamma and TNF-alpha and is modulated by metalloproteinase activity. *J Immunol* (2002) 168:604–12. doi: 10.4049/jimmunol.168.2.604

49. Pirvulescu MM, Gan AM, Stan D, Simion V, Calin M, Butoi E, et al. Subendothelial resistin enhances monocyte transmigration in a co-culture of human endothelial and smooth muscle cells by mechanisms involving fractalkine, MCP-1 and activation of TLR4 and gi/o proteins signaling. *Int J Biochem Cell Biol* (2014) 50:29–37. doi: 10.1016/j.biocel.2014.01.022

50. Chandrasekar B, Mummidi S, Perla RP, Bysani S, Dulin NO, Liu F, et al. Fractalkine (CX3CL1) stimulated by nuclear factor kappaB (NF-kappaB)-dependent inflammatory signals induces aortic smooth muscle cell proliferation through an autocrine pathway. *Biochem J* (2003) 373:547–58. doi: 10.1042/BJ20030207

51. Hadi T, Boytard L, Silvestro M, Alebrahim D, Jacob S, Feinstein J, et al. Macrophage-derived netrin-1 promotes abdominal aortic aneurysm formation by activating MMP3 in vascular smooth muscle cells. *Nat Commun* (2018) 9:5022. doi: 10.1038/s41467-018-07495-1

52. Petsophonsakul P, Furmanik M, Forsythe R, Dweck M, Schurink GW, Natour E, et al. Role of vascular smooth muscle cell phenotypic switching and calcification in aortic aneurysm formation. *Arterioscler Thromb Vasc Biol* (2019) 39:1351–68. doi: 10.1161/ATVBAHA.119.312787

53. Maguire EM, Pearce SWA, Xiao R, Oo AY, Xiao Q. Matrix metalloproteinase in abdominal aortic aneurysm and aortic dissection. *Pharm (Basel)* (2019) 12:118. doi: 10.3390/ph12030118

54. Cercek M, Matsumoto M, Li H, Chyu KY, Peter A, Shah PK, et al. Autocrine role of vascular IL-15 in intimal thickening. *Biochem Biophys Res Commun* (2006) 339:618–23. doi: 10.1016/j.bbrc.2005.11.050

55. Patel A, Jagadesham VP, Porter KE, Scott DJ, Carding SR. Characterisation of fractalkine/CX3CL1 and fractalkine receptor (CX3CR1) expression in abdominal aortic aneurysm disease. *Eur J Vasc Endovasc Surg* (2008) 36:20–7. doi: 10.1016/j.ejvs.2008.01.014

56. Yang Y, Yuan H, Yang T, Li Y, Gao C, Jiao T, et al. The expression regulatory network in the lung tissue of Tibetan pigs provides insight into hypoxia-sensitive pathways in high-altitude hypoxia. *Front Genet* (2021) 12:691592. doi: 10.3389/fgene.2021.691592

57. Gamberi T, Puglia M, Guidi F, Magherini F, Bini L, Marzocchini R, et al. A proteomic approach to identify plasma proteins in patients with abdominal aortic aneurysm. *Mol Biosyst* (2011) 7:2855–62. doi: 10.1039/c1mb05107e

58. Cao A, Galanello R. Beta-thalassemia. *Genet Med* (2010) 12:61–76. doi: 10.1097/GIM.0b013e3181cd68ed

59. Bobryshev YV, Lord RS. Vascular-associated lymphoid tissue (VALT) involvement in aortic aneurysm. *Atherosclerosis* (2001) 154:15–21. doi: 10.1016/s0021-9150(00)00441-x

60. Yuan Z, Lu Y, Wei J, Wu J, Yang J, Cai Z. Abdominal aortic aneurysm: Roles of inflammatory cells. *Front Immunol* (2020) 11:609161. doi: 10.3389/fimmu.2020.609161

61. Nordon IM, Hinchliffe RJ, Loftus IM, Thompson MM. Pathophysiology and epidemiology of abdominal aortic aneurysms. *Nat Rev Cardiol* (2011) 8:92–102. doi: 10.1038/nrcardio.2010.180

62. Daugherty A, Cassis LA, Lu H. Complex pathologies of angiotensin II-induced abdominal aortic aneurysms. *J Zhejiang Univ Sci B* (2011) 12:624–8. doi: 10.1631/jzus.B1101002

63. Zhou HF, Yan H, Stover CM, Fernandez TM, Rodriguez de Cordoba S, Song WC, et al. Antibody directs properdin-dependent activation of the complement alternative pathway in a mouse model of abdominal aortic aneurysm. *Proc Natl Acad Sci U.S.A.* (2012) 109:E415–22. doi: 10.1073/pnas.1119000109

64. Wu G, Chen T, Shahsafaei A, Hu W, Bronson RT, Shi GP, et al. Complement regulator CD59 protects against angiotensin II-induced abdominal aortic aneurysms in mice. *Circulation* (2010) 121:1338–46. doi: 10.1161/CIRCULATIONAHA.108.844589

65. Zagrapan B, Eilenberg W, Scheuba A, Klopf J, Brandau A, Story J, et al. Complement factor C5a is increased in blood of patients with abdominal aortic aneurysm and has prognostic potential for aneurysm growth. *J Cardiovasc Transl Res* (2021) 14:761–9. doi: 10.1007/s12265-020-10086-5

66. Martin-Ventura JL, Martinez-Lopez D, Roldan-Montero R, Gomez-Guerrero C, Blanco-Colio LM. Role of complement system in pathological remodeling of the vascular wall. *Mol Immunol* (2019) 114:207–15. doi: 10.1016/j.molimm.2019.06.016

67. Sundermann AC, Saum K, Conrad KA, Russell HM, Edwards TL, Mani K, et al. Prognostic value of d-dimer and markers of coagulation for stratification of abdominal aortic aneurysm growth. *Blood Adv* (2018) 2:3088–96. doi: 10.1182/bloodadvances.2017013359

68. Dai J, Louedec L, Philippe M, Michel JB, Houard X. Effect of blocking platelet activation with AZD6140 on development of abdominal aortic aneurysm in a rat aneurysmal model. *J Vasc Surg* (2009) 49:719–27. doi: 10.1016/j.jvs.2008.09.057

69. Touat Z, Ollivier V, Dai J, Huisse MG, Bezeaud A, Sebbag U, et al. Renewal of mural thrombus releases plasma markers and is involved in aortic abdominal aneurysm evolution. *Am J Pathol* (2006) 168:1022–30. doi: 10.2353/ajpath.2006.050868

70. Grzela T, Brawura-Biskupski-Samaha R, Jelenska MM, Szmidt J. Low molecular weight heparin treatment decreases MMP-9 plasma activity in patients with abdominal aortic aneurysm. *Eur J Vasc Endovasc Surg* (2008) 35:159–61. doi: 10.1016/j.ejvs.2007.09.008

71. Li H, Bai S, Ao Q, Wang X, Tian X, Li X, et al. Modulation of immune-inflammatory responses in abdominal aortic aneurysm: Emerging molecular targets. *J Immunol Res* (2018) 2018:7213760. doi: 10.1155/2018/7213760

72. Hendel A, Ang LS, Granville DJ. Inflammaging and proteases in abdominal aortic aneurysm. *Curr Vasc Pharmacol* (2015) 13:95–110. doi: 10.2174/1570161113011503031323 48

73. Curci JA, Thompson RW. Adaptive cellular immunity in aortic aneurysms: cause, consequence, or context? *J Clin Invest* (2004) 114:168–71. doi: 10.1172/JCI22309

74. Meng X, Yang J, Dong M, Zhang K, Tu E, Gao Q, et al. Regulatory T cells in cardiovascular diseases. *Nat Rev Cardiol* (2016) 13:167–79. doi: 10.1038/nrcardio.2015.169

75. Li J, Xia N, Li D, Wen S, Qian S, Lu Y, et al. Aorta regulatory T cells with a tissue-specific phenotype and function promote tissue repair through Tff1 in abdominal aortic aneurysms. *Adv Sci (Weinh)* (2022) 9:e2104338. doi: 10.1002/advs.202104338

76. Tchougounova E, Lundequist A, Fajardo I, Winberg JO, Abrink M, Pejler G. A key role for mast cell chymase in the activation of pro-matrix metalloprotease-9 and pro-matrix metalloprotease-2. *J Biol Chem* (2005) 280:9291–6. doi: 10.1074/jbc.M410396200

77. Sun J, Sukhova GK, Yang M, Wolters PJ, MacFarlane LA, Libby P, et al. Mast cells modulate the pathogenesis of elastase-induced abdominal aortic aneurysms in mice. *J Clin Invest* (2007) 117:3359–68. doi: 10.1172/JCI31311

78. Hiratzka LF, Bakris GL, Beckman JA, Bersin RM, Carr VF, Casey DE, et al. 2010 ACCF/AHA/AATS/ACR/ASA/SCA/SCAI/SIR/STS/SVM guidelines for the diagnosis and management of patients with thoracic aortic disease: a report of the American college of cardiology Foundation/American heart association task force on practice guidelines, American association for thoracic surgery, American college of radiology, American stroke association, society of cardiovascular anesthesiologists, society for cardiovascular angiography and interventions, society of interventional radiology, society of thoracic surgeons, and society for vascular medicine. *Circulation* (2010) 121:e266–369. doi: 10.1161/CIR.0b013e3181d4739e

79. Chou EL, Lindsay ME. The genetics of aortopathies: Hereditary thoracic aortic aneurysms and dissections. *Am J Med Genet C Semin Med Genet* (2020) 184:136–48. doi: 10.1002/ajmg.c.31771

80. Griffith M, Griffith OL, Coffman AC, Weible JV, McMichael JF, Spies NC, et al. DGIdb: mining the druggable genome. *Nat Methods* (2013) 10:1209–10. doi: 10.1038/nmeth.2689

frontiers | Frontiers in Immunology

TYPE Original Research
PUBLISHED 27 October 2022
DOI 10.3389/fimmu.2022.1026416

OPEN ACCESS

EDITED BY
Anette S. B. Wolff,
Haukeland University Hospital, Norway

REVIEWED BY
Marzia Rossato,
University of Verona, Italy
Kristin Tarbell,
Amgen, United States

*CORRESPONDENCE
Alessandra Petrelli
petrelli.alessandra@hsr.it

†These authors have contributed equally to this work and share first authorship

SPECIALTY SECTION
This article was submitted to Autoimmune and Autoinflammatory Disorders : Autoimmune Disorders, a section of the journal Frontiers in Immunology

RECEIVED 23 August 2022
ACCEPTED 11 October 2022
PUBLISHED 27 October 2022

CITATION
Bechi Genzano C, Bezzecchi E, Carnovale D, Mandelli A, Morotti E, Castorani V, Favalli V, Stabilini A, Insalaco V, Ragogna F, Codazzi V, Scotti GM, Del Rosso S, Mazzi BA, De Pellegrin M, Giustina A, Piemonti L, Bosi E, Battaglia M, Morelli MJ, Bonfanti R and Petrelli A (2022) Combined unsupervised and semi-automated supervised analysis of flow cytometry data reveals cellular fingerprint associated with newly diagnosed pediatric type 1 diabetes. *Front. Immunol.* 13:1026416. doi: 10.3389/fimmu.2022.1026416

Combined unsupervised and semi-automated supervised analysis of flow cytometry data reveals cellular fingerprint associated with newly diagnosed pediatric type 1 diabetes

Camillo Bechi Genzano[1†], Eugenia Bezzecchi[1,2†], Debora Carnovale[1], Alessandra Mandelli[1], Elisa Morotti[1,3], Valeria Castorani[1], Valeria Favalli[1,3], Angela Stabilini[1], Vittoria Insalaco[1], Francesca Ragogna[1], Valentina Codazzi[1], Giulia Maria Scotti[1], Stefania Del Rosso[5], Benedetta Allegra Mazzi[6], Maurizio De Pellegrin[7], Andrea Giustina[8,9], Lorenzo Piemonti[1,9], Emanuele Bosi[1,4,9], Manuela Battaglia[1], Marco J. Morelli[2], Riccardo Bonfanti[1,3,9] and Alessandra Petrelli[1*]

[1]Diabetes Research Institute, IRCCS Ospedale San Raffaele, Milan, Italy, [2]Center for Omics Sciences, IRCCS Ospedale San Raffaele, Milan, Italy, [3]Department of Pediatrics, IRCCS Ospedale San Raffaele, Milan, Italy, [4]Department of General Medicine, Diabetes and Endocrinology, IRCCS Ospedale San Raffaele, Milan, Italy, [5]Laboratory Medicine, Autoimmunity Section, IRCCS Ospedale San Raffaele, Milan, Italy, [6]Immuno-Hematology and Transfusion Medicine (ITMS), IRCCS Ospedale San Raffaele, Milan, Italy, [7]Pediatric Orthopedic and Traumatology Unit, IRCCS Ospedale San Raffaele, Milan, Italy, [8]Institute of Endocrine and Metabolic Sciences, IRCCS Ospedale San Raffaele, Milan, Italy, [9]Università Vita-Salute San Raffaele, Milan, Italy

An unbiased and replicable profiling of type 1 diabetes (T1D)-specific circulating immunome at disease onset has yet to be identified due to experimental and patient selection limitations. Multicolor flow cytometry was performed on whole blood from a pediatric cohort of 107 patients with new-onset T1D, 85 relatives of T1D patients with 0-1 islet autoantibodies (pre-T1D_LR), 58 patients with celiac disease or autoimmune thyroiditis (CD_THY) and 76 healthy controls (HC). Unsupervised clustering of flow cytometry data, validated by a

semi-automated gating strategy, confirmed previous findings showing selective increase of naïve CD4 T cells and plasmacytoid DCs, and revealed a decrease in CD56^{bright}NK cells in T1D. Furthermore, a non-selective decrease of CD3^{+}CD56^{+} regulatory T cells was observed in T1D. The frequency of naïve CD4 T cells at disease onset was associated with partial remission, while it was found unaltered in the pre-symptomatic stages of the disease. Thanks to a broad cohort of pediatric individuals and the implementation of unbiased approaches for the analysis of flow cytometry data, here we determined the circulating immune fingerprint of newly diagnosed pediatric T1D and provide a reference dataset to be exploited for validation or discovery purposes to unravel the pathogenesis of T1D.

KEYWORDS

type 1 diabetes, fingerprints, immune markers, pediatric diabetes, flow cytometry, computational biology

Introduction

Type 1 diabetes is a chronic autoimmune disease where the interaction between genes and environment shapes an immune-mediated attack of pancreatic β cells, eventually leading to chronic hyperglycemia and lifelong insulin dependence (1–3). Islet autoantibodies (Aabs) (4) mark the development of autoimmunity, so that the presence of ≥2 Aab in relatives of patients with type 1 diabetes is a highly sensitive predictor of the development of symptomatic diabetes (5), with a risk rising to almost 100% in pediatric subjects (6). However, while islet Aabs appear to be innocent bystanders in the development of type 1 diabetes, the chronic damage of insulin-producing β cells has historically been attributed to autoreactive T cells (7).

The development of type 1 diabetes has been associated with altered frequency and phenotype of both innate and adaptive immune cells (8), with a prominent role ascribed to subpopulations such as monocytes, dendritic cells (DCs), natural killer cells (NK cells), B cells and T cells, including regulatory T cells (Tregs) (9–15). However, despite numerous reports showing alterations of the circulating immune profile in patients with newly diagnosed type 1 diabetes, the technical limitations of cell analysis techniques may have prevented the identification of clinically relevant immune cell subsets with a "pro-diabetogenic" potential. Indeed, analysis of data obtained with multiparameter flow cytometry can be complex, as they are operator-dependent, ultimately affecting the quality and type of results. Furthermore, previous studies often lack proper control populations, preferring age and sex-matched healthy donors rather than relatives of patients with type 1 diabetes without persistent autoimmunity—but with a common genetic background— or patients with other autoimmune diseases. All these methodological biases have contributed to the generation of contradictory results and lack of data replicability.

In the present study, by validating unsupervised analysis of flow cytometry data with a semi-automated gating strategy and including proper control populations, we identify the peripheral cellular fingerprint of pediatric patients with newly diagnosed type 1 diabetes. Furthermore, we show that the frequency of naïve (N) CD4 T cells at disease onset is associated with partial remission, thus playing a potential role in a later stage of the autoimmune response.

Materials and methods

Subjects and data collection

A cohort of 326 five to eighteen-year-old children was enrolled at IRCCS Ospedale San Raffaele (OSR) from September 2018 to June 2021. The subject population was distributed as follows: 107 patients with newly diagnosed type 1 diabetes (T1D); 85 relatives of patients with type 1 diabetes (pre-T1D_LR) defined at low-risk of developing the disease as 0 or 1 islet Aab were detected; 58 patients with celiac disease or autoimmune thyroiditis (CD_THY) and 76 healthy controls (HC). The study was approved by the San Raffaele Hospital Ethics Committee (protocol TIGET004-DRI003). Table 1 describes the demographics and clinical characteristics of the four groups of individuals enrolled in this study. Exclusion criteria for the participation to the study were: age <5 and >18 years, antibiotic therapy in progress or concluded in the last 10 days, signs of infection (fever, cough, rhinitis) in the last 2 weeks. Children diagnosed with type 1 diabetes were hospitalized in the

TABLE 1 Characteristics of the study cohort.

	HC N=76	CD_THY N=58 (29 CD, 29 THY)	preT1D_LR N=85	T1D N=107
Age (years) (median - IQR)	13.8 (12.7 -14.9)	12.6 (9.8 -14.8)	12.9 (10.8 -15.5)	11.0 (9.0 -13.4)
Gender (M/F)	41/35 M=54%	16/42 M=28%	43/42 M=51%	66/41 M=62%
BMIp (median - IQR)	64.9 (22.9-77.83)	41.6 (23.7-68.3)	72.4 (30.95-82.72)	42.0 (6.4-73.1)
HbA1c (mmol/L) (median - IQR)	NA	NA	NA	103.0 (87.0-117.0)
n. of islet Aabs	0 Aab=74/76 1 Aab=2/76	0 Aab=50/53 1 Aab=2/53 2 Aab=1/53	0 Aab=77/85 1 Aab=8/85	0 Aab=3/107 1 Aab=16/107 2 Aab=32/107 >3 Aab=56/107
Anti-TPO	NA	10/11 THY 1/22 CD	NA	16/107
Anti-TG	0/59	1/7 THY 26/29 CD	2/84	15/107
HLA_DR3 and/or DR4	9/54	27/35	48/85	73/85
WBC (10x3 ul) (median - IQR)	6.1 (5.1-7.5)	6.0 (5.2-7.1)	6.5 (5.7-8.0)	5.7 (4.8-6.6)
Neutrophils (median - IQR)	3.0 (2.4-4.0)	3.1 (2.4-3.6)	3.3 (2.6-4.2)	2.3 (1.8-2.8)
Monocytes (median - IQR)	0.5 (0.4-0.6)	0.5 (0.4-0.6)	0.5 (0.5-0.62)	0.50 (0.40-0.59)
Lymphocytes (median - IQR)	2.2 (1.9-2.7)	2.2 (1.7-2.8)	2.5 (2.0-3.0)	2.6 (2.10-3.05)

Clinical and laboratory characteristics of healthy controls (HC), subjects with celiac or thyroid diseases (CD_THY), relatives of T1D patients with 0-1 autoantibodies (preT1D_LR), and subjects with type 1 diabetes (T1D). WBC, Neutrophils, Lymphocytes, Monocytes are expressed as 10x3/ul. BMIp, Body Mass Index for age percentile; Aabs, Autoantibodies; TPO, Thyroid peroxidase; TG, Transglutaminase; WBC, White blood cells; NA, not available.

Pediatric Department of OSR; blood samples were collected between 5 and 10 days after diagnosis. First- and second degree relatives of patients with type 1 diabetes with <2 detectable Aabs, which confers a low risk of developing the disease (16), were enrolled in this study. These individuals were enrolled in the Type 1 Diabetes TrialNet Pathway to Prevention Trial (TN01) (17) at the TrialNet Clinical Center of the San Raffaele Hospital. The complete TN01 protocol is available online (18). The study was approved by the OSR Ethics Committee (IRB# NHPROT32803-TN01). Seventy-six healthy non-diabetic children with no family history for type 1 diabetes were recruited at the pediatric Day hospital and Day surgery facilities of OSR, where they were admitted for suspected growth disorders or to undergo surgery for congenital diseases (i.e., flatfeet or hallux valgus). Fifty-eight children previously diagnosed with celiac disease (n=29) or autoimmune thyroiditis (n=29) who had a follow-up visit at the pediatric outpatient clinic of OSR were enrolled in this study. Detection of the islet Aabs GADA, IA2, ICA, mIAA, and ZnT8 was performed on subjects from all groups. The partial clinical remission of type 1 diabetes was assessed in 58 patients 12.2 months (IQR 11.1-13.2) after disease onset, using the insulin dose adjusted HbA1c (IDAA1c) calculated as HbA1c (%) + 4×insulin dose (U/kg per 24 hours); an IDAA1c equal to or less than 9 indicates the partial remission period (19). For the longitudinal analysis of relatives of patients with type 1 diabetes with pre-symptomatic stages of the disease, 2 groups of individuals enrolled in the TN01 trial who had cryopreserved PBMCs available in the local biobank were selected: 8 individuals who were Stage 0 (as they had 0 or 1 Aab) at T0 observation and persisted in Stage 0 at T1 observation; and 7 individuals that from Stage 0 at T0 transitioned to Stage ≥1 at T1 – i.e., developed two or more Aabs. Individuals from the two groups were sex- and age-matched (data not shown).

Preparation of cells for flow cytometry

Whole blood was collected into a Vacuette® blood collection tube with ACD-B anticoagulant solution (Greiner). After red blood cell lysis, the sample was washed and stained with a mix of monoclonal antibodies based on the specific panel. The list of anti-human monoclonal antibodies, including information on the company catalogue number, clone and concentration used for our assays is provided in Supplementary Table 1. Five panels of antibodies were designed and labelled as T cells, T&NK cells, B cells, Tregs and DCs/monos (Supplementary Figure 1A) encompassing main subsets of T cells, NK cells, B cells, Tregs, DCs and monocytes detected using 26 surface markers and the intracellular marker forkhead box P3 (FoxP3); for the Treg panel, intracellular staining was performed after fixation and permeabilization. The five panels were performed on all the blood samples; however, some samples are missing individual values due to technical errors, as indicated in Supplementary Figure 1B. In the longitudinal analysis, N CD4 T cells were identified using the following markers: CD3, CD4, CD45RA and CCR7. Cells were acquired on a BD FACSCanto-II flow cytometer equipped with FACSDiva software (Becton Dickinson, Franklin Lakes, NJ) within 24 hours. Rainbow calibration particles (Spherotech Inc., Lake Forest, IL) were

used to calibrate and normalize acquisition settings in each experiment.

Unsupervised clustering and semi-automated supervised gating

Unsupervised analysis and visual representation of cell populations was realized using the FlowSOM algorithm (20), included in the CyTOF/CATALYST pipeline (version 1.14.1) (21). Clusters showing similar marker expression profiles were manually merged. Collectively we identified 52 cell clusters, including 5 unclassified and 1 duplicate cluster (Supplementary Figure 2 A-E). Next, for data visualization, we applied the non-linear dimensionality reduction technique UMAP to the lineage marker levels, selecting a maximum of 500 cells per sample, using the *runDR()* function included in CyTOF workflow (22). To validate unsupervised clustering results, and to minimize manual biases, we set up a semi-automated supervised gating strategy using the OpenCyto R package (23) (gating strategies are shown in Supplementary Figures 3-4). Methodological details regarding unsupervised clustering and semi-automated supervised gating are contained in the Supplemental Material.

Statistics

Cell populations were compared between the four groups using a linear model by adding age, sex and operator variability as covariates. P-values were determined by performing the multiple pairwise-comparisons with Tukey *post-hoc* test, using the function glht() in multcomp R package (version 1.4-19). The correlation between the frequencies of cell populations identified through unsupervised and semi-automated supervised analysis was performed using the Spearman's rank-order correlation. Principal component analysis (PCA) (24) was performed on the circulating immunome, according to the frequencies of the 46 immunological populations identified by the unsupervised analysis (excluding unclassified and duplicate clusters). In all presented boxplots, medians are shown. The "hinges" represent the first and third quartile. The "whiskers" are the smallest and largest values without considering the outliers. To assess the frequency of $CD3^+CD56^+$ regulatory T cells, P-values were calculated by performing Students T test and Tukey *post-hoc* test for pairwise and multiple comparison respectively. A receiver operating characteristic (ROC) curve based on binary logistic regression was performed on 58 T1D subject to assess the predictive potential of the baseline frequency of N CD4 T cells on partial remission. In the longitudinal analysis, the Wilcoxon matched-pairs signed ranks test was used to analyze differences between paired samples. Statistical analyses were performed in R environment (version 4.0.3) and plotting was done using the ggplot2 R package (version 3.3.6). P-values less than 0.05 were regarded as statistically significant.

Results

Unsupervised clustering and semi-automated supervised analysis show an increase of N CD4 T cells and pDCs and a decrease of $CD56^{bright}$ NK cells in newly diagnosed type 1 diabetes

Unsupervised and semi-automated supervised analyses of five flow cytometry panels designed for the characterization of T cells, B cells, NK cells, DCs and monocytes were performed on whole blood of pediatric newly diagnosed T1D patients and on HC, CD_THY and pre-T1D_LR as control populations. Figure 1 illustrates the experimental workflow of the study. Unsupervised analysis allowed the identification of 46 immune cell clusters, whose frequency within HC is shown in Table 2. A very high overall correlation (r = 0.94) was found between unsupervised computational clustering and semi-automated analysis (Supplementary Figure 5A), with only 5 cell populations – i.e., $CD45RA^-$ $FoxP3^{lo}$ non Tregs, CM CD4 T cells, $CD45RA^+$ $FoxP3^{lo}$ resting Tregs, unswitched memory B cells and non-classical monocytes – displaying a correlation coefficient < 0.5 (Supplementary Figure 5B).

The T cell panel revealed 12 clusters (Figure 2A and Supplementary Figure 2A, bottom panel), with both unsupervised and semi-automated supervised analysis showing increased frequency of N CD4 T cells in T1D compared to the other groups (Figure 2B). The T&NK cell panel revealed 15 clusters (Figure 2C and Supplementary Figure 2B, bottom panel), showing a decreased frequency of $CD56^{bright}$ NK cells specifically associated with T1D in both unsupervised and semi-automated supervised analysis (Figure 2D). The DCs/monos panel, which revealed 7 clusters (Figure 2E and Supplementary Figure 2C, bottom panel), showed an enrichment of plasmacytoid Dendritic Cells (pDCs) in T1D compared to other groups both using unsupervised and semi-automated supervised analysis (Figure 2F). The B cell panel revealed 11 clusters (Supplementary Figure 2D, bottom panel and Supplementary Figure 6A). Unsupervised analysis showed a specific reduction of transitional B cells in T1D, which was not confirmed by semi-automated supervised analysis in the comparison with pre-T1D_LR individuals (Supplementary Figure 6B). Finally, the Treg panel revealed 7 clusters (Supplementary Figure 2E, bottom panel); however, no differential representation of any of these clusters was found between the 4 groups. The frequency of all the remaining cell clusters identified with unsupervised analysis is shown in Supplementary Figure 7.

To conclude, unsupervised clustering, validated by a highly consistent semi-automated gating analysis, shows

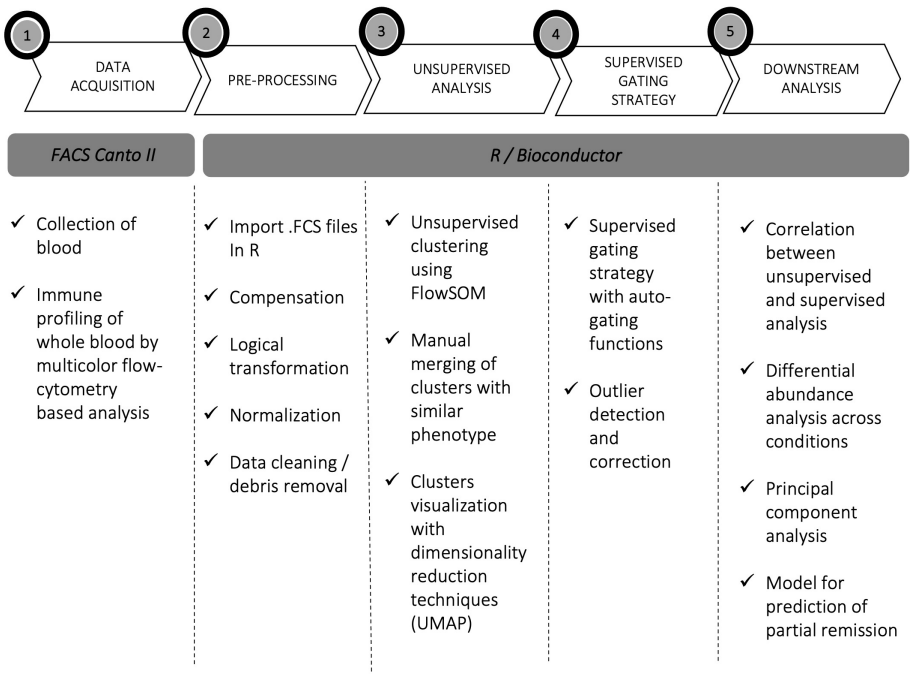

FIGURE 1
Experimental workflow. Experimental workflow of the study: acquisition (1), pre-processing (2), processing (3, 4), and downstream data analysis (5).

that the specific circulating immune profile of newly diagnosed type 1 diabetes is characterized by increased frequency of N CD4 T cells and pDCs, and decreased $CD56^{bright}$ NK cells.

Combined unsupervised and semi-automated supervised analyses show the circulating immune signature shared between type 1 diabetes and other autoimmune diseases

We found that specific cell clusters were consensually altered in both T1D and CD_THY as compared to HC and pre-T1D_LR, thus marking a feature of multiple autoimmune diseases rather than T1D. Unsupervised clustering showed a consensual reduction of EM CD8 T cells (Figure 3A) and $CD56^{dim}$ NK cells (Figure 3B), accompanied by an increase of $CD27^{+}CD28^{+}$ CD4 T cells (Figure 3C) in both T1D and CD_THY, which was confirmed by semi-automated supervised analysis. These data allow the identification of a circulating immune signature not exclusively associated with type 1 diabetes, but rather shared by other autoimmune diseases such as celiac disease and autoimmune thyroiditis.

T_{R3-56} cells are non-selectively reduced in newly diagnosed type 1 diabetes

We leveraged our dataset as a tool to validate previously reported data by testing the frequency of $CD3^{+}CD56^{+}$ regulatory T cells (25), defined as T_{R3-56} cells, recently described to be reduced in patients with newly diagnosed type 1 diabetes compared to HC. Unsupervised analysis allowed the identification of 2 clusters co-expressing CD3 and CD56 (Supplementary Figure 2B, upper panel), one also expressing CD8, CD27 and CD28 and the other CD8 and CD27, which were merged in a single cluster called $CD3^{+}CD56^{+}$ (Supplementary Figure 2B, lower panel). No difference in the frequency of this cluster was evident between the 4 groups (Supplementary Figure 7). The semi-automated analysis, using the same gating strategy as in the original work (25), confirmed that the frequency of T_{R3-56} cells was reduced in T1D compared to HC also in our cohort, (Figure 4A), showing similar phenotypical characteristics, such as the expression level of CD4 and CD8 (Figure 4B). However, although differences between HC and T1D persisted when other control groups were included in the analysis, T_{R3-56} cells were found non-selectively decreased in type 1 diabetes as no differences could be detected with CD_THY or pre-T1D_LR (Figure 4C).

10.3389/fimmu.2022.1026416

TABLE 2 Cell frequencies in healthy children.

Parent	Population	1st Qu.	Median	3rd Qu.	Mean
Lymphocytes	T cells	71.65%	75.67%	79.11%	74.99%
	B cells	10.93%	13.42%	17.12%	13.82%
Lympho-monocytes	HLADR+LIN-	10.55%	13.39%	16.15%	14.11%
T cells	CD4 T	54.21%	59.73%	65.17%	59.47%
	CD8 T	24.27%	28.46%	32.03%	28.49%
	CD4+ CD8+ T	0.26%	0.38%	0.54%	0.50%
	CD4- CD8- T	8.55%	10.68%	14.27%	11.73%
	CD3+ CD56+ T	1.93%	3.10%	5.02%	4.19%
CD4 T cells	CM CD4 T	9.43%	11.83%	13.69%	11.85%
	EM CD4 T	17.70%	22.30%	27.86%	23.74%
	N CD4 T	52.56%	59.97%	67.26%	58.94%
	TEMRA CD4 T	3.61%	5.03%	6.30%	5.44%
	CD127- CD45RA+ CD4 T	1.01%	1.73%	2.49%	1.95%
	CD127+ CD45RA- CD4 T	25.02%	30.98%	39.04%	32.29%
	CD127+ CD45RA+ CD4 T	57.09%	63.50%	69.95%	62.44%
	CD45RA- Foxp3hi activated Treg	0.61%	1.33%	1.74%	1.33%
	CD45RA- FoxP3lo non Treg	1.43%	1.86%	2.57%	1.97%
	CD45RA+ FoxP3lo resting Treg	1.68%	2.36%	2.96%	2.58%
	CD27- CD28- CD4 T	0.02%	0.04%	0.27%	0.48%
	CD27- CD28+ CD4 T	2.83%	4.66%	6.52%	5.00%
	CD27+ CD28+ CD4 T	93.34%	95.24%	96.58%	94.38%
EM CD4 T cells	EM CD57+ CD4 T	3.70%	5.56%	7.16%	6.11%
	EM PD1+ CD4 T	10.14%	16.23%	20.21%	15.78%
	PD1+ CD57+ EM CD4 T	1.12%	1.51%	2.50%	2.00%
TEMRA CD4 T cellsT cells	TEMRA CD57+ CD4 T	5.40%	8.32%	13.07%	10.52%
CD8 T cells	EM CD8 T	21.18%	26.10%	32.56%	27.18%
	N CD8 T	38.50%	48.48%	57.69%	47.20%
	TEMRA CD8 T	16.05%	20.03%	27.97%	22.47%
	CD27- CD28- CD8 T	1.84%	4.35%	10.00%	7.50%
	CD27- CD28+ CD8 T	0.82%	1.41%	2.26%	2.11%
	CD27+ CD28- CD8 T	9.42%	14.33%	19.01%	15.85%
	CD27+ CD28+ CD8 T	68.04%	77.64%	84.29%	74.52%
EM CD8 T cells	EM CD57+ CD8 T	7.87%	12.49%	18.98%	14.63%
	EM PD1+ CD8 T	6.77%	12.08%	18.09%	14.67%
	PD1+ CD57+ EM CD8 TCD8 T	1.39%	2.44%	4.65%	3.59%
TEMRA CD8 T cells	TEMRA CD57+ CD8 T	12.88%	20.37%	34.62%	25.18%
CD27+ CD28+ CD8 T cells	CD27+ CD28+ CD69+ CD8 T	2.19%	3.24%	6.61%	5.95%
B cells	Double-negative-1 B	1.31%	1.66%	2.20%	1.92%
Double-negative-1 B	Double-negative-2 B	11.10%	17.72%	26.13%	20.34%
IgD+ CD27- B cells	IgM-low naïve B	60.51%	66.46%	70.19%	64.85%
	Naïve B	29.81%	33.54%	39.49%	35.15%
IgM+ IgD+ B cells	Unswitched mem B	1.91%	3.35%	4.97%	3.63%
CD27- IgM+ IgD+ B cellsB cells	Transitional B	7.47%	8.00%	8.71%	7.92%
IgM- IgD+ B cells	IgD only switched mem Bmem B	12.85%	18.44%	32.02%	23.01%
IgM- IgD- B cells	Early plasmablasts	1.50%	2.30%	3.05%	2.60%
	Plasmablasts	3.32%	4.80%	7.68%	5.85%
	Switched mem B	64.78%	69.39%	77.40%	70.13%
CD3- Lymphocytes	$CD56^{dim}$ NK	30.64%	41.09%	49.35%	39.46%

(Continued)

TABLE 2 Continued

Parent	Population	1st Qu.	Median	3rd Qu.	Mean
	$CD56^{bright}$ NK	2.33%	3.37%	4.40%	3.59%
$CD56^{dim}$ NK	CD69+ $CD56^{dim}$ NK	2.51%	3.48%	4.93%	5.06%
$CD56^{bright}$ NK	CD69+ $CD56^{bright}$ NK	24.82%	28.02%	31.18%	29.46%
CD3+ CD56+ T cells	CD8+ CD3+ CD56+ T	47.41%	55.59%	71.09%	58.48%
CD14- HLADR+ LIN-	mDCs	41.07%	53.63%	63.95%	52.21%
	pDCs	8.57%	12.41%	15.72%	12.79%
mDCs	CD16 mDCs	58.35%	66.47%	74.12%	65.13%
	CD1c CD16 mDCs	2.87%	5.12%	8.02%	5.57%
	CD1c mDCs	10.46%	16.66%	21.49%	17.44%
HLADR+ LIN-	classical monocytes	42.50%	62.02%	74.95%	59.16%
	intermediate monocytes	3.90%	8.21%	19.69%	12.58%
	non-classical monocytes	6.89%	10.02%	14.61%	10.76%

Cell frequencies (% of parent) measured by unsupervised clustering within the healthy children cohort (HC, n = 76).

Age and peripheral lymphocyte count, but not diabetic ketoacidosis, drive a slight segregation of the circulating immunome in newly diagnosed pediatric type 1 diabetes

As we expected to observe a segregation of the circulating immunome of T1D patients compared to other groups, we performed a principal component analysis (PCA) (24) on the 46 detected clusters. Patients with T1D showed a weak segregation from other groups (which was more evident in the PC 1) explaining only 13% of the total variance (Figure 5A). Then, we tested whether, in newly diagnosed T1D patients, the following variables could affect the variance of the circulating immunome: age, sex, BMI percentile, type of Aab, white blood cell count, number of lymphocytes, monocytes and neutrophils, presence of diabetic ketoacidosis (DKA), family history of type 1 diabetes or other autoimmune diseases and presence of HLA-DR3 and/or DR4. We found that age (> or < the median, i.e., 11.0 years, Figure 5B) and lymphocyte count (> or < the median, i.e., 2.6 $\times 10^3$ cells/μL, Figure 5C), but not DKA (Figure 5D) or any the other tested parameters (data not shown), drove a slight, although evident, segregation of the circulating immunome.

Frequency of N CD4 T cells at disease onset is associated with partial remission

To determine whether immune cell subsets found to be altered in newly diagnosed T1D may have a pathogenic potential, we explored their relationship with partial remission. The IDAA1c estimates residual beta cell function, with IDAA1C ≤9 considered as surrogate marker of partial remission. We found that the frequency of N CD4 T cells, but not pDC or $CD56^{bright}$ NK cells, was increased at disease onset in individuals with IDAA1C >9 at the 12-month follow-up visit compared to those with IDAA1C ≤9 (Figure 4E). Notably, this was independent of age, as the age range of T1D patients with IDAA1C ≤9 vs. >9 was similar (Figure 4F). We also found that N CD4 T cells show the ability, albeit mild, to predict partial remission (AUC 0.68), indicating a potential biological relevance in symptomatic pediatric type 1 diabetes (Figure 4G). To test the possible involvement of N CD4 T cells in early disease stages, their frequency was tested in relatives of patients with type 1 diabetes who transitioned from Stage 0 (at T0) to Stage≥1 (at T1) and in a cohort of age and sex-matched relatives who maintained the Stage 0 status both at T0 and T1. No difference in the time span between T0 and T1 was observed between the two groups of relatives (i.e., mean of 2.5 years for Stage 0-T0 to Stage 0-T1 vs. mean of 2.7 years for Stage 0-T0 to Stage ≥1-T1, *ns*). Supervised analysis showed that the transition through pre-symptomatic stages of type 1 diabetes is not associated with a change in the frequency of N CD4 T cells (Figure 4H), indicating that this cell subset may be a player of the late phase of the autoimmune response associated with type 1 diabetes.

Discussion

In this study we unbiasedly identified the circulating immune fingerprint of pediatric patients with newly diagnosed type 1 diabetes compared to different control groups, including healthy controls, relatives with a low-risk of developing type 1 diabetes and patients with celiac disease and thyroiditis. We employed one of the most advanced (26), widely used (27), unsupervised clustering technique for the analysis of multiparameter flow cytometry data and validated the results with a fast and reproducible semi-automated gating method (26). Indeed, the pipelined semi-automated supervised analysis implemented in this study was highly reliable in reproducing

10.3389/fimmu.2022.1026416

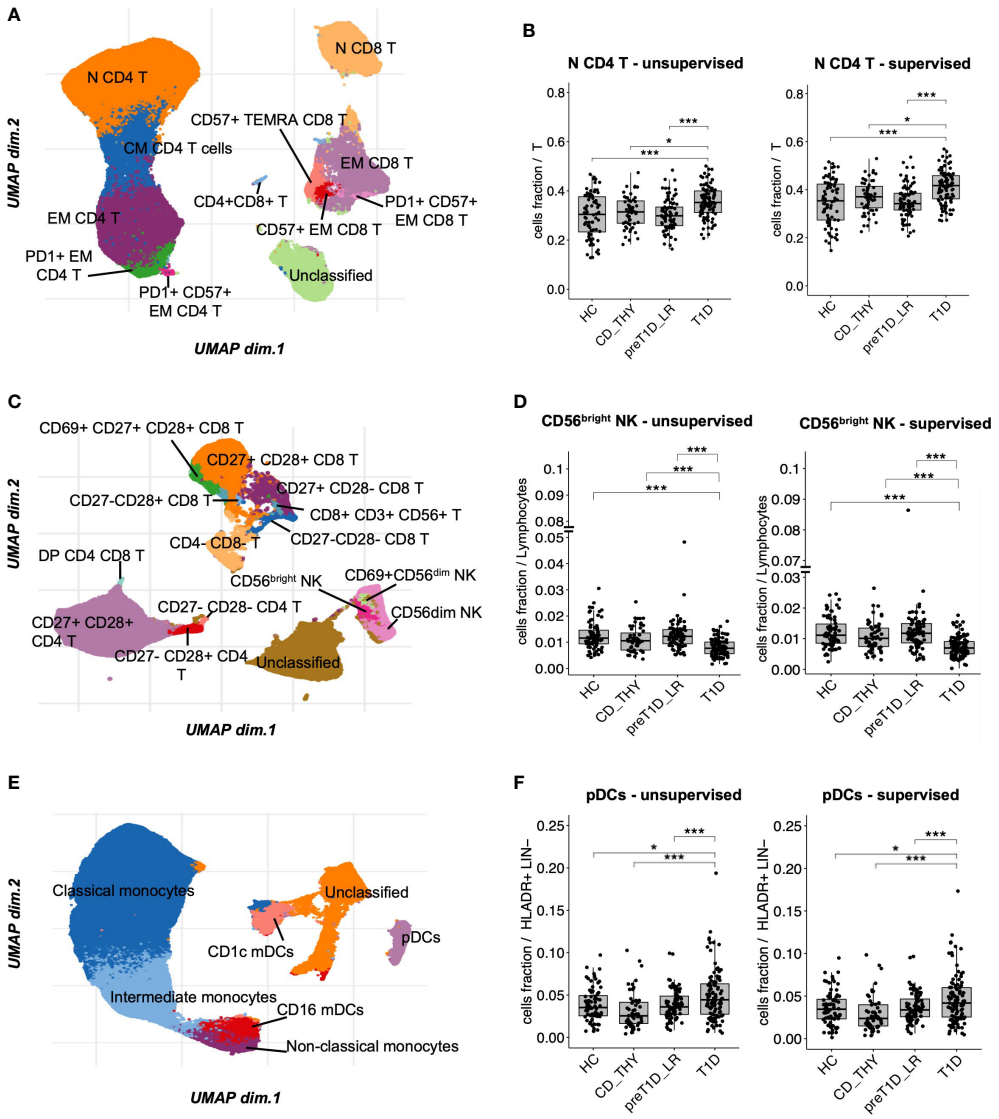

FIGURE 2
Unsupervised clustering shows increased frequency of N CD4 T cells and pDCs, and reduced frequency of CD56bright NK cells in T1D. UMAP data visualization of the cell clusters identified in the T cell **(A)**, T&NK cell **(C)** and DCs/monos **(E)** panels. Cell clusters differentially represented in T1D compared to all other groups in the T cell **(B)**, T&NK cell **(D)** and DC/mono **(F)** panels. HC, healthy controls; CD_THY, celiac or thyroid diseases; preT1D_LR, relatives with 0-1 autoantibodies; T1D, type 1 diabetes. Significant differences were determined by post hoc Tukey's test performed on the linear regression model with age, sex, and technician as covariates (*p < 0.05, ***p < 0.001).

results of the unsupervised clustering (r=0.94) for the vast majority of the cell populations–including rare cell subsets. The poorest correlations were observed in cell populations expressed as a smear, without a clear-cut discrimination between the negative and the positive edge. The interpretation of markers expressed as a continuous is subtle in flow cytometry data analysis and clustering machine-learning-based algorithms are in development to address this issue (28).

Three immune cell subsets, i.e. N CD4 T cells, pDCs and CD56^{bright} NK cells, were found differentially represented between new-onset type 1 diabetes and all other groups in both the analysis. Increased circulating frequency of N CD4 T cells has already been described by previous reports (8, 12); noteworthy, N CD4 T cells have been shown to be heterogeneous in phenotype, function, dynamics, gene expression profile and differentiation status, covering a whole spectrum of cells with different properties (29). Indeed, it is well-established that the major genetic determinants of type 1 diabetes risk are polymorphisms of class II HLA genes encoding DQ and DR (30), thus indicating a leading

10.3389/fimmu.2022.1026416

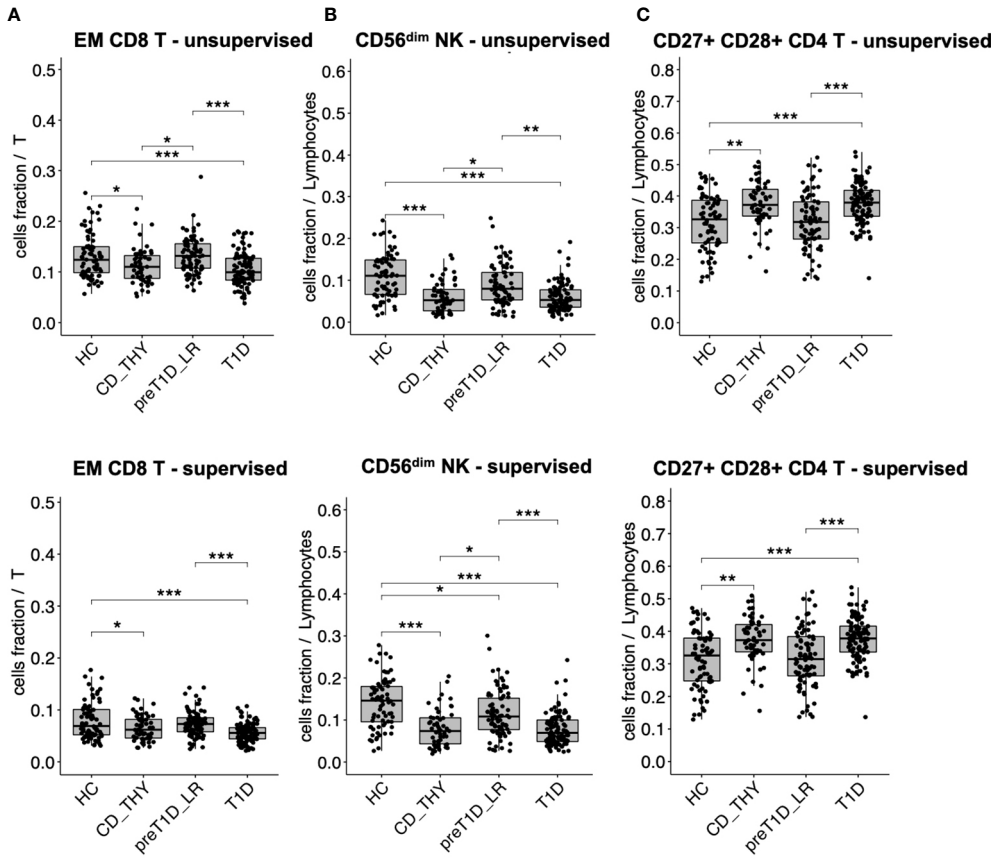

FIGURE 3
Cell populations altered in multiple autoimmune diseases. Cell subsets showing a reduced **(A, B)** or increased **(C)** frequency in the circulation of both patients with T1D and with celiac disease or autoimmune thyroiditis. HC, healthy controls; CD_THY, celiac or thyroid diseases; preT1D_LR, relatives with 0-1 autoantibodies; T1D, type 1 diabetes. Significant differences were determined by post hoc Tukey's test performed on the linear regression model with age, sex, and technician as covariates (*p < 0.05, **p < 0.01, ***p < 0.001).

contribution of the interactions between CD4 T cells and antigen presenting cells; our results suggest that the phenotypic and functional characterization of N CD4 T cells would allow the identification of candidate subsets with potential pathogenicity in the context of human type 1 diabetes. This hypothesis was further corroborated by the evidence that the frequency of N CD4 T cells at disease onset was associated with partial remission, independently of age, confirming, in a broader cohort, the observations of a recent report (31), and others associating the frequency of CD4 memory T cells with a longer partial remission (32). However, N CD4 T cell frequency was found unaltered in pre-symptomatic stages of type 1 diabetes, suggesting that the role of these cells may be crucial in a later phase of the autoimmune response.

Plasmacytoid DCs are mainly recognized for their swift and massive production of type I interferon (33) and are capable of activating several cell subsets, such as CD8 cytotoxic T cells and regulatory T cells (34, 35), and of stimulating B-cell activation, differentiation into plasma cells, and antibody production (36, 37). Our data confirm previous observations showing that the balance of peripheral dendritic cells is deeply altered at diabetes diagnosis, with a markedly elevated proportion of pDCs and reduction of mDCs compared with control subjects (38), and that pDCs are not increased in other autoimmune diseases (39, 40).

Although a small but distinct reduction in NK cell frequency has previously been found both in patients with other autoimmune diseases (41, 42) and with recent-onset diabetes (10), no differences were described in the repartition of the $CD56^{high}/CD16^{-}$ and $CD56^{dim}/CD16^{+}$ NK cell subsets (10). Here, we show a selective decrease of the $CD56^{bright}$ NK cell subset in newly diagnosed pediatric type 1 diabetes. The distribution of immune cells in peripheral blood tells only part of the story, as resident cell subsets located in the pancreas are the relevant players in the pathogenesis of type 1 diabetes. However, these changes in the blood could reflect similar

10.3389/fimmu.2022.1026416

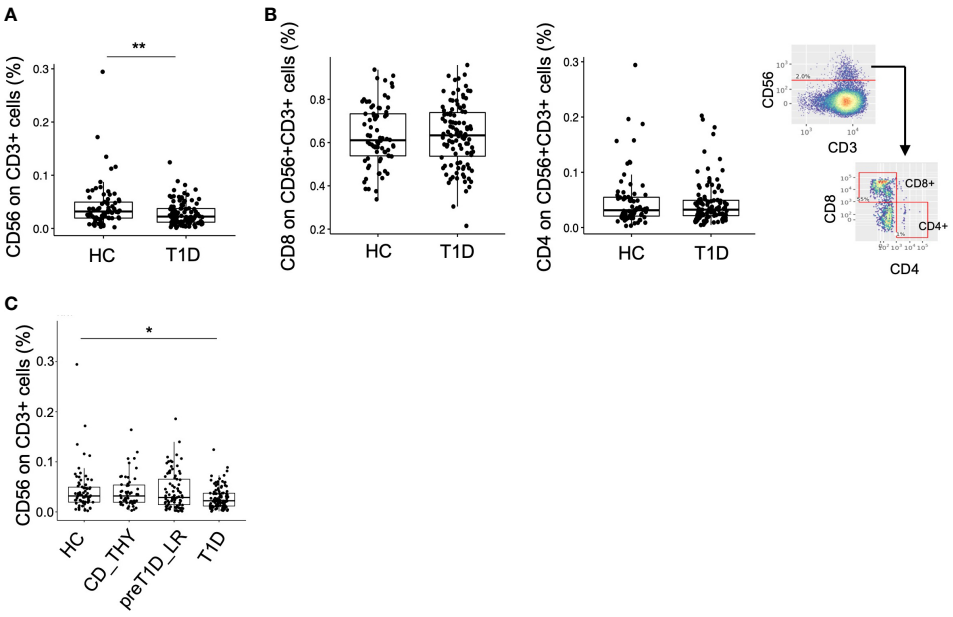

FIGURE 4
Validation of the TR3-56 cell biomarker in our cohort. Frequency of $CD56^{+}CD3^{+}$ cells (namely $T_{R3\text{-}56}$ cells) in HC and T1D using the semi-automated gating strategy **(A)**. Frequency of CD8 and CD4 on $TR_{3\text{-}56}$ cells and representative semi-automated gating strategy employed for the analysis. **(B)**. Frequency of $T_{R3\text{-}56}$ cells in HC, CD_THY, preT1D_LR and T1D **(C)**. Significant differences were determined by Student's t-test for pairwise comparisons and by Tukey *post-hoc* test on the linear regression model for multiple comparisons (*p < 0.05, **p < 0.01).

alterations in the tissue or could be the result of a relative sequestration/migration of specific populations into the pancreas. This may be the case of $CD56^{bright}$ NK cells, which are known to express high levels of CCR7 and CXCR3—thus preferentially migrating to secondary lymphoid organs—and to produce very high levels of cytokines (43). An increased homing to lymph nodes, with high local production of cytokines, and a consequent decrease in the peripheral blood of patients with new-onset type 1 diabetes could be hypothesized.

Besides validation of previously described data and discovery of new cellular biomarkers, our dataset clarified previous contrasting reports on specific cell subtypes. As an example, $CD45RA^{+}$ Tregs had been described as both normal (14) or altered (15) in type 1 diabetes; in our study, a normal frequency of this cell subpopulation was observed in newly diagnosed type 1 diabetes. In addition, the implemented pipeline of unbiased analyses, combined with the comparison with 3 control groups, allowed to elucidate how some of the previously reported type 1 diabetes-related immune alterations, such as a reduction of EM CD8 T (8) and $CD56^{dim}$ NK cells (44), are rather markers shared with other autoimmune diseases, or are not selectively altered in type 1 diabetes, as in the case of $T_{R3\text{-}56}$ cells (25). Therefore, the analytic approach proposed in this article appears to be robust, and our large cohort has the potential to be used by other investigators as a reference dataset.

Finally, we found that the peripheral immune profile could not discriminate patients with new-onset type 1 diabetes from other clinical groups, indicating that the non-(antigen)specific peripheral immune system is presumably inadequate for an exhaustive discrimination between individuals or diseases. However, age and lymphocyte count had an effect, although mild, on the segregation of the circulating immunome of patients with type 1 diabetes, confirming a recent study showing that a higher lymphocyte count is evident in younger patients with type 1 diabetes (13). Unexpectedly (45), DKA did not appear to have a major effect on the profile of the peripheral immunome, and this is likely due to the 5-to-10-day interval from diagnosis that we observe before the blood sample collection.

The extensive pediatric cohort of individuals, the strong consistency between unbiased analyses, and the proper assortment of different control groups are major strengths of our work. Nevertheless, although comprehensive for the well-defined lymphoid and myeloid markers, a limitation of this study is that we used five separate antibody panels, mainly comprised of lineage markers, which limits the chance to detect unconventional cell subsets. Furthermore, this work lacks an internal validation cohort, which would have allowed the identification and elimination of further possible biases.

10.3389/fimmu.2022.1026416

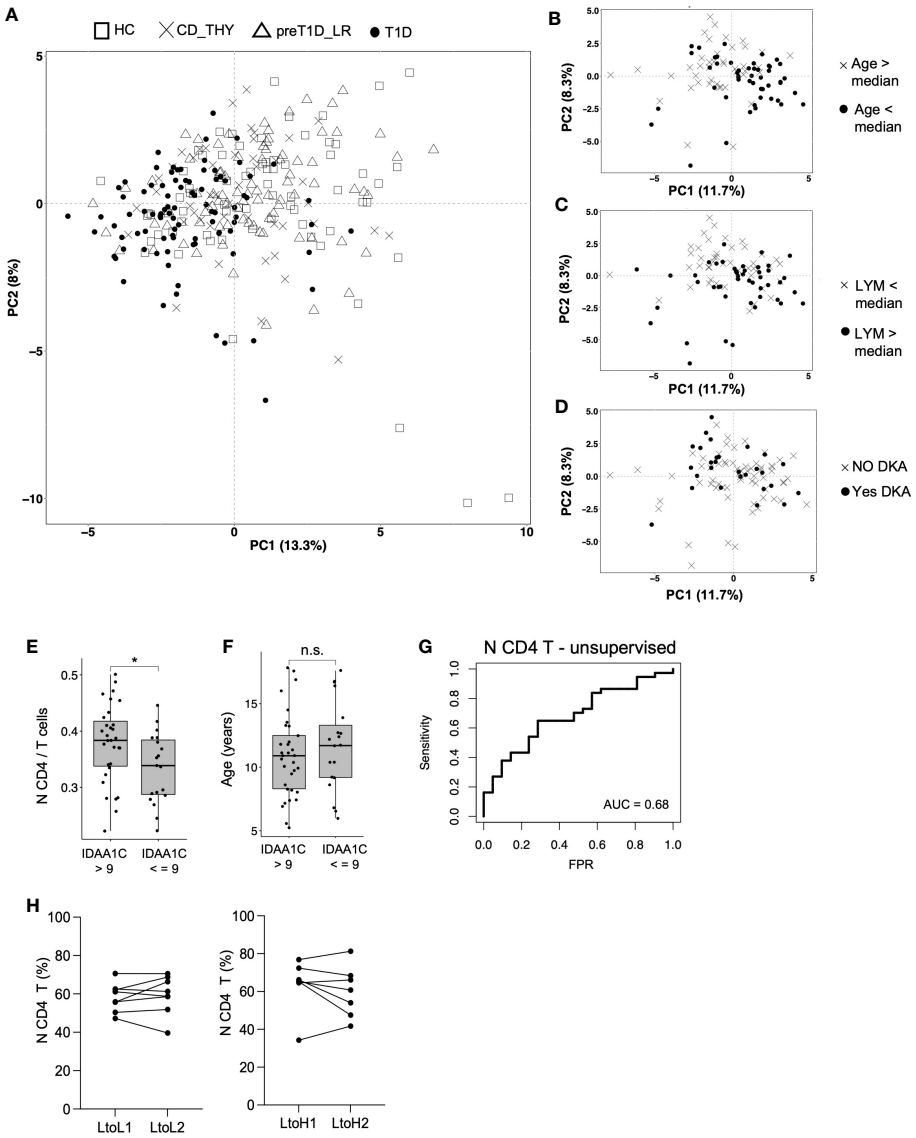

FIGURE 5
Frequency of N CD4 T cell at disease onset is associated with partial remission. Immunome-based principal component analysis performed on HC (n=73), CD_THY (n=47), preT1D-LR (n=82) and T1D (n=91) **(A)**; segregation of the circulating immunome of newly diagnosed T1D patients (n=91) based on median age **(B)**, median peripheral lymphocyte count **(C)** and presence of DKA **(D)**; comparison of the frequency of N CD4 T cell **(E)** and age **(F)** between newly diagnosed T1D patients with IDAA1C >9 (n=39) and IDAA1C ≤9 (n=21) at the 12-month follow-up visit; model for the prediction of partial remission based on the frequency N CD4 T cell at disease diagnosis **(G)**; N CD4 T cell frequency in relatives who maintained a stable Stage 0 status or during the transition from Stage 0 (0-1 Aab) to a Stage≥1 condition (≥2Aabs) **(H)**. LYM, lymphocytes; DKA, diabetic ketoacidosis; IDAA1c, insulin dose adjusted HbA1c; AUC, Area under the curve: N CD4 T cells: naïve CD4 T cells. Significant differences were determined by unpaired (4E, F) and paired (4H) Student's t-test for pairwise comparisons (*p < 0.05, ns, not significant.

This study provides an unbiased and reproducible characterization of the circulating immune cell profile uniquely associated with new-onset type 1 diabetes in a large pediatric cohort, representing a reference dataset to be exploited for validation or discovery purposes to elucidate the pathogenesis of type 1 diabetes.

Data availability statement

The original contributions presented in the study are included in the article/Supplementary Materials. Further inquiries can be directed to the corresponding author.

Ethics statement

The studies involving human participants were reviewed and approved by Ethics Committee Ospedale San Raffaele (protocols TIGET004-DRI003 and NHPROT32803-TN01). Written informed consent to participate in this study was provided by the participants' legal guardian/next of kin.

Author contributions

CBG and EB planned and performed the analyses, contributed to data interpretation and discussion, and drafted, revised, and approved the final version of the article. DC, AM, and VC performed data acquisition and analysis, and revised and approved the final version of the article. AS, VI, and FR performed sample storage and data management, and revised and approved the final version of the article. EM, VC, and VF provided biological samples, performed data acquisition, patient selections, contributed to data interpretation, and revised and approved the final version of the article. SDR and BAM performed data acquisition and analysis, contributed to data interpretation, and revised and approved the final version of the article. GMS supervised the statistical analysis, contributed to data interpretation, and revised and approved the final version of the article. DPM, AG, LP, EB, MB, MJM, and RB contributed to patient selection, provided biological samples, contributed to data interpretation, and revised and approved the final version of the article. AP designed and coordinated the study, interpretated the data, and drafted and revised the final version of the article. All authors contributed to the article and approved the submitted version.

Funding

This study was funded by the Italian Ministry of Health – Ricerca Finalizzata RF-2016-02364070. This study was funded by the Italian Ministry of Health – Ricerca Finalizzata RF-2016-02364070.

Acknowledgments

AP is supported by the Juvenile Diabetes Research Foundation JDRF (n. 3-APF-2019-744-AN) and Fondazione Italiana Diabete.

Conflict of interest

The authors declare that the research was conducted in the absence of any commercial or financial relationships that could be construed as a potential conflict of interest.

Publisher's note

Supplementary material

The Supplementary Material for this article can be found online at: https://www.frontiersin.org/articles/10.3389/fimmu.2022.1026416/full#supplementary-material

References

1. Eisenbarth GS. Type I diabetes mellitus. a chronic autoimmune disease. *N Engl J Med* (1986) 314:1360–8. doi: 10.1056/NEJM198605223142106

2. Atkinson MA, Eisenbarth GS. Type 1 diabetes: new perspectives on disease pathogenesis and treatment. *Lancet* (2001) 358:221–9. doi: 10.1016/S0140-6736(01)05415-0

3. Atkinson MA, Eisenbarth GS, Michels AW. Type 1 diabetes. *Lancet* (2014) 383:69–82. doi: 10.1016/S0140-6736(13)60591-7

4. Pietropaolo M, Eisenbarth GS. Autoantibodies in human diabetes. *Curr Dir Autoimmun* (2001) 4:252–82. doi: 10.1159/000060541

5. Insel RA, Dunne JL, Atkinson MA, Chiang JL, Dabelea D, Gottlieb PA, et al. Staging presymptomatic type 1 diabetes: a scientific statement of JDRF, the endocrine society, and the American diabetes association. *Diabetes Care* (2015) 38(10):1964–74. doi: 10.2337/dc15-1419

6. Yu L, Zhao Z, Steck AK. T1D autoantibodies: room for improvement? *Curr Opin Endocrinol Diabetes Obes* (2017) 24(4):285–91. doi: 10.1097/MED.0000000000000348

7. Roep BO, Peakman M. Diabetogenic T lymphocytes in human type 1 diabetes. *Curr Opin Immunol* (2011) 23:746–53. doi: 10.1016/j.coi.2011.10.001

8. Oras A, Peet A, Giese T, Tillmann V, Uibo R. A study of 51 subtypes of peripheral blood immune cells in newly diagnosed young type 1 diabetes patients. *Clin Exp Immunol* (2009) 198(1): 57–70. doi: 10.1111/cei.13332

9. Nieminen JK, Vakkila J, Salo HM, Nina Ekström N, Härkönen T, Ilonen J, et al. Altered phenotype of peripheral blood dendritic cells in pediatric type 1 diabetes. *Diabetes Care* (2012) 35(11):2303–10. doi: 10.2337/dc11-2460

10. Rodacki M, Svoren B, Butty V, Besse W, Laffel L, Benoist C, et al. Altered natural killer cells in type 1 diabetic patients. *Diabetes* (2007) 56(1):177–85. doi: 10.2337/db06-0493

11. Hanley P, Sutter JA, Goodman NG, Du Y, Sekiguchi DR, Meng W, et al. Circulating b cells in type 1 diabetics exhibit fewer maturation-associated phenotypes. *Clin Immunol* (2017) 183:336–34. doi: 10.1016/j.clim.2017.09.021

12. Hedman M, Faresjö M, Axelsson S, Ludvigsson J, Casas R. Impaired CD4 and CD8 T cell phenotype and reduced chemokine secretion in recent-onset type 1 diabetic children. *Clin Exp Immunol* (2008) 153(3):360–8. doi: 10.1111/j.1365-2249.2008.03720.x

13. Ratter-Rieck JM, Maalmi H, Trenkamp S, Zaharia OP, Rathmann W, Schloot NC, et al. Leukocyte counts and T-cell frequencies differ between novel subgroups of diabetes and are associated with metabolic parameters and biomarkers of inflammation. *Diabetes* (2021) 70(11):2652–62. doi: 10.2337/db21-0364

14. Brusko T, Wasserfall C, McGrail K, Schatz R, Lee Viener H, Schatz D, et al. No alterations in the frequency of FOXP3+ regulatory T-cells in type 1 diabetes. *Diabetes* (2007) 56(3):604–12. doi: 10.2337/db06-1248

15. Viisanen T, Gazali AM, Ihantola EL, Ekman I, Näntö-Salonen K, Veijola R, et al. FOXP3+ regulatory T cell compartment is altered in children with newly diagnosed type 1 diabetes but not in autoantibody-positive at-risk children. *Front Immunol* (2019) 10:19. doi: 10.3389/fimmu.2019.00019

16. Sosenko JM, Skyler JS, Mahon J, Krischer JP, Beam CA, Boulware DC, et al. Validation of the diabetes prevention trial-type 1 risk score in the TrialNet natural history study. type 1 diabetes TrialNet and diabetes. *Diabetes Care* (2011) 34:1785–7. doi: 10.2337/dc11-0641

17. Mahon JL, Sosenko JM, Rafkin-Mervis L, Krause-Steinrauf H, Lachin JM, Thompson C, et al. The TrialNet natural history study of the development of type 1 diabetes: objectives, design, and initial results. *Pediatr Diabetes* (2009) 10:97–104. doi: 10.1111/j.1399-5448.2008.00464.x

18. Clinical Trials. http://www.clinicaltrials.gov/show/NCT00097292.

19. Mortensen HB, Hougaard P, Swift P, Hansen L, Holl RW, Hoey H, et al. Hvidoere study group on childhood diabetes. new definition for the partial remission period in children and adolescents with type 1 diabetes. *Diabetes Care* (2009) 32(8):1384–90. doi: 10.2337/dc08-1987

20. Van Gassen S, Callebaut B, Van Helden MJ, Lambrecht BN, Demeester P, Dhaene T, et al. FlowSOM: Using self-organizing maps for visualization and interpretation of cytometry data. *Cytomet A* (2015) 87(7):636–45. doi: 10.1002/cyto.a.22625

21. Crowell HL, Chevrier S, Jacobs A, Sivapatham STumor Profiler Consortium, , Bodenmiller B, et al. An r-based reproducible and user-friendly preprocessing pipeline for CyTOF data. *F1000Res* (2020) 9:1263. doi: 10.12688/f1000research.26073.2

22. McInnes L, Healy J, Melville J. UMAP: Uniform manifold approximation and projection. *arXiv* (2018), 1802.03426. doi: 10.48550/arXiv.1802.03426

23. Finak G, Frelinger J, Jiang W, Newell EW, Ramey J, Davis MM, et al. OpenCyto: an open source infrastructure for scalable, robust, reproducible, and automated, end-to-end flow cytometry data analysis. *PloS Comput Biol* (2014) 10 (8):e1003806. doi: 10.1371/journal.pcbi.1003806

24. Jolliffe I. *Principal component analysis*. Berlin, Heidelberg: Springer (2011). International Encyclopedia of Statistical Science.

25. Terrazzano G, Bruzzaniti S, Rubino V, Santopaolo M, Palatucci AT, Giovazzino A, et al. T1D progression is associated with loss of CD3+CD56+ regulatory T cells that control CD8+ T cell effector functions. *Nat Metab* (2020) 2 (2):142–52. doi: 10.1038/s42255-020-0173-1

26. Liu P, Liu S, Fang Y, Xue X, Zou J, Tseng G, et al. Recent advances in computer-assisted algorithms for cell subtype identification of cytometry data. *Front Cell Dev Biol* (2020) 8:234. doi: 10.3389/fcell.2020.00234

27. Brummelman J, Haftmann C, Núñez NG, Alvisi G, Mazza EMC, Becher B, et al. Development, application and computational analysis of high-dimensional fluorescent antibody panels for single-cell flow cytometry. *Nat Protoc* (2019) 14 (7):1946–69. doi: 10.1038/s41596-019-0166-2

28. Greene E, Finak G, D'Amico LA, Bhardwaj N, Church CD, Morishima C, et al. New interpretable machine-learning method for single-cell data reveals correlates of clinical response to cancer immunotherapy. *Patterns* (2021) 2 (12):100372. doi: 10.1016/j.patter.2021.100372

29. Van den Broek T, Borghans JAM, van Wijk F. The full spectrum of human naive T cells. *Nat Rev Immunol* (2018) 18(6):363–73. doi: 10.1038/s41577-018-0001-y

30. Noble JA, Valdes AM. Genetics of the HLA region in the prediction of type 1 diabetes. *Curr Diabetes Rep* (2011) 11(6):533–42. doi: 10.1007/s11892-011-0223-x

31. Gomez-Muñoz L, Perna-Barrull D, Caroz-Armayones JM, Murillo M, Rodriguez-Fernandez S, Valls A, et al. Candidate biomarkers for the prediction and monitoring of partial remission in pediatric type 1 diabetes. *Front Immunol* (2022) 13:825426. doi: 10.3389/fimmu.2022.825426

32. Moya R, Robertson HK, Payne D, Narsale A, Koziol JType 1 Diabetes TrialNet Study Group, et al. A pilot study showing associations between frequency of CD4(+) memory cell subsets at diagnosis and duration of partial remission in type 1 diabetes. *Clin Immunol* (2016) 166-167:72–80. doi: 10.1016/j.clim.2016.04.012

33. Liu YJ. IPC: Professional type 1 interferon-producing cells and plasmacytoid dendritic cell precursors. *Annu Rev Immunol* (2005) 23:275–306. doi: 10.1146/annurev.immunol.23.021704.115633

34. Tel J, Schreibelt G, Sittig SP, Mathan TSM, Buschow SI, Cruz LJ, et al. Human plasmacytoid dendritic cells efficiently cross-present exogenous ags to CD8 + T cells despite lower Ag uptake than myeloid dendritic cell subsets. *Blood* (2013) 121:459–67. doi: 10.1182/blood-2012-06-435644

35. Ito T, Yang M, Wang YH, Lande R, Gregorio J, Perng OA, et al. Plasmacytoid dendritic cells prime IL-10-producing T regulatory cells by inducible costimulator ligand. *J Exp Med* (2007) 204:105–15. doi: 10.1084/jem.20061660

36. Jego G, Palucka AK, Blanck JP, Chalouni C, Pascual V, Banchereau J. Plasmacytoid dendritic cells induce plasma cell differentiation through type I interferon and interleukin 6. *Immunity* (2003) 19:225–34. doi: 10.1016/s1074-7613(03)00208-5

37. García-Marquez M, Shimabukuro-Vornhagen A, von Bergwelt-Baildon M. Complex interactions between b cells and dendritic cells. *Blood* (2013) 121:2367–8. doi: 10.1182/blood-2012-12-468017

38. Allen JS, Pang P, Skowera A, Ellis R, Rackham C, Lozanoska-Ochser B, et al. Plasmacytoid dendritic cells are proportionally expanded at diagnosis of type 1 diabetes and enhance islet autoantigen presentation to T-cells through immune complex capture. *Diabetes* (2009) 58(1):138–45. doi: 10.2337/db08-0964

39. Leskela S, Rodríguez-Muñoz A, de la Fuente H, Figueroa-Vega N, Bonay P, Martín P, et al. Plasmacytoid dendritic cells in patients with autoimmune thyroid disease. *J Clin Endocrinol Metab* (2013) 98(7):2822–33. doi: 10.1210/jc.2013-1273

40. Ciccocioppo R, Ricci G, Rovati B, Pesce I, Mazzocchi S, Piancatelli D, et al. Reduced number and function of peripheral dendritic cells in coeliac disease. *Clin Exp Immunol* (2007) 149(3):487–96. doi: 10.1111/j.1365-2249.2007.03431.x

41. Lee EK, Sunwoo JB. Natural killer cells and thyroid diseases. *Endocrinol Metab (Seoul)* (2019) 34(2):132–7. doi: 10.3803/EnM.2019.34.2.132

42. Agin M, Sevinc E, Dogan E, Sevinc N. Reduced levels of circulating natural killer cells in children with celiac disease. *Paediatr Indonesiana* (2020) 60:125–30. doi: 10.14238/pi60.3.2020.125-30

43. Poli A, Michel T, Thérésine M, Andrès E, Hentges F, Zimmer J. CD56bright natural killer (NK) cells: an important NK cell subset. *Immunology* (2009) 126 (4):458–65. doi: 10.1111/j.1365

44. Gomez-Muñoz L, Perna-Barrull D, Villalba A, Rodriguez-Fernandez S, Ampudia RM, Teniente-Serra A, et al. NK cell subsets changes in partial remission and early stages of pediatric type 1 diabetes. *Front Immunol* (2020) 11:611522. doi: 10.3389/fimmu.2020.611522

45. Kitabchi AE, Sttentz FB, Umpierrez GE. Diabetic ketoacidosis induces *in vivo* activation of human T-lymphocytes. *Biochem Biophys Res Commun* (2004) 315(2):404–7. doi: 10.1016/j.bbrc.2004.01.065

frontiers | Frontiers in Immunology

TYPE Case Report
PUBLISHED 20 January 2023
DOI 10.3389/fimmu.2023.1115691

OPEN ACCESS

EDITED BY
Joanna Davies,
San Diego Biomedical Research Institute,
United States

REVIEWED BY
Andreas B. Wild,
Universtätsklinikum Erlangen, Germany
Stefania Canè,
University of Verona, Italy

*CORRESPONDENCE
Guozhu Xie
xieguozhu@126.com
Dehua Wu
18602062748@163.com

†These authors have contributed equally to this work and share first authorship

SPECIALTY SECTION
This article was submitted to Immunological Tolerance and Regulation, a section of the journal Frontiers in Immunology

RECEIVED 04 December 2022
ACCEPTED 10 January 2023
PUBLISHED 20 January 2023

CITATION
Tan T, Lin X, Ling J, Wang R, Chen Y, Cai L, Sun J, Wu D and Xie G (2023) Case report: Abolishing primary resistance to PD-1 blockade by short-term treatment of lenvatinib in a patient with advanced metastatic renal cell carcinoma. *Front. Immunol.* 14:1115691. doi: 10.3389/fimmu.2023.1115691

Case report: Abolishing primary resistance to PD-1 blockade by short-term treatment of lenvatinib in a patient with advanced metastatic renal cell carcinoma

Tingting Tan[1,2†], Xiaotong Lin[1,2†], Jing Ling[1,2†], Rong Wang[1], Yue Chen[1], Longmei Cai[1], Jingyuan Sun[1], Dehua Wu[1,2*] and Guozhu Xie[1,2*]

[1]Department of Radiation Oncology, Nanfang Hospital, Southern Medical University, Guangzhou, Guangdong, China, [2]The First School of Clinical Medicine, Southern Medical University, Guangzhou, China

Anti-PD-1 immunotherapy has been extensively used in treatment of patients with advanced metastatic renal cell carcinoma (mRCC). Several prospective clinical trials showed that the combined treatment of anti-PD-1 antibody plus lenvatinib, a potent receptor tyrosine kinase inhibitor (TKI), exhibited high response rate compared with single-agent sunitinib. However, whether the patients with primary resistance to PD-1 blockade could benefit from the addition of lenvatinib is still unclear. Herein, we reported a patient with mRCC who was primary resistant to pembrolizumab and achieved a durable complete response after a short-term treatment with lenvatinib. This case report indicates that the patients with primary resistance to anti-PD-1 therapy could benefit from the short-term lenvatinib in combination with anti-PD-1 therapy, and provides a useful paradigm worthy of establishing a clinical trial for mRCC patients with primary resistance to anti-PD-1 therapy.

KEYWORDS

primary resistance, PD-1, lenvatinib, renal cell carcinoma, pembrolizumab

1 Introduction

Renal cell carcinoma (RCC) is a rapidly progressing malignant tumor of urinary system. Approximately one-third of patients with renal cell carcinoma have metastatic disease at initial presentation (1). Metastatic RCC (mRCC) has been notoriously resistant to conventional radiotherapy and chemotherapy. Currently, immune-checkpoint blockade (ICB) has been extensively used in treatment of patients with advanced mRCC. Recent studies showed that the ICB-based combination treatment had better outcomes than

sunitinib for patients with mRCC (2–6). Data from a prospective trial (NCT02853331) showed that the treatment with pembrolizumab plus axitinib resulted in 59.3% of overall objective response rate (ORR) among patients with previously untreated advanced mRCC (4). Another encouraging prospective trial (NCT02811861) showed 71.0% of ORR to the treatment with lenvatinib plus pembrolizumab for mRCC patients without previous systemic therapy (6). Notably, the combination of lenvatinib plus pembrolizumab even showed antitumor activity for patients with previously treated metastatic renal cell carcinoma (7). However, whether the patients with primary resistance to PD1 blockade could benefit from the addition of lenvatinib is still unclear.

Lenvatinib is a novel multitargeted receptor tyrosine kinase inhibitor (TKI) with activity against with VEGFR1-3, FGFR1-4, PDGFRα, RET and KIT proto-oncogenes (8). Compared with other TKIs, lenvatinib has the more potent activity against FGFR1-4 (9, 10), and has shown the higher efficacy as monotherapies than everolimus for RCC (11). However, high incidence rate of grade 3 and 4 adverse events was also observed in lenvatinib group compared with everolimus, which often led to treatment interruption of lenvatinib (11).

Previous studies in mouse tumor isograft models have demonstrated the immunomodulatory activity of lenvatinib in tumor microenvironment, including reducing tumor-associated immunosuppressive macrophages, increasing cytotoxic T cells, and activating interferon γ signaling (12, 13). In the human body, the immune system is able to recognize tumor antigens as not self and mounts an immune response against tumor cells. Once the immune response against tumor is primed in the body, it could be durable (14, 15). Given the potential role of lenvatinib in priming an antitumor immune response, there exists a possibility that just short-term use of lenvatinib could affect primary resistance of tumor to PD-1 blockade. Herein, we reported a patient who was primary resistant to pembrolizumab and achieved a durable complete response after a short-term treatment with lenvatinib.

2 Case presentation

A male patient received a diagnosis of renal cell carcinoma in December 2008 at 46 years of age. A computed tomography (CT) scan of the chest and abdomen revealed a left renal tumor with a 4.5cm maximum diameter which was confined to the renal capsule, and he underwent radical nephrectomy on December, 2008. The pathological examination showed a moderately to poorly differentiated renal clear cell carcinoma. All indications suggested a diagnosis of stage I RCC (T1bN0M0) according to the American Joint Committee on Cancer (AJCC) Cancer Staging Handbook, 6th edition. There was no residual tumor after surgery at the primary site, and the lymph nodes removed were not found to be involved. The patient underwent periodical CT examination after surgery.

The patient remained disease-free until contrast enhancement CT scan of upper abdomen revealed several new lesions at pancreas and liver on August 23, 2021 (Figure 1A), due to upper abdominal pain. Laparoscopic partial hepatectomy was performed for the largest intrahepatic lesions on August 26, 2021, and postoperative pathology confirmed liver metastasis of renal clear cell carcinoma (Figure 1B). The images of positron emission tomography CT (PET-CT) on September 09, 2021 showed three hypermetabolic lesions in pancreas and no hypermetabolism in the residual liver and other sites (Figure 1C). The pancreaticobiliary duct was seriously obstructed due to the compression by the metastatic tumor, a stent was implanted by endoscopic retrograde cholangio-pancreatography (ERCP) on September 17, 2021.

Immunohistochemical staining showed the tumor proportion score (TPS) of PD-L1 expression was 40% according to Allred criteria using the DAKO PD-L1 22C3 PharmDx assay (Agilent Technologies; Carpinteria, CA, USA) (Figure 1D). Since September 22, 2021, the patient received anti-PD-1 treatment with pembrolizumab (200 mg intravenously once every 3 weeks). The patient received a palliative radiotherapy to the pancreatic lesions on September 27, 2021. with a total of 40 Gy in five fractions once every other day using 6-MV photons by means of a coplanar nine-field intensity-modulated image-guided technique (IMRT).

After 3 cycles of pembrolizumab, a surveillance CT scan on November 05, 2021 showed disease progression, with several new metastases in liver (Figure 2A). The patient thus received the combined treatment with pembrolizumab (200 mg q3W) plus axitinib (5 mg q12h) from November 07, 2021. After 3-cycle treatment with pembrolizumab plus axitinib, a surveillance CT scan was performed on February 18, 2022, and showed further disease progression with significantly enlarged and increased number of metastases in liver compared with that on November 05, 2021 (Figure 2A). On February 22, 2022, axitinib was replaced by lenvatinib (12mg orally once daily) and pembrolizumab treatment was continuously administered as before. A follow-up CT scan in May 16, 2022 (3 months after lenvatinib initiation) showed the metastatic lesions in the liver had significantly decreased in size (Figure 2A). But at the same time, the patient experienced grade 3 adverse events (AEs) of proteinuria and hypertension according to the standard CTCAE5.0 criteria, so the dose of lenvatinib was reduced to 8mg once daily on June 23, 2022. Lenvatinib had to be discontinued due to aggravation of proteinuria on July 6, 2022, and pembrolizumab monotherapy was maintained. The whole process of treatment was shown in Figure 2B.

3 Results

Immunohistochemistry (IHC) showed the tumor proportion score (TPS) of PD-L1 expression was 40%, indicating potential response to anti-PD-1 therapy. However, for this patient, tumors did not respond to anti-PD-1 pembrolizumab monotherapy for 1.5 months, and disease continuously progressed even though axitinib was added to pembrolizumab for later 3.5 months (Figure 2A). After that, lenvatinib instead of axitinib was added to the treatment of pembrolizumab. Remarkably, an abdomen CT scan showed a dramatic treatment response of the patient's known lesions at 23 days after addition of lenvatinib to pembrolizumab (Figure 2A). All lesions had significantly regressed at next follow-up CT scan at 3 months after starting lenvatinib (May 16, 2022). Due to proteinuria and hypertension, the dose of lenvatinib was reduced to 8mg once daily on June 23, 2022. Lenvatinib was eventually discontinued on July 6, 2022, and pembrolizumab monotherapy was maintained after that. Nevertheless, all lesions had continuously regressed at multiple follow-up CT scans, and achieved complete response as shown by the CT scan images on September 29, 2022, and a sustained complete

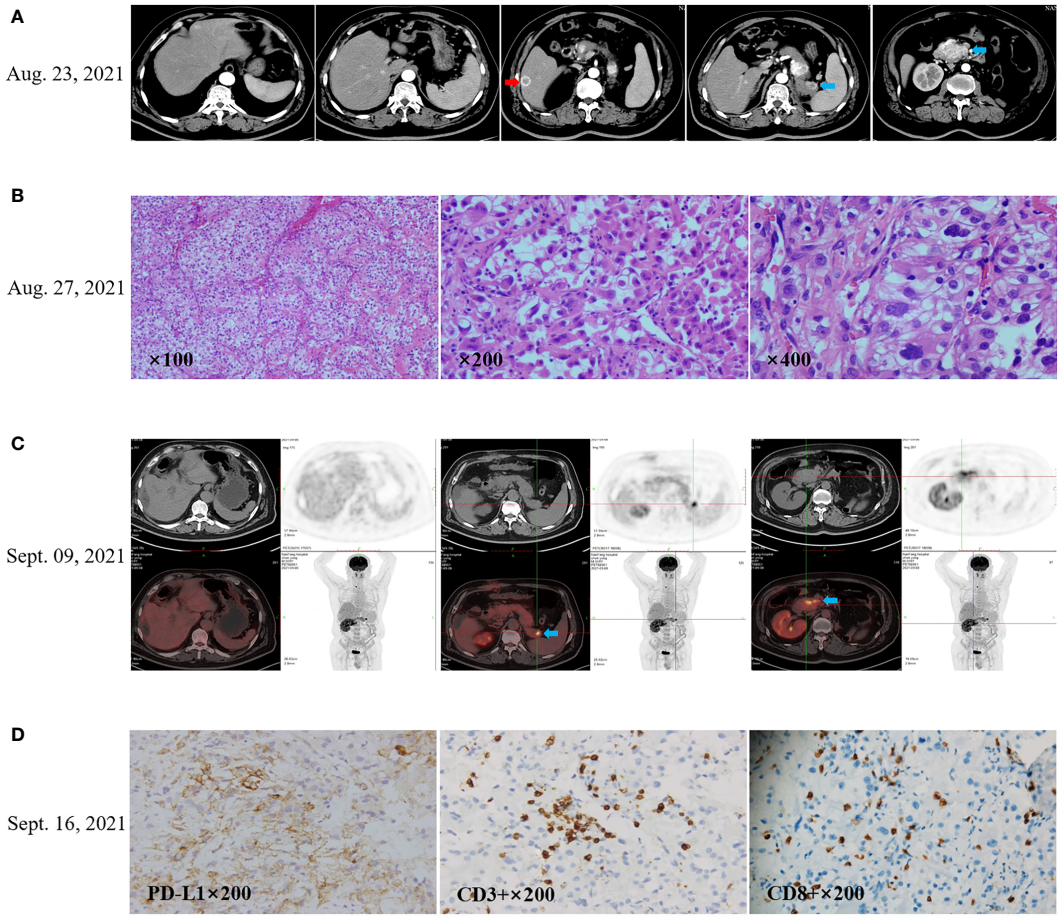

FIGURE 1
Recurrence after radical left nephrectomy of the patient's with renal clear cell carcinoma. **(A)** CT scan (August 23, 2021) showed the first recurrence after nephrectomy in 13 years. The red arrow indicates the prominent lesion in the liver, and the blue arrow indicates the pancreatic lesion. **(B)** Laparoscopic partial hepatectomy was performed for the largest intrahepatic lesions on August 26, 2021, and postoperative pathology confirmed liver metastasis of renal clear cell carcinoma. **(C)** The images of positron emission tomography CT (PET-CT) on September 09, 2021 showed hypermetabolic pancreatic lesions, no hypermetabolism in the residual liver, and no additional hypermetabolic lesions. **(D)** Immunohistochemistry showed that PD-L1 expression in the tumor tissue was 40% for tumor proportion score (TPS), $CD3^+$ TIL density was 100 cells/HPF, and $CD8^+$ TIL density was 50 cells/HPF.

response was observed in a recent CT scan images on December 2, 2022 (Figure 2A).

The patient experienced severe proteinuria (grade 3) and hypertension (grade 2) during lenvatinib treatment, and lenvatinib had to be discontinued on July 6, 2022. After 1 month of suspension of the use of lenvatinib, the patient's 24-hour urine protein test showed that urine protein gradually returned to normal (Figure 2C), hypertension symptom disappeared, and the patient no longer needed to take antihypertensive drugs. Additionally, ascites, bloating, diarrhea, fatigue, edema, and other lenvatinib-related adverse events were relieved. The body weight of patient was significantly increased (Figure 2D) and ECOG performance status was decreased from 3 points to 1 point, indicating the quality of life was significantly improved.

4 Discussion

ICB immunotherapy has become an important approach in the treatment of advanced cancers. However, the proportion of patients who can benefit from such therapy remains limited, with an estimated average response rate of 25% for patients with solid tumors, owing to primary or acquired resistance (16). Recently, Tae K. et al. proposed four distinct types of human cancer based on the presence of PD-L1 expression and tumor-infiltrating lymphocytes (TILs) in the tumor immune microenvironment (TIME), to better identify tumor response or resistance to anti-PD therapy. According to this classification, tumors could be divided into four types: PD-L1−/TIL− (type I); PD-L1+/TIL+ (type II); PD-L1−/TIL+ (type III); and PD-L1+/TIL− (type IV) (16). Primary resistance to anti-PD therapy was defined as the failure to initially respond to anti-PD therapy in the type II tumor, which has both PD-L1 expression and T cell infiltration (16). For this case, TPS of PD-L1 expression in tumor was 40%, and CD3+ TIL density was 100 cells/HPF (CD8+ TIL density was 50 cells/HPF), thus indicating a type II tumor with primary resistance to anti-PD therapy, which was evidenced by the fact that the tumor continuously progressed during pembrolizumab treatment for 5 months.

Multiple approaches are being developed to improve the response to anti-PD-1 therapy, including the combination treatment with other therapies. Combination with TKI targeted therapy has proved effective for RCC in several clinical trials. Pembrolizumab combined with axitinib was approved by the FDA in advanced RCC after the

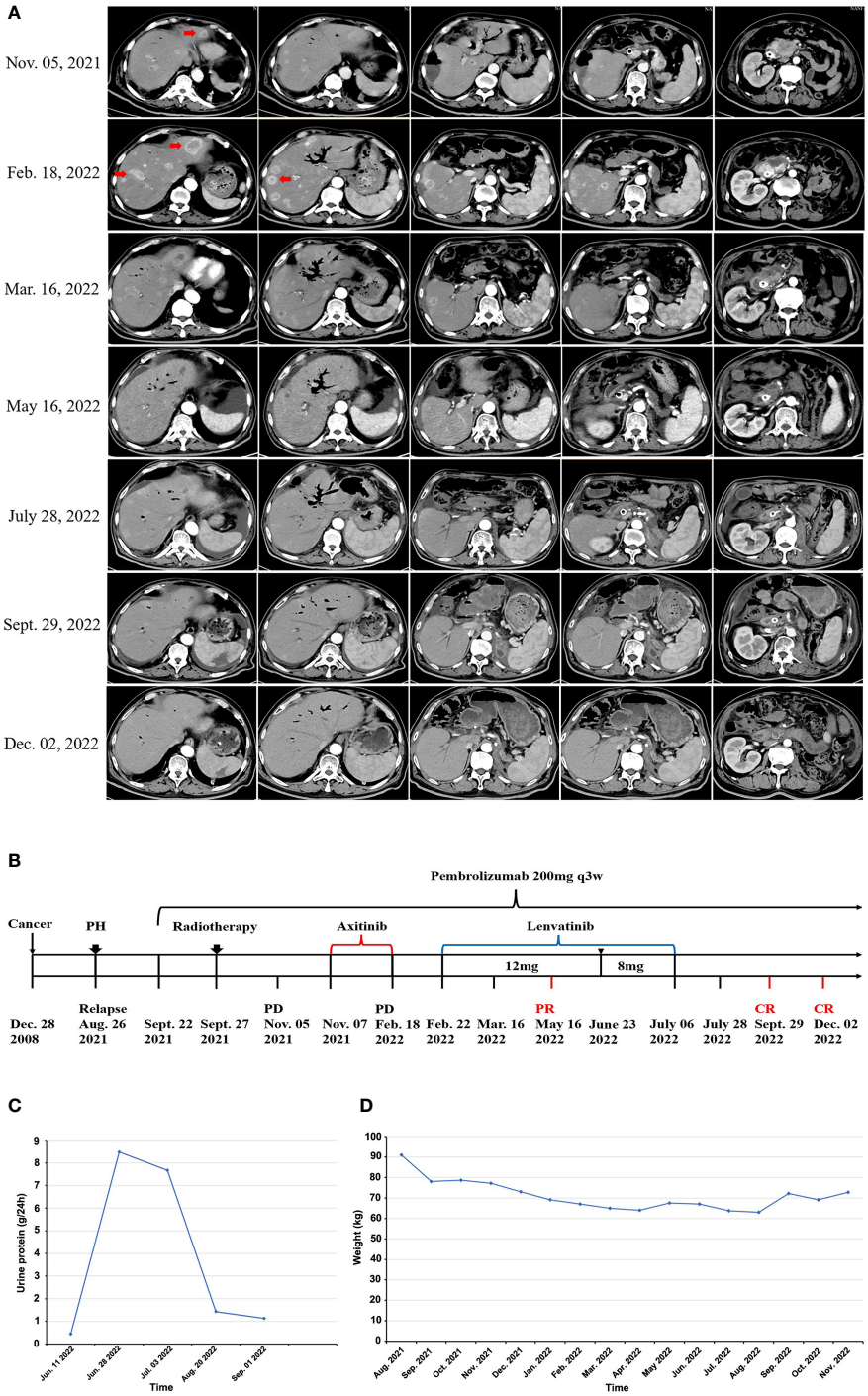

FIGURE 2
Short-term lenvatinib overcomes primary resistance of mRCC to anti-PD1 therapy. **(A)** After 3 cycles of pembrolizumab monotherapy, CT scan on November 05, 2021 showed disease progression, the patient was still resistant to the combination of axitinib with pembrolizumab, with significantly enlarged and increased number of metastases in liver (Feb 18, 2022), the addition of lenvatinib to pembrolizumab led to rapid tumor regression shown in a follow-up CT scan on March 16, 2022 (23 days after lenvatinib initiation), CT examination in May 2022 revealed almost complete response (CR) of the intrahepatic and pancreatic lesions, all lesions continued to regress in the two CT scans after lenvatinib was discontinued, with a sustained complete response as shown in the CT scan image on September 29, 2022 and December 02, 2022. **(B)** Diagram of the patient's entire treatment process, PH representing laparoscopic partial hepatectomy (August 26, 2021), representing lenvatinib dose reduction due to AEs (June 23, 2022). **(C)** After 1 month of suspension of the use of lenvatinib, the patient's 24-hour urine protein test showed that urine protein gradually returned to normal. **(D)** After discontinuation of lenvatinib, the patient gradually gained weight.

KEYNOTE-426 trial found that the combination was superior to monotherapy with sunitinib (4). However, for this case, the patient presented primary resistance to pembrolizumab monotherapy and even in combination with axitinib. Lenvatinib is a novel potent multitarget TKI that performs its action through the inhibition of VEGFR 1-3, FGFR 1-4, PDGFRα, RET and KIT (8). Lenvatinib plus pembrolizumab demonstrated a promising antitumor activity in mRCC patients (6). However, grade 3 or higher adverse

events occurred in up to 82.4% of the patients who received lenvatinib plus pembrolizumab. Notably, preclinical studies demonstrated that lenvatinib pretreatment could induce an immune-activating tumor microenvironment, resulting in significantly greater antitumor activity compared with anti-PD-1 treatment alone (12, 13), indicating a possibility that just short-term use of lenvatinib could initiate a potent and durable antitumor response to PD-1 blockade in patients with a type II tumor that is originally resistant to anti-PD therapy. Herein, we reported, for the first time, that a patient who was primary resistant to pembrolizumab plus axitinib, achieved a lasting response after a short-term treatment with lenvatinib. The miraculous effect observed herein provided further evidence for lenvatinib of modulating the tumor immune microenvironment and overcoming primary resistance of tumor to ICB.

For this case, radiotherapy was another factor that should be considered for contributing to the effect of anti-PD-1 therapy. Several cases had been reported that local radiotherapy, especially SBRT, could produce an abscopal effect by activation of the immune system. There are several prospective clinical trials investigating the abscopal effect (17–19). However, consistent results regarding occurrence of abscopal effect are highly variable. In general, these trials exploring expansion of abscopal effect still only provide relatively low occurrence rate of abscopal activity (19). For this case, a palliative radiotherapy (40Gy/8F) was delivered to metastatic lesions in pancreas. Unfortunately, disease, except for lesions in the irradiation field, continuously progressed during 5 months after radiotherapy until the treatment with lenvatinib. Therefore, tumor regression is unlikely to be an abscopal effect induced by radiotherapy. Additionally, the limitation of this case report is that it was not clear which markers were associated with the patient's durable response and what was the specific mechanism by which lenvatinib overcame primary resistance to perbrolizumab in this patient. It would be worthwhile to design a new clinical trial and a rigorous experiment to demonstrate.

5 Conclusion

This patient's surprising systemic response after short-term lenvatinib in combination with pembrolizumab provides new insights into the role of short-term lenvatinib in overcoming primary resistance of tumor to anti-PD-1 therapy.

Data availability statement

The original contributions presented in the study are included in the article/supplementary material. Further inquiries can be directed to the corresponding authors.

Ethics statement

The studies involving human participants were reviewed and approved by The Ethics Committee of the Nanfang Hospital. The patients/participants provided their written informed consent to participate in this study. Written informed consent was obtained from the individual(s) for the publication of any potentially identifiable images or data included in this article.

Author contributions

TT, XL, and JL designed the study and drafted the entire manuscript. RW and YC are responsible for patient information acquisition and postoperative follow-up. LC and JS are responsible for imaging and image processing. DW and GX conceived and designed the study, and guided the article revision. All authors contributed to the article and approved the submitted version.

Conflict of interest

The authors declare that the research was conducted in the absence of any commercial or financial relationships that could be construed as a potential conflict of interest.

Publisher's note

References

1. Bedke J, Gauler T, Grünwald V, Hegele A, Herrmann E, Hinz S, et al. Systemic therapy in metastatic renal cell carcinoma. *World J Urol* (2017) 35(2):179–88. doi: 10.1007/s00345-016-1868-5

2. Motzer RJ, Tannir NM, McDermott DF, Arén Frontera O, Melichar B, Choueiri TK, et al. Nivolumab plus ipilimumab versus sunitinib in advanced renal-cell carcinoma. *N Engl J Med* (2018) 378(14):1277–90. doi: 10.1056/NEJMoa1712126

3. Motzer RJ, Penkov K, Haanen J, Rini B, Albiges L, Campbell MT, et al. Avelumab plus axitinib versus sunitinib for advanced renal-cell carcinoma. *N Engl J Med* (2019) 380 (12):1103–15. doi: 10.1056/NEJMoa1816047

4. Rini BI, Plimack ER, Stus V, Gafanov R, Hawkins R, Nosov D, et al. Pembrolizumab plus axitinib versus sunitinib for advanced renal-cell carcinoma. *N Engl J Med* (2019) 380 (12):1116–27. doi: 10.1056/NEJMoa1816714

5. Rassy E, Flippot R, Albiges L. Tyrosine kinase inhibitors and immunotherapy combinations in renal cell carcinoma. *Ther Adv Med Oncol* (2020) 12:1758835920907504. doi: 10.1177/1758835920907504

6. Motzer R, Alekseev B, Rha S-Y, Porta C, Eto M, Powles T, et al. Lenvatinib plus pembrolizumab or everolimus for advanced renal cell carcinoma. *N Engl J Med* (2021) 384 (14):1289–300. doi: 10.1056/NEJMoa2035716

7. Lee C-H, Shah AY, Rasco D, Rao A, Taylor MH, Di Simone C, et al. Lenvatinib plus pembrolizumab in patients with either treatment-naive or previously treated metastatic renal cell carcinoma (Study 111/KEYNOTE-146): a phase 1b/2 study. *Lancet Oncol* (2021) 22(7):946–58. doi: 10.1016/S1470-2045(21)00241-2

8. Suyama K, Iwase H. Lenvatinib: A promising molecular targeted agent for multiple cancers. *Cancer Control* (2018) 25(1):1073274818789361. doi: 10.1177/1073274818789361

9. Matsuki M, Hoshi T, Yamamoto Y, Ikemori-Kawada M, Minoshima Y, Funahashi Y, et al. Lenvatinib inhibits angiogenesis and tumor fibroblast growth factor signaling pathways in human hepatocellular carcinoma models. *Cancer Med* (2018) 7(6):2641–53. doi: 10.1002/cam4.1517

10. Roskoski R JR. Classification of small molecule protein kinase inhibitors based upon the structures of their drug-enzyme complexes. *Pharmacol Res* (2016) 103:26–48. doi: 10.1016/j.phrs.2015.10.021

11. Motzer RJ, Hutson TE, Glen H, Michaelson MD, Molina A, Eisen T, et al. Lenvatinib, everolimus, and the combination in patients with metastatic renal cell carcinoma: A randomised, phase 2, open-label, multicentre trial. *Lancet Oncol* (2015) 16(15):1473–82. doi: 10.1016/S1470-2045(15)00290-9

12. Kato Y, Tabata K, Kimura T, Yachie-Kinoshita A, Ozawa Y, Yamada K, et al. Lenvatinib plus anti-PD-1 antibody combination treatment activates CD8+ T cells through reduction of tumor-associated macrophage and activation of the interferon pathway. *PloS One* (2019) 14(2):e0212513. doi: 10.1371/journal.pone.0212513

13. Kimura T, Kato Y, Ozawa Y, Kodama K, Ito J, Ichikawa K, et al. Immunomodulatory activity of lenvatinib contributes to antitumor activity in the Hepa1-6 hepatocellular carcinoma model. *Cancer Sci* (2018) 109(12):3993–4002. doi: 10.1111/cas.13806

14. Shrihari T. Innate and adaptive immune cells in tumor microenvironment. *Gulf J Oncol* (2021) 1:77–81.

15. Pandolfi F, Cianci R, Pagliari D, Casciano F, Bagalà C, Astone A, et al. The immune response to tumors as a tool toward immunotherapy. *Clin Dev Immunol* (2011) 2011:894704. doi: 10.1155/2011/894704

16. Kim TK, Vandsemb EN, Herbst RS, Chen L. Adaptive immune resistance at the tumour site: mechanisms and therapeutic opportunities. *Nat Rev Drug Discovery* (2022) 21(7):529–40. doi: 10.1038/s41573-022-00493-5

17. Willemijn SME, Peulen HMU, Lalezari F, van der Noort V, Vries JF, de Aerts GJ, et al. Effect of pembrolizumab after stereotactic body radiotherapy vs pembrolizumab alone on tumor response in patients with advanced non-small cell lung cancer: Results of the PEMBRO-RT phase 2 randomized clinical trial. *JAMA Oncol* (2019) 5(9):1276–82. doi: 10.1001/jamaoncol.2019.1478

18. Willemijn SME, Chen D, Verma V, Hobbs BP, Peulen HMU, Aerts GJV, et al. Pembrolizumab with or without radiotherapy for metastatic non-small-cell lung cancer: a pooled analysis of two randomised trials. *Lancet Respir Med* (2021) 9(5):467–75. doi: 10.1016/S2213-2600(20)30391-X

19. Craig DJ, Ambrose S, Stanbery L, Walter A, Nemunaitis J. Systemic benefit of radiation therapy *via* abscopal effect. *Front Oncol* (2022) 12:987142. doi: 10.3389/fonc.2022.987142

frontiers | Frontiers in Immunology

TYPE Original Research
PUBLISHED 20 January 2023
DOI 10.3389/fimmu.2022.1045731

OPEN ACCESS

EDITED BY
Stephen Robert Daley,
Queensland University of Technology, Australia

REVIEWED BY
Jeffrey B. Travers,
Wright State University, United States
Daniel González Maglio,
University of Buenos Aires, Argentina

*CORRESPONDENCE
Scott N. Byrne
scott.byrne@sydney.edu.au

SPECIALTY SECTION
This article was submitted to Immunological Tolerance and Regulation, a section of the journal Frontiers in Immunology

RECEIVED 16 September 2022
ACCEPTED 22 December 2022
PUBLISHED 20 January 2023

CITATION
Tse BCY, Ferguson AL, Koay YC, Grau GE, Don AS and Byrne SN (2023) Exposure to solar ultraviolet radiation establishes a novel immune suppressive lipidome in skin-draining lymph nodes. *Front. Immunol.* 13:1045731. doi: 10.3389/fimmu.2022.1045731

Exposure to solar ultraviolet radiation establishes a novel immune suppressive lipidome in skin-draining lymph nodes

Benita C. Y. Tse[1], Angela L. Ferguson[1], Yen Chin Koay[1,2], Georges E. Grau[1], Anthony S. Don[1] and Scott N. Byrne[1,3]*

[1]The University of Sydney, School of Medical Sciences, Faculty of Medicine and Health, Sydney, NSW, Australia, [2]Heart Research Institute, The University of Sydney, Sydney, NSW, Australia, [3]Westmead Institute for Medical Research, Centre for Immunology and Allergy Research, Sydney, NSW, Australia

The ability of ultraviolet radiation to suppress the immune system is thought to be central to both its beneficial (protection from autoimmunity) and detrimental (carcinogenic) effects. Previous work revealed a key role for lipids particularly platelet-activating factor and sphingosine-1-phosphate in mediating UV-induced immune suppression. We therefore hypothesized that there may be other UV-induced lipids that have immune regulatory roles. To assess this, mice were exposed to an immune suppressive dose of solar-simulated UV (8 J/cm^2). Lipidomic analysis identified 6 lipids (2 acylcarnitines, 2 neutral lipids, and 2 phospholipids) with significantly increased levels in the skin-draining lymph nodes of UV-irradiated mice. Imaging mass spectrometry of the lipids in combination with imaging mass cytometry identification of lymph node cell subsets indicated a preferential location of UV-induced lipids to T cell areas. *In vitro* co-culture of skin-draining lymph node lipids with lymphocytes showed that lipids derived from UV-exposed mice have no effect on T cell activation but significantly inhibited T cell proliferation, indicating that the lipids play an immune regulatory role. These studies are important first steps in identifying novel lipids that contribute to UV-mediated immune suppression.

KEYWORDS

immune regulation, immune suppression, lipids, ultraviolet radiation, mass spectrometry, extracellular vesicles

1 Introduction

Exposure to the ultraviolet (UV) radiation in sunlight suppresses the local cutaneous immune response and is a major risk factor for the development of UV-induced skin cancers (1). The formation of pyrimidine dimers (2, 3) and production of *cis*-urocanic acid (4) within the skin following UV exposure are well-established molecular signals

responsible for local immune suppression. However, UV is also capable of causing systemic immune suppression which is associated with protection from several autoimmune diseases (5). The suppressive signal generated in UV irradiated skin is transmitted to local draining lymph nodes by migrating Langerhans cells (LC) (6, 7) and mast cells (8). Recently arrived LCs interact with Natural Killer (NK) T cells to suppress the immune response in an IL-4-dependent manner (7) while IL-10-producing mast cells (9) interact with follicular B cells (8). Ultimately, these early cellular events lead to the generation of antigen-specific, long-lived UV-Tregs (10, 11) and UV-Bregs (12–15). The skin-draining lymph nodes are therefore a key anatomical site for UV-suppression of immunity.

Recently we showed that a single dose of solar-simulated UV altered lymphocyte recirculation between the skin-draining lymph nodes and the peripheral blood (16). This phenomenon was due to UV increasing the amount of the chemotactic lipid, sphingosine-1-phospate (S1P), in the lymph nodes. The increase in S1P led to a downregulation of sphingosine-1-phospate receptor 1 ($S1P_1$) receptors and a sequestration of naïve and central memory T cells in the lymph nodes. This provided the first evidence that UV can modulate the immune system by manipulating lipids in the skin-draining lymph nodes.

There is a growing recognition for the role of bioactive lipids and lipid metabolism in modulating the immune response. Lipid oxidation for example, is required for regulatory T cell proliferation (17–19) and the generation of memory T cells (20). In addition, bioactive lipids such as lysophosphatidylserine suppress $CD4^+$ T cell activation and proliferation by inhibiting IL-2 production and the upregulation of early activation markers such as CD69 (21, 22). Binding of lysophosphatidylserine also suppresses the generation of regulatory T cells (21), in which IL-2 inhibition is likely similarly involved. Indeed, UV radiation alters lipid in the skin by increasing production of sphingolipids, prostanoids and hydroxy fatty acids whilst reducing production of free fatty acids and triglycerides (23–25). Of particular importance, UV radiation of the skin triggers the release of the immunosuppressive lipid, platelet-activating factor (PAF) and its analogs. Activation of PAF receptors on dermal mast cells and Langerhans cells initiates their migration to the skin-draining lymph node (26, 27). Antagonism of PAF receptors and/or PAF-receptor deficiency attenuates UVB-induced systemic (28, 29), but not local immune suppression (30).

In light of our finding that UV upregulates S1P, in addition to other immune suppressive lipids such as PAF in the skin (31, 32), we hypothesized that exposure to UV may activate other immune modulating lipids in the skin-draining lymph nodes. In this study, we used non-targeted lipidomics to identify six novel UV-induced lipids in the skin draining lymph nodes. Using a combination of imaging mass spectrometry and cytometry of the nodes we were able to reveal that the upregulated lipids were preferentially expressed in the T cell areas following UV exposure. Finally, when the lipids induced by UV were isolated from the skin-draining lymph nodes and incubated with lymphocytes, they suppressed the proliferation of T cells. Thus, ultraviolet radiation induces immunosuppressive lipids where T cell activation occurs – in the skin-draining lymph nodes.

2 Materials and methods

2.1 Animals and UV radiation

Female C57BL/6 mice (Australian BioResources Ltd, Moss Vale, Australia) aged 7-10 weeks were housed at 22°C on a 12 h light-dark cycle with free access to water, and chow (Specialty Feeds, WA) provided ad libitum. The fluorescent lights used in the animal house did not emit any UV radiation. All mice were shaved and housed together and provided with sufficient nesting material for them to self-regulate their body temperature. Mice were shaved on the back and exposed to a single, immune suppressive 8 J/cm^2 dose of solar-simulated UV generated with a 1000 W xenon arc solar simulator (Oriel, Stratford, CT) with an output of 8% UVB and 92% UVA. Full details on the UV spectra has been published by us previously (33). In female C57BL/6 mice, a solar simulated UV dose of 3.64J/cm^2 is the minimum required to induce a statistically significant increase in skin thickness (the minimal edematous dose; MEdD) (33). Unlike humans, mice don't make a readily detectable erythemal response to UV, and so the MEdD is used as a surrogate for the minimal erythemal dose (MED). Thus, the dose used is 2.2MEdD which translates to approximately 15min of midday summer sun in Sydney, Australia. Control mice were shaved, sham-irradiated and co-housed with irradiated mice. The animal experiments were approved by the University of Sydney Animal Ethics committee (#1352).

2.2 Imaging mass cytometry

Skin-draining (inguinal) lymph nodes were collected 24 hours post-UV radiation and freshly frozen in embedding media containing 5% v/v carboxymethylcellulose and 10% v/v gelatin (both Sigma, St. Louis, USA) which is optimal for mass spectrometry imaging, generating significantly less background than OCT (34). 10 µm sections were fixed in 100% cold acetone for 10 minutes. For staining, the slide was rehydrated, blocked using an avidin-biotin blocking kit (Life Technologies, Carlsbad, USA) and 10% mouse serum containing anti-CD16/32 antibody (50 µg/mL, clone 93, Biolegend, San Diego, USA). 50 µL of a master mix containing anti-mouse CD45-FITC, CD35-biotin, CD62L-APC and CD11b-PE in 2% mouse serum was added and stained at 22°C for 2 hours. The CD45-FITC antibody was used to provide visual confirmation that the staining process was successful. The use of CD35-biotin, CD62L-APC and CD11b-PE

primary antibodies allowed for amplification of weaker antibody stains with a secondary metal-conjugated antibody and ensured that all our markers of interest could be included in the panel. Antibody clones and concentrations are stated in Table 1. The slide was then washed in Tris-buffered Saline and Tween (TBST; all from Sigma). A second master mix containing metal-conjugated antibodies was added to each section and incubated overnight at 4°C. The next morning, the slides were washed and fixed for 9 min using formalin (Fronine, Riverstone, Australia). Following fixation, the slide was washed in TBST and stained with iridium DNA intercalator for 30 min at 22°C. The slide was again washed first with TBST and then in distilled water. The slide was dried at 22°C and imaged within one week of staining. Imaging was conducted using the Hyperion Imaging System coupled to a Helios (Fluidgm, South San Francisco, USA).

2.3 Lipid extraction

Lipids were extracted from skin-draining lymph nodes as previously described (16). For lipidomic studies, 50 µL of pooled internal standards (all from Avanti Polar Lipids, Alabaster, USA) containing 20 µM C12 (18:1/12:0) glucosyl (β) ceramide (C12 GluCer), 20 µM C17 (18:1/17:0) ceramide (C17 Cer) and 4 µM of C17 (17:1) sphingosine (C17 Sph) were spiked into the extraction solution along with the lymph nodes. For T cell functional studies, no internal standards were added.

2.4 Non-targeted mass spectrometry

5 µL of lipid sample was injected into ThermoFisher Scientific Vanquish Ultra-High Pressure Liquid Chromatography (UHPLC) system coupled to a Waters Acquity UPLC C18 column (1.7 µm pore size, 2.1 x 100 mm). The HPLC operated with gradients of solvent A (60% acetonitrile, 40% water, 0.1% formic acid (Sigma) and 10 mM ammonium formate (Sigma)) and solvent B (90% isopropanol, 10% acetonitrile, 0.1% formic acid and 10 mM ammonium formate) (Organic solvents were from Fisher Chemical, New Hampshire, USA) (Table 2).

The lipid scan was conducted using a Thermo Fisher Scientific Q Exactive HF-X Hybrid Quadrupole-Orbitrap™ mass spectrometer in full scan/data-dependent MS/MS ($ddMS^2$) mode between *m/z* 220 and 1600. These scans were conducted in both positive and negative ion mode to ensure all classes of lipids are captured. Analysis of the peaks was conducted using Compound Discoverer (Thermo Fisher Scientific, Waltham, USA).

Molecules of interest were fragmented either by adding the lipids of interest onto the inclusion list, or by using a targeted-selected ion monitoring followed by $ddMS^2$ in both positive and negative ion mode. The fragmentation pattern was analyzed in LipidSearch 4.0 (Thermo Fisher) to identify the molecules. The identification was considered correct if: 1) An A or B grade was obtained in LipidSearch (grading indicates confidence in identifying the fatty acids and lipid group); 2) fragments were consistent with identification (e.g. fragments of headgroups and fatty acids were found); and 3) fragmentation and identification was consistent across 3 individual experiments.

2.5 Mass spectrometry imaging

The lymph nodes were cryosectioned at 10 µm thickness and mounted onto indium tin oxide (ITO) slides (Bruker Daltonics, Billerica, USA). The slide was prepared for matrix-assisted laser desorption/ionization (MALDI) mass spectrometry imaging following a previously established method (35) to sublimate recrystallized 2, 5-dihydroxybenzoic acid (DHB) (Sigma) onto the ITO slide. The slide was then loaded into the UltrafleXtreme (Bruker) mass spectrometer. Elemental red phosphorus (Sigma) was used to calibrate the instrument. The sections were then ablated at 15 µm raster width (i.e. 15 µm spatial resolution) and full scan analyzed at *m/z* 380-1800. The peaks and images were analyzed on SCiLS lab (Bruker).

2.6 Primary lymph node cell culture with lipids

Naïve skin-draining lymph nodes were collected inside biosafety cabinets under sterile conditions before being dissociated with 25 gauge needles (Terumo, Shibuya City, Japan) and cells passed through a cell strainer (Miltenyi, Bergisch Gladbach, Germany) to obtain single cell suspensions. Cells were then counted using a haemocytometer (Livingstone, Toronto, Canada) and viability assessed using trypan blue (Life Technologies, Carlsbad, USA).

For proliferation assays, cells were prepared for carboxyfluorescein succinimidyl ester (CFSE; Thermo Fisher) staining by washing once in RPMI 1640 medium (Life Technologies) then resuspending in pre-warmed RPMI to a concentration of 5×10^7 cells/mL. CFSE was added to the cells at a 1 in 1000 dilution (final concentration 5µM). The cells were immediately inverted and placed in a 37°C incubator for 10 minutes. Cells were inverted every 3-4 minutes and the staining stopped with the addition of cold complete RPMI (RPMI with 10% charcoal-stripped FCS (Thermo Fisher), 0.05 µM 2-mercaptoethanol (Sigma) and 1% penicillin-streptomycin (Invitrogen, Waltham, USA)) at 4 times the initial volume. Cells were washed twice more with complete RPMI.

For T cell activation assays, non-CFSE-labelled cells were seeded into U-bottom 96-well plates (Corning, New York, USA) at 2×10^5 cells/well. For T cell proliferation assays, CFSE-labelled cells were seeded into the plates at 5×10^5 cells/well. Dried lipid preparations were reconstituted in complete RPMI and added to

10.3389/fimmu.2022.1045731

TABLE 1 List of antibodies used for imaging mass cytometry.

Fluorochrome/Metal	Antibody	Clone	Concentration	Source
FITC	CD45	30-F11	5 μg/mL	BD
Biotin	CD35	8C12	1.25 μg/mL	BD
APC	CD62L	MEL-14	2 μg/mL	eBioscience
PE	CD11b	M1/70	2 μg/mL	Biolegend
Structural cell markers				
115In	Lyve1	Polyclonal	4 μg/mL	R&D
160Gd	Podoplanin	8.1.1	4 μg/mL	Biolegend
165Ho	CD31	390	4 μg/mL	BD
Pan-immune marker				
174Yb	anti-FITC/FITC-CD45	FIT-22	4 μg/mL	Biolegend
Myeloid markers				
142Nd	CD11c	N418	8 μg/mL	Biolegend
144Nd	Ly6G	1A8	2 μg/mL	Biolegend
146Nd	CD207 (Langerin)	4C7	4 μg/mL	Biolegend
154Sm	CD169	3D6.112	4 μg/mL	Biolegend
156Gd	Anti-PE/PE-CD11b	PE001	4 μg/mL	Biolegend
161Dy	F4/80	BM8	3 μg/mL	Biolegend
163Dy	CD64	X54-5/7.1	2 μg/mL	Biolegend
170Er	Anti-biotin/biotin-CD35	1D4-C5	1 in 200	DVS/Fluidgm
176Yb	Ly6C	HK1.4	2 μg/mL	Biolegend
T cell markers				
152Sm	CD3e	145-2C11	4 μg/mL	Biolegend
153Eu	CD4	RM4-5	1.8 μg/mL	Biolegend
168Er	CD8a	53-6.7	4 μg/mL	Biolegend
145Nd	CD69	H1.2F3	4 μg/mL	Biolegend
171Yb	CD44	IM7	2 μg/mL	BD
162Dy	Anti-APC/APC-CD62L	APC003	1 in 100	DVS/Fluidgm
158Gd	FoxP3	FJK-16s	1 in 200	DVS/Fluidgm
B cell markers				
149Sm	CD19	6D5	2 μg/mL	Biolegend
150Nd	IA-IE	M5/114.15.2	2 μg/mL	Biolegend
159Tb	B220	RA3-6B2	2 μg/mL	Biolegend
Pan-nuclei marker				
191Ir/193Ir	DNA intercalator		1.25 ng/mL	DVS/Fluidgm

10.3389/fimmu.2022.1045731

TABLE 2 LC gradients and flow-rate.

Time (min)	Flow-rate (mL/min)	% Solvent B
0.0	0.280	30
3.0	0.280	30
4.5	0.280	43
5.5	0.280	55
8.0	0.280	65
13.0	0.280	85
14.0	0.280	100
20.0	0.280	100
20.2	0.360	30
24.8	0.360	30
25.0	0.280	30

cells at a ratio of one lymph node amount of lipids to one lymph node number of cells as previously described (16). A final concentration of 0.27 µg/mL of anti-CD3 (clone 1452c11) and 0.17 µg/mL of anti-CD28 (Biolegend, clone 37.51) antibodies were added to the cells. The plates were incubated at 37°C with the activation plate analyzed after 24 hours and proliferation analyzed at 72 hours.

2.7 Large extracellular vesicle isolation and analysis

To assess large extracellular vesicles (LEVs), 6 hours post-UV (or sham-UV) treatment, skin-draining lymph nodes were collected in double filtered FACs buffer (phosphate-buffered saline (PBS) with 0.5% bovine serum albumin (BSA, Bovogen, Melbourne, Australia) and 0.4% ethylenediaminetetraacetic acid (EDTA)). Lymph node capsules were broken apart and a single-cell suspension achieved, retaining both the resulting cells and suspension. Lymph node cell viability was assessed by trypan blue staining and quantified using a haemocytometer. LEVs were harvested from all samples using multiple centrifugations: 1500x*g* for 15 minutes to remove cells, 13000x*g* for 2 minutes to remove cellular debris and platelets, and 18000x*g* for 60 minutes at 4°C to pellet LEVs. LEV pellets from each condition were then resuspended in a final volume of 100µl filtered PBS and kept at -80°C until they were prepared for flow cytometric analysis.

2.8 Flow cytometry staining

Cells were washed and pre-stained with Fixable Viability Dye eFluor 455UV (Thermo Fisher) and FcBlock (Biolegend) for 15 minutes at 22°C. Cells were then washed and 50 µL of primary antibody mix added (Table 3). Cells were stained in the dark at 4°C for 30 minutes. For the proliferation studies, cells were then washed, fixed in 50 µL of fixation buffer (Biolegend) for 20 minutes, washed and resuspended in FACs buffer ready for analysis. For the activation studies, cells were prepared for intracellular staining using a FoxP3/transcription factor staining buffer set (Thermo Fisher). Cells were fixed and permeabilized for 20 minutes at 22°C. Cells were then washed with permeabilisation buffer and resuspended in 50 µL of intracellular antibody mix. After 30 minutes of staining at 22° C, cells were washed again with permeabilization buffer and then resuspended in FACs buffer ready for analysis.

LEVs were stained with annexin-V AF488 (BD, Franklin Lakes, USA) and selected parent antibodies: T cells (CD4, Biolegend, clone RM4-5 or CD8, eBioscience, clone 53-6.7), B cells (CD19, eBioscience, clone 1D3), monocyte/macrophages (CD11b, Biolegend, clone M1/70), platelets (CD41, BD,clone MWReg30), endothelial cells (CD105, BD, clone MJ7/18), mast cells (CD117, Biolegend, clone ACK2) or keratinocytes (pan-keratin, CST, clone C11) for 25 minutes in binding buffer and enumerated on a BD LSRFortessa for 120 seconds at medium flow rate. Countbright, absolute counting beads (Invitrogen) were used as an internal standard to allow direct enumeration of EVs per microlitre of supernatant. LEVs were analyzed on a FSC vs SSC dot plot. To define the LEV gate, we used 0.22–1.34 µm latex beads (Nano Fluorescent Size Standard Kit, Yellow, Flow Cytometry Grade, Spherotech, Lake Forest, USA). Events falling within the LEV gate were then analyzed for parent-antibody and AnnexinV-AF488 fluorescence on a cytogram.

2.9 Statistics

For experiments with n values of greater than 6, comparisons between 2 groups were done by Student's t tests. For experiments with n values of 6, a Shapiro-Wilks normality test was performed (α=0.05; $p<0.05$) and for normally-distributed data, a Student's t test (comparing 2 groups) or ordinary one-way ANOVA with a Holm-Sidak multiple comparisons test (comparing more than 2 groups) were used. For groups that failed the Shapiro-Wilks normality test, and for experiments with n values less than 6 a non-parametric analysis using Mann-Whitney test (comparing 2 groups) or Kruskal-Wallis test with Dunn's multiple comparisons (comparing more than 2 groups) were used. Data from individual mice was expressed as a fold change (normalized) to the mean of the No UV control group in each experiment. Thus the relative expression/frequency of the No UV group would be a value of 1, enabling different experimental repeats to be pooled.

TABLE 3 List of flow cytometry antibodies.

Marker	Fluorochrome	Concentration	Clone	Company
Common to both lymph node cell panels				
CD16/32	Purified	5 µg/mL	93	Biolegend
Live/dead	eFluor 455UV	1 in 1000		Thermo Fisher
CD3ε	PE-CF594	1 µg/mL	145-2C11	BD
CD4	PerCP	1 µg/mL	RM4-5	Biolegend
Cell activation panel (24 hours)				
CD8α	FITC	2.5 µg/mL	5H10-1	Biolegend
CD62L	BV421	1 µg/mL	MEL-14	BD
CD44	BV786	0.2 µg/mL	IM7	BD
CD25	APC-eFluor780	2 µg/mL	PC61.5	eBioscience
FoxP3 (intracellular)	PE	1 in 50	150D	Biolegend
CD69	PE-Cy7	1 µg/mL	H1.2F3	Thermo Fisher
$S1P_1$	APC	1 in 100	713412	R&D
Cell proliferation panel (72 hours)				
CD8a	APC-Cy7	1 µg/mL	53-6.7	Biolegend
CD11c	APC	2 µg/mL	N418	eBioscience
CD19	PE	1 µg/mL	eBio1D3	eBioscience
B220	BUV737	1 µg/mL	RA3-6B2	BD
I-A/I-E	BV510	2.5 µg/mL	M5/114.15.2	Biolegend

3 Results

3.1 UV does not alter skin-draining lymph node architecture nor T cell distribution

We have previously demonstrated that exposure to UV results in local skin-draining lymph node hypertrophy (8, 16). To determine if this UV-induced lymph node hypertrophy is associated with changes in lymph node architecture, we performed imaging mass cytometry assessing 24 immune and structural markers. UV-exposure did not change gross lymph node architecture, with B cell follicles ($B220^+$), T cell areas ($CD3^+$), macrophage areas (defined by varying expressions of CD11b, CD169 and F4/80), lymphatics ($Lyve\text{-}1^+$) and high endothelial venules ($CD31^+$) all appearing to be similar to control unirradiated lymph nodes (Figure 1A)

UV-irradiated skin-draining lymph nodes preferentially sequester naïve and central memory T cells (16). Imaging mass cytometry revealed that $CD4^+$ and $CD8^+$ T cell distribution was similar between unirradiated control and UV lymph nodes with both T cell subsets abundant in the cortical area and $CD4^+$ T cells prominent in the interfollicular space closer to the lymphatic sinuses (Figure 1B). This is consistent with other studies demonstrating that $CD4^+$ T cell localize with lymph node resident cDC2s close to the lymphatic sinus, whereas $CD8^+$ T cells localize with the more centrally-located resident cDC1 population (36). In both groups there was a greater concentration of $CD44^+$ memory T cells adjacent to the follicles. Hence, UV-induced lymph node hypertrophy is not associated with changes in lymph node architecture.

3.2 UV-radiation alters the skin-draining lymph node lipidome

We next assessed if UV radiation of the skin alters lipids within the skin-draining lymph nodes. Lipids extracted from the skin-draining lymph nodes were analyzed using non-targeted mass spectrometry. Six identifiable lipids were significantly increased in the skin-draining lymph nodes following UV exposure (Figure 2A). These lipids were acylcarnitine (20:4) (neutral mass of 447.3348), acylcarnitine (20:3) (449.3505), diglyceride (18:1_20:4) (642.5221), phosphatidylcholine (o-38:6) (791.5823), triglyceride (16:1_14:1_18:2) (798.6743) and phosphatidylethanolamine (22:0_18:2) (799.6102). Thus the UV-altered lipids belonged to a variety of lipid classes.

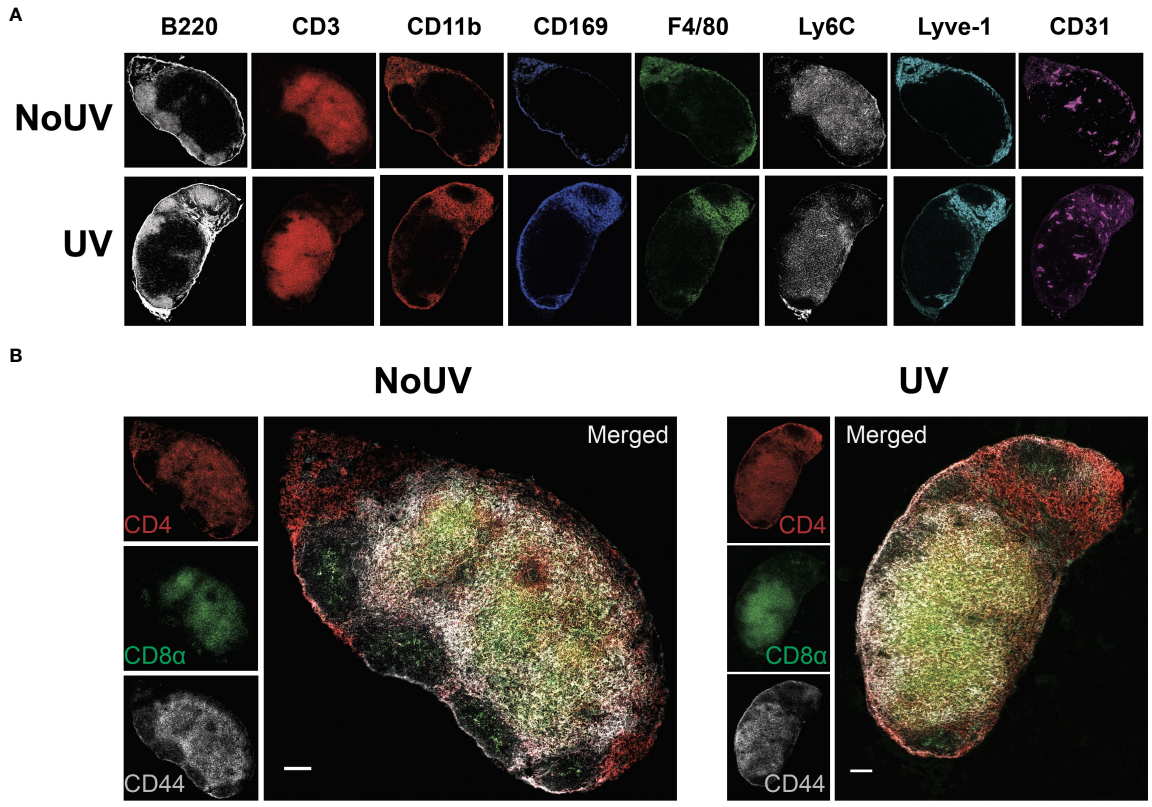

FIGURE 1
UV exposure does not alter skin-draining lymph node architecture. Skin-draining (inguinal) lymph nodes were collected from mice exposed (or not) to 8 J/cm^2 UV 24 h after exposure. Lymph node sections were stained and analyzed by imaging mass cytometry. **(A)** Representative images of immune and structural markers. **(B)** Representative images of CD4$^+$, CD8$^+$, and CD44$^+$ T cells. Scale bars represent 100 μm.

We next determined whether the UV altered lipids shared similar anatomical distribution across the lymph node. Since lipids cannot be imaged by immunohistochemistry or immunofluorescence, mass spectrometry imaging was conducted. Fresh-frozen lymph nodes were sectioned and sublimated with a lipid-ionizing DHB matrix. Lymph nodes were imaged by matrix-assisted laser desorption/ionization (MALDI) mass spectrometry imaging. In this method, the laser ablated a series of 15 μm pixels generating a non-targeted scan of detectable lipids at each pixel. A specific mass was selected and a gradient map generated to display the level of expression across the acquired area. We were able to detect 2 masses matching those of triglyceride (16:1_14:1_18:2; m/z 799.347) and phosphatidylethanolamine (22:0_18:2; m/z 800.327) with a hydrogen adduct (last 2 panels in Figure 2A showing the ammonium adduct, and imaging shown in Figure 2B). Both lipids appeared to localize to the same areas in the outer regions of each individual skin-draining lymph node, suggesting that the lipids may be draining into the lymph node. Mass spectrometry imaging data alone however did not reveal obvious differences in the lipid location between unirradiated control and UV-irradiated skin-draining lymph nodes.

To more closely interrogate the lymph node cells present in the high lipid areas, we mapped the location of the lipids to the serial section used for immune cell imaging. This revealed that the high lipid areas (as outlined in dotted lines) in the UV lymph nodes were more centrally located than in the control unirradiated lymph nodes (Figure 2B). To quantify this, B220 (B cell follicles), CD3 (T cell zones) and CD169 (macrophages in subcapsular sinus) expression within the high lipid "hotspot" areas were calculated as a percentage of the total area of the high lipid region of interest. The UV high lipid areas trended towards decreased CD169$^+$ and B220$^+$ expression whilst increasing CD3$^+$ expression [6 different lymph nodes from 6 individual mice (3 no UV and 3 UV) are shown in Figure 2C]. This data indicated that while no specific cell subset was associated with the high lipid regions, UV-induced lipids appear to preferentially locate more towards the T cell areas and away from the subcapsular sinus and B cell follicles.

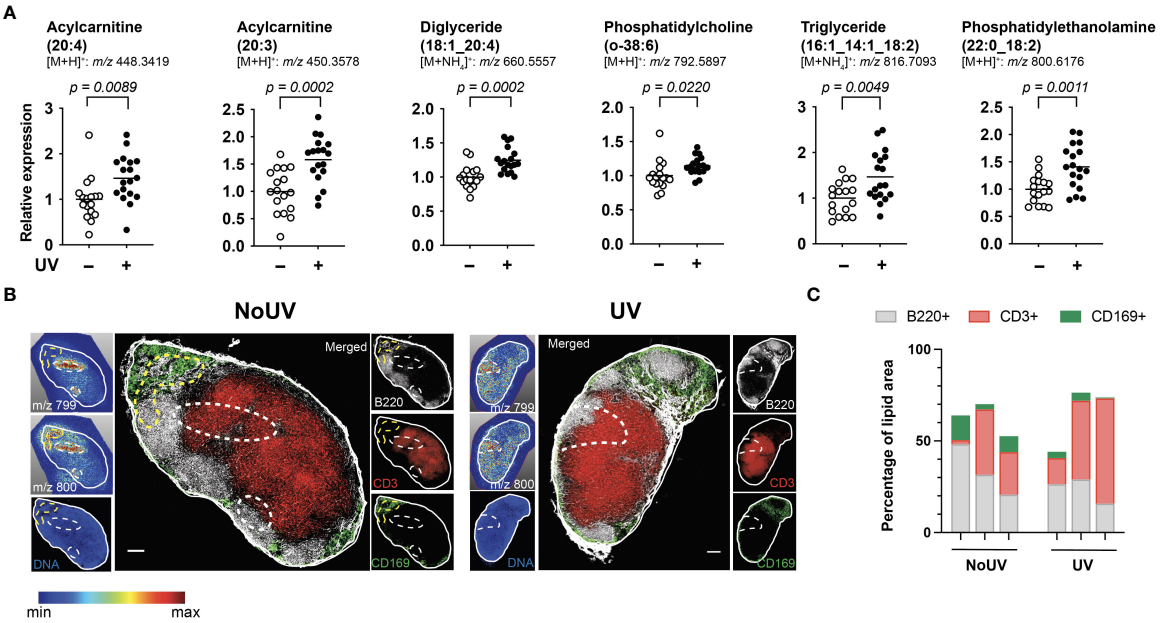

FIGURE 2
UV altered several lipids in the skin-draining lymph nodes with possible preferential localization to T cells areas. Skin-draining lymph nodes were collected from UV-irradiated and control mice 24 h after exposure. **(A)** Lipids extracted from skin-draining lymph nodes were analyzed by non-targeted mass spectrometry. Normalized relative expression of the lipids (acyl chain) across 3 independent UV experiments (each with n = 5-6 mice per group) are shown. Statistics were done by Student's t test with mean shown. **(B)** Mass spectrometry imaging and imaging mass cytometry were conducted on serial sections of lymph nodes. Representative lymph nodes shown with expression of lipids dictated by the gradient and dotted lines indicating high lipid areas. Scale bar represents 100 µm. **(C)** Areas of high lipid were quantified for the presence of CD169, B220 and CD3 expression for lymph nodes from 6 individual mice (3 NoUV and 3 UV).

3.3 UV-induced skin-draining lymph node lipids do not alter T cell subsets

Due to the preferential accumulation of UV-induced lipids in the T cell areas of lymph nodes, we next assessed whether UV-induced lipids affected lymphocyte activation and/or differentiation. To address this, we extracted the entire lipid fraction from the skin-draining lymph nodes of unirradiated control and UV-exposed mice. These bulk lipids were added to lymph node cells isolated from untreated skin-draining lymph nodes and incubated for 24 hours before T cell subsets were assessed by flow cytometry. The gating strategy to identify naïve, central memory, effector memory and regulatory T cells is shown in Figure 3A. To compare the effect of unirradiated control-derived and UV-derived lipids on T cell activation, the frequencies of subsets were normalized to the no lipid control. No differences were observed in the ability of lipids (from control or irradiated mice) to alter $CD4^+$ or $CD8^+$ T cells subsets, including Tregs (Figure 3B).

The failure of lipids alone to alter T cell subsets could be due to the absence of T cell stimulation. We therefore assessed whether lymph node lipids were able to suppress T cell activation in the presence of anti-CD3 and anti-CD28 antibodies. Similar to what was observed in the absence of T cell stimulation, adding lipids from unirradiated control or UV-irradiated mice did not affect $CD4^+$ or $CD8^+$ T cell activation in the presence of stimulation (Figure 3C). Hence, lipids from skin-draining lymph nodes, whether the skin is exposed to UV or not, do not alter T cell subsets.

3.4 UV-induced skin-draining lymph node lipids suppress T cell expansion

Clonal expansion is a requisite event for robust immune responses. Indeed, inhibition of T cell proliferation is a highly effective strategy underpinning the therapeutic success of immune suppressants (37). It was possible, therefore, that lipids from lymph nodes draining UV-exposed skin could be inhibiting T cell proliferation. To assess this, lipids isolated from the skin-draining lymph nodes of unirradiated control and UV-exposed mice were added to CFSE-labelled cells isolated from naïve skin-draining lymph nodes. Anti-CD3 and anti-CD28 antibodies were added to induce proliferation. 72 hours later, the cells were stained and analyzed by flow cytometry. As expected, the addition of anti-CD3 and anti-CD28 successfully caused $CD4^+$ and $CD8^+$ T cell proliferation. The addition of lipids derived from the skin-draining lymph nodes of mice exposed to UV, but not from

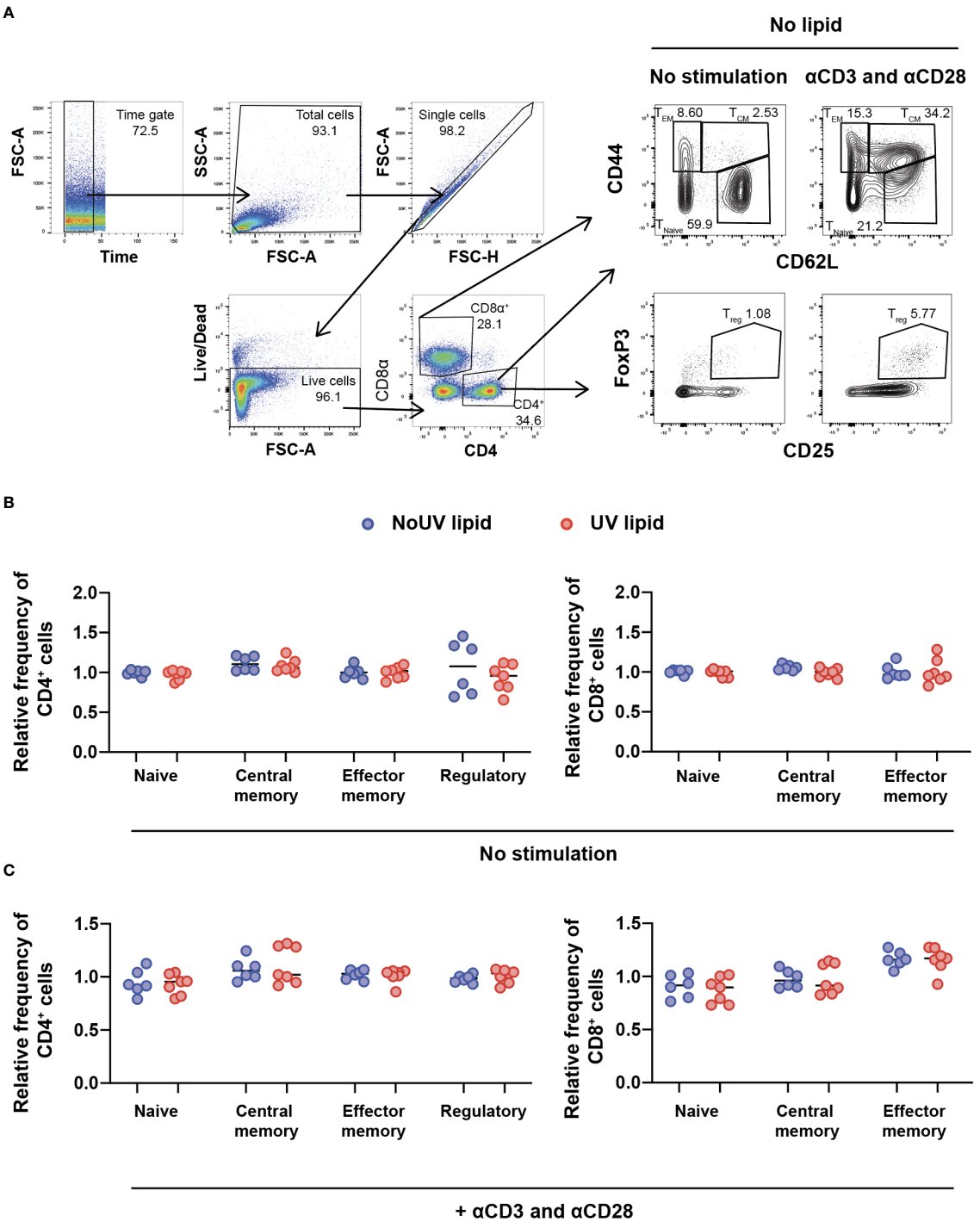

FIGURE 3
Lipids derived from UV-irradiated skin-draining lymph nodes have no effect on T cell subsets. Skin-draining lymph nodes were collected and lipids extracted. Lipids were then added to untreated skin-draining lymph node cells with or without anti-CD3 and anti-CD28 stimulation. Cells were cultured for 24 hours and stained for flow cytometry analysis. **(A)** Gating strategy for the identification of $CD4^+$ and $CD8^+$ T cell subsets. $CD62L^{hi}$ $CD44^{lo}$ T cells were defined as naïve, $CD62L^{hi}$ $CD44^{hi}$ T cells as central memory, $CD62L^{lo}$ $CD44^{hi}$ T cells as effector memory and $CD4^+$ $CD25^+$ $FoxP3^+$ cells as regulatory T cells. **(B)** T cell subsets following lipid co-culture without stimulation. **(C)** T cell subsets following lipid co-culture with stimulation. Relative frequency was calculated as a ratio to the no lipid control of each independent experiment. Median and individual mice (lipid donors, n = 6-7) from 2 independent UV-irradiation experiments are shown. Statistics were done by two-tailed unpaired Mann-Whitney test.

10.3389/fimmu.2022.1045731

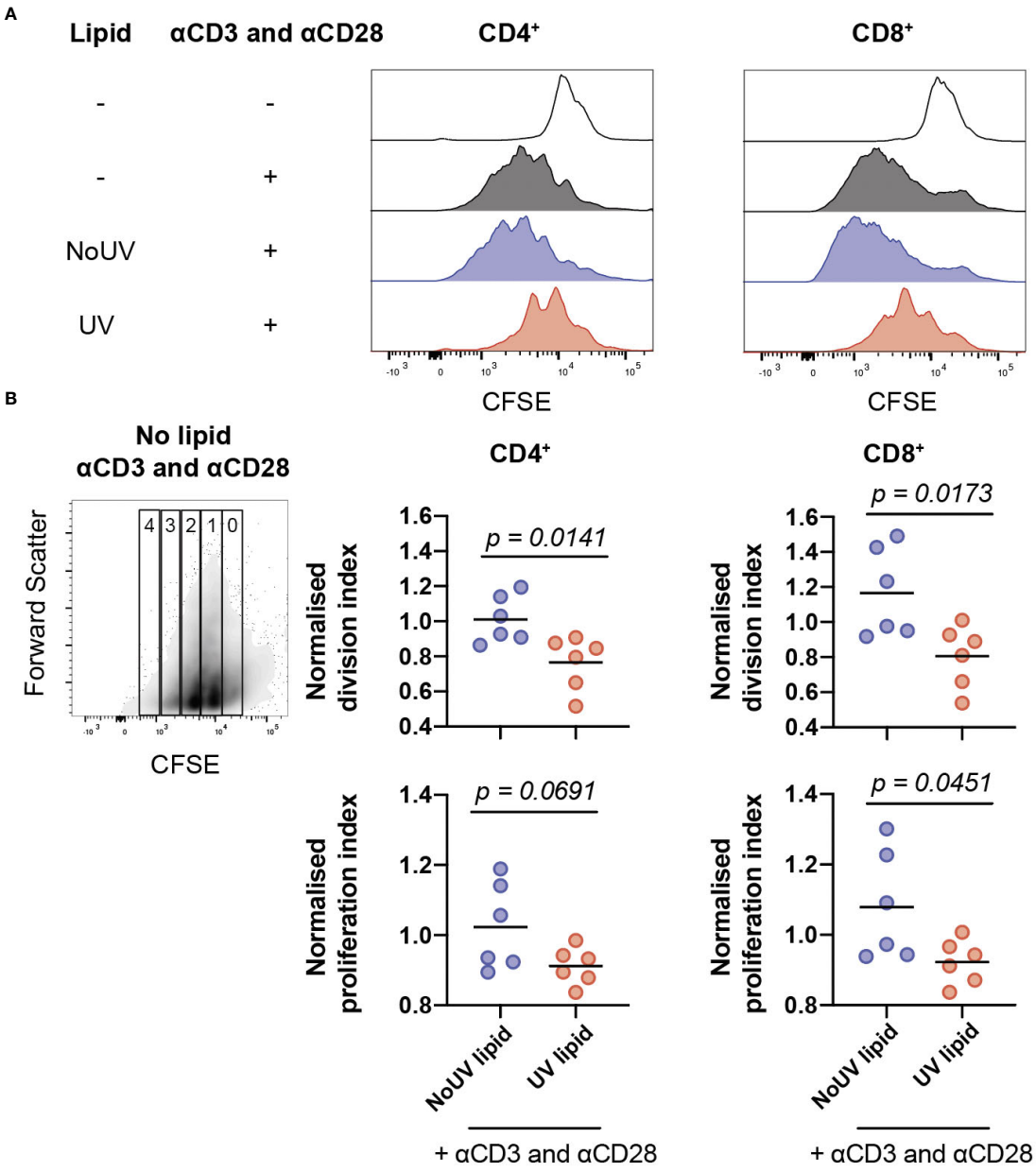

FIGURE 4
Lipids from UV-irradiated skin-draining lymph nodes suppress T cell proliferation. Skin-draining lymph nodes were collected and lipids extracted. Lipids were then added to CFSE-stained untreated skin-draining lymph node cells with or without anti-CD3 and anti-CD28. Cells were cultured for 72 h and assessed for CFSE expression by flow cytometry. **(A)** Representative histograms of CFSE expression in $CD4^+$ and $CD8^+$ T cells with and without lipids and/or stimulation. **(B)** Normalized division and proliferation index of $CD4^+$ and $CD8^+$ T cells with stimulation and either lipids from NoUV or UV mice. Division and proliferation indexes were normalized to the stimulated no lipid control of each independent experiment. Median and individual mice (lipid donors, n = 6) from 2 independent UV irradiation experiments are shown. Statistical analysis was by a two-tailed unpaired Student's t tests.

unirradiated control mice significantly inhibited both $CD4^+$ and $CD8^+$ T cell proliferation (Figure 4A).

To examine whether the lipids were reducing the number of cells proliferating or reducing the number of divisions each cell undergoes (or both), division index and proliferation index were calculated (38). Lipids from UV-exposed mice significantly decreased the division index for both helper and cytotoxic T cells (Figure 4B) indicating that the lipids suppressed the average number of divisions undertaken by all T cells. The proliferation index was also lower for $CD8^+$ T cells, but failed to reach statistical significance for $CD4^+$ T cells, meaning that once a $CD8^+$ T cell commenced proliferation, it underwent fewer

10.3389/fimmu.2022.1045731

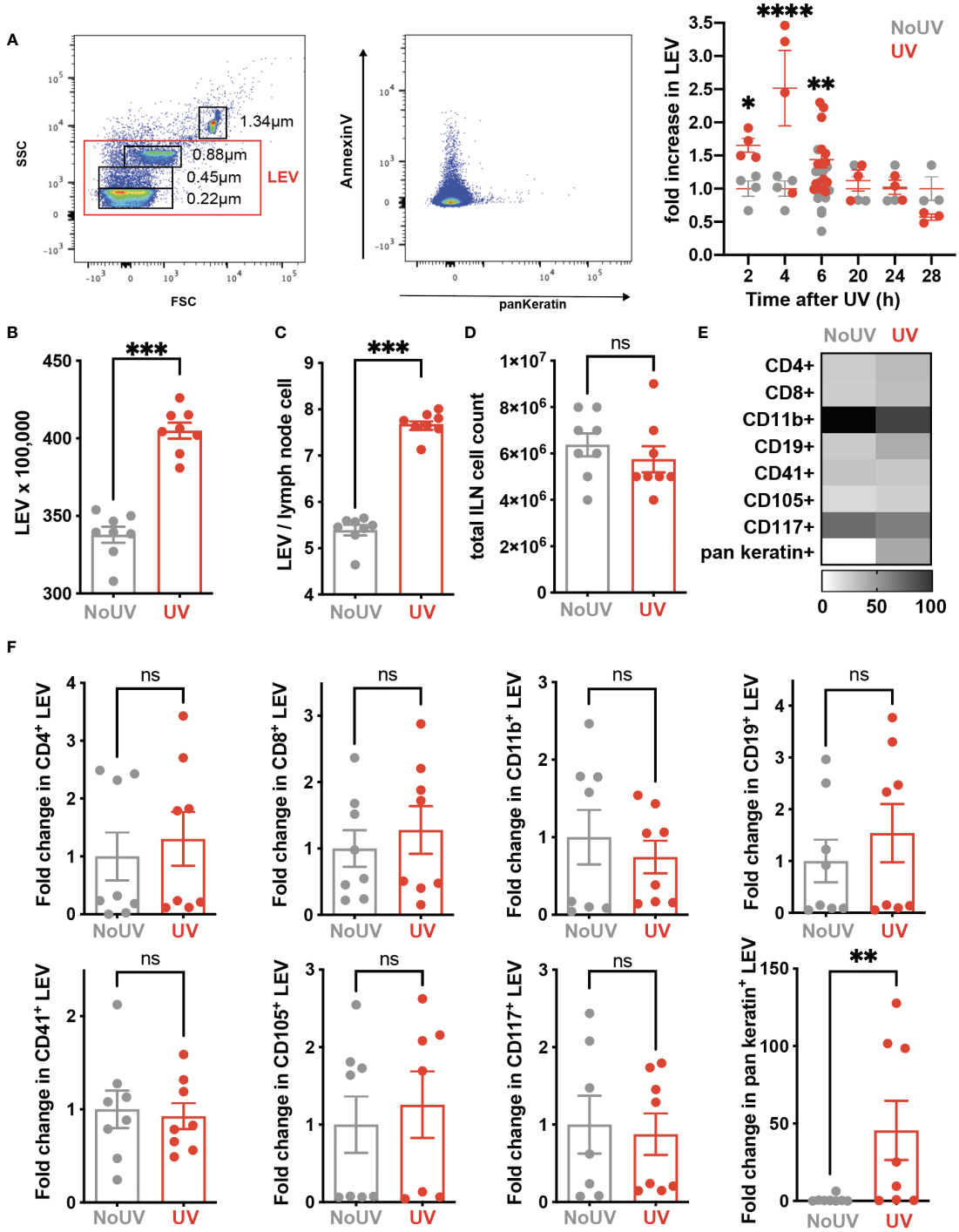

FIGURE 5
iLN LEV are increased at early but not late timepoints post UV exposure. **(A)** At the times indicated, or at 6h post UV, inguinal lymph nodes (iLN) were isolated and LEV isolated and analysed by flow cytometry. LEVs were gated using size beads (0.22, 0.45, 0.88, 1.34µm) to select particles 0.1-1µm (left plot), with a representative plot showing Keratin$^+$ LEVs (right plot). Fold increases in total iLN LEVs at 2, 4, 6, 20 and 24h post UV. At 6h post UV, total iLN LEVs were analyzed as **(B)** x100, 000 and **(C)** per iLN cell, calculated from **(D)** total iLN cell count. **(E)** Heatmap summarises changes in parent LEVs displayed as minimum-maximum percentile scaling where 100 is the maximum for each marker. **(F)** Each point represents an individual mouse UV-exposed (red) or not (grey). 'Parent' cell specific LEVs from T cells (CD4$^+$ and CD8$^+$), B cells (CD19$^+$), monocyte/macrophages (CD11b$^+$), platelets (CD41$^+$), endothelial cells (CD105$^+$) mast cells (CD117$^+$) and keratinocytes (pan-keratin$^+$) were assessed as fold change of absolute numbers x100,000. Statistical analysis was by a 2-way ANOVA with an uncorrected Fisher's LSD or Mann-Whitney test. *p< 0.05, **p< 0.01, ***p< 0.001, ****p<0.0001; ns, not significant.

divisions in the presence of lipids isolated from the lymph nodes of UV-exposed mice. Together, this indicates that UV-lymph node lipids significantly decrease the number of proliferating cells and, at least for $CD8^+$ cytotoxic T cells, reduce the number of divisions undertaken by cells that had commenced proliferation.

3.5 Skin-derived large extracellular vesicles rapidly appear in the lymph nodes following UV

Signals generated in UV-exposed skin leads to systemic immune suppression *via* the formation of microvesicles which are submicron (0.1-1μm) large extracellular vesicles (LEV) generated from the budding of cell membranes in response to stressors and danger-signals. LEVs derived from keratinocytes can be readily detected in the skin and plasma of mice and humans exposed to UVB radiation (39). Whether solar-simulated UV-induced skin LEVs find their way to draining lymph nodes has not been investigated before. Since LEVs can transport lipids as both cargo and on the membrane surface (40, 41), it is possible that skin-derived LEVs transport lipids to the skin-draining lymph nodes which could explain how UV alters the lymph node lipidome. To investigate this, groups of mice were exposed to UV before the LEVs in their skin-draining lymph nodes were analyzed by flow cytometry at various times. UV significantly increased the proportion of LEVs in the skin-draining lymph nodes at 2, 4 and 6h after UV (Figure 5A). Absolute numbers of LEVs were also increased 6h after UV exposure (Figure 5B). This increase preceded hypertrophy of the lymph nodes which typically occurs no earlier than 24h post exposure (Figures 5C, D) (8). Detailed flow cytometry analysis found that the only significant UV-induced increase was in $keratin^+$ LEV thus confirming their skin origin (Figure 5E). Indeed, $keratin^+$ LEV in the lymph nodes of control unirradiated mice were almost undetectable (Figure 5E). In addition, we found no change in LEV derived from other parent cells including T cells ($CD4^+$ and $CD8^+$ LEV), B cells ($CD19^+$ LEV), monocyte/macrophages ($CD11b^+$ LEV), platelets ($CD41^+$ LEV), endothelial cells ($CD105^+$ LEV) or mast cells ($CD117^+$ LEV) (Figures 5E, F with representative flow plots shown in Supplementary Figure 1). Thus, LEV from UV-exposed skin find their way to secondary lymphoid organs and represent an important way in which peripheral regulatory signals are transmitted to the immune system.

4 Discussion

The skin-draining lymph nodes are a major site of UV-induced immune suppression, where the activation of UV-Tregs, UV-Bregs and sequestration of naïve and central memory T cells occurs. Here we have demonstrated that UV upregulates 6 unique, previously undescribed UV-induced lipids, mostly in the T cell zones of lymph nodes, and that some of these lipids can suppress the expansion of T cells.

We previously showed that exposure to UVB prior to contact sensitization inhibits the expansion of effector T cells in the skin-draining lymph nodes (42). Until now, the mechanism behind this suppression was not known. There was no evidence for any of the described processes including prostaglandin E2 (PGE_2), pyrimidine dimers, *cis*-urocanic acid, reactive oxygen species, or the generation of functional Tregs (42, 43), to be responsible for this suppression. Here we show that lipids isolated from UV-irradiated skin-draining lymph nodes suppress T cell expansion. The lipid extraction method we used has been previously established as resulting in very minimal non-lipid material being extracted (44) and has been used in other similar lipid-tissue culture experiments (45), giving us confidence that the immune suppressive effects observed were indeed lipid-mediated. This suggests that UV-induced lipids in the local draining lymph nodes are at least in part responsible for a dampened T cell response post-UV exposure.

Our lipidomic analysis identified 2 acylcarnitines, a phosphatidylcholine, a diglyceride, a triglyceride and a phosphatidylethanolamine as being significantly increased in the skin-draining lymph nodes of UV-exposed mice. Previous studies have identified the lipids PGE2, PAF and arachidonic acid as being involved in UV-immune suppression (28). PGE2 is unlikely to be detected using untargeted mass spectrometry as it is too low in abundance. And due to its extremely short half-life, PAF is unlikely to be detectable under the experimental conditions used. However, the increased levels of acylcarnitine (20:4) we observed (Figure 2A) is a close surrogate for increased arachidonic acid as arachidonic acid is released from lipids that contain the arachidonyl fatty acid chain (20:4) in response to cell stimuli, usually associated with activation of phospholipase A2 (the enzyme that cleaves the 20:4 fatty acid from the lipid).

Whilst there is limited knowledge on how the specific lipids we identified affect cell-mediated immunity, the changes in acylcarnitines, diglycerides and triglycerides suggest that UV alters fatty acid metabolism. Indeed this is known to occur in the skin following UV exposure, whereby the expression of genes related to lipid synthesis are decreased (23, 24). Our group has also shown that UV exposure on the skin significantly increases total liver triglycerides (46). The possibility of UV modulating fatty acid metabolism is of particular importance as naïve T cells, but not effector T cells, use fatty acid oxidation and have high levels of acylcarnitine molecules (47, 48). Furthermore, regulatory T cells also use lipid oxidation to sustain proliferation (17–19). Since an increase in naïve T cells (16) and regulatory T cells (49) occurs in the skin-draining lymph nodes following UV irradiation, this potential change in lipid

metabolism may be an additional mechanism of maintaining naïve and regulatory T cells numbers in the lymph nodes.

Whilst the fragmentation data allowed for the identification of the lipid headgroup and acyl chains, the location of double bonds within the fatty acyl chain and the position of fatty acids on the glycerol headgroup cannot be distinguished by LC-MS/MS with electrospray ionization, as used for this study. This means that the specific lipids identified in this study cannot be synthesized currently as the exact structure is unknown. As the molecular structure affects the bioactivity of the lipid, this needs to be ascertained before functional studies can be conducted. Additionally, commercially available lipids typically contain identical fatty acids meaning that the UV-lipids identified in this study cannot be purchased, restricting the functional assays possible to interrogate whether the specific increases in lipids we have observed are responsible for inhibiting T cell expansion.

Visualization of UV-altered lipids using imaging mass spectrometry in combination with imaging mass cytometry was a powerful interrogation tool which revealed that lipids with masses close to triglyceride and phosphatidylethanolamine were found preferentially in T cell areas in the lymph nodes and further away from B cell follicles. In this study, mass spectrometry imaging was critical as lipids cannot be imaged by traditional immunohistochemical or immunofluorescent methods. However, mass spectrometry imaging does have some limitations. Mass accuracy is particularly important as it allows for the accurate identification of the lipid ion. However, the mass accuracies varied for the instrument used for lipidomic analysis (mass accuracy of 1 ppm) and imaging mass spectrometry (mass accuracy of ± 30 to 120 mDa). Since the imaging mass spectrometer had low mass accuracy and no fragmentation was done to ascertain the exact lipid identity, we cannot be certain that the same lipids identified in the lipidomic studies were imaged. Similarly, without an exact lipid identity, we are forced to assume that the imaged lipids were independent of each other and not isotopic ions (the same compound but with a series of ions differing by one *m/z* unit). In addition, the imaging mass spectrometer has lower sensitivity in comparison to the quadrupole-orbitrap mass spectrometer used for our lipidomics studies. This resulted in some of the low-abundance UV-induced lipids not being imaged.

This study has highlighted the ability of UV-induced lipids to suppress T cell proliferation in the skin-draining lymph nodes. A number of potential lipid candidates responsible for the suppression have been identified. Simultaneous sequestration of naïve and central memory T cells in the lymph nodes (16) will maximise the chances that the immune suppressive lipids we have discovered can influence T cell fate. The current limitations of lipid imaging resolution means that it is not yet known whether the associated cells are producing the lipid or are affected by the lipid. The conspicuous location of the lipids around the outer regions of the lymph nodes suggests that the lipids may be draining into the lymph nodes from the irradiated skin. Alternatively, exposure of the skin to UV, which enlarges dermal lymphatic vessels (50) and increases vascular flow, may result in increased drainage of cutaneous UV-induced lipids. This hypothesis would be consistent with free fatty acids and triglycerides being depleted in the epidermis following UV exposure (23). An alternative possibility that we considered and tested is that UV-induced skin lipids reach the lymph nodes packaged within large extracellular vesicles (LEV). UV induces LEV formation by keratinocytes in a PAF-dependent manner (51, 52) and in humans, LEV numbers within the skin and plasma (flow cytometrically identified by their surface expression of calcium-sensing receptors) are significantly increased post-UVB exposure (39). Our data shows that the same immune suppressive dose of solar simulated UV significantly increases the number of keratin-expressing LEVs in the local-draining lymph nodes 6 hours following exposure. Increases in skin-derived mast cells are not detectable in lymph nodes until 24h after UV exposure (8) so these events would appear to be distinct. To our knowledge this is the first-time antibodies to keratins have been used to identify skin-derived LEV. This approach is supported by proteomic data confirming the expression of keratins in LEVs (53). Showing that skin-derived LEVs are the source of the T cell-suppressing lipids in draining lymph nodes awaits next generation flow cytometers that can sort keratin+ LEVs for lipidomic analysis. In the meantime, studies inhibiting UV production of LEVs with topical acid sphingomyelinase inhibitors like imipramine could be performed. Indeed, this pharmacological strategy has already been shown to be effective in mice (39) and is currently being trialed in humans (NCT04520217).

Precisely how UV alters systemic immune responses is not well known. This is important if we are to harness the beneficial effects of UV to prevent and treat non-skin diseases like multiple sclerosis (5). The mechanisms appear to be different to that which mediate local immune suppression at the irradiated site. The release of skin-LEVs containing PAF (39) and alterations to S1P in lymph node nodes (16) are novel and major ways in which UV modulates distant, non-skin immune responses. Establishing a lymph node lipidome that suppresses T cell proliferation appears to be another.

Data availability statement

The original contributions presented in the study are included in the article/Supplementary Material. Further inquiries can be directed to the corresponding author.

Ethics statement

The animal study was reviewed and approved by The University of Sydney Animal Ethics Committee.

Author contributions

BT helped design and performed most of the experiments, analyzed and interpreted most of the data, prepared the majority of the figures and wrote the first draft of the manuscript. AF helped design and performed some of the experiments, analyzed and interpreted some of the data, and prepared some of the figures. YK and AD helped design, perform some of the experiments and interpret the results. GG helped design some of the experiments and interpret some of the data. SB supervised BT and AF, designed the experiments, analyzed and interpreted the data, finalized the figures and wrote the final draft of the manuscript. All authors contributed to the article and approved the submitted version.

Funding

BT was supported by an Australian Postgraduate Award. This work was supported by an Incubator Research Grant from Multiple Sclerosis Research Australia (#16-020) and with support from the Neil and Norma Hill Foundation.

Acknowledgments

We gratefully acknowledge subsidized access to Sydney Cytometry and Sydney Mass Spectrometry. We thank the support staff in these core facilities for their assistance.

Conflict of interest

The authors declare that the research was conducted in the absence of any commercial or financial relationships that could be construed as a potential conflict of interest.

Publisher's note

All claims expressed in this article are solely those of the authors and do not necessarily represent those of their affiliated organizations, or those of the publisher, the editors and the reviewers. Any product that may be evaluated in this article, or claim that may be made by its manufacturer, is not guaranteed or endorsed by the publisher.

Supplementary material

The Supplementary Material for this article can be found online at: https://www.frontiersin.org/articles/10.3389/fimmu.2022.1045731/full#supplementary-material

References

1. Fisher MS, Kripke ML. Systemic alteration induced in mice by ultraviolet light irradiation and its relationship to ultraviolet carcinogenesis. *Proc Natl Acad Sci USA* (1977) 74(4):1688–92. doi: 10.1073/pnas.74.4.1688

2. Kripke ML, Cox PA, Alas LG, Yarosh DB. Pyrimidine dimers in DNA initiate systemic immunosuppression in UV-irradiated mice. *Proc Natl Acad Sci USA* (1992) 89(16):7516–20. doi: 10.1073/pnas.89.16.7516

3. Kuchel JM, Barnetson RSC, Halliday GM. Cyclobutane pyrimidine dimer formation is a molecular trigger for solar-simulated ultraviolet radiation-induced suppression of memory immunity in humans. *Photochem Photobiol Sci* (2005) 4 (8):577–82. doi: 10.1039/b504068j

4. De Fabo EC, Noonan FP. Mechanism of immune suppression by ultraviolet irradiation in vivo. i. evidence for the existence of a unique photoreceptor in skin and its role in photoimmunology. *J Exp Med* (1983) 158(1):84–98. doi: 10.1084/jem.158.1.84

5. Hart PH, Norval M, Byrne SN, Rhodes LE. Exposure to ultraviolet radiation in the modulation of human diseases. *Annu Rev Pathol* (2019) 14:55–81. doi: 10.1146/annurev-pathmechdis-012418-012809

6. Moodycliffe AM, Kimber I, Norval M. Role of tumour necrosis factor-alpha in ultraviolet b light-induced dendritic cell migration and suppression of contact hypersensitivity. *Immunology.* (1994) 81(1):79–84.

7. Fukunaga A, Khaskhely NM, Ma Y, Sreevidya CS, Taguchi K, Nishigori C, et al. Langerhans cells serve as immunoregulatory cells by activating NKT cells. *J Immunol* (2010) 185(8):4633–40. doi: 10.4049/jimmunol.1000246

8. Byrne SN, Limon-Flores AY, Ullrich SE. Mast cell migration from the skin to the draining lymph nodes upon ultraviolet irradiation represents a key step in the induction of immune suppression. *J Immunol* (2008) 180(7):4648–55. doi: 10.4049/jimmunol.180.7.4648

9. Chacón-Salinas R, Limón-Flores AY, Chávez-Blanco AD, Gonzalez-Estrada A, Ullrich SE. Mast cell-derived IL-10 suppresses germinal center formation by affecting T follicular helper cell function. *J Immunol* (2011) 186(1):25–31. doi: 10.4049/jimmunol.1001657

10. Yamazaki S, Nishioka A, Kasuya S, Ohkura N, Hemmi H, Kaisho T, et al. Homeostasis of thymus-derived Foxp3+ regulatory T cells is controlled by ultraviolet b exposure in the skin. *J Immunol* (2014) 193(11):5488–97. doi: 10.4049/jimmunol.1400985

11. Maeda A, Beissert S, Schwarz T, Schwarz A. Phenotypic and functional characterization of ultraviolet radiation-induced regulatory T cells. *J Immunol* (2008) 180(5):3065–71. doi: 10.4049/jimmunol.180.5.3065

12. Byrne SN, Halliday GM. B cells activated in lymph nodes in response to ultraviolet irradiation or by interleukin-10 inhibit dendritic cell induction of immunity. *J Invest Dermatol* (2005) 124(3):570–8. doi: 10.1111/j.0022-202X.2005.23615.x

13. Byrne SN, Ahmed J, Halliday GM. Ultraviolet b but not a radiation activates suppressor b cells in draining lymph nodes. *Photochem Photobiol* (2005) 81 (6):1366–70. doi: 10.1562/2005-04-20-RA-495

14. Kok LF, Marsh-Wakefield F, Marshal JE, Gillis C, Halliday GM, Byrne SN. B cells are required for sunlight protection of mice from a CNS-targeted autoimmune attack. *J Autoimmun* (2016) 73:10–23. doi: 10.1016/j.jaut.2016.05.016

15. Matsumura Y, Byrne SN, Nghiem D, Miyahara Y, Ullrich SE. A role for inflammatory mediators in the induction of immunoregulatory b cells. *J Immunol* (2006) 177(7):4810–7. doi: 10.4049/jimmunol.177.7.4810

16. Tse BCY, Ireland RA, Lee JY, Marsh-Wakefield F, Kok LF, Don AS, et al. Exposure to systemic immunosuppressive ultraviolet radiation alters T cell recirculation through sphingosine-1-phosphate. *J Immunol* (2021) 207(9):2278–87. doi: 10.4049/jimmunol.2001261

17. Howie D, Ten Bokum A, Necula AS, Cobbold SP, Waldmann H. The role of lipid metabolism in T lymphocyte differentiation and survival. *Front Immunol* (2017) 8:1949. doi: 10.3389/fimmu.2017.01949

18. Macintyre AN, Gerriets VA, Nichols AG, Michalek RD, Rudolph MC, Deoliveira D, et al. The glucose transporter Glut1 is selectively essential for CD4 T cell activation and effector function. *Cell Metab* (2014) 20(1):61–72. doi: 10.1016/j.cmet.2014.05.004

19. Michalek RD, Gerriets VA, Jacobs SR, Macintyre AN, MacIver NJ, Mason EF, et al. Cutting edge: distinct glycolytic and lipid oxidative metabolic programs are essential for effector and regulatory CD4+ T cell subsets. *J Immunol* (2011) 186 (6):3299–303. doi: 10.4049/jimmunol.1003613

20. Pearce EL, Walsh MC, Cejas PJ, Harms GM, Shen H, Wang L-S, et al. Enhancing CD8 T-cell memory by modulating fatty acid metabolism. *Nature.* (2009) 460(7251):103–7. doi: 10.1038/nature08097

21. Barnes MJ, Cyster JG. Lysophosphatidylserine suppression of T-cell activation *via* GPR174 requires galphas proteins. *Immunol Cell Biol* (2018) 96 (4):439–45. doi: 10.1111/imcb.12025

22. Shinjo Y, Makide K, Satoh K, Fukami F, Inoue A, Kano K, et al. Lysophosphatidylserine suppresses IL-2 production in CD4 T cells through LPS3/GPR174. *Biochem Biophys Res Commun* (2017) 494(1-2):332–8. doi: 10.1016/j.bbrc.2017.10.028

23. Kim EJ, Jin X-J, Kim YK, Oh IK, Kim JE, Park C-H, et al. UV Decreases the synthesis of free fatty acids and triglycerides in the epidermis of human skin *in vivo*, contributing to development of skin photoaging. *J Dermatol Sci* (2010) 57(1):19–26. doi: 10.1016/j.jdermsci.2009.10.008

24. Kim EJ, Kim YK, Kim JE, Kim S, Kim M-K, Park C-H, et al. UV Modulation of subcutaneous fat metabolism. *J Invest Dermatol* (2011) 131(8):1720–6. doi: 10.1038/jid.2011.106

25. Tse BCY, Byrne SN. Lipids in ultraviolet radiation-induced immune modulation. *Photochem Photobiol Sci* (2020) 19(7):870–8. doi: 10.1039/d0pp00146e

26. Fukunaga A, Khaskhely NM, Sreevidya CS, Byrne SN, Ullrich SE. Dermal dendritic cells, and not langerhans cells, play an essential role in inducing an immune response. *J Immunol* (2008) 180(5):3057–64. doi: 10.4049/jimmunol.180.5.3057

27. Chacón-Salinas R, Chen L, Chávez-Blanco AD, Limón-Flores AY, Ma Y, Ullrich SE. An essential role for platelet-activating factor in activating mast cell migration following ultraviolet irradiation. *J Leukoc Biol* (2014) 95(1):139–48. doi: 10.1189/jlb.0811409

28. Walterscheid JP, Ullrich SE, Nghiem DX. Platelet-activating factor, a molecular sensor for cellular damage, activates systemic immune suppression. *J Exp Med* (2002) 195(2):171–9. doi: 10.1084/jem.20011450

29. Ocana JA, Romer E, Sahu R, Pawelzik SC, FitzGerald GA, Kaplan MH, et al. Platelet-activating factor-induced reduction in contact hypersensitivity responses is mediated by mast cells *via* cyclooxygenase-2-dependent mechanisms. *J Immunol* (2018) 200(12):4004–11. doi: 10.4049/jimmunol.1701145

30. Sahu RP, Yao Y, Konger RL, Travers JB. Platelet-activating factor does not mediate UVB-induced local immune suppression. *Photochem Photobiol* (2012) 88 (2):490–3. doi: 10.1111/j.1751-1097.2011.01071.x

31. Marathe GK, Johnson C, Billings SD, Southall MD, Pei Y, Spandau D, et al. Ultraviolet b radiation generates platelet-activating factor-like phospholipids underlying cutaneous damage. *J Biol Chem* (2005) 280(42):35448–57. doi: 10.1074/jbc.M503811200

32. Travers JB, Berry D, Yao Y, Yi Q, Konger RL, Travers JB. Ultraviolet b radiation of human skin generates platelet-activating factor receptor agonists. *Photochem Photobiol* (2010) 86(4):949–54. doi: 10.1111/j.1751-1097.2010.00743.x

33. Byrne SN, Spinks N, Halliday GM. Ultraviolet-a irradiation of C57BL/6 mice suppresses systemic contact hypersensitivity or enhances secondary immunity depending on dose. *J Invest Dermatol* (2002) 119(4):858–64. doi: 10.1046/j.1523-1747.2002.00261.x

34. Nelson KA, Daniels GJ, Fournie JW, Hemmer MJ. Optimization of whole-body zebrafish sectioning methods for mass spectrometry imaging. *J Biomol Tech.* (2013) 24(3):119–27. doi: 10.7171/jbt.13-2403-002

35. O'Rourke MB, Raymond BB, Djordjevic SP, Padula MP. A versatile cost-effective method for the analysis of fresh frozen tissue sections *via* matrix-assisted laser desorption/ionisation imaging mass spectrometry. *Rapid Commun Mass Spectrom.* (2015) 29(7):637–44. doi: 10.1002/rcm.7138

36. Gerner MY, Casey KA, Kastenmuller W, Germain RN. Dendritic cell and antigen dispersal landscapes regulate T cell immunity. *J Exp Med* (2017) 214 (10):3105–22. doi: 10.1084/jem.20170335

37. Haczku A, Alexander A, Brown P, Assoufi B, Li B, Kay AB, et al. The effect of dexamethasone, cyclosporine, and rapamycin on T-lymphocyte proliferation *in vitro*: comparison of cells from patients with glucocorticoid-sensitive and glucocorticoid-resistant chronic asthma. *J Allergy Clin Immunol* (1994) 93 (2):510–9. doi: 10.1016/0091-6749(94)90361-1

38. Roederer M. Interpretation of cellular proliferation data: avoid the panglossian. *Cytometry A.* (2011) 79(2):95–101. doi: 10.1002/cyto.a.21010

39. Liu L, Awoyemi AA, Fahy KE, Thapa P, Borchers C, Wu BY, et al. Keratinocyte-derived microvesicle particles mediate ultraviolet b radiation-induced systemic immunosuppression. *J Clin Invest* (2021) 131(10):e144963. doi: 10.1172/JCI144963

40. Record M, Silvente-Poirot S, Poirot M, Wakelam MJO. Extracellular vesicles: lipids as key components of their biogenesis and functions. *J Lipid Res* (2018) 59(8):1316–24. doi: 10.1194/jlr.E086173

41. Boilard E. Extracellular vesicles and their content in bioactive lipid mediators: more than a sack of microRNA. *J Lipid Res* (2018) 59(11):2037–46. doi: 10.1194/jlr.R084640

42. Rana S, Byrne SN, Macdonald LJ, Chan CY-Y, Halliday GM. Ultraviolet b suppresses immunity by inhibiting effector and memory T cells. *Am J Pathol* (2008) 172(4):993–1004. doi: 10.2353/ajpath.2008.070517

43. Rana S, Rogers LJ, Halliday GM. Systemic low-dose UVB inhibits CD8 T cells and skin inflammation by alternative and novel mechanisms. *Am J Pathol* (2011) 178(6):2783–91. doi: 10.1016/j.ajpath.2011.02.016

44. Bligh EG, Dyer WJ. A rapid method of total lipid extraction and purification. *Can J Biochem Physiol* (1959) 37(8):911–7. doi: 10.1139/y59-099

45. Travers JB, Weyerbacher J, Ocana JA, Borchers C, Rapp CM, Sahu RP. Acute ethanol exposure augments low-dose UVB-mediated systemic immunosuppression *via* enhanced production of platelet-activating factor receptor agonists. *J Invest Dermatol* (2019) 139(7):1619–22. doi: 10.1016/j.jid.2018.11.034

46. Ferguson AL, Kok LF, Luong JK, Van Den Bergh M, Bell-Anderson KS, Fazakerley DJ, et al. Exposure to solar ultraviolet radiation limits diet-induced weight gain, increases liver triglycerides and prevents the early signs of cardiovascular disease in mice. *Nutr Metab Cardiovasc Dis* (2019) 29(6):633–8. doi: 10.1016/j.numecd.2019.02.006

47. Angela M, Endo Y, Asou HK, Yamamoto T, Tumes DJ, Tokuyama H, et al. Fatty acid metabolic reprogramming *via* mTOR-mediated inductions of PPARgamma directs early activation of T cells. *Nat Commun* (2016) 7:13683. doi: 10.1038/ncomms13683

48. Raud B, McGuire PJ, Jones RG, Sparwasser T, Berod L. Fatty acid metabolism in CD8(+) T cell memory: Challenging current concepts. *Immunol Rev* (2018) 283(1):213–31. doi: 10.1111/imr.12655

49. Schwarz A, Maeda A, Wild MK, Kernebeck K, Gross N, Aragane Y, et al. Ultraviolet radiation-induced regulatory T cells not only inhibit the induction but can suppress the effector phase of contact hypersensitivity. *J Immunol* (2004) 172 (2):1036–43. doi: 10.4049/jimmunol.172.2.1036

50. Kajiya K, Detmar M. An important role of lymphatic vessels in the control of UVB-induced edema formation and inflammation. *J Invest Dermatol* (2006) 126 (4):919–21. doi: 10.1038/sj.jid.5700126

51. Bihl JC, Rapp CM, Chen Y, Travers JB. UVB generates microvesicle particle release in part due to platelet-activating factor signaling. *Photochem Photobiol* (2016) 92(3):503–6. doi: 10.1111/php.12577

52. Fahy K, Liu L, Rapp CM, Borchers C, Bihl JC, Chen Y, et al. UVB-generated microvesicle particles: A novel pathway by which a skin-specific stimulus could exert systemic effects. *Photochem Photobiol* (2017) 93(4):937–42. doi: 10.1111/php.12703

53. Willms E, Cabanas C, Mager I, Wood MJA, Vader P. Extracellular vesicle heterogeneity: subpopulations, isolation techniques, and diverse functions in cancer progression. *Front Immunol* (2018) 9:738. doi: 10.3389/fimmu.2018.00738

frontiers | Frontiers in Immunology

TYPE Original Research
PUBLISHED 15 February 2023
DOI 10.3389/fimmu.2023.1085742

OPEN ACCESS

EDITED BY
Stephen Robert Daley,
Queensland University of Technology,
Australia

REVIEWED BY
Jianlei Hao,
Jinan University, China
Alex Bobik,
Baker Heart and Diabetes Institute,
Australia

*CORRESPONDENCE
Katrin Peckert-Maier
katrin.peckert@uk-erlangen.de

†These authors have contributed equally to this work and share last authorship

SPECIALTY SECTION
This article was submitted to Immunological Tolerance and Regulation, a section of the journal Frontiers in Immunology

RECEIVED 31 October 2022
ACCEPTED 03 February 2023
PUBLISHED 15 February 2023

CITATION
Peckert-Maier K, Langguth P, Strack A, Stich L, Mühl-Zürbes P, Kuhnt C, Drassner C, Zinser E, Wrage M, Mattner J, Steinkasserer A, Royzman D and Wild AB (2023) CD83 expressed by macrophages is an important immune checkpoint molecule for the resolution of inflammation. *Front. Immunol.* 14:1085742. doi: 10.3389/fimmu.2023.1085742

CD83 expressed by macrophages is an important immune checkpoint molecule for the resolution of inflammation

Katrin Peckert-Maier[1*], Pia Langguth[1], Astrid Strack[1], Lena Stich[1], Petra Mühl-Zürbes[1], Christine Kuhnt[1], Christina Drassner[1], Elisabeth Zinser[1], Marius Wrage[2], Jochen Mattner[2], Alexander Steinkasserer[1], Dmytro Royzman[1†] and Andreas B. Wild[1†]

[1]Department of Immune Modulation, Universitätsklinikum Erlangen, Friedrich–Alexander Universität Erlangen–Nürnberg, Erlangen, Germany, [2]Mikrobiologisches Institut - Klinische Mikrobiologie, Immunologie und Hygiene, Universitäts-klinikum Erlangen and Friedrich-Alexander-Universität (FAU) Erlangen-Nürnberg, Erlangen, Germany

Excessive macrophage (Mφ) activation results in chronic inflammatory responses or autoimmune diseases. Therefore, identification of novel immune checkpoints on Mφ, which contribute to resolution of inflammation, is crucial for the development of new therapeutic agents. Herein, we identify CD83 as a marker for IL-4 stimulated pro-resolving alternatively activated Mφ (AAM). Using a conditional KO mouse (cKO), we show that CD83 is important for the phenotype and function of pro-resolving Mφ. CD83-deletion in IL-4 stimulated Mφ results in decreased levels of inhibitory receptors, such as CD200R and MSR-1, which correlates with a reduced phagocytic capacity. In addition, CD83-deficient Mφ upon IL-4 stimulation, show an altered STAT-6 phosphorylation pattern, which is characterized by reduced pSTAT-6 levels and expression of the target gene *Gata3*. Concomitantly, functional studies in IL-4 stimulated CD83 KO Mφ reveal an increased production of pro-inflammatory mediators, such as TNF-α, IL-6, CXCL1 and G-CSF. Furthermore, we show that CD83-deficient Mφ have enhanced capacities to stimulate the proliferation of allo-reactive T cells, which was accompanied by reduced frequencies of Tregs. In addition, we show that CD83 expressed by Mφ is important to limit the inflammatory phase using a full-thickness excision wound healing model, since inflammatory transcripts (e.g. *Cxcl1, Il6*) were increased, whilst resolving transcripts (e.g. *Ym1, Cd200r, Msr-1*) were decreased in wounds at day 3 after wound infliction, which reflects the CD83 resolving function on Mφ also *in vivo*. Consequently, this enhanced inflammatory milieu led to an altered tissue reconstitution after wound infliction. Thus, our data provide evidence that CD83 acts as a gatekeeper for the phenotype and function of pro-resolving Mφ.

KEYWORDS

CD83, macrophages, checkpoint molecule, resolution of inflammation, STAT-6, wound healing

Introduction

Macrophages (Mφ) constitute not only a vital part of the first defense line against invading pathogens, but they also resolve ongoing inflammation to re-establish tissue homeostasis. This variety of tasks requires a high level of phenotypic and functional plasticity to adapt to diverse environmental cues (1, 2). For example, Mφ undergo specific phenotypic and functional changes thereby contributing to proper wound healing upon skin injury. The wound healing process is generally characterized by overlapping phases, i.e. hemostasis, formation of inflammatory tissue, proliferation and remodeling of injured tissue (3, 4). Mφ are central for wound closure during all these stages, which is reflected by aberrant wound healing processes when Mφ have been depleted (4). Mφ not only dispose cellular debris during the inflammatory stage of wound healing, but later they adopt to a pro-resolving phenotype and secrete trophic factors, such as FGF or TGF-β, that induce proliferation of fibroblasts to promote complete wound closure (5).

These multifaceted Mφ phenotypes, which are required to adapt to *in vivo* challenges such as wound healing, are often classified into a spectrum between the two polar extremes of IFN-γ-stimulated, classically activated Mφ (CAM), and IL-4-treated, alternatively activated Mφ (AAM) (6). Pro-inflammatory CAM (MHCII^{high}, CD86^{high}, MerTK, CD40) predominantly boost inflammation by secretion of pro-inflammatory cytokines/chemokines, such as TNF-α, IL-6, IL-1β, CCL2, RANTES (7, 8). By contrast, alternatively activated Mφ (AAM) are often referred to as pro-resolving Mφ (MHC-II^{low}, CD86^{low}, CD206, PDL2, CD200R, MSR-1), that express specific mediators, such as CCL22, CCL17 or IL-10 (9, 10). Although the dichotomy of CAM and AAM does not suffice to grasp the entire complexity of Mφ polarization *in vivo*, it can be a valuable substitute for studying several aspects of Mφ biology *in vitro* (11). In this regard, genes that are associated uniquely with one of these phenotypes might emerge as important regulators of Mφ function.

Microarray analyses revealed that the *Cd83* transcript is specifically induced in AAM but not CAM (7). The corresponding membrane bound CD83 (mCD83) glycoprotein, which is expressed on activated immune cells, has been described to have potent immunomodulatory properties (12, 13). Furthermore, CD83 inhibits the ubiquitin-dependent degradation of MHC-II and CD86 on DCs as well as MHC-II on thymic epithelial cells, mediated by MARCH1 and MARCH8 respectively, thereby stabilizing the surface expression of these important molecules (14, 15). Moreover, CD83 expressed by DCs and regulatory T cells (Tregs) plays a central role in promoting resolution of inflammation (16, 17). In addition, a soluble isoform of CD83 (sCD83) has also been described, having profound immunomodulatory properties in murine autoimmune and transplantation models (12, 13, 18, 19). Recently, we reported that sCD83 induces pro-resolving Mφ, thereby improving corneal transplant survival (20) as well as skin wound healing processes (21).

However, the role of endogenously expressed mCD83 by Mφ is less well understood. An early study revealed that CD83 is preformed and stored intracellularly in human monocyte-derived cells, which allows for rapid surface display after stimulation with LPS. While LPS-stimulated DCs stably express CD83 for up to 48 hours, CD83 is only transiently detectable on monocytes and Mφ upon LPS stimulation, suggesting distinct regulatory mechanisms that might also affect cellular functions (22). Even more importantly, the role of CD83 expressed by AAM has not yet been addressed, despite the clear association with this Mφ phenotype (7).

Thus, we first analyzed CD83 expression kinetics in murine bone-marrow derived Mφ (BMDM) after stimulation with pro- and anti-inflammatory agents. Like in human Mφ, CD83 is expressed only transiently by BMDM after LPS stimulation, but shows stable surface display after stimulation with IL-4, suggesting an association with a pro-resolving phenotype. To further investigate the biological function of CD83 expressed by Mφ, we generated conditional knock-out (cKO) mice, specifically lacking CD83 expression by Mφ (CD83$^{\Delta M\varphi}$). BMDM from cKO mice show a striking reduction of MHC-II and CD86 expression, which could be explained by the missing inhibition of MARCH1, mediated by mCD83 (14). Stimulation of CD83-deficient Mφ with IL-4 resulted in a disturbed homeostatic IL-4 phenotype, characterized by lower expression levels of the inhibitory CD200R and scavenger receptor MSR-1, whilst DECTIN-1 was upregulated. We report data suggesting that this phenotype is associated with decreased IL-4 signaling activity. Functionally, CD83-deficient Mφ are characterized by their impaired phagoytic activity, by a pro-inflammatory cytokine signature as well as an enhanced allogeneic T cell stimulatory capacity. Using a full-thickness excisional wound healing model, we show that the specific deletion of CD83 in murine Mφ boosts the inflammatory phase within the wound area. This was hallmarked by an accelerated wound closure on day 3 in cKO mice compared to CD83wt control mice. As mentioned above during later phases of normal wound healing, i.e. without scar formation or fibrosis, Mφ adapt to an anti-inflammatory phenotype. However, we did not observe these phenotypic changes, since our analyses revealed increased expression of pro-inflammtory CAM-associated transcripts, e.g. *Il6* and *Cxcl1* as well as an decreased expression of AAM-associated transcripts including *Cd200r, Msr-1* as well as *Ym-1*. Thus, these data confirm our *in vitro* analyses showing an increased inflammatory phenotype of CD83-deficient macrophages. Finally, this pro-inflammatory milieu in wound areas of CD83-deficient cKO mice resulted in the upregulation of fibrosis associated transcripts, such as *Tgfb, Acta-2* and *Col1a1* on day 6.

Collectively, here we report for the first time data regarding the regulation of CD83 expression by murine Mφ and characterize CD83 as a checkpoint molecule modulating the function of murine Mφ.

Results

Stimulation of the IL-4 signaling pathway results in long-term and stable expression of CD83 on Mφ

Previous studies reported that CD83 is transiently expressed on human Mφ after LPS stimulation and that it is associated with IL-4 induced gene expression in murine Mφ (7, 22). However, temporal regulation of CD83 expression after both pro- and anti-inflammatory stimulation of murine Mφ has not yet been investigated. Thus, we incubated murine BMDM either with pro-inflammatory or with anti-

inflammatory mediators and assessed CD83 expression kinetics. Stimulation with IL-4 induced a strong and long-lasting CD83 expression on the cell surface of murine Mφ after 16 h, while neither LPS, IFN-γ nor TNF-α induced elevated surface expression levels (Figure 1A, left bar graph). Representative FACS histograms are shown in Figure 1A, right graph. In agreement with these results, we detected no *Cd83* regulation on mRNA level upon stimulation with IFN-γ or TNF-α after 16h (Figure 1B). In addition, LPS stimulation of murine Mφ results in significantly reduced *Cd83* mRNA levels in comparison to unstimulated Mφ (Figure 1B). Again, only IL-4 induced significant *Cd83* mRNA transcript levels after 16 h post stimulation (Figure 1B).

Subsequently, we investigated the temporal regulation of CD83 expression. Thus, we stimulated Mφ with LPS and other pro-inflammatory compounds and analyzed surface expression of CD83 over a 20 h time course (Figure 1C). LPS treatment caused an almost threefold increase of CD83 surface expression at the 2 h time point, followed by a rapid decline to baseline levels after six to eight hours. Similarly, the yeast cell wall component zymosan, which in contrast to LPS acts *via* TLR2, induced fourfold higher

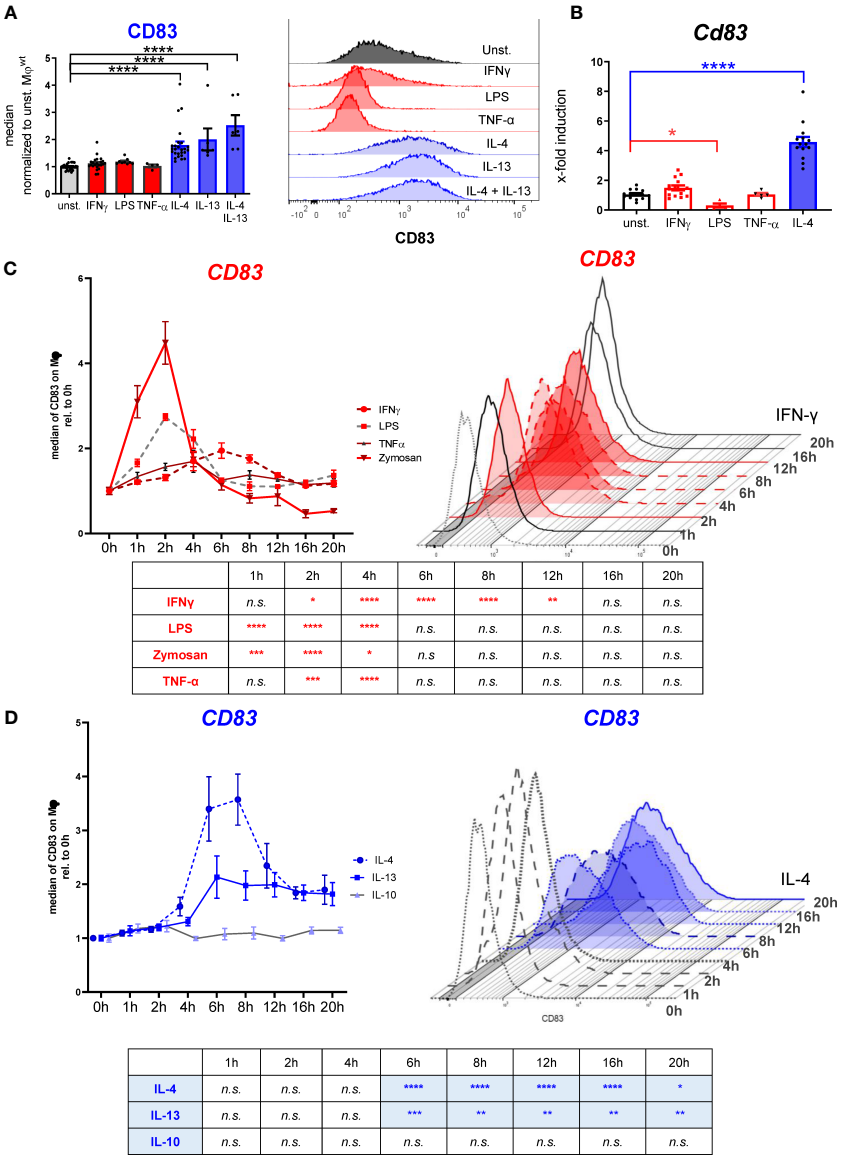

	1h	2h	4h	6h	8h	12h	16h	20h
IFNγ	n.s.	*	****	****	****	**	n.s.	n.s.
LPS	****	****	****	n.s.	n.s.	n.s.	n.s.	n.s.
Zymosan	***	****	*	n.s	n.s.	n.s.	n.s.	n.s.
TNF-α	n.s.	***	****	n.s.	n.s.	n.s.	n.s.	n.s.

	1h	2h	4h	6h	8h	12h	16h	20h
IL-4	n.s.	n.s.	n.s.	****	****	****	****	*
IL-13	n.s.	n.s.	n.s.	***	**	**	**	**
IL-10	n.s.	n.s.	n.s.	n.s.	n.s.	n.s.	n.s.	n.s.

FIGURE 1
Analyses of CD83 surface expression by murine bone-marrow derived Mφ using different stimuli. Murine bone-marrow derived macrophages were generated and CD83 expression levels were analyzed after inflammatory or alternative activation. **(A)** Flow cytometric analyses show no CD83 expression on murine Mφ upon stimulation with IFN-ɣ (300 U/ml), LPS (100ng/ml), TNF-α (300 U/ml) for 16h. In contrast, stimulation with IL-4 (40 ng/ml), IL-13 (40 ng/ml) or IL4+IL-13 resulted in high CD83 expression on the surface of Mφ at the 16h time point (n ≥ 4) (left bar graph); Representative FACS histograms are presented (right graph). **(B)** qPCR analyses of *Cd83* mRNA expression after different stimulations in murine Mφ. **(C)** Time-dependent regulation of CD83 expression on BMDM after inflammatory activation with IFN-ɣ (300 U/ml), LPS (100ng/ml), TNF-α (1000 U/ml) or Zymosan 10 µg/ml (n ≥ 4), analyzed by flow cytometry. **(D)** Time-dependent regulation of CD83 expression on BMDM upon stimulation with IL-4 (40 ng/ml), IL-13 (40 ng/ml) or IL-10 (10 ng/ml) (n ≥ 4), analyzed by flow cytometry. Gating strategy for the Mφ population is depicted in Supplementary Figure 2. Data are represented as mean ± SEM. Statistical analysis was performed using a Two-way ANOVA or the appropriate corresponding non-parametric test. Experiments were performed at least three times. n.s., not significant, which indicates there is no statistical signficance; * p<0.05; ** < 0.01; *** p < 0.001; **** p < 0.0001.

CD83 surface levels during the first two hours of stimulation. A slightly slower and less pronounced response was observed upon treatment with TNF-α, which resulted in a peak of CD83 expression after 4 h (Figure 1C). IFN-γ induced a rather delayed type of response, with a steady increase up to two-fold within the first six hours and a subsequent decrease until 16 h after stimulation (Figure 1C). Interestingly, IL-4 and IL-13 treatment caused a 2- to 3-fold CD83 induction as early as 4 h after stimulation, but in contrast to the pro-inflammatory mediators, this elevated expression did not revert to baseline levels even 20 h after stimulation (Figure 1D). Treatment with IL-10, another anti-inflammatory cytokine, had no influence on CD83 expression (Figure 1D). Thus, we observed a striking discrepancy in CD83 regulation after stimulation: while pro-inflammatory mediators induced a very rapid but transient increase in CD83 surface expression, stimulation of the IL-4R with either IL-4 or IL-13 resulted in a stable CD83 display on the cell surface. These data indicate an interesting functional role of CD83 in Mφ biology, especially for the resolving phenotype associated with IL-4 signaling.

Cell specific deletion of CD83 expression in Mφ interferes with their pro-resolving phenotype

Next, we aimed to characterize the biological function of CD83 expressed by murine Mφ by using a conditional knock-out (cKO) strategy. By crossing mice carrying floxed *Cd83* alleles with a CX3CR1-Cre line, we generated a conditional line with an abrogated CD83 expression specifically in Mφ (herein termed CD83$^{\Delta M\varphi}$). To test the efficacy of our KO strategy, we treated Mφ from CD83 cKO mice and wt mice with IFN-γ or IL-4 for 16 h and assessed the expression of *Cd83* by qPCR (Figure 2A). As depicted in Figure 2A, murine CD83wt Mφ stimulated with IL-4 show a highly significant induction of *Cd83* mRNA levels compared to unstimulated CD83wt Mφ, whilst no expression was observed in Mφ from cKO mice (Figure 2A). These results were confirmed by surface expression analyses of cKO derived Mφ after IL-4 treatment, whereas wt derived Mφ showed a significant and stable expression of CD83 (Figure 2B). Similarly, CD83 protein was also absent in cell lysates derived from cKO BMDMs as shown by Western blot analyses (Figure 2C).

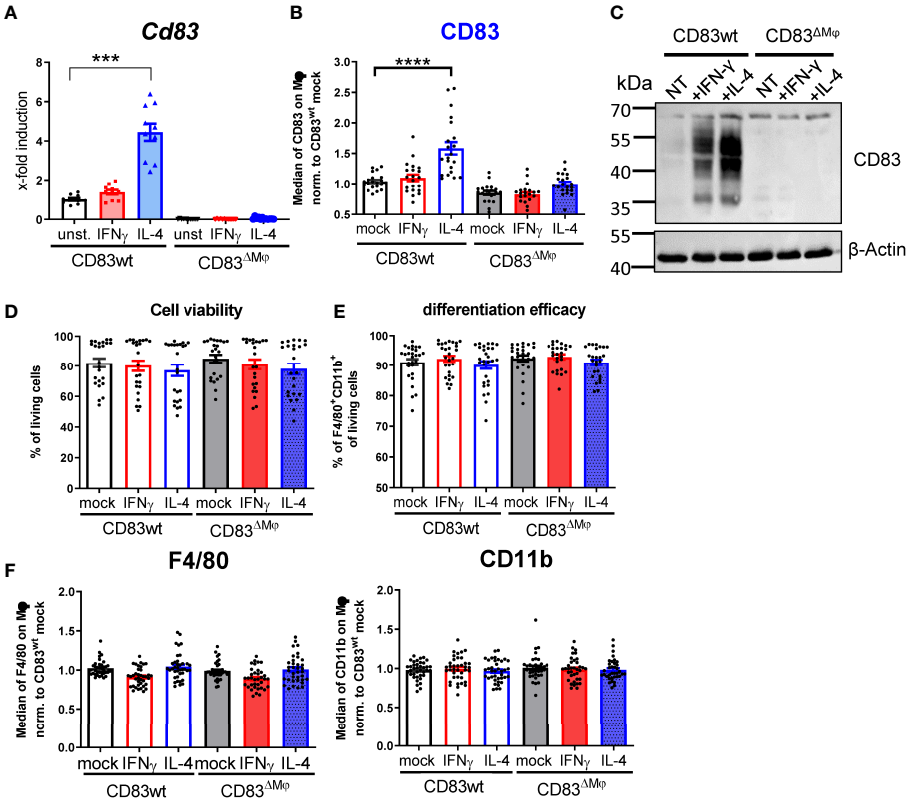

FIGURE 2
Analyses of CD83 deficient murine Mφ. Mφ were generated from CD83wt or CD83 cKO mice and subsequently stimulated with IFN-γ or IL-4 for 16h or left untreated. **(A)** *Cd83* expression levels were determined by qPCR and normalized to CD83wt BMDMs (n = 10). **(B)** Assessment of CD83 expression levels by flow cytometry (n = 20). **(C)** Assessment of knock-out efficiency in whole cell lysates from mock-, IFN-γ or IL-4 stimulated Mφ by Western blotting. β-actin served as a loading control. See full uncut gels in Supplemental Material (S1) **(D)** Cell viability assessment using flow cytometry (n = 24). **(E)** Differentiation efficacy assessing the percentage of F4/80^{+}CD11b^{+} cells by flow cytometry, representing the Mφ population (n ≥ 24). **(F)** Expression levels of F4/80 and CD11b within the Mφ population (n ≥ 40). The gating strategy for the Mφ population is depicted in Supplementary Figure 2. Statistical analyses were performed by One-way ANOVA or the appropriate corresponding non-parametric test. Data are represented as mean ± SEM. Experiments were performed at least three times. ***p<0.001; **** p< 0.0001. The absence of asterisks indicates that there is no statistical significance.

Interestingly, while stimulation with IFN-γ had no apparent effect on CD83 surface expression after 16 h, total protein levels were also elevated (Figure 2C), although to a lesser extent than IL-4 treatment. Next, we examined whether CD83-deletion affects cell viability (Figure 2D) or differentiation efficacy (Figure 2E), by flow cytometry and found that neither were affected. Furthermore, CD83 deletion has no effect on expression levels of F4/80 as well as CD11b on CD83$^{\Delta M\varphi}$ (Figure 2F). Thus, we conclude that CD83 deletion does not alter cell viability nor differentiation of murine mock-, IFN-γ- or IL-4-stimulated BMDM, generated from CD83wt or cKO mice.

In APCs, such as DCs and B cells, CD83 has been reported to stabilize surface MHC-II and CD86 expression by preventing their ubiquitin-dependent degradation (14, 17). Both molecules are hallmarks of a classic activation *via* IFN-γ, and consequently, we addressed the question how deletion of CD83 might affect their surface display. We observed an up-regulation of MHC-II and CD86 molecules on BMDM after stimulation with IFN-γ and to a lesser extent after IL-4 treatment (Figure 3A). In line with previous reports regarding the CD83-MARCH-MHC-II axis, Mφ from CD83$^{\Delta M\varphi}$ mice exhibited significantly lower surface expression levels of MHC-II and CD86 (Figure 3A). Since CD83 inhibits MHC-II ubiquitination *via* the interference with the ubiquitin-ligase March1 or March8 in DCs or thymic epithelial cells, respectively (14, 15), we tested which ubiquitin-ligase predominates in BMDM. Thus, BMDM were either left unstimulated or treated with IFN-γ, and we detected comparable levels of *Marchf1* transcripts. Since *Marchf8* expression is reduced by almost two orders of magnitude in comparison to *Marchf1* (see. Figure 3B), we conclude that CD86 as well as MHC-II stabilization is achieved by CD83-mediated inhibition of March1.

Next, we analyzed the overall phenotype of CD83-deficient Mφ. Since CD83 expression is tightly associated with an IL-4 mediated alternative activation (Figure 1C), we hypothesized that deletion of CD83 would mostly affect polarization of AAM. Indeed, we detected an altered phenotype in IL-4 stimulated CD83-deficient Mφ. This phenotype was characterized by significantly increased Dectin-1 expression on protein (Figure 3C, left bar graph) and mRNA level (Figure 3C, right bar graph), which is associated with a pro-inflammatory CAM polarization (23–26). Concomitantly, in IL-4-stimulated CD83-deficient Mφ we observed significantly reduced expression levels of the inhibitory receptor CD200R, which is known to limit pro-inflammatory cytokine secretion (27) (Figure 3D, left bar graph). Moreover, pro-resolving MSR-1 was also significantly decreased in IL-4 stimulated CD83-deficient Mφ, compared to CD83wt control Mφ. Furthermore, qPCR analyses of *Clec7a* (Figure 3C, right bar graph), *Cd200R* (Figure 3D, right bar

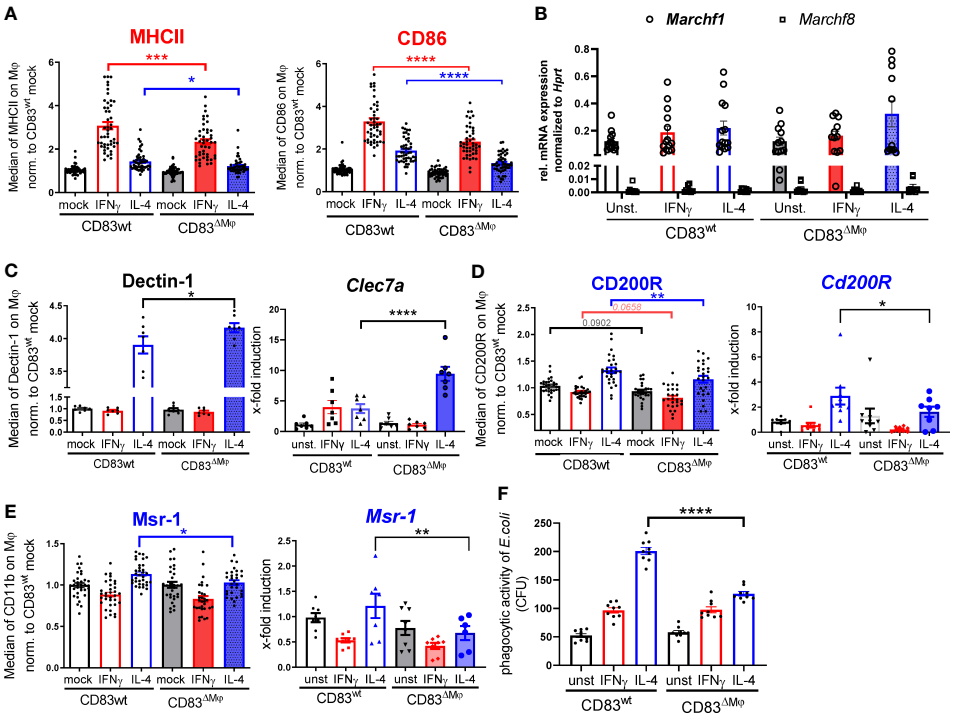

FIGURE 3
CD83 deficiency modulates the pro-resolving phenotype of IL-4 stimulated Mφ. BMDM were generated and differentiated into inflammatory CAM or AAM, using IFN-γ or IL-4 respectively, for 16h. **(A)** Assessment of surface MHC-II (n ≥ 47) and CD86 (n ≥ 47) expression levels by flow cytometry on stimulated murine wt and CD83-deficient Mφ. **(B)** qPCR analyses of *Marchf1* and *Marchf8* in Mφ derived from CD83wt or CD83 cKO mice (n = 5). **(C)** Analyses of Dectin-1 surface expression levels (left bar graph) and mRNA expression levels (right bar graph, *via* flow cytometry and qPCR, respectively). Significantly increased Dectin-1 expression levels on IL-4 stimulated CD83-deficient Mφ (n = 7). **(D)** Analyses of CD200R surface expression (left bar graph, n ≥ 29-31) and mRNA expression (right bar graph, n ≥ 8) revealed significantly decreased levels on IL-4 stimulated CD83-deficient Mφ **(E)** Analyses of MSR-1 surface expression (left bar graph, n ≥ 31) and Msr-1 mRNA expression (right bar graph, n = 6) revealed significantly decreased levels on IL-4 stimulated CD83-deficient Mφ. **(F)** Assessment of phagocytic activity *via* gentamicin protection assays revealed significantly decreased capacity to engulf *E.coli*. Statistical analyses were performed by One-way ANOVA or the appropriate corresponding non-parametric test. Data are represented as mean ± SEM. Experiments were performed at least three times. *p< 0.05; **p<0.01; ***p<0.001; **** p< 0.0001. The absence of asterisks indicates that there is no statistical significance.

graph) and *Msr-1* (Figure 3E, right bar graph) are in line with the protein data. Msr-1 is known to be upregulated on AAM being important to phagocytose *E.coli* bacteria. Since we observed a reduction in Msr-1 expression, we next checked whether CD83-deficient Mφ were impaired in their phagocytic activity to engulf *E.coli*. In fact, using a gentamicin protection assay revealed a significantly impaired phagocytic activity of IL-4 stimulated, CD83-deficient Mφ (Figure 3F). Collectively, these data suggest a profound functional change of IL-4 stimulated, CD83-deficient Mφ.

CD83-deficient Mφ show a reduced phosphorylation status of STAT-6 upon IL-4 stimulation

Since we detected a phenotypic change on IL-4-stimulated Mφ derived from CD83 cKO mice, we next examined whether members of the IL-4 signaling cascade are also modulated. IL-4 binds to IL-4Rα that recruits the IL-2Rγ chain, which leads to the activation of the tyrosine kinases Jak1/Jak3 and phosphorylation of STAT6, which form pSTAT6-dimers and translocate to the nucleus and initiate transcription of target genes (28, 29). To analyze possible differences between CD83wt and CD83 KO Mφ, we generated Mφ from CD83wt as well as CD83 cKO mice and stimulated them with IL-4 for 15 or 30 min. Subsequently, whole-cell lysates were prepared and analyzed by Western blot, in respect to pSTAT6 and STAT6 levels. In fact, we detected a decreased phosphorylation status of STAT6 upon IL-4 stimulation in CD83-deficient Mφ, compared to CD83wt Mφ (Figure 4A). Quantified ratios of pSTAT6 to STAT6 are shown in Figure 4B. Next, we analyzed the expression of STAT6 target gene *Gata3* (30), and its expression was downregulated in IL-4-stimulated CD83-deficient Mφ, when compared to wt derived Mφ (Figure 4C).

CD83-deficient Mφ show increased pro-inflammatory cytokine production and enhanced T cell stimulatory capacity

Next, we analyzed the impact of CD83-deficiency regarding the cytokine and chemokine production of IL-4- and IFN-γ-stimulated Mφ. As depicted in Figure 5A, IL-4-stimulated CD83-deficient Mφ showed a significantly increased secretion of pro-inflammatory mediators, including IL-6, TNF-α, CXCL1, and G-CSF (Figure 5A upper bar graphs). Additionally, we verified these data by qPCR and observed significantly increased expression levels of the corresponding transcripts *Il6*, *Tnfa*, *Cxcl1*, and *Csf3* (Figure 5A lower bar graphs). In addition, we detected significantly increased levels of RANTES/CCL5 (Figure 5, left bar graph) and of MCP-1/CCL2 in IFN-γ-stimulated CD83-deficient Mφ (Figure 5, right bar graph), suggesting that CD83 also influences the function of IFN-γ stimulated Mφ. Collectively, these data support our hypothesis that CD83 deficiency modulates activation and function of Mφ. Recently we reported that CD83-deficient DCs enhance antigen-specific T cell proliferation and increase secretion of pro-inflammatory cytokines compared to co-cultures with CD83wt DCs (17). Since the data described above indicate a modulated pro-resolving phenotype of CD83-deficient Mφ, we next assessed the T cell stimulatory capacity of IFN-γ- and IL-4-stimulated, in comparison to unstimulated Mφ, generated from CD83wt and CD83 cKO mice. Thus, we co-cultured the differently stimulated Mφ with allogeneic splenocytes, derived

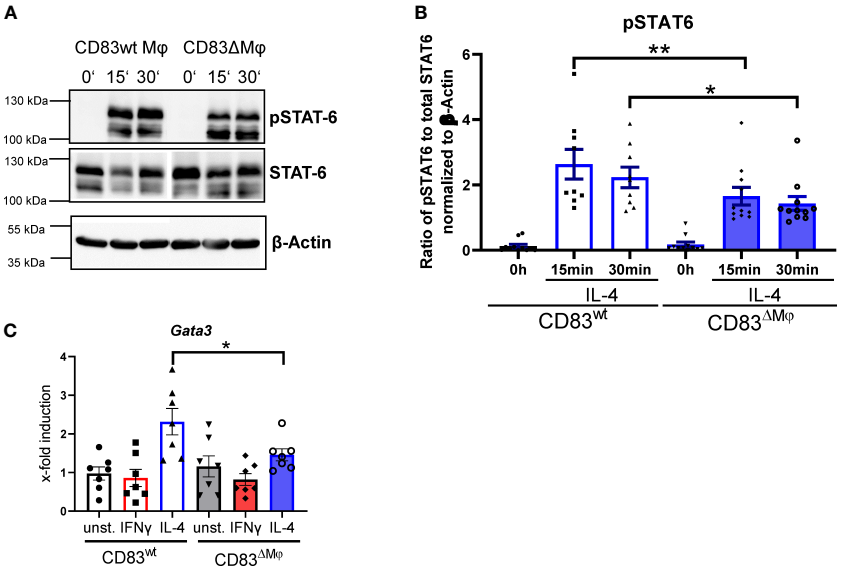

FIGURE 4
STAT6 phosphorylation is altered in CD83-deficient macrophages upon IL-4 stimulation. Bone-marrow derived Mφ were generated from CD83wt or CD83 cKO mice and stimulated with IL-4 for 15 or 30 min. Unstimulated Mφ served as control. Subsequently, whole cell lysates were prepared and analyzed by Western blot. **(A)** Representative Western blot showing pSTAT-6, STAT6 and β Actin levels in whole cell lysates derived from CD83wt and CD83ΔMφ animals **(B)** Quantification of the ratio of pSTAT-6 and STAT6 normalized to β-actin ($n \geq 9$). **(C)** qPCR analyses of *Gata3* mRNA levels in Mφ generated from cKO or wt mice, stimulated with IFNg or IL-4. Significantly reduced *Gata3* mRNA levels are observed in IL-4 stimulated CD83-deficient Mφ. Statistical analyses were performed by One-way ANOVA or the appropriate corresponding non-parametric test. Data are represented as mean ± SEM. Experiments were performed at least three times. *p< 0.05; **p<0.01. The absence of asterisks indicates that there is no statistical significance.

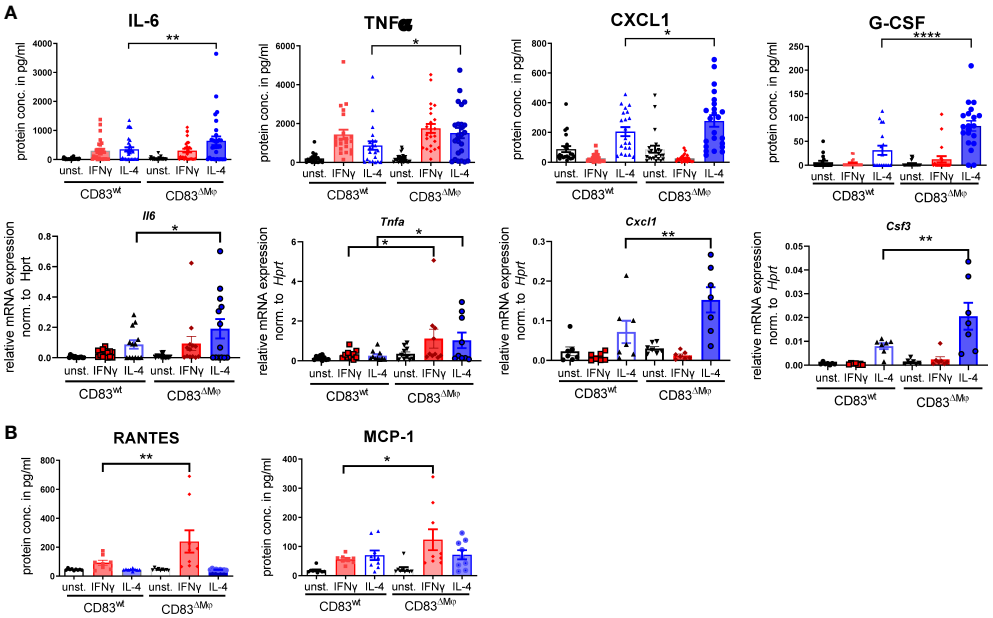

FIGURE 5
CD83-deficient IL-4- as well as IFN-γ-stimulated Mφ show a pro-inflammatory profile. Bone-marrow derived Mφ were generated and differentiated either into CAM or AAM, *via* IFN-γ or IL-4 respectively, or were left untreated for 16h. Afterwards, the supernatants were analyzed by CBA and cells *via* qPCR. **(A)** IL-4 stimulated CD83-deficient Mφ show increased secretion levels of IL-6, TNF-α, CXCL1 and G-CSF (upper bar graphs). qPCR analyses showed significantly increased mRNA levels of *Il-6, Tnfa, Cxcl1 and Csf3* in IL-4-stimulated CD83 KO Mφ (lower bar graphs). **(B)** CCL5/RANTES and MCP-1 expression levels are increased in supernatants of IFN-γ-stimulated CD83-deficient Mφ. Statistical analyses were performed by One-way ANOVA or the appropriate corresponding non-parametric test. Data are represented as mean ± SEM. Experiments were performed at least three times. *p< 0.05; **p<0.01; **** p< 0.0001. The absence of asterisks indicates that there is no statistical significance.

from BALB/c mice, and T cell proliferation was assessed *via* tritium incorporation. As depicted in Figure 6, T cell proliferation was enhanced in all co-cultures with CD83-deficient Mφ, regardless of their stimulus (Figures 6A–C). This observation is also reflected by enhanced clustering of T cells upon co-culture with CD83-deficient BMDMs (see representative microscopic images, Figures 6A–C). In MLRs with CD83-deficient Mφ we observed significantly increased proliferative response of alloreactive T cells (Figures 6A–C). Next, we investigated if the composition of T cell subsets, present in co-cultures with mock-, IFN-γ or IL-4-treated Mφ generated from CD83wt or CD83 cKO mice, would be altered. As depicted in Figure 6D, flow cytometric analyses revealed significantly reduced frequencies of $CD4^{+}Foxp3^{+}$ Tregs in co-cultures of allogeneic splenocytes with mock, IFN-γ or IL-4-stimulated CD83-deficient Mφ. This indicates that the reduced numbers of Tregs present in the co-cultures may account for the observed increased T cell proliferation (Figures 6A–C).

CD83-deficient Mφ accelerate the inflammatory phase of wound healing and promote upregulation of fibrosis associated transcripts

In order to investigate the *in vivo* relevance of CD83-deficiency in $CX3CR1^{+}$ Mφ, we performed full-thickness excisional wound healing experiments using cKO ($CD83^{\Delta M\varphi}$) in comparison to wildtype control mice (CD83wt). As depicted in Figure 7A, we induced 6 mm biopsy punches in the dorsal skin and monitored wound closure until day 6 and collected skin biopsies on day 3 as well as day 6 after wound infliction. As shown in Figure 7B, on day 3 the wound closure was significantly enhanced in $CD83^{\Delta M\varphi}$ mice when compared to CD83wt mice. This indicates a boost of the initial inflammatory phase, which is crucial for wound closure. This upregulated inflammatory phase was also confirmed by qPCR analyses, since transcripts such as *Il6* and *Cxcl1*, associated with a pro-inflammatory macrophage phenotype, were upregulated in $CD83^{\Delta M\varphi}$ mice (Figure 7C). Concomitantly, markers associated with pro-resolving Mφ, including *CD200r, Msr-1* as well as *Ym-1* were significantly reduced (Figure 7D). Surprisingly, regarding surface wound closure on day 6, no differences were detected between $CD83^{\Delta M\varphi}$ and wt animals. However, in samples derived from cKO animals we observed significantly increased expression levels of *Tgfb*, *Acta-2* as well as *Col1a1*. This indicates a higher prevalence of myofibroblasts and fibrosis associated transcript in $CD83^{\Delta M\varphi}$ mice, which are associated with disturbed wound healing processes (Figure 7E). Indeed, histological analyses of day 6 skin biopsies showed an altered reconstitution process, as indicated by an expanded epidermis, absent dermis and a prominent inflamed tissue area in $CD83^{\Delta M\varphi}$ mice (Figure 7F, upper panel). In contrast, histological analyses of skin biopsies from CD83wt mice showed a distinct epidermis alongside the dermis and a resolving inflammatory area (Figure 7F, lower panel). Of note, in CD83wt mice, hair follicles have already migrated into the former sites of excisional wounds, indicating a progressed stage of wound regeneration, which was not observed in $CD83^{\Delta M\varphi}$ mice.

10.3389/fimmu.2023.1085742

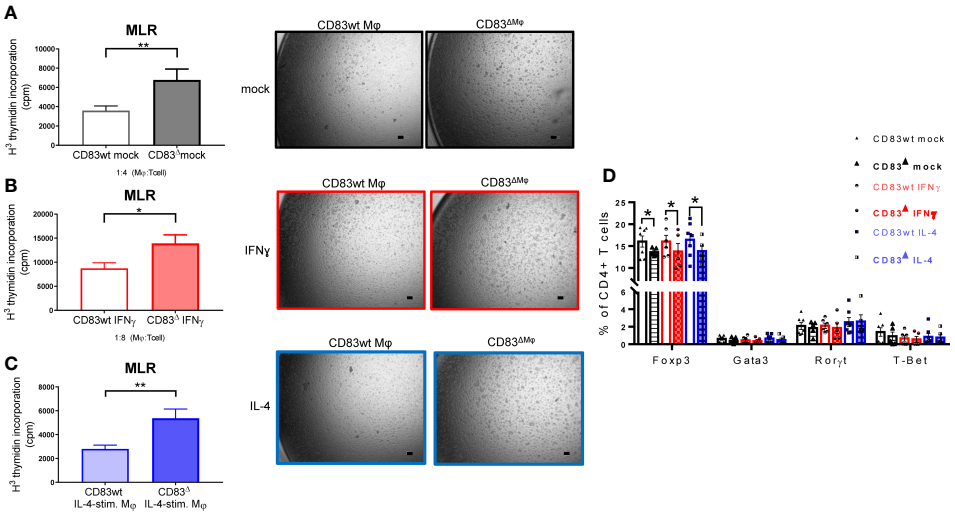

FIGURE 6
CD83-deficient Mφ show enhanced capacity to stimulate allo-reactive T cells. Mφ were generated from CD83wt and CD83 cKO mice and differentiated using IFNγ or IL-4. Afterwards, the medium was discarded and splenocytes derived from BALB/c mice ($4x10^5$ cells/well) were co-cultured with differentiated Mφ in 96-well plates, at different Mφ:splenocyte ratios, as indicated for 48h. T cell proliferation was assessed using tritium **(A–C)**. Co-cultures of unstimulated, IFN-γ- and IL-4 stimulated Mφ, derived from CD83-deficient Mφ, show enhanced proliferative responses, when compared to co-cultures with CD83wt derived Mφ (left bar graphs, **A–C**). This observation is reflected by decreased T cell clusters shown in representative microscopic images (**A–C**, right side). **(D)** Flow cytometric analyses revealed a significantly decreased frequencies of Tregs ($CD4^+Foxp3^+$ cells) in co-cultures of CD83-deficient Mφ with allo-reactive splenocytes. Statistical analyses were performed by using an Unpaired t-test **(A–C)** or Two-way ANOVA **(D)** or the appropriate corresponding non-parametric test ($n \geq 4$). Data are represented as mean ± SEM. Experiments were performed at least three times. *p< 0.05; **p<0.01. The absence of asterisks indicates that there is no statistical significance.

Discussion

Mφ are cells which show highly phenotypic plasticity in response to environmental cues. Despite a multitude of functionally diverse activation states observed *in vivo*, Mφ are often classified into two distinct polar extremes, namely IFN-γ-stimulated CAM with pro-inflammatory capacities and anti-inflammatory IL-4-treated AAM. CAM and AAM reveal striking differences in their transcriptome and subsequently provide specifically tailored effector functions during immune responses (8, 31). CAMs are essential during the initial inflammatory phase of wound healing. However, if they are still present during later stages, without switching to a pro-resolving, tissue repair AAM-associated phenotype, they are rather associated with incomplete/poor wound healing and fibrosis (32, 33). In contrast, anti-inflammatory AAMs are pivotal for resolution of inflammation and tissue regeneration during the later stage of wound healing (34, 35).

The crucial involvement of Mφ in numerous major health-threats, such as chronic inflammatory/autoimmune diseases and cancer, render these cells ideal targets for immunomodulatory interventions. Identification of novel immune checkpoint molecules on Mφ that stabilize either an inflammatory or pro-resolving phenotype and function can lead to the development of new therapeutic agents for the treatment of the respective disease.

One promising candidate is the CD83 protein, which has been described as an important checkpoint molecule that favors resolution of inflammation. In the context of autoimmune diseases and transplantation, several studies demonstrated that the sCD83 protein promotes resolution of inflammation and induces tissue tolerance (13, 18–20, 36–38). Studies using conditional KO (cKO) mice showed that deletion of CD83 in Tregs results in a pro-inflammatory Treg phenotype, which was characterized by increased levels of TNF-α and IL-1β concomitantly impaired secretion of pro-resolving molecules e.g. IL-10 and TGF-β (16). Analogously, conditional knockout mice with specific CD83 deletion in DCs showed excessive inflammatory autoimmune responses and impaired resolution of inflammation (17, 39). However, little was known regarding the regulation and function of CD83 expressed by Mφ.

An early study compared the expression pattern of CD83 upon LPS stimulation in human monocytes/macrophages as well as human DCs and showed that CD83 is highly and stably expressed on mDCs but not on Mφ (22). Furthermore, microarray analyses revealed that Mφ treated with IL-4, but not with IFN-γ+LPS, express *Cd83*, alongside typical AAM-associated gene transcripts, such as *Fizz1* and *Arg1* (7). This associates CD83 with the pro-resolving AAM phenotype, which is linked to tissue-repair and resolution of inflammation.

In order to investigate whether CD83-deletion interferes with the CAM or AAM phenotype, we subsequently performed different *in vitro* assays. Phenotypic analyses of CD83 cKO Mφ reinforced the concept of a tight connection between CD83 expression and an AAM-phenotype. In line with previous literature, CD83-deficient Mφ display decreased expression levels of the costimulatory molecule CD86 as well as MHC-II (Figure 3), which is most likely due to the missing blockade of the ubiquitin-ligase MARCH-1 in CD83 deficient Mφ (14). We attribute this effect to MARCH-1, as it is the prevailing MARCH-ubiquitinase expressed by Mφ, while MARCH-8, which is blocked by CD83 in thymic epithelial cells (15), is only marginally expressed. Furthermore, in IL-4 stimulated CD83-deficient Mφ we detected a striking reduction of the AAM-associated molecule CD200R, which is crucial to control

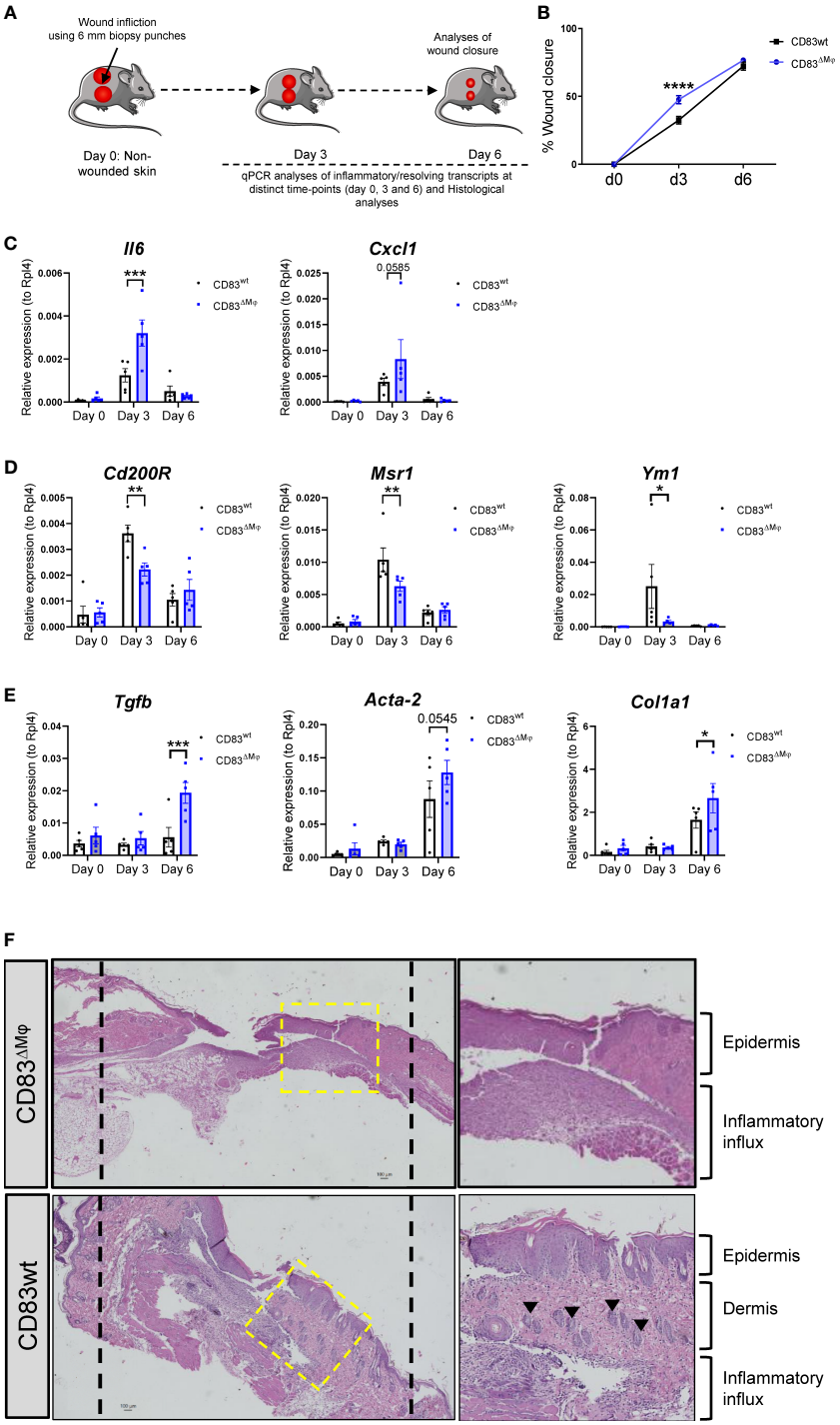

FIGURE 7
CD83-deficient Mφ accelerate the inflammatory phase of wound healing and promote upregulation of fibrosis associated transcripts **(A)** Experimental set-up for the full-thickness excisional wound healing model. Biopsy punches (6mm) were placed into the dorsal skin of CD83wt as well as CD83 cKO mice. **(B)** Wound closure was calculated relative to the initial d0 wound dimension. 8mm silicone rings (Thermo scientific) were mounted around the wound area, using vetbond (3M). Imaging was performed on day 0, 3, and 6 and wound diameters were determined by ImageJ. **(C–E)** qPCR analyses were performed using skin biopsies from day 0, 3 and 6 (n = 5 per group). **(F)** Representative H&E slides of day 6 wound biopsies from CD83wt as well as CD83 cKO mice. Statistical analyses were performed by using a Two-way ANOVA or the appropriate corresponding non-parametric test. Data are represented as mean ± SEM. *p< 0.05; **p<0.01; ***p<0.001; **** p< 0.0001. The absence of asterisks indicates that there is no statistical significance.

inflammatory responses by limiting pro-inflammatory cytokine secretion and cellular function (27, 40). This further supported the notion of a disturbed pro-resolving AAM-phenotype upon CD83 deletion. Scavenger receptors such as MSR-1 are involved in phagocytosis of cellular debris, which is a hallmark of AAM and crucial for proper resolution of inflammation (41, 42). Consequently, the reduction of MSR1 resulted in an impaired phagocytic activity upon IL-4 stimulation and additionally, CD83-deficient Mφ show a pronounced pro-inflammatory cytokine profile. Thus, we conclude that CD83 expressed by Mφ is crucial for the resolving AAM

phenotype and function, which is crucial for resolution of inflammation.

The modified alternative activation state of CD83 cKO Mφ towards pro-inflammatory features is further underpinned by the reduced phosphorylation status of STAT6, which is essential for the induction of AAM-related transcripts (43). In line with this knowledge, we found decreased expression levels of the STAT6 target gene *Gata3*, which is also a prominent marker of IL-4 stimulated AAM (30). Since STAT6 is responsible for the anti-inflammatory properties of murine Mφ (44), we conclude that the perturbed phenotype of IL-4 stimulated CD83-deficient Mφ is linked to the decreased STAT6 signaling activity. The notion that CD83 cKO derived Mφ are further modulated towards a defect in resolving functions is further underlined by the fact that we detected elevated expression levels of Dectin-1 after IL-4 treatment. Although induced by IL-4, expression of Dectin-1 is rather linked to a pro-inflammatory CAM phenotype (26, 45). This is in line with the observed enhanced production of pro-inflammatory cytokines as well as chemokines by CD83 cKO derived Mφ.

Interestingly, CD83 cKO BMDM induced higher proliferative responses upon co-culture with allogeneic T cells, regardless of the preceding stimulation. These results parallel those obtained from CD83-deficient DCs, also showing an over-activated phenotype characterized by an upregulation of co-stimulatory molecules and pro-inflammatory cytokines, resulting in an enhanced antigen-specific T cell stimulation (17). In the present study, we extend these findings to Mφ derived from CD83 cKO mice and reveal that CD83 deficiency affects regulatory T cell numbers in allogeneic co-cultures. This again substantiates the fact that membrane-bound CD83 expression by Mφ is an important checkpoint molecule that contributes to resolution of inflammation by Treg induction. In a recent study, we have shown that administration of the soluble CD83 molecule during differentiation of murine Mφ results in a modulation towards an anti-inflammatory phenotype, which is able to induce tissue tolerance in a corneal transplantation model *in vivo*, which goes along with a decreased capacity to stimulate allogeneic T cells (13). Moreover, we have shown that sCD83 modulates Mφ towards a pro-resolving, tissue-repair AAM-associated phenotype, able to restore tissue function and proper wound healing (21). Within the present study, we confirm the pro-resolving function of membrane-bound CD83 expressed by murine Mφ, using an *in vivo* wound healing model. Although wound closure of cKO mice was significantly accelerated on day 3, which can be explained by an enhanced pro-inflammatory phenotype of CD83-deficient Mφ, later phases of tissue repair and resolution of inflammation were hampered. This is reflected by significantly increased expression levels of fibrosis associated transcripts, including *Acta-2* and *Tgf-b*, which have been linked to fibrotic scar formation (33, 46). In addition, our histological analyses revealed a disturbed wound healing process in $CD83^{\Delta M\varphi}$ mice.

Collectively, our data indicate that CD83 expression by Mφ is vital for the transition of pro-inflammatory Mφ into a pro-resolving, tissue-repair associated phenotype (see also Figure 8) and identifies CD83 as a potential target for future therapeutic intervention strategies.

Materials and methods

Mice

To generate mice with CD83-deficient Mφ, we used a conditional knock-out strategy (CD83 cKO) by mating mice with floxed *Cd83* alleles (47), with the *Cx3cr1*-Cre line, which was kindly provided by Prof. Dr. Gerhard Krönke (Department of Medicine 3, University Hospital Erlangen, Erlangen, Germany). Cre-negative littermates as well as age-matched Cre-positive CD83wt mice served as controls (hereafter referred to as wt mice). Animal care and all experimental procedures of the present study were performed in accordance with the European Community Standards on the Care and Use of Laboratory Animals and were approved by the local ethics committee.

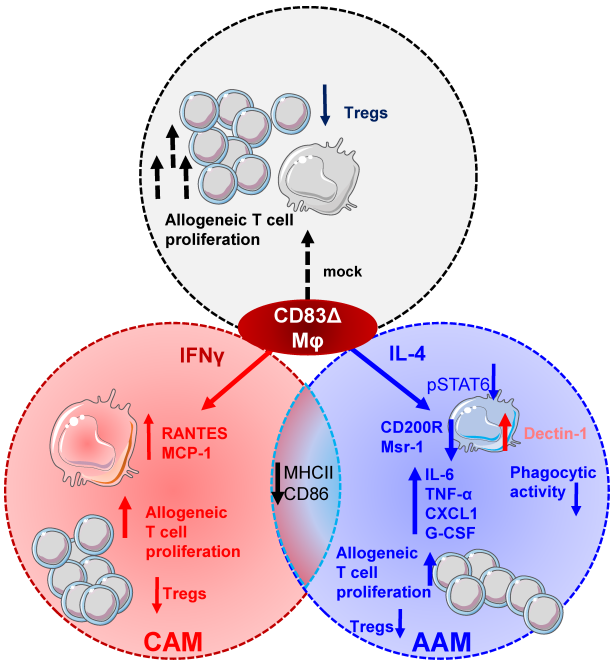

FIGURE 8
CD83 expressed by Mφ is an important immune checkpoint molecule that contributes to resolution of inflammation. CD83 is an early marker for IL-4 stimulated AAMs and its deletion in Mφ results in striking phenotypic and functional changes. CD83-deficient, IL-4 stimulated Mφ are characterized by a decreased STAT-6 phosphorylation status when compared to CD83wt Mφ. This goes along with reduced expression levels of AAM-associated marker molecules such as CD200R and Msr-1. Reduction in MSR-1 expression correlates with a reduced phagocytic activity of *E.coli* in CD83-deficient IL-4 stimulated Mφ. In contrast, CAM associated Dectin-1 expression is upregulated. Furthermore, CD83-deficient, IL-4 stimulated Mφ express increased levels of pro-inflammatory modulators, such as IL-6, TNF-α, CXCL1 and G-CSF. Functionally, Mφ generated from CD83 cKO mice show enhanced allogeneic T cell proliferative capacities and reduced frequencies of Tregs in Mφ - cell co-cultures. Finally, IFNγ-stimulated Mφ generated from cKO mice show an increased production of RANTES and MCP-1, indicating that CD83 also modifies the production of these pro-inflammatory chemokines.

Generation and stimulation of bone-marrow-derived Mφ

Bone-marrow derived Mφ were generated from murine bone-marrow precursor cells from CD83 cKO mice and wild type littermates, in D10 medium consisting of DMEM (Lonza), 10% FCS (Merck), Penicillin-Streptomycin-Glutamine-solution (Sigma Aldrich) and 50 µM β-mercaptoethanol. Bone-marrow cells were flushed from femur and tibia of mice and seeded for 1d in D10 medium containing M-CSF supernatant (10 - 30%). After overnight incubation, cells were harvested and seeded at a starting density of 3-4 x 10^6 cells per 10 cm^2 dish (Falcon) in D10 medium + M-CSF supernatant. Fresh D10 medium + M-CSF was added on day 3. On day 6, Mφ were harvested and stimulated as described below.

Stimulation of bone-marrow derived Mφ

On day 6, Mφ were harvested with 10 mM EDTA-PBS, washed with fresh medium and seeded in uncoated 24-well plates at a cell density of 2 x 10^6 cells per ml. For phenotypic and functional characterization of CD83, Mφ were generated from wt or cKO mice and seeded for differentiation into classically activated Mφ (CAM) or alternatively activated Mφ (AAM) using IFN-γ (300 U/ml) or IL-4 (40 ng/ml, PeproTech), respectively. For time kinetic experiments, Mφ were stimulated with inflammatory activators such as IFNγ (300 U/ml, PeproTech), LPS (100 ng/ml, *In vivo*gen) or TNF-α (1000U/ml) or alternatively with mediators, such as IL-4 (40 ng/ml), IL-13 (40 ng/ml) or IL-10 (10 ng/ml) for the indicated time period. Subsequently, cells were analyzed by flow cytometry.

Flow cytometric analyses

Live/dead discrimination was performed using either 7-AAD or LIVE/DEAD™ Fixable Aqua Dead Cell Stain (ThermoFisher Scientific). Surface staining of BMDMs and cells used in MLR assays was performed in PBS-diluted appropriate antibodies for 30 minutes. In the case of live/dead discrimination with 7-AAD, the dye was added just before the flow cytometry measurement. For intracellular staining, cells were permeabilized and fixed in Permeabilization Reagent (Thermo Fisher Scientific, 00-5523-00). The following antibodies were used from BioLegend, others are stated: F4/80 (BM8), CD11b (M1/70), CD200R (OX-110), Msr-1 (M204PA; Invitrogen), MHCII (M5/114.15.2), CD86 (GL-1), CD206 (C068C2), MERTK (2B10C42), CD83 (Michel-19) RORγT (Q31-378), GATA3 (L50-823;BDBiosciences), T-BET (O4-46,BD Pharmingen), FOXP3 (FJK-16s; Thermo Fisher Scientific). Afterwards, the cells were washed with PBS and subsequently analyzed by flow cytometry.

Cytometric bead array

Supernatants of BMDM were analyzed using the LEGENDplex™ Mouse Macrophage/Microglia or LEGENDplex™ Mu Pro-inflammatory Chemokine Panel (BioLegend), respectively, according to the manufacturer's instructions.

Mφ-allogeneic splenocyte cocultures (mixed lymphocyte reaction)

On day 6, BMDMs from wt controls and cKO mice were harvested, seeded in 96-well plates and stimulated with IFN-γ or IL-4 or left untreated. Allogeneic splenocytes derived from BALB/c mice (4 x 10^5 cells/well) were co-cultured with BMDMs in 96-well plates for 72 hours in D10 medium (37°C, 5.5% CO_2), at different Mφ: splenocyte ratios (1:2, 1:4, 1:8). To analyze the allogeneic T cell proliferation capacity, cell cultures were subsequently pulsed with [^{3}H]-thymidine (1 µC/well; PerkinElmer, Germany) for additional 8-16 h. Culture supernatants were harvested onto Glass Fiber Filter Mates using an ICH-110 harvester (Inotech, Switzerland), and filters were counted in a 1450-microplate (Wallac, Finland). Cells of cocultures were also harvested after 72 h and used for flow cytometric analyses to determine frequencies of different T cell subsets.

Phagocytosis assay

To analyze the ability of BMDMs to phagocytose and uptake *E.coli* bacteria, a gentamicin protection assay was performed. Bone marrow derived Mφ were generated from wt or cKO mice and seeded in 6 well plates in technical replicates in D10 medium without antibiotics. Cells were differentiated into CAM or AAM for 16h. Afterwards, Mφ were exposed to *E. coli* (DSM 1103) at an MOI = 10 for 1 hour. After rinsing the cultures three times in PBS to remove non-engulfed bacteria, cells were incubated for 1 h in fresh RPMI1640 medium containing 100 µg/ml of gentamicin to kill extracellular bacteria. Gentamicin was removed, and the cells were gently rinsed three times in PBS. BMDMs were lyzed by incubating them for three minutes in PBS containing 2 mM EDTA and 0.5% saponin, followed by transfer to Eppendorf tubes and high-speed vortexing for 30 s. Subsequently, cells were plated onto blood agar plates and the next day, *E.coli* colonies were counted.

Western blot analyses

To assess CD83 protein content in whole cell lysates of murine BMDM, Western blot analyses were performed. In addition, protein levels of pSTAT6 and STAT6 in lysates of CD83wt or CD83-deficient Mφ were also analyzed by Western blotting. Thus, protein-lysates (20-30 µg per lane) were separated *via* SDS – polyacrylamide gel electrophoresis and blotted onto a nitro-cellulose membrane (GE Healthcare). After blocking in blocking reagent (5% BSA-TBST) membranes were incubated with the following primary antibodies overnight (4°C): goat CD83 (Clone: AF1437, R&D systems), mouse β-actin (Clone: AC-74, Sigma Aldrich), rabbit p-STAT6 (Clone: D8S9Y, Cell Signaling), rabbit STAT6 (Clone: D3H4, Cell signaling). Specific signals were detected using the appropriate HRP-labeled secondary antibody and the ECL

Prime Western Blotting Detection Reagent (GE Healthcare). Quantification of Western Blots was performed using the ImageJ/Fiji software (48). The intensities of bands are visualized in bar graphs and represent the protein amount in arbitrary units. To analyze phosphorylation status of STAT6, band intensities of pSTAT6 were normalized to total STAT6 signals. β- Actin served as a loading control.

RNA isolation

Total RNA was isolated from mock-, IFN-γ or IL-4-stimulated BMDMs generated from CD83wt or CD83 cKO mice. Cell pellets were lysed in RLT+β-Mercaptoethanol extracted by RNeasy Plus Mini Kit (Qiagen) according to the manufacturer's instructions. In addition, wound biopsies were collected from CD83wt as well as cKO mice at day 0, day 3 or day 6, stored in RNAlater (Qiagen) at -80°C and subsequently used for further analyses. Homogenization of the tissue was performed in RLT+β mercaptoethanol using innuSPEED lysis Tube W (Analytic Jena). We performed three homogenization cycles à four minutes in the SpeedMill PLUS homogenizator (Analytic Jena).

qPCR

Total RNA was reversely transcribed using the First strand cDNA synthesis Kit (Thermo Fisher Scientific GmbH), as described by the manufacturer. Briefly, 0.5-1 µg RNA was reversely transcribed and diluted 1:5 after synthesis. qPCR analyses were performed using the Sybr Green Super mix (Biozym) on a CFX96 Real time system (BioRad) and normalized to reference gene transcript *Hprt*. All primers were designed and validated according to the Minimum Information for Publication of Quantitative Real-Time PCR Experiments guidelines. For primer sequences, see Table 1.

Full-thickness excisional wound model and analyses of wound closure

To investigate the role of CD83 expressed by Mφ in physiological wound healing responses, we used the full-thickness excisional wound healing model as described previously (21). Briefly, CD83wt mice as well as CD83cKO mice were anesthetized using a mixture of ketamine and xylazine (120 mg/kg and 20 mg/kg body weight, respectively). In

TABLE 1 Primer sequences used in qPCR experiments (Sigma Aldrich).

Gene	Orientation	Sequences
Cd83	Forward Reverse	5'-CGCAGCTCTCCTATGCAGTG-3' 5'-GTGTTTTGGATCGTCAGGGAATA-3'
Cd200R	Forward Reverse	5'-GGAGAACTTCTGCCCTAGCA-3' 5'-AGTGTTCACTTGTGTCAGAGGA-3'
Csf3	Forward Reverse	5'-AGATCACCCAGAATCCATGG-3' 5'-CCAGGGACTTAAGCAGGAAG-3'
Gata3	Forward Reverse	5'-CCAAGCGAAGGCTGTCGGCA-3' 5'-TCCTCCAGCGCGTCATGCAC-3'
Hprt	Forward Reverse	5'-GTTGGATACAGGCCAGACTTTGTT-3' 5'-GATTCAACTTGCGCTCATCTTAGGC-3'
Il6	Forward Reverse	5'-ACAAAGCCAGAGTCCTTCAGAG-3' 5'-GAGCATTGGAAATTGGGGTAGG-3'
Tnfa	Forward Reverse	5'-GTGATCGGTCCCCAAAGGG-3' 5'-CCAGCTGCTCCTCCACTTG-3'
Cxcl1	Forward Reverse	5'-ACTCAAGAATGGTCGCAAGG-3' 5'-GTCCCATCAGAGCAGTCTGT-3'
Msr-1	Forward Reverse	5'-AGGTGTTAAAGGTGATCGGG-3' 5'-ATCTTGATCCGCCTACACTC-3'
Ym1/Chil3	Forward Reverse	5'-GACTTGCGTGACTATGAAGC-3' 5'-TGAATATCTGACGGTTCTGAGG-3'
Tgfb	Forward Reverse	5'-TGGAGCAACATGTGGAACTCTA-3' 5'-AGACAGCCACTCAGGCGTATC-3'
Acta-2	Forward Reverse	5'-ATG CCT CTG GAC GTA CAA CTG-3' 5'-CAC ACC ATC TCC AGA GTC CA-3'
Col1a1	Forward Reverse	5'-GAAGCACGTCTGGTTTGGA-3' 5'-ACTCGAACGGGAATCCATC-3'

order to prevent wound healing by contraction and to give a defined scale for subsequent wound closure assessment, 8mm silicone rings (Thermo scientific) were mounted around the wound area, using vetbond (3M). Imaging was performed on day 0, 3, and 6 and wound diameters length (L) and width (W)) were determined by ImageJ and wound closure was calculated relative to the initial d0 wound dimension. Wound area (WA) on day X (dX) and wound closure (% of baseline) was calculated using the following equations:

$$Wound \quad area\,(WA) \;=\; (L/2) * (W/2) * \pi$$

$$Wound \quad closure \quad (\%) \;=\; (WA \quad d0 - WA \quad dX)/WA \quad d0 * 100$$

On day 3 and 6 biopsies were obtained as 8 mm punches (pfm medicals) around the former wound area. Samples were either fixed in 4% paraformaldehyde for histological assessment or stored in RNAlater (Qiagen) at - 80°C for subsequent RNA analyses.

Histology

For the histological assessment of wounds, skin biopsies were obtained on day 3 and day 6 after wound infliction using 8 mm biopsy punches around the wound area. Excised tissue was subsequently fixed in 4% paraformaldehyde and processed by conventional histological techniques, embedded in paraffin wax and sectioned at 5 µm thicknesses. Sections were mounted onto glass slides, de-paraffinized and stained with hematoxylin and eosin (HE).

Statistical analyses

All statistical analyses were performed using GraphPad Prism 9.3.1 and the two-tailed unpaired student's t- test or one- or two-way ANOVA for parametric data. Wherever necessary, we used non-parametric tests (Mann-Whitney-U or Kruskal-Wallis) when data was not normally distributed. Data are presented as mean values including the Standard Error Mean (SEM). P-values of *p<.05; **p<.01; ***p<.001; and ****p<.0001 were considered statistically significant.

Data availability statement

The original contributions presented in the study are included in the article/Supplementary Material. Further inquiries can be directed to the corresponding author.

Ethics statement

The animal study was reviewed and approved by Regierung von Unterfranken, Würzburg.

Author contributions

KP-M designed, conducted and analyzed the majority of the experiments and prepared the manuscript. PL, AStr, LS, PM-Z, CK, and AW performed experiments, analyzed data and edited the manuscript. MW and JM provided scientific insights and helped with the Gentamicin protection assays. ASte, EZ, DR, and AW conceived and designed the study, supervised experiments and prepared the manuscript. All authors contributed to the article and approved the submitted version.

Funding

This work was supported by the Deutsche Forschungsgemeinschaft (DFG) within grants CRC1181 project B03 and STE432/15-1 (both to ASte), ZI 1225/1-1 (to EZ), MA 2621/4-1 and MA 2621/5-1 (to JM and MW). By the Interdisciplinary Center of Clinical Research (IZKF) at the University Hospital Erlangen to ASte (grant A89), to AW (grant P062), to DR (grant ELAN P077), and to KP-M (grant P105). By the Else Kroner-Fresenius-Stiftung to AW (grant 2020_EKEA.81). KP-M was funded by the Bavarian Equal Opportunities Sponsorship – Realization Equal Opportunities for Women in Research and Teaching. ASte was further supported by the m4 Award (grant M4-2110-0003), sponsored by the Bavarian State Ministry of Economic Affairs and Media, Energy and Technology.

Acknowledgments

We would like to thank the staff of the central animal facility.

Conflict of interest

The authors declare that the research was conducted in the absence of any commercial or financial relationships that could be construed as a potential conflict of interest.

Publisher's note

Supplementary material

The Supplementary Material for this article can be found online at: https://www.frontiersin.org/articles/10.3389/fimmu.2023.1085742/full#supplementary-material

References

1. Ginhoux F, Jung S. Monocytes and macrophages: developmental pathways and tissue homeostasis. *Nat Rev Immunol* (2014) 14(6):392–404. doi: 10.1038/nri3671

2. Gordon S, Taylor PR. Monocyte and macrophage heterogeneity. *Nat Rev Immunol* (2005) 5(12):953–64. doi: 10.1038/nri1733

3. Sim SL, Kumari S, Kaur S, Khosrotehrani K. Macrophages in skin wounds: Functions and therapeutic potential. *Biomolecules* (2022) 12(11). doi: 10.3390/biom12111659

4. Mirza R, DiPietro LA, Koh TJ. Selective and specific macrophage ablation is detrimental to wound healing in mice. *Am J Pathol* (2009) 175(6):2454–62. doi: 10.2353/ajpath.2009.090248

5. Wynn TA, Vannella KM. Macrophages in tissue repair, regeneration, and fibrosis. *Immunity* (2016) 44(3):450–62. doi: 10.1016/j.immuni.2016.02.015

6. Mosser DM, Edwards JP. Exploring the full spectrum of macrophage activation. *Nat Rev Immunol* (2008) 8(12):958–69. doi: 10.1038/nri2448

7. Jablonski KA, Amici SA, Webb LM, Ruiz-Rosado Jde D, Popovich PG, Partida-Sanchez S, et al. Novel markers to delineate murine M1 and M2 macrophages. *PLos One* (2015) 10(12):e0145342. doi: 10.1371/journal.pone.0145342

8. Martinez FO, Gordon S. The M1 and M2 paradigm of macrophage activation: time for reassessment. *F1000Prime Rep* (2014) 6:13. doi: 10.12703/P6-13

9. Huber S, Hoffmann R, Muskens F, Voehringer D. Alternatively activated macrophages inhibit T-cell proliferation by Stat6-dependent expression of PD-L2. *Blood* (2010) 116(17):3311–20. doi: 10.1182/blood-2010-02-271981

10. Yao Y, Xu XH, Jin L. Macrophage polarization in physiological and pathological pregnancy. *Front Immunol* (2019) 10:792. doi: 10.3389/fimmu.2019.00792

11. Orecchioni M, Ghosheh Y, Pramod AB, Ley K. Macrophage polarization: Different gene signatures in M1(LPS+) vs. classically and M2(LPS-) vs. alternatively activated macrophages. *Front Immunol* (2019) 10:1084. doi: 10.3389/fimmu.2019.01084

12. Grosche L, Knippertz I, Konig C, Royzman D, Wild AB, Zinser E, et al. The CD83 molecule - an important immune checkpoint. *Front Immunol* (2020) 11:721. doi: 10.3389/fimmu.2020.00721

13. Peckert-Maier K, Royzman D, Langguth P, Marosan A, Strack A, Sadeghi Shermeh A, et al. Tilting the balance: Therapeutic prospects of CD83 as a checkpoint molecule controlling resolution of inflammation. *Int J Mol Sci* (2022) 23(2). doi: 10.3390/ijms23020732

14. Tze LE, Horikawa K, Domaschenz H, Howard DR, Roots CM, Rigby RJ, et al. CD83 increases MHC II and CD86 on dendritic cells by opposing IL-10-driven MARCH1-mediated ubiquitination and degradation. *J Exp Med* (2011) 208(1):149–65. doi: 10.1084/jem.20092203

15. von Rohrscheidt J, Petrozziello E, Nedjic J, Federle C, Krzyzak L, Ploegh HL, et al. Thymic CD4 T cell selection requires attenuation of March8-mediated MHCII turnover in cortical epithelial cells through CD83. *J Exp Med* (2016) 213(9):1685–94. doi: 10.1084/jem.20160316

16. Doebbeler M, Koenig C, Krzyzak L, Seitz C, Wild A, Ulas T, et al. CD83 expression is essential for treg cell differentiation and stability. *JCI Insight* (2018) 3(11). doi: 10.1172/jci.insight.99712

17. Wild AB, Krzyzak L, Peckert K, Stich L, Kuhnt C, Butterhof A, et al. CD83 orchestrates immunity toward self and non-self in dendritic cells. *JCI Insight* (2019) 4(20). doi: 10.1172/jci.insight.126246

18. Bock F, Rossner S, Onderka J, Lechmann M, Pallotta MT, Fallarino F, et al. Topical application of soluble CD83 induces IDO-mediated immune modulation, increases Foxp3 + T cells, and prolongs allogeneic corneal graft survival. *J Immunol* (2013) 191(4):1965–75. doi: 10.4049/jimmunol.1201531

19. Ge W, Arp J, Lian D, Liu W, Baroja ML, Jiang J, et al. Immunosuppression involving soluble CD83 induces tolerogenic dendritic cells that prevent cardiac allograft rejection. *Transplantation* (2010) 90(11):1145–56. doi: 10.1097/TP.0b013e3181f95718

20. Peckert-Maier K, Schonberg A, Wild AB, Royzman D, Braun G, Stich L, et al. Pre-incubation of corneal donor tissue with sCD83 improves graft survival via the induction of alternatively activated macrophages and tolerogenic dendritic cells. *Am J Transplant* (2022) 22(2):438–54. doi: 10.1111/ajt.16824

21. Royzman D, Peckert-Maier K, Stich L, König C, Wild AB, Tauchi M, et al. Soluble CD83 improves and accelerates wound healing by the induction of pro-resolving macrophages. *Front Immunol* (2022) 13. doi: 10.3389/fimmu.2022.1012647

22. Cao W, Lee SH, Lu J. CD83 is preformed inside monocytes, macrophages and dendritic cells, but it is only stably expressed on activated dendritic cells. *Biochem J* (2005) 385(Pt 1):85–93. doi: 10.1042/BJ20040741

23. Loures FV, Araujo EF, Feriotti C, Bazan SB, Costa TA, Brown GD, et al. Dectin-1 induces M1 macrophages and prominent expansion of CD8+IL-17+ cells in pulmonary paracoccidioidomycosis. *J Infect Dis* (2014) 210(5):762–73. doi: 10.1093/infdis/jiu136

24. Rahabi M, Jacquemin G, Prat M, Meunier E, AlaEddine M, Bertrand B, et al. Divergent roles for macrophage c-type lectin receptors, dectin-1 and mannose receptors, in the intestinal inflammatory response. *Cell Rep* (2020) 30(13):4386–4398.e5. doi: 10.1016/j.celrep.2020.03.018

25. Mata-Martinez P, Bergon-Gutierrez M, Del Fresno C. Dectin-1 signaling update: New perspectives for trained immunity. *Front Immunol* (2022) 13:812148. doi: 10.3389/fimmu.2022.812148

26. Li X, Luo H, Ye Y, Chen X, Zou Y, Duan J, et al. Betaglucan, a dectin1 ligand, promotes macrophage M1 polarization via NFkappaB/autophagy pathway. *Int J Oncol* (2019) 54(1):271–82. doi: 10.3892/ijo.2018.4630

27. Rygiel TP, Meyaard L. CD200R signaling in tumor tolerance and inflammation: A tricky balance. *Curr Opin Immunol* (2012) 24(2):233–8. doi: 10.1016/j.coi.2012.01.002

28. Bhattacharjee A, Shukla M, Yakubenko VP, Mulya A, Kundu S, Cathcart MK, et al. IL-4 and IL-13 employ discrete signaling pathways for target gene expression in alternatively activated monocytes/macrophages. *Free Radic Biol Med* (2013) 54:1–16. doi: 10.1016/j.freeradbiomed.2012.10.553

29. Gordon S, Martinez FO. Alternative activation of macrophages: mechanism and functions. *Immunity* (2010) 32(5):593–604. doi: 10.1016/j.immuni.2010.05.007

30. Lee CC, Lin JC, Hwang WL, Kuo YJ, Chen HK, Tai SK, et al. Macrophage-secreted interleukin-35 regulates cancer cell plasticity to facilitate metastatic colonization. *Nat Commun* (2018) 9(1):3763. doi: 10.1038/s41467-018-06268-0

31. Sica A, Mantovani A. Macrophage plasticity and polarization: in vivo veritas. *J Clin Invest* (2012) 122(3):787–95. doi: 10.1172/JCI59643

32. Kotwal GJ, Chien S. Macrophage differentiation in normal and accelerated wound healing. *Results Probl Cell Differ* (2017) 62:353–64. doi: 10.1007/978-3-319-54090-0_14

33. Zhang T, Wang XF, Wang ZC, Lou D, Fang QQ, Hu YY, et al. Current potential therapeutic strategies targeting the TGF-beta/Smad signaling pathway to attenuate keloid and hypertrophic scar formation. *BioMed Pharmacother* (2020) 129:110287. doi: 10.1016/j.biopha.2020.110287

34. Soliman AM, Barreda DR. Acute inflammation in tissue healing. *Int J Mol Sci* (2022) 24(1). doi: 10.3390/ijms24010641

35. Sugimoto MA, Sousa LP, Pinho V, Perretti M, Teixeira MM. Resolution of inflammation: What controls its onset? *Front Immunol* (2016) 7:160. doi: 10.3389/fimmu.2016.00160

36. Starke C, Steinkasserer A, Voll RE, Zinser E. Soluble human CD83 ameliorates lupus in NZB/W F1 mice. *Immunobiology* (2013) 218(11):1411–5. doi: 10.1016/j.imbio.2013.06.002

37. Royzman D, Andreev D, Stich L, Rauh M, Bauerle T, Ellmann S, et al. Soluble CD83 triggers resolution of arthritis and sustained inflammation control in IDO dependent manner. *Front Immunol* (2019) 10:633. doi: 10.3389/fimmu.2019.00633

38. Xiong L, Wang D, Lin S, Wang Y, Luo M, Gao L, et al. Soluble CD83 inhibits acute rejection by up regulating TGF-beta and IDO secretion in rat liver transplantation. *Transpl Immunol* (2021) 64:101351. doi: 10.1016/j.trim.2020.101351

39. Bates JM, Flanagan K, Mo L, Ota N, Ding J, Ho S, et al. Dendritic cell CD83 homotypic interactions regulate inflammation and promote mucosal homeostasis. *Mucosal Immunol* (2015) 8(2):414–28. doi: 10.1038/mi.2014.79

40. Caserta S, Nausch N, Sawtell A, Drummond R, Barr T, Macdonald AS, et al. Chronic infection drives expression of the inhibitory receptor CD200R, and its ligand CD200, by mouse and human CD4 T cells. *PLos One* (2012) 7(4):e35466. doi: 10.1371/journal.pone.0035466

41. Shichita T, Ito M, Morita R, Komai K, Noguchi Y, Ooboshi H, et al. MAFB prevents excess inflammation after ischemic stroke by accelerating clearance of damage signals through MSR1. *Nat Med* (2017) 23(6):723–32. doi: 10.1038/nm.4312

42. Taban Q, Mumtaz PT, Masoodi KZ, Haq E, Ahmad SM. Scavenger receptors in host defense: from functional aspects to mode of action. *Cell Commun Signal* (2022) 20 (1):2. doi: 10.1186/s12964-021-00812-0

43. Kapoor N, Niu J, Saad Y, Kumar S, Sirakova T, Becerra E, et al. Transcription factors STAT6 and KLF4 implement macrophage polarization via the dual catalytic powers of MCPIP. *J Immunol* (2015) 194(12):6011–23. doi: 10.4049/jimmunol.1402797

44. Li Y, Sheng Q, Zhang C, Han C, Bai H, Lai P, et al. STAT6 up-regulation amplifies M2 macrophage anti-inflammatory capacity through mesenchymal stem cells. *Int Immunopharmacol* (2021) 91:107266. doi: 10.1016/j.intimp.2020.107266

45. Liu M, Luo F, Ding C, Albeituni S, Hu X, Ma Y, et al. Dectin-1 activation by a natural product beta-glucan converts immunosuppressive macrophages into an M1-like phenotype. *J Immunol* (2015) 195(10):5055–65. doi: 10.4049/jimmunol.1501158

46. Pakyari M, Farrokhi A, Maharlooei MK, Ghahary A. Critical role of transforming growth factor beta in different phases of wound healing. *Adv Wound Care (New Rochelle)* (2013) 2(5):215–24. doi: 10.1089/wound.2012.0406

47. Krzyzak L, Seitz C, Urbat A, Hutzler S, Ostalecki C, Glasner J, et al. CD83 modulates b cell activation and germinal center responses. *J Immunol* (2016) 196 (9):3581–94. doi: 10.4049/jimmunol.1502163

48. Schindelin J, Arganda-Carreras I, Frise E, Kaynig V, Longair M, Pietzsch T, et al. Fiji: an open-source platform for biological-image analysis. *Nat Methods* (2012) 9(7):676–82. doi: 10.1038/nmeth.2019

frontiers | Frontiers in Immunology

TYPE Original Research
PUBLISHED 01 March 2023
DOI 10.3389/fimmu.2023.1128641

OPEN ACCESS

EDITED BY
Stephen Robert Daley,
Queensland University of Technology,
Australia

REVIEWED BY
Qizhen Shi,
Medical College of Wisconsin,
United States
Seema Patel,
Emory University, United States

*CORRESPONDENCE
Kathleen P. Pratt
kathleen.pratt@usuhs.edu

†These authors have contributed equally to this work

SPECIALTY SECTION
This article was submitted to Immunological Tolerance and Regulation, a section of the journal Frontiers in Immunology

RECEIVED 21 December 2022
ACCEPTED 20 February 2023
PUBLISHED 01 March 2023

CITATION
Gunasekera D, Vir P, Karim AF, Ragni MV and Pratt KP (2023) Hemophilia A subjects with an intron-22 gene inversion mutation show CD4+ T-effector responses to multiple epitopes in FVIII. *Front. Immunol.* 14:1128641. doi: 10.3389/fimmu.2023.1128641

Hemophilia A subjects with an intron-22 gene inversion mutation show CD4$^+$ T-effector responses to multiple epitopes in FVIII

Devi Gunasekera[1,2†], Pooja Vir[1,2†], Ahmad Faisal Karim[1,2†], Margaret V. Ragni[3] and Kathleen P. Pratt[1*]

[1]Department of Medicine, Uniformed Services University of the Health Sciences, Bethesda, MD, United States, [2]Henry Jackson Foundation for the Advancement of Military Medicine, Bethesda, MD, United States, [3]Department of Medicine, University of Pittsburgh, Pittsburgh, PA, United States

Background: Almost half of severe hemophilia A (HA) is caused by an intron 22 inversion mutation (Int22Inv), which disrupts the 26-exon *F8* gene. Inverted *F8* mRNA exons 1-22 are transcribed, while *F8B* mRNA, containing *F8* exons 23-26, is transcribed from a promoter within intron 22. Neither FVIII activity nor FVIII antigen (cross-reacting material, CRM) are detectable in plasma of patients with an intron-22 inversion.

Objectives: To test the hypothesis that (putative) intracellular synthesis of FVIII proteins encoded by inverted *F8* and *F8B* mRNAs confers T-cell tolerance to almost the entire FVIII sequence, and to evaluate the immunogenicity of the region encoded by the *F8* exon 22-23 junction sequence.

Patients/Methods: Peripheral blood mononuclear cells (PBMCs) from 30 severe or moderate HA subjects (17 with an Int22Inv mutation) were tested by ELISPOT assays to detect cytokine secretion in response to FVIII proteins and peptides and to map immunodominant T-cell epitopes. Potential immunogenicity of FVIII sequences encoded by the *F8* exon 22-23 junction region was also tested using peptide-MHCII binding assays.

Results: Eight of the Int22Inv subjects showed robust cytokine secretion from PBMCs stimulated with FVIII proteins and/or peptides, consistent with earlier publications from the Conti-Fine group. Peptide ELISPOT assays identified immunogenic regions of FVIII. Specificity for sequences encoded within *F8* mRNA exons 1-22 and *F8B* mRNA was confirmed by staining Int22Inv CD4$^+$ T cells with peptide-loaded HLA-Class II tetramers. FVIII peptides spanning the *F8* exon 22-23 junction (encoding M2124-V2125) showed limited binding to MHCII proteins and low immunogenicity, with cytokine secretion from only one Int22Inv subject.

Conclusions: PBMCs from multiple subjects with an Int22Inv mutation, with and without a current FVIII inhibitor, responded to FVIII epitopes. Furthermore, the FVIII region encoded by the exon 22-23 junction sequence was not remarkably

immunoreactive and is therefore unlikely to contain an immunodominant, promiscuous CD4$^+$ T-cell epitope. Our results indicate that putative intracellular expression of partial FVIII proteins does not confer T-cell tolerance to FVIII regions encoded by inverted *F8* mRNA or *F8B* mRNA.

KEYWORDS

hemophilia A, immune tolerance, intron-22 inversion mutation, epitope mapping, factor VIII

Introduction

Almost half of severe hemophilia A (HA) patients have a *F8* intron-22 inversion mutation (Int22Inv), which precludes expression of an intact, functional FVIII protein (1, 2). The *F8* gene consists of 26 exons encoding FVIII domains A1-A2-B-A3-C1-C2 (3). An additional transcription start site within intron 22 produces *F8B* mRNA, which consists of a short exon encoding eight non-FVIII amino acid residues followed by *F8* exons 23-26 encoding V2125-Y2332 (4). *F8B* mRNA is expressed in multiple tissues of individuals with and without HA, with the exception of HA patients having a deletion mutation within exons 23-26. In addition to *F8B* mRNA, individuals with an intron-22 inversion mutation express a truncated *F8* mRNA consisting of *F8* exons 1-22 (1, 2).

Approximately 30% of severe HA patients develop neutralizing anti-FVIII antibodies following replacement therapy with exogenous FVIII, which are clinically referred to as "inhibitors" (5–7) due to their interference with normal blood coagulation *via* blocking of FVIII cofactor activity. The development of anti-FVIII antibodies in HA patients follows a classic prime-boost response, with inhibitors generally developing within the initial 20 exposures to therapeutic FVIII (8). Initial inhibitor development after 150+ FVIII infusions is far less common. The role of CD4$^+$ T cells in providing ongoing help necessary for anti-FVIII antibody generation was clearly shown in a 1993 study of HA patients infected with HIV. For those with an inhibitor, their titers declined as their CD4$^+$ T-cell counts decreased (9). Proliferation and cytokine secretion of CD4$^+$ T cells from HA subjects in response to FVIII protein and synthetic peptides was demonstrated in subsequent studies (10–15). More recently, specific HLA-restricted T-cell epitopes have been identified, with several confirmed by isolation of T-cell clones responding to specific FVIII peptides (16–21). Thus, the essential role of CD4$^+$ T cells in development and persistence of inhibitor responses is well established.

A 2009 case-control study indicated that large *F8* gene deletions were associated with increased risk of developing an inhibitor (22), and a 2012 meta-analysis further indicated that inhibitor risk in HA-Int22Inv patients was somewhat lower than in severe HA patients with a large structural alteration of the *F8* gene, e.g., large deletion or early nonsense mutations (23). This provided some support for an earlier hypothesis that endogenous intracellular expression of FVIII partial proteins from these two mRNAs occurs, and that it may confer self-tolerance to the corresponding FVIII protein sequences, thereby decreasing the immunogenicity of FVIII replacement therapy in Int22Inv patients (24, 25). Since a substantial fraction of Int22Inv patients still develop inhibitors, a corollary of this hypothesis is that the FVIII C1 domain region encoded by mRNA spanning the exon 22-23 splice site (corresponding to FVIII residues ~I2103-A2146), which would be the only "non-self" region of therapeutic FVIII (Figure 1), is a promiscuous, highly immunogenic neo-epitope.

The present study tests this hypothesis and corollary by directly querying CD4$^+$ T-effector responses of HA subjects with and without an Int22Inv mutation to recombinant (r)FVIII proteins and synthetic peptides. A primary goal was to map immunodominant epitopes that elicit CD4$^+$ T-cell responses in the Int22Inv subjects and determine if the results indicate tolerance to FVIII regions encoded by inverted *F8* exons 1-22 and/or by *F8B*. In addition, peptide-HLA Class II binding assays were employed to test the ability of peptides encoded by the *F8* exon 22-23 junction region to be presented on a representative series of recombinant HLA-DRB1 proteins. The latter experiments would indicate if peptides encoded by this junction region, which cannot be expressed in patients with an Int22Inv mutation, could represent a promiscuous, immunodominant epitope responsible for inhibitor development in Int22Inv patients.

Materials and methods

Human subjects and blood samples

Blood samples from 11 severe and moderately severe HA subjects were donated as part of the "INHIBIT" feasibility study (5U34HL 114674, MVR, PI). Three of these were known Int22Inv subjects, while the HA-causing mutation was unknown for six of these subjects. PBMCs from severe HA and normal control subjects that were banked from earlier studies were also utilized (USU IRB#1, protocols MED-83-3442 and MED-83-3426). All subjects provided informed consent consistent with the Principles of Helsinki. Additional de-identified normal control samples were obtained from the NIH Blood Bank (Exempt E4). Both freshly prepared and frozen (7% DMSO in FBS) PBMC samples were analyzed.

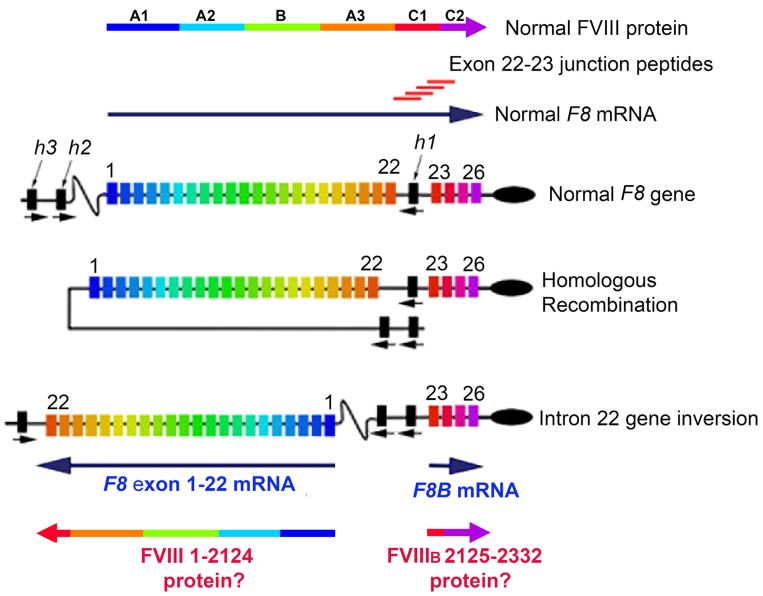

FIGURE 1
FVIII Structure, Int22Inv DNA, Int22Inv mRNA, and hypothesized partial FVIII proteins. Full-length FVIII consists of domains A1, A2, A3, B, C1 and C2, which are encoded by the 26-exon *F8* gene. Following a type 1 or type 2 intron 22 inversion mutation, the primary *F8* mRNA product consists of *F8* exons 1-22, which encode the FVIII A1, A2 and B domains, plus the C1 domain sequence through M2124 and then terminating at a stop codon within intron 22. The shorter transcript *F8B* is comprised of 24 nucleotides followed by *F8* exons 23-26, which encode FVIII residues 2125-2332. If these two partial FVIII proteins were expressed intracellularly, this could in principle promote tolerance to FVIII as a "self"-protein. The 20-mer exon 22-23 junction peptides, with *F8* sequences overlapping by 12 residues, were designed to allow peptides to bind to the HLA-DRB1 binding grooves in multiple possible registers, in order to evaluate their potential ability to be presented to $CD4^+$ T cells.

Inhibitor titers

Inhibitor titers, expressed as Bethesda units (BU)/mL, were from clinical records for the subjects, which reported results of CLIA-certified clotting or chromogenic substrate assays (26). Both clotting and chromogenic inhibitor assays are functional assays that measure the inhibition of FVIII cofactor activity in the presence of anti-FVIII antibodies. The clotting assay measures plasma clotting time [using a 1-stage assay (27)], while the chromogenic assay measures cleavage of a chromogenic substrate for factor X; normal factor X kinetics require a normal FVIII level. In either assay, serial dilutions of the patient plasma are mixed with a normal pooled plasma sample, and the residual FVIII activity, compared to a parallel assay using the normal pooled plasma plus buffer, is measured and reported in BU/mL. One BU/mL is the reciprocal of the patient plasma dilution that results in 50% normal FVIII activity in the assay. The lower limit of quantification is generally considered to be 0.6 BU/mL, and titers > 5.0 BU/mL are considered high-titer inhibitors.

Reagents, buffers and instruments

Recombinant (r)FVIII (Kogenate 27NZPO) was from Bayer (Leverkusen, Germany) or Baxter (Westlake Village, CA, USA; Recombinate TRH07504AA). Recombinant FVIII-C2 protein was purified in-house as described (28). Tetanus and Diptheria (TD) toxoid adsorbed was from Mass Biologics, (Boston, MA, USA) and Remel PHA (R30852801) (100µg/ml) were from Thermo Scientific (Rockford, IL, USA). Benzonase nuclease, 250 U/µl (021M0852) and 0.4% Trypan blue (T8154) were from Sigma Aldrich (St Louis, MO, USA). RPMI 1640 with 25 mM HEPES, DMEM/F-12(1(1:1), MEM nonessential amino acids (100X), 1X D-PBS (Ca/Mg-free) and 10X D-PBS were from Life Technologies (Grand Island, NY, USA). Ficoll-Paque PLUS was from GE Healthcare Life Sciences (Piscataway, NJ, USA). HCl was from JT Baker Tyco Products (Phillipsburg, NJ, USA). Human IFN-gamma ELISPOT pair (551849), Human IL-5 ELISPOT pair (551886), Human IL-10 ELISPOT pair (551883), AEC substrate set (551951) and TMB substrate were from BD Biosciences (San Jose, CA, USA). IL-7 (0.5ng/ml) was from Peprotech (Rocky Hill, NJ, USA). Fetal bovine serum was from Hyclone (Logan, UT, USA). ImmunO human serum type AB was from MP Biomedicals (Solon, OH, USA). Recombinant, extracellular domains of 10 HLA-DRB1 protein monomers, HLA Class II tetramers loaded with the relevant peptides and anti-HLA-DR antibody L243 were provided by the Tetramer Core Facility at the Benaroya Research Institute (Seattle, WA, USA). AIM-V medium and goat anti human IgG-HRP were from Invitrogen (Carlsbad, CA, USA). Sheep anti-human FVIII was from Cedarlane labs (Burlington, NC, USA). ELISA 12 well strips were from E & K Scientific (Santa Clara, CA, USA). Wallac enhancement solution, fluorescence assay buffer and europium-labeled straptavidin were from Wallac-Perkin Elmer (Turku, Finland). 96-well polypropylene plates and Corning Costar high-binding ELISA plates were from Sigma Aldrich (St. Louis, MO, USA), cat # CLS3799 and CLS2592, respectively). Recombinant human IL-2 (Chiron Il-2, Proleukin, 70 IU/ml) was from R & D systems, cat #202-IL-010)

FVIII peptides and peptide pools

Individual 20-mer peptides spanning the FVIII A2, C1 and C2 sequences, as well as equimolar pools containing 2-5 of these peptides, were from Anaspec, Inc. (Fremont, CA, USA, Table S1). Additional 15-mer peptides spanning the FVIII A1, A2, A3, C1 and C2 domain sequences, with 12-residue overlaps, were from Mimotopes, Inc. (Mulgrave, Victoria, Australia), which also provided large, medium and small equimolar pools of these peptides (Tables S2–S5). An intron 22-23 'junction peptide pool' was created by combining four 20-mer peptides (Mimotopes, Inc.) with overlapping sequences spanning the *F8* exon 22-23 – encoded region (FVIII 2103-2146) in DMSO (Table 1). All peptides were ordered at >70% advertised purity and their quality was verified by mass spectrometry.

Peptide-MHCII binding assays and predictions

Quantitative peptide-MHC competition binding assays were carried out to determine binding avidities of four 20-mer peptides spanning the *F8* exon 22-23 junction region to 10 HLA-DRB1 proteins using methodology described previously (29). Briefly, 1-µl aliquots of serially diluted (50nM – 50µM in DMSO) non-biotinylated FVIII peptides, were added to triplicate wells of 96-well polypropylene plates. Serially diluted non-FVIII reference peptides known to bind to specific HLA-DRB1 (Table S6) were added to separate wells as positive controls. The HLA-DRB1 proteins were diluted to 50 nM in 150 mM citrate-phosphate, pH 5.4, 0.75% n-octyl-beta-D-glucopyranoside, 1 mM PMSF. 50 µl of the HLA-DRB1 solution was added per well, and the plates were sealed and incubated at 37°C for 30 min to allow peptide binding to the HLA-DRB1 protein. Next, 1 µl of the appropriate biotinylated reference peptide, at a concentration in the known binding range for its respective HLA-DRB1 (Table S6), was added to each well, the solutions were mixed, and the plates were incubated at 37°C for 18-24 hrs. 100 µl aliquots of the anti-HLA-DR antibody L243 (10 µg/mL in 12.5 mM borate buffer, pH 8.2) were added to 96-well ELISA plates, and the plates were incubated at 4°C for 18-24 hrs, washed, and blocked with 1xDPBS containing 5% FBS for 3 hrs. The plates were washed again and 50 µl neutralization solution (50 mM Tris, pH 8.0, 0.75% n-octyl-beta-D-glucopyranoside) was added to each well. The contents of wells containing the peptide-HLA-DRB1 binding reactions were then transferred to wells of the ELISA plates containing the neutralization solution and the ELISA plates were incubated for 18-24 hrs at 4°C. After washing the plates 5X with 300 ul/well of 1XPBS, 0.05% Tween-20, 100 ul of Europium-labeled streptavidin (diluted 1:1,000 into Wallac assay buffer) was added to each well. The plates were covered with a black polystyrene lid, incubated at room temperature for 4 hrs and washed 5X with 300 ul/well of 1XPBS, 0.05% Tween-20. Wallac enhancement solution (100 µl/well) was then added, and the plates were incubated at room temperature for 30 min and then read on a Victor 2D time-resolved fluorometer. Sigmoidal binding curves were simulated and IC50 values calculated for the FVIII peptides, based on their competition with the reference peptides for each HLA-DRB1.

Predicted affinities of the four FVIII junction peptides for the 10 HLA-DRB1 alleles were obtained using the Immune Epitope Database (IEDB) server, using the NetMHCIIPan 4.0 prediction algorithm (30).

TABLE 1 FVIII peptides spanning the F8 exon 22-23 junction region.

2103-2122	IMYSLDGKKWQTYRGNSTGT
2111-2130	KWQTYRGNSTGTL**MV**FFGNV
2119-2138	STGTL**MV**FFGNVDSSGIKHN
2127-2146	FGNVDSSGIKHNIGNPPIIA

The bolded M and V indicate residues M2124 and V2125, which are the last amino acid encoded by exon 22 and the first amino acid encoded by exon 23, respectively.

In vitro expansion of FVIII-specific T cells

FVIII-specific $CD4^+$ T cells were expanded by culturing PBMCs with or without rFVIII, rFVIII-C2 protein, or pooled or individual FVIII peptides, as follows. One vial of frozen PBMCs (~10 million cells) was thawed by slowly adding 9 ml of AIM-V medium containing 10% human serum + 1.8 µl of 25K benzonase nuclease. The cells were washed with AIM-V medium containing 10% human serum and re-suspended in AIM-V medium containing 15% human serum, and then plated at $1x10^6$ cells per well in 48-well cell culture plates (1 mL/well) with one of the following: rFVIII protein (1 µg/mL ~8nM), rFVIII-C2 protein (2 µg/mL = 50 nM), pooled FVIII peptides (50 nM and 70 nM), FVIII pooled junction peptides (200 nM), or individual FVIII peptides (50 or 100 nM). Positive control wells were stimulated with 0.02Lf (5 µl/mL) TD toxoid, PHA (10 µg/mL) and negative controls with 5 µl DMSO. The plates were incubated for five days at 37°C in a 5% CO_2 incubator. At day 6, cells were harvested and re-suspended in AIM-V medium (no serum) containing 0.5ng/mL IL-7 and then directly plated on 96-well flat-bottom ELISPOT plates. For some individual peptide ELISPOT assays, expansions were continued for an additional 3 days, adding fresh AIM-V medium and IL-2 (3.5 IU/mL final concentration).

Epitope mapping by ELISPOT assays

ELISPOT plates were coated with capture antibody solutions (anti-IFN-γ, anti-IL-5 or anti-IL-10) diluted to 5 µg/ml in DPBS and incubated at 4C overnight. Wells were then washed once with 200 µl/well Blocking Solution (AIM-V medium containing 10% human serum). Another 200 µl Blocking Solution was then added to each well and the plates were incubated for 2 hrs at room temp and the Blocking solution discarded. The expanded PBMCs were then added in serial dilutions (carried out in duplicate when sufficient cells were available) with final concentrations of $2X10^5$, $1x10^5$ and $5x10^4$ cells/well, and incubated with the same antigenic stimulants as before. The plates were incubated for 24 hrs for IFN-γ

ELISPOTS or 48 hrs for IL-5 and IL-10 ELISPOTS at 37C, 5% CO_2. The suspended cells were then discarded and the plates washed with 200 µl/well dH_2O (2X) and 3x with PBS containing 0.05% Tween 20 (wash buffer I). The biotinylated anti-human antibody provided in the kits (0.25 µg/ml, diluted in PBS + 10% human serum) was then added and the plates were incubated for 2 hrs at room temperature. The plates were washed 3X with 200 µl/well wash buffer I, washed 2X with 200 µl/well PBS, and developed with streptavidin-HRP (BD Biosciences, #557630) diluted 1:100 in PBS containing 10% human serum for 1 hr at room temperature. Plates were then washed 4X with 200 µl/well wash buffer I, and washed 2X with 200 µl/well PBS. Spots were then developed by adding 100 µl/well of BD ELISPOT AEC substrate and incubated for 5-30 minutes in the dark. The wells were then washed 2X with 200 µl/well dH_20 and air-dried at room temp for 2 hrs. IFN-γ, IL-5 and IL-10-specific spot-forming cells (SFC) were then counted using software on a CTL Immunospot S6 Ultimate Image Analyzer. Stimulants were: rFVIII 5 µl/mL = 5 nM; rFVIII-C2 1µg/mL = 50 nM; FVIII peptides (pooled or individual): 50-100 nM; TT; 5 µl/mL; PHA: 5 µl/mL. The criteria for antigen-specific (positive) responses were: a minimum of 25 spots per million cells (based on spots per 200,000 cells/well) and wells with the stimulant had ≥3X the average number of spots counted for the unstimulated wells. In addition, antigen-specific responses to large FVIII peptide pools were "decoded", when sufficient cells were available, by subsequent ELISPOT assays using smaller peptide pools and then with individual peptides, to map immunogenic FVIII regions and specific epitopes contributing to the cytokine response.

Epitope mapping by HLA Class II tetramer staining

PBMCs were added to 48-well plates in 1ml of 10% human serum RPMI medium (1 million PBMCs per well) and then stimulated with individual or pooled 20-mer or 15-mer FVIII peptides (10 µM) and incubated for up to 19 days at 37C, 5% CO_2. At day 7, 50 µl of IL-2 was added (35 IU/mL final concentration) without removing any medium. At day 9, 400-500 µL supernatant was removed and replaced with fresh 15% human serum RPMI medium containing 50 µl IL-2 after which cells were fed with 50 µl IL-2 every 48-72 hours, splitting as needed. After 17-19 days, the cells were re-suspended, 100 µL aliquots were transferred to FACS tubes, and 1.5 µl of the appropriate peptide-loaded, PE-labeled HLA Class II tetramer (~10 µg/mL final concentration) was added. The tubes were incubated in the dark at 37C for 2 hrs and then put on ice. A mixture of anti-CD3-PerCP + anti-CD4 APC (3.75 µL each from stock solutions) was added to each tube, and tubes with no antibody added served as a negative staining control. The tubes were then incubated in the dark at 4C for 30 min. Additional tubes containing beads for compensation (ThermoFisher (ebiosciences), Rockville, MD, USA), were stained by adding 5 µL of anti-CD3-PerCP, 1.5 µl of anti-CD4-APC and 1.5 µl of anti-CD4-PE and tubes were incubated in the dark for 30 min. Sample and control cells were then washed and re-suspended in ice-cold FACS buffer, stored on ice in a covered container, and analyzed by flow cytometry and/or FACS acquisition. The gating strategy was: Singlets (FSC-H/FSC-A), Lymphocytes (SSC-A/FSC-A), followed by gating on anti-CD3-PerCP-high, followed by tetramer-PE/CD4-APC to detect antigen-specific CD4+ T cells.

Isolation of FVIII-specific T-cell clones

To isolate FVIII-specific T-cell clones, $CD4^{hi}Tetramer^{hi}$ cells were single-cell sorted into 96-well round-bottom plates containing 100 µl RPMI medium per well. To each well, (200,000) irradiated HLA-mismatched PBMC were added as feeder cells in a volume of 100 µL RPMI Medium containing 15% human serum AB plus PHA (5 µg/mL). The cells were incubated for 24 hrs at 37C, 5% CO_2, and then IL-2 (10 IU/mL) in 25 µl RPMI medium was added to each well. The cells were then incubated at 37C in 5% CO_2 for another 14-21 days. For wells containing expanding clones, tetramer staining was performed to confirm their specificity. If clones were not expanding, the cells were re-stimulated with irradiated, HLA-mismatched PBMCs and PHA as before, adding fresh medium and IL-2 (3.5 IU/mL final concentration) as needed to continue the expansion or else frozen in 10% DMSO in FBS.

Results

Peptide-MHCII binding assays and predictions

The experimental FVIII peptide-HLA-DRB1 affinities are in Table 2A and their predicted affinities are in Table 2B. Only HLA-DR0404, DR0701, DR0901 and DR1501 showed moderate or strong

TABLE 2A Experimental binding affinities (IC50 values) of FVIII exon 22-23 junction peptides.

FVIII peptide	DR0101	DR0301	DR0401	DR0404	DR0701	DR0901	DR1001	DR1101	DR1104	DR1501
2103-2122	n.b.	61.2	238.07	n.b.	n.b.	57.3	n.b.	50.58	n.b.	41.95
2111-2130	10.91	227.6	43.66	127.5	5.9	0.6	352.9	68.83	n.b.	9.09
2119-2138	n.b.	n.b.	74.46	0.9	1853.08	55.6	n.b.	n.b.	n.b.	2.97
2127-2146	n.b.	n.b.	n.b.	43.8	n.b.	60.9	n.b.	n.b.	n.b.	7.52

0-1.0 µM (Strong binding, dark gray); >1.0 and <10.0 µM (Moderate binding, medium gray); 10.0-50.0 µM (Weak binding, light gray); >50 µM (no binding, n.b.).

TABLE 2B Predicted binding affinities (IC50 values)* of FVIII exon 22-23 junction peptides.

FVIII peptide	DR0101	DR0301	DR0401	DR0404	DR0701	DR0901	DR1001	DR1101	DR1104	DR1501
2103-2122	0.415	2.074	2.045	2.172	1.315	0.974	0.768	1.082	1.063	0.356
2111-2130	0.189	6.081	0.515	1.816	0.256	0.323	0.318	1.764	2.908	0.857
2119-2138	0.188	3.948	0.164	0.186	0.161	0.26	0.145	1.897	1.934	0.209
2127-2146	0.45	4.058	1.053	2.044	0.983	1.384	1.113	2.195	2.799	1.452

* predictions run on the IEDB website (http://tools.iedb.org/mhcii) 11/27/22 and 1/16/23 using NetMHC Pan 4.0[15,16].
0-1.0 μM (Strong binding, dark gray); >1.0 and <10.0 μM (Moderate binding, medium gray).

binding affinity to one or more peptides spanning the *F8* exon 22-23-encoded region of FVIII, while weak binding was observed to HLA-DR0101 and DR0401. The MHCIIpan algorithm (30) predicted moderate-to-strong binding affinity to additional HLA-DR proteins. Based on the experimental results, ELISPOT assays were then carried out using PBMCs from nine HA subjects with an intron 22 inversion mutation who were also known to have *HLA-DR1, DR4, DR7, DR9* or *DR15* alleles.

Epitope mapping by ELISPOT assays

Several strategies were used to map T-cell epitopes, in order to test specific hypotheses and/or to rationally choose which peptides to utilize when there were not sufficient PBMCs to systematically test responses to larger and then smaller peptide pools followed by individual peptides (due to competing studies and resulting blood volume limitations in subjects with hemophilia A). The number of PBMCs per subject was highly variable, as samples were obtained from both adults and children, and the amounts of blood drawn also reflected the stated preferences of the subjects. Therefore, the number of experiments and replicate wells per experiment varied somewhat according to the number of cells available for the assays.

rFVIII and/or rFVIII-C2 domain protein ELISPOTs were included as a specific control in almost all ELISPOT experiments. For positive responders, IFN-γ secretion was generally more robust when cells were stimulated with 50 nM rFVIII-C2 than with 8 nM rFVIII. Unfortunately, FVIII protein becomes toxic to $CD4^+$ T cells at higher concentrations. The stronger responses to rFVIII-C2, and to pooled or individual FVIII peptides in some assays, may simply be due to stimulation of lower-avidity $CD4^+$ T cells by the higher concentrations of rFVIII-C2 and FVIII peptides. Of note, the rFVIII-C2 preps were routinely tested to confirm low endotoxin levels (31).

Exon 22-23 junction peptides

Potential $CD4^+$ T-cell responses to exon 22-23 junction sequences were tested using samples from nine HA subjects with an intron-22 inversion mutation who also had one of the *HLA-DRB1* alleles shown experimentally to bind peptides with these sequences: *HLA-DR1, DR4, DR7, DR9* or *DR15* (Table 2A). Eight of these subjects failed to show a response to the pooled FVIII exon 22-23 junction peptides when tested using IFN-γ ELISPOT assays (Table 3). Five of them had a current inhibitor and four had no inhibitor history. The one subject who showed a response to the junction peptides, G4, had a low-titer inhibitor. He had an intron 22 inversion mutation as well as a missense mutation, H1499Y, and his *HLA-DRB1* alleles were *HLA-DRB1*0301, 1501*. Therefore, additional MHCII binding predictions were made using the IEDB analysis resource Consensus tool (32, 33) with the input sequence FVIII 1485-1513, lpktsgkvellpkvhiyqkdlfptetsng, which contains all possible 15-mer sequences containing residue H1499. Interestingly, the IEDB prediction algorithm identified two overlapping 9-mer core sequences containing H1499 as potential *HLA-DRB1*1501*-restricted $CD4^+$ T-cell epitopes, ranking them in the top 15-20% based on predicted binding affinity (Table S7).

Systematic epitope mapping using pooled and individual FVIII peptides

Subjects P1 and P11 (both with an intron-22 inversion) generously donated sufficient blood to carry out fairly comprehensive epitope mapping by ELISPOT assays. P1 had a past inhibitor that had resolved (peak titer 15.2 BU/mL approximately 10 years prior to donating this sample). IFN-γ ELISPOT assays showed robust responses to both rFVIII and rFVIII-C2 protein (Figure 2A). His responses to A2 and C2 domain peptides were tested next, in order to test the hypotheses that tolerance to A2 epitopes was conferred by translation from the inverted *F8* mRNA (exons 1-22, containing the A2 domain sequence) and/or from *F8B* mRNA (exons 23-26, containing the C2 domain sequence). No responses to pooled A2 domain peptides were revealed under these assay conditions (not shown). However, his PBMCs responded to one of the pools of 20-mer peptides spanning the C2 domain sequence (Figure 2B). Decoding of this response by testing the individual peptides comprising this pool identified robust responses to peptides corresponding to C2-2210-2229, C2-2226-2245 and C2-2242-2261 (Figure 2C).

Subject P11 also had a previous inhibitor that resolved four years before donating this blood sample. His PBMCs showed robust IFN-γ secretion when stimulated with rFVIII, rFVIII-C2 protein, peptide pools spanning the FVIII A2 domain sequence, and peptide pools spanning the FVIII C2 domain sequence (Figures 3A–C). His PBMCs also responded to rFVIII stimulation with secretion of IL-5 and IL-10 (Figure 3D).

TABLE 3 IFN-γ ELiSpot responses of Int22Inv PBMCs to pooled junction peptides (FVIII 2103-2146).

Subject code	Age range	HLA-DRB1	Current inhibitor?	Past inhibitor that resolved?	Inhibitor peak (BU/mL)	F8 exon 22-23 junction peptide stimulation?
G1	18+	0701, 0701	N	N	0	N
G2	4-17	0901, 1101g	N	N	0	N
G3	18+	0701, 1301	Y	N	49	N
G4*	**18+**	**0302, 1501**	**Y**	**N**	**0.6**	**Y**
G5	4-17	0701, 1501	N	N	0	N
G6	18+	0801, 1503	Y	N	68	N
G7	4-17	0404, 1301	N	N	0	N
G8	4-17	0401, 0701	Y	N	1	N
G9	18+	0102, 1503	Y	N	>1000	N

*Subject G4 had an Int22Inv and a missense H1499Y mutation. His ELISPOT results were positive, showing 195 spots per million PBMCs, compared to the unstimulated background of 30 spots per million PBMCs.

Querying Int22Inv T-cell responses to a known *HLA-DRB1*1101*-restricted epitope in FVIII

IFN-γ ELISPOT assays were carried out to determine if PBMCs from six severe HA subjects with an *HLA-DR11* allele would respond to a known *HLA-DRB1*1101*-restricted T-cell epitope in the FVIII A2 domain, FVIII-589-608, which was identified in a HA subject with missense substitution R593C (20). The overlapping 20-mer peptides FVIII-A2-28 and/or A2-29 both contained the epitope of interest. Two of the subjects had an Int22Inv mutation, two had a frameshift mutation, and the HA-causing mutation was unknown for the other two. One of the Int22Inv subjects responded to peptide A2-29, and both of the Int22Inv subjects also showed a robust response to the FVIII-C2 protein (Figure S1). Together, these results indicated the Int22Inv mutation did not confer tolerance to either the FVIII A2 or C2 domains.

Mapping epitopes restricted to *HLA-DR3*

ELISPOT assays were first carried out for subject G21, who had an Int22Inv mutation and was monogenic for *HLA-DRB1*0301*. His PBMCs showed positive IFN-γ responses to rFVIII and to large peptide pools LP1, LP2 and LP3, which together span FVIII residues 1-737 (Figure 4A). The FVIII heavy chain consists of the A1 and A2 domains, residues 1-740. There were not enough PBMCs to allow systematic decoding *via* ELISPOT assays using smaller peptide pools and then individual peptides covering 740 residues. Therefore, the Immune Epitope Database (IEDB) server (33) was used to predict peptides within the FVIII A1 and A2 domains that would bind with high affinity to HLA-DR0301. Twenty-five 15-mer FVIII peptides from our library contained a total of 18 unique 9-mer motifs that were predicted to be in the top 2% for binding to HLA-DR0301 (Table S8). In several cases where overlapping 15-mer peptides contained the same motif the 2-3 peptides were pooled, generating a total of 18 individual or pooled FVIII peptides for further testing (Table S9). Stimulation of his PBMCs with four of these individual peptides, A1-41, A1-58, A2-47 and A2-59, produced IFN-γ secretion slightly above background levels (Figure 4B).

Next, PBMCs from three additional Int22Inv HA subjects who all had a current inhibitor and an *HLA-DR3* allele, G16, G17 and G18, were tested for IFN-γ responses to these 4 peptides by ELISPOT assays (Figure 4C). The strongest response was from G18, responding to peptide A2-59. Therefore, HLA-DR0301 tetramers loaded with the 4 pooled peptides, and with individual peptide A2-59, were ordered.

Other HA ELISPOT assays

PBMCs from 11 severe and moderate HA subjects, three of whom had a confirmed Int22Inv mutation, were tested for responses to rFVIII and rFVIII-C2 protein (Figure S2). Eight of them showed robust cytokine secretion in response to rFVIII and 9 responded to rFVIII-C2. In general, comparing results of ELISPOT experiments testing reactivity to rFVIII and rFVIII-C2, among the

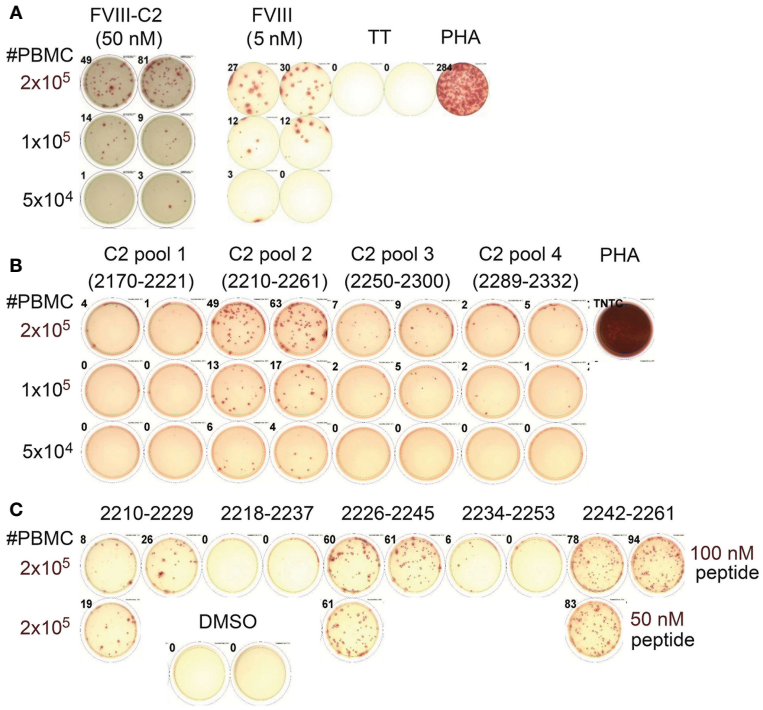

FIGURE 2
Mapping of CD4$^+$ T-cell epitopes in the FVIII C2 domain by peptide ELISPOT assays (Int22Inv subject P1). **(A)** This subject's PBMCs showed robust IFN-γ secretion when stimulated with rFVIII and rFVIII-C2 proteins. The FVIII-C2 ELISPOTs were carried out on different plates and read separately, hence the different background color in this image. **(B)** Decoding of his response to the FVIII C2 domain using pools of 20-mer peptides spanning the C2 domain sequence indicated that C2 pool #2 contained one or more immunodominant epitopes. **(C)** Further decoding by stimulations with the individual 20-mer peptides comprising C2 pool 2 indicated that he had specific responses to three epitopes in the FVIII C2 domain. His PBMCs did not respond to pooled peptides spanning the FVIII A2 domain (not shown).

positive responders IFN-γ secretion was usually more robust when cells were stimulated with 50 nM rFVIII-C2 than with 8 nM rFVIII. Unfortunately, FVIII protein becomes toxic to CD4 T cells at higher concentrations. The stronger responses to rFVIII-C2, and to pooled or individual FVIII peptides in some assays, may simply be due to stimulation of lower-avidity CD4 T cells by the higher concentrations of rFVIII-C2 and FVIII peptides. Of note, the rFVIII-C2 preps were routinely tested to confirm low endotoxin levels.

Non-HA control ELISPOT assays

Control ELISPOT experiments indicated that IFN-γ secretion from non-HA PBMCs in response rFVIII stimulation under these assay conditions (Figure S3) was rare, while responses of non-HA PBMCs to rFVIII-C2 protein (included as a control in several experiments) were seen more frequently but still were not common.

Background proliferation

Two severe HA and two non-HA control subjects showed high background IFN-γ secretion (seen in ELISPOT wells with DMSO alone added); they were therefore excluded from this study and are not included in any figures or tables.

Epitope mapping by HLA Class II tetramer staining and isolation of FVIII-specific T-cell clones

HLA-Class II tetramer staining was carried out using CD4$^+$ T cells isolated from four subjects with an Int22Inv mutation. Subject G16 was an adult inhibitor subject who had an *HLA-DRB1*0301, 1201g* haplotype. Subject G19 was an adult inhibitor subject with *HLA-DRB1*0302, 0901* haplotype. Subject G20 (age range 4-17 years) had the *HLA-DRB1*0301, 1101* haplotype and a current inhibitor. Subject G21 (age range 4-17 years) had the *HLA-DRB1*0301, 0301* haplotype and no inhibitor history. Tetramer staining was also carried out for subject G18, an adult with an intron 1 inversion mutation, a current inhibitor, and *HLA-DRB1*0301, 1401g* haplotype, in order to further test for *HLA-DRB1*0301*-restricted epitopes in FVIII. Tetramer staining of CD4$^+$ T cells isolated from these subjects' PBMCs was followed by sorting of tetramer-hi cells and expansion of clones in culture.

Tetramer staining to test for T-cell responses to epitopes in the FVIII A2 domain

PBMCs from Int22Inv subject G20 were queried using HLA-DR1101 tetramers loaded with peptide pool A2-6, which consisted

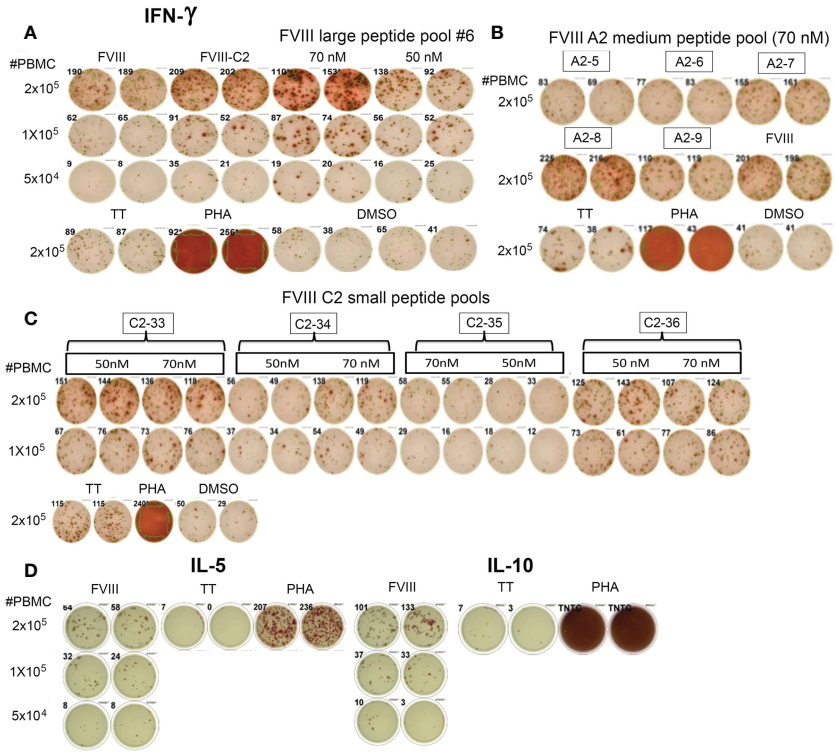

FIGURE 3
CD4$^+$ T cells from Int22Inv subject P11 respond to epitopes in the FVIII A2 and C2 domains. **(A)** He showed a strong IFN-γ response to rFVIII, rFVIII-C2 protein, and FVIII large peptide pool #6 (which contained peptides spanning the C2 domain sequence). **(B)** His PBMCs also responded to FVIII A2 domain medium peptide pools A2-7, A2-8 and A2-9. **(C)** Decoding of his response to rFVIII-C2 protein and FVIII large peptide pool #6 by stimulating his PBMCs with small peptide pools spanning the FVIII C2 domain sequence. His PBMCs responded to epitopes in pools C2-33, C2-34 and C2-36. **(D)** This subject also showed Th2 (IL-5) and Tr1 (IL-10) responses to rFVIII stimulation. His responses to multiple epitopes in the A2 and C2 domains indicate that the inverted *F8* mRNA containing exons 1-22 and *F8B* mRNA (encoding the putative FVIIIB protein containing the FVIII C2 domain sequence) did not confer tolerance to the FVIII A2 or C2 domains. TT = tetanus toxoid. PHA = phytohemagglutinin. Negative control: DMSO (5 µl/well). rFVIII: 5 nM, rFVIII-C2: 50 nM.

of four 20-mer peptides spanning FVIII residues 565-616. This region contains a known *HLA-DRB1*1101*-restricted T-cell epitope that was recognized by HA subjects with an R593C missense mutation (20). Figure 5A shows staining of representative T-cell clones with HLA-DR1101 tetramers loaded with peptide pool A2-6, obtained following expansion of CD4$^+$ T cells using this same peptide pool. Results clearly indicate recognition of one or more epitopes in the region FVIII 565-616.

Tetramer staining to test for T-cell responses to epitopes in the FVIII C2 domain

CD4$^+$ T-cell clones were isolated from Int22Inv subject G19 following expansion of CD4$^+$ T cells using a 20-mer peptide pool spanning the FVIII C2 domain region 2289-2332. Figures 5B–D shows tetramer staining of representative *HLA-DRB1*0901*-restricted T-cell clones recognizing these pooled peptides. A second staining of expanded clones using tetramers loaded with the individual FVIII-C2 peptides comprising this pool identified FVIII-2297-2316 as an *HLA-DRB1*0901*-restricted T-cell epitope recognized by CD4$^+$ T cells from this subject.

HLA-DR3-restricted T-cell clones recognizing another FVIII A2 domain epitope

PBMCs from three Int22Inv subjects and one intron 1 subject were stimulated with a pool of four immunogenic peptides identified by ELISPOT assays: A1-41, A1-58, A2-47 and A2-59 (Figure 4B). The expanded cells were then stained and single-cell sorted using HLA-DR0301 tetramers loaded with these pooled peptides (not shown). Clones were obtained from three of these subjects. Specificity of the staining was then confirmed using an HLA-DR0301 tetramer loaded with peptide A2-59. This tetramer produced strong staining for two clones expanded from Int22Inv subject G16, two clones from Int22Inv subject G21, and three clones from intron 1 inversion subject G18, confirming that this peptide contained a FVIII epitope. Representative tetramer staining results are in Figure 6. The gating strategy and staining of the remaining clones are in Figure S4.

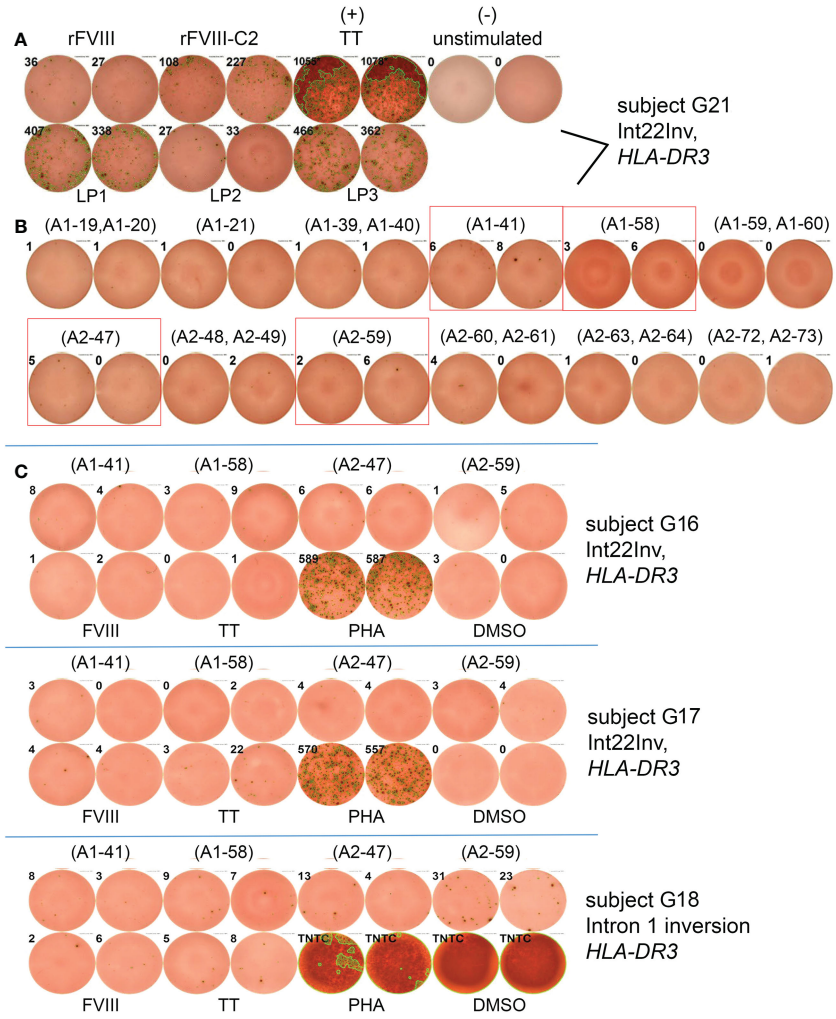

FIGURE 4
Epitope mapping of HLA-DRB1*0301-restricted responses to FVIII A1 and A2 domains by ELISPOT assays. **(A)** PBMCs from Int22Inv subject G21 responded to rFVIII and rFVIII-C2 domain protein, tetanus/diptheria toxin, and FVIII large peptide pools LP1, LP2 and LP3. Peptide pools LP1-LP3 consist of overlapping 15-mer peptides spanning the FVIII A1 and the A2 domains (Table S3). and LP2 **(B)** PBMCs from the same subject also responded to individual 15-mer FVIII peptides A1-41, A1-58, A2-47 and A2-59. Results for the remaining 6 peptides or peptide pools were negative and are not pictured. **(C)** PBMCs from an additional three Int22Inv subjects with an *HLA-DR3* allele (G16, G17 and G18) showed responses above background for one or more of the 4 FVIII A1 or A2 domain peptides. The response of the final subject to peptide FVIII-A2-59 (FVIII 605-619) was the most promising.

Positive and negative controls for tetramer-based assays

Positive controls stimulating PBMCs from subjects with tetanus-diptheria toxoid peptides demonstrated the validity of tetramer-based epitope mapping *via* isolation of multiple TT-specific T-cell clones (Figure S5). Negative controls for all tetramer experiments consisted of tetramers loaded with an irrelevant peptide to rule out nonspecific binding of the tetramer to $CD4^+$ T cells.

Summary of FVIII immunogenicity assays

Results of all assays, grouped by assay type and presented as per-subject results, as well as clinical and demographic data, are summarized in Table 4.

Discussion

The hypothesis that HA patients with an intron-22 inversion (Int22Inv) mutation have a lower risk of developing a neutralizing anti-FVIII antibody ("inhibitor") response (24, 25) has gained fairly wide traction in the hemophilia A community. Well-conducted earlier studies have indeed indicated that severe HA patients with an intron-22 inversion mutation had a lower inhibitor incidence compared to patients with other large structural changes in the *F8* gene such as large frameshifts or deletions, early stop codons, etc. (22, 23). However, an important point to note is that the sizes of these respective HA cohorts differ substantially: almost half of severe HA patients have an intron-22 inversion mutation, while the other large structural changes are a heterogeneous group of mutations that together comprise only ~6% of all mutations resulting in severe HA (34) (Ahmed and Pratt, J Thromb Haemost, *in press*).

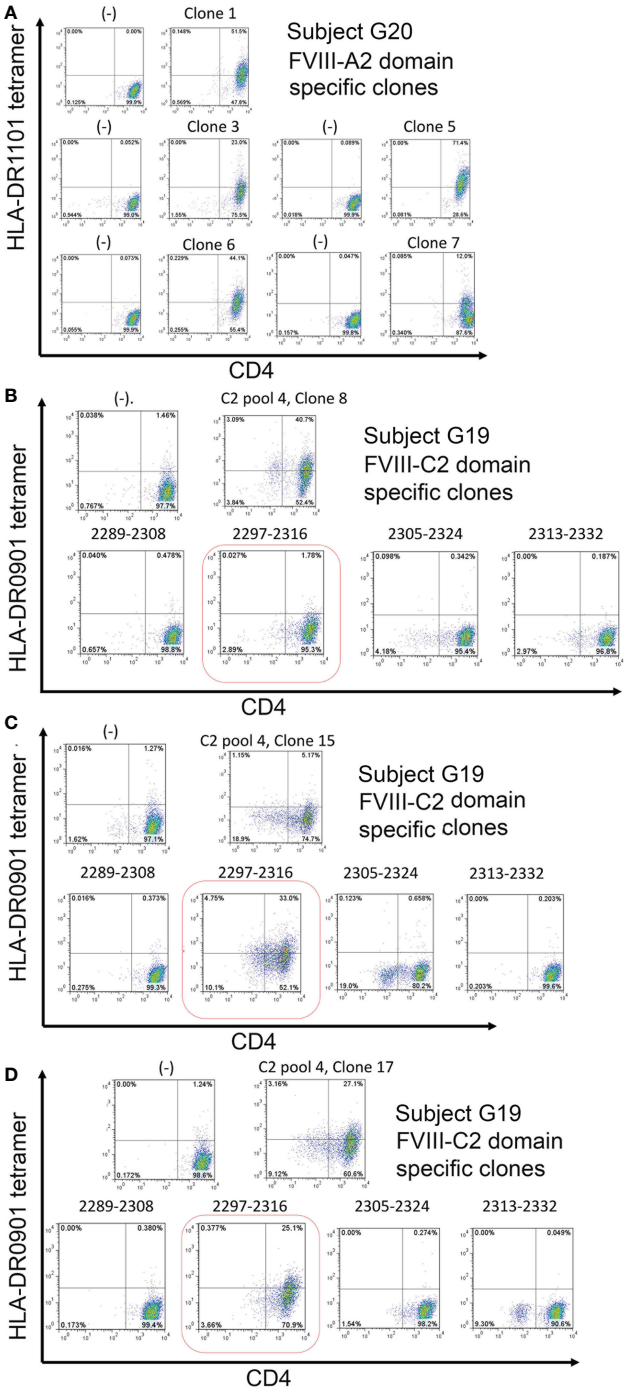

FIGURE 5
Tetramer staining identifies CD4$^+$ T-cell clones restricted to FVIII A2 and C2 domain peptides. **A.** CD4$^+$ T-cell clones restricted to one or more epitopes in the FVIII A2 domain were isolated from inhibitor subject G20 (Int22Inv, *HLA-DRB1*0301, 1101*) PBMCs by staining his CD4$^+$ T cells with DR1101 tetramers loaded with A2 peptide pool #6 (four 20-mer peptides spanning FVIII residues 565-616). The tetramer-hi cells were then single-cell sorted, expanded in culture, and the expanded clones were stained with the same tetramer, following standard protocols in our laboratory (29). All five clones showed high-avidity tetramer binding. **B, C, D.** CD4$^+$ T-cell clones recognizing pooled and individual peptides corresponding to the FVIII C2 domain were isolated from inhibitor subject G19 (Int22Inv, *HLA-DRB1*0302, 0901*) following a similar protocol. Clones recognizing C2 pool 4 peptides (spanning FVIII residues 2238-2332) were isolated. Decoding of this response using DR0901 peptides loaded with the individual peptides comprising this pool identified FVIII 2297-2316 as the immunodominant epitope. Negative controls: staining using the same HLA-DR tetramers loaded with irrelevant (tetanus) peptides did not produce tetramer-hi signals, indicating that these tetramers did not bind nonspecifically to CD4$^+$ T cells.

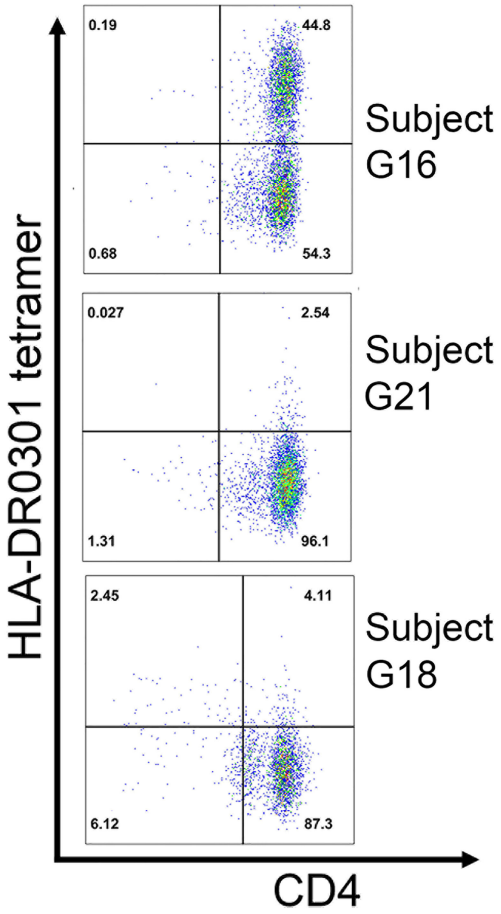

FIGURE 6
Confirmation of an HLA-DRB1*0301-restricted FVIII-A2 domain epitope by tetramer staining. T-cell clones expanded by stimulation with 15-mer peptide FVIII-A2-59 (FVIII 605-619) from three unrelated HA subjects: G16 (Int22Inv, current inhibitor), G18 (intron 1 inversion, current inhibitor), and G21 (Int22Inv, no inhibitor history). All three had an *HLA-DRB1*0301* allele, and their clones were stained with an HLA-DR0301 tetramer loaded with peptide FVIII-A2-59. The results indicate that this peptide contains an immunodominant, *HLA-DRB1*0301*-resticted T-cell epitope recognized by $CD4^+$ T cells from these subjects.

Furthermore, a significant fraction of patients with specific, rare large structural *F8* changes are related, compared to the overall low relatedness among the intron-22 inversion population. A family history of inhibitor development has been noted as a risk factor in multiple studies, indicating roles for other genetic factors influencing immune and/or inflammatory responses (35–37).

Individuals with an Int22Inv mutation express an mRNA from the inverted locus that contains *F8* exons 1-22 spliced to an additional 16 in-frame codons, followed by a stop codon (1, 2). An alternative *F8* isoform expressed in multiple human tissues, termed *F8B* mRNA, is a 2.6-kb transcript initiated from a start site within intron 22 and containing *F8* exons 23-26 (4). HA-Int22Inv patients do not circulate measurable FVIII antigenic material (often referred to as cross-reactive material, or FVIII-CRM+). Almost all of them have FVIII clotting activity (FVIII:C) levels <1% normal, i.e., by definition they have severe HA. (The rare exceptions, which generally report FVIII levels of 1-2% normal, are likely due to experimental variations or unusually high activity of other non-FVIII clotting factors). It has been hypothesized that partial FVIII proteins are expressed intracellularly from these two partial *F8* transcripts, and that they contain FVIII residues 1-2124 (encoded by *F8* exons 1-22) and FVIII residues 2125-2332 (encoded by *F8B* mRNA containing *F8* exons 23-26) (24, 38). It has been further hypothesized that this intracellular expression of the entire FVIII sequence, contained in 2 partial FVIII proteins, confers immune tolerance to these proteins, thereby explaining the apparently lower inhibitor risk associated with Int22Inv mutations (25). If such tolerance is conferred to Int22Inv patients, then their $CD4^+$ T-cell responses (providing help for anti-FVIII antibody production) to infused, therapeutic wild-type FVIII would be restricted to a neoepitope containing FVIII residues M2124 and V2125, as the mRNA encoding this short region is interrupted by the inversion mutation, precluding translation of this region (24, 25). In support of this hypothesis, Pandey et al. reported detection of intracellular FVIII-CRM^+ in both liver tissues and circulating cells from Int22Inv and nonhemophilic subjects, using antibody staining and LC-MS/MS analysis of cellular immunoprecipitates (24, 38). Our laboratory carried out similar experiments, using carefully validated antibodies to evaluate human and canine Int22-Inv liver tissues and cellular samples *via* immunofluorescence,

TABLE 4 Per-subject summary of clinical, demographic and experimental data.

Subject code in database	HA severity	HA mutation	Age range	HLA-DRB1	Current inhibitor?	Past inhibitor that resolved?	Inhibitor peak (BU/mL)*	FVIII protein response?	FVIII-C2 protein or peptide response?	FVIII-A1 and/or A2 peptide response?	Exon 22-23 junction peptide response?	Clones?
Exon 22-23 junction peptide ELISPOTS (Table 3)												
G1	severe	Int22Inv + frameshift	18+	0701, 0701	N	N	0				N	
G2	severe	Int22Inv	4-17	0901, 1101g	N	N	0				N	
G3	severe	Int22Inv	18+	0701, 1301	Y	N	49	N			N	
G4	severe	Int22Inv	18+	0302, 1501	Y	N	0.6	Y			Y	
G5	severe	Int22Inv	4-17	0701, 1501	N	N	0	N			N	
G6	severe	Int22Inv	18+	0801, 1503	Y	N	68	N			N	
G7	severe	Int22Inv	4-17	0404, 1301	N	N	0				N	
G8	severe	Int22Inv	4-17	0401, 0701	Y	N	1	N			N	
G9	severe	Int22Inv	18+	0102, 1503	Y	N	>1000	N	Y		N	
HLA-DR11, DR1 or DR15 alleles - A2-589-608 peptide ELISPOTS (Figure S1)												
G10	severe	Int22Inv	18+	1101, 1503	N	N	0	N	Y	Y		
G11	severe	unknown	4-17	1101, 1602	Y	N	47	N	Y	N		
G12	severe	Int22Inv	18+	1101, 1101	N	N	0	N	Y	N		
G13	severe	unknown	18+	1101, 1301	Y	N	32	N	N	N		
G14	severe	frameshift	4-17	0701, 1104	N	N	0	N		N		

(Continued)

10.3389/fimmu.2023.1128641

TABLE 4 Continued

Subject code in database	HA severity	HA mutation	Age range	HLA-DRB1	Current inhibitor?	Past inhibitor that resolved?	Inhibitor peak (BU/mL)*	FVIII protein response?	FVIII-C2 protein or peptide response?	FVIII-A1 and/or A2 peptide response?	Exon 22-23 junction peptide response?	Clones?
G15	severe	frameshift	4-17	0301, 1104	Y	Y	unknown	N		N		
HLA-DR3 - A1 and A2 domain peptide ELISPOTS (Figure 4)												
G16	severe	Int22Inv	18+	0301, 1201g	Y	N	31	N		N		
G17	severe	Int22Inv	18+	0301, 0804	Y	N	17	N		N		
G18	severe	Intron 1 inversion	18+	0301, 1401g	Y	N	80	N		Y		
G21	severe	Int22Inv	4-17	0301, 0301	N	N	0	Y		Y		
FVIII and FVIII-C2 protein ELISPOTS (Figure S2)												
P1	moderate	Int22Inv	18+	unknown	N	Y	15.2	Y	Y			
P2	moderate or severe	unknown	18+	unknown	unknown	unknown	unknown	Y	Y			
P3	severe	frameshift deletion	18+	unknown	Y	N	89.6	Y	Y			
P4	moderate or severe	unknown	18+	unknown	unknown	unknown	un known	Y	N			
P5	severe	Int22Inv (atypical)	18+	unknown	Y	N	716.8		Y			
P6	moderate or severe	unknown	18+	unknown	unknown	unknown	unknown		Y			
P7	severe	base substitution	18+	unknown	N	Y	51.2	Y	Y			
P8	moderate	unknown	18+	unknown	Y	N	384	N	N			
P9	moderate	unknown	18+	unknown	Y	N	4.6	Y	Y			
P10	severe	unknown	18+	unknown	N	Y	6	Y	Y			
P11	severe	Int22Inv	18+	unknown	N	Y	unknown	Y	Y			

(Continued)

10.3389/fimmu.2023.1128641

TABLE 4 Continued

Subject code in database	HA severity	HA mutation	Age range	HLA-DRB1	Current inhibitor?	Past inhibitor that resolved?	Inhibitor peak (BU/mL)*	FVIII protein response?	FVIII-C2 protein or peptide response?	FVIII-A1 and/or A2 peptide response?	Exon 22-23 junction peptide response?	Clones?
Tetramer isolation of CD4 T-cell clones (Figures 5, 6, S4, S5)												
G19	severe	Int22Inv	18+	0302, 0901	Y	N	3456					C2-specific
G20	severe	Int22Inv	4-17	0301, 1101	Y	N	0					A2-specific
G21	severe	Int22Inv	4-17	0301, 0301	N	N	0					A2-specific
G16	severe	Int22Inv	18+	0301, 1201g	Y	N	31					A2-specific
G18	severe	Intron 1 inversion	18+	0301, 1401g	Y	N	80					A2-specific
Normal control subjects (Figure S3)												
NC1	n/a	n/a	18+	unknown	n/a	n/a	n/a	N				
NC2	n/a	n/a	18+	unknown	n/a	n/a	n/a	N				
NC3	n/a	n/a	18+	unknown	n/a	n/a	n/a	N				
NC4	n/a	n/a	18+	unknown	n/a	n/a	n/a	N				
NC5	n/a	n/a	18+	unknown	n/a	n/a	n/a	N				
NC6	n/a	n/a	18+	unknown	n/a	n/a	n/a	N				

*Bethesda units (BU)/mL.

10.3389/fimmu.2023.1128641

immunohistochemistry, western blots and LC-MS/MS of immunprecipitates. We have been unable to detect intracellular expression of FVIII-CRM$^+$ proteins using these sensitive assays, leading us to suggest that antibodies used in the earlier studies were in fact binding nonspecifically to other antigens besides FVIII (39).

The most relevant data addressing the question of possible tolerance to FVIII is the actual patient outcomes. Our lab recently carried out a systematic regression analyses of data from >6,000 HA subjects enrolled in the "My Life Our Future" study in the U.S., of whom 1,075 had an Int22Inv mutation (Ahmed and Pratt, J Thromb Haemost, *in press*). A major conclusion of this study was that inhibitor risk associated with Int22Inv mutations was indistinguishable from that associated with other large structural changes in the *F8* gene. We attribute the apparent discrepancy of this result with reports from earlier case-control and meta-analysis studies (22, 23) to heterogeneity in the respective, much smaller cohorts (compared to the Int22Inv cohort) in each study that had mutations entailing large structural *F8* changes. Thus, the recently obtained statistical data from a large cohort in the U.S. indicate that individuals with an Int22Inv mutation are as likely to develop an inhibitor response as those with HA due to other major *F8* gene disruptions.

The present study directly addresses the question of whether Int22Inv patients are tolerized to FVIII, with the exception of a hypothesized neoepitope encoded by the *F8* exon 22-23 junction region. First, the binding affinities of 20-mer peptides spanning the exon 22-23 junction regions to ten recombinant HLA-DR proteins were determined using an established peptide-HLA competition binding assay (17, 29, 31). Predicted peptide-HLA-DR affinities were also obtained using a recent update of the same algorithm (MHCIIPan) used by Sauna et al. to predict the immunogenicity of this region (30). As in their study, medium-to-strong affinity binding of these peptides to multiple HLA-DR was predicted. However, the peptide binding assays revealed far fewer high- or medium-affinity interactions (Figure 2). Our experimental results showed high- or medium-affinity MHCII binding of these peptides by HLA-DR7, DR9 and DR15, but not by the other 7 HLA alleles that were tested; these 10 HLA-DR alleles were broadly representative of the U.S. population.

Although the IEDB and other prediction algorithms are extremely useful for applications such as determining prior exposure to a given pathogen or antigen, or peptide-based vaccine design, or for generating candidates for experimental tests of peptide immunogenicity, experimental validation is important before investing too many resources on the basis of predictions alone. MHC Class II and T-cell epitope prediction algorithms are continually being improved, and data such as those in the present study, characterizing both binding and non-binding of peptides to specific MHC alleles, can be utilized to train prediction algorithms and further improve their accuracy (40). Based on the present study's experimental results, we conclude that the exon 22-23 junction-encoded region, encompassing the FVIII C1 domain sequence extending 9-12 residues on either side of M2124-V2125, is unlikely to comprise an immunodominant, promiscuous T-cell epitope driving anti-FVIII immune responses in most HA-Int22Inv patients. The one subject who showed positive ELISPOT results (IFN-γ secretion in response to stimulation with exon 22-23 junction peptides), subject G4, had a current low-titer inhibitor, and this result indicated that an epitope in the exon 22-23 junction region contributed to his anti-FVIII immune response. He also had a missense *F8* mutation, H1499Y, although the relevance of this second mutation in an individual with an Int22Inv mutation is not clear, given that FVIII intact would not be expressed. The mutation H1499Y was not found in the CHAMPS hemophilia A mutation database (34) (accessed 01/24/2023, https://www.cdc.gov/ncbddd/hemophilia/champs.html), so we found no independent data regarding a potential association with inhibitor development. The remaining eight Int22Inv subjects (one also had a frameshift mutation) did not secrete IFN-γ in response to stimulation with the exon 22-23 junction peptides (Tables 3, 4).

Do individuals with an Int22Inv mutation have immune tolerance to FVIII proteins encoded by inverted *F8* exons 1-22 and/or *F8B* exons 23-36? This question was addressed by experiments to test the null hypothesis using independent, complementary methods: ELISPOT assays and HLA-DR tetramer staining. CD4$^+$ T-cell responses to rFVIII proteins and peptides were queried using PBMCs obtained from HA-Int22Inv subjects, as well as HA subjects with other *F8* mutations and healthy non-HA controls. Positive controls for these assays included stimulation with tetanus/diptheria toxin (TT) and phytohaemagluttinin (PHA), while negative controls included stimulation with the dimethylsulfoxide (DMSO) carrier solution for peptides, or incubating cells with an irrelevant peptide-loaded tetramer, or comparisons of Int22Inv cellular responses with those of healthy non-HA normal controls. The ELISPOT assays showed interferon-γ secretion in response to rFVIII and/or rFVIII-C2 proteins in almost all of the HA-Int22Inv experiments, whereas anti-FVIII responses were rare in the non-HA control samples. Further epitope mapping using pooled and individual FVIII peptides as stimulants clearly identified HA-Int22Inv immune responses to the FVIII A2 and C2 domains.

HLA Class II tetramer staining was carried out as a stringent, independent test to identify HLA-restricted CD4$^+$ T-cell responses to specific epitopes in FVIII, using PBMCS from Int22Inv subjects. An *HLA-DRB1*1101*-restricted epitope in FVIII was characterized earlier, identifying the wild-type FVIII A2 domain sequence 498-503 as a neoepitope recognized by CD4$^+$ T cells from two unrelated HA subjects with missense mutation FVIII-R593C (20). Thus, using tetramers loaded with FVIII-A2 peptides, we were able to test the hypothesis that a subject with an Int22Inv mutation and *HLA-DRB1*1101* allele would be tolerized to a confirmed *HLA-DRB1*1101*-restricted epitope that contributed to the anti-FVIII immune responses of HA subjects with a missense mutation at this site. Staining using HLA-DR1101 tetramers loaded with pooled A2 domain peptides, followed by isolation of multiple CD4$^+$ T-cell clones, indeed confirmed that Int22Inv subject G21 responded to one or more *HLA-DRB1*1101*-restricted epitopes within the FVIII A2 domain region 565-616 (Figure 5A).

Staining of CD4$^+$ T cells from a second Int22Inv subject, G19, using HLA-DR0901 tetramers loaded with pooled C2 domain peptides, produced positive staining using C2 peptide pool #4 (containing peptides spanning FVIII 2289-2332). Multiple clones were again isolated. Three of these pooled peptide responses were decoded by a second staining using tetramers loaded with the individual FVIII-C2 peptides comprising the pool. All three

decoding experiments identified FVIII-2297-2316 as an *HLA-DRB1*0901*-restricted T-cell epitope contributing to the anti-FVIII T-cell response of this subject (Figures 5B–D). Finally, FVIII-specific T-cell clones recognizing an *HLA-DRB1*0301*-restricted epitope in the FVIII A2 domain were isolated from two Int22Inv subjects and one intron 1 inversion subject with the same *HLA-DRB1* allele (Figure 6). One of the Int22Inv subjects had a current inhibitor, one had no inhibitor history, and the intron 1 inversion subject had a current inhibitor. Two of these subjects also responded to FVIII A2 domain epitopes in ELISPOT assays (Figure 4). To summarize, $CD4^+$ T-cell clones recognizing epitopes in the FVIII A2 or C2 domain were isolated from four unrelated Int22Inv subjects.

Approximately 20 years ago, the Conti-Fine group characterized $CD4^+$ T-cell responses to FVIII in HA and non HA subjects, primarily through T-cell proliferation and ELISPOT assays employing FVIII and pools of synthetic FVIII peptides spanning several FVIII domains (10, 12–15, 41). The present study builds on their earlier work, focusing on specific epitopes recognized by HA subjects with an Int22Inv mutation. We also tested the hypothesis that HA-Int22Inv patients have been tolerized to FVIII sequences encoded by mRNAs containing *F8* exons 1-22 and/or 23-26. Results of this study provide evidence in support of the null hypothesis: rather than being tolerized, $CD4^+$ T-effector cells from multiple Int22Inv subjects readily responded to multiple epitopes in FVIII. Together with recent statisitical/epidemiological evidence (Ahmed and Pratt, J Thromb Haemostas, *in press*) and our failure to detect FVIII-CRM^+ proteins in liver tissues or circulating cells from Int22Inv subjects (39), the present study indicates that Int22Inv patients should be monitored just as closely as other severe HA patients for development of an inhibitor, especially during initial FVIII infusions.

Data availability statement

The original contributions presented in the study are included in the article/Supplementary Material. Further inquiries can be directed to the corresponding author.

Ethics statement

The studies involving human participants were reviewed and approved by Uniformed Services University IRB #1. Written informed consent to participate in this study was provided by the participants or by their legal guardian/next of kin.

Author contributions

KP: Conceived the project and designed experiments, analyzed data, supervised the project and wrote the paper. DG, PV and AK: Performed experiments, analyzed data and edited the paper. MR: Enrolled subjects, consulted, and edited the paper. All authors contributed to the article and approved the submitted version.

Funding

Funded by R01 HL 130448 (KP), a Grifols investigator-initiated grant "Mechanisms of Immune Tolerance to Factor VIII" (KP), NHLBI U34 HL11674 (MR), 1RC2 HL 101851 (KP), and intramural funds to KP (Uniformed Services University). Grifols had no role in the study design, sample or data collection, sample analysis, interpretation, or writing of the manuscript.

Acknowledgments

We thank Dr. Eddie James (Benaroya Research Institute, Seattle WA) for help with HLA-DRB1 reagents and tests and Dr. Maochang Liu (Benaroya Research Institute) for carrying out pilot experiments. We thank Dr. Kateryna Lund (Uniformed Services University) for analysis of tetramer staining data. We thank all subjects for their generous blood donations and all clinical staff who participated in this study.

Conflict of interest

Author KP is an inventor on patents related to FVIII immunogenicity.

The remaining authors declare that the research was conducted in the absence of any commercial or financial relationships that could be construed as a potential conflict of interest.

Publisher's note

Author disclaimer

The opinions or assertions contained herein are the private ones of the author and are not to be construed as official or reflecting the views of the Department of Defense or the Uniformed Services University of the Health Sciences.

Supplementary material

The Supplementary Material for this article can be found online at: https://www.frontiersin.org/articles/10.3389/fimmu.2023.1128641/full#supplementary-material

References

1. Lakich D, Kazazian HHJr., Antonarakis SE, Gitschier J. Inversions disrupting the factor VIII gene are a common cause of severe haemophilia a. *Nat Genet* (1993) 5:236–41. doi: 10.1038/ng1193-236

2. Naylor J, Brinke A, Hassock S, Green PM, Giannelli F. Characteristic mRNA abnormality found in half the patients with severe haemophilia a is due to large DNA inversions. *Hum Mol Genet* (1993) 2:1773–8. doi: 10.1093/hmg/2.11.1773

3. Gitschier J, Wood WI, Goralka TM, Wion KL, Chen EY, Eaton DH, et al. Characterization of the human factor VIII gene. *Nature* (1984) 312:326–30. doi: 10.1038/312326a0

4. Levinson B, Kenwrick S, Gamel P, Fisher K, Gitschier J. Evidence for a third transcript from the human factor VIII gene. *Genomics* (1992) 14:585–9. doi: 10.1016/s0888-7543(05)80155-7

5. Gouw SC, Ter Avest PC, Van Helden PM, Voorberg J, Van Den Berg HM. Discordant antibody response in monozygotic twins with severe haemophilia a caused by intensive treatment. *Haemophilia* (2009) 15:712–7. doi: 10.1111/j.1365-2516.2009.01998.x

6. Gouw SC, Van Den Berg HM, Fischer K, Auerswald G, Carcao M, Chalmers E, et al. Intensity of factor VIII treatment and inhibitor development in children with severe hemophilia a: The RODIN study. *Blood* (2013) 121:4046–55. doi: 10.1182/blood-2012-09-457036

7. Johnsen JM, Fletcher SM, Dove A, Mccracken H, Martin BK, Kircher M, et al. Results of genetic analysis of 11 314 participants enrolled in the my life, our future hemophilia genotyping initiative in the united states. *J Thromb Haemost* (2022) 20:2022–34. doi: 10.1111/jth.15805

8. Reipert BM, Gangadharan B, Hofbauer CJ, Berg V, Schweiger H, Bowen J, et al. The prospective hemophilia inhibitor PUP study reveals distinct antibody signatures prior to FVIII inhibitor development. *Blood Adv* (2020) 4:5785–96. doi: 10.1182/bloodadvances.2020002731

9. Bray GL, Kroner BL, Arkin S, Aledort LW, Hilgartner MW, Eyster ME, et al. Loss of high-responder inhibitors in patients with severe hemophilia a and human immunodeficiency virus type 1 infection: A report from the multi-center hemophilia cohort study. *Am J Hematol* (1993) 42:375–9. doi: 10.1002/ajh.2830420408

10. Reding MT, Wu H, Krampf M, Okita DK, Diethelm-Okita BM, Key NS, et al. CD4+ T cell response to factor VIII in hemophilia a, acquired hemophilia, and healthy subjects. *Thromb Haemost* (1999) 82:509–15. doi: 10.1055/s-0037-1615873

11. Reding MT, Lei S, Lei H, Green D, Gill J, Conti-Fine BM. Distribution of Th1- and Th2-induced anti-factor VIII IgG subclasses in congenital and acquired hemophilia patients. *Thromb Haemost* (2002) 88:568–75.

12. Reding MT, Okita DK, Diethelm-Okita BM, Anderson TA, Conti-Fine BM. Human CD4+ T-cell epitope repertoire on the C2 domain of coagulation factor VIII. *J Thromb Haemost* (2003) 1:1777–84. doi: 10.1046/j.1538-7836.2003.00251.x

13. Hu GL, Okita DK, Conti-Fine BM. T Cell recognition of the A2 domain of coagulation factor VIII in hemophilia patients and healthy subjects. *J Thromb Haemost* (2004) 2:1908–17. doi: 10.1111/j.1538-7836.2004.00918.x

14. Reding MT, Okita DK, Diethelm-Okita BM, Anderson TA, Conti-Fine BM. Epitope repertoire of human CD4(+) T cells on the A3 domain of coagulation factor VIII. *J Thromb Haemost* (2004) 2:1385–94. doi: 10.1111/j.1538-7836.2004.00850.x

15. Hu G, Guo D, Key NS, Conti-Fine BM. Cytokine production by CD4+ T cells specific for coagulation factor VIII in healthy subjects and haemophilia a patients. *Thromb Haemost* (2007) 97:788–94.

16. Jacquemin M, Vantomme V, Buhot C, Lavend'homme R, Burny W, Demotte N, et al. CD4+ T-cell clones specific for wild-type factor VIII: A molecular mechanism responsible for a higher incidence of inhibitor formation in mild/moderate hemophilia a. *Blood* (2003) 101:1351–8. doi: 10.1182/blood-2002-05-1369

17. James EA, Kwok WW, Ettinger RA, Thompson AR, Pratt KP. T-Cell responses over time in a mild hemophilia a inhibitor subject: Epitope identification and transient immunogenicity of the corresponding self-peptide. *J Thromb Haemost* (2007) 5:2399–407. doi: 10.1111/j.1538-7836.2007.02762.x

18. Ettinger RA, James EA, Kwok WW, Thompson AR, Pratt KP. Lineages of human T-cell clones, including T helper 17/T helper 1 cells, isolated at different stages of anti-factor VIII immune responses. *Blood* (2009) 114:1423–8. doi: 10.1182/blood-2009-01-200725

19. Ettinger RA, James EA, Kwok WW, Thompson AR, Pratt KP. HLA-DR-restricted T-cell responses to factor VIII epitopes in a mild haemophilia a family with missense substitution A2201P. *Haemophilia* (2010) 16:44–55. doi: 10.1111/j.1365-2516.2008.01905.x

20. James EA, Van Haren SD, Ettinger RA, Fijnvandraat K, Liberman JA, Kwok WW, et al. T-Cell responses in two unrelated hemophilia a inhibitor subjects include an epitope at the factor VIII R593C missense site. *J Thromb Haemost* (2011) 9:689–99. doi: 10.1111/j.1538-7836.2011.04202.x

21. Ettinger RA, Paz P, James EA, Gunasekera D, Aswad F, Thompson AR, et al. T Cells from hemophilia a subjects recognize the same HLA-restricted FVIII epitope with a narrow TCR repertoire. *Blood* (2016) 128:2043–54. doi: 10.1182/blood-2015-11-682468

22. Ragni MV, Ojeifo O, Feng J, Yan J, Hill KA, Sommer SS, et al. Risk factors for inhibitor formation in haemophilia: A prevalent case-control study. *Haemophilia* (2009) 15:1074–82. doi: 10.1111/j.1365-2516.2009.02058.x

23. Gouw SC, Van Den Berg HM, Oldenburg J, Astermark J, De Groot PG, Margaglione M, et al. F8 gene mutation type and inhibitor development in patients with severe hemophilia a: Systematic review and meta-analysis. *Blood* (2012) 119:2922–34. doi: 10.1182/blood-2011-09-379453

24. Pandey GS, Yanover C, Miller-Jenkins LM, Garfield S, Cole SA, Curran JE, et al. Endogenous factor VIII synthesis from the intron 22-inverted F8 locus may modulate the immunogenicity of replacement therapy for hemophilia a. *Nat Med* (2013) 19:1318–24. doi: 10.1038/nm.3270

25. Sauna ZE, Lozier JN, Kasper CK, Yanover C, Nichols T, Howard TE. The intron-22-inverted F8 locus permits factor VIII synthesis: Explanation for low inhibitor risk and a role for pharmacogenomics. *Blood* (2015) 125:223–8. doi: 10.1182/blood-2013-12-530113

26. Miller CH, Boylan B, Shapiro AD, Lentz SR, Wicklund BMHemophilia Inhibitor Research Study, I. Limit of detection and threshold for positivity of the centers for disease control and prevention assay for factor VIII inhibitors. *J Thromb Haemost* (2017) 15:1971–6. doi: 10.1111/jth.13795

27. Potgieter JJ, Damgaard M, Hillarp A. One-stage vs. chromogenic assays in haemophilia a. *Eur J Haematol* (2015) 94(Suppl 77):38–44. doi: 10.1111/ejh.12500

28. Lin JC, Ettinger RA, Schuman JT, Zhang AH, Wamiq-Adhami M, Nguyen PC, et al. Six amino acid residues in a 1200 A2 interface mediate binding of factor VIII to an IgG4kappa inhibitory antibody. *PloS One* (2015) 10:e0116577. doi: 10.1371/journal.pone.0116577

29. Gunasekera D, Ettinger RA, Nakaya Fletcher S, James EA, Liu M, Barrett JC, et al. Factor VIII gene variants and inhibitor risk in African American hemophilia a patients. *Blood* (2015) 126:895–904. doi: 10.1182/blood-2014-09-599365

30. Reynisson B, Alvarez B, Paul S, Peters B, Nielsen M. NetMHCpan-4.1 and NetMHCIIpan-4.0: improved predictions of MHC antigen presentation by concurrent motif deconvolution and integration of MS MHC eluted ligand data. *Nucleic Acids Res* (2020) 48:W449–W54. doi: 10.1093/nar/gkaa379

31. Ettinger RA, Liberman JA, Gunasekera D, Puranik K, James EA, Thompson AR, et al. FVIII proteins with a modified immunodominant T-cell epitope exhibit reduced immunogenicity and normal FVIII activity. *Blood Adv* (2018) 2:309–22. doi: 10.1182/bloodadvances.2017013482

32. Wang P, Sidney J, Dow C, Mothe B, Sette A, Peters B. A systematic assessment of MHC class II peptide binding predictions and evaluation of a consensus approach. *PloS Comput Biol* (2008) 4:e1000048. doi: 10.1371/journal.pcbi.1000048

33. Wang P, Sidney J, Kim Y, Sette A, Lund O, Nielsen M, et al. Peptide binding predictions for HLA DR, DP and DQ molecules. *BMC Bioinf* (2010) 11:568. doi: 10.1186/1471-2105-11-568

34. Payne AB, Miller CH, Kelly FM, Michael Soucie J, Craig Hooper W. The CDC hemophilia a mutation project (CHAMP) mutation list: A new online resource. *Hum Mutat* (2013) 34:E2382–91. doi: 10.1002/humu.22247

35. Astermark J, Berntorp E, White GC, Kroner BLGroup, MS. The malmo international brother study (MIBS): Further support for genetic predisposition to inhibitor development in hemophilia patients. *Haemophilia* (2001) 7:267–72. doi: 10.1046/j.1365-2516.2001.00510.x

36. Hay CR. The epidemiology of factor VIII inhibitors. *Haemophilia* (2006) 12 (Suppl 6):23–8; discussion 8-9. doi: 10.1111/j.1365-2516.2006.01362.x

37. Gouw SC, van den Berg HM. The multifactorial etiology of inhibitor development in hemophilia: Genetics and environment. *Semin Thromb Hemost* (2009) 35:723–34. doi: 10.1055/s-0029-1245105

38. Pandey GS, Tseng SC, Howard TE, Sauna ZE. Detection of intracellular factor VIII protein in peripheral blood mononuclear cells by flow cytometry. *BioMed Res Int* (2013) 2013:793502. doi: 10.1155/2013/793502

39. Gunasekera D, Vir P, Karim AF, Ragni MV, Merricks EP, Nichols TC, et al. FVIII protein is not detectable in human PBMCs or livers from dogs with an intron-22 inversion mutation: Implications for FVIII immunogenicity and tolerance. *Blood* (2019) 134. doi: 10.1182/blood-2019-124880

40. Lundegaard C, Lund O, Nielsen M. Predictions versus high-throughput experiments in T-cell epitope discovery: Competition or synergy? *Expert Rev Vaccines* (2012) 11:43–54. doi: 10.1586/erv.11.160

41. Hu GL, Okita DK, Diethelm-Okita BM, Conti-Fine BM. Recognition of coagulation factor VIII by CD4+ T cells of healthy humans. *J Thromb Haemost* (2003) 1:2159–66. doi: 10.1046/j.1538-7836.2003.00366.x

frontiers | Frontiers in Immunology

TYPE Review
PUBLISHED 04 April 2023
DOI 10.3389/fimmu.2023.1154552

OPEN ACCESS

EDITED BY
Joanna Davies,
San Diego Biomedical Research Institute, United States

REVIEWED BY
Andreas B. Wild,
Universtätsklinikum Erlangen, Germany
Jianan Zhao,
Shanghai University of Traditional Chinese Medicine, China

*CORRESPONDENCE
Roland Michael Tisch
rmtisch@med.unc.edu

SPECIALTY SECTION
This article was submitted to Immunological Tolerance and Regulation, a section of the journal Frontiers in Immunology

RECEIVED 30 January 2023
ACCEPTED 17 March 2023
PUBLISHED 04 April 2023

CITATION
Ke Q, Greenawalt AN, Manukonda V, Ji X and Tisch RM (2023) The regulation of self-tolerance and the role of inflammasome molecules. *Front. Immunol.* 14:1154552. doi: 10.3389/fimmu.2023.1154552

The regulation of self-tolerance and the role of inflammasome molecules

Qi Ke[1], Ashley Nicole Greenawalt[1], Veera Manukonda[1], Xingqi Ji[1] and Roland Michael Tisch[1,2]*

[1]Department of Microbiology and Immunology, University of North Carolina at Chapel Hill, Chapel Hill, NC, United States, [2]Lineberger Comprehensive Cancer Center, University of North Carolina at Chapel Hill, Chapel Hill, NC, United States

Inflammasome molecules make up a family of receptors that typically function to initiate a proinflammatory response upon infection by microbial pathogens. Dysregulation of inflammasome activity has been linked to unwanted chronic inflammation, which has also been implicated in certain autoimmune diseases such as multiple sclerosis, rheumatoid arthritis, type 1 diabetes, systemic lupus erythematosus, and related animal models. Classical inflammasome activation-dependent events have intrinsic and extrinsic effects on both innate and adaptive immune effectors, as well as resident cells in the target tissue, which all can contribute to an autoimmune response. Recently, inflammasome molecules have also been found to regulate the differentiation and function of immune effector cells independent of classical inflammasome-activated inflammation. These alternative functions for inflammasome molecules shape the nature of the adaptive immune response, that in turn can either promote or suppress the progression of autoimmunity. In this review we will summarize the roles of inflammasome molecules in regulating self-tolerance and the development of autoimmunity.

KEYWORDS

autoimmunity, self-tolerance, inflammasomes, immunoregulation, inflammation

Introduction

A functioning immune system is characterized by the capacity to distinguish between self-antigens versus microbial pathogens and foreign molecules. Several mechanisms are in place regulating both innate and adaptive immunity to establish persistent self-tolerance. These mechanisms maintain self-tolerance by limiting the activation and maturation of innate effectors such as monocytes, macrophages and dendritic cells (DC), while regulating self-specific T and B cells *via* intrinsic and extrinsic events. Immunoregulation is a dominant mechanism by which self-tolerance is established and maintained. Multiple subsets of self-specific T cells, including forkhead box P3 (FoxP3)-expressing regulatory $CD4^+$ T cells ($Foxp3^+$Treg), as well as regulatory B cells, mediate immunoregulation *via* 1) secretion of anti-inflammatory cytokines (e.g. TGF β1, IL-10) and modulatory factors, and

2) cognate interactions with T and B cells and/or DC and macrophages serving as antigen-presenting cells (APC) by engagement of various ligand-receptor molecules. Subsets of DC and macrophages also contribute to immunoregulation through secretion of cytokines and factors. Breakdown of self-tolerance leads to autoimmunity, typically characterized by chronic inflammation driven by autoreactive T and B cells, autoantibodies, and/or activated macrophages, DC and other innate effectors (1). Autoimmune diseases are characterized as: 1) organ-specific autoimmunity, such as multiple sclerosis (MS), rheumatoid arthritis (RA) and type 1 diabetes (T1D), or 2) systemic autoimmune diseases, such as systemic lupus erythematosus (SLE) (2). Events leading to the failure of self-tolerance are complex and influenced in a polygenic manner, while involving a host of ill-defined environmental factors including microbial infections, toxins, ultraviolet (UV) irradiation, diet, and dysbiosis of the gut microbiota.

The immune system has also evolved to detect and rapidly respond to invading pathogens *via* innate cell-driven events. This early inflammation leads to subsequent expansion and differentiation of effector T and B cells, typically resulting in clearance of the pathogen, and establishment of long-lasting immune protection. Recognition of an invading microbial pathogen is mediated by surface and cytoplasmic pattern recognition receptors (PRRs) which recognize: 1) conserved pathogen-associated molecular patterns (PAMPs), and 2) endogenous-derived danger-associated molecular patterns (DAMPs) induced by tissue damage and cellular activities mediated by microbial virulence factors (3).

Inflammasomes are oligomeric complexes that play an important role in initiating inflammation in response to PAMPs and DAMPs (4). Appropriately regulated activation of inflammasomes protects against microbial infection. However, aberrant inflammasome activity has been associated with severe inflammation-driven pathologies (5–7), as well as autoinflammatory and autoimmune diseases (8). Notably, inflammasome receptor molecules regulate the properties of different immune cell effectors as well as non-immune cell types that is independent of classical activation and inflammation-inducing events (9). This alternative function of inflammasome molecules has also been directly linked to autoimmunity and sterile inflammation. In this review, we will discuss how inflammasomes contribute to autoimmunity: 1) by inflammation driven by classical inflammasome activation, and 2) *via* alternative functions inflammasome molecules display.

Inflammasome-mediated inflammation- an overview

Inflammasome-driven inflammation in the context of innate immunity generally entails the production of proinflammatory cytokines such as IL-1β and IL-18, as well as induction of programmed cell death. The typical inflammasome complex consists of three components; namely 1) a sensor molecule such as a nucleotide oligomerization domain-like receptor (NLR), Absent in melanoma 2-like receptors (ALR) or pyrin, 2) the adaptor molecule apoptosis-associated speck-like protein (ASC) that contains a caspase activation and recruitment domain (CARD), and 3) pro-caspase-1 (Figure 1) (4). The assembled inflammasome provides a platform for cleavage of pro-caspase-1 (4). Once activated *via* an autolytic processing event, caspase-1 mediates maturation of pro-IL-1β and pro-IL-18 precursors, as well as initiating pyroptosis (4).

Pyroptosis, a lytic form of programmed cell death, is induced through caspase-1-mediated cleavage of gasdermin D (GSDMD), which removes the autoinhibitory C-terminus portion of the protein (10). Cleaved GSDMD also forms pores in the cell membrane, which facilitate the secretion of mature IL-1β and IL-18 (11). Cleavage of GSDMD and induction of pyroptosis is also achieved by a nonconical pathway in which murine caspase-11 or human caspase-4/5 are activated by cytosolic lipopolysaccharide (LPS), a gram-negative bacteria endotoxin (11, 12). In addition to pyroptosis, certain inflammasome molecules such as NLR family pyrin domain containing 3 (NLRP3) and absent in melanoma 2 (AIM2), have been associated with PANoptosis-driven cell death in response to microbial infection and changes in cellular homeostasis (13). PANoptosis is regulated by the PANoptosome, which is a multimeric complex consisting in part of effector molecules involved in pyroptotic (caspase 1), apoptotic (caspase 8), and necroptotic (receptor-interacting protein kinase 1 (RIPK1), receptor-interacting protein kinase 3 (RIPK3)) cell death pathways (14). The composition of the PANoptosome varies with the nature of the stimulatory response, and complexes consisting of the ASC adaptor and NLRP3 or AIM2 sensor molecules have been identified (15).

Inflammasome activation is achieved in response to a broad range of stimuli derived from microbial infection, tissue damage, and/or dysregulation of metabolic events (Figure 1). The process of inflammasome activation typically entails two sets of signaling events that prime (signal 1), and activate (signal 2) the inflammasome (11). This multiple-step pathway ensures robust regulation of inflammasome activity. Signal one, induced by PRR (e.g. toll-like receptors (TLR)) primes inflammasome assembly *via* activation of NF-κB, upregulation of pro-IL-1β and pro-IL-18 expression, and induction of post-translational events that favor the formation of an inflammasome complex (11, 12). Signal two is specific for a given sensor molecule and induces inflammasome activation (12). Binding of an agonist to the leucine-rich repeat containing receptor (LRR) portion of the sensor protein leads to oligomerization *via* homotypic pyrin (PYD) interactions with the ASC adaptor molecule. ASC is important for linking the sensory protein with caspase-1 *via* CARD interactions (11, 12). Events driving caspase-1 activation, IL-1β and IL-18 maturation, and induction of pyroptosis and/or PANoptosis then follow (11, 12). To date, the role of inflammasomes in autoimmunity have largely focused on NLRP3 and AIM2, but other inflammasome molecules such as NLRP1, and NLR family CARD domain-containing protein 4 (NLRC4) have also been implicated in autoimmunity (16, 17). The respective inflammasomes are defined by the sensor protein.

NLRP3 has been the most extensively studied inflammasome, in general and in autoimmunity (18). NLRP3 agonists are structurally

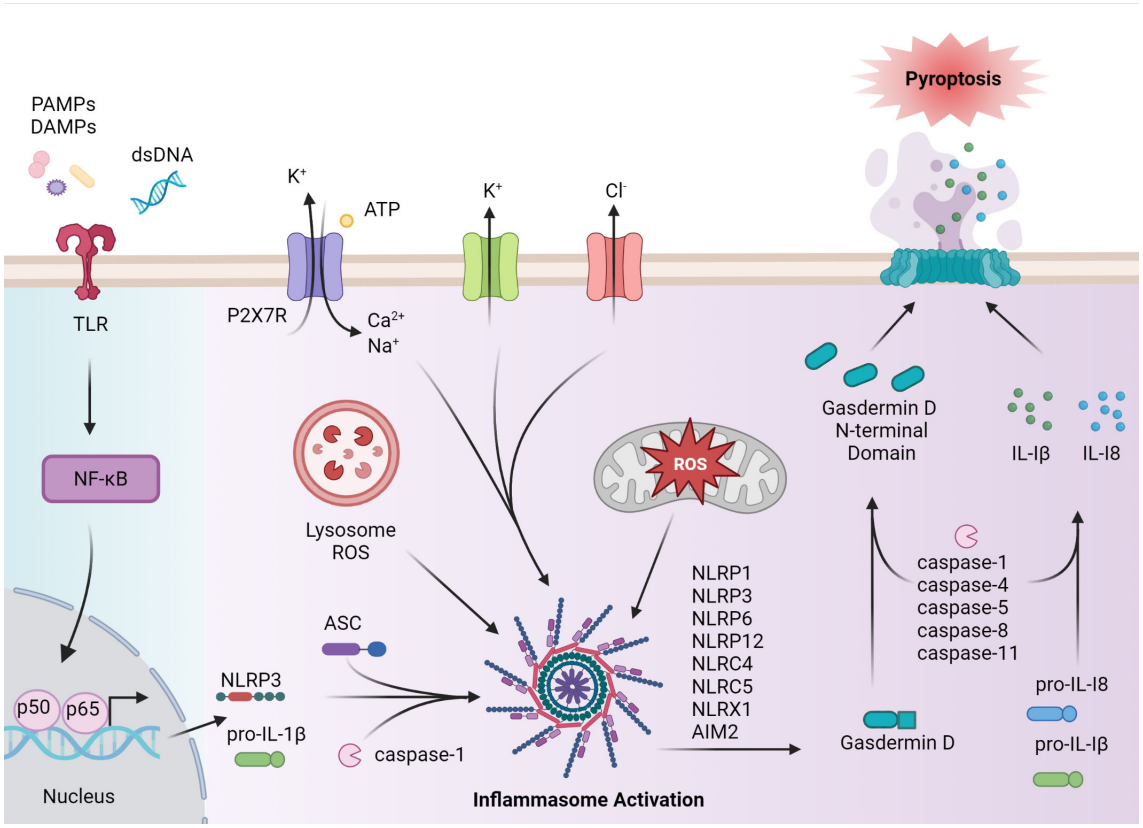

FIGURE 1
Inflammasome assembly and activation. Canonical activation of the inflammasome pathway begins with a primary signal, such as PAMPs, endogenous-derived DAMPs, or dsDNA, that are recognized by pattern recognition receptors (PRRs), such as toll-like receptors (TLRs). PRR activation induces NF-κB and subsequent expression of NLRP, pro-IL-1β and pro-IL-18, and post-translational events. Formation of the inflammasome complex occurs when the sensor protein, such as NLRP3, binds to ASC, driving caspase activation and inflammasome assembly. Caspase enzymes cleave pro-IL-1β and pro-IL-18 as well as the C terminus from gasdermin D, allowing the gasdermin D N-terminal domain to form pores necessary for pyroptosis. IL-1β and IL-18, as well as cellular contents are released to establish a proinflammatory response. In autoimmune disease, inflammasome activation can occur *via* activation in a noncanonical matter including agonist-induced ion flux and lysosomal and mitochondrial reactive oxygen species (ROS). The figure was prepared using Biorender software licensed to the UNC Lineberger Comprehensive Cancer Center.

and chemically diverse: such agonists include 1) PAMPs expressed by bacteria, virus, and fungi, and 2) DAMPs including cholesterol, extracellular ATP, microbial pore-forming toxins, and particulate matter such as uric acid crystals (19). Consequently, it is believed that these agonists are indirectly sensed by NLRP3. Here, agonist-induced K^+ and Cl^- effluxes, Ca^{2+} fluxes, lysosomal damage, and mitochondrial damage and/or dysfunction coupled with the release of reactive oxygen species (ROS) are directly sensed by NLRP3 (20). For instance, noncanonical-induced activation of GSDMD results in K^+ efflux, which activates NLRP3 and leads to caspase-1-mediated IL-1β and IL-18 production *via* the classical pathway (21–23). Gain of function variants in the *NLRP3* gene resulting in aberrant NLRP3 inflammasome activation cause a family of diseases referred to cryopyrin-associated periodic syndromes (CAPS), which are marked by reoccurring systemic inflammation (20). NLRP3 activation has also been linked to diseases of the central nervous system (CNS) such as Alzheimer's Disease (AD) (24, 25). In AD, the accumulation and subsequent uptake of amyloid-β by microglia residing in the brain results in lysosomal destabilization and NLRP3 activation (24). Production of IL-1β also has neurotoxic effects on microglia and astrocytes (25).

The process of NLRP1 activation is distinct from other inflammasomes (26). Here, motif-dependent ubiquitination followed by degradation of the N-terminal subunit by proteasome are required for activation of NLRP1 (27, 28). Various bacterial toxins and viral proteases have been reported to activate NLRP1 in mice and humans (29–33). However, since mice encode several NLRP1 orthologues with sequences that differ from the single human encoded *NLRP1* gene, specific PAMPs and DAMPs triggering NLRP1 activation are variable and not fully defined among the species (34–37). The NLRC4 inflammasome is also distinct compared to other inflammasomes, in which the sensor protein functions as an agonist receptor. Instead, the NLRC4 protein associates with NLR family apoptosis inhibitory proteins (NAIPs) that act as cytosolic innate immune receptors, and which bind bacterial flagellin and type III secretion system components (T3SS) (38, 39). Gain-of-function variants in *NLRC4* lead to periodic fever syndromes marked by increased systemic IL-18 (40).

AIM2 is responsive to cytosolic double-stranded DNA (dsDNA) from bacteria and DNA viruses. Notably, AIM2 binds both endogenous and microbe-derived dsDNA independent of nucleic acid sequence (41). Expression of AIM2 is upregulated by

type I interferon (IFN), and the AIM2 inflammasome is key in host defense against bacterial and viral pathogens such as *Francisella tularensis* and *Listeria monocytogenes*, and vaccinia virus and cytomegalovirus, respectively (42). In addition, the AIM2 inflammasome promotes caspase-1-driven death of intestinal epithelial cells and hematopoietic bone marrow cells upon recognition of dsDNA breaks due to ionizing radiation or chemotherapeutic drugs (43).

The roles of IL-1β and IL-18 in inflammation

Inflammasome generated IL-1β and IL-18 enhances both innate and adaptive immunity against microbial pathogens. However, dysregulated production of these two cytokines by inflammasomes is also linked to chronic autoimmune diseases.

IL-1β is produced largely by monocytes, macrophages, and DC (44). Local release of IL-1β amplifies inflammation by inducing increased expression of 1) adhesion molecules and chemokines for recruitment of immune effectors, as well as 2) proinflammatory mediators such as cyclooxygenase type 2 (COX-2) and prostaglandin-E2 (PGE2) (44–46). IL-1β production can also lead to systemic inflammation *via* induction of the acute phase response, vasodilatation, angiogenesis, and leukocyte activation (44, 45).

T cell responses are also regulated both indirectly and directly by IL-1β. For instance, IL-1β enhances the stimulatory capacity of DC by driving maturation and upregulation of co-stimulatory molecules needed for efficient T cell activation and expansion (47). Increased IL-12 secretion by IL-1β stimulated DC favors differentiation of antigen-stimulated T cells towards a type 1 phenotype, marked by IFNγ production by $CD4^+$ Th1 and $CD8^+$ Tc1 cells (48). On the other hand, IL-1β has direct effects on $CD4^+$ and $CD8^+$ T cells, influencing expansion and subset differentiation depending on the extracellular *milieu* (49). In mice, IL-1β synergizes with IL-6, IL-21 and IL-23 to induce the differentiation of $CD4^+$ T cells into IL-17-secreting Th17 cells (49). In humans, IL-1β has a more potent role in driving Th17 differentiation. Both Th1 and Th17 cells play key roles in several autoimmune diseases. Furthermore, IL-1β can suppress the function and/or reduce the stability of $Foxp3^+$Treg (50, 51). Dysregulation of the $Foxp3^+$Treg pool leading to skewed differentiation and pathogenic function of autoreactive effector T cells (Teff) is associated with a number of autoimmune diseases (52–56). $CD8^+$ T cell expansion and differentiation are also regulated by IL-1β (57).

IL-1β has regulatory effects on the B cell compartment by enhancing B cell proliferation and antibody production (45). In addition, IL-1β increases proliferation and secretion of IL-4 and IL-21 by $CD4^+$ T follicular helper cells (Tfh) (58). Tfh cells play a critical role in regulating antibody production by B cells and have also been implicated in the production of autoantibodies during autoimmunity (59).

IL-18 is expressed by a variety of cells such as Kupffer cells, macrophages, DC, and non-hematopoietic cells that include intestinal epithelial cells, keratinocytes and endothelial cells (60). Locally, IL-18 stimulates myeloid and endothelial cells to upregulate nitric oxide (NO) synthesis, and expression of cell adhesion molecules and chemokines to recruit and activate additional immune effectors at the site (60). In addition, IL-18 has potent regulatory effects on T cells and natural killer (NK) cells (60). IL-18 along with IL-12 drives the differentiation of Th1 cells and induces IFNγ production by $CD8^+$ T cells and NK cells (60, 61). Furthermore, IL-18 stimulation upregulates 1) perforin- and Fas ligand (FasL)-dependent cytotoxicity in $CD8^+$ T cells and NK cells, and 2) IL-17 secretion by γδ T cells (62). Not only is IL-18 linked to autoimmune diseases such as T1D and SLE, IL-18 has also been shown to play a key role in the maintenance of the intestinal epithelial barrier and regulation gut microbiota composition (63, 64). Dysbiosis of gut microbiota has been suggested as a risk factor for the development of autoimmunity (65, 66).

Classical inflammasome activation-dependent events in autoimmunity

In view of highly potent proinflammatory effects, it is not surprising that classical inflammasome activation is linked to a host of autoimmune diseases. Inflammasome activation is detected in innate and adaptive immune effectors thereby having indirect and direct effects that shape and maintain the proinflammatory response either locally and/or systemically in autoimmunity. In addition, inflammasome activation in non-immune cell types that makeup a given organ can initiate and/or exacerbate an autoimmune response. Finally, evidence indicates that inflammasome activation can have a protective role and contribute to maintenance of self-tolerance. In the following, we will describe the different roles classical inflammasome activation has in common tissue-specific and systemic autoimmune diseases (Table 1).

Multiple sclerosis and inflammasome-mediated neuroinflammation

MS is a demyelinating autoimmune disease marked by chronic inflammation of the CNS, leading to variable neurological symptoms and heterogenous clinical outcomes (143, 144). MS susceptibility and disease progression are influenced by both genetic and environmental factors (145). Although ill-defined, the autoimmune response in MS is believed to be initiated in the periphery, involving stimulation of $CD4^+$ and $CD8^+$ T cells specific for myelin proteins (146, 147). Differentiation of the encephalitogenic $CD4^+$ T cell pool is skewed towards Th1 and Th17 subsets. This pool coupled with $CD8^+$ T cells and B cells migrate across the CNS microvascular endothelium and into the brain and spinal cord (148, 149). The CNS infiltrate includes peripheral monocytes/macrophages and DC that further amplify the autoimmune response. Upon activation, microglia, which are tissue-resident macrophages as well as resident astrocytes also contribute to inflammation (144, 150) by production of: 1)

TABLE 1 Intrinsic-effects of classical inflammasome-mediated inflammation in autoimmunity.

Autoimmune Disease	Associated environmental trigger events	Genetic variants involved in inflammasome pathways	Inflammasome intrinsic effects on innate immune cells	Inflammasome intrinsic effects on adaptive immune cells	Inflammasome intrinsic effects on non-immune/ tissue resident cells
MS	Epstein-Barr virus (EBV), human herpes virus 6 (HHV-6), human endogenous retrovirus (HERV), cytomegalovirus (CMV), varicella zoster virus (VZV) (67, 68) *Helicobacter pylori, Chlamydia pneumoniae, Staphylococcus aureus* (69) Mouse hepatitis virus (MHV) (70), Semliki Forest virus (SFV) (71)	*NLRP1*: p.G587S (72), Gly587Ser (73), p.Ile601Phe, p.Ser1387Ile (74) *NLRP3*: Q705K (75), p.Leu832Ile (74) *NLRC4*: p.Arg310Ter, p.Glu600Ter (74) *NLRP9*: rs10423927 (76)	Microglia: ↑NLRP3, NLRC4 (77), ↑NLRP9 (76), ↓NLRX1 (78, 79), ↓NLRP12 (80, 81) PBMC: ↑Caspase-1 (82) DC/macrophage: ↑NLRP3 (83), ↓NLRC3 (84) Peripheral myeloid cells: ↑ GSDMD (85)	T cells: ↑ASC (86), ↓NLRP12 (87, 88)	Oligodendrocytes: ↑Caspase-1 (89) Astrocytes: ↑NLRP3, ↑NLRC4 (77), ↓NLRX1 (90)
RA	*Porphyromonas gingivalis*, *Prevotella nigrescens, Tannerella forsythensis, Prevotella intermedia* (91, 92) *Aggregatibacter actinomycetemcomitans, Treponema denticola* (93) Decreases in α-diversity (94, 95)	*NLRP3*: rs10754558 (96), rs4612666 (97, 98)	Monocytes/macrophages/ DC: ↑NLRP3, ↑ASC, ↑caspase-1 (99–104), ↑NLRC4 (105), ↑AIM2 (106, 107) Neutrophil: ↓NLRP3 (108)	T cells: ↑NLRP3 (109), ↓NLRP12 (110)	FLS: ↑AIM2 (111), ↓NLRP6 (112), ↑NLRP3 (113) (114), ↑NLRC5 (115),
T1D	Enteroviruses (116), *Mycobacterium avium* subspecies *paratuberculosis* (117)	*NALP1*: rs12150220 (118), rs11651270, rs2670660 (119) *NLRP3*: rs10754558 (120), rs3806265, rs4612666 (121) *NLRC4*: rs212704, rs385076 (122)	APC: ↑NLRP3 (123)		β cells: ↑NLRP3 (123) Intestinal tissues: ↓AIM2 (124), ↑NLRP3 (125, 126)
SLE	EBV, parvovirus B19 (B19V), HERVs (127) Gut virome (128) Dysbiosis in gut microbiota (129) Dysbiosis of oral microbiota (130)	*NLRP1*: rs12150220 (131), rs2670660 (131) *NLRP3*: rs4612666, rs10754558, rs6672995, rs3806268, rs35829419, rs4352135 (132)	Macrophages/PBMC/ monocytes: ↑NLRP3 (133–137), ↑AIM2 (135, 138, 139)	Tfh: ↓P2X7R and GSDMD-induced pyroptosis (140)	Glomerular podocytes: ↑ NLRP3 (141, 142)

Multiple sclerosis (MS); rheumatoid arthritis (RA); type 1 diabetes (T1D); systemic lupus erythematosus (SLE); experimental autoimmune encephalomyelitis (EAE); antigen presenting cells (APC); dendritic cells (DC); fibroblast-like synoviocytes (FLS); germinal center (GC); human peripheral blood mononuclear cells (PBMC); interferon (IFN).
"↑" indicates increased activity of a given molecule. "↓" indicates reduced activity of a given molecule.

proinflammatory cytokines such as IL-1β, which has neurotoxic and immunomodulatory effects in the CNS, as well as 2) chemokines that promote recruitment of immune effector cells (151, 152).

Studies of MS patients and rodent experimental autoimmune encephalomyelitis (EAE), a model of MS, demonstrate that inflammasomes such as NLRP3, are associated with various aspects of the autoimmune process (153–155) (Figure 2). mRNA expression of *NLRP3* and *IL1B* are detected in MS lesions as well as increased levels of IL-1β and IL-18 in blood and cerebrospinal fluid (CSF) (150, 156). Furthermore, the P2X7 purinergic receptor (P2X7R), a ligand-gated ion channel regulated by extracellular ATP that activates the NLRP3 inflammasome (157), is elevated in the spinal cord of MS patients. Indeed, increased extracellular levels of ATP and uric acid are found in the CSF and serum of MS patients (158, 159). ATP is normally abundant in the extracellular space of the CNS, where it functions as an excitatory neurotransmitter. Interestingly, various drugs used to clinically treat MS such as recombinant IFNβ, glatiramer acetate and natalizumab suppress *NLRP3* mRNA expression, and decrease IL-1β in the blood and CSF of MS patients (160–162). In the brain lesions of MS patients, NLRP9 protein is also up-regulated in microglia but not astrocytes, suggesting a role for NLRP9 in modulating the encephalitogenic response (76).

The functional role of inflammasomes and inflammasome-related molecules has been investigated using EAE and other demyelinating rodent models. Earlier studies have shown that the progression and severity of EAE are reduced in mice deficient in NLRP3 ($NLRP3^{-/-}$), ASC ($ASC^{-/-}$) and to a lesser extent caspase-1 ($Caspase1^{-/-}$) (83, 163). Attenuated EAE in $NLRP3^{-/-}$ and $ASC^{-/-}$ mice coincides with decreased infiltrates of Th1 and Th17 cells, macrophages and DC in the brain and spinal cord (83). This reduction in CNS infiltration is attributed to decreased production of IL-1β and IL-18 by APC (83). The latter are

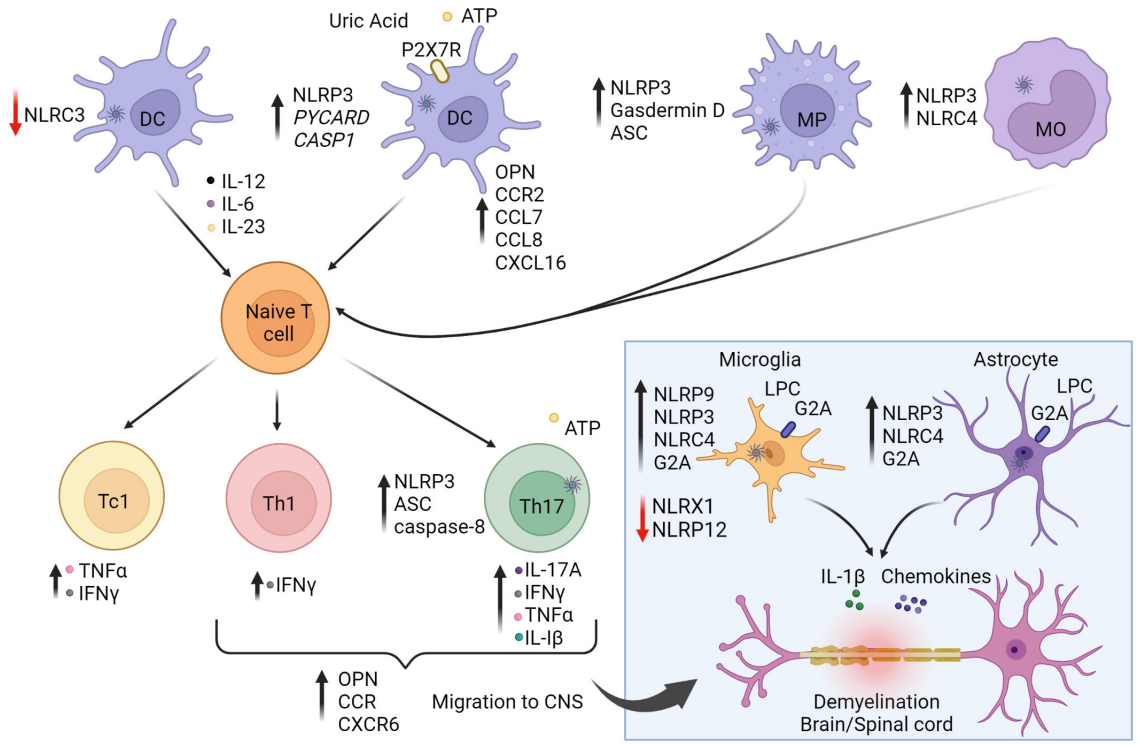

FIGURE 2
The role of inflammasomes in multiple sclerosis (MS) and experimental autoimmune encephalitis (EAE). The autoimmune response for MS is believed to begin in the periphery. Activation of NLRP3 and NLRC4 inflammasome pathways in antigen-presenting cells (APC) enhance stimulation and differentiation of pathogenic $CD4^+$ Th1/Th17 and $CD8^+$ Tc1 subsets. On the other hand, NLRC3 activation in dendritic cells (DC) is protective against disease by inhibiting DC maturation. Secretion of IL-1β and IL-18 increase T cell expression of osteopontin (OPN), CCR2 (binding CCL7/8), and CXCR6 (binding CXCL16) to promote infiltration to the central nervous system (CNS). Upon activation and differentiation, $CD4^+$ and $CD8^+$ T cells, and B cells migrate to the CNS. In the CNS, peripheral DC, macrophages (MP), and monocytes (MO) further amplify inflammation. CNS resident cells such as microglia and astrocytes also promote inflammation. Lysophosphatidylcholine (LPC) activates NLRP3 and NLRC4, causing secretion of IL-1β and chemokines, leading to further inflammation and demyelination. NLRP9 expression is increased in microglia. NLRX1 and NLRP12 serve to down-regulate neuroinflammation and provide protection against disease as indicated by the red arrows. Reduction of NLRX1 and NLRP12 can lead to exacerbated disease states. Purinergic receptor (P2X7R). The figure was prepared using Biorender software licensed to the UNC Lineberger Comprehensive Cancer Center.

needed to adequately activate and upregulate T cell expression of osteopontin (OPN), and chemokine receptors CCR2, and CXCR6 for efficient migration into the CNS (83). In addition, lack of NLRP3 and ASC expression also limits DC and macrophages to upregulate matching receptor/ligands for OPN (α4β1 integrin), CCR2 (CCL7/CCL8), and CXCR6 (CXCL16) (83), resulting in aberrant APC migration into the CNS. These findings support a role for APC-expressed NLRP3 in mediating chemotactic recruitment of immune effectors to the CNS.

Peripheral APC also regulate the progression of EAE *via* inflammasome-mediated pyroptosis. EAE is attenuated in mice lacking GSDMD expression by peripheral myeloid cells (85). On the other hand, selective deletion of GSDMD in microglia has no effect on EAE, indicating that pyroptosis of CNS-resident APC may have only a limited role. The T cell stimulatory capacity of $GSDMD^{-/-}$ APC is reduced, which is marked by diminished numbers and effector function of Th1 and Th17 cells in the CNS. Notably, selectively blocking GSDMD-mediated pyroptosis with the inhibitor disulfiram, also attenuates EAE, demonstrating a direct role for pyroptosis (85). It is believed that pyroptosis of APC heightens local inflammation to promote efficient T cell activation, and subset differentiation needed to generate a robust encephalitogenic T cell pool.

In addition to APC, inflammasome activity intrinsic to T cells impacts EAE progression (Figure 2). Selective ASC-deficiency in T cells attenuates EAE marked by reduced infiltration of $CD4^+$ T cells, B cells, and neutrophils (86). $ASC^{-/-}$ T cells are readily activated and undergo normal *in vitro* and *in vivo* differentiation into Th1, Th2, Th17 and $Foxp3^+$Treg subsets. However, ASC-deficiency affects the properties of Th17 but not Th1 cells. $ASC^{-/-}$ Th17 exhibit reduced survival and pathogenicity reflected by decreased secretion of IL-17A, IFNγ, TNFα, as well as IL-1β. Here, IL-1β plays a key role in an autocrine manner, by enhancing the survival and effector function of Th17 cells residing in the CNS. Interestingly, cleavage of pro-IL-1β in Th17 cells is mediated *via* a noncanonical pathway involving caspase 8 activation. In this scenario, increased extracellular ATP levels due to release by stressed and dying cells drives activation of the NLRP3-ASC-caspase-8 complex, establishing a feed-forward loop promoting Th17 cell-mediated pathogenicity.

In addition to NLRP3, the activity of other inflammasome molecules in non-immune CNS resident cell-types have been

found to promote neuroinflammation. Both NLRP3 and NLRC4 regulate the activity of microglia and astrocytes in a cuprizone model of inflammation-induced demyelination (77). Both cell types are known mediators of neuroinflammation through secretion of proinflammatory cytokines and chemokines. Cuprizone-induced pathology is prevented in NLRP3- and NLRC4-deficient mice characterized by microglia and astrocytes lacking IL-1β production, and exhibiting reduced expression of G2A, the receptor for lysophosphatidylcholine (LPC) (Figure 2). LPC, known for proinflammatory properties, is rapidly metabolized under homeostasis but accumulates under pathological conditions in the CNS (77). Following cuprizone treatment, LPC levels are increased, and LPC functioning as a DAMP, activates NLRP3 and NLRC4 expressed by microglia and astrocytes (77). In MS patients, expression of G2A and NLRC4 are increased, suggesting a role in the MS autoimmune response (77).

Interestingly, inflammasomes have also been shown to play a protective role in EAE. For instance, deficiency of NLRC3 exacerbates EAE (84). Lack of NLRC3 results in DC producing increased proinflammatory cytokines such as IL-12, IL-6, and IL-23, that in turn enhance differentiation of encephalitogenic Th1 and Th17 cells (84). NLRC3 negatively regulates DC maturation by inhibiting activation of the p38 signaling pathway (84). The ligand (s) regulating NLRC3 activity in DC is currently undefined (84). Also serving a protective function is NLR family member X1 (NLRX1), a more recently characterized NLR that is ubiquitously expressed and located in the mitochondria (78, 90). NLRX1 inhibits proinflammatory pathways, including type I IFN and TLR-mediated NF-κB signaling events, and may play a role in regulating mitochondria oxidative damage (78). Mice deficient of NLRX1 have increased T cell infiltration of the CNS, and consequently develop more severe EAE (79). Microglia exhibit a hyperactivated phenotype characterized by elevated expression of MHC class II molecules and production of IL-6 and chemokines, which in turn aid T cell recruitment and expansion (79). Accordingly, NLRX1 function is predicted to attenuate the proinflammatory properties of microglia. On the other hand, NLRX1-deficiency has no intrinsic effect on the pool of encephalitogenic T cells (79). NLRX1 may also play a protective function in astrocytes; NLRX1$^{-/-}$ astrocytes release excess glutamate in a Ca^{2+} dependent manner and contain reduced ATP levels compared to wild-type astrocytes, suggesting that NLRX1 promotes mitochondria ATP production (90). Furthermore, ROS levels in NLRX1 deficient astrocytes are increased compared to wild-type astrocytes, which may explain the reduced glutamate uptake (90). Recent evidence suggests that NLRX1 inhibits microglial activation in the early stages of EAE, which prevents activation of neurotoxic astrocytes (78).

NLRP12 has also been shown to regulate the progression and nature of CNS inflammation in EAE (87, 88, 153). NLRP12 mediates classical inflammasome driven inflammation in innate effector cells to certain microbes (164, 165), but also serves as a negative regulator of the NF-κB signaling pathway (80, 87, 88, 166, 167). In mice deficient of NLRP12, a more rapid and severe EAE develops (81). This exacerbated disease is characterized by increased mRNA levels encoding IL-1β and other proinflammatory molecules in the CNS, as well as activated microglia producing heightened levels of inducible NO synthase (iNOS), NO, TNFα, and IL-6 (81). A second study reported that EAE induction in NLRP12$^{-/-}$ mice results in neuroinflammation that promotes ataxia and poor balance, rather than the ascending paralysis that normally develops in wild-type mice (87). Furthermore, NLRP12-deficiency has intrinsic effects on T cells. In the absence of NLRP12 expression, T cells exhibit increased proliferation, and secretion of IFNγ, IL-17 and IL-4, that is in part due to hyperactivation of NF-κB (87). Therefore, NLRP12 negatively regulates various aspects of innate cell activation, as well as CD4$^+$ T cell expansion and effector function *via* blocking NF-κB signaling (88).

Rheumatoid arthritis and inflammasome-mediated joint inflammation

RA is a chronic autoimmune disease characterized by the inflammation of the joints, leading to synovial tissue proliferation, cartilage erosion and joint destruction (168–170). Pathology is in part driven by Th1 and Th17 CD4$^+$ T cells and B cells, as well as innate effectors such as monocytes, DC and neutrophils that traffick into the synovium (171–173). Joint-resident cells such fibroblast-like synoviocytes (FLS) also promote local inflammation (174). Normally, FLS play a key role in maintaining joint homeostasis *via* production of the extracellular matrix and matrix metalloproteinases (MMPs) (175).

The autoimmune response of RA also involves high levels of serum complement and the production of autoantibodies that target the Fc region of IgG (i.e. rheumatoid factor), cartilage components, nuclear proteins and proteins post-translationally modified by citrullination (176, 177). Key proinflammatory cytokines driving RA include IL-1β and IL-18, as well as IL-6 and TNFα (178). In addition to having immunomodulatory effects, IL-1β mediates cartilage erosion and prevents chondrocyte matrix formation (179). Furthermore, the severity of RA correlates with elevated serum IL-18 (180, 181). Moreover, during the early-stages of RA, FLS proliferate and differentiate into distinct subsets of activated synovial fibroblasts that produce inflammatory cytokines, matrix-degrading enzymes and proangiogenic factors which lead to the release of inflammatory mediators, bone destruction and angiogenesis (182–184). FLS also promote T cell survival, Tfh and Th17 cell differentiation, and can function as antigen presenters to autoreactive T cells (185–193). The etiology of RA is ill-defined but genetic and a host of environmental factors are known to influence disease susceptibility and progression. Evidence also suggests that inflammasomes likely have an important role in RA pathogenesis (Figure 3).

In RA patients, NLRP3 and NLRP3-inflammasome-related proteins are upregulated in a cell-specific manner among innate effectors. For instance, expression of NLRP3, ASC, and caspase-1 as well as IL-1β secretion is generally increased in monocytes, macrophages, and DC from RA patients (99–102) (Figure 3). CD4$^+$ T cells from RA patients also exhibit increased NLRP3 expression, which correlates with elevated serum IL-17A

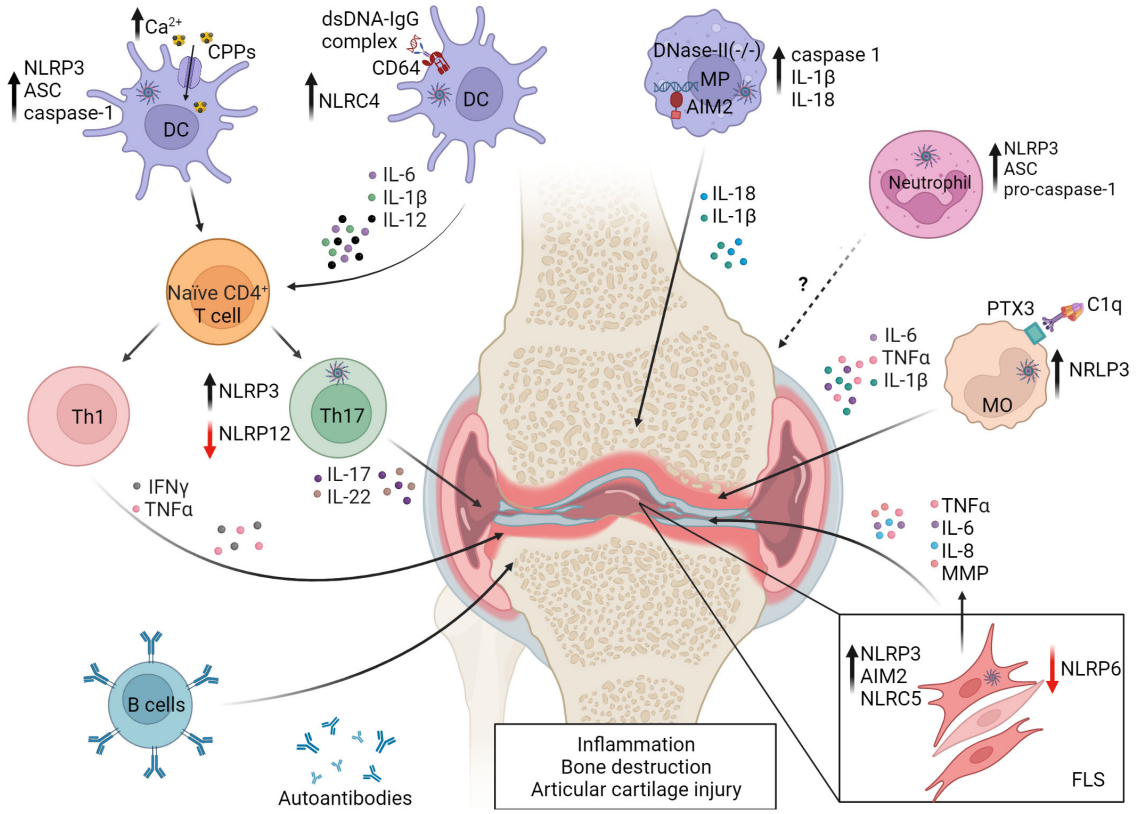

FIGURE 3
Events in dysregulated inflammasome activation in rheumatoid arthritis (RA). NLRP3 and NLRC4 activity are increased in monocytes (MO) and DC by Fc-receptor (FcR) binding of DNA-IgG immune complexes and complement component 1q (C1q) binding to pentraxin 3 (PTX3). Uptake of elevated levels of calciprotein particles (CPPs) in the joint by resident DC also leads to NLRP3 activation. Resulting pyroptosis and secretion of proinflammatory cytokines promote RA progression by favoring Th1 and Th17 differentiation and development of autoantibodies and RA factor producing plasma cells. NLRP3 activation is also increased in Th17 cells. Aberrant lysosomal processing of endocytosed dsDNA can lead to AIM2 activation in joint resident macrophages (MP). Neutrophils exhibit reduced expression of inflammasome molecules, which correlates with decreased disease severity. NLRP3, NLRC5 and AIM2 are associated with proinflammatory properties of fibroblast-like synoviocytes (FLS), while NLRP6 and NLRP12 serve protective roles, indicated by the red arrows. NLRP6 limits FLS cytokine production, and NLRP12 negatively regulates Th17 subset differentiation. Reduced expression of NLRP6 and NLRP12 leads to pathology. Matrix metalloproteinases (MMP). The figure was prepared using Biorender software licensed to the UNC Lineberger Comprehensive Cancer Center.

concentrations and disease activity (109) (Figure 3). Notably, differentiation of Th17 cells is inhibited by NLRP3 knockdown (109), suggesting that NLRP3 regulates the proinflammatory activity of both innate and adaptive effectors in RA. Interestingly, NLRP3 activation in monocytes is mediated *via* multiple mechanisms in RA patients. C1q binding to pentraxin 3, a key regulator of complement activity and which is increased on the surface of RA $CD14^+$ monocytes, leads to NLRP3 activation, enhanced IL-1β and IL-6 secretion, and GSDMD-induced pyroptosis (178). In addition, due to elevated extracellular Ca^{2+} in the joint and concomitant heightened activity of calcium-sensitive receptors, macropinocytosis of calciprotein particles (CPPs) is elevated by local monocytes (194). After uptake, CPPs disrupt lysosome integrity resulting in enhanced NLRP3 activation and IL-1β secretion (194).

Whereas NLRP3 and related inflammasome proteins are typically elevated in various innate and adaptive immune effectors, neutrophils from RA patients exhibit reduced NLRP3, ASC and pro-caspase-1 expression (108). Here, *NLRP3* mRNA levels in neutrophils negatively correlate with disease severity (108). This suggests that NLRP3 may serve a protective role in the context of neutrophil function *via* an ill-defined mechanism (108).

Various inflammasome molecules, in addition to NLRP3, have been found to be involved with RA (Figure 3). NLRC4 activity is increased in DC residing in the synovial membrane of RA patients (105). These DC secrete elevated IL-1β, have increased expression of CD64, an IgG Fc receptor, and display an enhanced capacity to stimulate Th1 and Th17 subset differentiation (105). This capacity is due to a novel mechanism of upregulation of NLRC4 expression and activity. Here, dsDNA-IgG complexes bind to CD64, are internalized, and the combination of CD64 signaling and intracellular sensing of the dsDNA increases NLRC4 activity (105). AIM2 expression is increased in synovial tissue of RA patients, and knockdown of *AIM2* mRNA inhibits *in vitro* proliferation of FLS derived from RA patients (111). On the other hand, NLRP6 levels are reduced in FLS from patients with RA versus osteoarthritis (112). Furthermore, increased ectopic expression of NLRP6 in RA patient-derived FLS blocks the production of inflammatory cytokines such as IL-1β, IL-6, and

TNFα, as well as MMP *via* inhibition of the NF-κB pathway. The latter indicates that NLRP6 serves a protective role in RA (112), and is consistent with NLRP6 having a negative regulatory function in colitis (195).

Animal studies further support the notion that the role for inflammasomes in RA is complex, and that cell type-dependent, inflammasome molecules can have distinct effects on immune cells and effector molecules depending on the RA model (103, 196) (Figure 3). Mice deficient of ASC are resistant to collagen induced arthritis (CIA), in part due to a reduced T cell stimulatory capacity of ASC$^{-/-}$ DC (103). However, CIA develops in both NLRP3$^{-/-}$ and Caspase1$^{-/-}$ mice suggesting that ASC has caspase 1-independent effects in DC (103). On the other hand, NLRP3 and caspase-1 play a key role in the spontaneous polyarthritis that develops in mice in which the RA susceptibility gene *A20/Tnfaip3* is selectively ablated in myeloid cells (A20myel-KO mice) (104). Here, macrophages lacking A20 have increased constitutive and LPS-induced expression of NLRP3 and pro-IL-1β. The latter is indicative of the established role A20 has as an inhibitor of NF-κB activation (197), which is needed for NLRP3 and pro-IL-1β transcription following inflammasome priming. Furthermore, activation of NLRP3 in A20-deficient macrophages results in enhanced caspase-1 activation, IL-1β secretion, and pyroptosis. Notably, pathology in A20myel-KO mice is blocked by ablation of NLRP3, caspase-1 and the IL-1 receptor (IL-1R), demonstrating a direct role for classical NLRP3 inflammasome activation in this spontaneous autoimmune model of cartilage destruction (104). NLRP3 is also associated with the proinflammatory properties of FLS. NLRP3 expression is increased in FLS isolated from mice with adjuvant-induced arthritis (AA) (113), and knockdown of *Nlrp3* mRNA expression in FLS reduces disease severity in a monosodium urate-induced model of gout arthritis in rats (114).

AIM2 has also been shown to have a key role in joint inflammation. Mice deficient in expression of lysosomal endonuclease DNase II and type I IFN receptor (IFNαR) develop polyarthritis marked by production of autoantibodies, and macrophage secreted proinflammatory cytokines such as IL-1β, IL-6 and TNFα (106). Lack of lysosomal endonuclease DNase II results in aberrant processing of dsDNA in lysosomal compartments, and translocation of undigested DNA into the cytoplasm of macrophages (106, 107). AIM2-deficiency limits joint inflammation marked by reduced caspase-1 activity, IL-1β and IL-18 expression, and macrophage infiltration (106, 107). Notably, however, autoantibody production is unaffected by AIM2-ablation indicating a tissue-specific role for AIM2. Furthermore, AIM2-ablation has no effect on the transfer of arthritogenic serum from K/BxN mice (107). In this passive model, arthritis is induced by the deposition of immune complexes within the joint, leading to complement fixation and ensuing pathology (106, 107). Therefore, AIM2 regulates inflammation when cytosolic DNA is the key driving event. A contribution for NLRC5 in joint inflammation has been reported (115). NLRC5 expression is elevated in the synovium and FLS in rat AA (115), and knockdown of *Nlrc5* mRNA blocks FLS proliferation and production of TNFα and IL-6, due to suppressed NF-κB activation (115).

Similar to NLRP6, NLRP12 has been shown to negatively regulate joint inflammation (110). The severity of antigen-induced arthritis in NLRP12$^{-/-}$ mice is increased, marked by elevated levels of joint infiltrating Th17 cells (110). Notably, *in vitro* Th17 cell differentiation is enhanced in NLRP12$^{-/-}$ CD4^{+} T cells marked by elevated IL-6-induced activation of signal transducer and activator of transcription (STAT) 3 (110).

Type 1 diabetes and inflammasome-mediated pancreatic islet inflammation

T1D is characterized by chronic inflammation of the pancreatic islets (insulitis) that results in the dysfunction and/or destruction of the insulin producing β cells (198–200). Despite life-long insulin therapy, T1D patients typically develop a variety of complications including retinopathy, neuropathy, and nephropathy related to hyperglycemia and inflammation. The autoimmune response involves islet infiltration of CD4^{+} and CD8^{+} T cells, B cells, macrophages, and DC. β cell-specific CD4^{+} and CD8^{+} T cells are generally believed to be the key drivers of pathology (198–200). Diabetogenic CD4^{+} and CD8^{+} T cells typically exhibit a type 1 effector phenotype, although Th17 cells are also implicated in the disease process (199). In addition to serving as APC, islet-infiltrating macrophages and DC, mediate β cell destruction through secretion of proinflammatory mediators and cytokines such as IL-1β, IFNγ and TNFα that have direct β cell-cytotoxic effects (199). The initiation and progression of T1D are influenced by genetic and poorly defined environmental factors (201–204). The latter include viral infections, and dysbiosis of gut microbiota, which are events that can be impacted by inflammasome activity (16, 201, 205).

Studies using murine models of T1D show that NLRP3 regulates the diabetogenic response (Figure 4). In non-obese diabetic (NOD) mice, which spontaneously develop β cell autoimmunity and overt diabetes, NLRP3 deficiency results in a reduced incidence of diabetes (123). This attenuated diabetes is due in part to NLRP3$^{-/-}$ APC having a decreased capacity to promote Th1 cell differentiation; Th17 cell differentiation, however, is unaffected. Importantly, NLRP3$^{-/-}$ β cells exhibit decreased production of IL-1β and chemokines such as CCL5, and CXCL10 (123). The latter limits migration into the islets by immune effectors including diabetogenic T cells (123) (Figure 4). Interestingly, limited IL-1β production leads to reduced activation of interferon regulatory factor 1 (IRF1) that is needed for β cell expression of CCL5 and CXCL10. Diminished IL-1β secretion by β cells is also expected to aid β cell viability and function, as well as enhance the maintenance and function of protective Foxp3^{+}Treg in the islets. Notably, upregulation of NLRP3 and IL-1β is also detected in human β cells upon LPS and ATP stimulation *in vitro* (206). A regulatory function for NLRP3 in the disease process is also seen in a multiple low dose streptozotocin (MLD-STZ)-induced model of T1D. Here, progression of β cell autoimmunity is reduced in MLD-STZ treated C57BL/6 mice lacking NLRP3 expression (207). In this model NLRP3 is activated in macrophages residing in the draining pancreatic lymph nodes (PLN) by mitochondrial DNA (mtDNA)

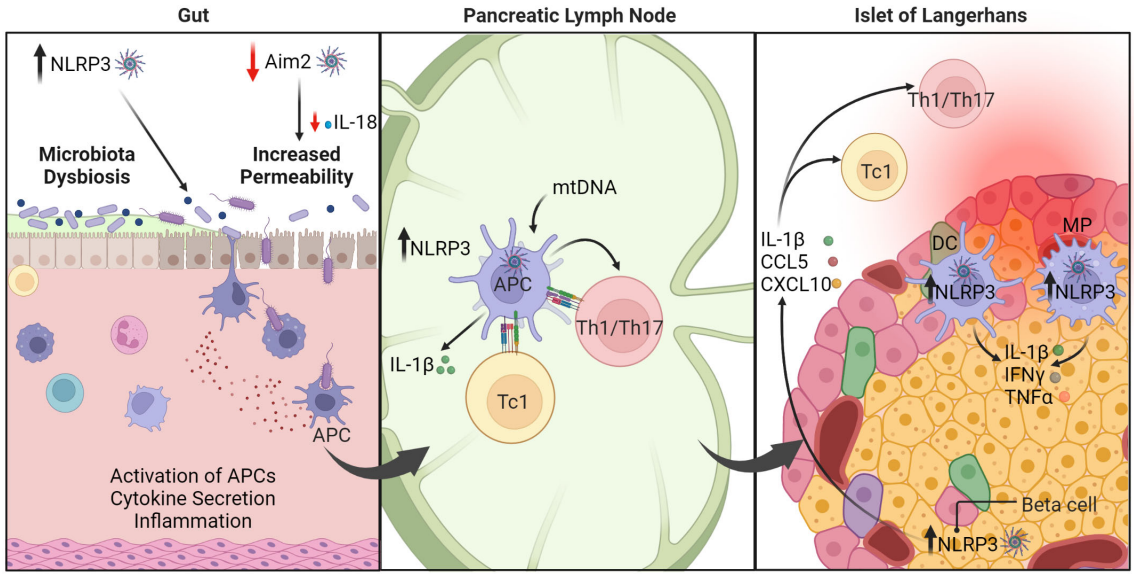

FIGURE 4
The roles of inflammasomes in type 1 diabetes (T1D). Under homeostasis, healthy intestinal epithelial cells maintain intestinal barrier function and regulate permeability to prevent passage of harmful elements such as microorganisms and toxins. AIM2 serves a protective function (indicated by the red arrow). Dysregulation of inflammasome function, such as AIM2 deficiency, leads to reduced production of IL-18, which is necessary for maintaining intestinal barrier function. Consequently, inflammasome dysregulation enhances intestinal permeability and triggers inflammation. On the other hand, NLRP3 is linked to dysbiosis within the gut microbiota, which can exacerbate T1D progression. In the pancreatic lymph node (PLN), upregulation of NLRP3 in APC promotes IL-1β production that ultimately drives differentiation of diabetogenic $CD8^+$ Tc1, $CD4^+$ Th1, and Th17 cells. In the pancreatic islets, NLRP3 hyperactivity in β cells induces release of cytokines and chemokines. These conditions combined with other immunomodulatory factors establish a positive feedback loop to further perpetuate pancreatic inflammation. Macrophage (MP), dendritic cell (DC), antigen-presenting cell (APC). The figure was prepared using Biorender software licensed to the UNC Lineberger Comprehensive Cancer Center.

that is released following STZ treatment. NLRP3 activation results in increased caspase-1 activity, and IL-1β production, which drives expansion of pathogenic Th1 and Th17 cells and the induction of diabetes. The PLN are a key site for priming of diabetogenic $CD4^+$ and $CD8^+$ T cells. Interestingly, plasma levels of mtDNA are increased in T1D versus healthy subjects, which is expected to contribute to systemic inflammasome activation (208). Indeed, circulatory mtDNA induced by MLD-STZ in mice activates NLRP3 in endothelial cells *via* Ca^{2+} influx and mitochondrial ROS generation, which leads to endothelial dysfunction and vascular inflammation (208). Vascular inflammation is a key driver of complications that develop in T1D. Together these studies indicate that NLRP3 promotes pathological events driving β cell autoimmunity. Nevertheless, mechanisms by which NLRP3 mediate effects are likely to be complex and cell dependent. For instance, disease progression in NOD mice is unaffected by caspase-1 deficiency (209, 210), and only minimally affected by IL-1R ablation (211).

In contrast to NLRP3-deficient C57BL/6 (207), MLD-STZ enhances diabetes development in AIM2-deficient C57BL/6 mice (124). Interestingly, disease exacerbation in the $AIM2^{-/-}$ mice is mediated by enhanced intestinal permeability, alterations in the gut microbiota, and increased bacterial translocation to the PLN where $CD4^+$ Th1 and $CD8^+$ Tc1 are readily expanded (Figure 4). Importantly, AIM2 deficiency results in decreased maturation of IL-18 which is needed to maintain intestinal barrier function (124). On the other hand, reduced NLRP3 expression in colonic NOD mouse tissue is associated with decreased microbiota dysbiosis, enhanced intestinal barrier function and diabetes prevention (125, 126). It is well established that dysbiosis within the gut microbiota significantly affects disease progression in NOD mice, and clinical findings suggest similar effects may also occur in T1D subjects (16, 205, 212–215). These studies provide evidence that inflammasomes may play a key role in regulating T1D progression in part *via* effects on gut microbiota and intestinal barrier function (16). Studies have reported that gut microbiota composition and/or intestinal barrier permeability are also influenced by other inflammasome molecules such as NLRP6 (216), NLRC4 (217), NLRX1 (218, 219), and NLRP12 (220, 221). Further investigation is necessary to elucidate the connection between inflammasomes, gut microbiota homeostasis, and autoimmunity.

Systemic lupus erythematosus and the role of inflammasome activity in widespread inflammation

SLE is a chronic autoimmune disease with diverse clinical manifestations. Development of SLE is influenced by genetic, hormonal, and environmental factors that lead to dysregulation of mechanisms of innate and adaptive-mediated self-tolerance. The autoimmune response is characterized by the generation of anti-nuclear autoantibodies, tissue deposition of immune complexes, increased type I IFN production, and inflammation in multiple

organs with the kidneys being the most commonly affected (222). $CD4^+$ T cells such as Tfh cells are key drivers of the autoantibody response, and Th17 cells, found infiltrating the kidneys and skin contribute to tissue damage (223). Innate effectors such as monocytes, macrophages, DC and neutrophils also play roles in mediating the systemic inflammation and tissue damage in SLE (223).

The etiology of SLE is not fully understood but evidence from humans and animal models indicate that inflammasomes contribute to disease progression (Figure 5). Inflammasome components are typically upregulated in kidney biopsies from SLE patients, and NLRP3, IL-1β and IL-18 are increased in SLE patient macrophages, peripheral blood mononuclear cells (PBMC), and serum (133, 134). A critical meditator of pathology in SLE are anti-nuclear autoantibodies (ANA) that target endogenous dsDNA and ribonucleoproteins (RNP) (224). Immune complexes (IC) of dsDNA upregulate NLRP3 and caspase-1 activity leading to increased IL-1β production by monocytes and macrophages of SLE patients (225). Here, the IC activates TLR9, a DNA sensor, which subsequently upregulates NF-κB and primes inflammasome assembly *via* increasing NLRP3 and pro-IL-1β (225). Upon IC binding, TLR9 also promotes mitochondrial ROS production and K^+ efflux and subsequent NLRP3 activation. Notably, SLE monocytes stimulated with dsDNA-antibody complexes readily promote differentiation of Th17 cells, which is also seen *in vivo* in lupus-prone NZBW/F1 mice injected with anti-dsDNA autoantibodies from SLE patients (224). Similarly, autoantibody complexes of U1-small nuclear RNP (U1-snRNP) activate the NLRP3 inflammasome involving cytoplasmic RNA sensors TLR7 and TLR8 signaling in human monocytes (226). Antibody complexes of endogenous snRNP also induce production of macrophage migration inhibitory factor (MIF) in human monocytes, which enhances NLRP3 activation and IL-1β production (227). Interestingly, the context of nucleic acid uptake appears to determine the identity of the inflammasome molecule being engaged. For instance, unbound dsDNA, normally found at high levels in SLE patient serum, is taken up by monocytes *via* macropinocytosis, which activates AIM2 as well as NLRP3 (135). Uptake of free nucleic acid, however, requires antibody to be internalized by macropinocytosis but not Fc receptor (FcR) (135). On the other hand, internalization of dsDNA/snRNP autoantibody

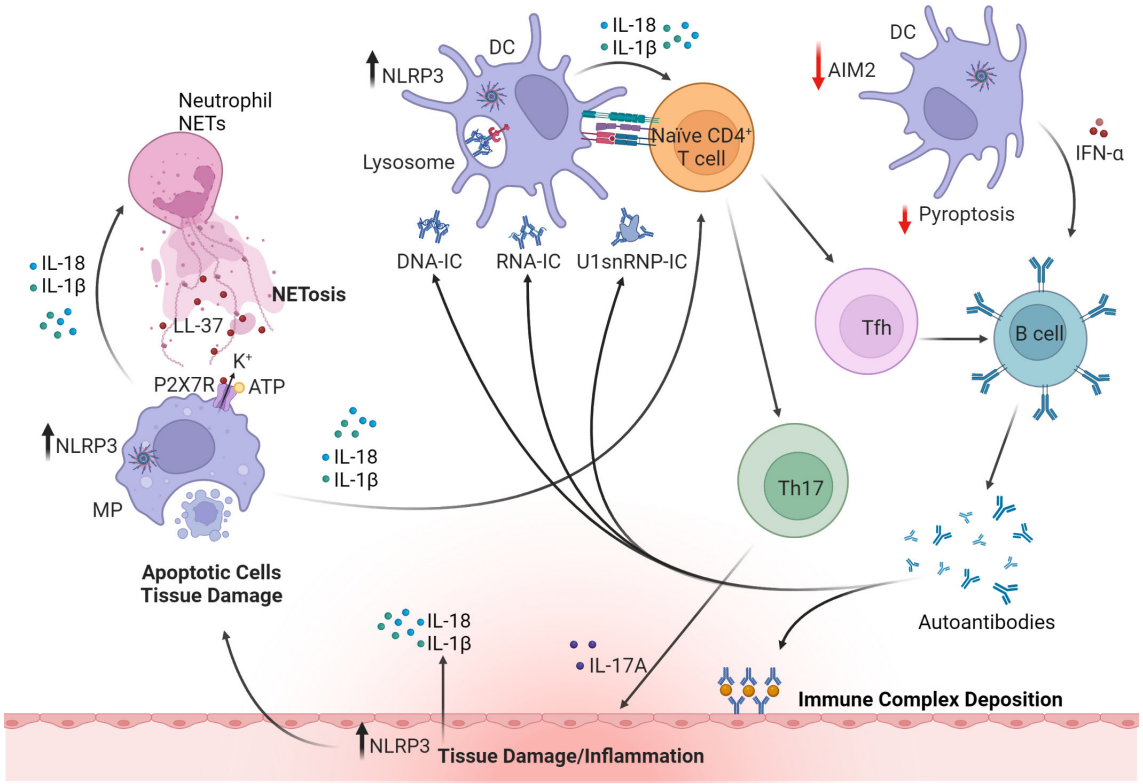

FIGURE 5
The roles of inflammasomes in systemic lupus erythematosus (SLE). Upregulation of NLRP3 inflammasome in macrophages (MP) and DC by DNA or RNA immune complexes (IC) or small nuclear ribonucleoprotein (snRNP) leads to release of proinflammatory cytokines such as IL-1β, IL-18 and IFNα. Dysregulation of inflammasomes in APC also promotes Th17 and Tfh cell differentiation. Tfh cells and IFNα facilitate B cell maturation and autoantibody production. However, production of IFNα is regulated by AIM2-mediated pyroptosis (indicated by red arrows). Deposition of IC, infiltrating Th17 cells, and production of autoantibodies and cytokines all contribute to tissue damage. IL-18 activates NETosis in neutrophils and in turn upregulates NLRP3 and IL-1β and IL-18 secretion in macrophages *via* cathelicidin antimicrobial peptide (LL37)-driven K^+ efflux mediated by the P2X7 receptor (P2X7R). These cytokines further induce pyroptosis and release of cellular and nuclear contents, leading to the production of anti-nuclear autoantibodies and further amplifying systemic inflammation. Inflammasome activation in cells of target tissues, such as kidney resident podocytes also contributes to disease pathology by producing IL-1β. The figure was prepared using Biorender software licensed to the UNC Lineberger Comprehensive Cancer Center.

complexes *via* FcR may favor activation of NLRP3, and possibly NLRC4 as seen in RA (105). In each of the aforementioned scenarios, IL-1β and IL-18 are secreted to maintain/amplify inflammation. Furthermore, induced pyroptotic death and release of cellular and nuclear contents lead to the production of ANA to further fuel the autoimmune response (228, 229).

Aberrant clearance of neutrophil extracellular traps (NETs) is also linked with the pathogenesis of SLE and inflammasome activation (Figure 5). NETs are a network of chromatin fibers containing antimicrobial peptides such as LL37 and enzymes that participate in host defense (230). NETs are primarily released by activated neutrophils that undergo NETosis, a programmed cell-death mechanism (231). Notably, NETs activate NLRP3 inflammasome and IL-1β and IL-18 secretion in macrophages from SLE patients *via* LL37-driven K^+ efflux mediated by the P2X7R (136). Furthermore, IL-18 activates NETs and promotes NETosis suggesting that a feed-forward loop exists that helps to maintain inflammation (136).

Monocytes from SLE patients versus healthy controls exhibit enhanced NLRP3 activation and IL-1β secretion (138, 139). This hyperactivity is attributed to chronic IFNα stimulation of monocytes. Elevated type I IFN-induced gene expression "signatures" correlate with the presence of autoantibodies, nephritis, and disease activity (232). Prolonged IFNα exposure *in vivo* induces NLRP3 hyperactivity by an IRF1 signaling pathway (138). However, consistent with other studies (233), short-term IFNα exposure of monocytes blocks NLRP3 activation (138). The latter, importantly, indicates that chronic type I IFN stimulation can have distinct effects on inflammasome activation.

The study of different murine lupus models provides further evidence that inflammasomes regulate SLE pathogenesis. Mice deficient in caspase-1 expression versus wild-type mice exhibit reduced autoantibody production, a limited IFN signature, as well as diminished NETosis and kidney pathology induced by pristane administration (136). In addition, blocking the P2X7R significantly impacts the development of spontaneous lupus in MRL/lpr mice. Here, limiting NLRP3 activation reduces the production of anti-dsDNA autoantibodies and IL-1β, and decreases Th17 cell expansion and the severity of nephritis (234). Furthermore, various drugs that inhibit NLRP3 inflammasome activation attenuate disease severity in different lupus mouse models (137, 235–237). On the other hand, nephritis induced by pristane treatment is exacerbated in mice in which myeloid cells selectively express a transgene encoding a hyperactive *Nlrp3*^{R258W} mutant protein (238).

In addition to immune effector cell types, inflammasome activation in target tissues also contributes to disease pathology (Figure 5). Endothelial cells, basement membrane, and podocytes form a glomerular filtration barrier, which is essential for maintaining kidney function (239). In NZM2328 mice, which spontaneously develop lupus nephritis, severe proteinuria correlates with increased activation of NLRP3 and caspase-1 as well as IL-1β secretion by glomerular podocytes (141, 142). NZM2328 mice treated with MCC950, an NLRP3 inhibitor, exhibit reduced NLRP3 activation by podocytes, and attenuated renal tissue damage and proteinuria (141, 142).

Depending on the lupus model, inflammasome molecules have also been shown to play a protective role. In C57BL/6$^{lpr/lpr}$ mice, which develop mild lupus, deficiency of NLRP3 or ASC exacerbates pathology marked by an increase in activated macrophages and DC and production of proinflammatory cytokines, and T and B cell proliferation but no effect is seen on autoantibody production (240). This enhanced pathology is marked by reduced SMAD2/3 phosphorylation during TGF-β receptor signaling, and consistent with the role of TGF-β1 as a key regulator of immune homeostasis (240). In this scenario, it is likely that NLRP3 or ASC serve functions independent of classical inflammasome activation (see below), consistent with the observation that IL-1R- or IL-18-deficiency in C57BL/6$^{lpr/lpr}$ mice does not exacerbate pathology.

Studies have indicated that AIM2 may also serve a protective role in lupus by negatively regulating type I IFN production. In B6.Nba2 mice, which spontaneously develop lupus nephritis, p202, another IFN-inducible p200 family member is up-regulated (241, 242). Notably, p202 blocks AIM2 inflammasome assembly, and pyroptosis-mediated cell death. Consequently, p202 or other dsDNA sensors such as cyclic GMP-AMP synthase (cGAS), bind cytosolic DNA to promote prolonged type I IFN production that would be normally terminated by AIM2-induced pyroptosis (243). Regulation of pyroptosis has also been found to impact other aspects of the autoimmune response driving lupus nephritis. Pristane-induced lupus nephritis is exacerbated in mice lacking T cell expression of the P2X7R (140). Here, the P2X7R normally mediates GSDMD-driven pyroptosis of Tfh cells, which then limits differentiation of autoantibody secreting plasma cells in the germinal centers. Together these findings demonstrate the complexity of the roles inflammasomes have in both promoting and suppressing the autoimmune response of SLE.

Alternative roles of inflammasome molecule-mediated regulation

Classical inflammasome activation and induction of a proinflammatory response contributes to autoimmunity in a variety of ways as described above. It is becoming apparent, however, that inflammasome molecules also serve regulatory functions independent of typical inflammation-driving events (Table 2). Caspase-1 for instance, in addition to being involved in the maturation of IL-1β and IL-18, has been shown to modulate protein secretion, cell death, and lysosomal function in many cell types such as neurons, hepatocytes, epithelial cells, and cardiomyocytes (244–251). These alternative roles for inflammasome molecules have been linked to regulation of immune effector cells such as T and B cells, as well as non-immune tissue-resident cell types. Accordingly, some of these events have been reported to be directly involved in the progression of autoimmunity, and/or can be expected to contribute to an autoimmune response.

ASC: A regulatory function in CD4$^+$ T cells

ASC has a T cell intrinsic effect regulating the production of IL-1β needed to maintain CNS-resident Th17 cells in EAE. Recent

TABLE 2 Alternative functions of inflammasome molecules in autoimmunity.

Inflammasome involved	Alternative mechanism	Associated diseases
ASC	Affects Th17, IL-1β maturation	MS
NLRP3	↑Th2 differentiation	MS
	↑TGF-β signaling	SLE
AIM2	↓Microglia inflammation	MS
	↑AIM2 in astrocytes in EAE model Maintains Foxp3$^+$Treg function Regulates Th1/Th17 differentiation	
	↑Tfh differentiation	SLE
	↑AIM2 in GC B cell, memory B cells, and plasma cells from SLE patients	

Multiple sclerosis (MS); experimental autoimmune encephalomyelitis (EAE); systemic lupus erythematosus (SLE); germinal center (GC).
"↑" indicates increased activity of a given molecule. "↓" indicates reduced activity of a given molecule.

findings indicate that ASC also regulates properties of murine CD4$^+$ T cells independent of classical inflammasome activation and IL-1β maturation (252). ASC is constitutively expressed in naïve CD4$^+$ T cells, and after anti-CD3/CD28 antibody stimulated TCR signaling, ASC is upregulated but no IL-1β or IL-18 secretion is detected (252). Naïve CD4$^+$ T cells lacking ASC expression normally differentiate *in vitro* into Th1, Th2, Th17, Th9, and Foxp3$^+$Treg subsets under polarizing conditions (252). Notably, recombination activation gene (Rag)-deficient mice develop more severe colitis after transfer of ASC$^{-/-}$ CD4$^+$ T cells versus wildtype, NLRP3$^{-/-}$, or Caspase1$^{-/-}$ CD4$^+$ T cells (252). This increased pathogenic function of ASC$^{-/-}$ CD4$^+$ T cells is marked by enhanced TCR signaling *in vitro*, elevated lymphopenic proliferation *in vivo*, and an increased metabolic state marked by higher glycolytic flux and increased glucose transporter 1 (Glut-1) surface expression (252). These findings suggest a negative regulatory function for ASC in CD4$^+$ T cell TCR signaling, proliferation, and metabolism. The mechanism(s) by which ASC regulates these events still needs to be defined. Nevertheless, one could envision a scenario in which dysregulation of alternative ASC function enhances the pathogenic potential of autoreactive CD4$^+$ (and possibly CD8$^+$) T cells to aid autoimmune disease progression.

NLRP3 and Th2 cell differentiation

NLRP3 has also been found to have T cell-intrinsic effects independent of classical inflammasome activation. Specifically, NLRP3 positively regulates Th2 subset differentiation (253). Upon TCR stimulation by anti-CD3/CD28 antibody, expression of NLRP3 is increased in both Th1 and Th2 cells, due in part to IL-2 induced STAT5 activity (253). However, NLRP3-deficiency reduces Th2 but not Th1 cell differentiation (253). Importantly, ASC or caspase-1 deficiency has no effect on NLRP3-mediated Th2 lineage differentiation ruling out a role for classical NLRP3 inflammasome activity (253). Findings indicate that NLRP3 functions as a transcription factor regulating *Il4* transcription (253). Here, NLRP3 forms a complex with the transcription factor IRF4, that enhances the binding of the IRF4 to the *Il4* promoter; however, NLRP3 alone is insufficient to mediate *Il4* transcription (253). Notably, induction of asthma, which is Th2 cell-dependent, is reduced in NLRP3-deficient mice (253). Furthermore, NLRP3$^{-/-}$ mice also more readily reject implanted B16F10 tumor cells due to an elevated Th1 cell response (253). In wildtype recipients, increased differentiation of Th2 cells permits the progression of B16F10 tumors (253). In the case of autoimmunity, aberrant Th2 cell differentiation has been associated with skewed development of Th1 and Th17 cells, which drive the pathology in MS, RA, T1D and SLE (254). Accordingly, aberrant expression and/or function of NLRP3 that is independent of inflammasome activity, may favor the development of pathogenic autoreactive Th1 and Th17 effectors. For instance, reduced IL-2 signaling and STAT5 activation, which is associated with T1D (255), would be expected to limit *Nlrp3* transcription and Th2 cell differentiation.

Roles of AIM2 independent of inflammasome activation

Studies demonstrate that AIM2 displays a number of alternative functions independent of inflammasome activation in various cell types, that affect the progression of autoimmunity. Recently, AIM2 was shown to have a T cell-intrinsic role in regulating peripheral Foxp3$^+$Treg (256). AIM2 is highly expressed in murine and human Foxp3$^+$Treg, and AIM2 expression is upregulated by TGF-β1 stimulation (256). TGF-β1 is required for peripheral differentiation of CD4$^+$ T cells into Foxp3$^+$Treg (257). In AIM2-deficient C57BL/6 mice, MOG_{35-55}-induced EAE is exacerbated characterized by increased Th1 and Th17 cell infiltration, and a reduction in the frequency of Foxp3$^+$Treg in the CNS (256). A diminished local pool of Foxp3$^+$Treg favors the expansion and effector function of encephalitogenic Teff (256, 257). Foxp3$^+$Treg are unaffected by ASC-deficiency, indicating that the role for AIM2 is inflammasome-independent (256). Notably, AIM2 in Foxp3$^+$Treg attenuates AKT activation, and downstream mTOR

and MYC signaling that leads to glycolysis (256). Normal Foxp3$^+$Treg differentiation and lineage maintenance is achieved under metabolic conditions favoring oxidative phosphorylation of lipids (256). On the other hand, glycolysis negatively impacts Foxp3$^+$Treg stability and function (256). AIM2 serves to maintain Foxp3$^+$Treg under proinflammatory conditions by forming a complex consisting of the adaptor protein receptor for activated C kinase 1 (RACK1), and the protein phosphatase 2 (PP2A) phosphatase that blocks AKT phosphorylation (256).

AIM2 has also been reported to regulate Tfh independent of inflammasome activation (258). Tfh from blood and skin lesions of SLE patients express elevated levels of AIM2. In mice in which AIM2 is conditionally ablated in T cells, the severity of pristane-induced lupus nephritis is reduced relative to control animals. The latter corresponds with a decreased Tfh pool. Notably, AIM2 regulates Tfh differentiation through an interaction with transcription factor c-MAF, that in turn is needed to promote *Il21* gene transcription (258). Interestingly, *Aim2* mRNA expression is upregulated by IL-21 stimulation suggesting that AIM2 participates in a feed-forward loop promoting Tfh differentiation and function.

In addition to T cells, AIM2 has been shown to have a B cell-intrinsic effect independent of inflammasome activation. SLE patients exhibit elevated AIM2 expression in germinal center (GC) B cells, memory B cells and antibody secreting plasma cells prepared from the tonsils, blood and/or skin lesions (259). Furthermore, pristane-induced lupus nephritis is attenuated in mice in which AIM2 is conditionally ablated in B cells. Limited disease is reflected by diminished numbers of GC B cells, and plasma cells. Findings suggest that AIM2 is an upstream regulator of the Blimp1-BCL6 transcriptional axis, which drives GC B cell and plasma cell differentiation (259).

AIM2 also serves a protective role in EAE by limiting the inflammatory properties of brain-resident microglia (151). Whereas ASC-deficiency in mice attenuates EAE as discussed above, AIM2-deficiency exacerbates EAE severity. Furthermore, selective ablation of AIM2 in microglia is sufficient to enhance the encephalitogenic response. In microglia, AIM2 negatively regulates a proinflammatory phenotype by suppressing the activity of DNA-dependent protein kinase (DNA-PK) and downstream activation of AKT3. Inhibition of AKT3 reduces phosphorylation of the key transcriptional factor IRF3, which blocks the production of chemokines, type I IFN, and the expression of antigen presentation molecules by microglia (151). AIM2 similarly inhibits DNA-PK and AKT activation in colon epithelial cells to protect mice from colitis and colon cancer (260). Interestingly, a recent study provides evidence that AIM2 has an alternative role in an EAE model independent of robust classical inflammasome activation (152). Through the use of a novel reporter mouse to track inflammasome activation *in situ*, AIM2 activation is seen to be prevalent in astrocytes but not CNS infiltrating monocytes and macrophages. Despite elevated AIM2 expression, no marked *Il1b* expression and cell death are detected in astrocytes (152). The role of AIM2 in this scenario needs to be further defined.

Targeting inflammasome molecules to prevent/treat autoimmunity

Inflammasome molecules offer an appealing target for immunotherapy and the treatment of autoimmunity. Several inhibitors targeting inflammasome-related molecules have been identified, developed, and tested in preclinical studies or clinical trials (Table 3). MCC950, a small-molecule inhibitor, specifically binds to the Walker B motif of the NACHT domain of NLRP3 to block function (287). Therapeutic efficacy and safety of MCC950 and analogs (Inzomelid and Somalix) have been assessed in several preclinical studies with promising results (288–294) (TrialTrovelID-368867; TrialTrovelID-360928). Nevertheless, a phase II clinical trial for RA showed that MCC950 has safety concerns related to elevated serum liver enzyme levels. Other NLRP3 inhibitors are currently being evaluated in animal studies of EAE (264, 266, 272, 279).

Caspase-1 is another key target for therapeutic intervention of autoimmunity. VX-765 (belnacasan), a caspase-1 inhibitor, blocks GSDMD-mediated pyroptosis, reduces inflammasome-associated proteins in the CNS, and attenuates EAE in mice (275). However, testing of the related caspase-1 inhibitor VX-740 was discontinued in a RA clinical trial due to the liver toxicity observed in animal models (295). Inhibiting GSDMD by necrosulfonamide reduces neuroinflammation and necroptosis in collagenase VII-induced mouse intracerebral hemorrhage model (277). In addition, dimethyl fumarate, an immunosuppressive drug used for the treatment of recurrent remission MS and plaque psoriasis promotes succination of GSDMD, which in turn disrupts the interaction with caspase-1 and blocks pyropotosis (278). Disulfiram, a drug used for alcohol addiction treatment, blocks pore formation by targeting Cys191/Cys192 in GSDMD (261).

IL-1β, which is associated with the pathogenesis of several autoimmune diseases, has been therapeutically targeted. Two FDA-approved biologics that block IL-1 activity have been clinically tested. Anakinra is a recombinant human IL-1R antagonist mainly applied for the treatment of RA. Due to a short half-life and low response rate compared to other treatments available, the usage of anakinra is limited, and efficacy is selective. For example, anakinra shows no efficacy for the treatment of T1D and Sjogren's disease. Canakinumab is an anti-IL-1β neutralizing monoclonal antibody and has shown efficacy in RA and systemic juvenile idiopathic arthritis but no benefit for recent onset T1D patients (285, 296). IL-18 blockers have also been established but have not been applied for the treatment of autoimmunity.

Summary/conclusions

The evidence at hand establishes roles for classical inflammasome activated inflammation and alternative pathways regulated by inflammasome molecules in autoimmunity. Inflammasome molecules have been implicated in human MS, RA, T1D and SLE, and shown in corresponding disease models to override and/or maintain self-tolerance (Table 1). Intrinsic and

TABLE 3 Therapeutic strategies targeting inflammasomes for autoimmunity.

Targeted inflammasome-associated molecule	Therapeutic	Disease	Ref
Upstream signal of NLRP3	Disulfiram	MS	(261)
NLRP3	MCC950	MS	(262)
		RA	(99)
		SLE	(141)
	1,2,4-trimethoxybenzene	MS	(263)
	OLT1177	MS	(264)
		RA	(265)
	RRx-001	MS	(266)
	JC171	MS	(267)
	Tranilast	RA	(268)
	A20	RA	(104)
	Curcumin	SLE	(236)
	Melatonin	SLE	(137)
	Piperine	SLE	(269)
	Citral	SLE	(270)
AIM2	Myricitrin	RA	(271)
ASC	IC100	MS	(272)
	Lonidamine	MS	(273)
	Spirodalesol analog 8A	MS	(274)
Caspase-1	VX-765	MS	(275)
	VX-740	RA	(276)
GSDMD	Necrosulfonamide	MS	(277)
	DMF	MS	(278)
NF-κB	BAY11-7082	MS	(279)
		SLE	(280)
	Methotrexate	RA	(281) NCT04464642
	Icariin	SLE	(282)
Interleukin-1	Anakinra	RA	(283)
	Canakinumab	RA	(284)
		T1D	(285)
	Gevokizumab	T1D	(286)

Multiple sclerosis (MS); rheumatoid arthritis (RA); type 1 diabetes (T1D); systemic lupus erythematosus (SLE); Gasdermin D (GSDMD).

extrinsic effects on both APC and other innate effectors as well as T and B cells enables inflammasome molecules to establish the nature and specificity of an autoimmune response. Similarly, inflammasome molecules have intrinsic and extrinsic effects that alter the cellular integrity of tissues, independent of immune effectors. In a given tissue, inflammasome activity can impact inflammation by initiating and/or further driving a local autoimmune response, which in turn may be influenced by induction of pyroptosis versus PANoptosis cell death pathways. Alternatively, dysregulated inflammasome function can have more broad effects. This is seen with aberrant inflammasome activity reducing intestinal barrier function, which results in shifts within the microbiota composition that can impact the production of systemically released metabolites and favor proinflammatory versus immunoregulatory events (214).

The key events that drive inflammasome molecule activity in autoimmunity are poorly understood. What is apparent, however, is that multiple pathways and mechanisms exist to induce activation,

in part reflecting the specificity of different inflammasome molecules. Poorly understood environmental factors known to influence MS, T1D, RA and SLE are likely involved in inducing inflammasome molecule activity. Release of PAMPs due to microbial infections or DAMPs due to cytotoxic effects of drugs, toxins, or UV irradiation for example, are obvious candidates to engage classical inflammasome-mediated inflammation. Polymorphisms in various inflammasome genes may also contribute to the polygenic influence on the development of MS, T1D, RA and SLE. Genetic analyses show that single nucleotide polymorphisms (SNPs) in genes encoding sensor molecules (i.e. *NLRP1*, *NLRP3*, *AIM2*) and inflammasome-related proteins (i.e. *PYCARD*, *CASP1*) are linked with susceptibility to and/or response to therapy for MS, T1D, RA and SLE (75, 78, 98, 119, 120, 153, 297–303). However, whether the disease-linked SNPs override the normally tight regulation of gene expression and/or function of inflammasome molecules needs to be ascertained. Inflammasome activity is also the consequence of collateral damage induced by autoimmunity. Autoimmune-mediated cytotoxicity leads to the release of DAMPs and a proinflammatory *milieu* induces local cellular stress affecting metabolism and mitochondrial function for instance, that drive inflammasome molecule activity.

The relative contribution(s) inflammasome molecule activity has in autoimmunity is poorly understood. Questions of whether inflammasome molecules mediate initiating events and/or modulate the progression and severity of autoimmunity need to be addressed. Environmental insults have typically been proposed to initiate autoimmunity where inflammasome activation is likely to occur (Table 1). Alternatively, sterile inflammation driven by metabolically stressed cells may stimulate dysregulated inflammasome activity and initiate autoimmunity. Pancreatic β cells are susceptible to metabolic stress due high levels of insulin expression and secretion (304, 305) that may lead to NLRP3 activation, for example. Reports showing that inflammasome expression and activity are upregulated in MS, T1D, RA and SLE patients suggest a role in at least supporting disease progression. Feed-forward loops in which inflammasome molecule activity are self-sustaining as well as promoting autoimmune reactivity and *vice versa* have been described. The use of murine models of spontaneous autoimmunity coupled with cell-specific and inducible expression systems will be helpful in further defining the contribution in the disease process for a given inflammasome molecule.

Of keen interest moving forward is defining regulation of inflammasome molecule-mediated events that are independent of classical activation of inflammation (Table 2). A hint to the complexity that is involved is exemplified by AIM2. As discussed above AIM2 regulates peripheral Foxp3$^+$Treg differentiation by blocking AKT signaling through a AIM2-RACK1-PP2A complex (256). On the other hand, AIM2 suppresses colon carcinoma by binding to and inhibiting DNA-PK and downstream AKT signaling events needed for colon epithelial cell transformation (260). Therefore, depending on the cell-type, AIM2 inhibits PI3K-AKT signaling but *via* distinct complexes and mechanisms. Furthermore, AIM2 is reported to interact with the c-MAF transcription factor to positively promote Tfh differentiation (258). The nature of the signaling events that stimulate alternative inflammasome molecule activity, and the outcome of that activity in immune and non-immune cell types are important issues that require continued investigation.

To date, the therapeutic benefit of inhibiting inflammasome activation has mostly been demonstrated in animal disease models with limited success in the clinic (Table 3). The general lack of efficacy may reflect the timing and relative contribution of an inflammasome molecule in a given autoimmune disease. For instance, inflammasome activation may play a prominent role early in a disease process. Therefore, targeting inflammasome activity once an autoimmune response is well established, which is typical in the clinic, may have only a minimal effect. There is the important concern that inhibiting a given inflammasome molecule, particularly long-term, may compromise immunity against pathogens. Therefore, both efficacy and safety may be enhanced by combining an inflammasome-based approach with other types of immunotherapies. For example, limiting ongoing inflammation by blocking inflammasome activity may enhance the efficacy of antigen-based immunotherapy and induction of protective Treg.

The etiology of MS, T1D, RA and SLE is highly complex, and ill-defined. Establishing the roles of inflammasome activity in autoimmunity will aid our understanding of the mechanisms that drive these disease processes, as well as provide the impetus for the development of novel strategies of immunotherapy for disease prevention and treatment.

Author contributions

QK, AG, VM, XJ and RT contributed to the preparation of the review article. All authors contributed to the article and approved the submitted version.

Funding

This work was supported by National Institutes of Health grants R01DK100256, R01AI139475, R01AI141631, R21AI115752 (RT).

Conflict of interest

The authors declare that the research was conducted in the absence of any commercial or financial relationships that could be construed as a potential conflict of interest.

Publisher's note

References

1. Davidson A, Diamond B. Autoimmune diseases. *N Engl J Med* (2001) 345(5):340–50. doi: 10.1056/nejm200108023450506

2. Papp G, Boros P, Nakken B, Szodoray P, Zeher M. Regulatory immune cells and functions in autoimmunity and transplantation immunology. *Autoimmun Rev* (2017) 16(5):435–44. doi: 10.1016/j.autrev.2017.03.011

3. Davis BK, Wen H, Ting JP. The inflammasome NLRS in immunity, inflammation, and associated diseases. *Annu Rev Immunol* (2011) 29:707–35. doi: 10.1146/annurev-immunol-031210-101405

4. Lamkanfi M, Dixit VM. Mechanisms and functions of inflammasomes. *Cell* (2014) 157(5):1013–22. doi: 10.1016/j.cell.2014.04.007

5. Cordero MD, Alcocer-Gómez E, Ryffel B. Gain of function mutation and inflammasome driven diseases in human and mouse models. *J Autoimmun* (2018) 91:13–22. doi: 10.1016/j.jaut.2018.03.002

6. Drutman SB, Haerynck F, Zhong FL, Hum D, Hernandez NJ, Belkaya S, et al. Homozygous NLRP1 gain-of-Function mutation in siblings with a syndromic form of recurrent respiratory papillomatosis. *Proc Natl Acad Sci USA* (2019) 116(38):19055–63. doi: 10.1073/pnas.1906184116

7. Romberg N, Vogel TP, Canna SW. NLRc4 inflammasomopathies. *Curr Opin Allergy Clin Immunol* (2017) 17(6):398–404. doi: 10.1097/aci.0000000000000396

8. Guo H, Callaway JB, Ting JP. Inflammasomes: Mechanism of action, role in disease, and therapeutics. *Nat Med* (2015) 21(7):677–87. doi: 10.1038/nm.3893

9. Deets KA, Vance RE. Inflammasomes and adaptive immune responses. *Nat Immunol* (2021) 22(4):412–22. doi: 10.1038/s41590-021-00869-6

10. Shi J, Zhao Y, Wang K, Shi X, Wang Y, Huang H, et al. Cleavage of GSDMD by inflammatory caspases determines pyroptotic cell death. *Nature* (2015) 526(7575):660–5. doi: 10.1038/nature15514

11. Malik A, Kanneganti TD. Inflammasome activation and assembly at a glance. *J Cell Sci* (2017) 130(23):3955–63. doi: 10.1242/jcs.207365

12. Broz P, Dixit VM. Inflammasomes: Mechanism of assembly, regulation and signalling. *Nat Rev Immunol* (2016) 16(7):407–20. doi: 10.1038/nri.2016.58

13. Pandian N, Kanneganti TD. Panoptosis: A unique innate immune inflammatory cell death modality. *J Immunol* (2022) 209(9):1625–33. doi: 10.4049/jimmunol.2200508

14. Samir P, Malireddi RKS, Kanneganti TD. The panoptosome: A deadly protein complex driving pyroptosis, apoptosis, and necroptosis (Panoptosis). *Front Cell Infect Microbiol* (2020) 10:238. doi: 10.3389/fcimb.2020.00238

15. Gullett JM, Tweedell RE, Kanneganti TD. It's all in the PAN: Crosstalk, plasticity, redundancies, switches, and interconnectedness encompassed by PANoptosis underlying the totality of cell death-associated biological effects. *Cells* (2022) 11(9). doi: 10.3390/cells11091495

16. Pearson JA, Wong FS, Wen L. Inflammasomes and type 1 diabetes. *Front Immunol* (2021) 12:686956. doi: 10.3389/fimmu.2021.686956

17. Tartey S, Kanneganti TD. Inflammasomes in the pathophysiology of autoinflammatory syndromes. *J Leukoc Biol* (2020) 107(3):379–91. doi: 10.1002/jlb.3mir0919-191r

18. Swanson KV, Deng M, Ting JP. The NLRP3 inflammasome: Molecular activation and regulation to therapeutics. *Nat Rev Immunol* (2019) 19(8):477–89. doi: 10.1038/s41577-019-0165-0

19. Jo EK, Kim JK, Shin DM, Sasakawa C. Molecular mechanisms regulating NLRP3 inflammasome activation. *Cell Mol Immunol* (2016) 13(2):148–59. doi: 10.1038/cmi.2015.95

20. Blevins HM, Xu Y, Biby S, Zhang S. The NLRP3 inflammasome pathway: A review of mechanisms and inhibitors for the treatment of inflammatory diseases. *Front Aging Neurosci* (2022) 14:879021. doi: 10.3389/fnagi.2022.879021

21. Hagar JA, Powell DA, Aachoui Y, Ernst RK, Miao EA. Cytoplasmic LPS activates caspase-11: Implications in TLR4-independent endotoxic shock. *Science* (2013) 341(6151):1250–3. doi: 10.1126/science.1240988

22. Yang Y, Wang H, Kouadir M, Song H, Shi F. Recent advances in the mechanisms of NLRP3 inflammasome activation and its inhibitors. *Cell Death Dis* (2019) 10(2):128. doi: 10.1038/s41419-019-1413-8

23. Kayagaki N, Wong MT, Stowe IB, Ramani SR, Gonzalez LC, Akashi-Takamura S, et al. Noncanonical inflammasome activation by intracellular LPS independent of TLR4. *Science* (2013) 341(6151):1246–9. doi: 10.1126/science.1240248

24. Halle A, Hornung V, Petzold GC, Stewart CR, Monks BG, Reinheckel T, et al. The Nalp3 inflammasome is involved in the innate immune response to amyloid-beta. *Nat Immunol* (2008) 9(8):857–65. doi: 10.1038/ni.1636

25. Saresella M, La Rosa F, Piancone F, Zoppis M, Marventano I, Calabrese E, et al. The NLRP3 and NLRP1 inflammasomes are activated in Alzheimer's disease. *Mol Neurodegener* (2016) 11:23. doi: 10.1186/s13024-016-0088-1

26. Sandstrom A, Mitchell PS, Goers L, Mu EW, Lesser CF, Vance RE. Functional degradation: A mechanism of NLRP1 inflammasome activation by diverse pathogen enzymes. *Science* (2019) 364(6435):eaau1330. doi: 10.1126/science.aau1330

27. Chui AJ, Okondo MC, Rao SD, Gai K, Griswold AR, Johnson DC, et al. N-terminal degradation activates the NLRP1b inflammasome. *Science* (2019) 364(6435):82–5. doi: 10.1126/science.aau1208

28. Xu H, Shi J, Gao H, Liu Y, Yang Z, Shao F, et al. The N-end rule ubiquitin ligase Ubr2 mediates NLRP1b inflammasome activation by anthrax lethal toxin. *EMBO J* (2019) 38(13):e101996. doi: 10.15252/embj.2019101996

29. Robert Hollingsworth L, David L, Li Y, Griswold AR, Ruan J, Sharif H, et al. Mechanism of filament formation in upa-promoted Card8 and NLRP1 inflammasomes. *Nat Commun* (2021) 12(1):189. doi: 10.1038/s41467-020-20320-y

30. Planès R, Pinilla M, Santoni K, Hessel A, Passemar C, Lay K, et al. Human NLRP1 is a sensor of pathogenic coronavirus 3cl proteases in lung epithelial cells. *Mol Cell* (2022) 82(13):2385–400.e9. doi: 10.1016/j.molcel.2022.04.033

31. Bauernfried S, Scherr MJ, Pichlmair A, Duderstadt KE, Hornung V. Human NLRP1 is a sensor for double-stranded rna. *Science* (2021) 371(6528):eabd0811. doi: 10.1126/science.abd0811

32. Tsu BV, Beierschmitt C, Ryan AP, Agarwal R, Mitchell PS, Daugherty MD. Diverse viral proteases activate the NLRP1 inflammasome. *Elife* (2021) 10:e60609. doi: 10.7554/eLife.60609

33. Robinson KS, Teo DET, Tan KS, Toh GA, Ong HH, Lim CK, et al. Enteroviral 3c protease activates the human NLRP1 inflammasome in airway epithelia. *Science* (2020) 370(6521):eaay2002. doi: 10.1126/science.aay2002

34. Levinsohn JL, Newman ZL, Hellmich KA, Fattah R, Getz MA, Liu S, et al. Anthrax lethal factor cleavage of NLRP1 is required for activation of the inflammasome. *PloS Pathog* (2012) 8(3):e1002638. doi: 10.1371/journal.ppat.1002638

35. Mitchell PS, Sandstrom A, Vance RE. The NLRP1 inflammasome: New mechanistic insights and unresolved mysteries. *Curr Opin Immunol* (2019) 60:37–45. doi: 10.1016/j.coi.2019.04.015

36. Okondo MC, Johnson DC, Sridharan R, Go EB, Chui AJ, Wang MS, et al. Dpp8 and Dpp9 inhibition induces pro-Caspase-1-dependent monocyte and macrophage pyroptosis. *Nat Chem Biol* (2017) 13(1):46–53. doi: 10.1038/nchembio.2229

37. Zhong FL, Robinson K, Teo DET, Tan KY, Lim C, Harapas CR, et al. Human Dpp9 represses NLRP1 inflammasome and protects against autoinflammatory diseases *via* both peptidase activity and fiind domain binding. *J Biol Chem* (2018) 293(49):18864–78. doi: 10.1074/jbc.RA118.004350

38. Miao EA, Mao DP, Yudkovsky N, Bonneau R, Lorang CG, Warren SE, et al. Innate immune detection of the type iii secretion apparatus through the NLRc4 inflammasome. *Proc Natl Acad Sci USA* (2010) 107(7):3076–80. doi: 10.1073/pnas.0913087107

39. Zhao Y, Yang J, Shi J, Gong YN, Lu Q, Xu H, et al. The NLRc4 inflammasome receptors for bacterial flagellin and type iii secretion apparatus. *Nature* (2011) 477(7366):596–600. doi: 10.1038/nature10510

40. Canna SW, de Jesus AA, Gouni S, Brooks SR, Marrero B, Liu Y, et al. An activating NLRc4 inflammasome mutation causes autoinflammation with recurrent macrophage activation syndrome. *Nat Genet* (2014) 46(10):1140–6. doi: 10.1038/ng.3089

41. Hornung V, Ablasser A, Charrel-Dennis M, Bauernfeind F, Horvath G, Caffrey DR, et al. AIM2 recognizes cytosolic dsDNA and forms a caspase-1-Activating inflammasome with ASC. *Nature* (2009) 458(7237):514–8. doi: 10.1038/nature07725

42. Man SM, Karki R, Kanneganti TD. AIM2 inflammasome in infection, cancer, and autoimmunity: Role in DNA sensing, inflammation, and innate immunity. *Eur J Immunol* (2016) 46(2):269–80. doi: 10.1002/eji.201545839

43. Hu B, Jin C, Li HB, Tong J, Ouyang X, Cetinbas NM, et al. The DNA-sensing AIM2 inflammasome controls radiation-induced cell death and tissue injury. *Science* (2016) 354(6313):765–8. doi: 10.1126/science.aaf7532

44. Garlanda C, Dinarello CA, Mantovani A. The interleukin-1 family: Back to the future. *Immunity* (2013) 39(6):1003–18. doi: 10.1016/j.immuni.2013.11.010

45. Dinarello CA. Immunological and inflammatory functions of the interleukin-1 family. *Annu Rev Immunol* (2009) 27:519–50. doi: 10.1146/annurev.immunol.021908.132612

46. Chan AH, Schroder K. Inflammasome signaling and regulation of interleukin-1 family cytokines. *J Exp Med* (2020) 217(1):e20190314. doi: 10.1084/jem.20190314

47. Waisman A, Lukas D, Clausen BE, Yogev N. Dendritic cells as gatekeepers of tolerance. *Semin Immunopathol* (2017) 39(2):153–63. doi: 10.1007/s00281-016-0583-z

48. Zaghouani H, Miller MM. Early-life T-helper 1 immunity. *Crit Rev Immunol* (2020) 40(5):407–11. doi: 10.1615/CritRevImmunol.2020035106

49. Martynova E, Rizvanov A, Urbanowicz RA, Khaiboullina S. Inflammasome contribution to the activation of Th1, Th2, and Th17 immune responses. *Front Microbiol* (2022) 13:851835. doi: 10.3389/fmicb.2022.851835

50. Zhang S. The role of transforming growth factor B in T helper 17 differentiation. *Immunology* (2018) 155(1):24–35. doi: 10.1111/imm.12938

51. Ikeda S, Saijo S, Murayama MA, Shimizu K, Akitsu A, Iwakura Y. Excess IL-1 signaling enhances the development of Th17 cells by downregulating TGFbeta-Induced Foxp3 expression. *J Immunol* (2014) 192(4):1449–58. doi: 10.4049/jimmunol.1300387

52. Zhu X, Zhu J. CD4 T helper cell subsets and related human immunological disorders. *Int J Mol Sci* (2020) 21(21). doi: 10.3390/ijms21218011

53. Bennett CL, Christie J, Ramsdell F, Brunkow ME, Ferguson PJ, Whitesell L, et al. The immune dysregulation, polyendocrinopathy, enteropathy, X-linked syndrome

(IPEX) is caused by mutations of Foxp3. *Nat Genet* (2001) 27(1):20–1. doi: 10.1038/83713

54. Brunkow ME, Jeffery EW, Hjerrild KA, Paeper B, Clark LB, Yasayko SA, et al. Disruption of a new Forkhead/Winged-helix protein, scurfin, results in the fatal lymphoproliferative disorder of the scurfy mouse. *Nat Genet* (2001) 27(1):68–73. doi: 10.1038/83784

55. Van Gool F, Nguyen MLT, Mumbach MR, Satpathy AT, Rosenthal WL, Giacometti S, et al. A mutation in the transcription factor Foxp3 drives T helper 2 effector function in regulatory T cells. *Immunity* (2019) 50(2):362–77.e6. doi: 10.1016/j.immuni.2018.12.016

56. Wildin RS, Ramsdell F, Peake J, Faravelli F, Casanova JL, Buist N, et al. X-Linked neonatal diabetes mellitus, enteropathy and endocrinopathy syndrome is the human equivalent of mouse scurfy. *Nat Genet* (2001) 27(1):18–20. doi: 10.1038/83707

57. Ben-Sasson SZ, Hogg A, Hu-Li J, Wingfield P, Chen X, Crank M, et al. IL-1 enhances expansion, effector function, tissue localization, and memory response of antigen-specific CD8 T cells. *J Exp Med* (2013) 210(3):491–502. doi: 10.1084/jem.20122006

58. Dolence JJ, Kobayashi T, Iijima K, Krempski J, Drake LY, Dent AL, et al. Airway exposure initiates peanut allergy by involving the IL-1 pathway and T follicular helper cells in mice. *J Allergy Clin Immunol* (2018) 142(4):1144–58 e8. doi: 10.1016/j.jaci.2017.11.020

59. Choi J, Crotty S. Bcl6-mediated transcriptional regulation of follicular helper T cells (T_{FH}). *Trends Immunol* (2021) 42(4):336–49. doi: 10.1016/j.it.2021.02.002

60. Kaplanski G. Interleukin-18: Biological properties and role in disease pathogenesis. *Immunol Rev* (2018) 281(1):138–53. doi: 10.1111/imr.12616

61. Novick D, Kim S, Kaplanski G, Dinarello CA. Interleukin-18, more than a Th1 cytokine. *Semin Immunol* (2013) 25(6):439–48. doi: 10.1016/j.smim.2013.10.014

62. Tsutsui H, Nakanishi K, Matsui K, Higashino K, Okamura H, Miyazawa Y, et al. IFN-gamma-inducing factor up-regulates fas ligand-mediated cytotoxic activity of murine natural killer cell clones. *J Immunol* (1996) 157(9):3967–73.

63. Nowarski R, Jackson R, Gagliani N, de Zoete MR, Palm NW, Bailis W, et al. Epithelial IL-18 equilibrium controls barrier function in colitis. *Cell* (2015) 163(6):1444–56. doi: 10.1016/j.cell.2015.10.072

64. Somm E, Jornayvaz FR. Interleukin-18 in metabolism: From mice physiology to human diseases. *Front Endocrinol (Lausanne)* (2022) 13:971745. doi: 10.3389/fendo.2022.971745

65. Dagar S, Singh J, Saini A, Kumar Y, Chhabra S, Minz RW, et al. Gut bacteriome, mycobiome and virome alterations in rheumatoid arthritis. *Front Endocrinol (Lausanne)* (2022) 13:1044673. doi: 10.3389/fendo.2022.1044673

66. Davis-Richardson AG, Triplett EW. A model for the role of gut bacteria in the development of autoimmunity for type 1 diabetes. *Diabetologia* (2015) 58(7):1386–93. doi: 10.1007/s00125-015-3614-8

67. Donati D. Viral infections and multiple sclerosis. *Drug Discovery Today Dis Models* (2020) 32:27–33. doi: 10.1016/j.ddmod.2020.02.003

68. Karampoor S, Zahednasab H, Ramagopalan S, Mehrpour M, Etemadifar M, Alsahebfosoul F, et al. Cytomegalovirus and varicella zoster virus seropositivity of Iranian patients with multiple sclerosis: A population-based study. *J Neuroimmunol* (2017) 309:4–6. doi: 10.1016/j.jneuroim.2017.04.004

69. Marrodan M, Alessandro L, Farez MF, Correale J. The role of infections in multiple sclerosis. *Mult Scler* (2019) 25(7):891–901. doi: 10.1177/1352458518823940

70. Lane TE, Hosking MP. The pathogenesis of murine coronavirus infection of the central nervous system. *Crit Rev Immunol* (2010) 30(2):119–30. doi: 10.1615/critrevimmunol.v30.i2.20

71. Morris MM, Dyson H, Baker D, Harbige LS, Fazakerley JK, Amor S. Characterization of the cellular and cytokine response in the central nervous system following semliki forest virus infection. *J Neuroimmunol* (1997) 74(1-2):185–97. doi: 10.1016/s0165-5728(96)00786-2

72. Bernales CQ, Encarnacion M, Criscuoli MG, Yee IM, Traboulsee AL, Sadovnick AD, et al. Analysis of NOD-like receptor NLRP1 in multiple sclerosis families. *Immunogenetics* (2018) 70(3):205–7. doi: 10.1007/s00251-017-1034-2

73. Maver A, Lavtar P, Ristić S, Stopinšek S, Simčič S, Hočevar K, et al. Identification of rare genetic variation of NLRP1 gene in familial multiple sclerosis. *Sci Rep* (2017) 7(1):3715. doi: 10.1038/s41598-017-03536-9

74. Popplewell LF, Encarnacion M, Bernales CQ, Sadovnick AD, Traboulsee AL, Quandt JA, et al. Genetic analysis of nucleotide-binding leucine-rich repeat (NLR) receptors in multiple sclerosis. *Immunogenetics* (2020) 72(6-7):381–5. doi: 10.1007/s00251-020-01170-w

75. Soares JL, Oliveira EM, Pontillo A. Variants in *NLRP3* and *NLRc4* inflammasome associate with susceptibility and severity of multiple sclerosis. *Mult Scler Relat Disord* (2019) 29:26–34. doi: 10.1016/j.msard.2019.01.023

76. Gil-Varea E, Urcelay E, Vilariño-Güell C, Costa C, Midaglia L, Matesanz F, et al. Exome sequencing study in patients with multiple sclerosis reveals variants associated with disease course. *J Neuroinflamm* (2018) 15(1):265. doi: 10.1186/s12974-018-1307-1

77. Freeman L, Guo H, David CN, Brickey WJ, Jha S, Ting JP. NLR members NLC4 and NLRP3 mediate sterile inflammasome activation in microglia and astrocytes. *J Exp Med* (2017) 214(5):1351–70. doi: 10.1084/jem.20150237

78. Gharagozloo M, Mahmoud S, Simard C, Yamamoto K, Bobbala D, Ilangumaran S, et al. NLRX1 inhibits the early stages of CNS inflammation and prevents the onset of spontaneous autoimmunity. *PloS Biol* (2019) 17(9):e3000451. doi: 10.1371/journal.pbio.3000451

79. Eitas TK, Chou WC, Wen H, Gris D, Robbins GR, Brickey J, et al. The nucleotide-binding leucine-rich repeat (NLR) family member NLRX1 mediates protection against experimental autoimmune encephalomyelitis and represses macrophage/microglia-induced inflammation. *J Biol Chem* (2014) 289(7):4173–9. doi: 10.1074/jbc.M113.533034

80. Tuladhar S, Kanneganti TD. NLRP12 in innate immunity and inflammation. *Mol Aspects Med* (2020) 76:100887. doi: 10.1016/j.mam.2020.100887

81. Gharagozloo M, Mahvelati TM, Imbeault E, Gris P, Zerif E, Bobbala D, et al. The nod-like receptor, NLRP12, plays an anti-inflammatory role in experimental autoimmune encephalomyelitis. *J Neuroinflamm* (2015) 12:198. doi: 10.1186/s12974-015-0414-5

82. Huang WX, Huang P, Hillert J. Increased expression of caspase-1 and interleukin-18 in peripheral blood mononuclear cells in patients with multiple sclerosis. *Mult Scler* (2004) 10(5):482–7. doi: 10.1191/1352458504ms1071oa

83. Inoue M, Williams KL, Gunn MD, Shinohara ML. NLRP3 inflammasome induces chemotactic immune cell migration to the CNS in experimental autoimmune encephalomyelitis. *Proc Natl Acad Sci USA* (2012) 109(26):10480–5. doi: 10.1073/pnas.1201836109

84. Fu Y, Zhan X, Wang Y, Jiang X, Liu M, Yang Y, et al. NLRc3 expression in dendritic cells attenuates CD4(+) T cell response and autoimmunity. *EMBO J* (2019) 38(16):e101397. doi: 10.15252/embj.2018101397

85. Li S, Wu Y, Yang D, Wu C, Ma C, Liu X, et al. Gasdermin D in peripheral myeloid cells drives neuroinflammation in experimental autoimmune encephalomyelitis. *J Exp Med* (2019) 216(11):2562–81. doi: 10.1084/jem.20190377

86. Martin BN, Wang C, Zhang CJ, Kang Z, Gulen MF, Zepp JA, et al. T Cell-intrinsic ASC critically promotes Th17-mediated experimental autoimmune encephalomyelitis. *Nat Immunol* (2016) 17(5):583–92. doi: 10.1038/ni.3389

87. Lukens JR, Gurung P, Shaw PJ, Barr MJ, Zaki MH, Brown SA, et al. The NLRP12 sensor negatively regulates autoinflammatory disease by modulating interleukin-4 production in T cells. *Immunity* (2015) 42(4):654–64. doi: 10.1016/j.immuni.2015.03.006

88. Gharagozloo M, Mahmoud S, Simard C, Mahvelati TM, Amrani A, Gris D. The dual immunoregulatory function of NLRP12 in T cell-mediated immune response: Lessons from experimental autoimmune encephalomyelitis. *Cells* (2018) 7(9):119. doi: 10.3390/cells7090119

89. Ming X, Li W, Maeda Y, Blumberg B, Raval S, Cook SD, et al. Caspase-1 expression in multiple sclerosis plaques and cultured glial cells. *J Neurol Sci* (2002) 197(1-2):9–18. doi: 10.1016/s0022-510x(02)00030-8

90. Mahmoud S, Gharagozloo M, Simard C, Amrani A, Gris D. NLRX1 enhances glutamate uptake and inhibits glutamate release by astrocytes. *Cells* (2019) 8(5). doi: 10.3390/cells8050400

91. Martinez-Martinez RE, Abud-Mendoza C, Patiño-Marin N, Rizo-Rodríguez JC, Little JW, Loyola-Rodríguez JP. Detection of periodontal bacterial DNA in serum and synovial fluid in refractory rheumatoid arthritis patients. *J Clin Periodontol* (2009) 36(12):1004–10. doi: 10.1111/j.1600-051X.2009.01496.x

92. Moen K, Brun JG, Valen M, Skartveit L, Eribe EK, Olsen I, et al. Synovial inflammation in active rheumatoid arthritis and psoriatic arthritis facilitates trapping of a variety of oral bacterial dnas. *Clin Exp Rheumatol* (2006) 24(6):656–63.

93. Reichert S, Haffner M, Keyßer G, Schäfer C, Stein JM, Schaller HG, et al. Detection of oral bacterial DNA in synovial fluid. *J Clin Periodontol* (2013) 40(6):591–8. doi: 10.1111/jcpe.12102

94. Romero-Figueroa MDS, Ramírez-Durán N, Montiel-Jarquín AJ, Horta-Baas G. Gut-joint axis: Gut dysbiosis can contribute to the onset of rheumatoid arthritis *via* multiple pathways. *Front Cell Infect Microbiol* (2023) 13:1092118. doi: 10.3389/fcimb.2023.1092118

95. Wang Y, Wei J, Zhang W, Doherty M, Zhang Y, Xie H, et al. Gut dysbiosis in rheumatic diseases: A systematic review and meta-analysis of 92 observational studies. *EBioMedicine* (2022) 80:104055. doi: 10.1016/j.ebiom.2022.104055

96. Addobbati C, da Cruz HLA, Adelino JE, Melo Tavares Ramos AL, Fragoso TS, Domingues A, et al. Polymorphisms and expression of inflammasome genes are associated with the development and severity of rheumatoid arthritis in Brazilian patients. *Inflammation Res* (2018) 67(3):255–64. doi: 10.1007/s00011-017-1119-2

97. Cheng L, Liang X, Qian L, Luo C, Li D. NLRP3 gene polymorphisms and expression in rheumatoid arthritis. *Exp Ther Med* (2021) 22(4):1110. doi: 10.3892/etm.2021.10544

98. Mathews RJ, Robinson JI, Battellino M, Wong C, Taylor JCBiologics in Rheumatoid Arthritis G, et al. Evidence of NLRP3-inflammasome activation in rheumatoid arthritis (RA); genetic variants within the NLRP3-inflammasome complex in relation to susceptibility to RA and response to anti-TNF treatment. *Ann Rheum Dis* (2014) 73(6):1202–10. doi: 10.1136/annrheumdis-2013-203276

99. Guo C, Fu R, Wang S, Huang Y, Li X, Zhou M, et al. NLRP3 inflammasome activation contributes to the pathogenesis of rheumatoid arthritis. *Clin Exp Immunol* (2018) 194(2):231–43. doi: 10.1111/cei.13167

100. Choulaki C, Papadaki G, Repa A, Kampouraki E, Kambas K, Ritis K, et al. Enhanced activity of NLRP3 inflammasome in peripheral blood cells of patients with active rheumatoid arthritis. *Arthritis Res Ther* (2015) 17(1):257. doi: 10.1186/s13075-015-0775-2

101. Ruscitti P, Cipriani P, Di Benedetto P, Liakouli V, Berardicurti O, Carubbi F, et al. Monocytes from patients with rheumatoid arthritis and type 2 diabetes mellitus display an increased production of interleukin (Il)-1β *via* the nucleotide-binding domain and leucine-rich repeat containing family pyrin 3(NLRP3)-inflammasome activation: A possible implication for therapeutic decision in these patients. *Clin Exp Immunol* (2015) 182(1):35–44. doi: 10.1111/cei.12667

102. Li Z, Guo J, Bi L. Role of the NLRP3 inflammasome in autoimmune diseases. *BioMed Pharmacother* (2020) 130:110542. doi: 10.1016/j.biopha.2020.110542

103. Ippagunta SK, Brand DD, Luo J, Boyd KL, Calabrese C, Stienstra R, et al. Inflammasome-independent role of apoptosis-associated speck-like protein containing a card (Asc) in T cell priming is critical for collagen-induced arthritis. *J Biol Chem* (2010) 285(16):12454–62. doi: 10.1074/jbc.M109.093252

104. Vande Walle L, Van Opdenbosch N, Jacques P, Fossoul A, Verheugen E, Vogel P, et al. Negative regulation of the NLRP3 inflammasome by A20 protects against arthritis. *Nature* (2014) 512(7512):69–73. doi: 10.1038/nature13322

105. Delgado-Arévalo C, Calvet-Mirabent M, Triguero-Martínez A, Vázquez de Luis E, Benguría-Filippini A, Largo R, et al. NLRC4-mediated activation of CD11c+ DC contributes to perpetuation of synovitis in rheumatoid arthritis. *JCI Insight* (2022) 7 (22). doi: 10.1172/jci.insight.152886

106. Jakobs C, Perner S, Hornung V. AIM2 drives joint inflammation in a self-DNA triggered model of chronic polyarthritis. *PloS One* (2015) 10(6):e0131702. doi: 10.1371/journal.pone.0131702

107. Baum R, Sharma S, Carpenter S, Li QZ, Busto P, Fitzgerald KA, et al. Cutting edge: AIM2 and endosomal tlrs differentially regulate arthritis and autoantibody production in DNAse ii-deficient mice. *J Immunol* (2015) 194(3):873–7. doi: 10.4049/jimmunol.1402573

108. Yang Z, Cao J, Yu C, Yang Q, Zhang Y, Han L. Caspase-1 mediated interleukin-18 activation in neutrophils promotes the activity of rheumatoid arthritis in a NLRP3 inflammasome independent manner. *Joint Bone Spine* (2016) 83(3):282–9. doi: 10.1016/j.jbspin.2015.07.006

109. Zhao C, Gu Y, Zeng X, Wang J. NLRP3 inflammasome regulates Th17 differentiation in rheumatoid arthritis. *Clin Immunol* (2018) 197:154–60. doi: 10.1016/j.clim.2018.09.007

110. Prado DS, Veras FP, Ferreira RG, Damasceno LEA, Melo PH, Zamboni DS, et al. NLRP12 controls arthritis severity by acting as a checkpoint inhibitor of Th17 cell differentiation. *FASEB J* (2020) 34(8):10907–19. doi: 10.1096/fj.202000795R

111. Chen Y, Fujuan Q, Chen E, Yu B, Zuo F, Yuan Y, et al. Expression of AIM2 in rheumatoid arthritis and its role on fibroblast-like synoviocytes. *Mediators Inflammation* (2020) 2020:1693730. doi: 10.1155/2020/1693730

112. Lin Y, Luo Z. NLRP6 facilitates the interaction between Tab2/3 and Trim38 in rheumatoid arthritis fibroblast-like synoviocytes. *FEBS Lett* (2017) 591(8):1141–9. doi: 10.1002/1873-3468.12622

113. Li XF, Shen WW, Sun YY, Li WX, Sun ZH, Liu YH, et al. MicroRNA-20a negatively regulates expression of NLRP3-inflammasome by targeting txnip in adjuvant-induced arthritis fibroblast-like synoviocytes. *Joint Bone Spine* (2016) 83 (6):695–700. doi: 10.1016/j.jbspin.2015.10.007

114. Tian J, Zhou D, Xiang L, Liu X, Zhang H, Wang B, et al. Mir-223-3p inhibits inflammation and pyroptosis in monosodium urate-induced rats and fibroblast-like synoviocytes by targeting NLRP3. *Clin Exp Immunol* (2021) 204(3):396–410. doi: 10.1111/cei.13587

115. Liu YR, Yan X, Yu HX, Yao Y, Wang JQ, Li XF, et al. NLRc5 promotes cell proliferation *via* regulating the NF-κB signaling pathway in rheumatoid arthritis. *Mol Immunol* (2017) 91:24–34. doi: 10.1016/j.molimm.2017.08.024

116. Filippi CM, von Herrath MG. Viral trigger for type 1 diabetes: Pros and cons. *Diabetes* (2008) 57(11):2863–71. doi: 10.2337/db07-1023

117. Sechi LA, Rosu V, Pacifico A, Fadda G, Ahmed N, Zanetti S. Humoral immune responses of type 1 diabetes patients to *Mycobacterium avium* subsp. *Paratuberculosis* lend support to the infectious trigger hypothesis. *Clin Vaccine Immunol* (2008) 15 (2):320–6. doi: 10.1128/cvi.00381-07

118. Magitta NF, Bøe Wolff AS, Johansson S, Skinningsrud B, Lie BA, Myhr KM, et al. A coding polymorphism in NALP1 confers risk for autoimmune addison's disease and type 1 diabetes. *Genes Immun* (2009) 10(2):120–4. doi: 10.1038/gene.2008.85

119. Sun X, Xia Y, Liu Y, Wang Y, Luo S, Lin J, et al. Polymorphisms in *NLRP1* gene are associated with type 1 diabetes. *J Diabetes Res* (2019) 2019:7405120. doi: 10.1155/2019/7405120

120. Pontillo A, Brandao L, Guimaraes R, Segat L, Araujo J, Crovella S. Two SNPs in *NLRP3* gene are involved in the predisposition to type-1 diabetes and celiac disease in a pediatric population from northeast Brazil. *Autoimmunity* (2010) 43(8):583–9. doi: 10.3109/08916930903540432

121. Sun X, Xu L, Xia Y, Luo S, Lin J, Xiao Y, et al. Rs3806265 and Rs4612666 of the *NLRP3* gene are associated with the titer of glutamic acid decarboxylase antibody in type 1 diabetes. *Front Endocrinol (Lausanne)* (2022) 13:835054. doi: 10.3389/fendo.2022.835054

122. Xu L, Sun X, Xia Y, Luo S, Lin J, Xiao Y, et al. Polymorphisms of the *NLRc4* gene are associated with the onset age, positive rate of gada and 2-h postprandial c-peptide in patients with type 1 diabetes. *Diabetes Metab Syndr Obes* (2020) 13:811–8. doi: 10.2147/dmso.S244882

123. Hu C, Ding H, Li Y, Pearson JA, Zhang X, Flavell RA, et al. NLRP3 deficiency protects from type 1 diabetes through the regulation of chemotaxis into the pancreatic islets. *Proc Natl Acad Sci USA* (2015) 112(36):11318–23. doi: 10.1073/pnas.1513509112

124. Leite JA, Pessenda G, Guerra-Gomes IC, de Santana AKM, André Pereira C, Ribeiro Campos Costa F, et al. The DNA sensor AIM2 protects against streptozotocin-induced type 1 diabetes by regulating intestinal homeostasis via the IL-18 pathway. *Cells* (2020) 9(4). doi: 10.3390/cells9040959

125. Wu C, Pan LL, Niu W, Fang X, Liang W, Li J, et al. Modulation of gut microbiota by low methoxyl pectin attenuates type 1 diabetes in non-obese diabetic mice. *Front Immunol* (2019) 10:1733. doi: 10.3389/fimmu.2019.01733

126. Jia LL, Zhang M, Liu H, Sun J, Pan LL. Early-life fingolimod treatment improves intestinal homeostasis and pancreatic immune tolerance in non-obese diabetic mice. *Acta Pharmacol Sin* (2021) 42(10):1620–9. doi: 10.1038/s41401-020-00590-4

127. Quaglia M, Merlotti G, De Andrea M, Borgogna C, Cantaluppi V. Viral infections and systemic lupus erythematosus: New players in an old story. *Viruses* (2021) 13(2). doi: 10.3390/v13020277

128. Chen C, Yan Q, Yao X, Li S, Lv Q, Wang G, et al. Alterations of the gut virome in patients with systemic lupus erythematosus. *Front Immunol* (2022) 13:1050895. doi: 10.3389/fimmu.2022.1050895

129. Li Y, Wang HF, Li X, Li HX, Zhang Q, Zhou HW, et al. Disordered intestinal microbes are associated with the activity of systemic lupus erythematosus. *Clin Sci (Lond)* (2019) 133(7):821–38. doi: 10.1042/cs20180841

130. Li BZ, Zhou HY, Guo B, Chen WJ, Tao JH, Cao NW, et al. Dysbiosis of oral microbiota is associated with systemic lupus erythematosus. *Arch Oral Biol* (2020) 113:104708. doi: 10.1016/j.archoralbio.2020.104708

131. Pontillo A, Girardelli M, Kamada AJ, Pancotto JA, Donadi EA, Crovella S, et al. Polimorphisms in inflammasome genes are involved in the predisposition to systemic lupus erythematosus. *Autoimmunity* (2012) 45(4):271–8. doi: 10.3109/08916934.2011.637532

132. Loras-Duclaux I, Descos B, Souillet G, Lachaux A, Badinand P, Montagnon N, et al. [Congenital intrinsic factor deficiency. apropos of 3 cases in a sibship]. *Arch Fr Pediatr* (1988) 45(3):197–9.

133. Huang T, Yin H, Ning W, Wang X, Chen C, Lin W, et al. Expression of inflammasomes NLRP1, NLRP3 and AIM2 in different pathologic classification of lupus nephritis. *Clin Exp Rheumatol* (2020) 38(4):680–90.

134. da Cruz HLA, Cavalcanti CAJ, de Azevedo Silva J, de Lima CAD, Fragoso TS, Barbosa AD, et al. Differential expression of the inflammasome complex genes in systemic lupus erythematosus. *Immunogenetics* (2020) 72(4):217–24. doi: 10.1007/s00251-020-01158-6

135. Inoue K, Ishizawa M, Kubota T. Monoclonal anti-dsDNA antibody 2c10 escorts DNA to intracellular DNA sensors in normal mononuclear cells and stimulates secretion of multiple cytokines implicated in lupus pathogenesis. *Clin Exp Immunol* (2020) 199(2):150–62. doi: 10.1111/cei.13382

136. Kahlenberg JM, Carmona-Rivera C, Smith CK, Kaplan MJ. Neutrophil extracellular trap-associated protein activation of the NLRP3 inflammasome is enhanced in lupus macrophages. *J Immunol* (2013) 190(3):1217–26. doi: 10.4049/jimmunol.1202388

137. Bonomini F, Dos Santos M, Veronese FV, Rezzani R. NLRP3 inflammasome modulation by melatonin supplementation in chronic pristane-induced lupus nephritis. *Int J Mol Sci* (2019) 20(14). doi: 10.3390/ijms20143466

138. Liu J, Berthier CC, Kahlenberg JM. Enhanced inflammasome activity in systemic lupus erythematosus is mediated *via* type I interferon-induced up-regulation of interferon regulatory factor 1. *Arthritis Rheumatol* (2017) 69(9):1840–9. doi: 10.1002/art.40166

139. Liu Y, Tao X, Tao J. Strategies of targeting inflammasome in the treatment of systemic lupus erythematosus. *Front Immunol* (2022) 13:894847. doi: 10.3389/fimmu.2022.894847

140. Faliti CE, Gualtierotti R, Rottoli E, Gerosa M, Perruzza L, Romagnani A, et al. P2X7 receptor restrains pathogenic tfh cell generation in systemic lupus erythematosus. *J Exp Med* (2019) 216(2):317–36. doi: 10.1084/jem.20171976

141. Fu R, Guo C, Wang S, Huang Y, Jin O, Hu H, et al. Podocyte activation of NLRP3 inflammasomes contributes to the development of proteinuria in lupus nephritis. *Arthritis Rheumatol* (2017) 69(8):1636–46. doi: 10.1002/art.40155

142. Fu R, Xia Y, Li M, Mao R, Guo C, Zhou M, et al. Pim-1 as a therapeutic target in lupus nephritis. *Arthritis Rheumatol* (2019) 71(8):1308–18. doi: 10.1002/art.40863

143. Noseworthy JH, Lucchinetti C, Rodriguez M, Weinshenker BG. Multiple sclerosis. *N Engl J Med* (2000) 343(13):938–52. doi: 10.1056/nejm200009283431307

144. Freeman LC, Ting JP. The pathogenic role of the inflammasome in neurodegenerative diseases. *J Neurochem* (2016) 136 Suppl 1:29–38. doi: 10.1111/jnc.13217

145. Ramagopalan SV, Sadovnick AD. Epidemiology of multiple sclerosis. *Neurol Clin* (2011) 29(2):207–17. doi: 10.1016/j.ncl.2010.12.010

146. Steinman L. No quiet surrender: Molecular guardians in multiple sclerosis brain. *J Clin Invest* (2015) 125(4):1371–8. doi: 10.1172/jci74255

147. Attfield KE, Jensen LT, Kaufmann M, Friese MA, Fugger L. The immunology of multiple sclerosis. *Nat Rev Immunol* (2022) 22(12):734–50. doi: 10.1038/s41577-022-00718-z

148. Bar-Or A. The immunology of multiple sclerosis. *Semin Neurol* (2008) 28 (1):29–45. doi: 10.1055/s-2007-1019124

149. Morales Y, Parisi JE, Lucchinetti CF. The pathology of multiple sclerosis: Evidence for heterogeneity. *Adv Neurol* (2006) 98:27–45.

150. Voet S, Mc Guire C, Hagemeyer N, Martens A, Schroeder A, Wieghofer P, et al. A20 critically controls microglia activation and inhibits inflammasome-dependent neuroinflammation. *Nat Commun* (2018) 9(1):2036. doi: 10.1038/s41467-018-04376-5

151. Ma C, Li S, Hu Y, Ma Y, Wu Y, Wu C, et al. AIM2 controls microglial inflammation to prevent experimental autoimmune encephalomyelitis. *J Exp Med* (2021) 218(5). doi: 10.1084/jem.20201796

152. Barclay WE, Aggarwal N, Deerhake ME, Inoue M, Nonaka T, Nozaki K, et al. The AIM2 inflammasome is activated in astrocytes during the late phase of EAE. *JCI Insight* (2022) 7(8). doi: 10.1172/jci.insight.155563

153. Gharagozloo M, Gris KV, Mahvelati T, Amrani A, Lukens JR, Gris D. NLR-dependent regulation of inflammation in multiple sclerosis. *Front Immunol* (2017) 8:2012. doi: 10.3389/fimmu.2017.02012

154. Geng YM, Wu BX. [One case of haemolysis after transcatheter closure of atrial septal defect]. *Zhonghua Xin Xue Guan Bing Za Zhi* (2012) 40(12):1062–3.

155. Cui Y, Yu H, Bu Z, Wen L, Yan L, Feng J. Focus on the role of the NLRP3 inflammasome in multiple sclerosis: Pathogenesis, diagnosis, and therapeutics. *Front Mol Neurosci* (2022) 15:894298. doi: 10.3389/fnmol.2022.894298

156. Keane RW, Dietrich WD, de Rivero Vaccari JP. Inflammasome proteins as biomarkers of multiple sclerosis. *Front Neurol* (2018) 9:135. doi: 10.3389/fneur.2018.00135

157. Voo VTF, O'Brien T, Butzkueven H, Monif M. The role of vitamin d and P2X7r in multiple sclerosis. *J Neuroimmunol* (2019) 330:159–69. doi: 10.1016/j.jneuroim.2019.03.004

158. Tavazzi B, Batocchi AP, Amorini AM, Nociti V, D'Urso S, Longo S, et al. Serum metabolic profile in multiple sclerosis patients. *Mult Scler Int* (2011) 2011:167156. doi: 10.1155/2011/167156

159. Lazzarino G, Amorini AM, Eikelenboom MJ, Killestein J, Belli A, Di Pietro V, et al. Cerebrospinal fluid atp metabolites in multiple sclerosis. *Mult Scler* (2010) 16 (5):549–54. doi: 10.1177/1352458510364196

160. Burger D, Molnarfi N, Weber MS, Brandt KJ, Benkhoucha M, Gruaz L, et al. Glatiramer acetate increases IL-1 receptor antagonist but decreases T cell-induced IL-1beta in human monocytes and multiple sclerosis. *Proc Natl Acad Sci USA* (2009) 106 (11):4355–9. doi: 10.1073/pnas.0812183106

161. Mellergård J, Edström M, Vrethem M, Ernerudh J, Dahle C. Natalizumab treatment in multiple sclerosis: Marked decline of chemokines and cytokines in cerebrospinal fluid. *Mult Scler* (2010) 16(2):208–17. doi: 10.1177/1352458509355068

162. Noroozi S, Meimand HAE, Arababadi MK, Nakhaee N, Asadikaram G. The effects of IFN-beta1 a on the expression of inflammasomes and apoptosis-associated speck-like proteins in multiple sclerosis patients. *Mol Neurobiol* (2017) 54(4):3031–7. doi: 10.1007/s12035-016-9864-8

163. Gris D, Ye Z, Iocca HA, Wen H, Craven RR, Gris P, et al. NLRP3 plays a critical role in the development of experimental autoimmune encephalomyelitis by mediating Th1 and Th17 responses. *J Immunol* (2010) 185(2):974–81. doi: 10.4049/jimmunol.0904145

164. Ataide MA, Andrade WA, Zamboni DS, Wang D, Souza Mdo C, Franklin BS, et al. Malaria-induced NLRP12/NLRP3-dependent caspase-1 activation mediates inflammation and hypersensitivity to bacterial superinfection. *PloS Pathog* (2014) 10 (1):e1003885. doi: 10.1371/journal.ppat.1003885

165. Vladimer GI, Weng D, Paquette SW, Vanaja SK, Rathinam VA, Aune MH, et al. The NLRP12 inflammasome recognizes Yersinia pestis. *Immunity* (2012) 37 (1):96–107. doi: 10.1016/j.immuni.2012.07.006

166. Williams KL, Lich JD, Duncan JA, Reed W, Rallabhandi P, Moore C, et al. The caterpiller protein monarch-1 is an antagonist of toll-like receptor-, tumor necrosis factor alpha-, and mycobacterium tuberculosis-induced pro-inflammatory signals. *J Biol Chem* (2005) 280(48):39914–24. doi: 10.1074/jbc.M502820200

167. Sun SC. Non-canonical NF-κB signaling pathway. *Cell Res* (2011) 21(1):71–85. doi: 10.1038/cr.2010.177

168. Smolen JS, Aletaha D, McInnes IB. Rheumatoid arthritis. *Lancet* (2016) 388 (10055):2023–38. doi: 10.1016/s0140-6736(16)30173-8

169. Aletaha D, Smolen JS. Diagnosis and management of rheumatoid arthritis: A review. *JAMA* (2018) 320(13):1360–72. doi: 10.1001/jama.2018.13103

170. Weyand CM, Wu B, Goronzy JJ. The metabolic signature of T cells in rheumatoid arthritis. *Curr Opin Rheumatol* (2020) 32(2):159–67. doi: 10.1097/bor.0000000000000683

171. Edilova MI, Akram A, Abdul-Sater AA. Innate immunity drives pathogenesis of rheumatoid arthritis. *BioMed J* (2021) 44(2):172–82. doi: 10.1016/j.bj.2020.06.010

172. Kotake S, Nanke Y, Yago T, Kawamoto M, Kobashigawa T, Yamanaka H. Elevated ratio of Th17 cell-derived Th1 cells (CD161(+)Th1 cells) to CD161(+)Th17 cells in peripheral blood of early-onset rheumatoid arthritis patients. *BioMed Res Int* (2016) 2016:4186027. doi: 10.1155/2016/4186027

173. Chen J, Li S, Shi J, Zhang L, Li J, Chen S, et al. Serum progranulin irrelated with Breg cell levels, but elevated in RA patients, reflecting high disease activity. *Rheumatol Int* (2016) 36(3):359–64. doi: 10.1007/s00296-015-3372-4

174. Smolen JS, Aletaha D, Barton A, Burmester GR, Emery P, Firestein GS, et al. Rheumatoid arthritis. *Nat Rev Dis Primers* (2018) 4:18001. doi: 10.1038/nrdp.2018.1

175. Pap T, Dankbar B, Wehmeyer C, Korb-Pap A, Sherwood J. Synovial fibroblasts and articular tissue remodelling: Role and mechanisms. *Semin Cell Dev Biol* (2020) 101:140–5. doi: 10.1016/j.semCDb.2019.12.006

176. Deane KD, Holers VM. The natural history of rheumatoid arthritis. *Clin Ther* (2019) 41(7):1256–69. doi: 10.1016/j.clinthera.2019.04.028

177. Carubbi F, Alunno A, Gerli R, Giacomelli R. Post-translational modifications of proteins: Novel insights in the autoimmune response in rheumatoid arthritis. *Cells* (2019) 8(7). doi: 10.3390/cells8070657

178. Wu XY, Li KT, Yang HX, Yang B, Lu X, Zhao LD, et al. Complement C1q synergizes with Ptx3 in promoting NLRP3 inflammasome over-activation and pyroptosis in rheumatoid arthritis. *J Autoimmun* (2020) 106:102336. doi: 10.1016/j.jaut.2019.102336

179. Alippe Y, Mbalaviele G. Omnipresence of inflammasome activities in inflammatory bone diseases. *Semin Immunopathol* (2019) 41(5):607–18. doi: 10.1007/s00281-019-00753-4

180. Kuwabara T, Ishikawa F, Kondo M, Kakiuchi T. The role of IL-17 and related cytokines in inflammatory autoimmune diseases. *Mediators Inflammation* (2017) 2017:3908061. doi: 10.1155/2017/3908061

181. Wahamaa H, Schierbeck H, Hreggvidsdottir HS, Palmblad K, Aveberger AC, Andersson U, et al. High mobility group box protein 1 in complex with lipopolysaccharide or IL-1 promotes an increased inflammatory phenotype in synovial fibroblasts. *Arthritis Res Ther* (2011) 13(4):R136. doi: 10.1186/ar3450

182. Croft AP, Campos J, Jansen K, Turner JD, Marshall J, Attar M, et al. Distinct fibroblast subsets drive inflammation and damage in arthritis. *Nature* (2019) 570 (7760):246–51. doi: 10.1038/s41586-019-1263-7

183. Lochhead RB, Ordoñez D, Arvikar SL, Aversa JM, Oh LS, Heyworth B, et al. Interferon-gamma production in Lyme arthritis synovial tissue promotes differentiation of fibroblast-like synoviocytes into immune effector cells. *Cell Microbiol* (2019) 21(2):e12992. doi: 10.1111/cmi.12992

184. Mousavi MJ, Karami J, Aslani S, Tahmasebi MN, Vaziri AS, Jamshidi A, et al. Transformation of fibroblast-like synoviocytes in rheumatoid arthritis; from a friend to foe. *Auto Immun Highlights* (2021) 12(1):3. doi: 10.1186/s13317-020-00145-x

185. Morgan R, Endres J, Behbahani-Nejad N, Phillips K, Ruth JH, Friday SC, et al. Expression and function of aminopeptidase N/CD13 produced by fibroblast-like synoviocytes in rheumatoid arthritis: Role of CD13 in chemotaxis of cytokine-activated T cells independent of enzymatic activity. *Arthritis Rheumatol* (2015) 67 (1):74–85. doi: 10.1002/art.38878

186. Harada S, Yamamura M, Okamoto H, Morita Y, Kawashima M, Aita T, et al. Production of interleukin-7 and interleukin-15 by fibroblast-like synoviocytes from patients with rheumatoid arthritis. *Arthritis Rheum* (1999) 42(7):1508–16. doi: 10.1002/1529-0131(199907)42:7<1508::Aid-anr26>3.0.Co;2-l

187. Liu R, Zhao P, Zhang Q, Che N, Xu L, Qian J, et al. Adiponectin promotes fibroblast-like synoviocytes producing IL-6 to enhance T follicular helper cells response in rheumatoid arthritis. *Clin Exp Rheumatol* (2020) 38(1):11–8.

188. Eljaafari A, Tartelin ML, Aissaoui H, Chevrel G, Osta B, Lavocat F, et al. Bone marrow-derived and synovium-derived mesenchymal cells promote Th17 cell expansion and activation through caspase 1 activation: Contribution to the chronicity of rheumatoid arthritis. *Arthritis Rheum* (2012) 64(7):2147–57. doi: 10.1002/art.34391

189. Lin J, Zhou Z, Huo R, Xiao L, Ouyang G, Wang L, et al. Cyr61 induces IL-6 production by fibroblast-like synoviocytes promoting Th17 differentiation in rheumatoid arthritis. *J Immunol* (2012) 188(11):5776–84. doi: 10.4049/jimmunol.1103201

190. Lee DG, Woo JW, Kwok SK, Cho ML, Park SH. Mrp8 promotes Th17 differentiation *via* upregulation of il-6 production by fibroblast-like synoviocytes in rheumatoid arthritis. *Exp Mol Med* (2013) 45(4):e20. doi: 10.1038/emm.2013.39

191. Wang B, Ma Z, Wang M, Sun X, Tang Y, Li M, et al. IL-34 upregulated Th17 production through increased IL-6 expression by rheumatoid fibroblast-like synoviocytes. *Mediators Inflammation* (2017) 2017:1567120. doi: 10.1155/2017/1567120

192. Gao S, Qi X, Li J, Sang L. Upregulated Kat7 in synovial fibroblasts promotes Th17 cell differentiation and infiltration in rheumatoid arthritis. *Biochem Biophys Res Commun* (2017) 489(2):235–41. doi: 10.1016/j.bbrc.2017.05.143

193. Tran CN, Davis MJ, Tesmer LA, Endres JL, Motyl CD, Smuda C, et al. Presentation of arthritogenic peptide to antigen-specific T cells by fibroblast-like synoviocytes. *Arthritis Rheum* (2007) 56(5):1497–506. doi: 10.1002/art.22573

194. Jäger E, Murthy S, Schmidt C, Hahn M, Strobel S, Peters A, et al. Calcium-sensing receptor-mediated NLRP3 inflammasome response to calciprotein particles drives inflammation in rheumatoid arthritis. *Nat Commun* (2020) 11(1):4243. doi: 10.1038/s41467-020-17749-6

195. Mukherjee S, Kumar R, Tsakem Lenou E, Basrur V, Kontoyiannis DL, Ioakeimidis F, et al. Deubiquitination of NLRP6 inflammasome by Cyld critically regulates intestinal inflammation. *Nat Immunol* (2020) 21(6):626–35. doi: 10.1038/s41590-020-0681-x

196. Joosten LA, Netea MG, Fantuzzi G, Koenders MI, Helsen MM, Sparrer H, et al. Inflammatory arthritis in caspase 1 gene-deficient mice: Contribution of proteinase 3 to caspase 1-independent production of bioactive interleukin-1beta. *Arthritis Rheum* (2009) 60(12):3651–62. doi: 10.1002/art.25006

197. Wertz IE, O'Rourke KM, Zhou H, Eby M, Aravind L, Seshagiri S, et al. De-ubiquitination and ubiquitin ligase domains of A20 downregulate NF-kappaB signalling. *Nature* (2004) 430(7000):694–9. doi: 10.1038/nature02794

198. Pugliese A. Autoreactive T cells in type 1 diabetes. *J Clin Invest* (2017) 127 (8):2881–91. doi: 10.1172/jci94549

199. Clark M, Kroger CJ, Tisch RM. Type 1 diabetes: A chronic anti-self inflammatory response. *Front Immunol* (2017) 8:1898. doi: 10.3389/fimmu.2017.01898

200. Tisch R, MCDevitt H. Insulin-dependent diabetes mellitus. *Cell* (1996) 85 (3):291–7. doi: 10.1016/s0092-8674(00)81106-x

201. van Belle TL, Coppieters KT, von Herrath MG. Type 1 diabetes: Etiology, immunology, and therapeutic strategies. *Physiol Rev* (2011) 91(1):79–118. doi: 10.1152/physrev.00003.2010

202. Atkinson MA. The pathogenesis and natural history of type 1 diabetes. *Cold Spring Harb Perspect Med* (2012) 2(11). doi: 10.1101/cshperspect.a007641

203. Katsarou A, Gudbjornsdottir S, Rawshani A, Dabelea D, Bonifacio E, Anderson BJ, et al. Type 1 diabetes mellitus. *Nat Rev Dis Primers* (2017) 3:17016. doi: 10.1038/nrdp.2017.16

204. Pearson JA, Agriantonis A, Wong FS, Wen L. Modulation of the immune system by the gut microbiota in the development of type 1 diabetes. *Hum Vaccin Immunother* (2018) 14(11):2580–96. doi: 10.1080/21645515.2018.1514354

205. Wen L, Ley RE, Volchkov PY, Stranges PB, Avanesyan L, Stonebraker AC, et al. Innate immunity and intestinal microbiota in the development of type 1 diabetes. *Nature* (2008) 455(7216):1109–13. doi: 10.1038/nature07336

206. Lebreton F, Berishvili E, Parnaud G, Rouget C, Bosco D, Berney T, et al. NLRP3 inflammasome is expressed and regulated in human islets. *Cell Death Dis* (2018) 9 (7):726. doi: 10.1038/s41419-018-0764-x

207. Carlos D, Costa FR, Pereira CA, Rocha FA, Yaochite JN, Oliveira GG, et al. Mitochondrial DNA activates the NLRP3 inflammasome and predisposes to type 1 diabetes in murine model. *Front Immunol* (2017) 8:164. doi: 10.3389/fimmu.2017.00164

208. Pereira CA, Carlos D, Ferreira NS, Silva JF, Zanotto CZ, Zamboni DS, et al. Mitochondrial DNA promotes NLRP3 inflammasome activation and contributes to endothelial dysfunction and inflammation in type 1 diabetes. *Front Physiol* (2019) 10:1557. doi: 10.3389/fphys.2019.01557

209. Schott WH, Haskell BD, Tse HM, Milton MJ, Piganelli JD, Choisy-Rossi CM, et al. Caspase-1 is not required for type 1 diabetes in the nod mouse. *Diabetes* (2004) 53 (1):99–104. doi: 10.2337/diabetes.53.1.99

210. Wen L, Green EA, Stratmann T, Panosa A, Gomis R, Eynon EE, et al. *In vivo* diabetogenic action of CD4+ T lymphocytes requires fas expression and is independent of IL-1 and IL-18. *Eur J Immunol* (2011) 41(5):1344–51. doi: 10.1002/eji.201041216

211. Thomas HE, Irawaty W, Darwiche R, Brodnicki TC, Santamaria P, Allison J, et al. IL-1 receptor deficiency slows progression to diabetes in the nod mouse. *Diabetes* (2004) 53(1):113–21. doi: 10.2337/diabetes.53.1.113

212. Burrows MP, Volchkov P, Kobayashi KS, Chervonsky AV. Microbiota regulates type 1 diabetes through toll-like receptors. *Proc Natl Acad Sci USA* (2015) 112(32):9973–7. doi: 10.1073/pnas.1508740112

213. Pearson JA, Kakabadse D, Davies J, Peng J, Warden-Smith J, Cuff S, et al. Altered gut microbiota activate and expand insulin B15-23-reactive CD8+ T cells. *Diabetes* (2019) 68(5):1002–13. doi: 10.2337/db18-0487

214. Mariño E, Richards JL, McLeod KH, Stanley D, Yap YA, Knight J, et al. Gut microbial metabolites limit the frequency of autoimmune T cells and protect against type 1 diabetes. *Nat Immunol* (2017) 18(5):552–62. doi: 10.1038/ni.3713

215. Markle JG, Frank DN, Mortin-Toth S, Robertson CE, Feazel LM, Rolle-Kampczyk U, et al. Sex differences in the gut microbiome drive hormone-dependent regulation of autoimmunity. *Science* (2013) 339(6123):1084–8. doi: 10.1126/science.1233521

216. Elinav E, Strowig T, Kau AL, Henao-Mejia J, Thaiss CA, Booth CJ, et al. NLRP6 inflammasome regulates colonic microbial ecology and risk for colitis. *Cell* (2011) 145 (5):745–57. doi: 10.1016/j.cell.2011.04.022

217. Fattinger SA, Geiser P, Samperio Ventayol P, Di Martino ML, Furter M, Felmy B, et al. Epithelium-autonomous Naip/NLRc4 prevents TNF-driven inflammatory destruction of the gut epithelial barrier in Salmonella-infected mice. *Mucosal Immunol* (2021) 14(3):615–29. doi: 10.1038/s41385-021-00381-y

218. Leber A, Hontecillas R, Zoccoli-Rodriguez V, Bienert C, Chauhan J, Bassaganya-Riera J. Activation of NLRX1 by NX-13 alleviates inflammatory bowel disease through immunometabolic mechanisms in CD4+ T cells. *J Immunol* (2019) 203 (12):3407–15. doi: 10.4049/jimmunol.1900364

219. Leber A, Hontecillas R, Tubau-Juni N, Zoccoli-Rodriguez V, Abedi V, Bassaganya-Riera J. NLRX1 modulates immunometabolic mechanisms controlling the host-gut microbiota interactions during inflammatory bowel disease. *Front Immunol* (2018) 9:363. doi: 10.3389/fimmu.2018.00363

220. Truax AD, Chen L, Tam JW, Cheng N, Guo H, Koblansky AA, et al. The inhibitory innate immune sensor NLRP12 maintains a threshold against obesity by regulating gut microbiota homeostasis. *Cell Host Microbe* (2018) 24(3):364–78.e6. doi: 10.1016/j.chom.2018.08.009

221. Chen L, Wilson JE, Koenigsknecht MJ, Chou WC, Montgomery SA, Truax AD, et al. NLRP12 attenuates colon inflammation by maintaining colonic microbial diversity and promoting protective commensal bacterial growth. *Nat Immunol* (2017) 18(5):541–51. doi: 10.1038/ni.3690

222. Tsokos GC, Lo MS, Costa Reis P, Sullivan KE. New insights into the immunopathogenesis of systemic lupus erythematosus. *Nat Rev Rheumatol* (2016) 12 (12):716–30. doi: 10.1038/nrrheum.2016.186

223. Moulton VR, Suarez-Fueyo A, Meidan E, Li H, Mizui M, Tsokos GC. Pathogenesis of human systemic lupus erythematosus: A cellular perspective. *Trends Mol Med* (2017) 23(7):615–35. doi: 10.1016/j.molmed.2017.05.006

224. Zhang H, Fu R, Guo C, Huang Y, Wang H, Wang S, et al. Anti-dsDNA antibodies bind to TLR4 and activate NLRP3 inflammasome in lupus monocytes/macrophages. *J Transl Med* (2016) 14(1):156. doi: 10.1186/s12967-016-0911-z

225. Shin MS, Kang Y, Lee N, Wahl ER, Kim SH, Kang KS, et al. Self double-stranded (ds)DNA induces IL-1beta production from human monocytes by activating NLRP3 inflammasome in the presence of anti-(ds)DNA antibodies. *J Immunol* (2013) 190(4):1407–15. doi: 10.4049/jimmunol.1201195

226. Shin MS, Kang Y, Lee N, Kim SH, Kang KS, Lazova R, et al. U1-small nuclear ribonucleoprotein activates the NLRP3 inflammasome in human monocytes. *J Immunol* (2012) 188(10):4769–75. doi: 10.4049/jimmunol.1103355

227. Shin MS, Kang Y, Wahl ER, Park HJ, Lazova R, Leng L, et al. Macrophage migration inhibitory factor regulates U1 small nuclear rnp immune complex-mediated activation of the NLRP3 inflammasome. *Arthritis Rheumatol* (2019) 71(1):109–20. doi: 10.1002/art.40672

228. Miao EA, Rajan JV, Aderem A. Caspase-1-Induced pyroptotic cell death. *Immunol Rev* (2011) 243(1):206–14. doi: 10.1111/j.1600-065X.2011.01044.x

229. Pisetsky DS, Lipsky PE. New insights into the role of antinuclear antibodies in systemic lupus erythematosus. *Nat Rev Rheumatol* (2020) 16(10):565–79. doi: 10.1038/s41584-020-0480-7

230. Brinkmann V, Zychlinsky A. Beneficial suicide: Why neutrophils die to make nets. *Nat Rev Microbiol* (2007) 5(8):577–82. doi: 10.1038/nrmicro1710

231. Papayannopoulos V. Neutrophil extracellular traps in immunity and disease. *Nat Rev Immunol* (2018) 18(2):134–47. doi: 10.1038/nri.2017.105

232. Eloranta ML, Ronnblom L. Cause and consequences of the activated type I interferon system in SLE. *J Mol Med (Berl)* (2016) 94(10):1103–10. doi: 10.1007/s00109-016-1421-4

233. Inoue M, Williams KL, Oliver T, Vandenabeele P, Rajan JV, Miao EA, et al. Interferon-beta therapy against EAE is effective only when development of the disease depends on the NLRP3 inflammasome. *Sci Signal* (2012) 5(225):ra38. doi: 10.1126/scisignal.2002767

234. Zhao J, Wang H, Dai C, Wang H, Zhang H, Huang Y, et al. P2X7 blockade attenuates murine lupus nephritis by inhibiting activation of the NLRP3/ASC/Caspase 1 pathway. *Arthritis Rheum* (2013) 65(12):3176–85. doi: 10.1002/art.38174

235. Zhu FG, Jiang W, Bhagat L, Wang D, Yu D, Tang JX, et al. A novel antagonist of toll-like receptors 7, 8 and 9 suppresses lupus disease-associated parameters in NZBW/F1 mice. *Autoimmunity* (2013) 46(7):419–28. doi: 10.3109/08916934.2013.798651

236. Zhao J, Wang J, Zhou M, Li M, Li M, Tan H. Curcumin attenuates murine lupus *via* inhibiting NLRP3 inflammasome. *Int Immunopharmacol* (2019) 69:213–6. doi: 10.1016/j.intimp.2019.01.046

237. Li D, Shi G, Wang J, Zhang D, Pan Y, Dou H, et al. Baicalein ameliorates pristane-induced lupus nephritis *via* activating Nrf2/Ho-1 in myeloid-derived suppressor cells. *Arthritis Res Ther* (2019) 21(1):105. doi: 10.1186/s13075-019-1876-0

238. Lu A, Li H, Niu J, Wu S, Xue G, Yao X, et al. Hyperactivation of the NLRP3 inflammasome in myeloid cells leads to severe organ damage in experimental lupus. *J Immunol* (2017) 198(3):1119–29. doi: 10.4049/jimmunol.1600659

239. Nawata A, Hisano S, Shimajiri S, Wang KY, Tanaka Y, Nakayama T. Podocyte and endothelial cell injury lead to nephrotic syndrome in proliferative lupus nephritis. *Histopathology* (2018) 72(7):1084–92. doi: 10.1111/his.13454

240. Lech M, Lorenz G, Kulkarni OP, Grosser MO, Stigrot N, Darisipudi MN, et al. NLRP3 and ASC suppress lupus-like autoimmunity by driving the immunosuppressive effects of TGF-beta receptor signalling. *Ann Rheum Dis* (2015) 74(12):2224–35. doi: 10.1136/annrheumdis-2014-205496

241. Panchanathan R, Xin H, Choubey D. Disruption of mutually negative regulatory feedback loop between interferon-inducible p202 protein and the E2f family of transcription factors in lupus-prone mice. *J Immunol* (2008) 180(9):5927–34. doi: 10.4049/jimmunol.180.9.5927

242. Haywood ME, Rose SJ, Horswell S, Lees MJ, Fu G, Walport MJ, et al. Overlapping BXSB congenic intervals, in combination with microarray gene expression, reveal novel lupus candidate genes. *Genes Immun* (2006) 7(3):250–63. doi: 10.1038/sj.gene.6364294

243. Yin Q, Sester DP, Tian Y, Hsiao YS, Lu A, Cridland JA, et al. Molecular mechanism for p202-mediated specific inhibition of AIM2 inflammasome activation. *Cell Rep* (2013) 4(2):327–39. doi: 10.1016/j.celrep.2013.06.024

244. Amer A, Franchi L, Kanneganti TD, Body-Malapel M, Ozören N, Brady G, et al. Regulation of Legionella phagosome maturation and infection through flagellin and host IPAF. *J Biol Chem* (2006) 281(46):35217–23. doi: 10.1074/jbc.M604933200

245. Bergsbaken T, Fink SL, den Hartigh AB, Loomis WP, Cookson BT. Coordinated host responses during pyroptosis: Caspase-1-dependent lysosome exocytosis and inflammatory cytokine maturation. *J Immunol* (2011) 187(5):2748–54. doi: 10.4049/jimmunol.1100477

246. Gross O, Yazdi AS, Thomas CJ, Masin M, Heinz LX, Guarda G, et al. Inflammasome activators induce interleukin-1α secretion *via* distinct pathways with differential requirement for the protease function of caspase-1. *Immunity* (2012) 36 (3):388–400. doi: 10.1016/j.immuni.2012.01.018

247. Keller M, Rüegg A, Werner S, Beer HD. Active caspase-1 is a regulator of unconventional protein secretion. *Cell* (2008) 132(5):818–31. doi: 10.1016/j.cell.2007.12.040

248. Luzio JP, Pryor PR, Bright NA. Lysosomes: Fusion and function. *Nat Rev Mol Cell Biol* (2007) 8(8):622–32. doi: 10.1038/nrm2217

249. Mezzaroma E, Toldo S, Farkas D, Seropian IM, Van Tassell BW, Salloum FN, et al. The inflammasome promotes adverse cardiac remodeling following acute myocardial infarction in the mouse. *Proc Natl Acad Sci USA* (2011) 108(49):19725–30. doi: 10.1073/pnas.1108586108

250. Syed FM, Hahn HS, Odley A, Guo Y, Vallejo JG, Lynch RA, et al. Proapoptotic effects of caspase-1/Interleukin-Converting enzyme dominate in myocardial ischemia. *Circ Res* (2005) 96(10):1103–9. doi: 10.1161/01.RES.0000166925.45995.ed

251. Zhang WH, Wang X, Narayanan M, Zhang Y, Huo C, Reed JC, et al. Fundamental role of the Rip2/Caspase-1 pathway in hypoxia and ischemia-induced neuronal cell death. *Proc Natl Acad Sci USA* (2003) 100(26):16012–7. doi: 10.1073/pnas.2534856100

252. Javanmard Khameneh H, Leong KWK, Mencarelli A, Vacca M, Mambwe B, Neo K, et al. The inflammasome adaptor ASC intrinsically limits CD4(+) T-cell proliferation to help maintain intestinal homeostasis. *Front Immunol* (2019) 10:1566. doi: 10.3389/fimmu.2019.01566

253. Bruchard M, Rebe C, Derangere V, Togbe D, Ryffel B, Boidot R, et al. The receptor NLRP3 is a transcriptional regulator of Th2 differentiation. *Nat Immunol* (2015) 16(8):859–70. doi: 10.1038/ni.3202

254. Raphael I, Nalawade S, Eagar TN, Forsthuber TG. T Cell subsets and their signature cytokines in autoimmune and inflammatory diseases. *Cytokine* (2015) 74 (1):5–17. doi: 10.1016/j.cyto.2014.09.011

255. Garg G, Tyler JR, Yang JH, Cutler AJ, Downes K, Pekalski M, et al. Type 1 diabetes-associated IL2ra variation lowers il-2 signaling and contributes to diminished CD4+CD25+ regulatory T cell function. *J Immunol* (2012) 188(9):4644–53. doi: 10.4049/jimmunol.1100272

256. Chou WC, Guo Z, Guo H, Chen L, Zhang G, Liang K, et al. AIM2 in regulatory T cells restrains autoimmune diseases. *Nature* (2021) 591(7849):300–5. doi: 10.1038/s41586-021-03231-w

257. Ziegler SF, Buckner JH. Foxp3 and the regulation of Treg/Th17 differentiation. *Microbes Infect* (2009) 11(5):594–8. doi: 10.1016/j.micinf.2009.04.002

258. Wu H, Deng Y, Long D, Yang M, Li Q, Feng Y, et al. The IL-21-Tet2-AIM2-C-Maf pathway drives the T follicular helper cell response in lupus-like disease. *Clin Transl Med* (2022) 12(3):e781. doi: 10.1002/ctm2.781

259. Yang M, Long D, Hu L, Zhao Z, Li Q, Guo Y, et al. AIM2 deficiency in b cells ameliorates systemic lupus erythematosus by regulating Blimp-1-Bcl-6 axis-mediated B-cell differentiation. *Signal Transduct Target Ther* (2021) 6(1):341. doi: 10.1038/s41392-021-00725-x

260. Wilson JE, Petrucelli AS, Chen L, Koblansky AA, Truax AD, Oyama Y, et al. Inflammasome-independent role of AIM2 in suppressing colon tumorigenesis *via* DNA-PK and AKT. *Nat Med* (2015) 21(8):906–13. doi: 10.1038/nm.3908

261. Hu JJ, Liu X, Xia S, Zhang Z, Zhang Y, Zhao J, et al. FDA-approved disulfiram inhibits pyroptosis by blocking gasdermin D pore formation. *Nat Immunol* (2020) 21 (7):736–45. doi: 10.1038/s41590-020-0669-6

262. Coll RC, Robertson AA, Chae JJ, Higgins SC, Muñoz-Planillo R, Inserra MC, et al. A small-molecule inhibitor of the NLRP3 inflammasome for the treatment of inflammatory diseases. *Nat Med* (2015) 21(3):248–55. doi: 10.1038/nm.3806

263. Pan RY, Kong XX, Cheng Y, Du L, Wang ZC, Yuan C, et al. 1,2,4-trimethoxybenzene selectively inhibits NLRP3 inflammasome activation and attenuates experimental autoimmune encephalomyelitis. *Acta Pharmacol Sin* (2021) 42(11):1769–79. doi: 10.1038/s41401-021-00613-8

264. Sanchez-Fernandez A, Skouras DB, Dinarello CA, Lopez-Vales R. Olt1177 (Dapansutrile), a selective NLRP3 inflammasome inhibitor, ameliorates experimental autoimmune encephalomyelitis pathogenesis. *Front Immunol* (2019) 10:2578. doi: 10.3389/fimmu.2019.02578

265. Marchetti C, Swartzwelter B, Koenders MI, Azam T, Tengesdal IW, Powers N, et al. NLRP3 inflammasome inhibitor Olt1177 suppresses joint inflammation in murine models of acute arthritis. *Arthritis Res Ther* (2018) 20(1):169. doi: 10.1186/s13075-018-1664-2

266. Chen Y, He H, Lin B, Chen Y, Deng X, Jiang W, et al. Rrx-001 ameliorates inflammatory diseases by acting as a potent covalent NLRP3 inhibitor. *Cell Mol Immunol* (2021) 18(6):1425–36. doi: 10.1038/s41423-021-00683-y

267. Guo C, Fulp JW, Jiang Y, Li X, Chojnacki JE, Wu J, et al. Development and characterization of a hydroxyl-sulfonamide analogue, 5-Chloro-N-[2-(4-Hydroxysulfamoyl-Phenyl)-Ethyl]-2-Methoxy-Benzamide, as a novel NLRP3 inflammasome inhibitor for potential treatment of multiple sclerosis. *ACS Chem Neurosci* (2017) 8(10):2194–201. doi: 10.1021/acschemneuro.7b00124

268. Huang Y, Jiang H, Chen Y, Wang X, Yang Y, Tao J, et al. Tranilast directly targets NLRP3 to treat inflammasome-driven diseases. *EMBO Mol Med* (2018) 10(4). doi: 10.15252/emmm.201708689

269. Peng X, Yang T, Liu G, Liu H, Peng Y, He L. Piperine ameliorated lupus nephritis by targeting Ampk-mediated activation of NLRP3 inflammasome. *Int Immunopharmacol* (2018) 65:448–57. doi: 10.1016/j.intimp.2018.10.025

270. Ka SM, Lin JC, Lin TJ, Liu FC, Chao LK, Ho CL, et al. Citral alleviates an accelerated and severe lupus nephritis model by inhibiting the activation signal of NLRP3 inflammasome and enhancing Nrf2 activation. *Arthritis Res Ther* (2015) 17:331. doi: 10.1186/s13075-015-0844-6

271. Shen C, Xu M, Xu S, Zhang S, Lin W, Li H, et al. Myricitrin inhibits fibroblast-like synoviocyte-mediated rheumatoid synovial inflammation and joint destruction by targeting AIM2. *Front Pharmacol* (2022) 13:905376. doi: 10.3389/fphar.2022.905376

272. Desu HL, Plastini M, Illiano P, Bramlett HM, Dietrich WD, de Rivero Vaccari JP, et al. Ic100: A novel anti-ASC monoclonal antibody improves functional outcomes in an animal model of multiple sclerosis. *J Neuroinflamm* (2020) 17(1):143. doi: 10.1186/s12974-020-01826-0

273. Chen C, Zhou Y, Ning X, Li S, Xue D, Wei C, et al. Directly targeting ASC by lonidamine alleviates inflammasome-driven diseases. *J Neuroinflamm* (2022) 19 (1):315. doi: 10.1186/s12974-022-02682-w

274. Liu W, Yang J, Fang S, Jiao C, Gao J, Zhang A, et al. Spirodalesol analog 8a inhibits NLRP3 inflammasome activation and attenuates inflammatory disease by directly targeting adaptor protein ASC. *J Biol Chem* (2022) 298(12):102696. doi: 10.1016/j.jbc.2022.102696

275. McKenzie BA, Mamik MK, Saito LB, Boghozian R, Monaco MC, Major EO, et al. Caspase-1 inhibition prevents glial inflammasome activation and pyroptosis in models of multiple sclerosis. *Proc Natl Acad Sci USA* (2018) 115(26):E6065–e74. doi: 10.1073/pnas.1722041115

276. Rudolphi K, Gerwin N, Verzijl N, van der Kraan P, van den Berg W. Pralnacasan, an inhibitor of interleukin-1beta converting enzyme, reduces joint damage in two murine models of osteoarthritis. *Osteoarthritis Cartilage* (2003) 11 (10):738–46. doi: 10.1016/s1063-4584(03)00153-5

277. Zhang X, Zhang Y, Wang F, Liu Y, Yong VW, Xue M. Necrosulfonamide alleviates acute brain injury of intracerebral hemorrhage *via* inhibiting inflammation and necroptosis. *Front Mol Neurosci* (2022) 15:916249. doi: 10.3389/fnmol.2022.916249

278. Humphries F, Shmuel-Galia L, Ketelut-Carneiro N, Li S, Wang B, Nemmara VV, et al. Succination inactivates gasdermin D and blocks pyroptosis. *Science* (2020) 369(6511):1633–7. doi: 10.1126/science.abb9818

279. Lang Y, Chu F, Liu L, Zheng C, Li C, Shen D, et al. Potential role of Bay11-7082, a NF-kappaB blocker inhibiting experimental autoimmune encephalomyelitis in C57BL/6j mice *via* declining NLRP3 inflammasomes. *Clin Exp Immunol* (2021) 207 (3):378–86. doi: 10.1093/cei/uxab022

280. Zhao J, Zhang H, Huang Y, Wang H, Wang S, Zhao C, et al. Bay11-7082 attenuates murine lupus nephritis *via* inhibiting NLRP3 inflammasome and NF-κB activation. *Int Immunopharmacol* (2013) 17(1):116–22. doi: 10.1016/j.intimp.2013.05.027

281. Pang Z, Wang G, Ran N, Lin H, Wang Z, Guan X, et al. Inhibitory effect of methotrexate on rheumatoid arthritis inflammation and comprehensive metabolomics analysis using ultra-performance liquid chromatography-quadrupole time of flight-mass spectrometry (Uplc-Q/Tof-Ms). *Int J Mol Sci* (2018) 19(10). doi: 10.3390/ijms19102894

282. Su B, Ye H, You X, Ni H, Chen X, Li L. Icariin alleviates murine lupus nephritis *via* inhibiting NF-κB activation pathway and NLRP3 inflammasome. *Life Sci* (2018) 208:26–32. doi: 10.1016/j.lfs.2018.07.009

283. Nikfar S, Saiyarsarai P, Tigabu BM, Abdollahi M. Efficacy and safety of interleukin-1 antagonists in rheumatoid arthritis: A systematic review and meta-analysis. *Rheumatol Int* (2018) 38(8):1363–83. doi: 10.1007/s00296-018-4041-1

284. Alten R, Gomez-Reino J, Durez P, Beaulieu A, Sebba A, Krammer G, et al. Efficacy and safety of the human anti-IL-1β monoclonal antibody canakinumab in rheumatoid arthritis: Results of a 12-week, phase ii, dose-finding study. *BMC Musculoskelet Disord* (2011) 12:153. doi: 10.1186/1471-2474-12-153

285. Moran A, Bundy B, Becker DJ, DiMeglio LA, Gitelman SE, Goland R, et al. Interleukin-1 antagonism in type 1 diabetes of recent onset: Two multicentre, randomised, double-blind, placebo-controlled trials. *Lancet* (2013) 381(9881):1905–15. doi: 10.1016/s0140-6736(13)60023-9

286. Seelig E, Timper K, Falconnier C, Stoeckli R, Bilz S, Oram R, et al. Interleukin-1 antagonism in type 1 diabetes of long duration. *Diabetes Metab* (2016) 42(6):453–6. doi: 10.1016/j.diabet.2016.08.005

287. Coll RC, Hill JR, Day CJ, Zamoshnikova A, Boucher D, Massey NL, et al. Mcc950 directly targets the NLRP3 ATP-hydrolysis motif for inflammasome inhibition. *Nat Chem Biol* (2019) 15(6):556–9. doi: 10.1038/s41589-019-0277-7

288. van der Heijden T, Kritikou E, Venema W, van Duijn J, van Santbrink PJ, Slutter B, et al. NLRP3 inflammasome inhibition by Mcc950 reduces atherosclerotic lesion development in apolipoprotein E-deficient mice-brief report. *Arterioscler Thromb VASC Biol* (2017) 37(8):1457–61. doi: 10.1161/atvbaha.117.309575

289. Zhang C, Zhu X, Li L, Ma T, Shi M, Yang Y, et al. A small molecule inhibitor Mcc950 ameliorates kidney injury in diabetic nephropathy by inhibiting NLRP3 inflammasome activation. *Diabetes Metab Syndr Obes* (2019) 12:1297–309. doi: 10.2147/dmso.s199802

290. Perera AP, Fernando R, Shinde T, Gundamaraju R, Southam B, Sohal SS, et al. Mcc950, a specific small molecule inhibitor of NLRP3 inflammasome attenuates colonic inflammation in spontaneous colitis mice. *Sci Rep* (2018) 8(1):8618. doi: 10.1038/s41598-018-26775-w

291. Mridha AR, Wree A, Robertson AAB, Yeh MM, Johnson CD, Van Rooyen DM, et al. NLRP3 inflammasome blockade reduces liver inflammation and fibrosis in experimental Nash in mice. *J Hepatol* (2017) 66(5):1037–46. doi: 10.1016/j.jhep.2017.01.022

292. Wang L, Lei W, Zhang S, Yao L. Mcc950, a NLRP3 inhibitor, ameliorates lipopolysaccharide-induced lung inflammation in mice. *Bioorg Med Chem* (2021) 30:115954. doi: 10.1016/j.bmc.2020.115954

293. Mangan MSJ, Olhava EJ, Roush WR, Seidel HM, Glick GD, Latz E. Targeting the NLRP3 inflammasome in inflammatory diseases. *Nat Rev Drug Discovery* (2018) 17 (8):588–606. doi: 10.1038/nrd.2018.97

294. Ltd IU. Safety and tolerability, pharmacokinetic and pharmacodynamic study with inzomelid. (2019).

295. Fischer U, Schulze-Osthoff K. Apoptosis-based therapies and drug targets. *Cell Death Differ* (2005) 12 Suppl 1:942–61. doi: 10.1038/sj.CDd.4401556

296. Ridker PM, Everett BM, Thuren T, MacFadyen JG, Chang WH, Ballantyne C, et al. Antiinflammatory therapy with canakinumab for atherosclerotic disease. *N Engl J Med* (2017) 377(12):1119–31. doi: 10.1056/NEJMoa1707914

297. Imani D, Azimi A, Salehi Z, Rezaei N, Emamnejad R, Sadr M, et al. Association of NOD-like receptor protein-3 single nucleotide gene polymorphisms and expression with the susceptibility to relapsing-remitting multiple sclerosis. *Int J Immunogenet* (2018) 45(6):329–36. doi: 10.1111/iji.12401

298. Jiang Q, Wang X, Huang E, Wang Q, Wen C, Yang G, et al. Inflammasome and its therapeutic targeting in rheumatoid arthritis. *Front Immunol* (2021) 12:816839. doi: 10.3389/fimmu.2021.816839

299. Sode J, Vogel U, Bank S, Andersen PS, Thomsen MK, Hetland ML, et al. Anti-TNF treatment response in rheumatoid arthritis patients is associated with genetic variation in the NLRP3-inflammasome. *PloS One* (2014) 9(6):e100361. doi: 10.1371/journal.pone.0100361

300. Kastbom A, Verma D, Eriksson P, Skogh T, Wingren G, Söderkvist P. Genetic variation in proteins of the cryopyrin inflammasome influences susceptibility and severity of rheumatoid arthritis (the Swedish tira project). *Rheumatol (Oxford)* (2008) 47(4):415–7. doi: 10.1093/rheumatology/kem372

301. Shaw PJ, MCDermott MF, Kanneganti TD. Inflammasomes and autoimmunity. *Trends Mol Med* (2011) 17(2):57–64. doi: 10.1016/j.molmed.2010.11.001

302. Wu Z, Wu S, Liang T. Association of NLRP3 Rs35829419 and Rs10754558 polymorphisms with risks of autoimmune diseases: A systematic review and meta-analysis. *Front Genet* (2021) 12:690860. doi: 10.3389/fgene.2021.690860

303. Smigoc Schweiger D, Goricar K, Hovnik T, Mendez A, Bratina N, Brecelj J, et al. Dual role of Ptpn22 but not NLRP3 inflammasome polymorphisms in type 1 diabetes and celiac disease in children. *Front Pediatr* (2019) 7:63. doi: 10.3389/fped.2019.00063

304. Griess K, Rieck M, Müller N, Karsai G, Hartwig S, Pelligra A, et al. Sphingolipid subtypes differentially control proinsulin processing and systemic glucose homeostasis. *Nat Cell Biol* (2023) 25(1):20–9. doi: 10.1038/s41556-022-01027-2

305. Rahman SMN, Giacca A. B-cell stress pathways in diabetes: Potential targets for therapy? *Endocrinology* (2022) 164(2). doi: 10.1210/endocr/bqac211

frontiers | Frontiers in Immunology

TYPE Review
PUBLISHED 05 May 2023
DOI 10.3389/fimmu.2023.1169232

OPEN ACCESS

EDITED BY
Joanna Davies,
San Diego Biomedical Research Institute, United States

REVIEWED BY
Vladimir Stanislavovich Rogovskii,
Pirogov Russian National Research Medical University, Russia
Jose Maria Soares Junior,
University of São Paulo, Brazil

*CORRESPONDENCE
Tailang Yin
reproductive@whu.edu.cn
Su Liu
sunnysue0309@163.com

RECEIVED 19 February 2023
ACCEPTED 24 April 2023
PUBLISHED 05 May 2023

CITATION
Wang J, Yin T and Liu S (2023) Dysregulation of immune response in PCOS organ system.
Front. Immunol. 14:1169232.
doi: 10.3389/fimmu.2023.1169232

Dysregulation of immune response in PCOS organ system

Jingxuan Wang[1], Tailang Yin[1*] and Su Liu[2*]

[1]Reproductive Medicine Center, Renmin Hospital of Wuhan University, Wuhan, China, [2]Shenzhen Key Laboratory of Reproductive Immunology for Peri-implantation, Shenzhen Zhongshan Institute for Reproduction and Genetics, Shenzhen Zhongshan Urology Hospital, Shenzhen, China

Polycystic ovary syndrome (PCOS) is the most common reproductive endocrine disorder affecting women, which can lead to infertility. Infertility, obesity, hirsutism, acne, and irregular menstruation are just a few of the issues that PCOS can be linked to. PCOS has a complicated pathophysiology and a range of clinical symptoms. Chronic low-grade inflammation is one of the features of PCOS. The inflammatory environment involves immune and metabolic disturbances. Numerous organ systems across the body, in addition to the female reproductive system, have been affected by the pathogenic role of immunological dysregulation in PCOS in recent years. Insulin resistance and hyperandrogenism are associated with immune cell dysfunction and cytokine imbalance. More importantly, obesity is also involved in immune dysfunction in PCOS, leading to an inflammatory environment in women with PCOS. Hormone, obesity, and metabolic interactions contribute to the pathogenesis of PCOS. Hormone imbalance may also contribute to the development of autoimmune diseases. The aim of this review is to summarize the pathophysiological role of immune dysregulation in various organ systems of PCOS patients and provide new ideas for systemic treatment of PCOS in the future.

KEYWORDS

polycystic ovary syndrome, immune cells, cytokines, ovary, endometrium, vaginal microorganisms

1 Introduction

Polycystic ovary syndrome (PCOS) is a common endocrine and metabolic disorder in women of childbearing age, which is closely related to female infertility, with an incidence of 5% -15% (1). The diagnosis of PCOS is a diagnosis of exclusion and should present with at least two of the three main symptoms: 1) clinical and/or biochemical hyperandrogenism (HA); 2) ovulatory dysfunction (OD); and 3) polycystic ovarian morphology (PCOM) (2). Clinical manifestations like insulin resistance (IR), obesity, hirsutism, and acne may also be present (3). Women with PCOS are more likely to develop type II diabetes, endometrial cancer, underlying cardiovascular disease, mood disorders, and depression. Additionally, multiple pregnancies, abortions, preeclampsia and pregnancy-induced hypertension, gestational diabetes, and other problems are more likely to occur in PCOS women (4).

Currently, the etiology of PCOS remains unknown, as its symptoms are complex and diverse and cannot be completely cured clinically (5).

Primordial follicles consist of an oocyte resting at diplotene stage in meiosis I diplotene and a single layer of flattened anterior granulosa cells surrounding it. The majority of primordial follicles are more likely to stay dormant until death than to be activated (6). Activated primordial follicles form primary follicles, at which point pregranulosa cells will transform into a single layer of cuboidal granulosa cells (GC). The transformation of main follicles into secondary (preantral) follicles occurs with GC proliferation, differentiation, and oocyte growth. At the same time, theca cells begin to form around the outer granulosa cells and can produce androgens and serve as raw materials for estrogen production by GC (7). Accumulation of follicular fluid between GCs increases in response to estrogen and follicle-stimulating hormone, and follicular enlargement is called antral follicle (7). Atresia develops in the majority of antral follicles, and only antral follicles that react to follicle-stimulating hormone (FSH) and luteinizing hormone (LH) are likely to be selected for ovulation (7, 8). Due to the high expression of LH receptors in a subset of antral follicles that line the follicular wall, preovulatory LH spikes activate these follicles, causing them to ultimately ovulate the dominant follicle (9). PCOS is an important syndrome causing anovulation. Women with PCOS have larger-than-normal ovaries and more than 12 follicles that range in size from 2 to 9 millimeters (10). PCOS is characterized by an elevated density of small preantral follicles compared to normal ovaries (11), arrested follicular maturation with accumulation of follicular fluid and dilatation of antrum. Follicles gradually expand, apoptosis occurs in the GC layer and finally atresia occurs, resulting in the disappearance of GC in the follicular wall and the appearance of thin-walled cysts. The causes of ovarian folliculocytosis in PCOS patients are very complex and have been shown to be related to factors such as abnormal anti-mullerian hormone (AMH) secretion by GC, excessive androgen production by membranous cells, and insufficient FSH secretion leading to follicular maturation failure (12).

Regarding the pathogenesis of PCOS, recent studies have suggested that it is associated with genetic and environmental factors, intrauterine environment, endocrine, immune and metabolic dysfunction (13). Hyperandrogenism, obesity and IR interact in PCOS and are involved in immune disorders and systemic inflammation in PCOS (14). Obesity, as a metabolic disease, occurs in nearly 50% of women with PCOS and is one of the causes contributing to chronic low-grade systemic inflammation (15). BMI has already been shown to correlate with endometrial proliferation in women with PCOS. In PCOS patients, BMI is positively correlated with expression of endometrial marker of proliferation Ki-67 (MKI67) (16). Numerous studies have recently concentrated on the impact of chronic inflammation and low-grade inflammation on immunity, with hyperandrogenism playing a significant role in the emergence of immunological problems in PCOS. The prevalence of PCOS is strongly correlated with a number of inflammatory factors, including IL-6, TNF-α, IL-1, IL-18, IL-17, and inflammasomes (17). Additionally, PCOS was associated with a considerably higher proportion of various immune cell subsets (16). A low grade chronic inflammatory state in PCOS patients is caused by the accumulation of numerous inflammatory cells and multiple inflammatory cytokines (18). This article reviews the literature on the relationship between PCOS and immune cells and cytokines and their metabolic effects in various organ systems of the female body, and explores the immune response mechanism of PCOS.

2 Method

In this review, a literature search was performed in PubMed, Elsevier, and Wiley Online Library, including literatures published in English and available up to March 2023. The following key word were used for the search alone or in combination: polycystic ovarian syndrome (PCOS), obesity, insulin resistance, hyperandrogenism, inflammation, immune regulation, androgens, estrogens, cytokines, macrophages, monocytes, dendritic cells, natural killer cells, vaginal microorganisms, intestinal microorganisms, nonalcoholic fatty liver disease, autoimmune thyroid disease, subclinical hypothyroidism, adrenal androgens, dehydroepiandrosterone, dehydroepiandrosterone sulfate, COVID-19, obstructive sleep apnea. Literatures were selected for review based on their titles and abstracts which were relevant to the topic. The references of the articles correlating to this review were further searched and selected.

3 The impact of sex hormones on immune responses in women

By boosting the amount of immune cells that are in circulation and regulating the generation of cytokines in the body, sex hormones have an impact on the immune system (19). Typically, androgens have anti-inflammatory effects and can suppress immune cell activity (20). For example, androgen ablation increases the number of mature dendritic cells (mDCs) as well as expression of dendritic cell (DC) costimulatory markers in lymph nodes (21). Androgen causes a significant decrease in cell-surface toll-like receptor 4 (TLR4) expression in macrophage-like cell lines (22). In addition, androgens can also regulate adaptive immunity in humans by inhibiting Th1, Th2 and Th17 activity, but inducing Treg activity (23). However, the anti-inflammatory effects of androgens are not absolute. Hyperandrogenism in PCOS may change inflammation by influencing macrophage numbers and phenotypes. Higher M1 (inflammatory) and M2 (anti-inflammatory) macrophage ratios could be observed in 5α-dihydrotestosterone (DHT) -treated rat ovaries and PCOS female ovaries (24). Androgen receptor (AR) is expressed by normal skin, fibroblasts, epithelial cells, and macrophages in acute trauma (25). It is reported that castrated rats treated with androgens before urethroplasty have a prolonged inflammatory phase during healing, with upregulation of macrophages and TNF-α levels in urethral wounds (26). Estrogen has a more complex regulatory effect on the immune system (27, 28). Because estrogen levels fluctuate throughout the menstrual cycle, estrogen can suppress

pro-inflammatory pathways at high levels during periovulation and indicate pro-inflammatory pathways when levels fall to the early follicular phase (29). Through the estrogen receptor α (ER α), estrogen can take role in the activation of the macrophage immunophenotype. Estrogen influences macrophage metabolic remodeling, enabling macrophages to cooperate with various activation pathways in different microenvironments (28). When estrogen levels are physiological, the immune system responses more strongly to bacterial endotoxins. Contrarily when levels are supraphysiological, the capacity of macrophages to bind lipopolysaccharide (LPS) is enhanced. It potentially leads to a more severe inflammatory response after bacterial infection (28). This reflects the dual effects of estrogen on the immune system in different microenvironments. Specifically, in autoimmune diseases like systemic lupus erythematosus (SLE), estrogen stimulates the expression of IL-6, which drives naive CD4 cells to differentiate into Th17 cells and inhibits TGF β of IL-6, which drives naive (30). In SLE, activation of IFN (α or γ) signaling upregulates estrogen receptor α (ERα) expression and stimulates target gene expression. Elevated levels of estrogen and IFN-α engage positive feedback loops that further intensify the inflammatory response in SLE (30, 31).

4 The impact of obesity on immune system

Obesity is a metabolic systemic disorder that affects metabolic homeostasis and causes low-grade inflammatory responses (32). It has been demonstrated that immune system deficiencies are related to obesity. A large number of neutrophils, M1 macrophages, and T cells could be observed in adipose tissues (33). Adipose tissue macrophages (ATM) play a dominant role in participating in systemic inflammatory responses. Increased secretion of monocyte chemoattractant protein-1 (MCP-1/CCL2) and leukotriene B4 (LTB4) by adipocytes promotes migration and infiltration of macrophages. Macrophages and adipocytes that accumulate abundantly in adipose tissue secrete adipose inflammatory cytokines TNF-α, IL-6, and IL-1β, activating the nuclear factor kappa-B (NF-κB) pathway to produce large amounts of inflammatory factors. Leptin secreted by adipose tissue is also one of the causes involved in immune disorders in obese individuals (34). In addition, adipose tissue was enriched for large numbers of $CD4^+$ T cells as well as IFN-γ secreted by them. Macrophages and adipocytes overexpressing class II major histocompatibility complex (MHC II) and costimulatory molecules (e.g., CD80 and CD86) in adipose tissue act as antigen-presenting cells (APCs) to promote $CD4^+$ T cell proliferation and Th1 differentiation and produce excessive IFN-γ in adipose tissue (35). Furthermore, leptin secreted by adipocytes can stimulate Th1 cells to secrete IFN-γ in excess and induce MHC II overexpression in adipocytes, further aggravating the inflammatory response (36).

5 PCOS-related immune dysregulation in the female reproductive system

The immune system orchestrates the HPO axis to participate in normal female physiological processes, such as ovulation, fertilization, pregnancy, and embryo implantation. Immune cells like neutrophils, T cells, and macrophages are recruited to the ovaries during fertilization and migration (37). It has been proved that luteal production and regression are influenced by macrophage, T cell, and granulocyte infiltration (38). Endometrial immune environment is important to the maintenance of normal pregnancy. On the one hand, Endometrial immune cells protect against pathogen infiltration, on the other hand, the immune system exerts immune tolerance functions and contributes to the implantation of embryos and normal pregnancy (39). The composition and function of the microorganisms in the genital tract are also influenced by mucosal local immunity. Immune regulation issues in PCOS-affected women further promote the development of chronic inflammation (40). The mechanisms involved in immune as well as metabolic disorders in PCOS in the reproductive system will be investigated below.

5.1 PCOS-related immune dysregulation in the ovary

Ovarian tissue is mainly composed of ovarian parenchyma and ovarian stroma. The parenchyma is composed of ovarian follicles, whereas the stroma is composed of immune cells, blood vessels, nerves, lymphatic vessels, and ovarian-specific components (41). Macrophages, dendritic cells, neutrophils, eosinophils, mast cells, B cells, T cells, and natural killer (NK) cells are among the immune cells found in the ovary. Ovarian immune cells have multiple functions, including phagocytosis and antigen presentation, remodeling of tissues by proteolytic enzymes, and secretion of soluble signals, including cytokines, chemokines, and growth factors (41, 42).

PCOS patients are in a state of chronic low-grade inflammation, which may trigger a cascade of events that further promote the content of ovarian androgens and affect ovulation. PCOS patients present with an abnormal androgen response to gonadotropin-releasing hormone (GnRH) stimulation leading to ovarian androgen overproduction (43). Immune cells and cytokines interact with androgens resulting in disruption of ovarian immune balance in PCOS. For example, González's results showed that mononuclear cells (MNCs) entering the ovary may cause a local inflammatory response that stimulates ovarian androgen production in women with PCOS (44). Li et al. showed that the IFN-γ levels were decreased in PCOS rats induced by dehydroepiandrosterone (DHEA). It is possible that DHEA inhibited proliferation and promoted apoptosis of ovarian granulosa cells and down-regulated IFN-γ expression (43).

Follicles represent the basic functional units of the ovary (7). Follicular fluid (FF) which is composed of follicular cell secretion and theca vascular exudate, which contains gonadotropins secreted by the pituitary gland and steroid hormones secreted by the ovary, changes with follicular development (45). In recent years, there have been plenty of studies demonstrating that abnormal inflammation can alter normal ovarian follicular dynamics, leading to impaired oocyte quality, anovulation, and associated infertility (46). DCs are specialized innate immune cells that sense danger signals, absorb and process antigens, and transmit them to T lymphocytes (47). Prior to impending ovulation, DC are important components of bone marrow-derived leukocytes in the microenvironment of mature oocytes and their abundance and maturity may be related to ovarian function in women with PCOS (48). Evidence has shown that the mean fluorescence intensity (MFI) of human leukocyte antigen DR (HLA-DR) expression reflects a positive correlation between DC maturity and ovarian response as measured by serum E2 levels on the day of human chorionic gonadotropin (hCG) administration. E2 production measured 48 h prior to oocyte retrieval was associated with the presence of more mature DCs, while this association was strengthened when analyzing patients undergoing *in vitro* fertilization (IVF) due to male factor infertility (i.e., normal ovarian function). This suggests that maturity of DC in FF is positively correlated with gonadotropin response and may favor an aseptic inflammatory process leading to ovulation in follicles (48). In addition, the percentage of $CD11c^+$ $HLADR^+$ DCs was significantly lower in FF of PCOS patients than in normal controls. It is also possible that reduced DCs may influence the activation of Th17/Th1 cells, leading to failure of dominant follicle selection and developmental processes (49).

Th cells play a role in adaptive immunity by producing cytokines.Th1 mainly secrete IL-2 and IFN-γ to promote cellular immunity, and Th2 mainly secrete IL-4 to regulate humoral immunity (50). Local coordination of T lymphocytes impacts survival of granulosa cells and embryo quality in female ovaries. Changes in T cell distribution can promote follicular survival either by providing trophic growth factors or inhibiting adverse immune activity, or conversely by transmitting cytotoxic signals to induce oocyte or granulosa cell death and promote follicular regression (51). Early studies have found that memory T lymphocytes in the theca layer of PCOS ovaries are reduced compared to non-PCOS ovaries (52). Qin, et al. showed that Th1 cytokines (IFN-γ, IL-2) production in FF lymphocytes was significantly higher in PCOS patients than in controls, and Th1 cytokines predominate in FF of PCOS patients as analyzed by flow cytometry. On the contrary, the production of Th2 cytokines (IL-4, IL-10) was not statistically significant between the two groups, suggesting that the imbalance of Th1/Th2 cell ratio may affect egg quality and ovulation (53). Li et al. showed that the percentage of total $CD4^+$ T cells and $CD8^+$ T cells was significantly decreased while the expression of PD-1 was increased in FF of the infertile PCOS patients. The failure of dominant follicle selection and development was caused by higher PD-1 levels, which further supported the pathogenic function of local T cell imbalance in PCOS (54).

Granulocyte colony-stimulating factor (G-CSF) is a cytokine that stimulates neutrophil proliferation and differentiation, which is mainly secreted by granulosa cells before ovulation. G-CSF produced by granulosa cells may recruit leukocytes to the thecal layer during ovulation to accelerate ovulation (55). G-CSF concentrations in follicular fluid and serum were also significantly higher in PCOS patients than in controls. The neutrophil count and neutrophil/leukocyte ratio of PCOS patients were significantly higher than those of controls, further supporting the theory of chronic inflammation in PCOS (55, 56). Other studies have shown that IL-18 levels in FF of PCOS patients are higher than those in controls, especially the level of IL-18 in FF of overweight PCOS patients is significantly higher than that in normal weight PCOS patients (57). More studies showed increased levels of IL-1β, IL-6, and TNF in FF of PCOS patients (17, 58, 59). The reason for this is that inflammatory cytokines in follicular fluid alternately alter the follicular microenvironment, activating the NF-κB inflammatory pathway. The inflammatory cascade may affect granulosa cell proliferation, inhibit oocyte maturation, and aggravate ovulatory dysfunction more severely (58) (Table 1).

5.2 PCOS-related immune dysregulation in the endometrium

The human endometrium is a steroid-dependent tissue, and hormonal changes during the ovulatory cycle can affect the growth and remodeling of endometrial cell components and tissues (60). In

TABLE 1 The immune cells and cytokines in follicular fluid of PCOS.

Immune cells	Related immune cells or cytokines	Function	References
$CD11c^+HLA\text{-}DR^+DCs$	Th17, Th1	Failure of dominant follicle selection and developmental processes	(49)
Th1	IFN-γ, IL-2	Affection on egg quality and ovulation caused by Th1/Th2 cell ratio imbalance	(53)
Th2	IL-4, IL-10		
$CD4^+$ T cells, $CD8^+$ T cells	PD-1	Failure of dominant follicle selection and development	(54)
Immune factor			
G-CSF	Neutrophil	Chronic inflammation in PCOS	(55, 56)
IL-18, IL-1β, IL-6, and TNF-α		Activation of NF-κB inflammatory pathway	(17, 57–59)

addition to guarding against infections, female reproductive system immune cells also enable embryo implantation and establish immunological tolerance to sperm and embryo/fetus (61). As steroid hormones (progestins, androgens, and estrogens) change with the menstrual cycle, it has been demonstrated in an increasing number of studies that immune cells and inflammatory factors have an impact on the reproductive system's ability to function. Steroid hormones either directly or indirectly affect the expression of chemokines IL- 8 and MCP-1) as well as the survival and apoptosis of resident endometrial cells (stromal cells, epithelial cells, and endothelial cells) and immune cells (39, 62). $CD56^+$ uterine natural killer cells (uNK), $CD68^+$ macrophages and $CD8^+$ cytotoxic T lymphocytes are all common endometrial/decidual immune cells (63), and They regulate endometrial function by releasing cytokines, such as IL-15, IL-10 and IFN-γ (64).

The endometrium of women with PCOS has continuous estrogen exposure during both the proliferative and secretory phases, while diminished progesterone action during the secretory phase is likely to impair endometrial receptivity and lead to long-term endometrial hyperplasia, bleeding, and cancer (65). In addition to sex hormones, metabolic disorders and chronic inflammatory conditions caused by obesity and hyperinsulinemia promote oxidative stress imbalance in PCOS endometrium and affect progesterone receptor activity in PCOS endometrium. Women with PCOS had a poorer reaction to progesterone than did women without the condition, and they had thicker surface epithelium and more stromal cells than women without PCOS, but considerably fewer blood vessels overall (66). uNK cells are one of the most important immune cells of human uterine leukocytes. The main endometrial NK cells are $CD16^-$ NK cells, accounting for 70-80% of secretory endometrial lymphocytes (67). The percentage change of uNK with hormones during the menstrual cycle may play a key role in implantation and maintenance of pregnancy, especially the number of decidualized endometrium is further increased in the first trimester (67, 68). Female sex hormones appear to regulate uNK recruitment indirectly by modulating chemokine and interleukin expression. It has been shown that the percentage of $CD56^+/CD16^-$ NK cells and $CD56^{bright}/CD16^-$ NK cells decreased in the late secretory endometrium of PCOS women, while the proportion of $CD3^+$ lymphocytes significantly increased. Meanwhile, $CD56^+$ and $CD56^{bright}$ NK cells were reduced, the expression of IL-15, IL-18, and CXCL10 was also significantly lower in PCOS than that of the control group, which may be related to chronic oligo-ovulation or hyperandrogenism in PCOS patients (68). $CD68^+$ macrophages are seen in the endometrium throughout the menstrual cycle, particularly in the late luteal phase (69). Endometrial macrophages may be involved in the onset of menses, repair and remodeling of the functional layer of the endometrium, and play an important role in the preparation of a receptive endometrium during the "window of implantation" and endometrial decidualization (61). Macrophages within the endometrium have been identified as an important source of proinflammatory and chemotactic factors that specifically express role-specific markers at different stages of the menstrual cycle (70). It has been shown that endometrial $CD68^+$ macrophages and $CD163^+$ M2 macrophages are significantly increased in PCOS patients, which may be related to insulin resistance and the release of inflammatory factors in PCOS (71). One of the main endocrine features of PCOS is hyperandrogenism, while androgens can induce TNF-α production by macrophages. Recent studies have observed that the proliferative endometrial TNF-α level is significantly increased in PCOS patients (72, 73). Therefore, the increased number of macrophages in the endometrium of PCOS patients may be responsible for the increased TNF-α (72). DCs are mainly located in the functional and basal layers of the endometrium and are broadly classified according to their developmental pathways: plasmacytoid DCs (pDCs) and Myeloid DCs. Myeloid DCs have a high correlation with the endometrium and can be divided into immature DCs (iDCs) and mDCs according to maturation status (74). In response to foreign antigens or inflammatory signals, mDCs present antigens together with MHC molecules to T cells, effectively initiating adaptive immunity (71, 75). Studies have shown that the increased percentage of endometrial $CD1a^+$ iDCs, $CD83^+$ mDCs in normal weight PCOS patients, and confirmed that the dysfunction of DCs may be related to the pathogenesis of PCOS. Granulocyte-macrophage colony-stimulating factor (GM-CSF) can promote DC and endometrial macrophage maturation (71). Studies have found that GM-CSF down-regulation in endometrial stromal fibroblasts (eSF) of women with PCOS, which may be associated with poor endometrial receptivity and DC cell migration (76). Endometrial T cells include CD4 Th1, Th2 CD8, Treg, and Th17 cells, mainly located in the decidual stroma and glandular epithelium (77). Decidual tissues had the highest concentration of $CD8^+$ T lymphocytes. Endometrial $CD8^+$ T cells are elevated in PCOS patients, indicating that the immune environment of the endometrium is altered and T cells may be involved in endometrial immunoregulatory mechanisms in PCOS (71). Previous studies have also shown that high levels of MCP-1 increased the terminal differentiation of $CD4^+$ T cells into Th2 cells, while the basal level of MCP-1 was also increased in PCOS patients. It indicates that T cells may play a role in the pathogenesis of the condition (76).

Cytokines and chemokines in the endometrium also affect the endometrial immune microenvironment in PCOS patients. At present, IL-1 and vascular endothelial growth factor (VEGF) are closely related to endometrial receptivity. The expression levels of IL-1 and VEGF in endometrium of PCOS rats were significantly lower than those of the control group, suggesting that the endometrial receptivity of PCOS rats was significantly lower than that of the normal control group (78). It has been found that the key elements of TLR -mediated NF-κB signaling pathway were dysregulated in endometrial tissue of PCOS women, and the expression of TLR4 protein was increased in the endometrium. IRF-7 and NF-κB signaling may be activated and TRL4 positively regulated by hyperandrogenism, which may also boost the expression of cytokines like IFN-α and TNF-α in the endometrium (79). In addition, the inflammatory environment in the endometrium of women with PCOS is also thought to be associated with the overexpression of other cytokines, such as IL-6, IL-8, IL-18, and CRP (76, 80, 81) (Figure 1).

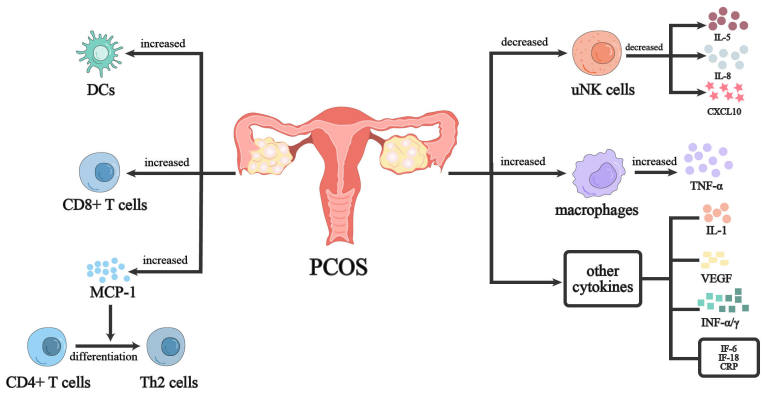

FIGURE 1
Immunoregulation of endometrium in PCOS women. PCOS women have a imbalanced immune environment in the endometrium. Both the proliferation and differentiation of T cells in PCOS women's endometrium as well as the proliferation of innate immune cells such uNK cells and dendritic cells are influenced. At the same time, cytokines secreted by immune cells are dysregulated. Further evidence of the inflammatory milieu in PCOS women's endometrium came from the upregulation of inflammatory molecules like TNF, CRP, and IL-6.

5.3 PCOS-related immune dysregulation in the vaginal mucosa

Healthy female vagina is colonized by multiple normal microbial and fungal groups, which are divided into beneficial microorganisms and opportunistic pathogens inhabiting the vaginal environment, with lactobacilli as the dominant genus (82, 83). The effects of estrogen and progesterone on vaginal epithelial cells, PH, sexual activity, menstruation, and antibiotic usage are the key factors affecting the vaginal microbiome (83). The body benefits from the homeostasis of vaginal bacteria since they are a crucial part of the microenvironment of the reproductive tract (40). Increasing evidence suggests that the composition of a woman's vaginal microbiota can significantly impact her sexual and reproductive health, including her risk of adverse delivery outcomes, including miscarriage and premature delivery, as well as infection with HIV and other sexually transmitted pathogens (84–86). The stratified squamous epithelial cells that cover the mucus layer are part of the vaginal ecosystem, along with vaginal bacteria, neutrophils, macrophages, classical dendritic cells, Langerhans cells, NK cells, T and B lymphocytes, and other innate and adaptive immune cells (86). The vagina contains many immune-related cells and receptors that detect pathogenic organisms primarily through microbial motif pattern recognition of pattern recognition receptors (PRRs), such as TLRs or dectin-1 receptors (40). Additionally, vaginal defense is aided by mannose-binding lectin (MBL), vaginal antimicrobial peptide (AMP), immunoglobulin A, and immunoglobulin G (IgA, IgG) (40).

The impact of PCOS on women's vaginal health is mainly reflected in the disruption of homeostasis of the vaginal microenvironment. Hong's study showed that the vaginal microbiome is associated with clinical manifestations of PCOS, such as acanthosis nigricans, intermenstrual bleeding, etc. When compared to healthy women, PCOS patients with high testosterone levels had a higher relative abundance of *L. crispatus* and a lower relative abundance of *L. iners*. On the other hand, their relative abundance of *Mycoplasma* and *Prevotella* was significantly higher than that of controls (87). Another study also demonstrated that *L. crispatus* and *L. iners* populations were more sensitive to testosterone levels in women with PCOS (88). Tu showed that there was a significant decrease in lactobacilli in lower genital tract (LGT) organisms in PCOS patients, while *Gardnerella vaginalis* was significantly enriched in both the vagina and cervix of PCOS patients, in addition to several potential pathogens including *Gardnerella*, *Prevotella*, *Veillonellaceae*, *Streptococcus*, and *Dialister* species (89). *Gardnerella*, *Prevotella*, and other species produce sialidase, IgA protease, and short-chain fatty acids, which lead to local IgA inactivation and, respectively, improve their adherence to epithelial cells, evade antibody-mediated inhibition, and modulate the immune environment (90, 91). Prevotella also contributes to activation of Th17 immune responses via APCs, promotes increases in cytokines such as IL-23A, IL-6, IL-1A, and IL-1B that promote Th17 immune responses, and recruits and activates Th cells in inflamed vaginal mucosa (92). Bacterial products of certain anaerobes have been shown to induce the production of short-chain fatty acids from pro-inflammatory cytokines by TLR stimulation, dendritic cell activation and maturation, and by producing specifically short immune cell migration, apoptosis, and phagocytosis (93). This suggests that disturbances in vaginal microbial homeostasis in PCOS may be associated with impaired mucosal immunity.

6 PCOS-related immune dysregulation in the cardiovascular system

Increasing evidence suggests that women with PCOS are at increased risk for coronary artery disease (CAD) and cardiovascular disease (CVD) (15, 94, 95). Insulin resistance is one of the most important pathogenesis of PCOS and an important cause affecting cardiometabolism in women with PCOS (96). IR increases a woman's risk of CVD by being linked to a number of

cardiometabolic disorders, including dyslipidemia, hypertension, diabetes mellitus, and metabolic syndrome (97). Oxidative stress and chronic inflammation have been implicated in the pathogenesis of IR in PCOS, including increased reactive oxygen species (ROS) production by peripheral blood leukocytes, activation of leukocyte-endothelial interactions, and increased levels of the pro-inflammatory transcription NF-κβ, as well as pro-inflammatory cytokines and C-reactive protein (98). The low-grade chronic inflammatory state of PCOS is likely to provide a pathophysiological basis for the development of CVD, particularly the development of atherosclerosis. Microparticles (MPs) are subcellular vesicles that can be released practically by any cell and range in size from 100 to 1000 nm. They are a major indicator for identifying cardiometabolic risk in PCOS (99). MPs derived from leukocytes (LMPs) may originate from neutrophils, monocytes/macrophages, and lymphocytes, alter endothelial function, participate in coagulation and platelet activation, and promote the recruitment of inflammatory cells into the vessel wall, contributing to atherosclerotic lesion progression (100). A study showed higher levels of LMPs in PCOS patients, suggesting that MP may be closely associated with the development of atherosclerosis in PCOS patients (100). CRP plays a role in and triggers atherothrombotic processes as one of the recognized markers that can forecast cardiovascular events. In CAD patients with low-grade or persistent inflammation, CRP can be used in combination with the biomarkers MCP-1 and galectin 3 to predict recurrent events (101). MCP-1 can recruit monocytes to the vessel wall via its C-C chemokine receptor type 2 (CCR-2) on monocytes as a chemokine (102). Hu et al. showed that serum concentrations of CRP and MCP-1 were significantly higher in PCOS patients compared with controls. The possible mechanism is that elevated CRP levels promote monocyte accumulation in the atherogenic arterial wall by increasing monocyte chemotactic activity in response to MCP-1 (103). A meta-analysis showed that women with PCOS had significantly higher levels of CRP, Hcy, PAI-1 antigen, PAI-1 activity, VEGF, ADMA, AGEs, and Lp (a). Although it is unclear how IL-6 and TNF-α are related to CVD events in PCOS, these inflammatory factors are probably significant indicators for predicting CVD in PCOS (104, 81).

7 PCOS-related immune dysregulation in the digestive system

7.1 Intestine

The gut microbiota (GM) is a complex community with physiological roles such as constituting the gut barrier, stimulating the immune system, and anabolism (105). The impact of PCOS on the gastrointestinal tract is mainly reflected in the disruption of gut microbial diversity and homeostasis, while the gut microbiota affects the development of the immune system and regulates immune mediators, which in turn affect the intestinal barrier (106).

According to growing evidence showing the GM in PCOS patients differs from those of healthy women, suggesting that microbial imbalance or "dysbiosis" in the gut may contribute to the pathology of PCOS (107–109). Qi et al. showed that bile acids are involved in regulating IL-22 production to affect ovarian function in PCOS. IL-22 mRNA, tauroursodeoxycholic acid (TUDCA) levels, and GATA3 levels were significantly decreased in mice transplanted with stool from individuals with PCOS. In addition, serum IL-22 levels in PCOS-like mouse models also decreased. Similar to the mice research, PCOS patients had significantly lower serum and follicular fluid levels of IL-22 than in controls. Because mice preferentially conjugate bile acids with taurine, humans predominantly use glycine. Intestinal and serum IL-22 levels and intestinal GATA 3 mRNA levels increased in PCOS-like mouse models after glycodeoxycholic acid (GDCA) administration. Secretion of IL-22 protein and Il22 mRNA levels were significantly increased in group 3 innate lymphoid cells (ILC3s) cultured *in vitro* in the presence of TUDCA or GDCA. The reason for this is that bile acids induce IL-22 secretion by intestinal ILC3s via the GATA 3 signaling pathway, which in turn improves the PCOS phenotype (110). Lindheim et al. showed a significantly lower abundance of *Tenericutes* in the gut of PCOS patients compared to healthy women and a negative correlation with total blood lymphocyte counts (107). More studies have shown that LPS produced by intestinal flora has endotoxin effect, and LPS-binding protein can bind to TRL4 on the surface of innate immune cells and mediate PCOS-related inflammatory response, further aggravating IR symptoms in PCOS patients (111, 112).

7.2 Liver

Nonalcoholic fatty liver disease (NAFLD) encompasses a spectrum of diseases ranging from simple steatosis without inflammation or fibrosis to nonalcoholic steatohepatitis (NASH), to fibrosis, cirrhosis, and finally hepatocellular carcinoma (113, 114). The etiology of PCOS and NAFLD share the same features: they are all strongly associated with IR, hyperandrogenism, and obesity (113, 115, 116). In recent years, increasing evidence suggests an association between NAFLD and PCOS, but there are few studies on immunomodulation in NAFLD in PCOS women. Increased plasma levels of IL-6 and TNF-α have now been demonstrated in NAFLD and NASH patients, and increased production of TNF-α and IL-6 by peripheral blood mononuclear cells from NASH patients (117). Mohammadi et al. showed that the levels of IL-6 and CRP were significantly increased in PCOS rats, while the levels of IL-6 and CRP were significantly decreased in curcumin-treated PCOS rats (118). Increases in IL-6 and TNF-α are likely related to depletion of DCs located in the central and periportal veins aggravating aseptic inflammation in the liver and enhancing TLR4 and TLR9 activity and expression in innate effector cells (119, 120). Chen et al. showed that nine differentially expressed genes (DEGs), TREM1, S100A9, FPR1, NCF2, FCER1G, CCR1, S100A12, MMP9, and IL1RN, were significantly upregulated in PCOS and NAFLD, whereas these DEGs have been demonstrated to be associated with immune and inflammatory responses (121).

8 PCOS-related immune dysregulation in the endocrine system

PCOS is one of the common reproductive endocrine system diseases in women. In this section, we only discuss dysregulated immune response in other endocrine system rather than reproductive system.

8.1 Thyroid

Recent research has demonstrated that autoimmunity, particularly autoimmune thyroid disease (AITD) and subclinical hypothyroidism (SCH), may be strongly linked to PCOS etiology. AITD, the most widespread autoimmune antibody disease, is more prevalent in women with PCOS than in non-PCOS women and is the most frequent cause of hypothyroidism or subclinical hypothyroidism in the adult population (122–125). AITDs include Hashimoto's thyroiditis (HT) and Grave' s disease (GD). The pathogenesis of GD and HT may be related to triggering of T cell- and B cell-mediated immune responses, which may eventually develop generalized hypothyroidism (125, 126). More women may have only higher antibody levels without significant thyroid dysfunction, leading to SCH (126). Several studies have demonstrated that autoimmune antibodies such as anti-TPO, anti-TG, anti-TSH are significantly elevated in women with PCOS (127, 128). The cause of AITD in women with PCOS is likely to be associated with hyperandrogenism. Androgen levels rise *in vivo* as a result of increased GnRH and LH pulse frequency in women with PCOS (126). Excessive androgens can enhance T suppressor cell activity or promote Th1 responses, and Th1-mediated autoimmunity leads to thyroid cytolysis and hypothyroidism, leading to HT (125). Aromatase converts androgens to estrogens, which causes compensatory increases in estrogen levels. Additionally, binding to estrogen receptors appears to have proliferative effects on B lymphocytes, T lymphocytes, and macrophages (126). Women with PCOS tend to have inadequate progesterone secretion, estrogen increases IL-6 expression in T cells, and the absence of progesterone suppression may lead to overstimulation of the immune system, making these patients more susceptible to autoimmune diseases (128).

8.2 Adrenal gland

The ovary is the main source of androgens in women with PCOS. Indeed, it has long been shown that adrenal androgen secretion is also increased in PCOS (129). DHEA and dehydroepiandrosterone sulfate (DHEA-S) are the two primary adrenal androgens in PCOS women. Acne vulgaris, as one of the common dermatologic manifestations of PCOS, has also been shown to be associated with higher concentrations of dehydroepiandrosterone sulfate (130). Peripheral conversion to testosterone nevertheless contributes to hyperandrogenism despite minimal adrenal androgen activity (131). It is reported that adrenal androgen (AA) has been reported in 20% to 30% of PCOS patients (132). A meta-analysis showed that DHEA levels were significantly higher in women with PCOS compared to healthy controls (133). Corticosteroid-steroidogenesis may therefore be an independent factor for hyperandrogenism in some women with PCOS and may be a genetic, stable trait (134). DHEA as well as DHEA-S have been demonstrated to have immunomodulatory functions in human cytological experiments, mainly affecting immune cell numbers by modulating cytokine levels (135). DHEA is involved in ovarian immune regulation and affects the balance of Th1 and Th2 immune responses in the ovary. It enhances Th1 responses while weakening Th2 responses by reducing the release of IL-2 and IL-10 (i.e., Th2-related cytokines) and the expression of the activation marker CD69 on $CD4^+$ T cells, resulting in a new balance of Th1/Th2 immune responses (136). This shows that adrenal androgens may be associated with the immunological response in PCOS, but further research is needed to determine the precise mechanism.

In addition, according to a study, there is a unique clinical phenotype of PCOS. This phenotype is characterized by age-specific hyperandrogenism, but the patient's hyperandrogenism initially decreases to the normal range by approximately 35 years of age. The hyper-/hypoandrogenic PCOS phenotype (HH-PCOS) is known for having comparatively low androgen levels compared to the traditional PCOS phenotype (137). Gleicher et al. found that women with the HH-PCOS phenotype showed an activated immune system, particularly a strong association with anti-thyroid autoimmunity in the form of anti-TPO antibodies (138). Whereas adrenal autoimmunity is highly associated with other autoimmune abnormalities, antiadrenal and antithyroid autoimmunity is frequently observed in the same patient (123). Insufficient cortisol (C) production in the zona fasciculata can be detected in HH-PCOS. It is tempting to speculate that the putative autoimmune attack on the adrenal gland is not limited to decreased androgen production in the zona reticularis, but also affects the adjacent zona fasciculata (139). This suggests that HH-PCOS is likely an immune/inflammatory disease and is associated with autoimmunity.

9 PCOS-related immune dysregulation in the other system

On account of the global outbreak of novel coronavirus pneumonia, COVID-19 has been increasingly investigated in PCOS. PCOS patients may have a higher susceptibility to COVID-19, which is also increased by the presence of comorbidities such as NAFLD, obesity, alterations in the gut microbiome (140, 141). Hyperandrogenism in PCOS may be one of the main causes of high susceptibility to COVID-19. Androgens modulate immune responses, decrease NK cell activity, reduce TRL4 expression on macrophage surfaces, and also suppress pro-inflammatory responses by reducing extracellular signal-regulated kinase and leukotriene formation in neutrophils (142). In PCOS mice, elevated androgens upregulated SARS-CoV-2 receptor angiotensin converting enzyme 2 (ACE2), which acts synergistically with host transmembrane protease serine 2 (TMPRSS2) to increase SARS-CoV-2 viral entry into tissues (141,

143). Vitamin D can regulate the immune function of the body and play an important role in inducing macrophage differentiation, inhibiting the maturation of dendritic cells and blocking the adaptive response to antigen presentation, and enhancing the development of Treg cells (144). Furthermore, vitamin D can also down-regulate the synthesis of pro-inflammatory factors (IL-1, IL-6, IL-12, TNF-α and IL-17) and increase the expression of anti-inflammatory factors (IL-1). Macrophage activation correlates well with the severity of COVID-19 (145). Vitamin D has been linked to COVID-19 in a growing number of studies (146–148), although further research is needed to determine its significance for PCOS patients. One study showed that vitamin D was significantly lower in women with PCOS and was negatively correlated with BMI. Women with PCOS had higher levels of the pro-inflammatory macrophage-derived biomarkers CXCL5, CD163, and matrix metalloproteinase 9 (MMP9), but CD200 expression was lower. Pro-inflammatory expression of these macrophage-derived proteins was linked to obesity. CD80 was identified as one of the specific markers of activated Treg in circulation (149), whereas IL-12 induced Th1 cell differentiation and stimulated IFN-γ synthesis (150). Vitamin D deficiency has been associated with decreased CD80, IFN-γ, and IL-12 in PCOS in women with PCOS (151). These findings imply that one of the potential high-risk variables contributing to PCOS patients' susceptibility to COVID-19 infection may be vitamin D deficiency.

Obstructive sleep apnea (OSA) is also an obesity-related disorder and is generally more prevalent in men than in women (152). OSA is characterized by repeated partial or complete airway collapse that may lead to intermittent hypoxia. Intermittent hypoxia further contributes to oxidative imbalance, producing reactive oxygen species, numerous cytokines such as IL-2, IL-4, IL-6, lipid peroxidation, and free DNA (153). There has long been much evidence that women with PCOS have a higher prevalence of OSA than the normal population (154–156). Although androgen excess may influence the prevalence and severity of OSA in both men and women, it does not necessarily cause OSA in women with PCOS because androgen levels in this population are still lower than those in men (157, 158). Nevertheless, hormones may play a protective role in the development of OSA. For instance, IL-6 secretion is elevated in sleep apnea, yet estrogen can inhibit IL-6 secretion (157). The true predisposing factors for OSA in women with PCOS may be IR and obesity (152). Obesity/insulin-resistance may be the main cause of sleep apnea, which in turn may accelerate these metabolic abnormalities because of the gradual rise of cytokines, such as IL-6 and TNF-α (159).

10 Discussion

PCOS has a range of effect on organ system in addition to the female reproductive system. Immune system function is impacted by hormonal disorders, and PCOS patients suffer low-grade chronic inflammation due to abnormal cytokine secretion, immune cell dysfunction, and hormonal disorders. At the same time, the etiology of chronic inflammation in PCOS is also influenced by obesity and metabolic disorders (particularly insulin resistance). In a vicious circle involving hormones, obesity, and IR, inflammatory cells and inflammatory markers accumulate up in PCOS women and disrupt the immune microenvironment of PCOS. In addition to having an impact on the reproductive system of PCOS patients, where it affects ovulation, endometrial receptivity, and folliculogenesis, abnormal immune function also contributes to the dysfunction of other systems in PCOS women. Patients with PCOS exhibit microbial dysbiosis, CVD, NAFLD, and OSA, all of which are closely associated with immunological regulation. Compared to healthy women, women with PCOS are even more susceptible to inflammatory illnesses and COVID-19.

One of the PCOS diagnosis criteria and one of its most prevalent symptoms is hyperandrogenism. Sexually dimorphic immunoreactivity typically uses androgens as anti-inflammatory hormones and estrogens as pro-inflammatory hormones. Furthermore, considering women experience menstruation cycles, changes in sex hormones have an impact on the growth of female follicles and ovulation. However, androgens are not just straightforward anti-inflammatory hormone in PCOS. In PCOS patients with hyperandrogenism, DEGs are highly enriched in immune and inflammatory responses (160). Nevertheless, there is controversy over how androgens affect fat tissue in PCOS. There is a stronger correlation between visceral and abdominal obesity in women with PCOS, as well as a significantly higher incidence of NAFLD. Obesity is a chronic inflammatory disorder in which necrotic adipocytes attract inflammatory cells and release inflammatory cytokines like TNF-α; PCOS is also associated with higher levels of M1 macrophages and inflammatory cytokines like TNF-α and IL-6. More significantly, obesity by itself is not a PCOS diagnostic indicator. Moreover, there is evidence that an excess of androgen is not responsible for chronic inflammation in PCOS but instead has anti-inflammatory benefits when obesity is present (161).

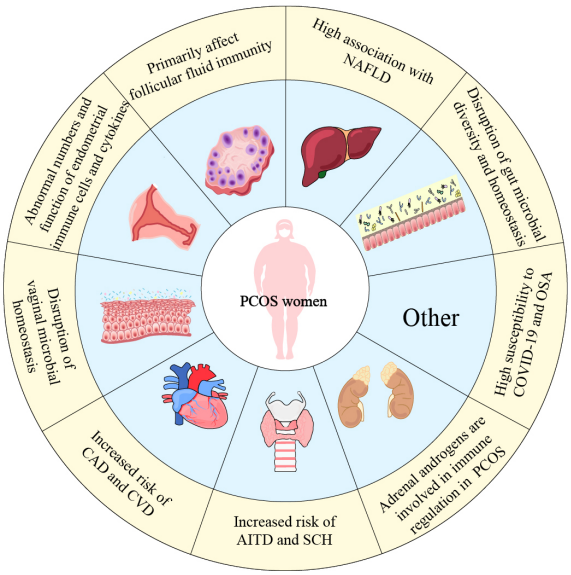

FIGURE 2
The dysfunction of organ systems related to immune dysregulation in PCOS women. This figure summarizes immune dysfunction in PCOS women in various systems. Not only the female reproductive system, the impact of PCOS is even reflected in the cardiovascular, intestinal, thyroid and other organs.

From the viewpoint of organs and tissues from the systemic system, we outline the pathogenic function of immune imbalance in PCOS women in this review. It is more convincing to demonstrate that PCOS is a systemic metabolic syndrome as well as an illness of the reproductive system. The review does, however, have some constraints. The manuscript is solely based on the author's collection of literature, and the opinion that was eliminated has some subjectivity in the author's opinion. The significance of immune cell and immune factor imbalance in PCOS has been summarized in earlier research. This manuscript begins with immune cells and immune factors as well. However, it concentrates more on the relationship with systemic organs and examines how obesity, hormones, and metabolic disorders interact with immune cells and immune factors in PCOS inflammation.

In addition to helping to evaluate chronic low-grade inflammation, understanding the immune cell phenotype and cytokine expression in PCOS patients can help predict the development of other diseases. Consequently, figuring out the pathogenic function of immune regulation in PCOS is crucial for both treatment and preventing further complications in the future (Figure 2).

Author contributions

JW and TY conceived the original idea of the manuscript. JW drafted the manuscript and develop the figures. JW, TY and SL revised the first version of the manuscript. SL provided critical feedback and helped revise the manuscript. All authors contributed to the article and approved the submitted version.

Funding

This work was funded by Shenzhen Natural Science Foundation (JCYJ20220530172814032) and the Hubei Provincial Natural Science Foundation of China (2022CFB200).

Conflict of interest

The authors declare that the research was conducted in the absence of any commercial or financial relationships that could be construed as a potential conflict of interest.

Publisher's note

References

1. Wang J, Wu D, Guo H, Li M. Hyperandrogenemia and insulin resistance: the chief culprit of polycystic ovary syndrome. *Life Sci* (2019) 236:116940. doi: 10.1016/j.lfs.2019.116940

2. Baracat EC, Baracat MCP, José M ,SJJr. Are there new insights for the definition of PCOS? *Gynecological Endocrinol* (2022) 38:703–4. doi: 10.1080/09513590.2022.2121387

3. Pugeat M, Ducluzeau PH. Insulin resistance, polycystic ovary syndrome and metformin. *Drugs* (1999) 58 Suppl 1:41–6. doi: 10.2165/00003495-199958001-00010

4. Palomba S, de Wilde MA, Falbo A, Koster MPH, La Sala GB, Fauser BCJM. Pregnancy complications in women with polycystic ovary syndrome. *Hum Reprod Update* (2015) 21:575–92. doi: 10.1093/humupd/dmv029

5. Coutinho EA, Kauffman AS. The role of the brain in the pathogenesis and physiology of polycystic ovary syndrome (PCOS). *Med Sci (Basel)* (2019) 7:84. doi: 10.3390/medsci7080084

6. Atwood CS, Vadakkadath Meethal S. The spatiotemporal hormonal orchestration of human folliculogenesis, early embryogenesis and blastocyst implantation. *Mol Cell Endocrinol* (2016) 430:33–48. doi: 10.1016/j.mce.2016.03.039

7. Gershon E, Dekel N. Newly identified regulators of ovarian folliculogenesis and ovulation. *Int J Mol Sci* (2020) 21:4565. doi: 10.3390/ijms21124565

8. Matsuda F, Inoue N, Manabe N, Ohkura S. Follicular growth and atresia in mammalian ovaries: regulation by survival and death of granulosa cells. *J Reprod Dev* (2012) 58:44–50. doi: 10.1262/jrd.2011-012

9. Rimon-Dahari N, Yerushalmi-Heinemann L, Alyagor L, Dekel N. Ovarian folliculogenesis. *Results Probl Cell Differ* (2016) 58:167–90. doi: 10.1007/978-3-319-31973-5_7

10. Rotterdam ESHRE/ASRM-Sponsored PCOS Consensus Workshop Group. Revised 2003 consensus on diagnostic criteria and long-term health risks related to polycystic ovary syndrome. *Fertil Steril* (2004) 81:19–25. doi: 10.1016/j.fertnstert.2003.10.004

11. Webber LJ, Stubbs S, Stark J, Trew GH, Margara R, Hardy K, et al. Formation and early development of follicles in the polycystic ovary. *Lancet* (2003) 362:1017–21. doi: 10.1016/s0140-6736(03)14410-8

12. Chang RJ, Cook-Andersen H. Disordered follicle development. *Mol Cell Endocrinol* (2013) 373:51–60. doi: 10.1016/j.mce.2012.07.011

13. Rosenfield RL, Ehrmann DA. The pathogenesis of polycystic ovary syndrome (PCOS): the hypothesis of PCOS as functional ovarian hyperandrogenism revisited. *Endocr Rev* (2016) 37:467–520. doi: 10.1210/er.2015-1104

14. Zhai Y, Pang Y. Systemic and ovarian inflammation in women with polycystic ovary syndrome. *J Reprod Immunol* (2022) 151:103628. doi: 10.1016/j.jri.2022.103628

15. Rudnicka E, Suchta K, Grymowicz M, Calik-Ksepka A, Smolarczyk K, Duszewska AM, et al. Chronic low grade inflammation in pathogenesis of PCOS. *Int J Mol Sci* (2021) 22:3789. doi: 10.3390/ijms22073789

16. Hu C, Pang B, Ma Z, Yi H. Immunophenotypic profiles in polycystic ovary syndrome. *Mediators Inflammation* (2020) 2020:5894768. doi: 10.1155/2020/5894768

17. Rostamtabar M, Esmaeilzadeh S, Tourani M, Rahmani A, Baee M, Shirafkan F, et al. Pathophysiological roles of chronic low-grade inflammation mediators in polycystic ovary syndrome. *J Cell Physiol* (2021) 236:824–38. doi: 10.1002/jcp.29912

18. Luan Y-Y, Zhang L, Peng Y-Q, Li Y-Y, Liu R-X, Yin C-H. Immune regulation in polycystic ovary syndrome. *Clin Chim Acta* (2022) 531:265–72. doi: 10.1016/j.cca.2022.04.234

19. Bhatia A, Sekhon HK, Kaur G. Sex hormones and immune dimorphism. *ScientificWorldJournal* (2014) 2014:159150. doi: 10.1155/2014/159150

20. Trigunaite A, Dimo J, Jørgensen TN. Suppressive effects of androgens on the immune system. *Cell Immunol* (2015) 294:87–94. doi: 10.1016/j.cellimm.2015.02.004

21. Koh YT, Gray A, Higgins SA, Hubby B, Kast WM. Androgen ablation augments prostate cancer vaccine immunogenicity only when applied after immunization. *Prostate* (2009) 69:571–84. doi: 10.1002/pros.20906

22. Rettew JA, Huet-Hudson YM, Marriott I. Testosterone reduces macrophage expression in the mouse of toll-like receptor 4, a trigger for inflammation and innate immunity. *Biol Reprod* (2008) 78:432–7. doi: 10.1095/biolreprod.107.063545

23. Kanda N, Hoashi T, Saeki H. The roles of sex hormones in the course of atopic dermatitis. *Int J Mol Sci* (2019) 20:4660. doi: 10.3390/ijms20194660

24. Lima PDA, Nivet A-L, Wang Q, Chen Y-A, Leader A, Cheung A, et al. Polycystic ovary syndrome: possible involvement of androgen-induced, chemerin-mediated

ovarian recruitment of monocytes/macrophages. *Biol Reprod* (2018) 99:838–52. doi: 10.1093/biolre/ioy096

25. Ashcroft GS, Mills SJ. Androgen receptor-mediated inhibition of cutaneous wound healing. *J Clin Invest* (2002) 110:615–24. doi: 10.1172/JCI15704

26. Hofer MD, Cheng EY, Bury MI, Xu W, Hong SJ, Kaplan WE, et al. Androgen supplementation in rats increases the inflammatory response and prolongs urethral healing. *Urology* (2015) 85:691–7. doi: 10.1016/j.urology.2014.11.025

27. Hases L, Archer A, Williams C. ERβ and inflammation. *Adv Exp Med Biol* (2022) 1390:213–25. doi: 10.1007/978-3-031-11836-4_12

28. Trenti A, Tedesco S, Boscaro C, Trevisi L, Bolego C, Cignarella A. Estrogen, angiogenesis, immunity and cell metabolism: solving the puzzle. *Int J Mol Sci* (2018) 19:859. doi: 10.3390/ijms19030859

29. Straub RH. The complex role of estrogens in inflammation. *Endocr Rev* (2007) 28:521–74. doi: 10.1210/er.2007-0001

30. Moulton VR. Sex hormones in acquired immunity and autoimmune disease. *Front Immunol* (2018) 9:2279. doi: 10.3389/fimmu.2018.02279

31. Panchanathan R, Shen H, Zhang X, Ho S-M, Choubey D. Mutually positive regulatory feedback loop between interferons and estrogen receptor-alpha in mice: implications for sex bias in autoimmunity. *PloS One* (2010) 5:e10868. doi: 10.1371/journal.pone.0010868

32. Dao MC, Saltzman E, Page M, Reece J, Mojtahed T, Wu D, et al. Lack of differences in inflammation and T cell-mediated function between young and older women with obesity. *Nutrients* (2020) 12:237. doi: 10.3390/nu12010237

33. Trim WV, Lynch L. Immune and non-immune functions of adipose tissue leukocytes. *Nat Rev Immunol* (2022) 22:371–86. doi: 10.1038/s41577-021-00635-7

34. Yong W, Wang J, Leng Y, Li L, Wang H. Role of obesity in female reproduction. *Int J Med Sci* (2023) 20:366–75. doi: 10.7150/ijms.80189

35. Morris DL, Cho KW, Delproposto JL, Oatmen KE, Geletka LM, Martinez-Santibanez G, et al. Adipose tissue macrophages function as antigen-presenting cells and regulate adipose tissue CD4+ T cells in mice. *Diabetes* (2013) 62:2762–72. doi: 10.2337/db12-1404

36. Deng T, Lyon CJ, Minze LJ, Lin J, Zou J, Liu JZ, et al. Class II major histocompatibility complex plays an essential role in obesity-induced adipose inflammation. *Cell Metab* (2013) 17:411–22. doi: 10.1016/j.cmet.2013.02.009

37. Galvão AM, Ferreira-Dias GM, Chełmonska-Soyta A, Wocławek-Potocka I, Skarżyński DJ. Immune-endocrine cross-talk in reproductive biology and pathology. *Mediators Inflammation* (2014) 2014:856465. doi: 10.1155/2014/856465

38. Walusimbi SS, Pate JL. Physiology and endocrinology symposium: role of immune cells in the corpus luteum. *J Anim Sci* (2013) 91:1650–9. doi: 10.2527/jas.2012-6179

39. Vanderstraeten A, Tuyaerts S, Amant F. The immune system in the normal endometrium and implications for endometrial cancer development. *J Reprod Immunol* (2015) 109:7–16. doi: 10.1016/j.jri.2014.12.006

40. Smith SB, Ravel J. The vaginal microbiota, host defence and reproductive physiology. *J Physiol* (2017) 595:451–63. doi: 10.1113/JP271694

41. Kinnear HM, Tomaszewski CE, Chang FL, Moravek MB, Xu M, Padmanabhan V, et al. The ovarian stroma as a new frontier. *Reproduction* (2020) 160:R25–39. doi: 10.1530/REP-19-0501

42. Norman RJ, Brannstrom M. White cells and the ovary–incidental invaders or essential effectors? *J Endocrinol* (1994) 140:333–6. doi: 10.1677/joe.0.1400333

43. Li Y, Zheng Q, Sun D, Cui X, Chen S, Bulbul A, et al. Dehydroepiandrosterone stimulates inflammation and impairs ovarian functions of polycystic ovary syndrome. *J Cell Physiol* (2019) 234:7435–47. doi: 10.1002/jcp.27501

44. González F. Inflammation in polycystic ovary syndrome: underpinning of insulin resistance and ovarian dysfunction. *Steroids* (2012) 77:300–5. doi: 10.1016/j.steroids.2011.12.003

45. Abdalla M, Deshmukh H, Atkin SL, Sathyapalan T. miRNAs as a novel clinical biomarker and therapeutic targets in polycystic ovary syndrome (PCOS): a review. *Life Sci* (2020) 259:118174. doi: 10.1016/j.lfs.2020.118174

46. Boots CE, Jungheim ES. Inflammation and human ovarian follicular dynamics. *Semin Reprod Med* (2015) 33:270–5. doi: 10.1055/s-0035-1554928

47. Balan S, Saxena M, Bhardwaj N. Dendritic cell subsets and locations. *Int Rev Cell Mol Biol* (2019) 348:1–68. doi: 10.1016/bs.ircmb.2019.07.004

48. Fainaru O, Hantisteanu S, Rotfarb N, Michaeli M, Hallak M, Ellenbogen A. CD11c+HLADR+ dendritic cells are present in human ovarian follicular fluid, and their maturity correlates with serum estradiol levels in response to gonadotropins. *Fertil Steril* (2012) 97:702–6. doi: 10.1016/j.fertnstert.2011.12.030

49. Zhang T, Tian F, Huo R, Tang A, Zeng Y, Duan Y-G. Detection of dendritic cells and related cytokines in follicular fluid of patients with polycystic ovary syndrome. *Am J Reprod Immunol* (2017) 78. doi: 10.1111/aji.12717

50. Lu X, Cui J, Cui L, Luo Q, Cao Q, Yuan W, et al. The effects of human umbilical cord-derived mesenchymal stem cell transplantation on endometrial receptivity are associated with Th1/Th2 balance change and uNK cell expression of uterine in autoimmune premature ovarian failure mice. *Stem Cell Res Ther* (2019) 10:214. doi: 10.1186/s13287-019-1313-y

51. Kryczek I, Frydman N, Gaudin F, Krzysiek R, Fanchin R, Emilie D, et al. The chemokine SDF-1/CXCL12 contributes to T lymphocyte recruitment in human pre-ovulatory follicles and coordinates with lymphocytes to increase granulosa cell survival and embryo quality. *Am J Reprod Immunol* (2005) 54:270–83. doi: 10.1111/j.1600-0897.2005.00307.x

52. Wu R, Fujii S, Ryan NK, van der Hoek KH, Jasper MJ, Sini I, et al. Ovarian leukocyte distribution and cytokine/chemokine mRNA expression in follicular fluid cells in women with polycystic ovary syndrome. *Hum Reprod* (2007) 22:527–35. doi: 10.1093/humrep/del371

53. Qin L, Xu W, Li X, Meng W, Hu L, Luo Z, et al. Differential expression profile of immunological cytokines in local ovary in patients with polycystic ovarian syndrome: analysis by flow cytometry. *Eur J Obstet Gynecol Reprod Biol* (2016) 197:136–41. doi: 10.1016/j.ejogrb.2015.12.003

54. Li Z, Peng A, Feng Y, Zhang X, Liu F, Chen C, et al. Detection of T lymphocyte subsets and related functional molecules in follicular fluid of patients with polycystic ovary syndrome. *Sci Rep* (2019) 9:6040. doi: 10.1038/s41598-019-42631-x

55. Kahyaoglu I, Yılmaz N, Timur H, Inal HA, Erkaya S. Granulocyte colony-stimulating factor: a relation between serum and follicular fluid levels and in-vitro fertilization outcome in patients with polycystic ovary syndrome. *Cytokine* (2015) 74:113–6. doi: 10.1016/j.cyto.2014.09.002

56. Brannstrom M, Pascoe V, Norman RJ, McClure N. Localization of leukocyte subsets in the follicle wall and in the corpus luteum throughout the human menstrual cycle. *Fertil Steril* (1994) 61:488–95. doi: 10.1016/S0015-0282(16)56581-9

57. Zhang H, Wang X, Xu J, Zhu Y, Chen X, Hu Y. IL-18 and IL-18 binding protein concentration in ovarian follicular fluid of women with unexplained infertility to PCOS during *in vitro* fertilization. *J Reprod Immunol* (2020) 138:103083. doi: 10.1016/j.jri.2020.103083

58. Liu Y, Liu H, Li Z, Fan H, Yan X, Liu X, et al. The release of peripheral immune inflammatory cytokines promote an inflammatory cascade in PCOS patients via altering the follicular microenvironment. *Front Immunol* (2021) 12:685724. doi: 10.3389/fimmu.2021.685724

59. Adams J, Liu Z, Ren YA, Wun W-S, Zhou W, Kenigsberg S, et al. Enhanced inflammatory transcriptome in the granulosa cells of women with polycystic ovarian syndrome. *J Clin Endocrinol Metab* (2016) 101:3459–68. doi: 10.1210/jc.2015-4275

60. Giudice LC. Endometrium in PCOS: implantation and predisposition to endocrine CA. *Best Pract Res Clin Endocrinol Metab* (2006) 20:235–44. doi: 10.1016/j.beem.2006.03.005

61. Agostinis C, Mangogna A, Bossi F, Ricci G, Kishore U, Bulla R. Uterine immunity and microbiota: a shifting paradigm. *Front Immunol* (2019) 10:2387. doi: 10.3389/fimmu.2019.02387

62. Kayisli UA, Guzeloglu-Kayisli O, Arici A. Endocrine-immune interactions in human endometrium. *Ann N Y Acad Sci* (2004) 1034:50–63. doi: 10.1196/annals.1335.005

63. Palomba S, Piltonen TT, Giudice LC. Endometrial function in women with polycystic ovary syndrome: a comprehensive review. *Hum Reprod Update* (2021) 27:584–618. doi: 10.1093/humupd/dmaa051

64. Liu S, Diao L, Huang C, Li Y, Zeng Y, Kwak-Kim JYH. The role of decidual immune cells on human pregnancy. *J Reprod Immunol* (2017) 124:44–53. doi: 10.1016/j.jri.2017.10.045

65. Piltonen TT. Polycystic ovary syndrome: endometrial markers. *Best Pract Res Clin Obstet Gynaecol* (2016) 37:66–79. doi: 10.1016/j.bpobgyn.2016.03.008

66. Baracat MCP, Baracat EC, Simões RS, Simões MJ, Maciel GAR, Azziz R, et al. Hormonal and metabolic factors influence the action of progesterone on the endometrium of women with polycystic ovary syndrome. *Diagnostics (Basel)* (2023) 13:382. doi: 10.3390/diagnostics13030382

67. Kitaya K, Yamaguchi T, Honjo H. Central role of interleukin-15 in postovulatory recruitment of peripheral blood CD16(-) natural killer cells into human endometrium. *J Clin Endocrinol Metab* (2005) 90:2932–40. doi: 10.1210/jc.2004-2447

68. Matteo M, Serviddio G, Massenzio F, Scillitani G, Castellana L, Picca G, et al. Reduced percentage of natural killer cells associated with impaired cytokine network in the secretory endometrium of infertile women with polycystic ovary syndrome. *Fertil Steril* (2010) 94:2222–2227, 2227.e1–3. doi: 10.1016/j.fertnstert.2010.01.049

69. Salamonsen LA, Woolley DE. Menstruation: induction by matrix metalloproteinases and inflammatory cells. *J Reprod Immunol* (1999) 44:1–27. doi: 10.1016/s0165-0378(99)00002-9

70. Thiruchelvam U, Dransfield I, Saunders PTK, Critchley HOD. The importance of the macrophage within the human endometrium. *J Leukoc Biol* (2013) 93:217–25. doi: 10.1189/jlb.0712327

71. Liu S, Hong L, Mo M, Xiao S, Chen C, Li Y, et al. Evaluation of endometrial immune status of polycystic ovary syndrome. *J Reprod Immunol* (2021) 144:103282. doi: 10.1016/j.jri.2021.103282

72. Oróstica L, Astorga I, Plaza-Parrochia F, Vera C, García V, Carvajal R, et al. Proinflammatory environment and role of TNF-α in endometrial function of obese women having polycystic ovarian syndrome. *Int J Obes (Lond)* (2016) 40:1715–22. doi: 10.1038/ijo.2016.154

73. Oróstica L, Poblete C, Romero C, Vega M. Pro-inflammatory markers negatively regulate IRS1 in endometrial cells and endometrium from women with obesity and PCOS. *Reprod Sci* (2020) 27:290–300. doi: 10.1007/s43032-019-00026-3

74. Schulke L, Manconi F, Markham R, Fraser IS. Endometrial dendritic cell populations during the normal menstrual cycle. *Hum Reprod* (2008) 23:1574–80. doi: 10.1093/humrep/den030

75. Vallvé-Juanico J, Houshdaran S, Giudice LC. The endometrial immune environment of women with endometriosis. *Hum Reprod Update* (2019) 25:564–91. doi: 10.1093/humupd/dmz018

76. Piltonen TT, Chen JC, Khatun M, Kangasniemi M, Liakka A, Spitzer T, et al. Endometrial stromal fibroblasts from women with polycystic ovary syndrome have impaired progesterone-mediated decidualization, aberrant cytokine profiles and promote enhanced immune cell migration. *vitro. Hum Reprod* (2015) 30:1203–15. doi: 10.1093/humrep/dev055

77. Zolfaghari MA, Arefnezhad R, Parhizkar F, Hejazi MS, Motavalli Khiavi F, Mahmoodpoor A, et al. T Lymphocytes and preeclampsia: the potential role of T-cell subsets and related MicroRNAs in the pathogenesis of preeclampsia. *Am J Reprod Immunol* (2021) 86:e13475. doi: 10.1111/aji.13475

78. Zhao D-M, Shan Y-H, Li F-H, Jiang L, Qu Q-L. Correlation between endometrial receptivity with expressions of IL-1 and VEGF in rats with polycystic ovary syndrome. *Eur Rev Med Pharmacol Sci* (2019) 23:5575–80. doi: 10.26355/eurrev_201907_18291

79. Hu M, Zhang Y, Li X, Cui P, Sferruzzi-Perri AN, Brännström M, et al. TLR4-associated IRF-7 and NFκB signaling act as a molecular link between androgen and metformin activities and cytokine synthesis in the PCOS endometrium. *J Clin Endocrinol Metab* (2021) 106:1022–40. doi: 10.1210/clinem/dgaa951

80. Long X, Li R, Yang Y, Qiao J. Overexpression of IL-18 in the proliferative phase endometrium of patients with polycystic ovary syndrome. *Reprod Sci* (2017) 24:252–7. doi: 10.1177/1933719116653681

81. Escobar-Morreale HF, Luque-Ramírez M, González F. Circulating inflammatory markers in polycystic ovary syndrome: a systematic review and metaanalysis. *Fertil Steril* (2011) 95:1048-1058.e1–2. doi: 10.1016/j.fertnstert.2010.11.036

82. Chen C, Song X, Wei W, Zhong H, Dai J, Lan Z, et al. The microbiota continuum along the female reproductive tract and its relation to uterine-related diseases. *Nat Commun* (2017) 8:875. doi: 10.1038/s41467-017-00901-0

83. Chee WJY, Chew SY, Than LTL. Vaginal microbiota and the potential of lactobacillus derivatives in maintaining vaginal health. *Microb Cell Fact* (2020) 19:203. doi: 10.1186/s12934-020-01464-4

84. Moosa Y, Kwon D, de Oliveira T, Wong EB. Determinants of vaginal microbiota composition. *Front Cell Infect Microbiol* (2020) 10:467. doi: 10.3389/fcimb.2020.00467

85. Elovitz MA, Gajer P, Riis V, Brown AG, Humphrys MS, Holm JB, et al. Cervicovaginal microbiota and local immune response modulate the risk of spontaneous preterm delivery. *Nat Commun* (2019) 10:1305. doi: 10.1038/s41467-019-09285-9

86. Torcia MG. Interplay among vaginal microbiome, immune response and sexually transmitted viral infections. *Int J Mol Sci* (2019) 20:266. doi: 10.3390/ijms20020266

87. Hong X, Qin P, Huang K, Ding X, Ma J, Xuan Y, et al. Association between polycystic ovary syndrome and the vaginal microbiome: a case-control study. *Clin Endocrinol (Oxf)* (2020) 93:52–60. doi: 10.1111/cen.14198

88. Hong X, Qin P, Yin J, Shi Y, Xuan Y, Chen Z, et al. Clinical manifestations of polycystic ovary syndrome and associations with the vaginal microbiome: a cross-sectional based exploratory study. *Front Endocrinol (Lausanne)* (2021) 12:662725. doi: 10.3389/fendo.2021.662725

89. Tu Y, Zheng G, Ding G, Wu Y, Xi J, Ge Y, et al. Comparative analysis of lower genital tract microbiome between PCOS and healthy women. *Front Physiol* (2020) 11:1108. doi: 10.3389/fphys.2020.01108

90. Anahtar MN, Gootenberg DB, Mitchell CM, Kwon DS. Cervicovaginal microbiota and reproductive health: the virtue of simplicity. *Cell Host Microbe* (2018) 23:159–68. doi: 10.1016/j.chom.2018.01.013

91. Lewis WG, Robinson LS, Perry J, Bick JL, Peipert JF, Allsworth JE, et al. Hydrolysis of secreted sialoglycoprotein immunoglobulin a (IgA) in ex vivo and biochemical models of bacterial vaginosis. *J Biol Chem* (2012) 287:2079–89. doi: 10.1074/jbc.M111.278135

92. Larsen JM. The immune response to prevotella bacteria in chronic inflammatory disease. *Immunology* (2017) 151:363–74. doi: 10.1111/imm.12760

93. Brotman RM, Ravel J, Bavoil PM, Gravitt PE, Ghanem KG. Microbiome, sex hormones, and immune responses in the reproductive tract: challenges for vaccine development against sexually transmitted infections. *Vaccine* (2014) 32:1543–52. doi: 10.1016/j.vaccine.2013.10.010

94. Wekker V, van Dammen L, Koning A, Heida KY, Painter RC, Limpens J, et al. Long-term cardiometabolic disease risk in women with PCOS: a systematic review and meta-analysis. *Hum Reprod Update* (2020) 26:942–60. doi: 10.1093/humupd/dmaa029

95. Wild RA, Carmina E, Diamanti-Kandarakis E, Dokras A, Escobar-Morreale HF, Futterweit W, et al. Assessment of cardiovascular risk and prevention of cardiovascular disease in women with the polycystic ovary syndrome: a consensus statement by the androgen excess and polycystic ovary syndrome (AE-PCOS) society. *J Clin Endocrinol Metab* (2010) 95:2038–49. doi: 10.1210/jc.2009-2724

96. Sangaraju SL, Yepez D, Grandes XA, Talanki Manjunatha R, Habib S. Cardio-metabolic disease and polycystic ovarian syndrome (PCOS): a narrative review. *Cureus* (2022) 14:e25076. doi: 10.7759/cureus.25076

97. Osibogun O, Ogunmoroti O, Michos ED. Polycystic ovary syndrome and cardiometabolic risk: opportunities for cardiovascular disease prevention. *Trends Cardiovasc Med* (2020) 30:399–404. doi: 10.1016/j.tcm.2019.08.010

98. Victor VM, Rovira-Llopis S, Bañuls C, Diaz-Morales N, Martinez de Marañon A, Rios-Navarro C, et al. Insulin resistance in PCOS patients enhances oxidative stress and leukocyte adhesion: role of myeloperoxidase. *PloS One* (2016) 11:e0151960. doi: 10.1371/journal.pone.0151960

99. Ma J, Zhang H, Tang K, Huang B. Tumor-derived microparticles in tumor immunology and immunotherapy. *Eur J Immunol* (2020) 50:1653–62. doi: 10.1002/eji.202048548

100. Carvalho LML, Ferreira CN, Sóter MO, Sales MF, Rodrigues KF, Martins SR, et al. Microparticles: inflammatory and haemostatic biomarkers in polycystic ovary syndrome. *Mol Cell Endocrinol* (2017) 443:155–62. doi: 10.1016/j.mce.2017.01.017

101. Blanco-Colio LM, Méndez-Barbero N, Pello Lázaro AM, Aceña Á, Tarín N, Cristóbal C, et al. MCP-1 predicts recurrent cardiovascular events in patients with persistent inflammation. *J Clin Med* (2021) 10:1137. doi: 10.3390/jcm10051137

102. Namiki M, Kawashima S, Yamashita T, Ozaki M, Hirase T, Ishida T, et al. Local overexpression of monocyte chemoattractant protein-1 at vessel wall induces infiltration of macrophages and formation of atherosclerotic lesion: synergism with hypercholesterolemia. *Arterioscler Thromb Vasc Biol* (2002) 22:115–20. doi: 10.1161/hq0102.102278

103. Hu W, Qiao J, Yang Y, Wang L, Li R. Elevated c-reactive protein and monocyte chemoattractant protein-1 in patients with polycystic ovary syndrome. *Eur J Obstet Gynecol Reprod Biol* (2011) 157:53–6. doi: 10.1016/j.ejogrb.2011.03.015

104. Toulis KA, Goulis DG, Mintziori G, Kintiraki E, Eukarpidis E, Mouratoglou S-A, et al. Meta-analysis of cardiovascular disease risk markers in women with polycystic ovary syndrome. *Hum Reprod Update* (2011) 17:741–60. doi: 10.1093/humupd/dmr025

105. Wang H-X, Wang Y-P. Gut microbiota-brain axis. *Chin Med J (Engl)* (2016) 129:2373–80. doi: 10.4103/0366-6999.190667

106. Takiishi T, Fenero CIM, Câmara NOS. Intestinal barrier and gut microbiota: shaping our immune responses throughout life. *Tissue Barriers* (2017) 5:e1373208. doi: 10.1080/21688370.2017.1373208

107. Lindheim L, Bashir M, Münzker J, Trummer C, Zachhuber V, Leber B, et al. Alterations in gut microbiome composition and barrier function are associated with reproductive and metabolic defects in women with polycystic ovary syndrome (PCOS): a pilot study. *PloS One* (2017) 12:e0168390. doi: 10.1371/journal.pone.0168390

108. Guo Y, Qi Y, Yang X, Zhao L, Wen S, Liu Y, et al. Association between polycystic ovary syndrome and gut microbiota. *PloS One* (2016) 11:e0153196. doi: 10.1371/journal.pone.0153196

109. Parker J, O'Brien C, Hawrelak J. A narrative review of the role of gastrointestinal dysbiosis in the pathogenesis of polycystic ovary syndrome. *Obstet Gynecol Sci* (2022) 65:14–28. doi: 10.5468/ogs.21185

110. Qi X, Yun C, Sun L, Xia J, Wu Q, Wang Y, et al. Gut microbiota-bile acid-interleukin-22 axis orchestrates polycystic ovary syndrome. *Nat Med* (2019) 25:1225–33. doi: 10.1038/s41591-019-0509-0

111. He F-F, Li Y-M. Role of gut microbiota in the development of insulin resistance and the mechanism underlying polycystic ovary syndrome: a review. *J Ovarian Res* (2020) 13:73. doi: 10.1186/s13048-020-00670-3

112. Wang Y, Xiao H, Liu Y, Tong Q, Yu Y, Qi B, et al. Effects of bu shen hua zhuo formula on the LPS/TLR4 pathway and gut microbiota in rats with letrozole-induced polycystic ovary syndrome. *Front Endocrinol (Lausanne)* (2022) 13:891297. doi: 10.3389/fendo.2022.891297

113. Carreau A-M, Pyle L, Garcia-Reyes Y, Rahat H, Vigers T, Jensen T, et al. Clinical prediction score of nonalcoholic fatty liver disease in adolescent girls with polycystic ovary syndrome (PCOS-HS index). *Clin Endocrinol (Oxf)* (2019) 91:544–52. doi: 10.1111/cen.14062

114. Won YB, Seo SK, Yun BH, Cho S, Choi YS, Lee BS. Non-alcoholic fatty liver disease in polycystic ovary syndrome women. *Sci Rep* (2021) 11:7085. doi: 10.1038/s41598-021-86697-y

115. de Zegher F, Diaz M, Ibañez L. From adolescent PCOS to adult MAFLD: opposing effects of randomised interventions. *BMJ Open Gastroenterol* (2021) 8:e000574. doi: 10.1136/bmjgast-2020-000574

116. Asfari MM, Sarmini MT, Baidoun F, Al-Khadra Y, Ezzaizi Y, Dasarathy S, et al. Association of non-alcoholic fatty liver disease and polycystic ovarian syndrome. *BMJ Open Gastroenterol* (2020) 7:e000352. doi: 10.1136/bmjgast-2019-000352

117. Utzschneider KM, Kahn SE. Review: the role of insulin resistance in nonalcoholic fatty liver disease. *J Clin Endocrinol Metab* (2006) 91:4753–61. doi: 10.1210/jc.2006-0587

118. Mohammadi S, Karimzadeh Bardei L, Hojati V, Ghorbani AG, Nabiuni M. Anti-inflammatory effects of curcumin on insulin resistance index, levels of interleukin-6, c-reactive protein, and liver histology in polycystic ovary syndrome-induced rats. *Cell J* (2017) 19:425–33. doi: 10.22074/cellj.2017.4415

119. Arrese M, Cabrera D, Kalergis AM, Feldstein AE. Innate immunity and inflammation in NAFLD/NASH. *Dig Dis Sci* (2016) 61:1294–303. doi: 10.1007/s10620-016-4049-x

120. Henning JR, Graffeo CS, Rehman A, Fallon NC, Zambirinis CP, Ochi A, et al. Dendritic cells limit fibroinflammatory injury in nonalcoholic steatohepatitis in mice. *Hepatology* (2013) 58:589–602. doi: 10.1002/hep.26267

121. Chen Y, Ma L, Ge Z, Pan Y, Xie L. Key genes associated with non-alcoholic fatty liver disease and polycystic ovary syndrome. *Front Mol Biosci* (2022) 9:888194. doi: 10.3389/fmolb.2022.888194

122. Romitti M, Fabris VC, Ziegelmann PK, Maia AL, Spritzer PM. Association between PCOS and autoimmune thyroid disease: a systematic review and meta-analysis. *Endocr Connect* (2018) 7:1158–67. doi: 10.1530/EC-18-0309

123. Sen A, Kushnir VA, Barad DH, Gleicher N. Endocrine autoimmune diseases and female infertility. *Nat Rev Endocrinol* (2014) 10:37–50. doi: 10.1038/nrendo.2013.212

124. Singla R, Gupta Y, Khemani M, Aggarwal S. Thyroid disorders and polycystic ovary syndrome: an emerging relationship. *Indian J Endocrinol Metab* (2015) 19:25–9. doi: 10.4103/2230-8210.146860

125. Ho C-W, Chen H-H, Hsieh M-C, Chen C-C, Hsu S-P, Yip H-T, et al. Increased risk of polycystic ovary syndrome and it's comorbidities in women with autoimmune thyroid disease. *Int J Environ Res Public Health* (2020) 17:2422. doi: 10.3390/ijerph17072422

126. Singh J, Wong H, Ahluwalia N, Go RM, Guerrero-Go MA. Metabolic, hormonal, immunologic, and genetic factors associated with the incidence of thyroid disorders in polycystic ovarian syndrome patients. *Cureus* (2020) 12:e11681. doi: 10.7759/cureus.11681

127. Mohammed S, Awooda HA, Rayis DA, Hamdan HZ, Adam I, Lutfi MF. Thyroid function/antibodies in sudanese women with polycystic ovarian disease. *Obstet Gynecol Sci* (2017) 60:187–92. doi: 10.5468/ogs.2017.60.2.187

128. Al-Saab R, Haddad S. Detection of thyroid autoimmunity markers in euthyroid women with polycystic ovary syndrome: a case-control study from syria. *Int J Endocrinol Metab* (2014) 12:e17954. doi: 10.5812/ijem.17954

129. Gonzalez F. Adrenal involvement in polycystic ovary syndrome. *Semin Reprod Endocrinol* (1997) 15:137–57. doi: 10.1055/s-2007-1016296

130. Franik G, Bizoń A, Włoch S, Kowalczyk K, Biernacka-Bartnik A, Madej P. Hormonal and metabolic aspects of acne vulgaris in women with polycystic ovary syndrome. *Eur Rev Med Pharmacol Sci* (2018) 22:4411–8. doi: 10.26355/eurrev_201807_15491

131. Yesiladali M, Yazici MGK, Attar E, Kelestimur F. Differentiating polycystic ovary syndrome from adrenal disorders. *Diagnostics (Basel)* (2022) 12:2045. doi: 10.3390/diagnostics12092045

132. Yildiz BO, Azziz R. The adrenal and polycystic ovary syndrome. *Rev Endocr Metab Disord* (2007) 8:331–42. doi: 10.1007/s11154-007-9054-0

133. Benjamin JJ KM, Koshy T KNM, DHEA RP. And polycystic ovarian syndrome: meta-analysis of case-control studies. *PloS One* (2021) 16:e0261552. doi: 10.1371/journal.pone.0261552

134. Zhou R, Bird IM, Dumesic DA, Abbott DH. Adrenal hyperandrogenism is induced by fetal androgen excess in a rhesus monkey model of polycystic ovary syndrome. *J Clin Endocrinol Metab* (2005) 90:6630–7. doi: 10.1210/jc.2005-0691

135. Bongiovanni B, Diaz A, Santucci N, D'Attilio LD, Bottasso O, Hernández Pando R, et al. The immunoregulatory actions of DHEA in tuberculosis, a tool for therapeutic intervention? *Front Endocrinol (Lausanne)* (2022) 13:892270. doi: 10.3389/fendo.2022.892270

136. Zhang J, Qiu X, Gui Y, Xu Y, Li D, Wang L. Dehydroepiandrosterone improves the ovarian reserve of women with diminished ovarian reserve and is a potential regulator of the immune response in the ovaries. *Biosci Trends* (2015) 9:350–9. doi: 10.5582/bst.2015.01154

137. Gleicher N, Darmon S, Patrizio P, Barad DH. Reconsidering the polycystic ovary syndrome (PCOS). *Biomedicines* (2022) 10:1505. doi: 10.3390/biomedicines10071505

138. Gleicher N, Kushnir VA, Darmon SK, Wang Q, Zhang L, Albertini DF, et al. New PCOS-like phenotype in older infertile women of likely autoimmune adrenal etiology with high AMH but low androgens. *J Steroid Biochem Mol Biol* (2017) 167:144–52. doi: 10.1016/j.jsbmb.2016.12.004

139. Gleicher N, Kushnir VA, Darmon SK, Wang Q, Zhang L, Albertini DF, et al. Suspected ontogeny of a recently described hypo-androgenic PCOS-like phenotype with advancing age. *Endocrine* (2018) 59:661–76. doi: 10.1007/s12020-017-1498-8

140. Atkinson L, Kite C, McGregor G, James T, Clark CCT, Randeva HS, et al. Uncertainty, anxiety and isolation: experiencing the COVID-19 pandemic and lockdown as a woman with polycystic ovary syndrome (PCOS). *J Pers Med* (2021) 11:952. doi: 10.3390/jpm11100952

141. Ilias I, Goulas S, Zabuliene L. Polycystic ovary syndrome: pathways and mechanisms for possible increased susceptibility to COVID-19. *World J Clin cases* (2021) 9:2711–20. doi: 10.12998/wjcc.v9.i12.2711

142. Klein SL, Flanagan KL. Sex differences in immune responses. *Nat Rev Immunol* (2016) 16:626–38. doi: 10.1038/nri.2016.90

143. Huffman AM, Rezq S, Basnet J, Yanes Cardozo LL, Romero DG. SARS-CoV-2 viral entry proteins in hyperandrogenemic female mice: implications for women with PCOS and COVID-19. *Int J Mol Sci* (2021) 22:4472. doi: 10.3390/ijms22094472

144. Xu Y, Baylink DJ, Chen C-S, Reeves ME, Xiao J, Lacy C, et al. The importance of vitamin d metabolism as a potential prophylactic, immunoregulatory and neuroprotective treatment for COVID-19. *J Transl Med* (2020) 18:322. doi: 10.1186/s12967-020-02488-5

145. Merad M, Martin JC. Pathological inflammation in patients with COVID-19: a key role for monocytes and macrophages. *Nat Rev Immunol* (2020) 20:355–62. doi: 10.1038/s41577-020-0331-4

146. Teshome A, Adane A, Girma B, Mekonnen ZA. The impact of vitamin d level on COVID-19 infection: systematic review and meta-analysis. *Front Public Health* (2021) 9:624559. doi: 10.3389/fpubh.2021.624559

147. Rawat D, Roy A, Maitra S, Shankar V, Khanna P, Baidya DK. Vitamin d supplementation and COVID-19 treatment: a systematic review and meta-analysis. *Diabetes Metab Syndr* (2021) 15:102189. doi: 10.1016/j.dsx.2021.102189

148. Mansur JL, Tajer C, Mariani J, Inserra F, Ferder L, Manucha W. Vitamin d high doses supplementation could represent a promising alternative to prevent or treat COVID-19 infection. *Clin Investig Arterioscler* (2020) 32:267–77. doi: 10.1016/j.arteri.2020.05.003

149. Trzupek D, Dunstan M, Cutler AJ, Lee M, Godfrey L, Jarvis L, et al. Discovery of CD80 and CD86 as recent activation markers on regulatory T cells by protein-RNA single-cell analysis. *Genome Med* (2020) 12:55. doi: 10.1186/s13073-020-00756-z

150. Nguyen KG, Vrabel MR, Mantooth SM, Hopkins JJ, Wagner ES, Gabaldon TA, et al. Localized interleukin-12 for cancer immunotherapy. *Front Immunol* (2020) 11:575597. doi: 10.3389/fimmu.2020.575597

151. Moin ASM, Sathyapalan T, Butler AE, Atkin SL. Vitamin d association with macrophage-derived cytokines in polycystic ovary syndrome: an enhanced risk of COVID-19 infection? *Front Endocrinol (Lausanne)* (2021) 12:638621. doi: 10.3389/fendo.2021.638621

152. Kahal H, Kyrou I, Tahrani AA, Randeva HS. Obstructive sleep apnoea and polycystic ovary syndrome: a comprehensive review of clinical interactions and underlying pathophysiology. *Clin Endocrinol (Oxf)* (2017) 87:313–9. doi: 10.1111/cen.13392

153. Fan C, Huang S, Xiang C, An T, Song Y. Identification of key genes and immune infiltration modulated by CPAP in obstructive sleep apnea by integrated bioinformatics analysis. *PloS One* (2021) 16:e0255708. doi: 10.1371/journal.pone.0255708

154. Ehrmann DA. Metabolic dysfunction in pcos: relationship to obstructive sleep apnea. *Steroids* (2012) 77:290–4. doi: 10.1016/j.steroids.2011.12.001

155. Nitsche K, Ehrmann DA. Obstructive sleep apnea and metabolic dysfunction in polycystic ovary syndrome. *Best Pract Res Clin Endocrinol Metab* (2010) 24:717–30. doi: 10.1016/j.beem.2010.08.001

156. Kumarendran B, Sumilo D, O'Reilly MW, Toulis KA, Gokhale KM, Wijeyaratne CN, et al. Increased risk of obstructive sleep apnoea in women with polycystic ovary syndrome: a population-based cohort study. *Eur J Endocrinol* (2019) 180:265–72. doi: 10.1530/EJE-18-0693

157. Vgontzas AN, Legro RS, Bixler EO, Grayev A, Kales A, Chrousos GP. Polycystic ovary syndrome is associated with obstructive sleep apnea and daytime sleepiness: role of insulin resistance. *J Clin Endocrinol Metab* (2001) 86:517–20. doi: 10.1210/jcem.86.2.7185

158. Kahal H, Kyrou I, Uthman O, Brown A, Johnson S, Wall P, et al. The association between obstructive sleep apnea and metabolic abnormalities in women with polycystic ovary syndrome: a systematic review and meta-analysis. *Sleep* (2018) 41. doi: 10.1093/sleep/zsy085

159. Vgontzas AN, Bixler EO, Chrousos GP. Metabolic disturbances in obesity versus sleep apnoea: the importance of visceral obesity and insulin resistance. *J Intern Med* (2003) 254:32–44. doi: 10.1046/j.1365-2796.2003.01177.x

160. Gao Q, Ma C, Meng S, Wang G, Xing Q, Xu Y, et al. Exploration of molecular features of PCOS with different androgen levels and immune-related prognostic biomarkers associated with implantation failure. *Front Endocrinol (Lausanne)* (2022) 13:946504. doi: 10.3389/fendo.2022.946504

161. González F, Sia CL, Stanczyk FZ, Blair HE, Krupa ME. Hyperandrogenism exerts an anti-inflammatory effect in obese women with polycystic ovary syndrome. *Endocrine* (2012) 42:726–35. doi: 10.1007/s12020-012-9728-6

frontiers | Frontiers in Immunology

TYPE Original Research
PUBLISHED 13 July 2023
DOI 10.3389/fimmu.2023.1209190

OPEN ACCESS

EDITED BY
Joanna Davies,
San Diego Biomedical Research Institute,
United States

REVIEWED BY
Wayne Robert Thomas,
University of Western Australia, Australia
Francisca Palomares,
Unversidad de Sevilla, Spain

*CORRESPONDENCE
Marta Gorzkiewicz
gorzkiewiczmarta@cm.umk.pl

RECEIVED 20 April 2023
ACCEPTED 29 June 2023
PUBLISHED 13 July 2023

CITATION
Gorzkiewicz M, Łoś-Rycharska E, Gawryjołek J, Gołębiewski M, Krogulska A and Grzybowski T (2023) The methylation profile of *IL4*, *IL5*, *IL10*, *IFNG* and *FOXP3* associated with environmental exposures differed between Polish infants with the food allergy and/or atopic dermatitis and without the disease.
Front. Immunol. 14:1209190.
doi: 10.3389/fimmu.2023.1209190

The methylation profile of *IL4*, *IL5*, *IL10*, *IFNG* and *FOXP3* associated with environmental exposures differed between Polish infants with the food allergy and/or atopic dermatitis and without the disease

Marta Gorzkiewicz[1]*, Ewa Łoś-Rycharska[2], Julia Gawryjołek[2], Marcin Gołębiewski[3,4], Aneta Krogulska[2] and Tomasz Grzybowski[1]

[1]Department of Forensic Medicine, Ludwik Rydygier Collegium Medicum in Bydgoszcz, Nicolaus Copernicus University in Toruń, Toruń, Poland, [2]Department of Pediatrics, Allergology and Gastroenterology, Ludwik Rydygier Collegium Medicum in Bydgoszcz, Nicolaus Copernicus University in Toruń, Toruń, Poland, [3]Department of Plant Physiology and Biotechnology, Nicolaus Copernicus University in Toruń, Toruń, Poland, [4]Interdisciplinary Centre of Modern Technologies, Nicolaus Copernicus University in Toruń, Toruń, Poland

Objectives: Epigenetic dynamics has been indicated to play a role in allergy development. The environmental stimuli have been shown to influence the methylation processes. This study investigated the differences in CpGs methylation rate of immune-attached genes between healthy and allergic infants. The research was aimed at finding evidence for the impact of environmental factors on methylation-based regulation of immunological processes in early childhood.

Methods: The analysis of methylation level of CpGs in the *IL4*, *IL5*, *IL10*, *IFNG* and *FOXP3* genes was performed using high resolution melt real time PCR technology. DNA was isolated from whole blood of Polish healthy and allergic infants, with food allergy and/or atopic dermatitis, aged under six months.

Results: The significantly lower methylation level of *FOXP3* among allergic infants compared to healthy ones was reported. Additional differences in methylation rates were found, when combining with environmental factors. In different studied groups, negative correlations between age and the *IL10* and *FOXP3* methylation were detected, and positive - in the case of *IL4*. Among infants with different allergy symptoms, the decrease in methylation level of *IFNG*, *IL10*, *IL4* and *FOXP3* associated with passive smoke exposure was observed. Complications during pregnancy were linked to different pattern of the *IFNG*, *IL5*, *IL4* and *IL10* methylation depending on allergy status. The *IFNG* and *IL5* methylation rates were higher among exclusively breastfed infants with atopic dermatitis compared to the non-breastfed. A decrease in the *IFNG* methylation was noted among allergic patients fed exclusively with milk

formula. In different study groups, a negative correlation between *IFNG*, *IL5* methylation and maternal BMI or *IL5* methylation and weight was noted. Some positive correlations between methylation rate of *IL10* and child's weight were found. A higher methylation of *IL4* was positively correlated with the number of family members with allergy.

Conclusion: The *FOXP3* methylation in allergic infants was lower than in the healthy ones. The methylation profile of *IL4*, *IL5*, *IL10*, *IFNG* and *FOXP3* associated with environmental exposures differed between the studied groups. The results offer insights into epigenetic regulation of immunological response in early childhood.

KEYWORDS

DNA methylation, environmental exposure, allergy, *IL4*, *IL5*, *IL10*, *IFNG*, *FOXP3*

1 Introduction

Food allergy (FA) is a complex, multifactorial disease that is becoming a worldwide health problem. Its prevalence is increasing in both Western and developing countries affecting up to 10% of the populations, with the greatest incidence observed among younger children (1, 2). Cow's milk and egg allergy are two of the most common food allergies in most countries (2) and most of them resolve within the first few years of life (3, 4).

In normal conditions, antigen-presenting immune cells including dendritic cells (5), macrophages (6), and T regulatory (Tregs) cells (7) inhibit an inappropriate immune response to food antigens, whereas in allergic individuals, it comes to dysregulation of normal immune tolerance and in consequence, to FA development (1). It was found that IgE-mediated food allergy results from a Th2 immune response of the adaptive immune system to specific food-derived antigens (8). By extension, Th1/Th2 lineage determination mediated by multitude of factors, including the cytokine environment, is critical to the development of food allergy (9). Th1 cells are mainly responsible for interferon gamma (IFNG) production and mounting a protective response against infectious agents. Interleukin 4 (IL4), interleukin 5 (IL5) and interleukin 10 (IL10) are secreted by Th2 cells, which are involved in allergic responses and humoral immunity (10). Any disruption of the cytokine secretion, especially increased IL4 and/or decreased IFNG, are considered to be a major factor contributing to allergy development (11). The IL5 contributes to the development of allergic diseases via a very complicated process of inflammation engaging the T cells and granulocytes (12). The IL10 is a regulator of the immune response and repressor of inflammation. A modulation of the Th1 and Th2 responses by T cell-derived IL10 may lead to the acquisition of immunotolerance (13). The expression pattern of transcription factor Forkhead Box Protein 3 (FOXP3) in Tregs was shown to be associated with the IgE-dependent food allergy and acquisition of tolerance in infants with cow's milk allergy (14, 15).

It is suggested that FA mechanisms may involve the interactions between genetics, epigenetics and environmental factors. The epigenetic changes are believed to provide a possible account of the influence of ambient exposures on gene expression, dysregulating immune processes as a result (1, 9). The differences between methylation profiles of single-food and multi-food-allergic individuals were observed, suggesting that the epigenome changes play a significant role in differentiation of B cells in allergic processes (16). The potential of analysis of 96 CpG's methylation status to predict a clinical response to food challenge in food-sensitized infants was demonstrated (17). It was found that DNA methylation status of Th1/Th2- related genes like *IL4*, *IL5*, *IL10* and *IFNG* was different between children with cow's milk allergy and those tolerant to cow's milk (18). Similarly, the association of the *FOXP3* gene methylation with milk's allergy status in young allergic patients was observed (19). The study by Syed et al. (20) showed an *FOXP3* methylation decline throughout the peanut oral immunotherapy course.

There are few papers on the role of DNA methylation of Th1/Th2 loci in the food allergy/atopic dermatitis development in infants. The studies performed thus far focused preferentially on the dynamics of RNA and protein levels depending on allergy status. Besides, the studies were very small in terms of sample sizes. In the case of infants, the cord blood has often been used to infer differences between the healthy and allergic participants, whereas in older children or adults, the peripheral blood mononuclear cells (PBMC), single blood cells lineages or purified T-cell populations were examined. It cannot be ruled out that cord blood might contain contamination with maternal cells. In turn, PBMC's collection requires large amounts of blood to be drawn, which can be difficult in the case of infants.

The first objective of the current investigation was to examine the methylation level of CpG's spanning promoter sequences of the *IL4*, *IL5*, *IL10* and *IFNG* genes and Treg-specific demethylated

Abbreviations: FA, food allergy; AD, atopic dermatitis; CMA, cow's milk allergy; Tregs, T regulatory (Treg) cells; IFNG, interferon gamma; IL4, interleukin 4; IL5, interleukin 5; IL10, interleukin 10; FOXP3, forkhead box protein 3; PBMC, peripheral blood mononuclear cells; TSDR, treg-specific demethylated region.

region (TSDR) within the *FOXP3* gene in whole blood collected from infants. The supplementary goal was to check if a few drops of blood deposited on the FTA card would be sufficient for testing, which would be extremely beneficial in the case of the youngest patients. For the purpose of determining methylation status, a very simple and cost-effective real-time PCR technology was employed. The next goal was to detect any differences in methylation of selected loci between infants with and without allergy, in order to infer whether the TH1/TH2 methylation profile from whole blood may be predictive in allergy development. Additionally, the study was aimed at finding evidence for the impact of environmental factors on methylation dynamics in allergic and healthy groups that would help in better understanding of molecular basis of allergy.

2 Materials and methods

2.1 Subject recruitment

As patients, we enrolled infants with atopic dermatitis (AD) and/or food allergy (FA) under six months of age that were hospitalized in the Department of Pediatrics, Allergology and Gastroenterology, Collegium Medicum, Nicolaus Copernicus University, Poland and from Gastrological and Allergological Outpatient Clinics in Bydgoszcz, Poland. As controls, during the same study period, healthy infants without symptoms indicating allergy visiting the medical centre were also recruited. The inclusion and exclusion criteria as well as medical data were described in detail previously (21).

Finally, after rejection of participants who did not meet all the requirements, the study sample consisted of 89 controls and 138 patients with allergy suspicion (for simplicity, this group was further referred to as allergic patients) including 15, 38 and 85 with atopic dermatitis (AD), food allergy (FA) or atopic dermatitis/food allergy (ADFA), respectively. For some analyses infants with ADFA were coupled with those with FA or AD (FA+ADFA group and AD+ADFA group, respectively).

2.2 Sample collection

Peripheral blood samples from patients and healthy subjects were collected on FTA cards during medical appointments and delivered in short order to the laboratory for further processing.

2.3 Methylation analysis

We investigated the methylation profiles of selected CpG's sites located in *IL4* (Chr5:132673908, Chr5:132673939, Chr5:132673992, Chr5:132674040), *IL5* (Chr5:132556873, Chr5:132556876, Chr5:132556881, Chr5:132556887, Chr5:132556894, Chr5:132556902, Chr5:132556906, Chr5:132556911, Chr5:132556913, Chr5:132556929, Chr5:132556932, Chr5:132556947, Chr5:132556950, Chr5:132556956, Chr5:132556958, Chr5:132556962, Chr5:132556978), *IL10* (Chr1:206772789, Chr1:206772819, Chr1:206772821, Chr1:206772842), *IFNG* (Chr12:68159573, Chr12:68159617, Chr12:68159623) gene promoters and in the TSDR of *FOXP3* gene (ChrX:49260767, ChrX:49260786, ChrX:49260795, ChrX:49260803, ChrX:49260807, ChrX:49260813, ChrX:49260816, ChrX:49260826, ChrX:49260834).

DNA from whole blood deposited on FTA card was extracted by GeneMATRIX Bio-Trace DNA Purification Kit (EurX) according to the manufacturer's instructions. DNA concentration was estimated with Quantifiler Duo Quantification kit (Thermo Fisher Scientific). 500 ng of DNA was bisulfite-converted using the EpiTect Fast DNA Bisulfite Kit (Qiagen) following the manufacturer's protocol. PCR was performed in a 10 µL reaction volume. 10 ng of converted DNA were added to each well which contained 1 × HRM Master Mix® (Thermo Fisher Scientific) and 0.2 µM of each primer (for details see Supplementary Table S1). The amplification consisted of 10 min at 95°C and 40 cycles of the following steps: denaturation 95°C, 15 s and annealing/extension 61°C (exception: 60°C in case of *IL4* reaction), 1 min. High resolution melting analyses were performed at the temperature ramping and fluorescence acquisition setting recommended by the manufacturer. Real Time PCR amplification of the DNA (for quantification purposes as well as methylation analysis) was carried out using ViiA7 apparatus (Thermo Fisher Scientific) equipped with the Ruo software (Version 1.1). The EpiTect PCR Control DNA Set consisting of Human Methylated and Non-Methylated DNA standards were purchased from Qiagen, and mixed to receive the standard curve containing 0, 10, 25, 50, 75 and 100% of methylated template. The methylation level of each test sample was determined by interpolation of the data generated from the linear regression analysis of the standard curve as described in (22). Additionally, the methylation analysis products were verified by direct sequencing using Sanger method.

2.4 Statistical analysis

The normality of data was checked with the Shapiro–Wilk test and homogeneity of variance by Levene's test. Clinical categorical data were analysed using two-tailed Fisher's exact and/or Chi-square tests. The Kruskal–Wallis one way ANOVA test was used to evaluate the differences among continuous variables. Bonferroni correction for multiple comparisons was applied. Correlations between demographic/clinical variables and methylation levels in different compartments were tested using Spearman's rho. For all statistical tests a significance level of 0.05 (p) was used. All analyses were conducted by SPSS for Windows (PS IMAGO PRO 8.0).

3 Results

The characteristics of the study and control groups are given in Table 1. Generally, the study and control cohorts are similar, but some significant differences were observed, including mother's weight/BMI (which is higher in the control group) and familial history of allergy. The significant findings described in sections below were shown in figures (numbered 1-10). All results of

10.3389/fimmu.2023.1209190

TABLE 1 The characteristics of the study and control group.

Variables		Control group n = 89	Allergic group n = 138	FA group n = 38	ADFA group n = 85	AD group n = 15
Child's age (weeks), mean ± SD		14.87 ± 6.62	16.63 ± 6.89	16.13 ± 6.65	16.58 ± 7.01	18.20 ± 7.01
Sex, n (%)	**Females**	46 (51.7)	57 (41.3)	17 (44.7)	34 (40.0)	6 (40)
	Males	43 (48.3)	81 (58.7)	21 (55.3)	51 (60.0)	9 (60)
Child's birth weight (kg), mean ± SD		3.36 ± 0.59	3.47 ± 0.46	3.36 ± 0.53	3.50 ± 0.43	3.59 ± 0.37
Child's current weight (kg), mean ± SD		7.09 ± 1.37	7.18 ± 1.33	6.09 ± 1.35	6.42 ± 1.36	6.96 ± 1.58
Exclusive breastfeeding, n (%)		38 (42.7)	57 (41.3)	15 (39.5)	36 (42.3)	6 (40.0)
Exclusive milk formula feeding, n (%)		42 (47.1)	67 (48.5)	20 (52.6)	39 (45.9)	8 (53.3)
Place of residence, n (%)	**village**	9 (10.1)	7 (5.1)	2 (5.3)	4 (4.7)	2 (5.3)
	suburbs	14 (15.7)	36 (26.1)	12 (31.6)	20 (23.5)	12 (31.6)
	city	66 (74.2)	95 (68.8)	24 (63.2)	61 (71.8)	24 (63.2)
Mother's age (years), mean ± SD		29.37 ± 5.11	30.04 ± 4.89	29.50 ± 5.01	30.71 ± 4.65	27.67 ± 5.33
Father's age (years), mean ± SD		31.96 ± 5.08	32.35 ± 5.10	31.74 ± 5.36	32.96 ± 4.84	30.40 ± 5.59
Mother's weight (kg), mean ± SD *		65.35 ± 12.21	62.20 ± 10.17	65 ± 9.16	61.70 ± 10.72	58.15 ± 7.47
Mother's BMI, mean ± SD **		23.71 ± 4.12	22.52 ± 3.41	23.49 ± 3.24	22.25 ± 3.53	21.76 ± 2.76
Siblings, n (%)		35 (39.3)	59 (42.8)	16 (42.1)	37 (43.5)	6 (40)
Animals at home, n (%)		33 (37.1)	60 (43.5)	20 (52.6)	32 (37.6)	8 (53.3)
Passive smoking exposure, n (%)	**During pregnancy**	17 (19.1)	29 (21)	9 (23.7)	16 (18.8)	4 (26.7)
	After birth	25 (28.1)	35 (25.4)	9 (23.7)	19 (22.4)	7 (46.7)
Pregnancy complications, n (%)		33 (37.1)	45 (32.6)	14 (36.8)	24 (28.2)	7 (46.7)
Number of family members with allergy, n (%) **	**0**	46 (51.7)	56 (40.6)	18 (47.4)	26 (30.6)	12 (80)
	1	32 (36)	40 (29)	12 (31.6)	27 (31.8)	1 (6.7)
	2	11 (12.4)	33 (23.9)	7 (18.4)	25 (29.4)	1 (6.7)
	3	0 (0)	9 (6.5)	1 (2.6)	7 (8.2)	1 (6.7)

* significant p value for comparisons between control and allergic groups.
** significant p value for comparisons between control and allergic groups/FA, AD and ADFA groups.

statistical analyses were presented in Supplementary Tables S2–S13).

3.1 Methylation status, presence of allergy and the type of symptoms

The present study concentrates on methylation profiles of gene promoters of the immune response-attached factors IL4, IL5, IL10, IFNG and TSDR of FOXP3. The assessments of the methylation level in particular loci were based on relevant standard curves. A similar distribution of methylation for allergic and healthy donors was observed. Methylation interquartile values were fluctuated depending on locus: for *IFNG* ranging from approximately 82% to 100%, for *FOXP3* from 90% to 100%, for *IL4* from 56% to 100%, for *IL10* from 31% to 47% and for *IL5* from 0% to 16%. In the case of the first three loci, most values were between 95% and 100%, whereas the *IL5* methylation rate mostly assumed a value near 0%. Some outstanding values for all loci were also observed. The methylation rates of the *IL4*, *IL5*, *IL10*, *IFNG* and *FOXP3* genes are presented in Figure 1. No significant differences were found between controls and all allergic patients with the exception of the *FOXP3* gene for which lower percentage of methylation in allergic infants was observed ($H_{K\text{-}W}$=5.651; p=0.017). On the other hand, the distributions of the methylation level for all genes did not differ between healthy participants and those with FA, AD and ADFA, analysed separately.

3.2 The impact of environmental exposures on methylation dynamics in the *IL4*, *IL5*, *IL10*, *IFNG* and *FOXP3* genes

3.2.1 Demographic/social data

Comparison of the percentage of methylation between the healthy and allergic groups (analysed separately or together) in

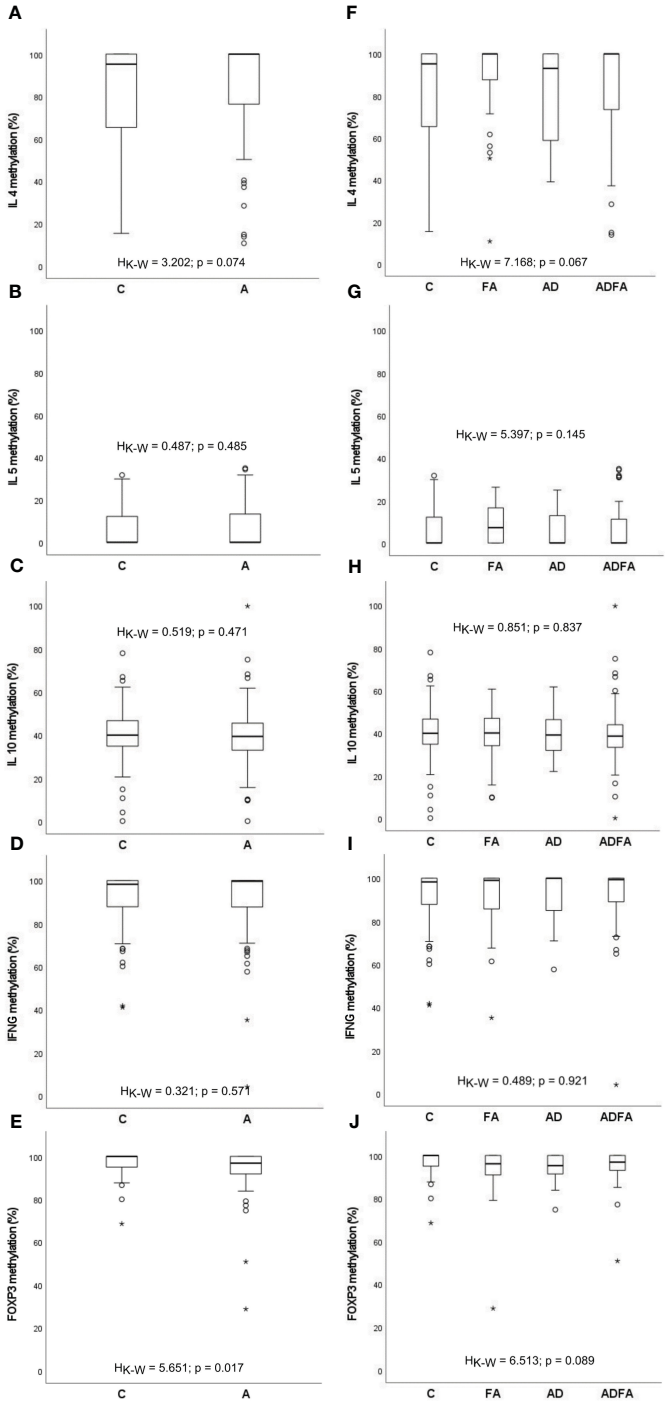

FIGURE 1
DNA methylation rate of the *IL4*, *IL5*, *IL10*, *IFNG* and *FOXP3* genes observed in the study population. **(A-E)** comparisons between control and allergic groups, **(F-J)** comparisons between control group and groups with FA, AD and ADFA. °C and * – the outliers, H_{K-W} – Kruskal-Wallis ANOVA coefficient, level of significance p<0.05.

the context of gender did not exhibit any significant distinctions. No statistically significant differences in methylation levels of the genes between any studied groups were found, regardless of having siblings or animals. Similarly, no connection between the methylation status and place of residence (village, suburbs or city) was detected.

However, some relations between the infants' and parents' age and the methylation profile of the genes were observed (Figures 2, 3, respectively). It turned out that the older the child, the lower was the *IL10* methylation in the control group (rho=-0.300, p=0.004). Besides, the older the mother or father, the lower was the *FOXP3* methylation in controls (rho=-0.229, p=0.031 and rho=-0.268,

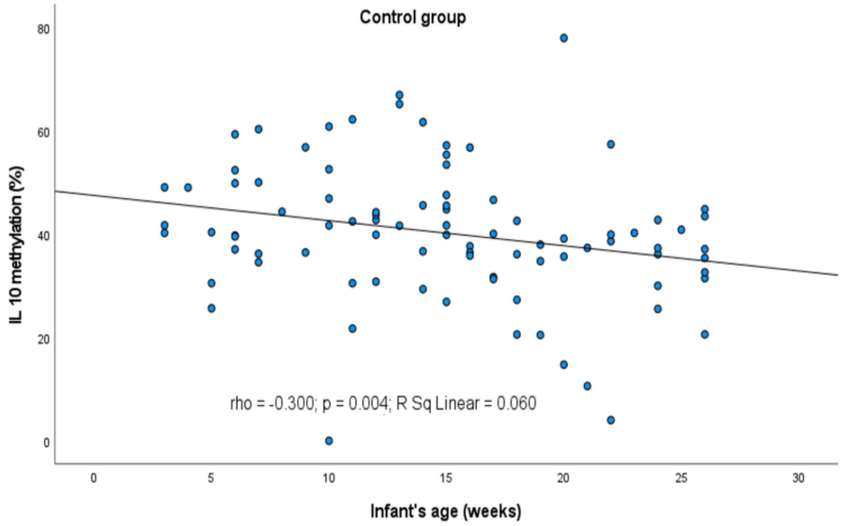

FIGURE 2
Significant correlation between DNA methylation level of *IL10* promoter and infant's age. rho – Spearmans' rho coefficient, level of significance p<0.05.

p=0.011, respectively). In turn, the opposite relationship between the *IL4* methylation and age of mother and father in the AD group was shown (rho=0.569, p=0.027 and rho=0.521, p=0.047, respectively).

3.2.2 Cigarette smoking

When cigarette smoking exposure is taken into account, some differences in the methylation levels appeared in a manner that in infants subjected to second-hand smoke the methylation level has mainly declined (Figure 4). In details, the *IFNG* methylation level decrease was observed in participants with any allergy (H_{K-W}=5.359, p=0.021), the *IL10* methylation level was lower among FA+ADFA patients (H_{K-W}=5.116, p=0.024), whereas the *FOXP3* methylation level was higher among those with ADFA (H_{K-W}=4.670, p=0.031), while smoking exposure was taking place after the birth of an infant.

The same relationship was found between the percentage of methylation and smoking exposure during pregnancy. The methylation rate of *IFNG* promoter was lower in allergic children and in the group consisting of FA+ADFA donors (H_{K-W}=5.785, p=0.016 and H_{K-W}=4.130, p=0.042, respectively). Similarly, methylation level of *IL4* and *FOXP3* genes diminished among

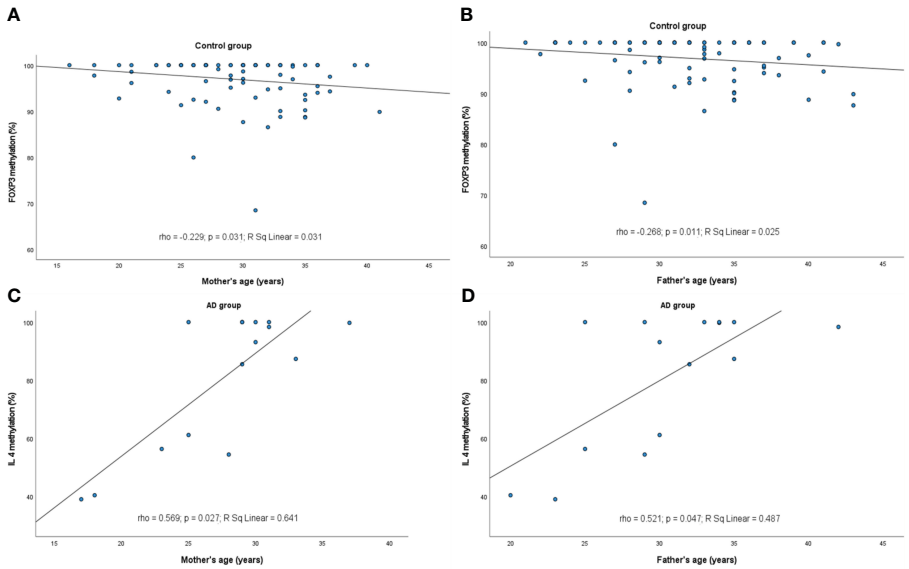

FIGURE 3
Significant correlations between DNA methylation level and parent's age: **(A)** *FOXP3* methylation rate in control group and maternal age, **(B)** *FOXP3* in control group and paternal age, **(C)** *IL4* in AD group and maternal age, **(D)** *IL4* in AD group and paternal age. rho – Spearmans' rho coefficient, level of significance p<0.05.

10.3389/fimmu.2023.1209190

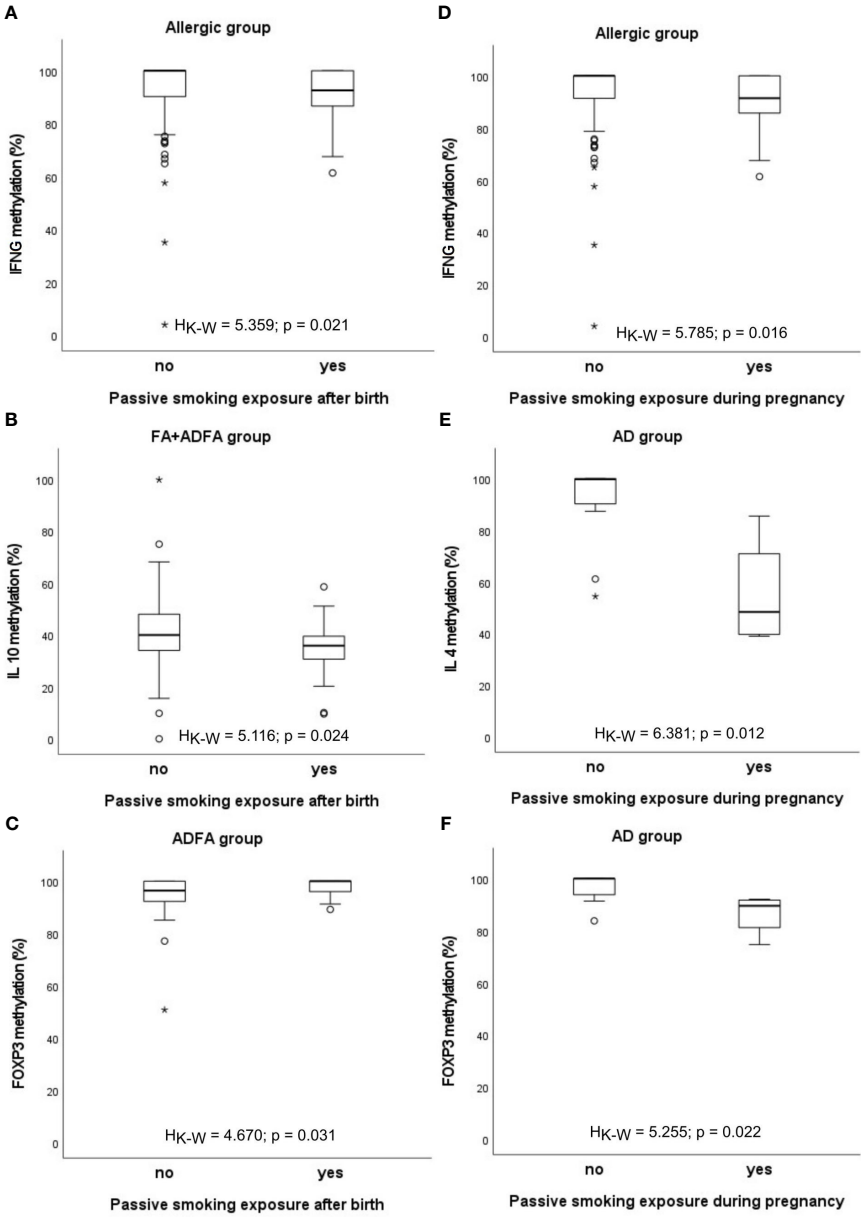

FIGURE 4
Significant associations between DNA methylation level and infant's passive smoking exposure: **(A-C)** after birth, **(D-F)** during pregnancy. °C and * – the outliers, H_{K-W} – Kruskal-Wallis ANOVA coefficient, level of significance p<0.05.

children with AD (H_{K-W}=6.381, p=0.012 and H_{K-W}=5.255, p=0.022, respectively).

3.2.3 Complications during pregnancy

Abnormal course of pregnancy was shown to be associated with changes of methylation degree. Different abnormalities were diagnosed in mothers including gestational diabetes, hypothyroidism, hypertension, anaemia, oligoamnios, hydramnion, bacterial infections, mycoses and others. One of the most frequently diagnosed complications of pregnancy in the study was gestational diabetes but few cases were limited only to this disease. The presence of several comorbidities was prevalent so it was decided to carry out statistical analyzes for pregnancy complications in general, without separating them into individual disease entities.

In the healthy group, significantly lower methylation of *IFNG* (H_{K-W}=5.828, p=0.016), *IL5* (H_{K-W}=5.231, p=0.022) and *IL10* (H_{K-W}=4.618, p=0.032) promoters was found (Figure 5).

Similar statistically significant relations between an abnormal pregnancy and methylation status were observed for *IL5* in infants with allergy (H_{K-W}=5.298, p=0.021) and in those from the FA +ADFA group (H_{K-W}=5.131, p=0.024), whereas for *IL4* in patients with ADFA (H_{K-W}=4.301, p=0.038) and among the FA+ADFA infants (H_{K-W}=4.118, p=0.042) (Figure 6).

3.2.4 The type of infant feeding

The possible impact of the type of feeding on the level of methylation was analysed (Figure 7). It was shown that percentage of methylation of *IFNG* is higher among exclusively breastfed infants with AD compared to those who were not breastfed at all (H_{K-W}=4.449, p=0.035) and lower among exclusively milk formula-fed compared to those who were never fed by milk formula (H_{K-W}=6.303, p=0.012). The opposite observation in patients with FA was found (H_{K-W}=3.139, p=0.076; H_{K-W}=4.515, p=0.034, respectively), whereby results for exclusively breastfed infants were not significant. Additionally, the significantly decreased methylation of *IL5* among infants with AD who were exclusively breastfed, was observed (H_{K-W}=3.926, p=0.048). A similar, but not significant trend was noted for milk formula feeding (H_{K-W}=2.084, p=0.149).

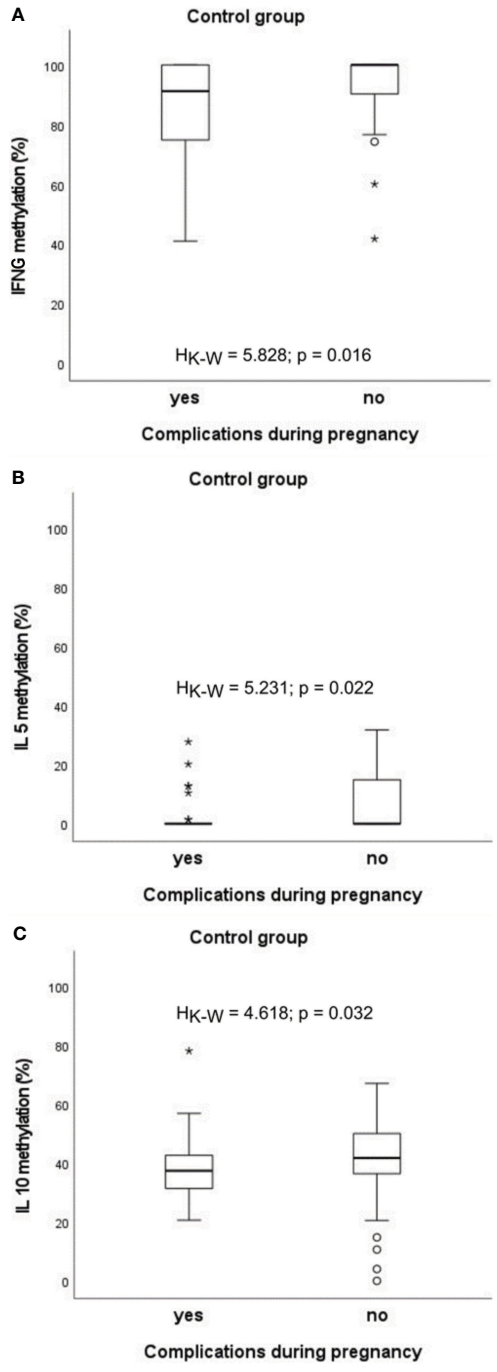

FIGURE 5
Significant associations between DNA methylation level and the presence of complications during pregnancy in the control group: **(A)** in case of *IFNG*, **(B)** in case of *IL5*, **(C)** in case of *IL10*. °C and * – the outliers, H_{K-W} – Kruskal-Wallis ANOVA coefficient, level of significance p<0.05.

3.2.5 BMI/weight of mother or infant

Analyses of correlation between methylation profiles and values of maternal weight/BMI are presented in Figure 8 and child's weight in Figure 9 as well.

A slight negative correlation between the mother BMI and methylation profile was observed. The higher the BMI value, the lower was the methylation level of: *IFNG* (rho=-0.238, p=0.028) and *IL5* (rho=-0.330, p=0.028) in controls. The same trend was observed for the *IL5* methylation status in controls in the case of the mother's weight (rho=-0.299, p=0.005).

In the allergic and FA+ADFA groups, the increase in the level of the *IL10* methylation was observed with an increase in the birth weight of the child (rho=0.203, p=0.017 and rho=0.205, p=0.023, respectively).

The current child's weight was positively correlated with *IL10* methylation level in patients with allergy (rho=0.203, p=0.017).

3.2.6 History of familial allergy

A weak positive correlation between the number of allergic family members and the *IL4* methylation was observed in the healthy subjects (rho=0.226, p=0.033), AD patients (rho=0.585, p=0.022) and AD+ADFA patients (rho=0.202, p=0.044) (Figure 10).

4 Discussion

4.1 Methylation status, presence of allergy and the type of symptoms

Previous studies have shown that epigenetic changes, especially the pattern of DNA methylation, were associated with food allergy and other allergic diseases, as reviewed in (23). Methylation in CpG islands within gene promoters is believed to silence gene expression. Also, a strong correlation with gene expression has been shown for DNA methylation in regions located even up to 2 kb from known CpG islands (24).

All researches the papers of which are cited in the current work examined fresh blood samples but we used blood spotted on FTA cards. Since DNA extraction and even transport to the place of proper storage cannot always be performed at the time of sample collection (i.e. immediately after the visit), whole blood samples must be stored in conditions preventing the decline of the yield and quality of DNA, including DNA methylation. FTA classic cards are commonly used for blood, saliva and sperm transport and storage providing reliable results of classic DNA analysis like genotyping or

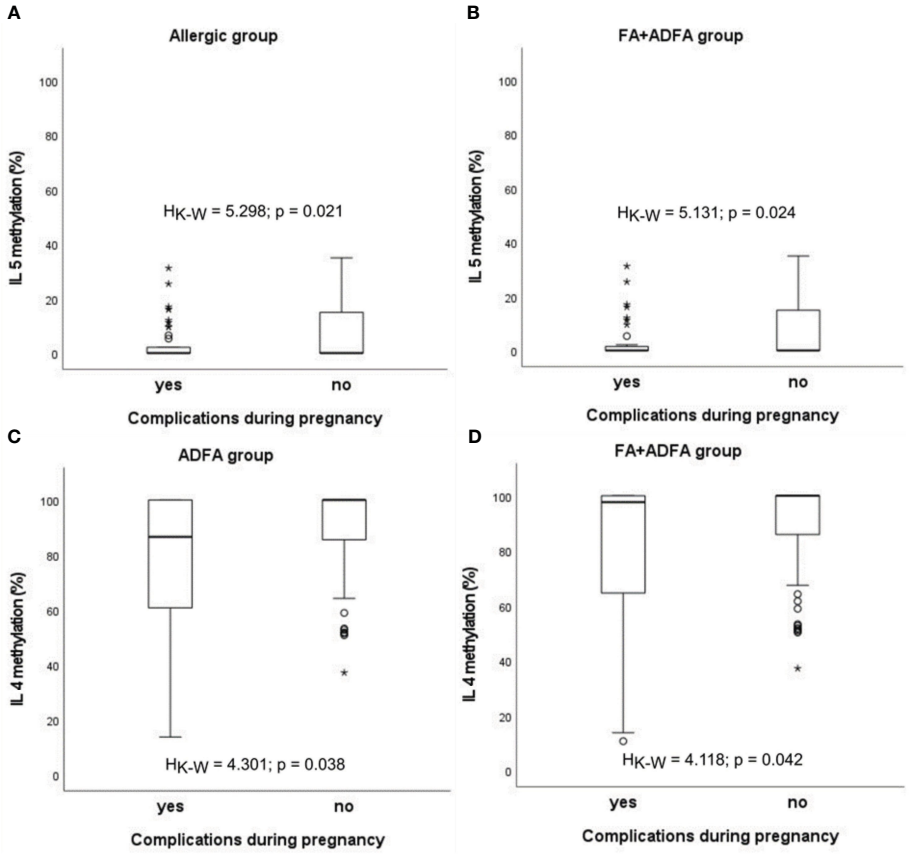

FIGURE 6
Significant associations between DNA methylation level and the presence of complications during pregnancy in patients: **(A, B)** in case of *IL5*, **(C, D)** in case of *IL4*. °C and * – the outliers, H_{K-W} – Kruskal-Wallis ANOVA coefficient, level of significance p<0.05.

sequencing. More recently, their usefulness was confirmed for epigenetic analysis (25–27).

Since different methylation profiles may act as potential biomarkers of modifiable disease pathways, the methylation profiles of selected CpG's sites spanning regulatory regions of the *IL4*, *IL5*, *IL10*, *IFNG* and *FOXP3* genes from infants with FA, AD and with symptoms of both (ADFA), as well as healthy subjects were investigated. To simplify the workflow as much as possible, the MS-HRM methodology was used that enables assessment of the overall methylation percentage of the entire amplicon in a particular sample by comparison with melting standard curves created by different dilution ratios of methylated and unmethylated control DNAs. Using this method, even small differences (5%–10%) in DNA methylation could be detected, allowing to assess the contribution of methylated DNA from subpopulations of cells within heterogeneous populations (28).

Comparing the distribution of methylation of the TH1/TH2 cytokine and *FOXP3* genes from patients with those from the control group demonstrated a significant difference for the *FOXP3* gene only. It was shown that lower percentage of methylation occurred in allergic infants. But measuring the methylation level in the CpG loci of healthy infants up against the ones with FA, AD or ADFA, respectively, did not differ significantly. In other studies methylation of the same loci had the values ranging from approximately 35% to 85% for *IL4*, *IL5* and *IFNG* (18) and from 75% to 100% for *FOXP3* (19) depending on the allergy status. It has been proved that DNA methylation profiles of CpGs in the promoter region of *IL4*, *IL5*, *IL10* and *IFNG* (18) as well as the demethylation status of TSDR in *FOXP3* (19) clearly separated patients with cow's milk allergy from controls and children who outgrew CMA. The *IL4* and *IL5* DNA methylation was significantly lower, and the *IL10*, *IFNG* and *FOXP3* DNA methylation was higher in active IgE-mediated CMA patients compared to the other two groups. The discrepancy between methylation rates obtained in this and other studies (18, 19) can result from distinct material used for examination, since we used whole blood samples, whereas other groups tested peripheral blood mononuclear cells (PBMCs) isolated from whole blood samples. Blood is a complex mixture of many different specialized cell types with varying methylation profiles (29). It can influence detected methylation level and, for example, may have a dilution effect. For example, normal proportion of T cells equals 20% of white blood cells (29), so analysing PBMC will give distinct methylation values for TH1/TH2-derived loci in comparison to whole blood. On the other hand, Yu et al. (30) identified relative hypermethylated states in gene promoters of neonatal CD4+ T cells, compared to those of adults. Others reported that neonatal CD4/CD45RO- T cells, but not CD8+ T cells, are hypermethylated at CpG within and adjacent

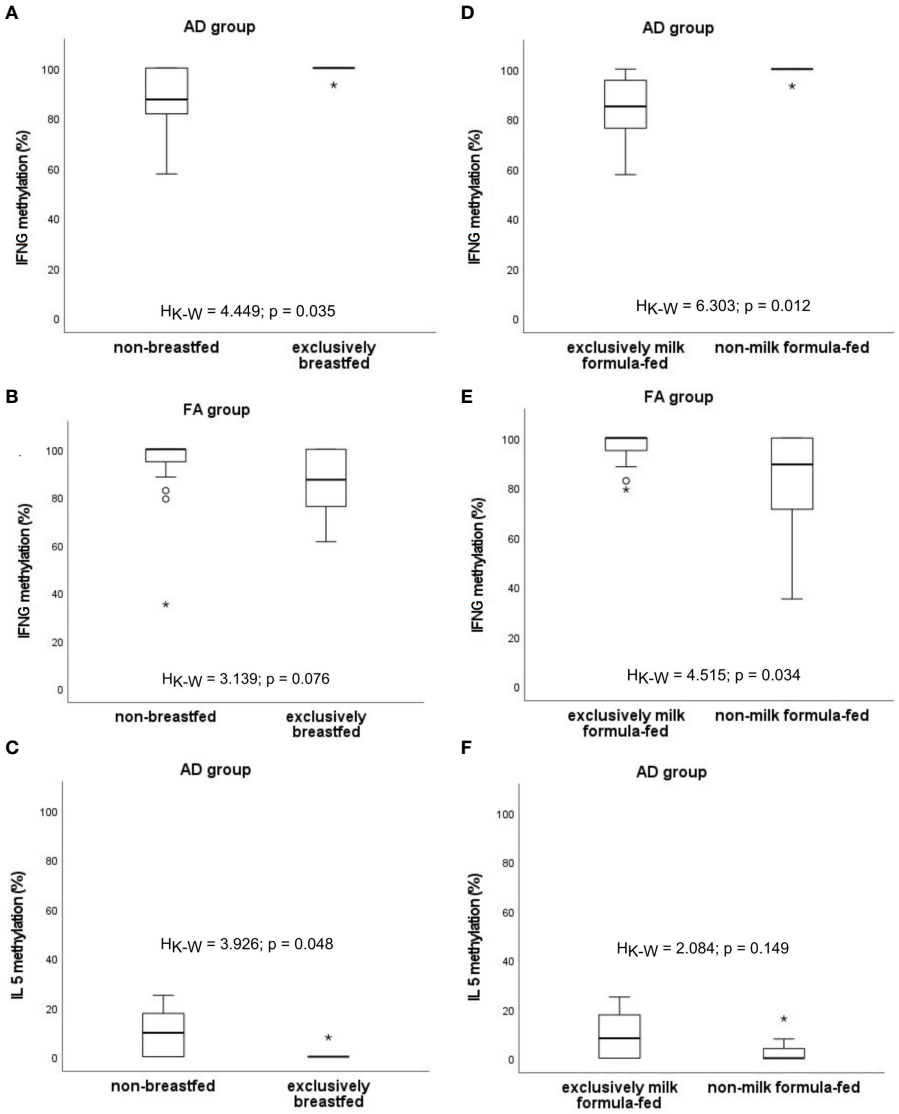

FIGURE 7
Significant associations between DNA methylation level and the type of infant feeding: **(A–C)** excusively breastfed vs. non-breastfed, **(D–F)** excusively milk formula-fed vs. non-milk formula-fed. °C and * – the outliers, H_{K-W} – Kruskal-Wallis ANOVA coefficient, level of significance p<0.05.

to the *IFNG* promoter (31, 32). There is the opposite pattern of CpGs in both the promoter and the transcribed region in NK and B cells (hypo and hypermethylated, respectively) (33). The methylation differences spanning CpGs within and adjacent to the *IFNG* promoter were also noticed between neonatal CD4/CD45RO- T cells and CD8+ T cells and NK cells. The former were hypermethylated, whereas the latter were less methylated and were comparable with those of adults (31, 32). Hypermethylation of *IFNG* promoter down-regulated gene expression in neonatal T-cells, but for *IL4* a converse correlation was found in neonatal CD4+ T cells, compared to those of adults (30). It is possible that the pattern similar to adults occurs also in older children. It is worth mentioning that in the case of *IL4*, we reported a very wide range of methylation rate suggesting the methylation in this locus changes in a more individual manner. In turn, the level of methylation obtained in this study for *IL10* in whole blood fluctuated mainly between 31% and 47% but did not differ regardless of the presence of allergies. A similar range of values was shown for healthy controls and children who outgrew CMA, although the two groups could be distinguished from each other (18). In the case of allergic donors, a higher level of methylation has been shown (55-85%) (18). Cytokine IL10 is mainly expressed by monocytes, Th2 and regulatory T cells which have an inhibitory effect over the expression of Th1 cytokines (34). There are contradictory results on the presence of correlation between methylation of *IL10* promoter and the level of cytokine expression. The discrepancies concerned both the presence or absence of correlation, but also different CpG dinucleotides in the promoter of the *IL10* gene and different regulatory regions (promoter/intron) subjected to methylation (18, 35–39). Zheng et al. (40) have described in detail the intricate networks of relationships surrounding the dynamics of epigenetic changes associated with IL10. Moreover, IL10 can cause various effects

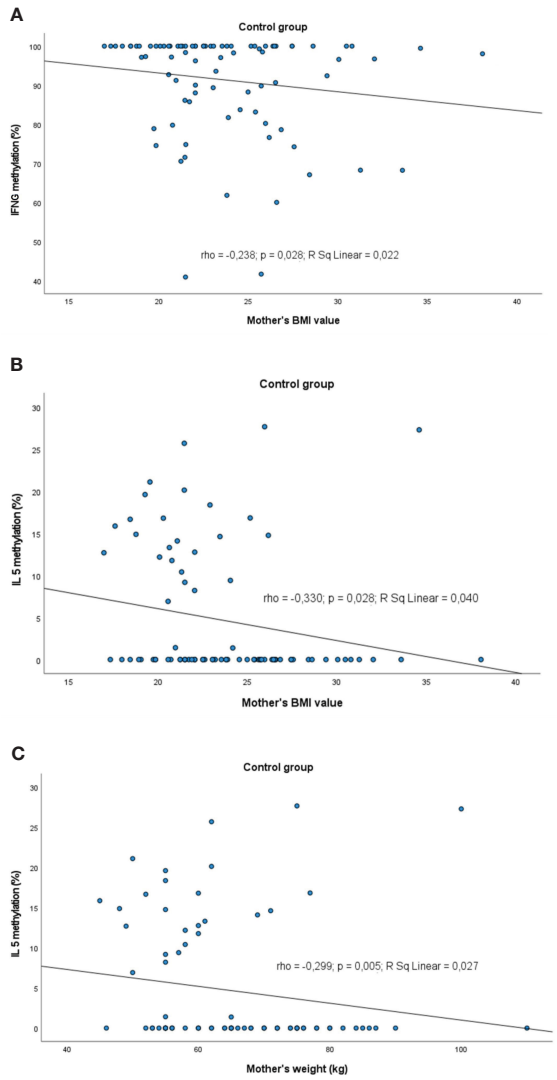

FIGURE 8
Significant correlations between DNA methylation level and maternal weight/BMI: **(A)** correlation between *IFNG* and maternal BMI in control group, **(B)** correlation between *IL5* methylation and maternal BMI in control group, **(C)** correlation between *IL5* methylation and maternal weight in control group. rho – Spearmans' rho coefficient, level of significance p<0.05.

depending on timing, dose, and location of expression; in some cases, the expected immunosuppressive activities are observed, while in others IL10 enhances immune or inflammatory responses (41). Coming back to our *FOXP3* methylation picture, lower methylation levels were observed among infants with allergies, in contrast to the results of others (19). We tested the blood of infants with active allergic symptoms at the time of inclusion. Some of these children developed tolerance at a later stage, and in some of them the initial diagnosis was verified (data not shown). The research of Paparo et al. (19) encompassed infants with CMA at diagnosis aged 5.5 months, the subject's outgrown CMA and healthy participants aged 16.9 and 9 months, respectively. The same research group was examined by Canani et al. (18). Therefore, it is possible that differences in the methylation rates of *FOXP3* and TH1/TH2 cytokine genes, at least partially, result from distinct age of donors. In addition, it was pointed that the role of FOXP3 expression in unstimulated and milk-allergen stimulated different T-cell populations could not be the same and has to be elucidated (42). Another explanation for the lower *FOXP3* methylation could be that in the developing immune system, the inflammatory processes associated with the development of allergies start to arouse an earlier response, whereas nothing is happening in healthy children. All in all, these mechanisms are still unknown.

The above facts can explain the differences in the percentage of methylation between experiments. One could note it may be difficult to achieve sufficient signal strength of methylation changes in minor fraction, for example, Treg cells within the total white cell compartment. On the other hand, a diagnostic test that requires isolation of specific cell populations would be of far less utility in comparison to the one demanding only a small amount of unsorted whole blood, such as from finger prick. We have made such an attempt in this study. The lack of differences in our study may result from a dilution effect as mentioned above, but not only. It should be noted that in the case of *FOXP3* only, we certainly tested the same CpG's set as elswere (19) because we used the same primers for amplification. For the remaining loci, we can confirm that we tested a similar region, the promoters, but are not sure if an identical set of CpG's. It is documented that not all CpG's in regulatory regions have the same methylation level in different donors [i.e. neonatal and adult T-cells differ in *IFNG* gene promoter particular CpG's methylation pattern (32)], or in normal and affected conditions [i.e. the upstream CpGs at -408, -387, -385, and -355 bp had similar hypermethylated status in both the patients with rheumatoid arthritis and healthy donors, whereas the proximal CpG at -145 was hypomethylated to a much greater extent in the patients than in the controls (37)]. Another issue mentioned above concerns the age of the surveyed children, which varies in different publications. It has been found that methylation profiles of many loci are changing with age. Mulder et al. (43) characterized the genome-wide DNA methylation directions across age period spanning multiple time-points from birth to late adolescence. They have found that sites with decreasing levels of methylation around the age of 6 years were functionally enriched for immune-developmental pathways, whereas sites with increasing levels of methylation for the neurodevelopmental ones. It turned out that 11% of CpGs were undergoing methylation changes in a non-linear manner, mostly involving changes from birth to the age of 6 years, after which DNA methylation status was more stable. One should not forget about the differences in methylation patterns depending on the population origin, resulting from epigenome-wide studies in different populations, including Europeans, Africans, Latin Americans or Arabs. Additionally, health disparities between human populations may be partially elucidated by methylation differences (44). It was proposed that differences in the development of specific T cell memory to food and inhalant allergens during the first 2 years of infant's life may explain a disparate picture of allergic disease prevalence in Swedish and Estonian populations (45).

4.2 The impact of environmental exposures on methylation dynamics in the *IL4*, *IL5*, *IL10*, *IFNG* and *FOXP3* genes

4.2.1 Methylation status and demographic/social data

The potential relationships between the methylation profile of the TH1/TH2 cytokine genes and *FOXP3* and some social data were analysed. The two factors of having no siblings nor animals were correlated with methylation dynamics in all studied groups. For example, Čelakovská et al. (46) reported that persistent AD lesions occurred more often in patients that had become sensitized to animal dander. Allergy to cats, dogs, or both is considered a major risk factor for the development of asthma and rhinitis, and to a lesser extent is associated with atopic dermatitis or some forms of food allergy, however, such associations are controversial [reviewed in (47)]. One could expect that place of residence (village, suburbs or city) may influence the methylation status but we have not found evidence for that. It can be assumed that heavy metals, dust and other pollutants in the air such as particulate matter (PM) are more common in cities. Many studies supported the hypothesis that these factors could influence DNA methylation patterns as reviewed in (48–50). It was shown, for example, that PM2.5 exposure level was positively correlated with methylation level in the *IFNG* promoter region and decreased cytokine expression (51). The cited studies concerned older participants. Perhaps the infants we examined were exposed to these factors for too short, or even protected against them.

The impact of age on methylation processes was also confirmed in this study. We observed that the older the child, the lower was the *IL10* methylation rate in the control group. The same relation between parents' age and *FOXP3* methylation in controls was detected. Similar but weaker association of mother's age with methylation of *FOXP3* in allergic infants was noted. On the other hand, in patients with AD, the methylation of *IL4* promoter was increasing along with father's or mother's age. A report based on the results of genome-wide DNA methylation profiling of 168 newborns indicated that maternal, and to a lesser extent paternal age contributes to differences in CpG methylation levels at birth. There is a general trend towards hypomethylation of CpG islands, especially in genes associated with oncogenesis and cancer progression in newborn blood cells with increasing parental age (52). It was reported that DNAm gestational age acceleration of the offspring at birth was associated with maternal age of over 40 years at delivery. In contrary, DNAm GA deceleration of the offspring at birth was associated with insulin-treated gestational diabetes mellitus (GDM) in a previous pregnancy and Sjögren's syndrome. GAA means an older DNAm GA than chronological GA, whereas GAD means younger DNAm GA than chronological GA (53). Older maternal age was significantly associated with reduced methylation at four adjacent CpGs near the second exon of KLHL35 in Norwegian newborns, while no corresponding effect of paternal age on methylation levels at these sites was found (54). Studies on protein expression level of TH1/TH2 genes in children aged 1-96 months demonstrated that the expression of IFNG and IL4 was increasing progressively with age, whereas the levels of IL5 and IL10 tended to be regulated on an individual basis during infancy and early childhood. The IL4 mRNA expression levels were diminished in neonates, then they tended to be increased after birth and remained relatively stable in infancy and childhood. Interestingly, no correlation was observed between IL4 protein expression and IL4 mRNA levels (55). A significant age correlation of IFNG, IL4 and IL5 release in blood samples of atopic and non-atopic children after stimulation with staphylococcal enterotoxin B was reported (56). There are no systemic studies on TH1/TH2 genes methylation alterations with age, but the correlation between methylation of the promoters and mRNA/protein expression levels may be indirect evidence of such a link. A significant influence of age on DNA methylation and mRNA levels of different genes (i.e. ELOV2, HOXC4 and PI4KB) in white blood cells of adults was found (57).

The changes in DNA methylation pattern occur naturally with aging, including global hypomethylation and region-specific

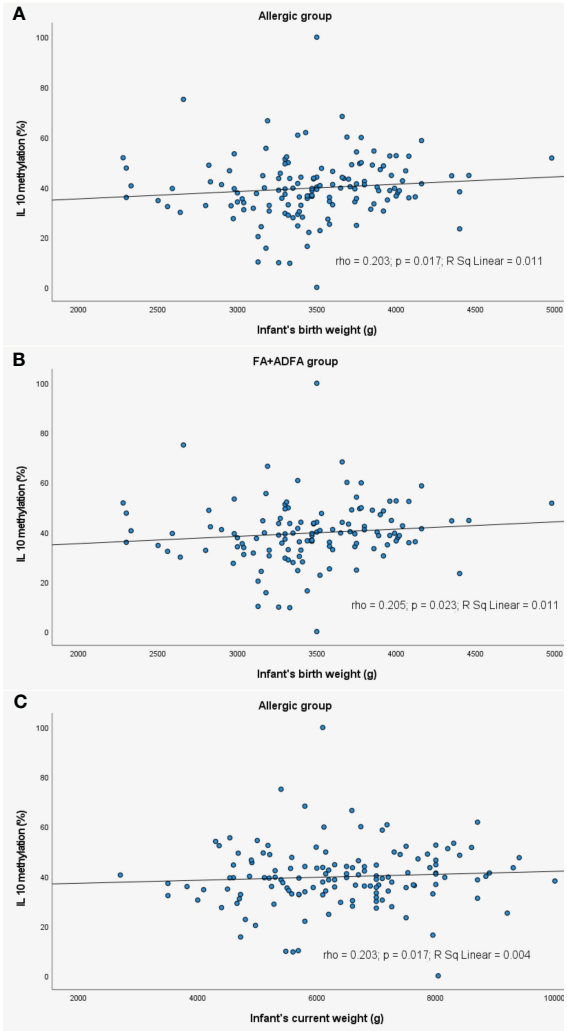

FIGURE 9
Significant correlations between DNA methylation level and infant's weight: **(A)** correlation between *IL10* methylation and infant's birth weight in allergic group, **(B)** correlation between *IL10* methylation and infant's birth weight in FA+ADFA group, **(C)** correlation between *IL10* methylation and infant's current weight in allergic group. rho – Spearmans' rho coefficient, level of significance p<0.05.

hypermethylation. The dynamics of methylation processes is more rapid in children than adults (58), with the majority of changes in childhood taking place during the first five years of life (59). It is well established that DNA methylation biomarkers can determine biological age of any tissue during the development as well as across the entire human lifespan. There is also growing evidence suggesting epigenetic age acceleration to be strongly linked to common diseases or occurring in response to various environmental factors (44, 60). The decrease in DNA methylation level of *IL10* gene associated with infant's age that we found in control group may be a result of natural maturation process. The lack of such relationship among allergic infants may come from alterations in epigenetic mechanism linked to allergy. The association of changes in *FOXP3* and *IL4* methylation level with parental age is more difficult to elucidate. Epidemiological studies (53, 61, 62) have shown that exposure to adverse environmental events in the prenatal period predicts increased risk of aging-related diseases, which are consistent with the Developmental Origins of Health and Diseases (DOHaD) hypothesis, suggesting that prenatal exposures alter developmental trajectories (63). One option is that placenta epigenetic aging of older mothers is a player as its associations with pre-pregnancy conditions and birth outcomes in children were reported. Accordingly, neonate methylomes contain molecular memory of the individual *in utero* experience (62, 64). It is assumed that each generation begins with a "renewed" epigenome. After fertilization the maternal and paternal genomes undergo a rapid demethylation of most of the genome followed by remethylation. Embryogenesis up until the blastocyst stage is crucial in determining the epigenetic marks needed for later development. The *in utero* period is developmentally plastic life stage, during which environmental exposures may impart long-lasting effects on future phenotype via epigenetic programming. However, there is evidence that the methylation patterns present in the parents are not totally erased and reset during gametogenesis and fertilization at a proportion of loci, including both imprinted and non-imprinted genes (44, 52, 65). So age-related DNA methylation changes also take place in germ cells and might be possibly transmitted to the offspring and may contribute to the increased disease risk in offspring of older parents (52, 66, 67). As information on maternal or paternal DNA methylation status is unavailable, the comparison between parental and offspring's methylation profile is impossible. The epigenetic inheritance or *in utero* environment effects seem to be important players in shaping the offspring epigenome but other confounding factors cannot be excluded and further studies are needed to clarify this issue.

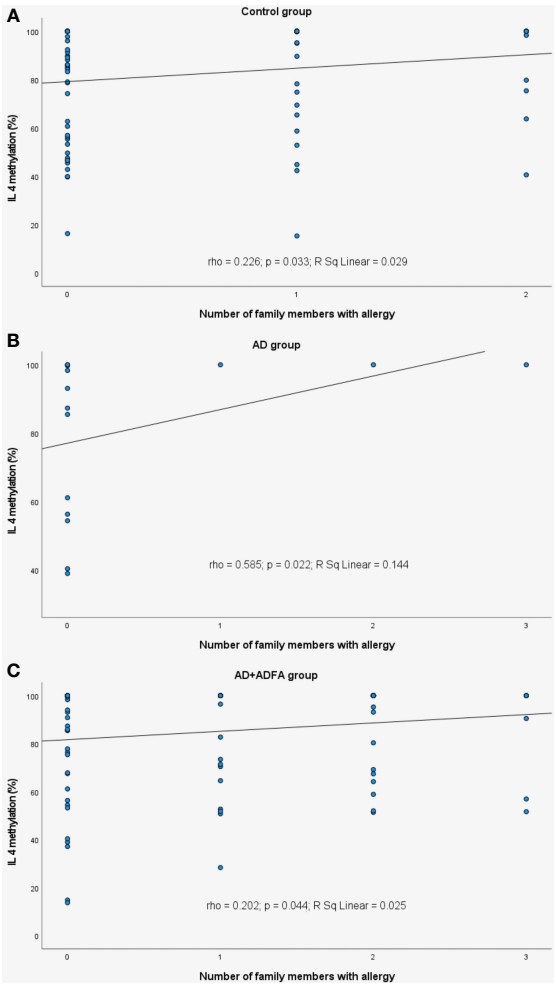

FIGURE 10
Significant correlations between DNA methylation level of *IL4* and the number of family allergic members: **(A)** in control group, **(B)** in AD group, **(C)** in AD+ADFA group. rho – Spearmans' rho coefficient, level of significance p<0.05.

4.2.2 Cigarette smoking

It was found that methylation levels of some loci declined among infants exposed to second-hand smoke both during pregnancy and after birth. Methylation of *IFNG* was lower within an overall allergic group, methylation of *IL4* and *IL10* was diminished among patients with AD and FA+ADFA. Whereas *FOXP3* exhibited contradictory results depending on the time of smoking exposure. Multiple independent studies on different populations have shown a significant impact of smoking on blood methylome (68). Due to very few cases of active maternal smoke exposures in our study, we resigned from analysing potential links with methylation patterns. However, it is documented that maternal smoking during pregnancy causes many undesirable effects on the offspring including low birth weight, some types of cancers, respiratory dysfunctions, and it leads to obesity and elevated blood pressure (69, 70). Epigenetic mechanisms are suggested since a set of genes with methylation changes present at birth in children whose mothers smoked during pregnancy was identified (71). The association of maternal smoking, birth weight and gestational age with significant DNA methylation differences in neonatal blood was confirmed (72, 73). Functional network analysis suggested a role in activating the immune system (73).

4.2.3 The presence of complications during pregnancy

Interestingly, a link was found between blood methylation status in infants and the occurrence of complications during pregnancy. Abnormal state has been associated with the decrease

in methylation of *IFNG*, *IL4*, *IL5* promoters in the healthy group. Also, statistically significant relations for *IL5* in infants with allergy and those with FA or ADFA, as well as for *IL4* in patients with ADFA or FA+ADFA were observed. The presence of pregnancy anomalies was associated with partial demethylation of the analysed loci in infant blood, although not always in a significant manner. These findings are in agreement with other observations of the relationships between maternal environmental exposures during pregnancy and the risk of illness in offspring. The prenatal period is believed to programme epigenetics of foetus, which in turn influences the risk for a range of disorders that develop later in life, including food allergy (examples are discussed (74, 75).

One of the most frequently diagnosed complications of pregnancy in our study was gestational diabetes but in most cases they were accompanied by other disorders like thyroidism, hypertension, bacterial infections and mycoses, and others. Little is known about the biological processes that link the occurrence of these pregnancy complications with adverse child outcomes; altered biological aging of the growing fetus up to birth is one molecular pathway of increasing interest (62). It was shown that maternal dysglycaemia was associated with significant changes in the methylation profile of the infants. Moreover, the epigenetic changes caused by a dysglycaemic prenatal environment appeared to be modifiable by a lifestyle intervention in pregnancy (76). Interestingly, compared to those who did not develop gestational diabetes mellitus, women diagnosed with GDM were older, had a higher BMI, and were more likely to be multiparous (76). As mentioned earlier in this work, DNAm GA deceleration of the offspring at birth was associated with insulin-treated gestational diabetes mellitus (GDM) in a previous pregnancy and Sjögren's syndrome (53). It was observed that prenatal exposure to gestational diabetes and preeclampsia, but not to hypertension, was associated with reduced biological maturity (decelerated gestational biological age) at birth among female neonates (62). On the other hand, there was evidence that offspring of mothers with hypertensive disorders of pregnancy (compared with those whose mothers who did not experience HDP) had a slightly faster increase in methylation between birth and age 7 (77).

Ours and other researchers' findings suggest that the epigenetic dynamics is an important biological pathway associated with pregnancy conditions playing a role in mediating the effects of these conditions on perinatal and child health outcomes. Further research on the functional relevance of methylation changes at specific sites is required.

4.2.4 The type of infant feeding

Some differences in methylation profiles were shown to be associated with the type of feeding within groups of allergic and healthy infants. In the case of exclusive breastfeeding, demethylation of *IFNG* was observed among patients with FA, whereas hypermethylation was characteristic for infants with AD. Contradictory results were obtained for infants exclusively fed with milk formula. Additionally, breastfeeding seemed to be linked with a lower *IL5* methylation rate in AD infants. There is no consensus among researchers about the effects of diet during pregnancy and in early childhood on allergy development. It was suggested that observed discrepancies in the results which were varying from a protective or neutral effect to a disease-promoting effect can result from other modulating factors affecting the immunological processes, for example age, gender, family history of allergies, coexistence of other allergies or genetic background (74). We have also observed the influence of some of these factors on the methylation dynamics as is discussed elsewhere in this work. It has been confirmed that improving the diet and exercise influence methylation biomarkers of healthy aging (78). Exclusive breastfeeding is suggested to prevent the risks of overweight/obesity of children and adults through DNA methylation mechanisms occurring early in life (79). Modifications of methylation patterns in blood playing important roles in various biological pathways including development and function of the immune system have also been associated with the duration of breastfeeding (80). L-Arginine is an important nutrient in the infant diet that by methylation mechanisms is acting as a regulator of the maturation process of the immune system in neonates, including the maturation of CD4+ T cells. Interestingly, after L-arginine treatment, more CpG dinucleotides were hypomethylated and more genes appeared to be activated in neonatal T-cells as compared with adult (76). Besides these findings, the role of breastfeeding in modulating the epigenetic pathways remains unclear. Introducing milk formula into the child's diet and maternal supplementation during breastfeeding are suggested to influence baby's methylome. Prenatal *L. reuteri* supplementation was shown to change DNA methylation patterns in CD4+ T cells of newborns enhancing immune activation at birth, resulting in affecting immune maturation and allergy development (81). It was observed that hydrolysed casein formula containing probiotics for infants drew higher *IL4*/*IL5* and lower *IL10*/*IFNG* DNA methylation patterns in CD4+ T cells than soya formula (30). L-arginine treatment induced greater hypomethylation of CpG dinucleotides and gene activation in neonatal T-cells as compared with adult. Among the most stimulated were genes regarding immune-related pathways (30). The L-arginine intake influenced the *IL10* promoter DNA hypomethylation inducing increase in IL10 production by neonatal CD4+ T cells (82). ω-3 PUFA seemed to have immunomodulatory properties via modifying DNA methylation since altered LINE1 repetitive sequences' methylation in children of women who smoked during pregnancy, as well as modulated DNA methylation levels in the promoters of genes encoding IFNG and IL13 were observed (83). Vitamin C was found to prevent offspring DNA methylation changes associated with maternal smoking during pregnancy (84). Furthermore, gestational vitamin D deficiency is considered to increase IL4 concentration and decrease the Th1/Th2 ratio and IFNG production. The maternal deficit of vitamin D was shown to cause an increase in the activity of DNA methyltransferase and hypermethylation of *IFNG* locus. The process can be reversed by vitamin D supplementation during pregnancy (85). Acevedo et al. (86) compiled studies on the effects of breastfeeding on the onset and course of allergic diseases. The authors indicated that some findings have supported the protective effects of breastfeeding on food allergy, atopic dermatitis and overall positive effect on gut and respiratory health, while some of them showed no or even an increased risk in children who were breastfed. The inconsistencies between studies are

most likely due to differences in duration of breastfeeding, the amount of milk given, genetic predisposition and methodology. One cannot ignore the fact that the composition of milk may differ between individuals and across populations, and it may depend on maternal nutritional status, smoking, having pets, and geographic location, etc.

4.2.5 BMI/weight of mother or infant

We also demonstrated the effects of birth/current weight of the child as well as mother BMI on CpG methylation status that is consistent with other findings. It was reported elsewhere that pre-gestational maternal obesity contributed to decreased basal expression of pro-inflammatory mediators in monocytes and in the latter, to suppressed expression of the key inflammatory regulator IL10 in activated macrophages. Alterations in the expression of *IL-1β* and *IL10* were associated with DNA methylation dynamics in their promoter regions (87). We found that with an increase in maternal BMI/weight value DNA methylation of some loci in offspring blood has become lower. Changes toward demethylation of *IFNG* and *IL5* associated with higher BMI were observed in controls and of *IL10* in allergic infants. A similar negative correlation appeared for mother's weight and *IL5* methylation status in healthy infants. There are many reports confirming positive or negative correlations, depending on the locus, between maternal BMI/adiposity and DNA methylation in neonates (88–95). Lifestyle interventions in pregnant women with obesity contributed to epigenetic changes in offspring, potentially influencing its lean mass and early growth (96).

Additionally, we have found that the *IL10* methylation level was increasing along with a child's birth weight in a group consisting of all patients as well as FA+ADFA participants. Similarly, the current child's weight was positively correlated with the *IL10* methylation level in allergic infants. DNA hypermethylation found in cells of blood or adipose tissue of obese individuals is the consequence of obesity (97). In another study, the association between increased BMI and accelerated epigenetic aging in the blood cells of middle-aged individuals was noted (98).

The results of epigenome-wide association studies (EWAS) regarding paternal prenatal body mass index (BMI) in relation to DNA methylation in offspring blood at birth and in childhood do not confirm any association between these variables, even at imprinted regions (88, 99). It supports the hypothesis of the uterine microenvironment playing a role in methylation shaping.

4.2.6 Family history of allergy

We detected a weak positive correlation between the number of allergic family members and *IL4* promoter methylation within certain subgroups such as the healthy group, patients with AD and ADFA or with AD only. It seems likely that history of familial allergy may increase the risk of allergy symptoms in the next child. The heritability of epigenetic marks and their association with DNA variants were documented (100–102). A neonatal epigenome is shaped by both intrauterine environmental and underlying genetic factors (100). It is the evidence that allele-specific DNA methylation is widespread across the genome, most of which can be strongly influenced by the sequence of adjacent SNPs (101, 102). Average heritability for DNA methylation is estimated at approximately 20% (103). There are studies indicating food allergies heritability estimates ranging from 15% to 30% for food specific IgE (104). The recent rise in prevalence of food allergies suggests a low to moderate impact of genetic factors and highlights the environmental exposure issues. Only a proportion of children subjected to variation in these exposures develop clinical food allergy, suggesting that some individuals are more genetically susceptible than others, but only in certain environments (23). The sequence information is inherited from the parents but epigenetic pattern is arising *de novo* during development of the embryo, except for a group of promoter sequences (CpG islands) needed for the expression of the developmental genes (105). On the other hand, research on animal models indicated that epigenetic patterns affected by external factors can persist across generations depending upon the timing of exposures (23). The genes are capable of 'learning' or 'adapting' to the environment over time and highlighted that the very complex interplay between genetic and ambient components during early immune development is at the root of the allergy (23). The risk of FA among one-year-old allergic infants was higher when there was any allergy in one immediate member of family and increased even to 80% when two such members were present in comparison to children without family history of allergy (106).

Limitations of this study include a low number of participants, especially patients with AD and the fact that we tested the blood of infants with active allergic symptoms at the time of inclusion, in some of them the initial diagnosis was verified. The age may be a weakness of this study in terms of establishing a diagnosis, but it was also a strong point. The knowledge on DNA methylation mechanisms in the food allergy/atopic dermatitis development in infants is obscure. Our research partially fills the gap because we test the blood of infants at a time when the infants methylome begins to form outside the womb in response to external factors. Besides, the comparisons between infants of similar age is very beneficial. Additionally, the effects of cell mixture on the measurement of DNA methylation in whole blood must be considered. On the other hand, counting of cell type may also be predictive in allergic processes. More extensive validation of methylation analysis of whole blood is required.

In conclusion, the potential of examination of a few drops of whole blood to detect methylation changes in the immune-attached genes using a cost-effective MS-HRM PCR methodology was demonstrated. It was found that methylation rate in *FOXP3* TSDR region in allergic infants was lower than in the healthy ones. It was also shown that methylation profile of *IL4*, *IL5*, *IL10*, *IFNG* and *FOXP3* was associated with environmental exposures and the direction of methylation dynamics differed depending on the presence and types of allergy symptoms. These results indicate that the interpretation of methylation pattern in the context of an allergic disease should take into account ambient factors having impact on epigenetic variation in early childhood. Undoubtedly, the development and maturation of the immune system is a very complicated process influenced by both individual genetic background and the environmental exposures regulating action of different types of cells. Further studies are needed to clarify this network.

Data availability statement

The raw data supporting the conclusions of this article will be made available by the authors, without undue reservation.

Ethics statement

The studies involving human participants were reviewed and approved by Bioethics Committee of Ludwik Rydygier Collegium Medicum in Bydgoszcz Nicolaus Copernicus University in Toruń, Poland. Written informed consent to participate in this study was provided by the participants' legal guardian/next of kin.

Author contributions

AK, EŁ-R, MG contributed to the conception, design, data collection, data analysis, and manuscript writing. MG was responsible for statistical analyses and interpretation and drafted the manuscript. JG contributed to the data collection. TG supervised the study. TG, MGo helped with manuscript writing and editing. All authors contributed to the article and approved the submitted version.

Funding

This study was supported by National Science Centre, Poland, award number 2017/25/B/NZ5/00141.

Acknowledgments

The authors would like to thank Aneta Jakubowska, Mariola Mrozek and Elżbieta Szymkuć for their hard work in conducting the laboratory procedures; and all of the participating families for their patience and dedication to the study.

Conflict of interest

The authors declare that the research was conducted in the absence of any commercial or financial relationships that could be construed as a potential conflict of interest.

Publisher's note

Supplementary material

The Supplementary Material for this article can be found online at: https://www.frontiersin.org/articles/10.3389/fimmu.2023.1209190/full#supplementary-material

References

1. Quake C, Nadeau K. The role of epigenetic mediation and the future of food allergy research. *Semin Cell Dev Biol* (2015) 43:125–30. doi: 10.1016/j.semcdb.2015.07.002

2. Loh W, Tang MLK. The epidemiology of food allergy in the global context. *Int J Environ Res Public Health* (2018) 15(9):2043. doi: 10.3390/ijerph15092043

3. Peters RL, Koplin JJ, Gurrin LC, Dharmage SC, Wake M, Ponsonby AL, et al. The prevalence of food allergy and other allergic diseases in early childhood in a population-based study: HealthNuts age 4-year follow-up. *J Allergy Clin Immunol* (2017) 140 (1):145–153.e8. doi: 10.1016/j.jaci.2017.02.019

4. Alduraywish SA, Lodge CJ, Vicendese D, Lowe AJ, Erbas B, Matheson MC, et al. Sensitization to milk, egg and peanut from birth to 18 years: a longitudinal study of a cohort at risk of allergic disease. *Pediatr Allergy Immunol* (2016) 27(1):83–91. doi: 10.1111/pai.12480

5. Ruiter B, Shreffler WG. The role of dendritic cells in food allergy. *J Allergy Clin Immunol* (2012) 129(4):921–8. doi: 10.1016/j.jaci.2012.01.080

6. Kumar S, Dwivedi PD, Das M, Tripathi A. Macrophages in food allergy: an enigma. *Mol Immunol* (2013) 56(4):612–8. doi: 10.1016/j.molimm.2013.06.009

7. Palomares O. The role of regulatory T cells in IgE-mediated food allergy. *J Investig Allergol Clin Immunol* (2013) 23:371–82.

8. Yu W, Freeland DMH, Nadeau KC. Food allergy: immune mechanisms, diagnosis and immunotherapy. *Nat Rev Immunol* (2016) 16(12):751–65. doi: 10.1038/nri.2016.111

9. Zhou X, Han X, Lyu SC, Bunning B, Kost L, Chang I, et al. Targeted DNA methylation profiling reveals epigenetic signatures in peanut allergy. *JCI Insight* (2021) 6(6):e143058. doi: 10.1172/jci.insight.143058

10. Mosmann TR, Sad S. The expanding universe of T-cell subsets Th1, Th2 and more. *Immunol Today* (1996) 17:138–46. doi: 10.1016/0167-5699(96)80606-2

11. Romagnani S. Immunologic influences on allergy and the TH1/TH2 balance. *J Allergy Clin Immunol* (2004) 113(3):395–400. doi: 10.1016/j.jaci.2003.11.025

12. Yanagibashi T, Satoh M, Nagai Y, Koike M, Takatsu K. Allergic diseases: from bench to clinic - contribution of the discovery of interleukin-5. *Cytokine* (2017) 98:59–70. doi: 10.1016/j.cyto.2016.11.011

13. Mori F, Barni S, Cianferoni A, Pucci N, de Martino M, Novembre E. Cytokine expression in CD3+ cells in an infant with food protein-induced enterocolitis syndrome (FPIES): case report. *Clin Dev Immunol* (2009) 2009:679381. doi: 10.1155/2009/679381

14. Krogulska A, Polakowska E, Wąsowska-Królikowska K, Małachowska B, Młynarski W, Borowiec M. Decreased FOXP3 mRNA expression in children with atopic asthma and IgE-mediated food allergy. *Ann Allergy Asthma Immunol* (2015) 115 (5):415–21. doi: 10.1016/j.anai.2015.08.015

15. Sardecka-Milewska I, Łoś-Rycharska E, Gawryjołek J, Toporowska-Kowalska E, Krogulska A. Role of FOXP3 expression and serum vitamin d and c concentrations when predicting acquisition of tolerance in infants with cow's milk allergy. *J Investig Allergol Clin Immunol* (2020) 30(3):182–90. doi: 10.18176/jiaci.0422

16. Imran S, Neeland MR, Koplin J, Dharmage S, Tang ML, Sawyer S, et al. Epigenetic programming underpins b-cell dysfunction in peanut and multi-food allergy. *Clin Transl Immunol* (2021) 10(8):e1324. doi: 10.1002/cti2.1324

17. Martino D, Dang T, Sexton-Oates A, Prescott S, Tang ML, Dharmage S, et al. Blood DNA methylation biomarkers predict clinical reactivity in food-sensitized infants. *J Allergy Clin Immunol* (2015) 135(5):1319–28.e1-12. doi: 10.1016/j.jaci.2014.12.1933

18. Berni Canani R, Paparo L, Nocerino R, Cosenza L, Pezzella V, Di Costanzo M, et al. Differences in DNA methylation profile of Th1 and Th2 cytokine genes are associated with tolerance acquisition in children with IgE-mediated cow's milk allergy. *Clin Epigenetics.* (2015) 7(1):38. doi: 10.1186/s13148-015-0070-8

19. Paparo L, Nocerino R, Cosenza L, Aitoro R, D'Argenio V, Del Monaco V, et al. Epigenetic features of FoxP3 in children with cow's milk allergy. *Clin Epigenet* (2016) 8:86. doi: 10.1186/s13148-016-0252-z

20. Syed A, Garcia MA, Lyu SC, Bucayu R, Kohli A, Ishida S, et al. Peanut oral immunotherapy results in increased antigen-induced regulatory T-cell function and hypomethylation of forkhead box protein 3 (FOXP3). *J Allergy Clin Immunol* (2014) 133(2):500–10. doi: 10.1016/j.jaci.2013.12.1037

21. Łoś-Rycharska E, Gołębiewski M, Sikora M, Grzybowski T, Gorzkiewicz M, Popielarz M, et al. A combined analysis of gut and skin microbiota in infants with food allergy and atopic dermatitis: a pilot study. *Nutrients* (2021) 13(5):1682. doi: 10.3390/nu13051682

22. Tse MY, Ashbury JE, Zwingerman N, King WD, Taylor SA, Pang SC. A refined, rapid and reproducible high resolution melt (HRM)-based method suitable for quantification of global LINE-1 repetitive element methylation. *BMC Res Notes.* (2011) 4:565. doi: 10.1186/1756-0500-4-565

23. Martino DJ, Saffery R, Allen KJ, Prescott SL. Epigenetic modifications: mechanisms of disease and biomarkers of food allergy. *Curr Opin Immunol* (2016) 42:9–15. doi: 10.1016/j.coi.2016.05.005

24. Irizarry RA, Ladd-Acosta C, Wen B, Wu Z, Montano C, Onyango P, et al. The human colon cancer methylome shows similar hypo- and hypermethylation at conserved tissue-specific CpG island shores. *Nat Genet* (2009) 41(2):178–86. doi: 10.1038/ng.298

25. Serra O, Frazzi R, Perotti A, Barusi L, Buschini A. Use of FTA® classic cards for epigenetic analysis of sperm DNA. *Biotechniques* (2018) 64(2):45–51. doi: 10.2144/btn-2017-0101

26. Peng F, Feng L, Chen J, Wang L, Li P, Ji A, et al. Validation of methylation-based forensic age estimation in time-series bloodstains on FTA cards and gauze at room temperature conditions. *Forensic Sci Int Genet* (2019) 40:168–74. doi: 10.1016/j.fsigen.2019.03.006

27. Walker RM, MacGillivray L, McCafferty S, Wrobel N, Murphy L, Kerr SM, et al. Assessment of dried blood spots for DNA methylation profiling. *Wellcome Open Res* (2019) 4:44. doi: 10.12688/wellcomeopenres.15136.1

28. Wojdacz TK, Dobrovic A, Hansen LL. Methylation-sensitive high-resolution melting. *Nat Protoc* (2008) 3(12):1903–8. doi: 10.1038/nprot.2008.191

29. Accomando WP, Wiencke JK, Houseman EA, Nelson HH, Kelsey KT. Quantitative reconstruction of leukocyte subsets using DNA methylation. *Genome Biol* (2014) 15(3):R50. doi: 10.1186/gb-2014-15-3-r50

30. Yu HR, Hsu TY, Tsai CC, Huang HC, Cheng HH, Lai YJ, et al. The functional DNA methylation signatures relevant to altered immune response of neonatal T cells with l-arginine supplementation. *Nutrients* (2021) 13(8):2780. doi: 10.3390/nu13082780

31. White GP, Hollams EM, Yerkovich ST, Bosco A, Holt BJ, Bassami MR, et al. CpG methylation patterns in the IFNgamma promoter in naive T cells: variations during Th1 and Th2 differentiation and between atopics and non-atopics. *Pediatr Allergy Immunol* (2006) 17(8):557–64. doi: 10.1111/j.1399-3038.2006.00465.x

32. White GP, Watt PM, Holt BJ, Holt PG. Differential patterns of methylation of the IFN-gamma promoter at CpG and non-CpG sites underlie differences in IFN-gamma gene expression between human neonatal and adult CD45RO- T cells. *J Immunol* (2002) 168(6):2820–7. doi: 10.4049/jimmunol.168.6.2820

33. Jones B, Chen J. Inhibition of IFN-gamma transcription by site-specific methylation during T helper cell development. *EMBO J* (2006) 25(11):2443–52. doi: 10.1038/sj.emboj.7601148

34. Fiorentino DF, Bond MW, Mosmann TR. Two types of mouse T helper cell. IV. Th2 clones secrete a factor that inhibits cytokine production by Th1 clones. *J Exp Med* (1989) 170(6):2081–95. doi: 10.1084/jem.170.6.2081

35. Dong J, Ivascu C, Chang HD, Wu P, Angeli R, Maggi L, et al. IL10 is excluded from the functional cytokine memory of human CD4+ memory T lymphocytes. *J Immunol* (2007) 179(4):2389–96. doi: 10.4049/jimmunol.179.4.2389

36. Alipour S, Nouri M, Khabbazi A, Samadi N, Babaloo Z, Abolhasani S, et al. Hypermethylation of IL10 gene is responsible for its low mRNA expression in behçet's disease. *J Cell Biochem* (2018) 119(8):6614–22. doi: 10.1002/jcb.26809

37. Fu LH, Ma CL, Cong B, Li SJ, Chen HY, Zhang JG. Hypomethylation of proximal CpG motif of interleukin-10 promoter regulates its expression in human rheumatoid arthritis. *Acta Pharmacol Sin* (2011) 32(11):1373–80. doi: 10.1038/aps.2011.98

38. Hwang W, Lee CG, Lee C, Verma R, Rudra D, Park ZY, et al. Locus-specific reversible DNA methylation regulates transient IL10 expression in Th1 cells. *J Immunol* (2018) 200(5):1865–75. doi: 10.4049/jimmunol.1701162

39. Larsson L, Thorbert-Mros S, Rymo L, Berglundh T. Influence of epigenetic modifications of the interleukin-10 promoter on IL10 gene expression. *Eur J Oral Sci* (2012) 120(1):14–20. doi: 10.1111/j.1600-0722.2011.00917.x

40. Zheng Z, Huang G, Gao T, Huang T, Zou M, Zou Y, et al. Epigenetic changes associated with interleukin-10. *Front Immunol* (2020) 11:1105. doi: 10.3389/fimmu.2020.01105

41. Moore KW, de Waal Malefyt R, Coffman RL, O'Garra A. Interleukin-10 and the interleukin-10 receptor. *Annu Rev Immunol* (2001) 19:683–765. doi: 10.1146/annurev.immunol.19.1.683

42. Yamawaki K, Inuo C, Nomura T, Tanaka K, Nakajima Y, Kondo Y, et al. Multicolor flow-cytometric analysis of milk allergen-specific T-helper type 2 cells revealed coexpression of interleukin-4 with Foxp3. *Ann Allergy Asthma Immunol* (2015) 115(6):503–8. doi: 10.1016/j.anai.2015.09.020

43. Mulder RH, Neumann A, Cecil CAM, Walton E, Houtepen LC, Simpkin AJ, et al. Epigenome-wide change and variation in DNA methylation in childhood: trajectories from birth to late adolescence. *Hum Mol Genet* (2021) 30(1):119–34. doi: 10.1093/hmg/ddaa280

44. Kader F, Ghai M. DNA Methylation-based variation between human populations. *Mol Genet Genomics* (2017) 292(1):5–35. doi: 10.1007/s00438-016-1264-2

45. Böttcher MF, Jenmalm MC, Voor T, Julge K, Holt PG, Björkstén B. Cytokine responses to allergens during the first 2 years of life in Estonian and Swedish children. *Clin Exp Allergy* (2006) 36(5):619–28. doi: 10.1111/j.1365-2222.2006.02484.x

46. Čelakovská J, Ettlerová K, Ettler K, Vaněčková J, Bukač J. Sensitization to aeroallergens in atopic dermatitis patients: association with concomitant allergic diseases. *J Eur Acad Dermatol Venereol.* (2015) 29(8):1500–5. doi: 10.1111/jdv.12891

47. Konradsen JR, Fujisawa T, van Hage M, Hedlin G, Hilger C, Kleine-Tebbe J, et al. Allergy to furry animals: new insights, diagnostic approaches, and challenges. *J Allergy Clin Immunol* (2015) 135(3):616–25. doi: 10.1016/j.jaci.2014.08.026

48. Ferrari L, Carugno M, Bollati V. Particulate matter exposure shapes DNA methylation through the lifespan. *Clin Epigenet* (2019) 11(1):129. doi: 10.1186/s13148-019-0726-x

49. Ghazi T, Naidoo P, Naidoo RN, Chuturgoon AA. Prenatal air pollution exposure and placental DNA methylation changes: implications on fetal development and future disease susceptibility. *Cells* (2021) 10(11):3025. doi: 10.3390/cells10113025

50. Isaevska E, Moccia C, Asta F, Cibella F, Gagliardi L, Ronfani L, et al. Exposure to ambient air pollution in the first 1000 days of life and alterations in the DNA methylome and telomere length in children: a systematic review. *Environ Res* (2021) 193:110504. doi: 10.1016/j.envres.2020.110504

51. Li Y, Mu Z, Wang H, Liu J, Jiang F. The role of particulate matters on methylation of *IFN-γ* and *IL4* promoter genes in pediatric allergic rhinitis. *Oncotarget* (2018) 9(25):17406–19. doi: 10.18632/oncotarget.24227

52. Adkins RM, Thomas F, Tylavsky FA, Krushkal J. Parental ages and levels of DNA methylation in the newborn are correlated. *BMC Med Genet* (2011) 12:47. doi: 10.1186/1471-2350-12-47

53. Girchenko P, Lahti J, Czamara D, Knight AK, Jones MJ, Suarez A, et al. Associations between maternal risk factors of adverse pregnancy and birth outcomes and the offspring epigenetic clock of gestational age at birth. *Clin Epigenetics.* (2017) 9:49. doi: 10.1186/s13148-017-0349-z

54. Markunas CA, Wilcox AJ, Xu Z, Joubert BR, Harlid S, Panduri V, et al. Maternal age at delivery is associated with an epigenetic signature in both newborns and adults. *PloS One* (2016) 11(7):e0156361. doi: 10.1371/journal.pone.0156361

55. Härtel C, Adam N, Strunk T, Temming P, Müller-Steinhardt M, Schultz C. Cytokine responses correlate differentially with age in infancy and early childhood. *Clin Exp Immunol* (2005) 142(3):446–53. doi: 10.1111/j.1365-2249.2005.02928.x

56. Smart JM, Kemp AS. Ontogeny of T-helper 1 and T-helper 2 cytokine production in childhood. *Pediatr Allergy Immunol* (2001) 12:181–7. doi: 10.1034/j.1399-3038.2001.012004181.x

57. Mansego ML, Milagro FI, Zulet MÁ, Moreno-Aliaga MJ, Martínez JA. Differential DNA methylation in relation to age and health risks of obesity. *Int J Mol Sci* (2015) 16(8):16816–32. doi: 10.3390/ijms160816816

58. Alisch RS, Barwick BG, Chopra P, Myrick LK, Satten GA, Conneely KN, et al. Age-associated DNA methylation in pediatric populations. *Genome Res* (2012) 22(4):623–32. doi: 10.1101/gr.125187.111

59. Pérez RF, Santamarina P, Tejedor JR, Urdinguio RG, Álvarez-Pitti J, Redon P, et al. Longitudinal genome-wide DNA methylation analysis uncovers persistent early-life DNA methylation changes. *J Transl Med* (2019) 17(1):15. doi: 10.1186/s12967-018-1751-9

60. Salameh Y, Bejaoui Y, El Hajj N. DNA Methylation biomarkers in aging and age-related diseases. *Front Genet* (2020) 11:171. doi: 10.3389/fgene.2020.00171

61. Cameron N, Demerath EW. Critical periods in human growth and their relationship to diseases of aging. *Am J Phys Anthropol.* (2002) Suppl 35:159–84. doi: 10.1002/ajpa.10183

62. Ladd-Acosta C, Vang E, Barrett ES, Bulka CM, Bush NR, Cardenas A, et al. Environmental influences on child health outcomes program. analysis of pregnancy complications and epigenetic gestational age of newborns. *JAMA Netw Open* (2023) 6(2):e230672. doi: 10.1001/jamanetworkopen.2023.0672

63. Barker DJ. The fetal and infant origins of adult disease. *BMJ Clin Res* (1990) 301(6761):1111. doi: 10.1136/bmj.301.6761.1111

64. Teh AL, Pan H, Chen L, Ong ML, Dogra S, Wong J, et al. The effect of genotype and *in utero* environment on interindividual variation in neonate DNA methylomes. *Genome Res* (2014) 24(7):1064–74. doi: 10.1101/gr.171439.113

65. Perng W, Nakiwala D, Goodrich JM. What happens *In utero* does not stay *In utero*: a review of evidence for prenatal epigenetic programming by per- and polyfluoroalkyl substances (PFAS) in infants, children, and adolescents. *Curr Environ Health Rep* (2023) 10(1):35–44. doi: 10.1007/s40572-022-00387-z

66. Atsem S, Reichenbach J, Potabattula R, Dittrich M, Nava C, Depienne C, et al. Paternal age effects on sperm FOXK1 and KCNA7 methylation and transmission into the next generation. *Hum Mol Genet* (2016) 25(22):4996–5005. doi: 10.1093/hmg/ddw328

67. Potabattula R, Dittrich M, Böck J, Haertle L, Müller T, Hahn T, et al. Allele-specific methylation of imprinted genes in fetal cord blood is influenced by cis-acting genetic variants and parental factors. *Epigenomics* (2018) 10(10):1315–26. doi: 10.2217/epi-2018-0059

68. Heikkinen A, Bollepalli S, Ollikainen M. The potential of DNA methylation as a biomarker for obesity and smoking. *J Intern Med* (2022) 292(3):390–408. doi: 10.1111/joim.13496

69. Brion MJ, Leary SD, Lawlor DA, Smith GD, Ness AR. Modifiable maternal exposures and offspring blood pressure: a review of epidemiological studies of maternal age, diet, and smoking. *Pediatr Res* (2008) 63(6):593–8. doi: 10.1203/PDR.0b013e31816fdbd3

70. Cupul-Uicab LA, Skjaerven R, Haug K, Melve KK, Engel SM, Longnecker MP. *In utero* exposure to maternal tobacco smoke and subsequent obesity, hypertension, and gestational diabetes among women in the MoBa cohort. *Environ Health Perspect* (2012) 120(3):355–60. doi: 10.1289/ehp.1103789

71. Joubert BR, Håberg SE, Nilsen RM, Wang X, Vollset SE, Murphy SK, et al. 450K epigenome-wide scan identifies differential DNA methylation in newborns related to maternal smoking during pregnancy. *Environ Health Perspect* (2012) 120(10):1425–31. doi: 10.1289/ehp.1205412

72. Hannon E, Schendel D, Ladd-Acosta C, Grove J, Hansen CS, Hougaard DM, et al. Variable DNA methylation in neonates mediates the association between prenatal smoking and birth weight. *Philos Trans R Soc Lond B Biol Sci* (2019) 374 (1770):20180120. doi: 10.1098/rstb.2018.0120

73. Küpers LK, Xu X, Jankipersadsing SA, Vaez A, la Bastide-van Gemert S, Scholtens S, et al. DNA Methylation mediates the effect of maternal smoking during pregnancy on birthweight of the offspring. *Int J Epidemiol.* (2015) 44(4):1224–37. doi: 10.1093/ije/dyv048

74. Hong X, Wang X. Early life precursors, epigenetics, and the development of food allergy. *Semin Immunopathol* (2012) 34(5):655–69. doi: 10.1007/s00281-012-0323-y

75. Williams L, Seki Y, Delahaye F, Cheng A, Fuloria M, Hughes Einstein F, et al. DNA Hypermethylation of CD3(+) T cells from cord blood of infants exposed to intrauterine growth restriction. *Diabetologia* (2016) 59(8):1714–23. doi: 10.1007/s00125-016-3983-7

76. Antoun E, Kitaba NT, Titcombe P, Dalrymple KV, Garratt ES, Barton SJ, et al. UPBEAT consortium. maternal dysglycaemia, changes in the infant's epigenome modified with a diet and physical activity intervention in pregnancy: secondary analysis of a randomised control trial. *PloS Med* (2020) 17(11):e1003229. doi: 10.1371/journal.pmed.1003229

77. Kazmi N, Sharp GC, Reese SE, Vehmeijer FO, Lahti J, Page CM, et al. Hypertensive disorders of pregnancy and DNA methylation in newborns. *Hypertension* (2019) 74(2):375–83. doi: 10.1161/HYPERTENSIONAHA.119.12634

78. Fiorito G, Caini S, Palli D, Bendinelli B, Saieva C, Ermini I, et al. DNA Methylation-based biomarkers of aging were slowed down in a two-year diet and physical activity intervention trial: the DAMA study. *Aging Cell* (2021) 20(10):e13439. doi: 10.1111/acel.13439

79. Briollais L, Rustand D, Allard C, Wu Y, Xu J, Rajan SG, et al. DNA Methylation mediates the association between breastfeeding and early-life growth trajectories. *Clin Epigenetics.* (2021) 13(1):231. doi: 10.1186/s13148-021-01209-z

80. Naumova OY, Odintsova VV, Arincina IA, Rychkov SY, Muhamedrahimov RJ, Shneider YV, et al. A study of the association between breastfeeding and DNA methylation in peripheral blood cells of infants. *Rus J Genet* (2019) 55(6):749–55. doi: 10.1134/S1022795419060103

81. Forsberg A, Huoman J, Söderholm S, Bhai Mehta R, Nilsson L, Abrahamsson TR, et al. Pre- and postnatal lactobacillus reuteri treatment alters DNA methylation of infant T helper cells. *Pediatr Allergy Immunol* (2020) 31(5):544–53. doi: 10.1111/pai.13240

82. Yu HR, Tsai CC, Chang LS, Huang HC, Cheng HH, Wang JY, et al. L-Arginine-Dependent epigenetic regulation of interleukin-10, but not transforming growth factor-β, production by neonatal regulatory T lymphocytes. *Front Immunol* (2017) 8:487. doi: 10.3389/fimmu.2017.00487

83. Lee HS, Barraza-Villarreal A, Hernandez-Vargas H, Sly PD, Biessy C, Ramakrishnan U, et al. Modulation of DNA methylation states and infant immune system by dietary supplementation with ω-3 PUFA during pregnancy in an intervention study. *Am J Clin Nutr* (2013) 98(2):480–7. doi: 10.3945/ajcn.112.052241

84. Shorey-Kendrick LE, McEvoy CT, Ferguson B, Burchard J, Park BS, Gao L, et al. Vitamin c prevents offspring DNA methylation changes associated with maternal smoking in pregnancy. *Am J Respir Crit Care Med* (2017) 196(6):745–55. doi: 10.1164/rccm.201610-2141OC

85. Jiao X, Wang L, Wei Z, Liu B, Liu X, Yu X. Vitamin d deficiency during pregnancy affects the function of Th1/Th2 cells and methylation of IFN-γ gene in offspring rats. *Immunol Lett* (2019) 212:98–105. doi: 10.1016/j.imlet.2019.06.012

86. Acevedo N, Alashkar Alhamwe B, Caraballo L, Ding M, Ferrante A, Garn H, et al. Perinatal and early-life nutrition, epigenetics, and allergy. *Nutrients* (2021) 13 (3):724. doi: 10.3390/nu13030724

87. Cifuentes-Zúñiga F, Arroyo-Jousse V, Soto-Carrasco G, Casanello P, Uauy R, Krause BJ, et al. IL10 expression in macrophages from neonates born from obese mothers is suppressed by IL4 and LPS/INFγ. *J Cell Physiol* (2017) 232(12):3693–701. doi: 10.1002/jcp.25845

88. Sharp GC, Lawlor DA, Richmond RC, Fraser A, Simpkin A, Suderman M, et al. Maternal pre-pregnancy BMI and gestational weight gain, offspring DNA methylation and later offspring adiposity: findings from the Avon longitudinal study of parents and children. *Int J Epidemiol.* (2015) 44(4):1288–304. doi: 10.1093/ije/dyv042

89. Liu X, Chen Q, Tsai HJ, Wang G, Hong X, Zhou Y, et al. Maternal preconception body mass index and offspring cord blood DNA methylation: exploration of early life origins of disease. *Environ Mol Mutagen* (2014) 55(3):223–30. doi: 10.1002/em.21827

90. Morales E, Groom A, Lawlor DA, Relton CL. DNA Methylation signatures in cord blood associated with maternal gestational weight gain: results from the ALSPAC cohort. *BMC Res Notes.* (2014) 7:278. doi: 10.1186/1756-0500-7-278

91. Richmond RC, Sharp GC, Ward ME, Fraser A, Lyttleton O, McArdle WL, et al. DNA Methylation and BMI: investigating identified methylation sites at HIF3A in a causal framework. *Diabetes* (2016) 65(5):1231–44. doi: 10.2337/db15-0996

92. Burris HH, Baccarelli AA, Byun HM, Cantoral A, Just AC, Pantic I, et al. Offspring DNA methylation of the aryl-hydrocarbon receptor repressor gene is associated with maternal BMI, gestational age, and birth weight. *Epigenetics* (2015) 10(10):913–21. doi: 10.1080/15592294.2015.1078963

93. Sharp GC, Salas LA, Monnereau C, Allard C, Yousefi P, Everson TM, et al. Maternal BMI at the start of pregnancy and offspring epigenome-wide DNA methylation: findings from the pregnancy and childhood epigenetics (PACE) consortium. *Hum Mol Genet* (2017) 26(20):4067–85. doi: 10.1093/hmg/ddx290

94. Andraos S, de Seymour JV, O'Sullivan JM, Kussmann M. The impact of nutritional interventions in pregnant women on DNA methylation patterns of the offspring: a systematic review. *Mol Nutr Food Res* (2018) 62(24):e1800034. doi: 10.1002/mnfr.201800034

95. Küpers LK, Fernández-Barrés S, Mancano G, Johnson L, Ott R, Vioque J, et al. Maternal dietary glycemic index and glycemic load in pregnancy and offspring cord blood DNA methylation. *Diabetes Care* (2022) 45(8):1822–32. doi: 10.2337/dc21-2662

96. Jönsson J, Renault KM, García-Calzón S, Perfilyev A, Estampador AC, Nørgaard K, et al. Lifestyle intervention in pregnant women with obesity impacts cord blood DNA methylation, which associates with body composition in the offspring. *Diabetes* (2021) 70(4):854–66. doi: 10.2337/db20-0487

97. Wahl S, Drong A, Lehne B, Loh M, Scott WR, Kunze S, et al. Epigenome-wide association study of body mass index, and the adverse outcomes of adiposity. *Nature* (2017) 541(7635):81–6. doi: 10.1038/nature20784

98. Nevalainen T, Kananen L, Marttila S, Jylhävä J, Mononen N, Kähönen M, et al. Obesity accelerates epigenetic aging in middle-aged but not in elderly individuals. *Clin Epigenetics.* (2017) 9:20. doi: 10.1186/s13148-016-0301-7

99. Sharp GC, Alfano R, Ghantous A, Urquiza J, Rifas-Shiman SL, Page CM, et al. 36 other members of the pregnancy and childhood epigenetics (PACE) consortium. paternal body mass index and offspring DNA methylation: findings from the PACE consortium. *Int J Epidemiol.* (2021) 50(4):1297–315. doi: 10.1093/ije/dyaa267

100. Ollikainen M, Smith KR, Joo EJ, Ng HK, Andronikos R, Novakovic B, et al. DNA Methylation analysis of multiple tissues from newborn twins reveals both genetic and intrauterine components to variation in the human neonatal epigenome. *Hum Mol Genet* (2010) 19(21):4176–88. doi: 10.1093/hmg/ddq336

101. Schalkwyk LC, Meaburn EL, Smith R, Dempster EL, Jeffries AR, Davies MN, et al. Allelic skewing of DNA methylation is widespread across the genome. *Am J Hum Genet* (2010) 86(2):196–212. doi: 10.1016/j.ajhg.2010.01.014

102. Kerkel K, Spadola A, Yuan E, Kosek J, Jiang L, Hod E, et al. Genomic surveys by methylation-sensitive SNP analysis identify sequence-dependent allele-specific DNA methylation. *Nat Genet* (2008) 40(7):904–8. doi: 10.1038/ng.174

103. McRae AF, Powell JE, Henders AK, Bowdler L, Hemani G, Shah S, et al. Contribution of genetic variation to transgenerational inheritance of DNA methylation. *Genome Biol* (2014) 15(5):R73. doi: 10.1186/gb-2014-15-5-r73

104. Tsai HJ, Kumar R, Pongracic J, Liu X, Story R, Yu Y, et al. Familial aggregation of food allergy and sensitization to food allergens: a family-based study. *Clin Exp Allergy* (2009) 39(1):101–9. doi: 10.1111/j.1365-2222.2008.03111.x

105. Dor Y, Cedar H. Principles of DNA methylation and their implications for biology and medicine. *Lancet* (2018) 392(10149):777–86. doi: 10.1016/S0140-6736(18)31268-6

106. Koplin JJ, Allen KJ, Gurrin LC, Aldurawish RL, Lowe AJ, Tang ML, et al. The impact of family history of allergy on risk of food allergy: a population-based study of infants. *Int J Environ Res Public Health* (2013) 10(11):5364–77. doi: 10.3390/ijerph10115364

Frontiers in Immunology

Explores novel approaches and diagnoses to treat immune disorders.

The official journal of the International Union of Immunological Societies (IUIS) and the most cited in its field, leading the way for research across basic, translational and clinical immunology.

Discover the latest Research Topics

See more →

Frontiers

Avenue du Tribunal-Fédéral 34
1005 Lausanne, Switzerland
frontiersin.org

Contact us

+41 (0)21 510 17 00
frontiersin.org/about/contact